WATER QUALITY MODELLING OF EUTROPHIED RESERVOIRS IN SOUTH AFRICA

by

Ansie Venter, MSc (Chem)
Potchefstroom University for Christian Higher Education

Thesis Presented for the Degree of
Doctor of Philosophy
at the University of Cape Town

Department of Civil Engineering
University of Cape Town

February 1996

DECLARATION BY CANDIDATE

I, Ansie Venter, hereby declare
that this degree is my own work and that it has
not been submitted for a degree at another University

Signed by candidate

February 1996

ACKNOWLEDGEMENTS

Financial support from the Department of Civil Engineering is gratefully acknowledged.

The Water Research Commission initiated the project and financed part of the research.

Staff of the Weather Bureau in Pretoria supplied meteorological data.

Mr Jan Schutte and his team of the Directorate of Hydrology, Department of Water Affairs and Forestry, Pretoria, provided water quality data.

The IWQS (Mr Bosman and Mr Quibell) supplied data on Roodeplaat Dam, as well as general support and advice.

Dr Ashton of Watertek (CSIR) provided data and general information.

The original MINLAKE model was obtained from St Anthony Falls Hydraulic Laboratory, University of Minnesota, USA, at no cost.

The preliminary project was conducted in cooperation with Ninham Shand Inc.

Stewart Scott Inc. kindly let me use their printing facilities.

Many useful discussions were held with Professors Kilner and Kratz, and Professor Loewenthal provided general moral support.

Professor Mark Wentzel was always ready with invaluable advice and a sympathetic ear.

Special thanks go to Professor Emeritus GvR Marais, who gave me the full benefit of a life-time of experience.

SYNOPSIS

BACKGROUND AND OBJECTIVES

Reservoirs are the main source of potable and irrigation water in South Africa, and many reservoirs are also important recreational sites. Eutrophication has been identified as one of the major water quality problems in South African waters. The nutrients that cause eutrophication (phosphate and nitrogen) arise from both non-point (diffuse) and point sources. Diffuse sources are mainly runoff from agricultural activities and from informal settlements with inadequate sanitation facilities. Point sources are mainly effluent discharges from industrial and waste water treatment plants.

Governmental agencies in South Africa became concerned about the increase in eutrophication-related water quality problems during the early 1970's. The first step taken to control eutrophication was introduction of an effluent phosphate standard that limited the phosphorus concentration in effluents being discharged in certain sensitive catchments to a maximum of 1 mg PO_4-P l^{-1}. This standard applied only to point sources, because of an initial belief that the contribution from non-point sources was relatively minor, and the absence of practical economic measures to control phosphorus discharges from non-point sources.

Subsequent to introduction of the 1 mg P Standard several modelling studies were undertaken, as there was a need to describe the response of eutrophic reservoirs to altered phosphate inputs. Most of the work was done on the hypertrophic Hartbeespoort Dam reservoir. The models utilised were empirical, zero-dimensional models that treated the reservoir as a completely mixed reactor. Usually these models considered only the steady state, or at most, annual changes.

The models simulated annual mean phosphate-P concentrations with varying degrees of success, but a significant relationship between observed and simulated chlorophyll-a concentrations could not be obtained, i.e. these models could not be used to predict

the response of eutrophic reservoirs to different management strategies aimed at alleviating eutrophication-related water quality problems. Consequently, a further study was initiated by the Water Research Commission to test the applicability of more sophisticated hydrodynamic and water quality models, developed in the USA and Australia, to stratified reservoirs under South African climatic conditions. Several models of varying complexity were available. From these four models were selected for study.

The models that were tested were the one-dimensional models DYRESM (developed in Australia), and MINLAKE (developed in the USA), and the two-dimensional models CE-QUAL and WASP (developed in the USA). The DYRESM model can simulate hydrodynamic behaviour only, whereas MINLAKE, CE-QUAL and WASP can simulate both hydrodynamic and water quality behaviour. Common characteristics of these models are:

- Daily meteorological and inflow water quality data are needed to run these models.
- Experience has shown that these models can be subdivided into two parts, hydrodynamic and water quality. The hydrodynamic behaviour is relatively independent of the water quality behaviour, but the water quality behaviour is significantly affected by the hydrodynamic behaviour. Because of this behaviourial characteristic, satisfactory simulation of the hydrodynamic behaviour can be achieved without satisfactory simulation of the water quality response. However, simulation of the water quality behaviour of a reservoir is not possible unless the hydrodynamic behaviour is simulated correctly.

This report covers the extensive study that conducted on the MINLAKE model. The study is justified in view of the potential of the MINLAKE model to evaluate different treatment options: of the four models selected, it is the only model that can simulate more than one algal class. Thus it is an ideal tool to assess the effect of a chosen treatment option on, for example, algal succession.

In a preliminary study the water temperature and total dissolved salts (TDS) concentration of a typical South African reservoir (Roodeplaat Dam) could be simulated successfully with the MINLAKE model. However, during the preliminary study it also became clear that the model would have to be modified to simulate the water quality behaviour of Roodeplaat Dam (and probably any South African reservoir) over an extended period of time. It was recognised that, due to the complex nature of water quality processes, modification of the water quality part of the MINLAKE model would require an intensive investigation - all the processes would have to be critically assessed with respect to their constants and formulation. Accordingly, the Water Research Commission appointed the Department of Civil Engineering, University of Cape Town, as a consultant in January 1993, with the specific aim to:

- Modify the MINLAKE model so that it can simulate the water quality behaviour of Roodeplaat Dam
- Assess the sensitivity of the modified model output to reduced data input
- Apply the modified model to another dam.

SIMULATION OF THE WATER QUALITY BEHAVIOUR OF ROODEPLAAT DAM WITH THE MODIFIED MINLAKE MODEL

When the original MINLAKE model was applied to Roodeplaat Dam, it simulated the water quality behaviour poorly. It was postulated that the poor simulation results were due to any or all of the following:

- In the original MINLAKE model, 20 kinetic processes, acting on 15 constituents, are represented in the form of mathematical equations. Because of the complex nature of these processes, many of the processes cannot be formulated precisely. It was necessary to use simplified mathematical representations incorporating kinetic process coefficients which must be specified by the user. Many of these coefficients are algal and climate-specific. It was possible that the initial values chosen for Roodeplaat Dam were not optimal values.

- The original MINLAKE model was developed and tested on Lake Riley, an eutrophic lake situated in a cold temperate climate in the northern hemisphere. In contrast, Roodeplaat Dam is hypertrophic and is situated in a warm temperate/subtropical climate in the southern hemisphere. Possibly certain processes of little consequence in modelling a reservoir in a cold temperate climate, but of significance in modelling a hypertrophic reservoir in a warm/subtropical climate, are not represented in the MINLAKE model.

Kinetic process coefficients:

Regarding the kinetic process coefficients, the original MINLAKE model requires 32 kinetic coefficients, of which 21 are algal and climate specific. Virtually none of the coefficients have been determined experimentally for Roodeplaat Dam. Experimental determination of these coefficients was outside the scope of this study, thus a literature study was undertaken to find values of the coefficients that would be valid for the algal species and subtropical climatic conditions of Roodeplaat Dam. This proved to be a difficult task, as the majority of the values reported in the literature were determined in a cold temperate climate, and therefore were probably not valid for Roodeplaat Dam. In particular, very little information was available on the dominant blue-green algal species in Roodeplaat Dam (*Microcystis aeruginosa*). Considerable time was spent in an exhaustive literature survey to obtain estimates of the algal and climate specific coefficients for Roodeplaat Dam. From an extensive modelling exercise, it is believed that the values of the coefficients for Roodeplaat Dam derived from the literature are near optimal values. Very likely these values will be valid for other reservoirs in the same climatic region.

Additional processes:

To simulate the water quality behaviour of Roodeplaat Dam to an acceptable level, it was necessary to add a number of processes not included in the original MINLAKE model, such as denitrification and sediment phosphate adsorption. Also, it was necessary to modify a number of process rates (e.g. the rate of nutrient release from the bottom sediments), to enable simulation of the effect of anaerobic conditions in the hypolimnion on these process rates. Due to the complex interaction between the

various reservoir processes, extreme care needed to be taken when changing and/or adding any processes - considerable time was spent in examining the processes and the various interactions in detail, to ensure optimal representation and formulation of the processes.

The modified MINLAKE model, utilising the derived values of the kinetic coefficients for the algal and climatic conditions of Roodeplaat Dam, now simulates both the hydrodynamic and water quality behaviour of Roodeplaat Dam remarkably well. The following variables are simulated from the surface to the bottom of the reservoir, for a period of 18 months:

	Water temperature
	Mixing depth
	Water level (stage), and
Concentrations of:	Chlorophyll-a (up to three algal classes)
	Dissolved phosphate
	Soluble detritus
	Particulate detritus
	Dissolved oxygen
	Total inorganic suspended sediment (TSS)
	Total dissolved salts (TDS)
	Nitrate and ammonia
	Zooplankton.

The model has not been calibrated to simulate zooplankton concentration. Also, neither the original nor the modified MINLAKE model simulates dissolved iron and manganese. These metals do not pose a water quality problem in Roodeplaat Dam, but may be of importance in reservoirs that drain Table Mountain sandstone formations. Conceptually it should not be too difficult to add the relevant processes to the modified MINLAKE model to remedy this shortcoming.

Of special interest is the successful simulation of algal succession in Roodeplaat Dam from blue-green algae during summer to green algae during late winter to blue-green algae during summer. The modified MINLAKE model is the only dynamic water quality model calibrated for a South African reservoir that can simulate more than one algal class, i.e. can simulate algal succession.

Conclusions on simulation of water quality:

The following conclusions were drawn with the aid of the model:

- During periods of overturn wind action is the dominant mixing process from the surface to the bottom of the reservoir.

- During periods of stratification, wind action is the dominant mixing process in the epilimnion only. In the hypolimnion the effect of the wind is counteracted by the thermal stability of the system, where eddy (turbulent) diffusivity becomes the dominant mixing process. It is essential that hypolimnetic eddy diffusivity be represented as correctly as possible, especially in systems where there is substantial release of nutrients from the bottom sediments, because eddy diffusivity is the main physical process for mixing the released nutrients into the overlying water.

- In the hypertrophic Roodeplaat Dam the bottom sediments are a major source of nutrients, this is possibly due to the age of the dam.

- In hypertrophic reservoirs it is essential to take cognisance of the effect of anaerobic periods in the hypolimnion on processes and their rates, such as the rate of nutrient release by bottom sediments, detrital decay, etc.

- Two principal management options exist to prevent or relieve anaerobic conditions in the hypolimnion, e.g. destratification or hypolimnetic aeration. The bottom sediments can be a major source of nutrients in eutrophic reservoirs, so destratification may have a detrimental effect on the trophic (algal) response

of a system. Hypolimnetic aeration may be a more appropriate option. When considering destratification/hypolimnetic aeration as management options, it is essential to consider not only the effect on the hydrodynamic behaviour, but also on the water quality behaviour, i.e. the trophic response of the reservoir.

- The factors that govern algal succession in Roodeplaat Dam could be identified with the aid of the model. In this dam, dissolved phosphate is always available in excess and thus nitrogen is the main limiting nutrient. Also, due to self shading and turbidity, light becomes an additional regulator of algal growth in the upper layers of the dam. Furthermore, both water temperature and light have a dominating influence on the algal succession in the dam.

- The values of the algal and climate-specific coefficients determined for Roodeplaat Dam should be valid for other reservoirs in the same climatic region so that, once the appropriate data bases have been set up, minimum effort would be required to calibrate the modified MINLAKE model to these reservoirs. Once the model has been calibrated for a particular reservoir, the way is prepared to test the effects of various management options on the hydrodynamic and water quality response of the reservoir.

- Possible areas of extension of the modified MINLAKE model are incorporation of silica as a nutrient to enable simulation of diatoms, and incorporation of relevant processes to enable simulation of iron and manganese.

ASSESSING THE SENSITIVITY OF THE MODIFIED MODEL OUTPUT TO REDUCED DATA INPUT

The time-series meteorological and inflow water quality data required by dynamic water quality models usually are very similar, and because model predictions have a time step of one day, daily meteorological and inflow water quality data are needed. For instance, the MINLAKE model requires the following input data on a daily basis:

Meteorological data:

- Air temperature
- Dew point (other models may require relative humidity)
- Precipitation
- Wind speed
- Wind direction
- Percentage sunshine
- Shortwave radiation

Inflow water quality data:

- Flow rate
- Water temperature
- Dissolved phosphate
- Detritus
- Dissolved oxygen
- Total inorganic suspended sediment
- Total dissolved salts
- Nitrate and ammonia
- Chlorophyll-a (up to three classes)

Monitoring of these variables is not always done at the specific reservoir, or may not be on a daily basis, or a limited range of variables may be measured. As a consequence, infilling of incomplete data often has to be done to obtain a set of daily data, or data obtained from a nearby or regional site have to be substituted. To address these difficulties, a study was undertaken to ascertain whether model output would be significantly affected by reduced data input and to determine which of the input variables affects model output the most.

For meteorological data, the effect of using weekly or monthly data instead of daily data was assessed. For inflow water quality data, two approaches were assessed:

- Assuming the data for the first day of the week are representative of the data for the rest of the week (this is referred to as 'weekly data')

- Establishing a linear regression between the each water quality variable and flow rate and using this instead of daily observed data, that is, the daily inflow water quality data are calculated from the flow rate.

Conclusions on the effect of reduced data input on model output:

- Regarding meteorological data, with the possible exception of wind speed data, weekly data can be used for all the variables instead of daily data. In some instances, monthly data or data from a nearby site can be used for some of the variables.

- In South Africa, wind speed is usually measured at a height of 1.8 meters, whereas models such as DYRESM and MINLAKE require wind speed measurements at a height of 10 meters. It is of the utmost importance to correctly convert the observed wind speed to wind speed at the required height of 10 meters.

- Regarding river flow rate, this needs to be measured daily, as infilling of many of the inflow water quality variables is done from the daily flow rate.

- Regarding inflow water quality, a final conclusion that would be valid for all reservoirs could not be drawn. It appears that, for reservoirs such as Roodeplaat Dam, where the internal nutrient load due to nutrient release from the bottom sediments is high in comparison with the inflow nutrient load, instead of daily input inflow water quality data, weekly data, or daily data calculated from the flow rate with the aid of a simple regression, can be used. However, it is unlikely that this conclusion will be valid for reservoirs where the inflow nutrient load is comparable to the internal nutrient load.

APPLICATION OF THE MODIFIED MINLAKE MODEL TO ANOTHER RESERVOIR

To assess the generality of the modified model it should be applied to another reservoir. Unfortunately it has not as yet been possible to establish the required data bases for another South African reservoir. However, the original model was tested on Lake Riley in the USA, and data bases for this lake were available, therefore it was decided to apply the modified model to Lake Riley.

Excellent results were obtained. The finding that the modified model gives good results for a reservoir in a warm temperate/subtropical climate, as well as for a lake in a cold temperate climate, would indicate that the modified model has validity over a wide range of conditions. This implies that the model can be applied to other reservoirs in South Africa, irrespective of the climatic region where the reservoir is situated.

TABLE OF CONTENTS

3 CONCEPTUAL REPRESENTATION OF A HYDRODYNAMIC AND WATER QUALITY MODEL

4 GENERAL FORMULATION OF AN EUTROPHICATION MODEL

8 DISCUSSION OF THE SIMULATION RESULTS OBTAINED WITH THE MODIFIED MINLAKE MODEL ON ROODEPLAAT DAM RESERVOIR

9 VERIFICATION OF THE MODIFIED MINLAKE MODEL

10 SENSITIVITY OF MODEL OUTPUT TO INPUT DATA FREQUENCY

APPENDICES

LIST OF FIGURES

LIST OF TABLES

LIST OF SYMBOLS

α	=	molecular diffusion coefficient (m^2 day^{-1}).
α_i	=	ratio of interfacial to bed shear stress
β	=	fraction of incoming solar radiation (H_s) absorbed in the surface layer.
β	=	average density gradient in reservoir (10^{-3}kg m^{-4}).
γ	=	Bowen coefficient (= 0.66)
γ	=	rate of initial mixing (= q_a/q_o)
γ	=	wet and dry bulb hygrometric constant (Penman 1948)
δ	=	thickness of the diffusional layer (m).
$\Delta\rho$	=	density difference between epilimnion and hypolimnion (kg m^{-3})
$\Delta\rho_0$	=	excess density of inflow relative to ρ_a (g m^{-3})
$\Delta\rho_0$	=	excess density of underflow relative to ρ_a (g m^{-3})
ΔH	=	surface heat flux (kcal m^{-2} d^{-1})
$_\Delta\rho$	=	density difference (kg $m^{-3)}$
$_\Delta P$	=	change in phosphate concentration due to sediment exchange of phosphate (mg l^{-1})
$\partial N/\partial t$	=	increase in nitrogen concentration with time
$\partial P/\partial t$	=	increase in phosphorus concentration with time
$\partial s/\partial z$	=	concentration gradient of substance s in the z direction.
$\partial\Theta/\partial t$	=	change in temperature with time t (°C s^{-1})
$\partial\Theta/\partial z$	=	vertical temperature gradient (°C m^{-1})
$_\Delta t$	=	time step.
$\partial u/\partial z$	=	horizontal velocity shear (m s^{-1}).
$_\Delta V$	=	incremental volume (m^3)
ε	=	internal energy dissipation rate
ε	=	emissivity of the atmosphere (= 0.97)
ε_w	=	emissivity of water (≈ 0.97)
ϵ	=	coefficient of eddy viscosity (g s^{-1} cm^{-1})
ϵ_0	=	relative density difference between inflow and ambient water (= $\Delta\rho_0/\rho_a$)
ϵ_d	=	density difference downstream of plunge point (underflow) relative to ambient water density (g m^{-3}) = $\Delta\rho_0/\rho_a$
η	=	total extinction coefficient (m^{-1}).
θ	=	Arrhenius temperature coefficient
Θ_z	=	temperature at depth z (°C).
Θ	=	angle of the bed slope
κ	=	Von Karman constant (= 0.4)
μ	=	rate of growth with nutrients limitation i.e. specific growth rate (day^{-1})
μ	=	absolute viscosity (Nsm^{-2})
μ_{max}	=	maximum specific growth rate (day^{-1})
ρ	=	density of water (g m^{-3})
ρ	=	reaction rate
$\rho_{(aerobic)}$	=	reaction rate under fully aerobic conditions
$\rho_{(anaerobic)}$	=	reaction rate under fully anaerobic conditions
ρ_a	=	density of air (g m^{-3})
ρ_a	=	ambient water density (g m^{-3}).
ρ_a/ρ_w	=	density of air/density of water (= 0.0012)
$\rho_a+\rho_0$	=	density of inflow water (g m^{-3})

ρ_o	=	reference density (= 1000 kg m^{-3})
ρ_s	=	sediment density (g cm^{-3})
ρ_w	=	density of water (g m^{-3})
σ	=	critical ratio for deepening of the mixed layer
σ	=	Stefan-Boltzman constant (= 1.171 * 10^{-8} kcal m^{-2} $°K^{-4}$)
σ_1, σ_2	=	empirical constants
τ	=	optical depth (m) (= $\eta z/\ln 2$)
τ	=	shear stress at the air-water interface (kg m^{-2} s^{-1}).
υ	=	theoretical maximum rate of photosynthesis
υ_a/υ_w	=	viscosity of air/viscosity of water (= 15).
A	=	Area through midpoint of a layer (m^2)
A, A_s	=	reservoir surface area (km^2, m)
A	=	sediment interface (m^2).
a,b	=	empirical constants.
A_d	=	cross-sectional area at depth d (m^2)
A_z	=	sediment cross-sectional area at depth z (m^2)
A_z	=	reservoir cross-sectional area at depth z (m^2, cm^2)
BAA	=	sediment phosphate adsorption rate (g $m^2 day^{-1}$)
BBOT	=	dissolved BOD released from bottom sediment under anaerobic conditions (g $m^2 day^{-1}$)
BBOTOK	=	anaerobic switching constant for release of dissolved BOD from bottom sediment (see BBOT) (mg $O_2 l^{-1}$)
BOD	=	detritus as BOD
BODK20	=	detrital decay rate (day^{-1})
BODPK	=	decomposition rate for particulate BOD (detritus) (day^{-1})
BODSK	=	dissolved BOD decay rate (day^{-1})
BODSOK	=	aerobic switching constant for detrital decay (mg O_2 l^{-1})
BRNH	=	sediment ammonium release rate (mg NH_4 m^{-2} day^{-1})
BRNHK	=	anaerobic switching constant for sediment ammonium release ($mgO_2 l^{-1}$)
BRNO	=	sediment nitrate release rate (mg NO_3 m^{-2} day^{-1})
BRNOK	=	aerobic switching constant for sediment nitrate release (mg $O_2 l^{-1}$)
BRPK	=	switching constant for sediment phosphate release/adsorption (mg $O_2 l^{-1}$)
BRR	=	sediment phosphate release rate (g $m^2 day^{-1}$)
c	=	wind coefficient
c	=	specific heat capacity of water (cal g^{-1} $°C^{-1}$)
c	=	empirical constant
C	=	cloud cover ratio.
C	=	empirical coefficient for wind sheltering
C	=	intracellular carbon concentration (μmoles C $cell^{-1}$)
C	=	concentration or intrinsic property of the fluid such as temperature (mg l^{-1} or °C)
CA	=	phytoplankton concentration (mg l^{-1})
C_D	=	drag coefficient
CD	=	concentration of detritus carbon (mg l^{-1})
Chla	=	chlorophyll-a concentration (mg l^{-1}).
$Chla_t$	=	threshold chlorophyll-a concentration (g m^{-3} day^{-1})

C_m	=	maximum intracellular carbon concentration (μmoles C cell^{-1})
C_s	=	saturated dissolved oxygen concentration at 0°C and 1 atmosphere
C_{s20}	=	saturated dissolved oxygen concentration at 20°C and 1 atmosphere (mg l^{-1})
d	=	particle diameter (cm)
d	=	Secchi disc depth (m).
d	=	depth of inflow or outflow (m)
D	=	molecular diffusivity (m^2s^{-1}) (= 6.92 * 10^{-15} T_K/μ)
D	=	depth of neutral buoyancy (m)
D	=	depth of mixed layer (m)
dh/dt	=	rate of entrainment (m s^{-1})
DMU	=	dry matter in upper layer of sediment (kg kg^{-1})
DN	=	detritus nitrogen in lake water (mg l^{-1}).
dO/dt	=	change in oxygen concentration (mg l^{-1})
DO	=	concentration of dissolved oxygen in the overlying water (mg l^{-1})
DO_{sat}	=	saturated dissolved oxygen concentration (mg l^{-1})
DO_{SL}	=	oxygen concentration in the first layer (mg l^{-1})
DP	=	detritus phosphorus (intracellular phosphorus) (mg l^{-1})
E	=	mass flux of water (evaporation rate) (cm s^{-1} or m d^{-1}).
E	=	entrainment coefficient.
e_a	=	saturated vapour pressure of the air (mbar).
EBRR	=	equilibrium concentration for sediment phosphate release (mg P l^{-1})
EDNK	=	denitrification inhibition constant (mg NO_3l^{-1})
e_s	=	saturated vapour pressure at the water surface (mbar or N m^{-2})
f	=	ratio of total phosphorus to exchangeable phosphorus in the sediment
f	=	bed friction coefficient.
f(T)	=	temperature function.
f(W)	=	horizontal wind velocity function (= cW)
$f(W_z)$	=	wind function (= cW_z)
f_b	=	bed friction coefficient
FC	=	modifying factor for cloud cover
F_D	=	densimetric Froude number
f_i	=	friction coefficient for interface
F_p	=	densimetric Froude number at plunge point
f_t	=	total friction coefficient (= f_b + f_i)
FVBOD	=	fall velocity of particulate detritus (m^2day^{-1})
FVCHLA	=	algal settling rate (m day^{-1})
g	=	acceleration due to gravity (m s^{-2})
GROMAX	=	maximum nutrient saturated growth rate (day^{-1})
GRZ	=	zooplankton grazing rate (g m^{-3} day^{-1})
h	=	depth of the reservoir (m)
H	=	total depth of the reservoir (m)
H(z)	=	solar radiation at depth z (kcal m^{-2} d^{-1})
H_a	=	atmospheric long wave radiation (kcal m^{-2} d^{-1}).

H_b	=	back radiation (kcal m^{-2} d^{-1})
H_c	=	convective heat loss (cal cm^{-2} d^{-1})
h_d	=	underflow depth (m)
H_e	=	evaporative heat loss (cal cm^{-2} d^{-1})
Hkmax	=	Maximum hypolimnetic diffusion coefficient (m^2 day^{-1})
H_N	=	net surface heat exchange (kcal m^{-2} d^{-1})
h_p	=	plunge depth (m)
h_{pm}	=	plunge depth for steep slope (m)
h_{ps}	=	plunge depth for mild slope (m)
H_s	=	incident solar radiation (W m^{-2} or kcal m^{-2} d^{-1}).
HSC1	=	half saturation coefficient for light limited growth (μE $m^{-2}s^{-1}$)
HSC2	=	light inhibition coefficient (μE $m^{-2}s^{-1}$)
HSCN	=	half saturation coefficient for nitrogen uptake (mg l^{-1})
HSCNH	=	half saturation coefficient for preferential uptake of ammonia over nitrate (mg l^{-1})
HSCPA	=	half saturation coefficient for phosphorus uptake (mg l^{-1})
H_{sn}	=	net solar radiation (kcal m^{-2} d^{-1})
H_w	=	thermal energy flux (cal cm^{-2} s^{-1})
I	=	photosynthetically active radiation (PAR) (Einstein m^{-2} h^{-1})
I	=	light intensity (μE m^{-2} s^{-1})
I_k	=	optimum light intensity corresponding to P_{max} (μE m^{-2} s^{-1})
I_o	=	subsurface light intensity (W m^{-2}).
J_{sz}	=	mean flux of substance s in the z (vertical) direction due to turbulent mixing
k	=	Von Karman's constant (≈ 0.40)
K	=	vertical turbulent diffusion coefficient (m^2 day^{-1})
K(T)	=	temperature coefficient at ambient temperature
k_1	=	cloud height coefficient
K_1	=	half saturation coefficient for light controlled algal growth (μE m^{-2} s^{-1})
k_1,k_2	=	decay rates for BOD fractions
k_2	=	extinction coefficient due to chlorophyll-a (m^2 (g chla)$^{-1}$)
K_2	=	Light inhibition coefficient (μE m^{-2} s^{-1})
K4	=	biodegradation rate of detritus (h^{-1})
K5	=	biodegradation rate of organic phosphorus in the sediment
K6	=	Arrhenius temperature coefficient for biodegradation
K_b	=	sediment oxygen demand (g O_2 m^{-2} day^{-1})
k_E	=	surface exchange coefficient
k_g	=	contribution of gilvin (gelbstoff) to the total extinction coefficient (m^{-1})
K_H	=	eddy diffusion coefficient (cm^2 s^{-1})
K_{Ho}	=	neutral (or surface) value of the eddy diffusion coefficient (cm^2 s^{-1})
KI	=	Michaelis constant for light intensity (kcal m^{-2} 24 h^{-1}).
K_L	=	oxygen mass transfer coefficient (m s^{-1} or m day^{-1})
K_m	=	mortality coefficient (day^{-1}).
KN	=	half-saturation constant for uptake of soluble inorganic nitrogen (g m^{-3})
KNF	=	temperature dependent rate constant

KNFIX = nitrogen fixation coefficient (day^{-1})
KONH = aerobic switching constant for nitrification (mg $O_2 l^{-1}$)
KONO = anaerobic switching constant for denitrification (mg $O_2 l^{-1}$)
K_o = aerobic/anaerobic switching constant (mg l^{-1}).
K_{opt} = temperature coefficient at optimum temperature
k_{ph} = contribution of phytoplankton to the total extinction coefficient (m^{-1}).
K_Q = minimum nutrient concentration in algal cell required for algal growth (mg nutrient (mg chla)$^{-1}$)
K_r = respiration coefficient (day^{-1})
K_s = half-saturation coefficient for nutrient uptake (mg l^{-1}).
K_{sed} = sedimentation coefficient
K_{sz} = eddy transport coefficient of substance s in the z direction ($cm^2\ s^{-1}$)
k_T = reaction rate at ambient temperature (°C)
k_{tr} = contribution of tripton to the total extinction coefficient (m^{-1})
k_{Tr} = reaction rate at reference temperature (usually 20°C)
KTR = threshold concentration for grazing (g m^{-3})
k_w = extinction coefficient of pure water (m^{-1}) (*cf* Table 3.3)
K_z = eddy diffusion coefficient at depth z ($cm^2\ s^{-1}$)
L = latent heat of vaporization (kcal m^{-3})
L = length of reservoir (m)
L_{det} = particulate BOD (mg l^{-1}).
L_{sol} = soluble BOD (mg l^{-1})
L_T = average length of reservoir in thermocline region (m).
LUL = upper unstabilized layer (100 mm)
L_v = latent heat of vaporization (J kg^{-1})
M = mortality rate (mg l^{-1} day^{-1})
M_v = molecular weight of water vapour (= 18 * 10^{-3} kg mol^{-1})
MYZ = growth rate of zooplankton (day^{-1})
MYZMAX= maximum growth rate of zooplankton (day^{-1})
n, ß = constants.
N = algal concentration (mg l^{-1})
N = empirical mass transfer coefficient (wind function coefficient).
N = Brunt-Väisälä frequency (buoyancy frequency) (s)
NFIX = rate of nitrogen fixation (g m^{-3} day^{-1})
NH = ammonium concentration (mg l^{-1})
NH_4 = concentration of ammonium nitrogen (g m^{-3} or mg l^{-1})
NH_4L = threshold limit concentration of ammonium (mg l^{-1}).
N_{int} = Intracellular nitrogen concentration (mg l^{-1})
NIT = nitrate-N concentration (mg l^{-1})
NITR = nitrification rate (g m^{-3} day^{-1})
NITRK= nitrification rate coefficient (day^{-1})
N_{max} = maximum intracellular nitrogen concentration (mg N (mg chla)$^{-1}$)
N_{min} = minimum intracellular nitrogen concentration required for algal growth (mg N mg-1 Chla)
NO = nitrate concentration (mg l^{-1})
NPHYT= observed concentration of nitrogen fixing algae (g m^{-3}).
N_r = nitrogen released from sediment
NS = soluble inorganic nitrogen concentration (g m^{-3})

O	=	oxygen concentration (mg l^{-1})
P	=	potential energy of column of water.
P	=	atmospheric pressure (mbars)
P(I)	=	specific rate of photosynthesis (mmol O_2 mg $chla^{-1}$ h^{-1})
p(z,t)	=	photosynthetic production of oxygen at depth *z* and time *t*
P_0	=	atmospheric pressure at sea level (1013 mbar)
PE	=	exchangeable phosphorus in upper layer of sediment (mg l^{-1})
PHYT	=	algal concentration (g m^{-3})
PHYTN	=	concentration of nitrogen fixing algae (g m^{-3}).
P_{int}	=	Intracellular phosphorus concentration (mg l^{-1})
Plw	=	phosphorus in the interstitial water in the sediment (mg l^{-1})
$p_m(t)$	=	maximum oxygen production occurring at or just below the surface at time *t* (mg O_2 h^{-1})
P_{max}	=	maximum specific photosynthetic oxygen production rate at light saturating conditions (mg O_2 (mg Chla)$^{-1}$ h^{-1})
PMAX	=	maximum intracellular phosphorus storage capacity (mg P (mg Chla)$^{-1}$)
P_{min}	=	minimum intracellular phosphorus concentration required for algal growth (mg P (mg Chla)$^{-1}$)
PN	=	nitrogen content in phytoplankton (mg l^{-1})
P_o	=	turbulent Prandtl number (≈ 1)
PO_4	=	dissolved phosphate concentration (mg l^{-1})
PP	=	phosphorus content in phytoplankton (mg l^{-1})
+PR	=	sediment release rate of phosphate (g m^{-2} d^{-1})
- PR	=	sediment adsorption rate of phosphate (g m^{-2} d^{-1})
P_s	=	energy introduced by inflowing streams
P_s	=	atmospheric pressure at the site (mbar)
PS	=	soluble phosphorus concentration (g m^{-3})
P_w	=	saturated water vapour pressure at 20°C (= 23.35 mbar).
P_w	=	energy introduced by wind at the surface of the lake
q	=	inflow flux per unit span
Q	=	river inflow rate (m^3s^{-1}).
Q	=	rate of inflow/outflow (m^3 s^{-1}).
Q	=	intracellular nutrient concentration (mg l^{-1})
Q	=	volumetric discharge (m^3 s^{-1})
q_{lo}	=	flow rate per unit span downstream of plunge point (underflow)
q_o	=	inflow flux per unit span
q_a	=	inflow rate of ambient water per unit span into plunge region
QBNO	=	Arrhenius temperature coefficient for sediment nitrate release
QBOD	=	Arrhenius temperature coefficient for detrital decay
QBRNH	=	Arrhenius temperature coefficient for sediment ammonium release
QBRR	=	temperature coefficient for sediment phosphate release/adsorption
QCHLA	=	Arrhenius temperature coefficient for processes relating to algal
Q_N	=	Arrhenius temperature coefficient for denitrification
Q_m	=	maximum nutrient concentration that can be stored in the algal cell (mg nutrient (mg Chla)$^{-1}$)
QNNH	=	Arrhenius temperature coefficient for nitrification

r	=	solar reflectivity (W m^{-2} or kcal m^{-2} d^{-1}).
r	=	rate of surface renewal.
R	=	net incoming solar radiation (cal cm^{-2} s^{-1})
R	=	Bowen's ratio (= H_c/H_e)
R	=	gas constant (= 8.314 J $°K^{-1}$ mol^{-1})
R	=	respiration rate (mg l^{-1} day^{-1})
r_{bio}	=	rate of decay (mg l^{-1} $24h^{-1}$)
$r_{bio,max}$	=	maximum specific rate of decay (mg l^{-1} $24h^{-1}$)
REL	=	sediment release rate of phosphate (g m^{-2} d^{-1})
RELK	=	sediment release coefficient
Ri	=	Richardson number
R_{max}	=	maximum respiration rate at optimum temperature
R_z	=	solar radiation flux at depth z (cal cm^{-2} s^{-1})
S	=	nutrient concentration in reservoir water (mg l^{-1})
S	=	bed slope
S	=	surface area of the lake (m^2)
S	=	rate of sedimentation (m day^{-1})
S	=	stability (Eq 4.65).
S	=	dissolved nutrient concentration (mg l^{-1})
S_1	=	coefficient (= 0.2 ~ 0.3)
S_2	=	coefficient (= 0.6 ~ 0.9)
SA	=	phytoplankton settling rate (h^{-1})
SB20	=	sediment oxygen demand (g $m^2 day^{-1}$)
SETTL	=	rate of removal of phosphate by settling (g m^{-3} d^{-1}).
S_N	=	nitrogen in upper layer of sediment (g l^{-1})
SOD	=	sediment oxygen demand (g O_2 m^{-2} day^{-1})
S_q	=	sediment concentration (mg l^{-1})
SS	=	inorganic suspended sediment concentration (mg l^{-1})
t	=	time (s or day^{-1})
T	=	ambient water temperature (°C)
T_a	=	air temperature (°C or °K)
T_E	=	equilibrium temperature (°K)
T_K	=	water temperature (°K)
TKE	=	wind-induced turbulent kinetic energy
T_m	=	characteristic mixing time scale (s)
T_{max}	=	upper temperature for where algal growth rate has declined to 10% of the maximum growth rate (°C)
T_{min}	=	lower temperature where algal growth rate has declined to 10% of the maximum growth rate (°C)
T_{opt}	=	optimum temperature for algal growth (°C)
T_s	=	surface water temperature (°C)
T_w	=	water temperature (°K).
U	=	wind speed (m s^{-1}).
U	=	specific uptake rate (day^{-1})
U'	=	nitrogen uptake rate (day^{-1})
u_*	=	shear velocity (m s^{-1})
u_{*a}	=	shear velocity of air (m s^{-1})
u_{*s}	=	surface shear velocity (m s^{-1}).

u_{*w}	=	water shear velocity (m s^{-1})
U_{10}	=	wind speed measured at 10 meter height (m s^{-1}).
u_d	=	mean velocity of the underflowing water (m s^{-1})
U_{max}	=	maximum specific uptake rate (day^{-1})
UN(NIT)	=	uptake rate of nitrate (day^{-1})
Unmax	=	maximum nitrogen uptake rate (mg N mg^{-1} Chla day^{-1})
U_{NO}	=	nitrate uptake rate (day^{-1})
Upmax	=	maximum phosphorus uptake rate (mg P mg^{-1} Chla day^{-1})
u_w	=	surface drift velocity (m s^{-1}).
v	=	vertical velocity of a suspended substance (m day^{-1})
	=	0 for dissolved substances and temperature
V	=	volume of the lake (m^3)
V	=	volume of layer (m^3)
V	=	volume (m^3)
V_{SS}	=	sediment fall velocity (m s^{-1})
W	=	mean maximum wind speed (m^3s^{-1})
W	=	wind speed over water surface (m s^{-1}).
W_L	=	work required (rate of change of potential energy)
W_z	=	wind speed at height z (m s^{-1})
XDNK	=	denitrification rate (day^{-1})
XK1	=	light extinction coefficient for pure water (m^{-1})
XK2	=	light extinction coefficient for chlorophyll-a (m_2g $Chla^{-1}$)
XKM	=	algal mortality rate (day^{-1})
XKNH	=	nitrification rate (day^{-1})
XKR	=	euphotic zone algal respiration rate (day^{-1})
XKR1	=	algal respiration rate (day^{-1})
XNH	=	nitrification inhibition constant (mg NH_4l^{-1})
XNMAX	=	maximum intracellular nitrogen storage capacity (mg N (mg Chla)$^{-1}$)
XNMIN	=	minimum intracellular nitrogen concentration required for algal growth (mg N (mg Chla)$^{-1}$)
YCBOD	=	mass ratio of chlorophyll to detritus (mg Chla mg BOD^{-1})
YCHO2	=	mass ratio of dissolved oxygen produced during photosynthesis, and oxygen utilized during respiration (mg Chla $mg^{-1}O_2$)
YNHBOD	=	mass ratio of ammonium released per dissolved oxygen utilized during detrital decay (mg NH_4 mg BOD^{-1})
$YNHO_2$	=	oxygen utilized in nitrification (mg l^{-1})
YPBOD	=	mass ratio of phosphorus produced from detrital decay (mg P (mg Chla)$^{-1}$)
z	=	depth from the surface (cm or m)
z_e	=	depth of the epilimnion in summer (m)
z_e	=	equilibrium surface roughness height ($\approx$ 0.25 cm)
Z_g	=	depth of centre of gravity of mixed layer (m).
ZOO	=	zooplankton concentration (g m^{-3}).

CHAPTER 1

INTRODUCTION

South Africa is a dry country with a highly seasonal rainfall pattern. The major part of the country (86% of the total area) experiences summer rainfall (DWAF 1986, Bureau of Information 1991). Rainfall is distributed unevenly over the country, declining from more than 1000 mm annually on the East Coast to as low as 50 mm on the West Coast (Fig 1.1). Even though the average annual rainfall is 500 mm (compared with a world average of 860 mm), barely one third of the country receives an annual rainfall of 500 mm - 500 mm being the lower limit for successful dry-land crop production (DWAF 1986, Bureau of Information, 1990).

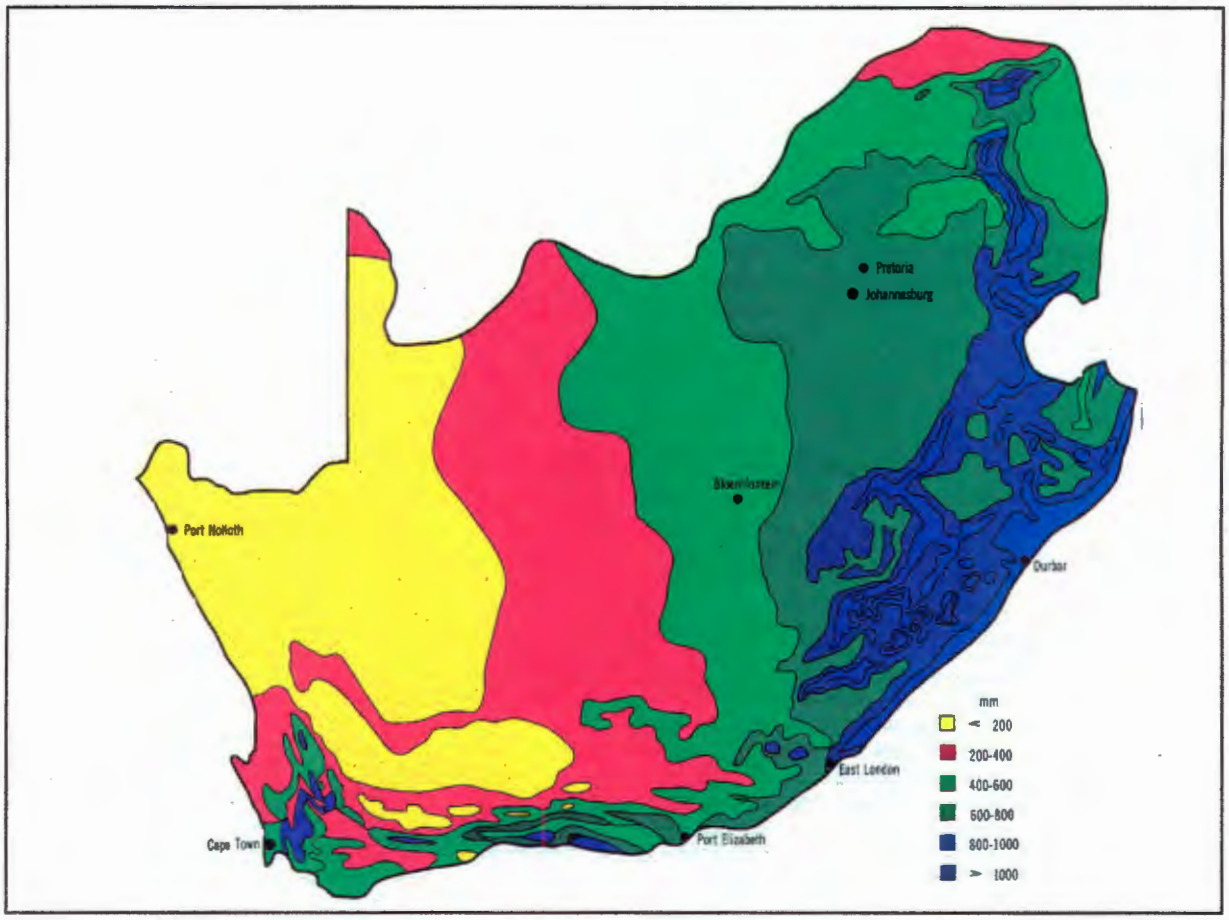

Figure 1.1
Rainfall distribution in South Africa (DWAF 1986).

Reservoirs are the main source of potable and irrigation water in South Africa, and many reservoirs are important recreational sites. Demands on the reservoirs are continually increasing, due to the increase in population with an associated increase in urbanisation and industrialisation, and rising standards of living (DWAF 1986). Over the period 1979 - 1989 the population has increased by 2.1% per year to an estimated total of just over 30 million people in 1989 (Bureau of Information, 1991). The total water demand of South Africa in 1990 was 18 500 million m^3 a^{-1}: The estimated total water demand for the year 2010 is 25 888 million m^3 a^{-1} (Barta 1994, Pitman 1995). Comparing this value with the potential surface water storage of 33 million m^3 a^{-1}, one can see that improved methods of water utilization and water reuse will be cardinal issues in ensuring adequate water provision into the 21st Century.

Apart from the availability of water, maintenance of the quality of the water is of increasing importance. Increased industrialisation, urbanisation, use of artificial fertilizers and pesticides in agriculture, and an increase in the number of informal (squatter) settlements have resulted in a continuous deterioration of surface water quality in virtually all the regions in South Africa. The principle water quality problems in South Africa are (Hattingh 1978, DWAF 1986):

- **Salinisation** - increased concentrations of dissolved salts in flows and return flows due to agricultural, municipal, mining, and industrial use. This gives rise to problems for domestic, industrial and agricultural users of water, because of scaling and corrosion of water reticulation systems, adverse effects on the quality of some industrial products, damage to crops and soil, and other effects.

- **Eutrophication** - stimulation of algal growth in reservoirs by input of nutrients such as nitrogen and phosphorus. The level of eutrophication in a particular reservoir is determined also by climatic factors and the shape and depth of the reservoir. Eutrophication gives rise to the following problems (DWAF 1986, Rossouw 1986a):
    - Increased water treatment costs.
    - Higher levels of expertise are required to design and operate water treatment plants to produce safe potable water.
    - Taste and odour problems in drinking water.
    - Carcinogenic trihalomethanes may be formed during chlorination of water from eutrophied sources.
    - Health problems such as skin irritation and gastroenteritis.
    - Loss of livestock due to ingestion of toxic algae.
    - Deoxygenation of hypolimnetic waters.
    - Aesthetic degradation of water surfaces.
    - Decrease in the value of lake side properties due to aesthetic degradation of surface water.
    - Interference with recreational use of impoundments.
    - Interference with irrigation, e.g. *Cladophera* growing in irrigation channels.

- **Microbiological contamination of surface waters** - arises principally from areas with inadequate or no sanitation provisions. It particularly affects users who take their water for domestic purposes directly from a water body without the water being treated.

- **Turbidity** - originates mainly from storm water flows which carry high concentrations of total inorganic suspended sediment (TSS), derived from surface erosion. Turbidity reduces light penetration in the receiving reservoirs thereby affecting the extent and intensity of eutrophication. Settlement of the larger particles gradually reduces the operational volume of the reservoir.

- **Organic pollution** - arises principally from waste water streams that are partially treated or not treated at all, as well as from municipalities, informal settlements and industries, and from organic material generated in the reservoir by algal growth. In South Africa organic pollution from municipalities and industries is relatively minor because of the strict requirements for waste water treatment before discharge. However, organic pollution from informal settlements can be significantly high.

- **Metals, trace metal contaminants and pesticides** - these arise mainly from industrial and agricultural activities. According to DWAF (1986), these cause water quality problems in a limited number of water bodies only. Usually metals such as iron and manganese will be in particle form in the inflow, and settle out in the bottom sediment of the reservoir. Under low redox potential (eg under anaerobic conditions in the hypolimnion[1] during the stratified period), these metals can solubilise into the overlying water mass. Should it be necessary to abstract water from the hypolimnion for potable use, additional water treatment processes will be needed to remove these metals.

Salinisation and eutrophication are regarded as the main water quality problems in South Africa. Regarding eutrophication, the nutrients phosphate and nitrogen originate from two main sources: non-point (diffuse) and point sources. Diffuse sources are mostly runoff from agricultural activities and from informal settlements with inadequate sanitation facilities. Point sources are mainly effluent discharges from industrial and waste water treatment plants. The nutrient contribution from these return flows is significantly reduced where modern biological nutrient removing plants have been installed.

Governmental agencies in South Africa became concerned about the increase in eutrophication related water quality problems during the early 1970's (Jones and Lee

---

[1] During summer, because of the effect of radiation and wind, the water in the reservoir physically divides into two layers - a warm upper layer, called the epilimnion, and a colder lower layer, called the hypolimnion.

1984), leading to an investigation into the possible causes, consequences and control of eutrophication in South Africa. Two significant reports were published; the first report by Toerien (1977) reviewed eutrophication and provided tentative guidelines for its control in South Africa. The second report by Walmsley and Butty (1980), based on an eutrophication study of 21 reservoirs in South Africa (Walmsley and Butty 1980a), described a relationship between phosphorus load and chlorophyll concentration that fitted available data on South African reservoirs, and provided further guidelines for the control of eutrophication. The first step to control eutrophication was the introduction of an effluent phosphate standard that limited the phosphorus concentration in effluents being discharged in certain sensitive catchments to a maximum of 1 mg l^{-1} ortho-phosphate (as P). It should be noted that this standard applied only to point sources. No standards were set for non-point sources, partly because of the difficulties in evaluating the magnitude of these sources, an initial belief that the contribution from non-point sources was relatively minor, and the unavailability of practical economic measures to control phosphorus discharges from non-point sources.

The effect of the phosphorus standard on water quality in reservoirs has been monitored to determine whether a stricter standard, additional legal controls, or other management strategies may be required (DWAF 1986). However, the effect of changes in management strategies is often difficult to envisage, because of the complex interactions between the various processes that contribute to the water quality of a water body, and also because any treatment may have secondary, unforeseen effects. As a result, considerable world-wide effort has been put into studies to identify and quantify the input, mechanisms, and processes relevant to the water quality in reservoirs, and to aggregate these into a system that simulates the water quality response of a reservoir, i.e. a mathemetical model. With such a model the response of a reservoir to various management options can be evaluated and thus it can serve as an invaluable aid in determining the best strategy to improve water quality. The model can also serve as an aid in long-range planning, the design of treatment facilities, or the problem of legislation for discharge consents and standard setting. It may also be employed in the design and operation of real-time control and forecasting systems. (Orlob, 1983).

The first mathematical models originated in the United States during the 1920's. However, it was only from about 1960 onward that the field of water quality modelling expanded rapidly. This was due to the development of more sophisticated computers which resulted in more complex models that allowed a better fundamental understanding of the behaviour of reservoirs. In addition, there was a dire need to control ever the increasing water pollution that resulted mostly from eutrophication (Orlob 1983).

In South Africa, water quality modelling of reservoirs also had its origin in the need to describe the response of eutrophic reservoirs to phosphate inputs. Subsequent to the reports of Toerien (1977), and Walmsley and Butty (1980a), where eutrophication was identified as a serious water quality problem, and after introduction of the 1 mg l^{-1} P standard, a number of modelling studies were undertaken (Thornton and Walmsley 1982, Jones and Lee 1984, Walmsley and Thornton 1984, Grobler 1985). Most of the work was done on the hypertrophic Hartbeespoort Dam Reservoir. The models utilised were empirical, zero-dimensional models that treated the reservoir as a completely stirred reactor. Most of these models considered only the steady state, or at the most, annual changes.

These models simulated annual mean phosphate-P concentrations with varying degrees of success, the most successful predictions being obtained with the Reservoir Eutrophication Model of Grobler (1985). However, a significant relationship between observed and simulated chlorophyll-a concentrations could not be obtained with these models (Chutter 1989), i.e these models could not be used to predict the response of eutrophic reservoirs to different management strategies to alleviate eutrophication related water quality problems. Also, because these models assumed complete mixing, they could not supply information on the actual water quality at an abstraction point at a specific depth - information was supplied only on overall average states. In view of these shortcomings, a further study was initiated by the Water Research Commission to test the applicability of more sophisticated hydrodynamic and water quality models (developed elsewhere), to stratified reservoirs under South African climatic conditions.

Several models of varying complexity that described the hydrodynamic and water quality response of a reservoir from the surface to the bottom of the reservoir were available. From these four models were selected for study, three of the models from the United States, and one from Australia. The models from the United States appear to have been developed for reservoirs in cold temperate climates, whereas the one from Australia was developed under climatic conditions similar to those in South Africa, i.e warm temperate/subtropical. However, the Australian model (DYRESM) can only simulate water temperature and salinity. The models from the United States (MINLAKE, CE-QUAL-W2 and WASP4) incorporated both the hydrodynamic and water quality aspects.

The models were studied simultaneously over a period of several years. The DYRESM, CE-QUAL-W2 and WASP4 models were studied by a consulting firm, Ninham Shand, and the MINLAKE model by the University of Cape Town. Some of the comparative findings are discussed briefly in Chapter 2. The rest of this report covers the extensive study that was made of the MINLAKE model - the extent of the study being justified in view of the potential of the MINLAKE model. The MINLAKE model is the only one of the models selected that can simulate more than one algal class, thereby making it an ideal tool to estimate, for instance, the effect of certain management options on algal succession.

To evaluate a model effectively, a critical study of the concepts underlying the model and formulation of the processes is necessary. Accordingly, the structure of the report evolved as follows:

- Chapter 2 deals briefly with historical and present water quality modelling in South Africa. The objective here is to place the modelling effort with MINLAKE into perspective and to indicate why the MINLAKE model was selected for detailed study.
- Chapter 3 reviews the conceptual aspects, processes and products of water quality modelling in general, highlighting requirements for modelling water quality in eutrophic reservoirs in warm temperate climates.

- Chapter 4 presents general formulations of the hydrodynamic and water quality processes identified in Chapter 3.
- In Chapter 5 formulations in the MINLAKE model are compared with the conceptual representation in Chapter 3 as well as general formulations in Chapter 4.
- Modifications to the formulations in the original MINLAKE model as well as formulation of the processes that had to be added to enable simulation the water quality behaviour in the Southern African climate are presented in Chapter 5.
- Calibration of the hydrodynamic and water quality parts of the modified MINLAKE model on Roodeplaat Dam is reported in Chapters 6 and 7 and the results obtained are discussed in Chapter 8.
- In Chapter 9 the modified MINLAKE model is applied to Lake Riley in the United States; this lake was used to calibrate the original MINLAKE model. The objective here was to check if the modified model retained the capacity to simulate the response of Lake Riley, i.e. if the modified model had achieved greater generality by successfully simulating lakes in both the warm temperate and cool temperate climates.
- Water quality models such as MINLAKE require meteorological and river water quality data on a daily basis. However, for many South African reservoirs daily sets of input data would not be available, thus a study was done to determine the sensitivity of the model output to weekly, or even monthly data. The results of this study are given in Chapter 10.
- In Chapter 11 the use of the model to test a few typical treatment options for Roodeplaat Dam is illustrated. Conclusions and recommendations are given in Chapter 12.

CHAPTER 2

AN OVERVIEW OF WATER QUALITY MODELLING IN SOUTH AFRICA

2.1 INTRODUCTION

Management-orientated prediction of the consequences of eutrophication in South Africa has gone through several stages (Rossouw 1990), starting with a report by Toerien (1977) that reviewed eutrophication and gave tentative guidelines for its control in South Africa. Thereafter an extensive survey was conducted on the water quality status of 22 South African reservoirs, resulting in a second report on guidelines for the control of eutrophication in South African reservoirs (Walmsley and Butty 1980, 1980a).

On the basis of these reports, the Department of Water Affairs and Forestry decided to implement measures to control the causes of eutrophication rather than the consequences (Rossouw 1990). Initially attention was focused on reducing the phosphorus load entering reservoirs, because, at that stage, phosphorus has been identified as the plant nutrient that most often limits algal growth in fresh waters, and because phosphorus was considered to be easiest to control (Toerien 1977). [1] It was assumed that point sources were responsible for 80% to 90% of the phosphorus loads to reservoirs in the so called 'sensitive' catchments (Taylor *et al* 1984). Seven sensitive catchments were specified in the *Government Gazette* No 9925 of May 1984 (Grobler 1986), and legislation was introduced whereby all treated municipal and industrial waste water that were returned to water bodies in these catchments were legally required to comply to a 1 mg l^{-1} phosphorus standard.

---

[1] It should be noted, however, that later studies (Reynolds 1984) indicated that, due to the occurrence of the process of denitrification, nitrogen often is the limiting nutrient in lakes and reservoirs situated in subtropical climates.

The standard of 1 mg was based on the technical and economical feasibility of phosphorus removal from the effluent of typical waste water treatment plants, and in particular, removal of phosphorus by construction of the new generation of waste water treatment plants, the biological phosphorus removal plants. The standard was severely criticized by industries and local authorities who argued that (1) Compliance to the 1 mg P standard would require tertiary waste water treatment, which would have serious economic implications, specially for small local authorities. (2) The 1 mg P standard was a uniform standard that did not take into account the varying assimilative capacity of individual water bodies - the assimilative capacity of a reservoir being affected by a multitude of factors such as internal and external nutrient load, reservoir morphology, and even climate, i.e. each dam has a unique assimilative capacity. (3) Some of the impoundments-drainage basin systems may be dominated by non-point source phosphorus loads which will not be controlled by the 1 mg P standard. For example, a study by Bath (1989) demonstrated that in the Berg River basin more than 80% of the phosphorus entering the river was derived from runoff from the intensive farming activities in this basin. Many of the small local authorities, who could least afford the treatment required to comply to the standard, are situated in such drainage basins (Grobler 1986).

In contrast, limnologists criticized the 1 mg P standard as not being stringent enough to prevent eutrophication in many water bodies.

From the views expressed above it became evident that a rational policy on the control of phosphorus would emerge only if the contribution of phosphorus from non-point sources were identified and quantified, and if the trophic response of a reservoir to phosphorus loads could be predicted. Both these problems have received attention in South Africa, both often considered simultaneously.

Regarding the external phosphorus load, it was noted earlier that phosphorus originates from either point or non-point sources. Point sources can be readily identified and quantified by regular monitoring. In contrast, non-point sources are difficult to locate and quantify: often the greater part of phosphorus load resulting from

surface runoff are present in the flood flow from a storm event, whereas the load during non-flood flow can drop to very low values. In the summer rainfall areas where the rainfall is principally via rainstorms a reliable assessment of the phosphorus load demands a high density of monitoring over a flood hydrograph period. As the time and place of a storm event cannot be predicted ahead of time, the information on phosphorus loading will always have some uncertainty. As an alternative, basin wide macroscopic statistical approaches to evaluate the phosphorus load have been developed. (Grobler 1985, 1986). However, the very nature of the method employed leaves the estimates with an unknown measure of uncertainty.

With regard to the eutrophic response of reservoirs in South Africa a number of mathematical reservoir models have been applied. In the following sections the models that have found application are briefly reviewed.

2.2 REGRESSION MODELS

A number of these models have been applied in South Africa, using either existing models such as the Vollenweider model (Thornton and Walmsley 1982), the Dillon and Rigler model (Thornton and Walmsley 1982), or the OECD (Organisation for Economic Cooperation and Development) model (Jones and Lee 1984); or developing new models such as the Reservoir Eutrophication Model (REM) model (Grobler 1985, 1986), or TROPHIC (NIWR 1985). As phosphorus was regarded as the principal nutrient that limited algal growth, the major aim of these studies was to find a relationship between the phosphorus load that enters a reservoir, and algal growth in that reservoir.

2.2.1. The Vollenweider Model

This model is a zero-dimensional (budget) model, i.e. the reservoir is treated as a uniformly mixed reactor and the system is taken to be completely mixed at all times. It related the steady state in-lake phosphorus concentration to phosphorus loading, whereafter a statistical relationship was developed between the natural logarithm of

the average summer epilimnetic chlorophyll-a concentration and the natural logarithm of the predicted steady state in-lake total phosphorus concentration. Only the steady state, or at the utmost, annual changes are considered. The following conceptual assumptions are made in the model (Thornton and Walmsley 1982, Henderson-Sellers 1984, Grobler 1985):

- The lake is treated as a completely mixed reactor of constant volume, i.e. inflow and outflow rates are equivalent and input phosphorus is immediately mixed throughout the lake.
- The outflow phosphorus concentration is equal to the concentration prevailing in the lake.
- No internal loading of phosphorus to the water column from the sediments.
- Phosphorus sedimentation is proportional to the phosphorus concentration in the water.
- Seasonal fluctuations in phosphorus loading may be ignored.

For lakes in the northern temperate climate a good statistical relationship was found between the average summer epilimnetic chlorophyll-a concentration and the predicted total phosphorus concentration.($r = 0.86$, $n = 60$, and $P < 0.001$). The regression line for the relationship was:

$$Chla = 0.367\ P_{TP}^{0.91} \qquad (2.1)$$

Chla = average summer epilimnetic chlorophyll-a concentration (mg m^{-3})

P_{TP} = predicted steady state total phosphorus concentration in the lake (mg l^{-1}).

When the Vollenweider model was applied to South African reservoirs, phosphorus concentrations predicted by the model were usually higher than the observed concentrations in the reservoir (Thornton and Walmsley 1982). The over-prediction was

attributed to the way phosphorus sedimentation was simulated in the Vollenweider model (Grobler 1985):

$$P_{sed} = s\,P \qquad (2.2)$$

P_{sed} = phosphorus sedimentation (mass/time)
s = sedimentation rate ($time^{-1}$)
P = mass of total phosphorus in the water body above the sediments (mass).

In the Vollenweider model, the sedimentation rate (**s** in Eq 2.2) is entered as a constant. However, a constant phosphorus sedimentation rate is regarded as not applicable to South African conditions (Grobler 1985). As a result, studies were conducted with other models (eg the Dillon and Rigler model, and the OECD model) that do not utilise a constant sedimentation rate.

2.2.2 The Dillon and Rigler Model

This model is based on the Vollenweider model. However, the submodel for phosphorus sedimentation is not based on a constant sedimentation rate (**s** in Eq 2.1), but on a phosphorus retention coefficient which is defined as the amount of phosphorus remaining in a water body expressed as a fraction of the amount of phosphorus that entered the water body. In a study by Thornton and Walmsley (1982),[2] this model gave good correlation between simulated and observed in-lake steady state phosphorus concentrations, but they concluded that, even though the model has some potential for predicting in-lake phosphorus concentrations of South African impoundments, it requires further development before it can be used to predict the trophic status of these impoundments.

---

[2] Observed in-lake steady state concentrations were taken as the measured annual phosphorus concentrations of the surface waters.

2.2.3 The OECD Model

The OECD model (Organisation for Economic Cooperation and Development) also is based on the Vollenweider model. The main difference is in the sedimentation submodel. Based on a study done by Vollenweider on 21 lakes, the sedimentation rate (s in Eq 2.2) in the original Vollenweider model was substituted by $T_w^{-0.5}$, with T_w the water retention time of the reservoir (Grobler 1985). Thereafter, statistical regressions were developed to relate the predicted total phosphate concentration to the trophic state of the water body, as measured by chlorophyll-a, Secchi depth and hypolimnetic oxygen depletion rate (Jones and Lee 1984). The regressions were based on data on about 350 Nordic lakes, Alpine lakes, shallow lakes and reservoirs, and lakes in the United States (Walmsley and Thornton 1984). A relationship for shallow lakes and reservoirs was developed, as well as a combined relationship for general application. The relationship for shallow lakes and reservoirs is:

$$Chla = 0.54\ P_{TP}^{0.72} \qquad (2.3)$$

The combined relationship is:

$$Chla = 0.37\ P_{TP}^{0.79} \qquad (2.4)$$

Chla = average summer epilimnetic chlorophyll-a concentration (mg m^{-3})
P_{TP} = predicted steady state total phosphorus concentration in the lake (mg l^{-1}).

When this model was applied to South African reservoirs, utilising data on the 21 reservoirs in the study by Walmsley and Butty (1980a), the model was found to generally over-predict chlorophyll-a levels resulting from a particular phosphorus load (Jones and Lee 1984). According to the developers, the deviant behaviour could be attributed to the following (Jones and Lee 1984, Walmsley and Thornton 1984):

- The predicted chlorophyll-a concentrations were obtained from a regression equation that is based on mean, summer epilimnetic concentrations, whereas the observed values in the study by Walmsley and Butty (1980a) were annual average chlorophyll-a concentrations obtained from depth-integrated samples, which would be lower than mean summer epilimnetic concentrations.

- The model provides only for phosphorus as limiting nutrient. Nitrogen limited systems tend to give low observed chlorophyll-a concentrations relative to phosphorus concentration.

- The phosphorus-chlorophyll-a relationship in the model was developed on lakes with relatively clear water, and thus the relationship will be modified by high turbidity, a factor particularly relevant to South African reservoirs.

- The model is not applicable to reservoirs with a dendritic shape where nutrient loading affects only one arm.

- The model is not suitable for dams where internal phosphorus loading from sediments occurs.

2.2.2. The Reservoir Eutrophication Model (REM)

Grobler and Silberbauer (1984) came to the conclusion that the steady state modelling approach utilising OECD type models had limited value as an aid in decision making in South Africa, for the following reasons (Grobler 1986):

- South Africa experiences highly variable hydrological conditions, therefore the amount of water stored in reservoirs, the inflow to, and the outflow from, these reservoirs also are highly variable, invalidating the steady state assumption.

- Non-point sources vary as a function of runoff, which is not constant. Thus, the constant phosphate sedimentation rate utilised in the OECD type models is not suitable - a variable sedimentation rate should be more appropriate.

Consequently, a dynamic Reservoir Eutrophication Model (REM) that employs a variable phosphate sedimentation rate was developed for South African reservoirs (Grobler 1985). Variable time-series of outflow, reservoir volumes, and point and non-point source phosphate loads are required as input (Grobler 1986). Model output is on a monthly basis.

The model consists of various submodels as indicated in Fig 2.1. The phosphate budget submodel is based on the conservation of mass and is similar to that in the Vollenweider model, except that instead of a constant sedimentation rate (s in Eq 2.2), the rate of sedimentation is expressed as a function of ambient phosphate concentration in a reservoir (Grobler 1986):

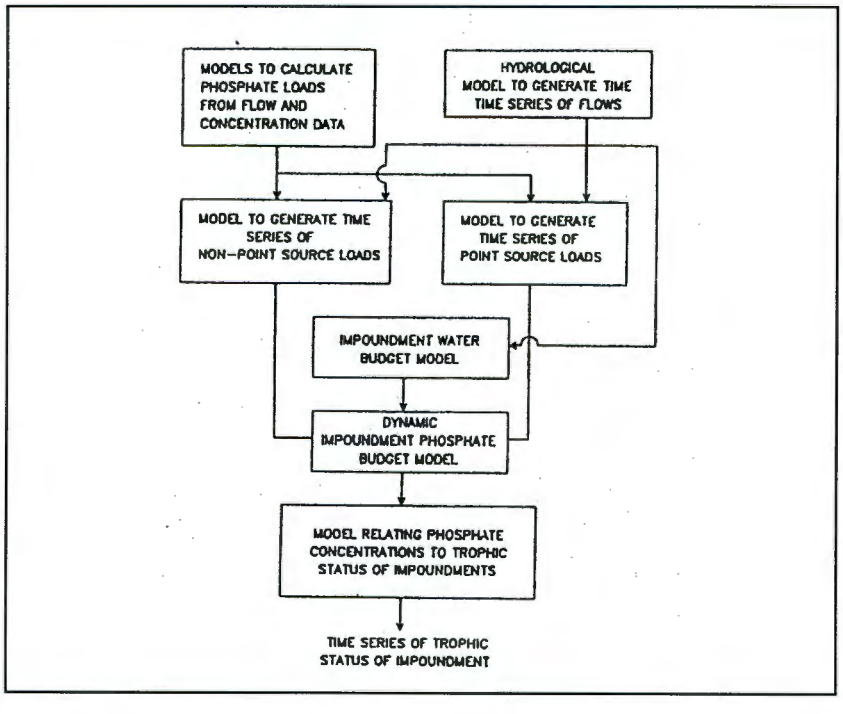

Figure 2.1
Diagram indicating submodels in the Reservoir Eutrophication Model (REM)

$$s = \frac{k}{(C_o - C)} \quad (2.5)$$

s = sedimentation rate
k = reservoir specific parameter
C_o = maximum phosphate concentration (mg l^{-1})
C = ambient phosphate concentration (mg l^{-1}).

To relate phosphate concentrations to trophic status (Fig 2.1), the REM model employs the relationship for shallow reservoirs developed in the OECD model (Eq 2.3) (Meyer and Rossouw 1992):

$$Chla = 0.54\ P_{TP}^{0.72} \quad (2.6)$$

Chla = average summer epilimnetic chlorophyll-a concentration (mg m^{-3})
P_{TP} = predicted total phosphorus concentration in the lake (mg l^{-1}).

To facilitate use of the model, the model was incorporated in a user-friendly decision support system (DSS), consisting of three components - a model base, a data base and a computer program (Rossouw 1990, 1991). The model base contains the different sub-models indicated in Fig 2.1. The data base contains the hydrological, point source, catchment, and reservoir data of a specific reservoir. The computer program links the data base and the model base, and provides the interface with the user.

The REM model, as incorporated in the DSS system, is known as REMDSS. This system has been used extensively in a number of studies by the Department of Water Affairs and Forestry, mainly to assess the impact of the 1 mg P l^{-1} effluent standard on reservoirs in sensitive catchments (Rossouw 1990). However, in a study conducted

by Rossouw and Meyer (1992) where each of the three submodels in the REM model (see Fig 2.1) was evaluated, they demonstrated that the REM model does not describe the historical characteristics of two South African reservoirs (Hartbeespoort and Witbank Dams) accurately. Hence there is concern about the accuracy of chlorophyll-a levels as simulated with this model, which infers that application of the REM model may lead to incorrect conclusions regarding the impact of proposed management strategies for phosphorus control.

In an attempt to improve the chlorophyll-a submodel in the REM model, Rossouw and Meyer (1992) used a multi-factorial statistical approach. Instead of expressing chlorophyll-a concentration as a function of phosphate concentration only, as was done in the REM model (Eq 2.6), they developed a regression between the natural logarithm of chlorophyll-a concentration and the natural logarithms of total phosphorus, Kjeldahl nitrogen, nitrates, nitrites, phosphate, and ammonia concentrations. Although the resulting model has to be calibrated individually for each reservoir, it reproduced historical behaviour more reliably than the REM model, and hence should simulate future conditions with greater accuracy for the two reservoirs being studied.

2.2.5 Inherent shortcomings of regression models

The models described thus far are all regression models that establish a functional relationship between chlorophyll-a and nutrient concentrations from observation in a number of reservoirs. Thereafter the established regression is employed to predict future chlorophyll-a concentrations from nutrient concentrations for any reservoir. Nutrients other than phosphorus are seldom considered. These models are popular because they are simple to use and do not require extensive data. However, they suffer from a number of inherent shortcomings (Rossouw 1990, 1991, James 1993):

- They do not provide for light limited algal growth, a factor that may be important in South African reservoirs that often are highly turbid.
- Usually, these models consider phosphorus as the only limiting nutrient. However, in warmer climates nitrogen often becomes the limiting nutrient due to denitrification in the hypolimnion during the stratified period.
- Internal cycling of nutrients due to release from the bottom sediments is not taken into account. In highly eutrophic systems this may be of considerable importance.
- Regression models zero-dimensional models, i.e the reservoir is considered as a uniformly stirred reactor and the system is taken to be completely mixed at all times. Site-specific factors such as climate, hydrology, etc that cause most South African reservoirs to stratify on an annual basis are ignored - stratification is of great significance in determining water quality in reservoirs, thus it is important to be able to predict temperature patterns throughout the depth of the reservoir. Also, in some instances the water quality at a specific abstraction point is of more importance than the average water quality.

Regression models in fact do not provide a description of the behaviour of a system. They are concerned only with measured inputs and outputs, and are based on best-fit relationships of data (Cochrane *et al* 1987). Often they are reservoir specific and cannot be used in other case studies without modification (Orlob 1983, Henderson-Sellers 1984).

2.3 MECHANISTIC MODELS

Models that do provide a description of the mechanisms acting within the reservoir are called *mechanistic models*. These models provide mathematical descriptions of theoretical principles, i.e. formulation is based on identification of causal relationships that describe the phenomena that govern the behaviour of the system (Orlob 1983). This includes the causal relationship between the hydrodynamic and water quality behaviour of a reservoir, i.e. the effect of local climate and hydrology on water quality processes is taken into account. Often these models are divided into a hydrodynamic

and a water quality part that can be separated partially but do interact. The hydrodynamic part deals with physical processes in which input of wind, radiation, air temperature, turbidity, salt concentrations, river inflow, river discharge and reservoir morphology influences mixing, temperature distribution, salinity distribution and other lesser physical parameters within the water mass. The water quality part deals with biochemical and chemical processes within the water body, such as algal growth, nutrient distribution (including internal nutrient cycling), and oxygen distribution and the effect of the latter on other processes. Experience has shown that whereas the effect of the water quality processes on the hydrodynamic behaviour is relatively small, the hydrodynamic processes have significant effect on the water quality behaviour.

Mechanistic water quality models often are one- or two-dimensional, [3] thus they can simulate the changing distribution of water quality with depth that results from the annual stratification that occurs in most South African reservoirs. Efforts to apply the mechanistic model approach in South Africa are very recent, since about 1984. Impetus for their application in South Africa came principally from the Water Research Commission as stated in Chapter 1.

2.3.1 The Hartbeespoort Dam Ecosystem Model (TROPHIC)

The *TROPHIC* model was developed at the South African Council for Scientific and Industrial Research (NIWR 1985, Clarke *et al* 1987, Cochrane *et al* 1987). It represents an intermediate stage between the use of simplistic regression-type budget models and more sophisticated multi-dimensional models in South Africa. *TROPHIC* is a mechanistic model in that it describes phosphorus cycling in Hartbeespoort Dam in South Africa (a highly eutrophic impoundment). In the model the reservoir is divided seasonally into an epilimnion and hypolimnion, i.e. it is a compartmental model. Phosphorus, phytoplankton, zooplankton and fish are simulated. The hydrodynamic

---

[3] In one-dimensional models horizontal distribution of a substance is assumed to be homogeneous, only the vertical distribution can vary with time. In two-dimensional models distribution of a substance can vary in both the horizontal and vertical directions - see further discussion in paragraph 3.2

behaviour of the dam is not simulated; the hydrodynamic state is obtained by entering monthly values of mean water temperature and surface temperature, mean wind speed, mean monthly maximum water depth, and mean height of the oxycline above the deepest point. Though the model runs on daily iterations to enable simulation of algal and zooplankton growth rates, model output is on a monthly basis.

The TROPHIC model (in its unstratified form) was used to investigate and make recommendations about various management options for Hartbeespoort Dam (Clarke *et al* 1987).

The TROPHIC model is relatively simplistic compared to one- or two-dimensional mechanistic models, but it did show that mechanistic models may be the more appropriate ones in evaluating the trophic response of a dam to various management strategies, because these models contribute to an understanding of the quantitative behaviour of the dam, and the causal relationships that exist between hydrodynamic and water quality processes.

The experience gained from the TROPHIC model served as a spur to study the application of one- and two-dimensional models in South Africa. A number of these water quality models have been developed in other countries, and four of these were selected for further study, viz (1) the two-dimensional models CE-QUAL-W2 and WASP4 (2) the one-dimensional models DYRESM and MINLAKE.

A brief review of these models and their preliminary findings will now be given to bring into perspective the more detailed study of one of the models, the MINLAKE model.

2.3.2 CE-QUAL-W2 Model

This model has been under continuous development since 1975 (Cole 1991). The original model, developed by Edinger and Buchak, was known as LARM (Laterally Averaged Reservoir Model). Addition of the water quality algorithms by the Water Quality Modelling Group at the US Army Engineer Waterways Experiment Station

resulted in the present version of CE-QUAL-W2 (Cole 1991). It is a dynamic, two-dimensional model, with a variable temporal resolution. Up to 20 constituents, including bacterial activity, can be simulated.

An advantage of a two-dimensional model is its ability to simulate the movement of water quality constituents in two dimensions (vertical and horizontal, but not lateral) in the reservoir. This is particularly valuable in describing the transient behaviour during flood events, as well as describing the change in water quality along the longitudinal axis of long, narrow dams.

The main deficiency of the model is its inability to simulate more than one algal class, i.e. algal succession cannot be simulated. This decreases the suitability of this model to simulate the trophic response in South African reservoirs - often more than one algal class is present in South African reservoirs.

Regarding the calibration of CE-QUAL-W2 to a South African reservoir, this was done for Inanda Reservoir in Natal, and the Vaal Barrage. For Inanda Reservoir, the following variables were simulated over a period of 200 days (Görgens *et al,* 1993):

- Water temperature
- Total dissolved salts (TDS)
- Total inorganic suspended sediment (TSS)
- Phosphate
- Algae
- Dissolved oxygen

For the Vaal Barrage, the following variables were simulated over a period of 140 days (Görgens *et al,* 1993):

- Water temperature
- Electrical conductivity
- Total dissolved salts (TDS)

The advantage of using a two-dimensional model on a long, narrow reservoir such as Inanda Dam, to simulate, for instance, movement of phosphate along the reservoir, was demonstrated in this study (Görgens *et al,* 1993).

2.3.3 WASP4 Model

This is a two-dimensional water quality and hydrodynamic model developed by the US Environmental Research Laboratory in Athens, USA. The model consists of two stand-alone computer programs, DYNHYD5 for simulation of hydrodynamic behaviour, and WASP4 for simulation of water quality behaviour. The model was applied to Roodeplaat Dam for a period of 100 days, and to the Vaal Barrage for a period of 138 days. In both instances, DYNHYND5 successfully simulated the hydrodynamic behaviour of these water bodies. However, due to errors in the source code of the WASP4 model, a series of problems was encountered when simulation of the water quality behaviour was attempted. It was decided that the model would be retested once new source code and documentation are available (Görgens 1993).

2.3.4 DYRESM Model

This model was developed in 1978 by the Centre of Water Research at the University of Western Australia (Görgens *et al* 1993). It is a dynamic, one-dimensional model, with a temporal resolution that ranges from 15 minutes to one day. Only water temperature and salinity can be simulated, i.e. only the hydrodynamic behaviour is simulated. Further work is being done by the Centre of Water Research at the University of Australia to extend the model to enable simulation of water quality processes also. The algorithms describing the water quality processes are derived mainly from those in the MINLAKE model (Hamilton and Schladow 1994).

A great advantage of the DYRESM model is its ability to simulate bubble plume destratification, thus the model can be used in the design, testing, and optimization of potential destratification systems, and in simulating existing bubble plume systems (Görgens *et al* 1993). However, because the model simulates water temperature and

salinity only, the effect of destratification on water quality cannot be simulated, therefore this model is not suitable for modelling the trophic response of a reservoir to different management strategies.

Regarding calibration of the DYRESM model to South African reservoirs, the model simulated observed salinity and temperature profiles successfully in Laing Dam for a period of 10 months (Ninham Shand 1989). A number of future operational testing scenarios was tested, which served as basis for recommendations regarding the operation of the dam.

The model was also calibrated for Roodeplaat Dam Reservoir (Görgens *et al*, 1993). Only water temperature was simulated, for a period of two years. The temperature simulation gave vertical temperature profiles in the reservoir almost identical to those simulated by the MINLAKE model.

2.3.5 MINLAKE Model

This model simulates both the hydrodynamic and water quality behaviour of a reservoir. The present version of the model was released in 1988 (Riley and Stefan 1988). The model was developed by St Anthony Falls Hydraulic Laboratory at the University of Minnesota in the USA. It is a dynamic, one-dimensional model with a fixed temporal resolution of one day. The water quality aspect is particularly well developed - up to 15 constituents, including zooplankton, can be modelled. Although bacterial activity cannot be modelled, up to three algal classes can be simulated simultaneously. The ability of the model to simulate three algal classes was particularly important as this provided a way for modelling algal succession, an important seasonal phenomenon in many South African reservoirs. It also means that the model can be used to evaluate the response of the reservoir to treatment options aimed at changing algal dominance from undesirable blue-green algae to more acceptable green algae.

Regarding calibration of the MINLAKE model to a South African reservoir, in a preliminary study (Görgens *et al* 1993), the model was calibrated for Roodeplaat Dam

Reservoir for a period of two years. For this period, water temperature and total dissolved salts (TDS) could be simulated successfully. Regarding simulation of the water quality response of Roodeplaat Dam Reservoir, during the preliminary study it became clear that, to simulate the water quality behaviour of Roodeplaat Dam Reservoir, and hence, any South African reservoir, over an extended period of time (ie, longer than six months), the original MINLAKE model would have to be modified substantially. This was mainly due to the fact that the original MINLAKE model was developed in a northern temperature climate, while most South African reservoirs are classified as subtropical, and processes that are of importance in warmer climates, such as denitrification, and nutrient-sediment kinetics under aerobic/anaerobic conditions, have not been included in the model.

The balance of this report covers the extensive study that has been made on the MINLAKE model. One dimensional water quality modelling is a relatively new field in South Africa. Therefore, to assist the many users unfamiliar with this kind of model, the conceptual basis and possible formulation of the processes relevant to one dimensional hydrodynamic and water quality models are described in some detail. The MINLAKE model was calibrated on Roodeplaat Dam as it has been classified as highly eutrophic and as it was the only facility in South Africa that had most of the data sets required as input by the model.

CHAPTER 3

CONCEPTUAL REPRESENTATION OF A HYDRODYNAMIC AND WATER QUALITY MODEL

3.1 INTRODUCTION

The conceptual representation of a model is a verbal description of the system which serves as a framework for subsequent mathematical formulation and structuring of the model. To set up the conceptual representation on which the subsequent mathematical model is based, the physical orientation of the reservoir in space should be determined, i.e. whether the reservoir should be represented by a zero, one, two, or three dimensional model. Thereafter the processes operating on and in the system and the compounds on which these act are identified, and the various interactions between processes, as well as the interactions between processes and compounds, are delineated descriptively. In this chapter possible spatial representations of lakes and reservoirs are presented, as well as a conceptual description of eutrophication.

In lakes and reservoirs abiotic effects (wind, radiation, and inorganic and organic materials) serve as energy and matter inputs. The abiotic acts on, and interacts with the biotic (growth of algae, bacteria and higher life forms); which, in turn, affects abiotic responses (precipitation and dissolution of salts, etc.). These systems are extremely complex and no total description is possible, therefore our objective is restricted to conceptualisation and description of the phenomenon of eutrophication and its causative factors in reservoirs in warm temperate regions.

Eutrophication is defined as the process where, due to a high input of otherwise limiting nutrients, the production of organic matter exceeds that which can be oxidized by respiration, predation, and bacterial processes (Weiss 1969, Henderson-Sellers 1984, Reynolds 1984). One of the most important characteristics of an eutrophic reservoir is the significant reduction in oxygen concentration in the lower levels of the

reservoir (the hypolimnion) during summer (Weiss 1969, Reynolds 1984). In some reservoirs the hypolimnion may become completely depleted of oxygen as a result of processes associated with eutrophication.

Eutrophication affects the quality of the water; this in turn affects the subsequent use of the water. Since use of the water is the primary objective for storing water in a reservoir, the quality of the water at different levels in the reservoir may be of significant importance, so that one must consider the water quality as in integral part of the eutrophication response of a reservoir.

The conceptual framework of an eutrophication/water quality model to be presented here is a reflection of the experience gained on the behaviour of lakes and reservoirs by many investigators over many years. Very little, if anything, new is presented on the important processes acting in the system. It is principally in the focus on the behaviour of these systems in warm temperate climates that there may be a contribution.

Past work on describing the eutrophic response of lakes and reservoirs has shown that the response is dominated by two categories of behaviour that affect each other interactively - hydrodynamic and water quality. Whereas the hydrodynamic behaviour affects the water quality behaviour profoundly, the effect of the water quality behaviour on the hydrodynamic response is relatively minor, and often insignificant. This allows the description of the hydrodynamic behaviour to be made virtually independently of the water quality behaviour as a necessary precursor to description of the water quality behaviour. Accordingly, after discussion of the spatial representation of reservoirs, the hydrodynamic behaviour is considered before the water quality behaviour.

3.2 DETERMINING THE SPATIAL REPRESENTATION OF A MODEL

Ideally, a model should describe any variable to be modelled as a function of three-dimensional space (x,y,z), and as a function of time (t). However, such a description would require an extensive set of observed data to calibrate the model. Collection of such a data set may be beyond the capabilities of the user. Also, a computer with extensive storage and computing facilities would be needed.

Depending on the goals and objectives of the study, it may be possible to describe the behaviour of the system adequately by defining the variables as functions of two, one, or even zero dimensional space. Thus models are classified according to their spatial dimension, i.e. zero dimensional models, compartmental models, and one, two or three dimensional models.

3.2.1 Zero dimensional models

In zero dimensional models the reservoir is equated to a continuously stirred tank reactor (CSTR) and it is assumed that nutrients, temperature, etc are uniformly distributed throughout the system (Rossouw 1986). Zero dimensional models are also known as budget models or input-output models. A well known example of a zero dimensional model is the Vollenweider model. These models are least demanding in terms of data input, and in an information-poor situation often a zero-dimensional model is the only one that can be applied.

3.2.2 Compartmental models.

In compartmental models the water body is divided into two horizontal layers. If stratification occurs, these layers coincide with the epilimnion and the hypolimnion. The water body may also be divided into segments if nutrient concentrations vary horizontally (James 1993). These models are an improvement on zero-dimensional models in so far as they can be used to simulate stratified reservoirs.

3.2.3 One dimensional models.

In one dimensional models the water body is divided into a number of horizontal layers. The division can be done either according to the *Eularian* approach, or according to the *Langrangian* approach (Henderson-Sellers 1984):

Eularian: All the layers, except the top layer, are of equal thickness, but varying area. The change in the depth of the reservoir with changing volume is simulated by shrinking and deleting, or expanding and subdividing the top layer, while the other layers

remain constant. The number of layers, therefore, may change during the simulation period, but the thicknesses of all the layers, apart from the top layer, remain constant.

Langrangian: The number of layers stays the same during the entire simulation period, but the thicknesses of the individual layers may change to enable simulation of varying lake depth due to differences between inflow or outflow, causing changes in stored volume.

With both the Eularian and the Langrangian approach, uniform, homogeneous distribution of each substance, including temperature, is assumed within each layer. Provision is made for transport between layers by advection and diffusion, that is, due to these transport processes, temperature, or the concentration of a substance, can change in the vertical direction only.

A large amount of work has been done on one dimensional models. Experience has shown that one dimensional models are applicable where horizontal homogeneity can be assumed in small to medium sized reservoirs that stratify (Orlob 1983, Henderson-Sellers 1984). One dimensional models cannot be applied under the following conditions:

- According to Orlob (1983), and Tchobanoglous *et al* (1985), lakes that are greater than 50 km along the major axis are not suitable for simulation by one dimensional models. The reasons for this are twofold:

  - Internal waves and seiches are caused in a reservoir by wind blowing over the surface of the reservoir. Seiches are defined as horizontal density oscillations, eg, horizontal oscillation of the thermocline (Fischer *et al* 1979). The greater the surface area of the lake, the greater the effect of the wind, causing larger internal waves and seiches. In large lakes these internal waves may become so big that horizontal homogeneity is destroyed (Fischer *et al* 1979), making the lake unsuitable for simulation by a one dimensional model.

- Hydraulic currents caused by water flowing into a lake are affected by the earth's rotation - in the northern hemisphere the currents will be deflected to the right, and in the southern hemisphere to the left. This effect is known as the *Coriolis* effect. In large lakes these deflections may become so severe that horizontal homogeneity is destroyed, making the lake unsuitable for simulation by a one dimensional model.

- In large lakes with varying bottom topography horizontal homogeneity may be violated in the layers near the bottom of the lake (Henderson-Sellers 1984).

- For a one-dimensional model the effects of hydraulic currents due to inflow and outflow should be negligible. In reservoirs that are relatively narrow and deep, or where the total volume is relatively small compared with the peak rate of inflow, the amount of mixing caused by inflow and outflow may be significant, exceeding turbulent mixing caused by wind (Orlob 1983, Henderson-Sellers 1984). This is often the case with pumped storage reservoirs, in which the volume of water in the reservoir changes significantly on a daily basis, and with reservoirs of small capacity relative to river inflow (Henderson-Sellers 1984).

The behaviour of most reservoirs can be described by a one dimensional model, and one dimensional models have found wide application. However, the capabilities and limitations of any modelling approach always should be kept in mind (Henderson-Sellers 1984). Before applying a one dimensional model to a reservoir, the modeller must ensure that the reservoir satisfies the criteria for one dimensional modelling as set out in the preceding paragraphs.

3.2.4 Two dimensional models.

A two dimensional model allows temperature and concentration gradients in both the vertical and longitudinal direction, but not in the lateral direction. Change in the vertical direction is simulated by dividing the reservoir into a number of horizontal layers according to either the Eularian or Langrangian approach, similar to one dimensional models (Orlob 1983). Change in the longitudinal direction is simulated by dividing the reservoir into a number of vertical segments.

Two dimensional models find application in long, narrow reservoirs with strong through flows (Orlob 1983), such as reservoirs situated in rivers, or reservoirs with a dendritic form (Henderson-Sellers 1984). The input required greatly exceeds that of one dimensional models, and from a practical viewpoint two dimensional models tend to be restricted to specific reservoirs.

3.2.5 Three dimensional models.

A three dimensional model allows changes in temperature and concentration in vertical, longitudinal and lateral directions to be simulated. These are achieved by dividing the reservoir spatially into a three dimensional Eularian grid. Variables are calculated at each node for successive time steps (Orlob 1983). Three dimensional models are elaborate and demanding in data input, and would find application in simulation of the hydrodynamic behaviour of large bodies of water in which the Coriolis effect and internal seiching are significant.

As stated earlier, the behaviour of most reservoirs can be described by a one dimensional model, and thus, in this study, attention will be focused on one-dimensional models. This means that hydrodynamic processes not applicable to the one-dimensional approach, such as the Coriolis effect and basin wide internal waves, will not be discussed.

3.3 HYDRODYNAMIC PROCESSES

3.3.1 Background

Consider a small to medium size reservoir: The water mass in such a reservoir may exhibit distinctive physical structures because of the effect of various abiotic factors (Fig 3.1), the unique density properties of water, and the depth and the size of the reservoir. Over the course of a year, the water body undergoes distinct cyclical, seasonally linked, changes due principally to the input of energy (heat and wind).

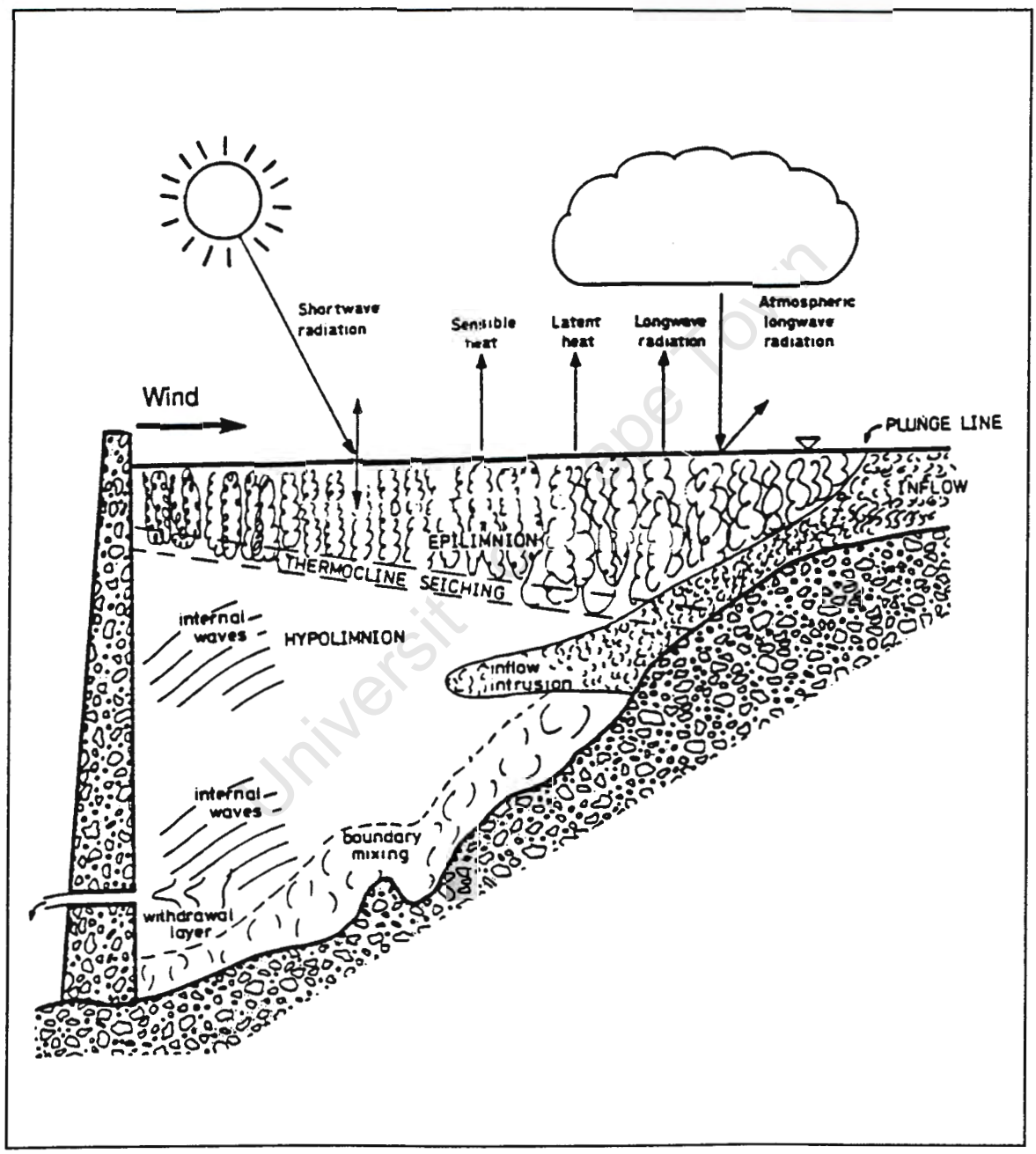

Figure 3.1
Diagrammatic representation of the hydrodynamic forces that act on a reservoir

During winter, there is very little, or no change in water temperature with depth (Fig 3.2c), and the reservoir is said to be in a *fully mixed* state (Henderson-Sellers 1984).

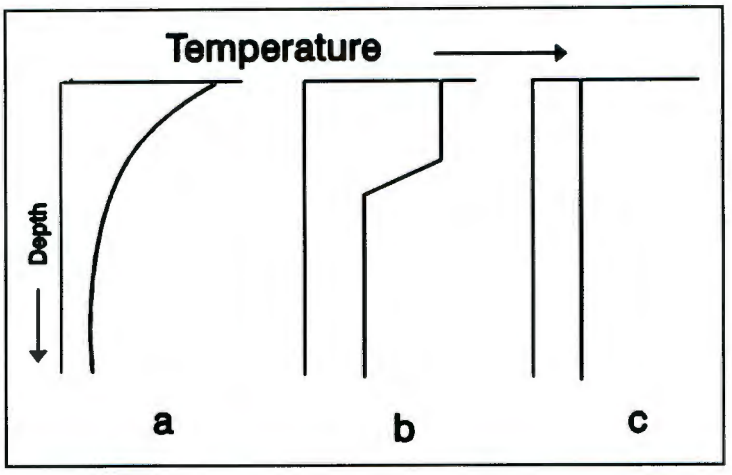

Figure 3.2
Vertical distribution of temperature under
a) the influence of radiation only,
b) the influence of both wind and radiation,
c) when the reservoir is fully mixed.

With the onset of summer, the increase in solar radiation causes a corresponding increase in water temperature through the exchange of heat energy at the air-water interface. The water density decreases accordingly. If there is no movement in the water column heat would be absorbed exponentially by the water (similarly to light), leading to a distribution of temperature with depth similar to that shown in Fig 3.2a - because heating by absorption of radiation is greatest in the surface layer and progressively less in the layers lower down, the water nearer the surface is slightly warmer and therefore less dense, or more buoyant (Barnes and Mann 1991). Although some heat is lost from the surface through conductive (sensible), and latent (evaporative) heat loss, as well as by long wave radiation (Fig 3.1), essentially the structure depicted in Fig 3.2a will remain stable as long as the input of short wave radiation remains stable, and as long as there is no disturbance in the water column. However, it is virtually impossible to have totally quiescent conditions in the water column. Wind blowing across the reservoir exerts a frictional drag at the water surface, leading to turbulent mixing in the water body. Initially the increased heat at the surface is transported deeper down by turbulent mixing, however, as the water temperature

increases, mixing becomes increasingly difficult. This can be attributed to the density properties of water at different temperatures - the rate of change of water density is not constant with increasing temperature, the higher the temperature, the greater the change in density per degree change in temperature (Fig 3.3), and the greater the resistance to mixing. For example, it takes about 30 times more energy to completely mix equal volumes of water at 24 and 25°C as it takes to mix the same volumes of water at 4 and 5°C (Goldman and Horne 1983). Because of the greater energy needed at higher temperatures to mix water layers of different temperatures, normally the turbulent energy generated by wind blowing across the water surface is sufficient only to mix the increasingly warmer water at the surface with the water immediately below; usually there is not enough energy available to mix the warmer water in the upper part with the colder water deeper down, i.e. mixing is effectively limited to the warmer, upper part of the reservoir. As a result, the water temperature in this part increases steadily, thereby increasing the density difference between the upper part of the reservoir and the water deeper down. Thus an increasing amount of energy also will be needed to mix the water in the warm upper part of the reservoir with the colder water beneath. Strong winds or a storm event with high river inflow may impart sufficient energy to cause mixing throughout the reservoir depth.

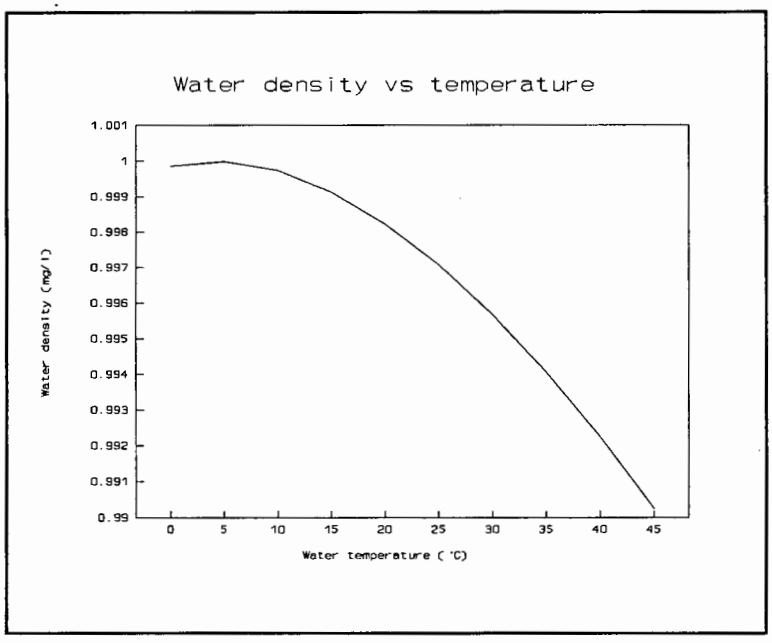

Figure 3.3
Change in water density with temperature

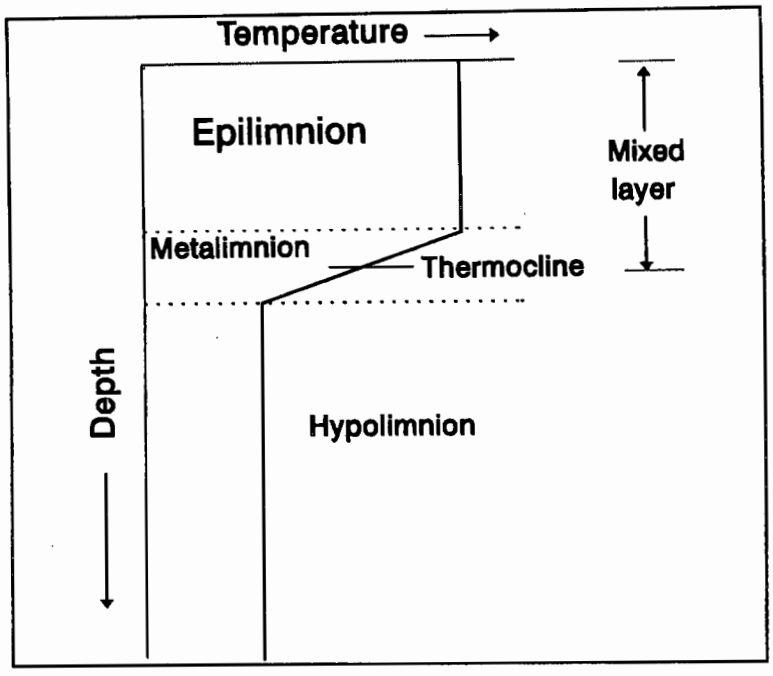

Figure 3.4
The physical state of the reservoir under stratified conditions

As a result of this resistance to mixing, particularly in summer with greater density differences per degree difference in temperature, the reservoir divides into upper and lower temperature regimes (Fig 3.2b), i.e. instead of being in a fully mixed state, it is in a state of *stratification*. The warmer upper part is called the *epilimnion* (Fig 3.4), and the lower colder layer at the bottom is the *hypolimnion*. Between these two layers is a region where the temperature gradient is very steep, i.e. if T denotes temperature and z denotes depth, dT/dz (the rate of change of temperature with depth) is very large in this region, which is known as the *metalimnion.* Often this region is referred to as the *thermocline*, but the thermocline is more precisely defined as that depth in the metalimnion where the temperature-depth curve exhibits an inflection point (Henderson-Sellers 1984). The region above the thermocline is known as the *mixed layer*. Often the mixed layer is taken as being equivalent to the epilimnion; in terms of our definition this is not correct, as the mixed layer encompasses the epilimnion plus the upper part of the metalimnion.

With the onset of winter, solar radiation decreases, and heat loss through the water surface exceeds heat input. The temperature of the water near the surface decreases, and the density increases. This causes the water nearest the surface to be heavier than the water immediately underneath and therefore it sinks down, mixing with the warmer water underneath, thereby gradually decreasing the water temperature in the epilimnion. This means that less energy is needed for mixing in the epilimnion, and also that the density difference between the epilimnion and the hypolimnion decreases. Consequently less energy is needed to mix epilimnetic and hypolimnetic water, and turbulence generated under normal wind conditions, plus convective mixing due to sinking of cooler water from the surface, is sufficient to cause epilimnetic mixing to extend eventually down to the bottom of the reservoir, resulting in a homogeneous distribution of temperature/density from the top to the bottom of the reservoir. This process is known as *overturn*. Once the reservoir has overturned, it has returned to a fully mixed state (Fig 3.2c).

The conditions for mixing and stratification are governed principally by radiation (and thus by water and air temperatures), and wind speed, with factors such as water surface area (and thus wind fetch length), depth of the water body, and turbidity contributing also. Because so many factors are involved, it is not a simple matter to determine *ab initio* whether the water body will be in a mixed or stratified state, or the time frame in which these two conditions will be present. According to Hanson *et al* (1987), and James (1993), lakes up to 2 metres deep stratify briefly and are mixed almost daily; lakes 3 - 7 metres deep stratify for a few days to a few weeks; and lakes deeper than 8 metres stratify on a seasonal basis. However, it would seem that these observations were made in water bodies in cold temperate regions; the situation may be different for lakes and reservoirs in warm temperate/subtropical climates, as the degree of stratification varies with lake morphometry and climatic conditions. Thus reservoirs of similar depth, but in different climates may have a different time scale for stratification -in warm/subtropical climates reservoirs tend to stratify for longer periods, depending on the wind conditions (Hanson 1987, James 1993). For example, Marais (1970) reports that small lakes of 1-2 metres deep in Zambia showed a daily cycle of mixing and stratification during the cooler subtropical season, and continuous stratification during the hotter season.

Reservoirs and lakes that are permanently stratified are termed *meromictic. Oligomictic* lakes generally are tropical and have rare periods of circulation. Reservoirs that turn over once a year only are known as *monomictic*. Those in warm temperate regions, where the annual overturn occurs during autumn, are called *warm monomictic*, and lakes in the Arctic region where the annual overturn occurs during spring, due to melting of the ice cover, are termed *cold monomictic*. Lakes and reservoirs that turn over twice a year (during autumn and during spring) are termed *dimictic*, and lakes that never stratify due to frequent circulation because of, for instance, high winds, are termed *polymictic*.

With this background we will now identify the various components and processes that affect the hydrodynamic behaviour of a reservoir.

3.3.2 Identification of hydrodynamic processes

In lakes and reservoirs of small to medium size (less than 50 km along the major axis), it has been found that the temperature over any horizontal plane parallel to the surface is virtually homogeneous during the stratified period, i.e. the temperature gradient is almost exclusively in the vertical direction (Orlob 1983). Even though storm events and wind disturbances cause longitudinal and lateral disturbances, these effects are transient and are rapidly dissipated under the influence of gravitation, making vertical temperature variations dominant (Imberger and Patterson 1981). The principal water quality gradients also are in the vertical rather than the longitudinal direction (James 1993), and thus it has been found that lakes and reservoir of small to medium size can be adequately represented by a one-dimensional structure, the exception being reservoirs with a short retention time (Orlob 1983). Accordingly, in this study the one-dimensional approach is followed, i.e. only vertical temperature and water quality gradients are taken into account; phenomena, such as the Coriolis effect and large internal waves and seiches are not considered.

To assist in identifying the processes that govern the hydrodynamic behaviour of a reservoir, the reservoir is divided into a number of horizontal layers. Consider the forces that act on one horizontal layer of water at, for instance, the surface of the reservoir. Of these forces, solar radiation and wind action have been identified as the most important (Orlob 1983, Henderson-Sellers 1984).

Regarding solar radiation, heat energy from short wave solar radiation will enter the top of the layer. Some of the heat energy is absorbed in this layer, and the remainder will penetrate further and pass through the bottom of the layer into the layer directly below, and so on. Due to absorption of heat energy (from solar radiation) in the layer, the water temperature of the layer will increase. Only shortwave radiation (solar radiation) can penetrate into the water and cause heating below the surface - other radiation such as long wave radiation and back radiation affects the surface only.

Regarding wind action, wind blowing over the surface of the water exerts a frictional drag on the water surface, causing shear stress in the water near the surface. Some of the turbulence resulting from the shear stress is dissipated in overcoming viscosity, whereas the rest may cause mixing of layers of different temperature/density.

The hydrodynamic forces exerted by inflows and outflows have a lesser effect than the forces generated by solar radiation and wind action (Stefan and Ford 1975, Goldman and Horne 1983), nevertheless these also must be taken into account. Water flowing into the layer will disperse into the layer if the temperature, and thus the density, of the inflowing water is the same as that in the layer, otherwise the inflowing water will continue to move downward out of the layer, until it finds a layer of similar density, where it will disperse. While moving downward, turbulence is created due to shear stress between the moving water and the sloping sides of the reservoir. This turbulence may cause some mixing.

Regarding outflows, if water is withdrawn at the level of the hypothetical layer, the resultant water movement will cause a certain degree of mixing. Any movement at the bottom/top of the layer will be propagated to the layer below/above and so on.

The major processes associated with the forces identified above are:

- Exchange of heat energy
- Convective mixing
- Advective mixing
- Mixing due to wind action

3.3.2.1 Exchange of heat energy:

According to Henderson-Sellers (1984), the major heat exchanges occur at the air-water interface. Except for very small reservoirs, the energy flow into and out of the sides and bottom of the reservoir is relatively small compared to the exchange at the water surface, and is seldom taken into account in calculation of vertical temperature profiles.

The following energy exchanges take place at the water surface: Absorption of short wave radiation, back radiation, atmospheric radiation, evaporative (latent) heat loss, as well as convective (sensible) heat loss (Fig 3.1).

Absorption of short wave radiation:

Some of the incoming short wave radiation from the sun is reflected at the water surface; the amount reflected will depend on the turbidity of the water, the angle of the sun and cloud cover (Henderson-Sellers 1984). Some of the remaining radiation is absorbed by the surface layer. The rest penetrates to greater depth, being absorbed along its path, until eventually all the short wave radiation is absorbed by the water. The depth to which short wave radiation will penetrate before it is totally absorbed depends on various factors such as the turbidity of the water. Only short wave radiation can penetrate below the surface layer, and thus short wave radiation is the main mechanism for heating the water body (see absorption of atmospheric long wave radiation below).

Evaporative heat loss:

During the evaporation process, when the state of the water changes from a liquid to a vapour, heat energy is lost from the reservoir in the form of latent heat of evaporation (Orlob 1983). The evaporation process directly affects the surface layer of the reservoir only, and will depend on wind speed, and relative humidity/water vapour pressure (Henderson-Sellers 1984).

Sensible heat loss/gain:

This process is also referred to as convective heat loss/gain - sensible heat is transferred between the air and water by conduction, and transported to or from the air-water interface by convection associated with a moving air mass (Orlob 1983). This process affects the surface layer of the water only, and will depend on the temperature of the surface layer, air temperature, and wind speed (Henderson-Sellers 1984).

Back radiation:

All material above absolute zero temperature emits long wave radiation, thus long wave radiation will be emitted from the water surface to the atmosphere (Henderson-Sellers 1984). This process represents a loss of energy from the reservoir.

Absorption of atmospheric long wave radiation:

Long wave radiation emitted from the earth is absorbed by the atmosphere and clouds, whereupon it is re-emitted. The amount of radiation re-emitted by the atmosphere will depend on cloud cover and the temperature of the atmosphere (Dake and Harleman 1969, Henderson-Sellers 1984). The long wave radiation re-emitted by the atmosphere will be absorbed only by the surface water in the reservoir, because long wave radiation, unlike short wave radiation, cannot penetrate deeper into the water body. This process represents a gain of heat energy by the reservoir.

3.3.2.2 Convective mixing:

In late summer the air temperature drops below that of the water and the water at the surface starts to lose heat to the atmosphere. As a result, the uppermost water of the epilimnion becomes colder, and thus denser. The colder water is negatively buoyant

and therefore sinks, causing mixing by entrainment (Fischer *et al* 1979, Henderson-Sellers 1984). In combination with wind action, convective mixing causes deepening of the thermocline until the thermocline reaches the bottom of the reservoir, i.e. the reservoir is in *fully mixed* state again. This process is known as *convective overturn*.

3.3.2.3 Advective mixing:

The term 'advective mixing' describes mixing in a reservoir due to inflows and withdrawals:

Advective mixing due to inflows:

Usually the density of water flowing into a reservoir differs from the density of the water at the surface of the reservoir. If the inflowing water is less dense than the surface water in the reservoir, the inflowing water will disperse on top of the surface water of the reservoir. If the inflowing water is denser than the reservoir surface water, the inflowing water will plunge beneath the surface at a point known as the *plunge line* or the *plunge point* (Fig 3.1). Thereafter the inflowing water becomes a density current that entrains ambient water (Farrell and Stefan 1988). The amount of entrainment at the interface between the reservoir and the inflowing water depends on the amount of turbulence created by the roughness and slope of the submerged river bed (Fischer *et al* 1979). The inflowing water will flow along the bed until it reaches a level where the density of the reservoir water equals that of the inflowing water, whereafter the inflowing water disperses horizontally at this level. The depth where the inflowing water disperses is known as the *plunging depth.*

Mixing due to withdrawals:

When the reservoir is in fully mixed condition, the water is of uniform density, and water being withdrawn will flow radially towards the outlet port, equally symmetric from all directions (Fischer *et al* 1979, Henderson-Sellers 1984). During stratified periods, if the outlet port is situated in the epilimnion, and if the discharge is small, the stable boundary formed by the thermocline may prevent vertical motion extending into the hypolimnion. Similarly, if the outlet port is located in the hypolimnion, the thermal/density stability in the hypolimnion may be large enough to prevent large

vertical motions, and the water that is discharged will come from a thin horizontal layer at the level of the outlet port (Fischer *et al* 1979).

In most large reservoirs hydraulic currents caused by inflows and outflows are negligible and there is no need to take the resultant shear-induced mixing into account. The exception is reservoirs with short retention times (10 days or less), and reservoirs with significant throughflow (Goldman and Horn 1983, Henderson-Sellers 1984, James 1993).

3.3.2.4 Mixing due to wind action:

Mixing due to wind action can be divided into two categories, i.e. mixing due to weak winds, and mixing due to strong winds (Fischer *et al* 1979).

Weak winds:

A wind blowing over the surface of the reservoir exerts a drag force on the surface, causing waves to form and break, and producing shear near the water surface. Both the breaking waves and mean shear generate turbulence in the upper layers of the water (Sundaram and Rehm 1971, Fischer *et al* 1979). The turbulence can be dissipated in overcoming viscosity, or if sufficiently strong, entrains water at the thermocline into the epilimnion, thereby deepening the epilimnion. Usually, most of the turbulence generated by weak winds is used in overcoming viscosity, leaving insufficient turbulence to cause deepening of the epilimnion.

The effect of strong winds:

A strong wind causes the water in the epilimnion to move in the direction of the wind. However, it has been observed that in spite of the water movement in the epilimnion, the water surface remains nearly horizontal, thus, to counter the flow in the epilimnion, the water in the hypolimnion must flow in the reverse direction (Fischer *et al* 1979). The resultant whole basin circulation may last for a few days, allowing an appreciable shear to develop across the thermocline, thereby causing mixing of hypolimnetic and epilimnetic waters due to entraining, effectively deepening the epilimnion. With continuous winds, the shear will increase over time, causing the thermocline to tilt, until

the hydrostatic pressure gradient resulting from the tilting thermocline just balances the surface stress. Thereafter the whole basin circulation changes to two closed gyres (non-overturning motions), one in the epilimnion, and one in the hypolimnion, with opposite rotation. At this stage the shear at the thermocline has decreased to a very small value, and, as with weak winds, all the turbulence generated by the shear is either dissipated internally by overcoming viscosity, or causes the epilimnion to deepen by entrainment (Fischer *et al* 1979).

It is possible that shear production at the thermocline may be sustained long enough for the thermocline to tilt, but it may not be sustained long enough for the whole basin circulation to change to two closed gyres. After the wind ceases, the tilted thermocline will return to its original horizontal position, and in doing so, starts to oscillate around its original position. This phenomena is known as *seiching*. In basins with mildly sloping sides, basin-scale motions such as seiching cause severe shear at the boundary formed by the sides and bottom of the reservoir, leading to further turbulence (Imberger and Hamblin 1982). Especially in reservoirs of small to medium size, such boundary mixing may be significant in the vertical transport of heat and mass in the hypolimnion (Fischer *et al* 1979, Imberger and Hamblin 1982).

The mechanisms discussed above - wind stirring, mixing caused by shear production at the thermocline, and boundary mixing - all contribute in generating turbulence that may cause deepening of the epilimnion. However, deepening of the epilimnion is not a function of turbulence only, it is the result of the non-linear interaction between turbulence and stability due to density gradients (Sundaram and Rehm 1971). In fact, according to Henderson-Sellers (1984), the stability of the reservoir, as manifested in the distribution of water temperature with depth, is the most important factor that governs the behaviour of a reservoir. The more stable the reservoir, the greater the amount of energy that must be input to cause deepening of the epilimnion. Also, the stability of the reservoir will determine whether wind stirring or shear production will cause deepening of the epilimnion; if the stability is high, deepening is caused mainly by wind stirring, under less stable conditions, deepening is caused by shear production at the thermocline (Fischer *et al* 1979, Spigel and Imberger 1980, James

1993). Also, a strong temperature/density gradient, i.e. stable conditions in the reservoir, tends to inhibit vertical movement, and generally horizontal currents are several orders of magnitude larger than vertical currents (Fischer *et al* 1979, Goldman and Horn 1983, Henderson-Sellers 1984). Thus horizontal and longitudinal gradients are dispersed so much faster than the vertical gradients that their effect becomes of secondary importance.

First attempts at describing the vertical transport of heat (and mass) and the resultant formulation of the thermocline were based on conservation of mass (the *diffusion concept*). However, due to some inherent shortcomings of this concept, models based on the diffusion concept could not simulate thermocline formation adequately. This resulted in the diffusion concept being supplemented by the *integral energy concept*, which is based on conservation of energy (Stefan and Ford, 1975).

3.3.2.5 Diffusion concept of vertical transport of heat:

In reservoirs, three processes contribute to the vertical transport of heat by diffusion - advective dispersion, molecular diffusion and eddy (turbulent) diffusion. Advective dispersion represents the contribution of inflows to the heat budget. However, because inflowing water disperses in a layer of similar temperature, no temperature difference exists between the inflowing water and the water in the reservoir at the point of dispersal, and hence heat diffusion through vertical advective dispersal is negligible (Powell and Jassby 1974). Turbulence created by inflows may contribute to vertical heat transport, but this is greatly inhibited by stratification, and can be modelled effectively as part of the entrainment between the inflowing water and the reservoir water (Patterson *et al* 1984).

Regarding eddy and molecular diffusion, in reservoirs, eddy diffusion is up to an order of magnitude greater than molecular diffusion (Sundaram and Rehm 1971, Harleman 1982). Eddy diffusion has been identified as the main process for the vertical transport of heat and mass, specially in the hypolimnion (Mortimer 1942, Jassby and Powell 1975).

According to Mortimer (1942), the fundamental assumption (experimentally verified) of the laws of diffusion and heat conduction is that the amount of substance or heat passing across a boundary of unit area in unit time is the product of the appropriate coefficient of conduction or diffusion, and the gradient of temperature, or concentration, existing at the boundary along an axis normal to it. Because eddy diffusion is the main diffusion process in reservoirs, the only diffusion coefficient that needs to be taken into account is the eddy diffusion coefficient.

The value of the eddy diffusion coefficient is several hundred times greater in the epilimnion than in the hypolimnion. Within the epilimnion the eddy diffusion coefficient is a function of wind stirring only, and, for all practical purposes, can be regarded as constant. However, the hypolimnion is effectively sheltered from the effect of wind by the thermocline, and thus turbulent mixing in the hypolimnion is due to internal currents that are an indirect response to surface wind stress and advection (Sundaram and Rehm 1971, Imboden 1978, Ford and Stefan 1980). Also, the thermal stability of the hypolimnion during stratification tends to dampen any water movement. Consequently the hypolimnetic eddy diffusion coefficient becomes a function of both water movement and thermal stability (Henderson-Sellers 1984). Furthermore, it has been observed that the hypolimnetic eddy diffusion coefficient is not constant, but increases with reservoir size and mean depth (Mortimer 1942, Orlob and Selna 1970, Jassby and Powell 1975, Henderson-Sellers 1984). This can probably be attributed to the effect of wind fetch length on turbulent mixing.

Predictive models based on the diffusion concept experienced limited success (Ford and Stefan 1980). Although the seasonal temperature cycle of stratified lakes could be simulated to a certain degree, the diffusion concept turned out to be an unsuitable basis for water quality modelling (Fischer *et al* 1979). The inherent limitation of the diffusion concept is that the time scale associated with diffusion in reservoirs is of the order of several days (Harleman 1982), whereas simulation of biological constituents and processes requires a daily time step at most (Imberger *et al*, 1978). Furthermore, the operation of a reservoir often requires daily management, but a time step of several days means that models based on the diffusion concept can be used only in seasonal water management of reservoirs (Stefan and Ford 1975).

A further drawback of the diffusion concept is that it provides little insight into the dynamics of the reservoir, and the interactions between various processes, particularly the interaction between turbulence and density gradients that leads to formation of the thermocline (Ford and Stefan 1980, Patterson *et al* 1984). The deficiencies of the diffusion concept led to development of another concept, the *integral energy* concept, based on the principle of conservation of energy, instead of conservation of mass as is the case with the diffusion concept.

3.3.2.6 Integral energy concept of turbulent transport:

According to Stefan and Ford (1975) the integral energy concept should be seen as supplemental, rather than competitive, to the diffusion concept. The integral energy concept was pioneered by Turner and Kraus (1967) on the basis of experimental results. The fundamental basis of this concept is that turbulent mixing and transport across a density gradient, such as that represented by a thermocline in a reservoir, can be explained on the basis of an energy consideration (Linden 1973). The energy required to lift relatively heavy water from below the epilimnion, and to accelerate stationary water, is expressed as the rate of change in potential energy (CWR 1991). The rate of change of potential energy serves as a measure of the stability of the reservoir - the more stable the reservoir, the bigger the temperature/density difference between the epilimnion and the hypolimnion, and the more energy would be required for mixing.

Energy available for mixing is expressed in terms of turbulent kinetic energy; turbulence due to wind stirring, shear production at the thermocline, and advection contribute to the turbulent kinetic energy budget. It is postulated that mixing due to entrainment of colder, denser hypolimnetic water into the mixed layer or epilimnion, and thus deepening of the epilimnion, is dependent on a certain critical ratio of turbulent kinetic energy and rate of change in potential energy in the epilimnion (Stefan and Ford 1975, Imberger *et al* 1978, Imboden 1978). If less than the critical amount of turbulent kinetic energy is supplied, virtually no mixing takes place, and the incoming turbulent kinetic energy is dissipated in overcoming viscosity. If more than the critical amount is supplied, turbulent entrainment and mixing will occur until the

excess kinetic energy is spent, i.e. the critical ratio is restored again. On the basis of experimental evidence, the value of the critical ratio is estimated to be close to unity (Stefan and Ford 1975, Linden 1973).

The main difference between the diffusion concept and the integral energy concept is in the importance attached to transport of turbulent kinetic energy (Ford and Stefan 1980) - in the diffusion concept transport of turbulent kinetic energy and formation of the thermocline is linked to eddy diffusivity, whereas in the integral energy concept, transport of turbulent kinetic energy and formation of the thermocline is linked to the amount of entrainment that occurs at the bottom of the mixed layer. The latter concept provides a better description of the interaction between turbulence and stability, and the resultant thermocline formation. Also, because wind stirring is the main contributor to turbulent kinetic energy budget (Imboden 1978), the inherent time-scale associated with the integral energy concept is that of wind speed measurement, i.e. one day or less. This means that hydrodynamic models based on the integral energy concept would form suitable bases for water quality models, as simulation of nutrient and algal dynamics requires a time scale of one day or less (Harleman 1982).

A shortcoming of the integral energy concept is that it does not take hypolimnetic diffusion into account, and thus early models based on this concept could not simulate hypolimnetic temperature profiles adequately (Harleman 1982, Henderson-Sellers 1984). This deficiency was overcome by introducing eddy diffusion in the hypolimnion, analogous to the diffusion concept (Imberger *et al* 1978, Ford and Stefan, 1980).

To summarize; models based on the integral energy concept, that include hypolimnetic diffusion, describe the vertical distribution of temperature with a higher degree of accuracy, have a better predictive capability, and are more dynamic than models based on the diffusion concept. Furthermore, models based on the integral energy concept provide more insight into the dynamics of the reservoir, and the interactions between various processes, and form a more suitable basis for water quality models (Harleman 1982, Ford and Stefan 1980).

3.4 WATER QUALITY PROCESSES

3.4.1 Background

In the previous section a conceptual description was given of the hydrodynamic behaviour of reservoirs. Underlying the hydrodynamic description was the assumption that the hydrodynamic response is relatively insensitive to the water quality response. In contrast, the water quality response is extremely sensitive to the hydrodynamic response. This can be ascribed to the seasonal cycle of stratification and overturn - because of the density difference between the epilimnion and the hypolimnion during the period of stratification, the thermocline effectively forms a physical barrier that restricts movement of heat, nutrients, and oxygen between the epilimnion and the hypolimnion. This is of particular significance in the water quality behaviour of the reservoir: algae need nutrients and light for growth, but, because light is absorbed by water, algal growth is limited to the upper part of the water body. Regarding nutrients, often the bottom sediments are the main source of nutrients, but, because of the barrier formed by the thermocline, effectively these nutrients are trapped in the hypolimnion, and are not available to the algae which are mainly in the epilimnion.

The greatest significance of the barrier formed by the thermocline, however, is the effect it has on the distribution of oxygen. The main source of oxygen in a reservoir is that transferred from the atmosphere, as well as oxygen generated during the algal growth process. Under stratified conditions the hypolimnion is effectively sealed off from both these sources, thus there is no means of replenishing oxygen that is consumed in the hypolimnion during, for instance, bacterial degradation of organic matter. If the concentration of organic matter in the hypolimnion is high, bacterial degradation may cause the oxygen in the hypolimnion to be depleted, thereby resulting in anaerobic[1] conditions in the hypolimnion. Under anaerobic conditions

---

[1]In this study the term *anaerobic* refers to a condition where no oxygen or nitrate is present, or where the potential rate of oxygen/nitrate consumption exceeds the rate of oxygen/nitrate replenishment. The term *aerobic* refers to a condition where oxygen is present, and the term *anoxic* refers to a condition where nitrate is present, but no oxygen.

phosphate, ammonium, manganese and iron salts are released from the bottom sediment, and nitrate is denitrified. High concentrations of manganese and iron may render the water unfit for human use. The phosphate and ammonium salts accumulate in the hypolimnion until overturn, when it is mixed homogeneously throughout the reservoir, causing an increase in nutrient concentration in the upper part of the reservoir, which may lead to excessive algal growth. Clearly, anaerobic conditions in the hypolimnion may cause severe water quality problems. In fact, according to Mortimer (1942), reservoirs where the hypolimnion becomes anaerobic should be considered as fundamentally different from reservoirs where the hypolimnion does not become anaerobic. Anaerobic reservoirs are characterised by high internal cycling of nutrients, which may cause excessive algal growth after overturn. This has severe implications for the management of such reservoirs, as the trophic state of a reservoir where the hypolimnion becomes anaerobic, is not determined by incoming nutrient load only, but also by the load from internal nutrient cycling, and the response of the reservoir to the nutrient load. To a certain extent, the response of each reservoir will be unique, as, for instance, factors such as the degree of stratification (if the reservoir does stratify), and the vertical distribution of oxygen will be strongly influenced by the size and the shape of the reservoir (Mortimer 1942), as well as climate. In the warm/subtropical regions of Africa the degree of stratification is much stronger than in temperate regions, because of higher epilimnetic water temperatures. Also, the density difference between the epilimnion and the hypolimnion is increased further by the high concentration of inorganic suspended sediment (TSS) that is a characteristic of many reservoirs in this region (Allanson *et al* 1990). The greater degree of stratification means that transport of heat, nutrients and oxygen between the epilimnion and the hypolimnion is restricted even more. Also, the higher water temperature causes biological rates such as bacterial decomposition of organic matter to increase, leading to more rapid hypolimnetic oxygen depletion (and thus greater internal cycling of nutrients) than would be the case for a reservoir with a similar concentration of organic matter, but situated in a cooler region (Henderson-Sellers 1984). Furthermore, it has been found that the morphology of the reservoir and wind mixing are amongst the crucial factors that determine whether algal concentration will reach nuisance proportions (Zohary and Breen 1989).

From the above, in the conceptual representation of a water quality model for reservoirs, the following categories of processes can be identified, and would need consideration:

- Processes affecting dissolved oxygen concentration
- Microbial decomposition of organic matter
- Processes affecting algal concentration

These categories are strongly interlinked and are presented separately only for convenience.

3.4.2 Processes affecting oxygen concentration

The concentration of dissolved oxygen in water can be expressed in two ways - in mg l^{-1}, or as a percentage saturation. The former is a direct measure of the amount of oxygen in the water. It is a useful measure as it allows assessment as to whether there is sufficient oxygen to sustain the different forms of aerobic aquatic life at different temperatures. Also, it allows formulation of the transition behaviour from, say, aerobic to anoxic or anaerobic states.

Expressing dissolved oxygen concentration as percentage saturation is useful under oxygen unsaturated conditions, as it gives an indication of the fraction of oxygen present relative to its saturation state. Saturation state is the maximum concentration of oxygen that can dissolve in water at a given time, and is a function of temperature, as well as pressure (Henderson-Sellers 1984, Jeffries and Mills 1990). The percentage saturation has merit as a practical rapid operational tool, not so much for quantitative study.

The saturation concentration of oxygen in a water in contact with air is dependent on both the water temperature and atmospheric pressure. It is affected to a relatively minor degree by dissolved salts concentration (provided the dissolved salts concentration $< 2\,000$ mg l^{-1}).

The saturated oxygen concentration in water decreases with increasing temperature. For example, in Figure 3.5 the saturated concentration of oxygen in distilled water at 1 atmosphere (sea level) changes from greater than 14 mg O l^{-1} at 0°C to about 7.5 mg O l^{-1} at 30°C. Thus, from the temperature effect alone, waters in the upper layers of a reservoir situated in a warm/subtropical climate will be saturated at a much lower oxygen concentration than will be the case for a reservoir situated in a cold temperate climate, i.e. at saturation there is a much lower oxygen reserve for oxidative processes in a reservoir situated in a hot climate, compared to a reservoir in a colder climate.

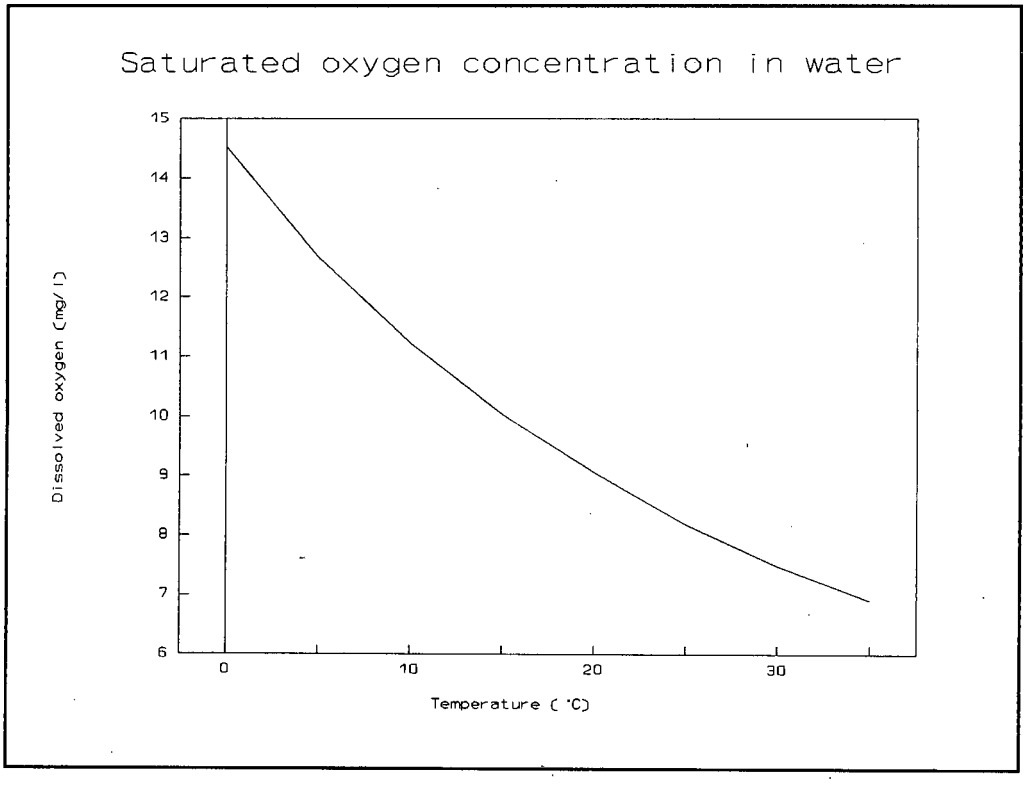

Figure 3.5.
Saturated oxygen concentration in water at 1 atmosphere for a range of temperatures

The effect of atmospheric pressure is to lower the saturation concentration as the elevation increases above sea level. The dissolved oxygen concentration at, say, 20°C, for any atmospheric pressure is expressed by Henry's Law which states that the mass of any gas that dissolves in a given volume of liquid, at a constant temperature, is directly proportional to the partial pressure the gas exerts above the liquid (James 1993). As a consequence, for a reservoir at a high altitude where the atmospheric pressure (and hence the oxygen partial pressure) is lower, the oxygen saturation concentration is lower compared to a reservoir at sea level. For instance, in South African reservoirs such as Roodeplaat Dam Reservoir situated at an altitude of 1200 metre above sea level, the saturated oxygen concentration will be 14% lower than in reservoirs at sea level. Again this means that oxygen depletion will occur more readily in high altitude reservoirs, because of the lower oxygen reserve at saturation (Goldman and Horne 1983, Henderson-Sellers 1984).

Dissolved oxygen plays an important role in many chemical and biological processes in a reservoir - it serves as an electron acceptor, and affects the solubility and availability of many nutrients, and thereby the productivity of the water body. Both the oxygen concentration, as well its distribution in the water column is important. The oxygen concentration can range from zero to supersaturation. When the concentration approaches zero, below a certain concentration the rates of the aerobic processes decline, whereas anoxic/anaerobic process rates increase concomitantly. For example, if anoxic/anaerobic conditions develop at the sediment-water interface, nutrients such as phosphates and ammonium are released. In the upper layers of the reservoir oxygen supersaturation can occur; invariably it is the result of oxygen generation through photosynthesis by the algae - the algae produce pure oxygen thereby increasing its partial pressure in the water. Thus, under conditions of supersaturation, the partial pressure of oxygen in water is higher than the partial pressure of oxygen in the atmosphere above the water surface, therefore oxygen readily precipitates out of the water to the atmosphere upon any significant disturbance of the water mass, for instance wind action.

Sources of oxygen in an open body of water are mainly:

- Transfer of atmospheric oxygen to the water mass
- Production of oxygen by algal photosynthesis

Sinks of oxygen arise mainly from chemical and biological oxidation processes (Klapper 1991).

3.4.2.1 Atmospheric oxygen transfer: This phenomenon has first been conceptualised by the classic two-film theory of Lewis and Whitman (1924). However, because the theory of Lewis and Whitman is applicable only under conditions of hydrodynamically smooth (laminar) flow over the water surface, Danckwerts (1951) developed a theory to account for atmospheric oxygen transfer into a water body under hydrodynamically rough flow conditions.

According to the theory of Lewis and Whitman (1924), when a gas and a liquid come into contact, two thin stagnant films form on both the gas and the liquid side of the interface. These films are practically free from mixing by convection, consequently gas is transferred through the films by the relatively slow process of molecular diffusion. The films therefore constitute the controlling resistance to absorption of gas by liquid. In some instances one of the films may be of much greater importance than the other; the less important film can then be neglected and the process be conceptualised as if only one film exists. For instance, in the case of absorption of atmospheric oxygen by water, the diffusional resistance of the water sublayer (film) will be greater than that of the atmospheric sublayer as the rate of molecular diffusion in air is 10^3 to 10^4 times greater than that in water (Lewis and Whitman 1924, Emerson 1975). Also, because of the low solubility of oxygen in water, it diffuses so slowly through the water layer that the overall reaction rate is controlled by rate of diffusion through the water sublayer (Lewis and Whitman 1924). The atmospheric film therefore is of much less importance, and only the film on the water side of the interface needs to be considered.

Treating the transfer of atmospheric oxygen into a water body in terms of the water film only, the transfer across the air-water interface can be divided into three stages (Bratby 1977):

a) Oxygen molecules from the air are initially transferred to the air-water interface until a stage is reached where the molecules leaving the air and dissolving in the interface are equal to those coming out of solution and re-entering the gas phase, that is, the interface becomes saturated with oxygen. The rate at which oxygen molecules are transferred to the interface to achieve saturation is very rapid.

b) Oxygen molecules dissolved to saturation at the interface pass through the film on the water side of the interface by molecular diffusion. The water film has special properties being composed of water molecules which, because of the air phase on the other side of the interface, are orientated with their negative oxygen ends facing the interface. For all practical purposes the film can be taken as being of the order of 13 molecules thick.

c) Below the water film oxygen is distributed throughout the water body by diffusion and convection.

Danckwerts (1951) postulated that, under turbulent conditions, the interfacial film is constantly being eroded and the liquid at the surface continually replaced with fresh liquid from the main body of liquid. Under these circumstances, the rate of gas transfer is no longer a function of molecular diffusion, but a function of surface renewal. Thus there are two extreme modes of transfer - that proposed by Lewis and Whitman (1924), applicable under laminar flow conditions, and that proposed by Danckwerts (1951), applicable under turbulent flow conditions.

There is a vast literature on the transfer of oxygen in water, all in some measure contain the conceptual ideas of Lewis and Whitman, and Dankwerts, linking these to some external force driving the process. Considering the transfer of atmospheric

oxygen into a water body such as a lake or a reservoir, it is postulated that a sublayer exists at the water surface, that has a thickness which is inversely proportional to wind shear velocity. The flow over the surface of a reservoir is hydrodynamically smooth up to wind speeds of about 3 m s^{-1}. Under smooth flow, viscous conditions prevail in the water sublayer, and the rate at which oxygen enters the water body is controlled by the rate of molecular diffusion through the undisturbed water sublayer (Emerson 1975, O'Connor 1983, Livingstone and Imboden 1993).

With increasing wind speed a certain critical shear velocity is reached where air flow over the water surface changes from aerodynamically smooth to turbulent. This transition occurs at a shear velocity of approximately 10 cm s^{-1}, which is equivalent to a wind speed of 3 m s^{-1} (Emerson 1975, O'Connor 1983). At wind speeds > 3 m s^{-1} the thickness of the sublayer at the water surface layer is not inversely proportional to the wind shear velocity, but decreases more rapidly with increasing wind shear velocity, due to the wind-induced drift current in the upper layer of the water body which causes erosion of the sublayer at the water surface, i.e. as postulated by Danckwerts (1951), the water in the sublayer is continually disrupted, removed, and replaced with water from the rest of the water body (Emerson 1975, Cohen 1983, O'Connor 1983). The oxygen concentration in the bulk of the water body is lower than in the sublayer, thus this continual replacement exposes layers of lower oxygen concentration. This leads to an increased rate of oxygen transfer from the atmospheric layer to the water layer, as the rate of transfer is proportional to the concentration difference between these layers (Bratby 1977, O'Connor 1983). Under these circumstances the rate of transfer is a function of both diffusion and the renewal rate of the sublayer (Eckenfelder *et al* 1967, Cohen 1983, O'Connor 1983).

At wind speeds above 10 - 13 m s^{-1}, wave breaking may occur. This may lead to a further increase in transfer of oxygen from the atmosphere, due to enhanced mixing in the surface layer, the presence of spray and the disintegration of wave crests (Cohen 1983). On the other hand, wind shear may be reduced by the sheltering effect of the wave crests, thereby decreasing the rate of oxygen transfer (Emerson 1975). The effect of wind speeds > 10 - 13 m s^{-1} on atmospheric oxygen transfer has not

been studied as intensively as the effect of wind speeds between 3 and 10 m s^{-1}, possibly because the wind speeds most frequently found over land (and thus over inland waters) are below 5 m s^{-1}. For instance, at Roodeplaat Dam Reservoir the average wind speed at 10 metre height during October 1980 to March 1981 (summer) was 4.8 m s^{-1}, and during winter (April 1981 to September 1981) 5.2 m s^{-1}.

From a practical point of view, the effects of turbulence, layer thickness, and the resistance these layers offer to the transfer of oxygen from the atmosphere, can be parameterized in terms of a *mass transfer coefficient* (analogous to the diffusion coefficient in Fickian diffusion). Sometimes the mass transfer coefficient is referred to as the *reaeration coefficient* (James 1993). As the mass transfer coefficient is a non-linear function of wind speed, it will vary between reservoirs, and must be determined for each reservoir.

3.4.2.2 Oxygen produced by algal photosynthesis:

Photosynthetic oxygen is produced during daylight only, and only in the euphotic zone, i.e. the zone where there is sufficient light for photosynthesis - *cf* paragraph 3.4.3.1. Due to the high turbidity in many South African reservoirs, the euphotic zone does not usually extend into the hypolimnion, thus photosynthetic oxygen production tends to be limited to the epilimnion. The hypolimnion remains virtually in a state of continual darkness with no oxygen production. In stratified hypertrophic systems with high algal concentrations and low wind speeds, photosynthetic production of oxygen may cause the surface layer of water to be supersaturated, for instance, in Hartbeespoort Dam Reservoir oxygen concentrations as high as 40 mg l^{-1} have been recorded during periods of high algal growth (Scott *et al* 1977).

3.4.2.3 Sinks of oxygen:

Oxygen in the water is consumed by the metabolic processes of aerobic micro-organisms for two purposes, growth and maintenance (endogenous respiration). Oxygen consumed by respiration processes can be considerable, but in eutrophic reservoirs the oxygen consumption for growth of the organisms using detritus as a food source (i.e. microbial decay of organic matter) is of far greater significance (see discussion in paragraph 3.4.3).

A further important sink of oxygen is the so-called *sediment oxygen demand* - this term refers to the consumption of oxygen in the bottom sediment due to chemical oxidation and microbial decay of organic matter. In eutrophic reservoirs with a high concentration of organic matter in the sediments, sediment oxygen utilization due to microbial decay of organic matter is far greater than oxygen utilized during chemical oxidation (Wang 1979, Tomaszek 1991). Furthermore, sediment oxygen demand appears to be affected by sediment composition, as well as the oxygen concentration of the overlying water - a decrease in oxygen uptake rate by the sediments has been observed for dissolved oxygen concentrations below 1.5 mg l^{-1} (Tomaszek 1991).

Reactions such as nitrification also will affect oxygen concentration in the water column (see paragraph 3.4.5.2), but the effect of these reactions is relatively small compared to the effect of surface reaeration and microbial decay.

It is not only the concentration of oxygen that determines the trophic state of a reservoir, but also the vertical distribution of oxygen. The vertical distribution is very much affected by the physical state of the reservoir. The main processes that cause an increase in oxygen concentration (surface reaeration and photosynthesis) occur in the upper part of the reservoir. When the reservoir is stratified, any increase in oxygen concentration is limited to the epilimnion only. In the hypolimnion processes such as microbial decay of organic matter, which leads to a decrease in oxygen concentration, are dominant. Although oxygen can be distributed throughout the reservoir by eddy diffusion, during the stratified period the metalimnion forms an effective barrier, preventing transfer of oxygen between the epilimnion and the hypolimnion. As a consequence, in eutrophic reservoirs it often happens that the hypolimnion is depleted of oxygen, while the epilimnion is supersaturated due to photosynthetic production of oxygen by algae. Only when the reservoir has overturned may the oxygen be distributed approximately homogeneously throughout the reservoir.

3.4.3 Microbial decay of organic matter

In reservoirs, organic matter is present in dissolved and particulate form. Conventionally, dissolved organic matter refers to organic particles that are so small that they pass through a filter of 45 μm mesh size (Jeffries and Mills 1990, Barnes and Mann 1991), so that 'dissolved organic matter' is not necessarily all truly dissolved. In reservoirs dissolved organic matter originates from organic matter in river inflow, direct runoff from land, extracellular release from phytoplankton during the growth process, and from degradation and leaching of particulate organic matter (Robarts and Ashton 1988, Barnes and Mann 1991). Usually the degradation process is the major source of dissolved organic matter in eutrophic reservoirs (Rheinheimer 1971, Jørgensen 1980, Grobbelaar and Toerien 1985), but in some South African reservoirs, eg Hartbeespoort Dam, the load of dissolved organic matter from incoming rivers equals the internal load from degradation of organic material (Ashton 1994).

Particulate organic matter consists mainly of detritus that is formed when algal cells die. Some particulate organic matter also originates from aggregation and flocculation of dissolved organic matter. The organic particles float in the water, slowly moving down until they settle in the bottom sediment. The settling velocity depends on the density and viscosity of the water, the size and shape of the particles, and turbulence in the water.

Decay of organic matter proceeds via various chemical and bacterial processes, but usually the latter dominates (Ashton 1994). Particulate organic matter is made up mainly of macro-molecules such as proteins, carbohydrates and fats. These macro-molecules cannot be utilized directly by bacteria (Nedwell and Brown 1982), and have to be broken down through the action of exoenzymes into smaller fractions such as amino-acids, and various other dissolved organic compounds, which then serve as substrate for heterotrophic bacteria.

The substrate serves a dual purpose in the metabolic function of bacteria:

- It supplies material from which bacteria synthesize new cell material.
- It provides energy for cell synthesis.

Part of the dissolved organic matter is broken up by the bacteria to give hydrogen ions, carbon dioxide molecules, and electrons. Because the organic molecule releases electrons it is termed the *electron donor*, and upon yielding electrons the molecule is said to be *oxidized*. The electrons is transferred to a molecule that has the capacity to receive electrons. This molecule, known as the *electron acceptor*, is *reduced* upon receiving electrons. During this oxidation-reduction (redox) reaction free energy is released, and it is this energy that is utilized to synthesize new bacterial cell material from the remainder of the dissolved organic matter (Dold *et al* 1980, Tchobanoglous and Schroeder 1985). Generally, the quantity of free energy released depends on both the electron donor and acceptor. In reservoirs, usually the electron donor is dissolved organic carbon only, but several compounds can act as an electron acceptor. The electron acceptor that contributes the most free energy to the redox reaction will dominate until it is depleted, whereafter the next most energy efficient electron acceptor will take over. In reservoirs, electron acceptors will be consumed in the following order: oxygen, manganese oxides, nitrates, ferric oxides, sulphates, and carbon dioxide (Nedwell and Brown 1982, Baudo *et al,* 1990). If nitrate serves as an electron acceptor, the process is known as *denitrification* (see discussion in paragraph 3.4.4.2). Furthermore, because oxygen is the most favoured electron acceptor in terms of energy, it has been found that the rate of the redox reaction is much faster under aerobic than under anaerobic conditions, and both aerobic and anaerobic rates are highly dependant on temperature (Jørgensen 1980). With oxygen as an electron acceptor, the oxygen concentration that is consumed during the redox reaction can serve as a measure of the number of electrons accepted in the reduction of oxygen to water. Thus the mass of oxygen required in the metabolic process gives a direct stoichiometric measure of the electrons that were donated by the biodegradable dissolved organic matter. This mass of oxygen is known as the *biochemical oxygen demand* (BOD) (Tchobanoglous and Schroeder 1985). Often BOD is used as a measure of the concentration of dissolved organic carbon.

However, it must be kept in mind that dissolved organic carbon is not degraded completely by bacteria, as a fraction of the dissolved organic carbon compounds consists of refractory organic carbon compounds that are relatively resistant to bacterial decomposition (Jørgensen 1980). Thus BOD is not an exact measurement of the concentration of dissolved organic carbon. Even during decay of the biodegradeble part of dissolved organic matter some of it is readily converted back to particulate organic matter by physical and biological mechanisms (Mann 1988). Most of the earlier work on decay of organic matter has concentrated on the fragmentation and decay of particulate organic matter, but Mann (1988) suggests that the role of dissolved organic matter is much more important than previously thought, and concludes that the conversion of dissolved organic matter to particulate organic matter by bacterial action and the resultant utilization in higher trophic levels is an urgent topic for further study.

This concept of Mann, i.e. that the decay of organic matter in reservoirs involves more than just the decay of particulate organic matter (POM), but that the reformation of POM during the bacterial decay of DOM should be taken into account also, can be seen as analogous to the approach of Dold *et al* (1991) and Van Haendel *et al* (1981) to bacterial decay of actived sludge. They showed that the classical approach to conceptualization of the metabolic behaviour of micro-organisms - the synthesis-endogenous respiration approach - is adequate to formulate the kinetic behaviour of organisms under aerobic and anoxic states, but that the description becomes totally inadequate if a temporary anaerobic state is imposed on the system in an aerobic/anoxic/anaerobic sequence.

They also found that, even though succesful modelling of the aerobic/anoxic system could be attained with the classical approach, the endogenous respiration rates between pure and mixed cultures differed so markedly that a different basic behaviour pattern exists between pure and mixed cultures. To resolve this they proposed a new approach (an approach that appears to also have merit in the mixed culture situation in reservoirs): Bacterial organisms are generated (synthesized) from soluble substrate, and after solubilization of particulate substrate. The generated organisms are subject

to predation and thus form the substrate for higher organisms, resulting in a death-regeneration mode of behaviour.

Dold and Van Haendel concluded that in mixed cultures the oxygen demand accredited to endogenous respiration *per se* is minor and can be lumped with the major oxygen demand due to death and regeneration of organic mass. With aerobic/anoxic conditions the synthesis/endogenous respiration and death/regeneration approaches are linearly related. Behaviour under aerobic and anoxic conditions is different only in the rates of reaction. However, if anaerobic states are introduced, the synthesis/endogenous respiration approach fails completely to describe the kinetic behaviour, whereas the death/regeneration approach gives a reliable description - death continues under anaerobic conditions, but synthesis cannot occur due to the absence of oxygen and nitrate, thus there is an accumulation of organic material during this period, leading to an upsurge of oxygen demand when oxygen becomes available.

This approach led to successful simulation of the activated sludge process under aerobic, anoxic, and anaerobic conditions. This approach may be extrapolated to the situation in lakes and reservoirs: In reservoirs that become anaerobic during the hydrological cycle it is possible that consideration of the decay of particulate organic matter only will not be sufficient, and that the cycle will have to be extended to include decay of dissolved organic matter and the resultant formation of particulate organic matter. This approach will be investigated further in this study.

3.4.4 Processes that affect algal concentration

Algal concentration in a reservoir is increased by the process of algal growth, and decreased by processes such as respiration, mortality, and sedimentation. Regarding the process of algal growth, algae are photo-autotrophic organisms, i.e. during a process known as *photosynthesis* they absorb energy from the visible spectrum of solar radiation, and use the energy to form complex organic compounds from carbon dioxide and water, with the release of molecular oxygen (Freedman 1989). The

complex organic compounds, as well as *nutrients* such as phosphorus and nitrogen, are the building blocks for new cell material. Furthermore, as with all biological rates, algal growth rate is affected by temperature.

3.4.4.1 The process of photosynthesis:

A detailed description of the photosynthetic process is beyond the scope of this study, but a basic understanding of the process will facilitate conceptualization and formulation of the model.

The overall photosynthetic process can be summarized as follows (Reynolds 1984):

$$6CO_2 + 6H_2O \xrightarrow{light} C_6H_{12}O_6 + 6O_2 \qquad (3.1)$$

Consider the photosynthetic process in more detail: Algal cells contain pigments that allow absorption of light energy in the spectrum between 390 - 710 nm. The light energy in this region is defined as *photosynthetically active radiation (PAR)*. Different algal species have different pigment compositions, for instance, all freshwater algae contain chlorophyll-a and ß-carotene, but green algae contain chlorophyll-b also, and blue-green algae contain phycocyanin also. The different pigments absorb light at different wavelengths between 400 and 700 nm.

The photosynthesis process comprises two photochemical reactions that occur in series, referred to as *photosystem 1* (PSI) and *photosystem 2* (PSII) (Kirk 1983, Reynolds 1984). Each photosystem has its own pigments that harvest light energy. When light energy is absorbed by photosystem 1, electrons are released from photosystem 1. (Eventually photosystem 1 will return to its original state by taking up electrons released from photosystem 2 at a later stage). The electrons released from photosystem 1 are transferred via a series of electron carriers to a phosphate compound, nicotinamide adenine dinucleotide phosphate (NADP), which is reduced to $NADPH_2$ upon electron uptake.

When light energy is absorbed by photosystem 2, it also loses electrons. These electrons are transferred via a series of electron carriers to photosystem 1, which returns to its original state upon electron uptake. Photosystem 2 returns to its original state by removing electrons from water via a series of electron carriers. Oxygen is liberated from the water upon electron removal.

During electron transport between photosystem 1 and 2, a high energy phosphate compound, adenosine triphosphate, or ATP is formed. ATP, together with $NADPH_2$ formed in photosystem 1, are used in an enzymatic reaction to convert carbon dioxide to carbohydrate (Kirk 1983, Reynolds 1984).

Adequate supplies of both light and carbon dioxide are a prerequisite for photosynthesis. Because the conversion of carbon dioxide to carbohydrate is an enzymatic process, the rate of photosynthesis will be affected by temperature (Kirk 1983, Reynolds 1984).

Effect of light intensity on the rate of photosynthesis:

The rate of photosynthesis increases linearly with increasing light intensity (irradiance) up to a certain level of irradiance, at higher levels the rate of photosynthesis reaches an upper plateau and at yet higher levels the rate decreases again (Fig 3.6). In the range of irradiances where there is a linear increase in the rate of photosynthesis, the photosynthetic rate is said to be *light limited*. In the range of irradiances where the photosynthetic rate has levelled off to a constant upper value, photosynthesis is said to be *light saturated*, and the photosynthetic rate is referred to as the maximum specific photosynthetic rate, P_m (Kirk 1983, Reynolds 1984). At yet higher levels of irradiance, the photosynthetic rate may start to decrease again, a phenomenon known as *photoinhibition*.

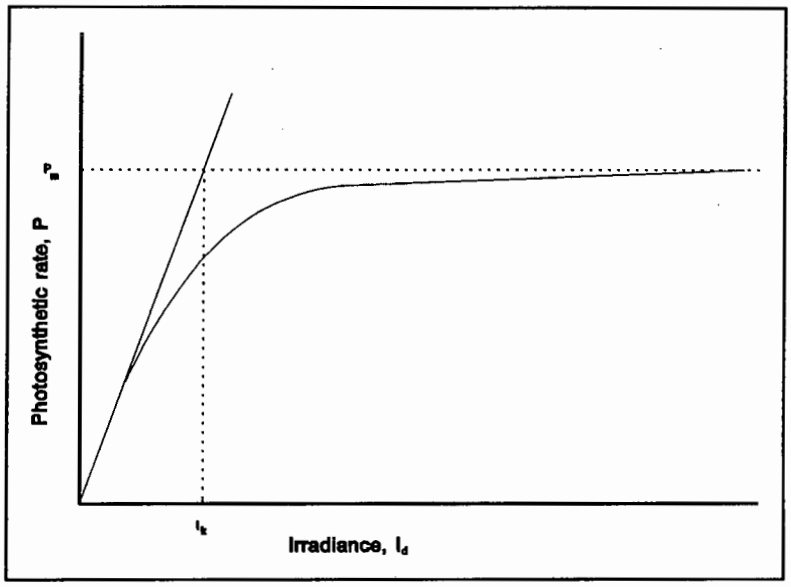

Figure 3.6.
Idealized curve of specific photosynthetic rate (P), as a function of irradiance (I_k) (After Kirk, 1983).

As the irradiance increases, there is a gradual onset of saturation, and it is difficult to determine the specific irradiance value that indicates the onset of the maximum specific rate of photosynthesis. This difficulty has lead to specification of an irradiance, I_k, which is the irradiance where the maximum rate, P_m would be reached if the rate of photosynthesis was to continue to increase linearly with increasing irradiance, instead of gradually levelling off (Fig 3.6). The irradiance where the rate of photosynthesis will reach a maximum, as well as the irradiance where photoinhibition will commence, differs markedly between algal species. It is affected by temperature also (Kirk 1983).

The effect of carbon dioxide concentration on the rate of photosynthesis:
The compounds $NADPH_2$ and ATP are formed during the process of photosynthesis. In a subsequent enzymatic reaction, these two compounds are utilized in converting carbon dioxide to carbohydrate. The rate of formation of $NADPH_2$ and ATP is a function of light intensity. Under high light intensities the concentration of $NADPH_2$ and ATP may become so high that there is not enough carbon dioxide available to utilize the supply of $NADPH_2$ and ATP. Under these circumstances the availability of carbon dioxide becomes the rate limiting step in the over-all photosynthesis process.

Regarding the availability of carbon dioxide; when carbon dioxide gas dissolves in water it forms molecularly dissolved CO_2 species, a part of which hydrolyses to form H_2CO_3 (carbonic acid) species. The H_2CO_3 interacts with the water species (H_2), H^+, OH^-) to form two ionic species, HCO_3^- (bicarbonate) and CO_3^{2-} (carbonate) species. The totality of species constitute the carbonate weak acid/base system. The ratio of dissolved CO_2 to carbonic acid (H_2CO_3) is fixed:

$$CO_2 : H_2CO_3 = 99.3 : 0.7$$

Due to this fixed ratio, the practice is to combine the two and express the sum as $H_2CO_3^*$, i.e.

$$H_2CO_3 + CO_2 \text{ (dissolved)} = H_2CO_3^*$$

Because $H_2CO_3^*$ is constituted dominantly of dissolved CO_2, $H_2CO_3^*$ is widely termed "free CO_2 (carbon dioxide)". The relative proportions of $H_2CO_3^*$, HCO_3^-, and CO_3^{2-} species in aqueous solution can be determined via dissociation equations and total carbonate species concentration, C_T. These relative proportions are dependent on pH, and are constant at each particular pH value (Fig 3.7). The $H_2CO_3^*$ species is present in significant proportions up to about pH 7; at pH 8 it has decreased to form less than 0.003 percent of the total carbonate species concentration, C_T (Loewenthal and Marais 1976, Henderson-Sellers 1984).

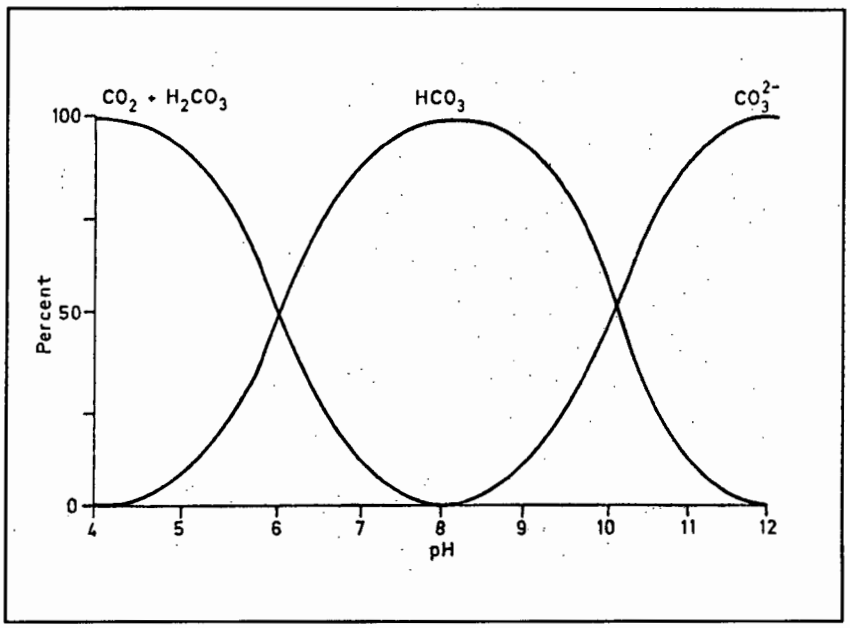

Figure 3.7
Theoretical relative proportions of the forms of CO_2 in relation to pH (After Henderson-Sellers, 1984).

Many inland waters have a pH > 7, thus in these waters the carbonate species are principally in the HCO_3^- (bicarbonate) form, and the fraction of $H_2CO_3^*$ is relatively low. Although free CO_2 ($H_2CO_3^*$) is the only form of inorganic carbon that can be utilized in photosynthesis, some algae have the ability to convert bicarbonate to carbon dioxide intracellularly; the bicarbonate ions (HCO_3^-) combine with H^+ to give H_2CO_3, which is dehydrated in an enzymatic reaction to give CO_2. The H^+ ions that combine with HCO_3^- are obtained from the intracellular dissociation of water (H_2O, H^+, OH^-), leading to an increase in OH^- ions. These ions are excreted from the cells to balance the uptake of HCO_3^-, causing an increase in the pH of the surrounding water.

Even though some algae have the ability to convert bicarbonate (HCO_3^-) to free carbon dioxide ($H_2CO_3^*$) for utilization in the photosynthetic process, free carbon dioxide is utilized more effectively, i.e. for the same concentrations of free carbon dioxide and bicarbonate, a higher photosynthetic rate is obtained with free carbon dioxide. This phenomenon can be attributed to the energy that is required to transport

the bicarbonate ion into the plant, whereas carbon dioxide diffuses in freely (Kirk 1983). However, some blue-green algae such as *Anabaena cylindrical*, have the same photosynthetic rate irrespective whether the source of inorganic carbon is free carbon dioxide or bicarbonate ions (Kirk 1983). This gives these algae a competitive edge over, for instance, certain green algae that cannot utilize bicarbonate at all, or that cannot utilize bicarbonate as effectively as free carbon dioxide. Also, as described in the previous paragraph, uptake of bicarbonate ions gives rise to release of OH^- ions from the cell, thereby causing an increase in the pH of the surrounding water. According to Kirk (1983), algae such as *Anabaena cylindrical* that can utilize bicarbonate effectively, also photosynthesize optimally at pH values in the region of 9.0, thus he is of the opinion that the ability of certain blue-green algae to photosynthesize in water of high pH (i.e. virtually zero free carbon dioxide) could be one of the main reasons for their dominance in eutrophic lakes in late summer. This theory is supported by Shapiro (1990).

The actual concentration of free carbon dioxide affects the rate of photosynthesis also. The rate varies with carbon dioxide concentration according to the Michaelis-Menten/Monod concept that was originally developed for enzyme kinetics; at low carbon dioxide concentrations the rate of photosynthesis increases linearly with an increase in carbon dioxide concentration (first order reaction). However, with increasing carbon dioxide concentration, the rate of photosynthesis gradually levels off, until it becomes constant, i.e. a zero order reaction (*cf* Fig 3.9).

The effect of temperature on the rate of photosynthesis:

An integral part of the photosynthetic process, conversion of carbon dioxide to carbohydrate, is an enzymatic reaction, thus the rate of photosynthesis will be affected by temperature. The effect of temperature on the rate of photosynthesis can be divided into two categories: the effect of an immediate change in temperature, and the effect of a gradual change, allowing the algae to adapt to the new temperature.

Regarding the effect of an immediate change: at low irradiances, where the rate of photosynthesis increases linearly with increased irradiance (Fig 3.6), an increase in temperature has little effect on the rate of photosynthesis. This behaviour is due the fact that, in this range of irradiances, the rate of photosynthesis is determined by light reactions, which are not very sensitive to temperature (Kirk 1983). However, the enzymatic conversion of carbon dioxide to carbohydrate is sensitive to temperature. At low temperatures this reaction very likely is inhibited, but the reaction rate increases with increasing temperature (Kirk 1983). At higher irradiances where photosynthesis is light saturated, enzymatic conversion of carbon hydroxide to carbohydrate determines the rate of photosynthesis, therefore, as indicated in Fig 3.8, the species-specific maximum rate of photosynthesis, as well as I_k, which corresponds to the onset of light saturation, increases with an increase in temperature (Kirk 1983, Reynolds 1984, Allanson *et al* 1990).

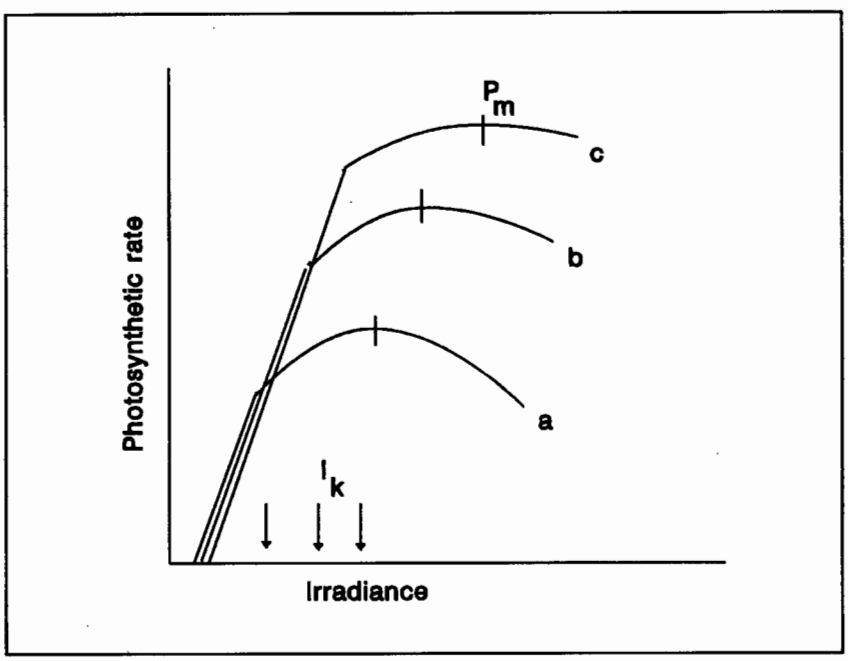

Figure 3.8
Hypothetical curves of photosynthetic rate vs irradiance, indicating the effect of increasing temperature: curves a,b, and c are in order of increasing temperature

Regarding the effect of a gradual change in temperature - a gradual change gives algae the opportunity to adapt to the change in temperature. It has been found that, for a specific algal species adapted to warm water, both the optimum temperature for photosynthesis and the maximum rate of photosynthesis are higher than that of the same algal species growing in cold water. Also, photoinhibition occurs at lower irradiances in algae growing in cold water. (Kirk 1983, Allanson *et al*, 1990)

The effect of temperature on photosynthesis must not be confused with the effect of temperature on algal growth rate. Algal growth rate is a function of photosynthesis as well as several other processes (De Wet 1986), thus the effect of temperature on photosynthesis and on algal growth rate is similar, but not equal (Reynolds 1984). The effect of temperature on reaction rates is expressed in terms of the Q_{10} value, i.e. the factor by which the rate increases for every 10°C increase in temperature. According to Reynolds (1984), on average the Q_{10} values of algal growth are higher than those of photosynthesis.

3.4.4.2 The processes of nutrient uptake and algal growth rate:

The elements that form the algal cell can be divided into macronutrients and micronutrients. Each macronutrient, C, O, H, N, P, S, K, Mg, Ca, Na, and Cl, constitutes > 0.1% of the ash-free dry weight of the cell, whereas micronutrients such as Fe, Mn, Cu, B, Zn, Mo, V, and Co, usually contribute << 0.1% by weight (Reynolds 1984). Without these elements no algal growth will occur. The two main theories that link algal growth rate to uptake of nutrients are the *Monod concept* and the *Droop concept*.

The Monod concept is based on Michaelis-Menten enzyme kinetics. It treats nutrient uptake and algal growth rate as one process and describes algal growth rate as a function of external nutrient concentration only. According to the Monod theory, at low nutrient concentrations the growth rate will increase linearly as the nutrient concentration in the surrounding water increases, i.e. first order kinetics. At very high external nutrient concentrations, the growth rate becomes a constant, equal to the maximum growth rate, i.e. zero order kinetics (Fig 3.9) (Droop 1983, Rossouw 1986a).

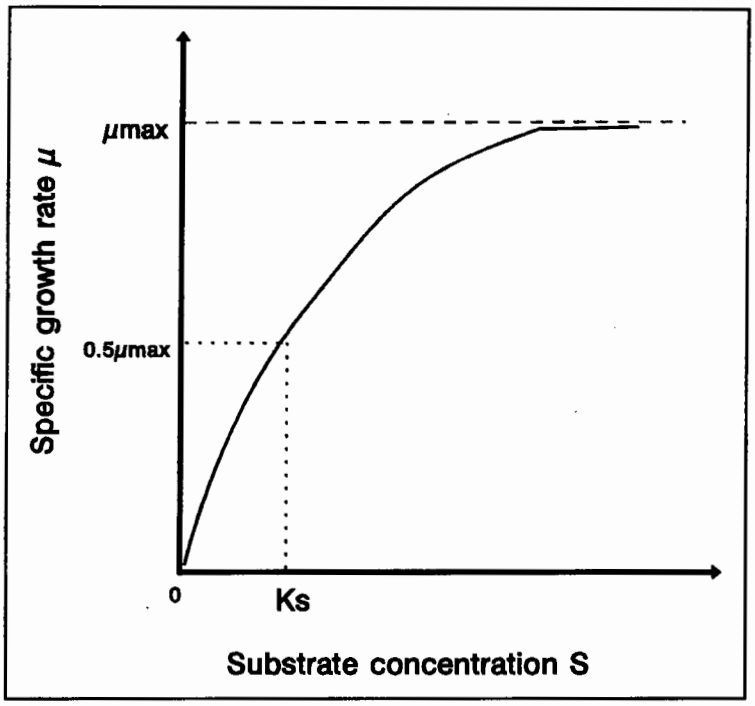

Figure 3.9
Algal growth rate as a function of external nutrient concentration according to the Monod concept

The main deficiencies of the Monod concept are the following:

- It does not provide for the effect known as *luxury uptake*
- It assumes that the stiochiometric composition of the cell remains constant, irrespective of the external nutrient condition
- It is applicable to steady state conditions only.

Luxury uptake refers to the ability of algal cells to take up and store nutrients in excess of their immediate need. The stored nutrients are used for algal growth during periods of low external nutrient concentration. In practice this means that algal growth will continue for some time after depletion of nutrients in the surrounding water, contrary to Monod's concept in which algal growth rate is a function of external nutrient concentration only.

Regarding the stiochiometric composition of the cell, contrary to Monod's assumption, it has been observed that cell composition varies greatly depending on external conditions and the growth rate (Droop 1973, Rossouw 1986a).

Withe regard to steady state conditions, under steady state conditions any change in external conditions would lead to an immediate change in the algal growth rate. However, in natural waters changes in the external environment occur at the same time scale as the internal response of the algal cells, thus there is an appreciable time lag between external change and the internal response (Harris 1984).

The deficiencies of the Monod Concept are addressed in Droop's Concept of algal growth (Droop 1973, 1983). Basically this concept, also known as the cell quota concept, is a refinement of the Monod Concept - Monod treated nutrient uptake and growth as a single process, whereas Droop treated nutrient uptake and algal growth as a two-step process. Based on experimental results, he postulated that the specific nutrient uptake rate is a function of external, as well as internal nutrient concentration, but that the specific algal growth rate is a function of the internal nutrient concentration only (Droop 1983). The specific nutrient uptake rate will increase with increasing external nutrient concentration, until, at high external nutrient concentrations, the specific uptake rate becomes constant and equal to the maximum uptake rate. This assumption is similar to the Monod Concept as illustrated in Fig 3.9 (Droop 1983). However, Droop extended the theory of nutrient uptake by postulating that the specific nutrient uptake rate will decrease as the nutrient concentration in a cell increases, until a maximum cellular nutrient concentration is reached. Each algal species has a characteristic maximum cellular concentration for a particular nutrient. The specific uptake rate of cells with low internal nutrient concentrations can be an order of magnitude faster than that of nutrient saturated cells (Rossouw 1986a).

Regarding the specific algal growth rate, Droop postulated that a certain minimum intracellular nutrient concentration is needed before algal growth can occur, and that the specific algal growth rate will be a function of the intracellular nutrient concentration in excess of the minimum intracellular nutrient concentration (Droop 1983, Rossouw 1986a).

Droop's theory rectifies the shortcomings of Monod's Theory in that it makes provision for non-steady state conditions by treating nutrient uptake and algal growth separately. Also, because the intracellular nutrient concentration can vary between a minimum and maximum intracellular nutrient concentration, provision is made for varying cell stoichiometry and luxury uptake.

3.4.4.3 Effect of temperature on algal growth rate:

According to Orlob (1983) accurate modelling of algal growth kinetics will not be possible if the response of algal growth rate to water temperature is not taken into account. Algal growth rates increase in a non-linear, exponential fashion with increasing water temperature. Generally, the increase is expressed as a Q_{10} value, i.e. the factor by which the rate increases per 10 degC increase in temperature. The growth rate will increase with increasing temperature until a maximum rate is reached at an optimal temperature which is species specific. The optimal temperature occurs between 25 and 40°C and may cover a range of several degrees, rather than a single optimal temperature (Reynolds 1984, Davison 1991). The growth rate declines as the temperature changes from the optimal temperature to higher or lower limits (Lehman *et al* 1975) - the upper temperature where algal growth rate has declined to 10% of the maximum growth rate is defined as the maximum temperature for algal growth, and the lower temperature where algal growth rate has declined to 10% of the maximum growth rate is defined as the minimum temperature for algal growth.

The effect of temperature on algal growth rate must not be confused with the effect of temperature on photosynthesis. Algal growth rate is a function of photosynthesis as well as several other processes, thus the effect of temperature on algal growth rate and photosynthesis is similar, but not necessarily equal (De Wet 1986, Reynolds 1984). Generally the Q_{10} values for algal growth are higher than those of photosynthesis.

3.4.4.4 Processes leading to a decrease in algal concentration:

Various processes lead to a decrease in algal concentration, the most important are hydraulic washout, sedimentation, mortality, predation, and respiration (Henderson-Sellers 1984, Reynolds 1984).

When water is discharged from the reservoir, algae may be washed out with the discharge, depending on the position of the discharge outlet. At high discharge rates, specially during winter when algal growth rates are at a minimum, washout rates may exceed the growth rates of many algal species, leading to a decrease in algal concentration. The decrease may be so severe that the bloom that often occurs during spring is delayed or prevented, because of the low pre-existing stock of algae (Reynolds 1984).

Regarding loss of algae through sedimentation, some algae such as *Microcystis aeruginosa* can regulate their buoyancy, but others, notable the diatoms, are heavier than water and thus have a tendency to sink (James 1993). The sinking velocity of the algal particles is a function of the shape of the particle (which is not easily defined), the viscosity of the water, advection by water currents, and turbulence (Orlob 1983, Henderson-Sellers 1984, James 1993). Eventually the algal particles sink down to the bottom sediments, though, of course, as soon as the algae sink out of the euphotic zone, photosynthesis cannot occur, leading to a decrease in algal cells. However, in shallow water bodies resuspension may occur, thereby bringing once-sedimented algae back into the euphotic zone, where re-growth may be possible.

Concerning algal mortality, death of algal cells may be due to various causes - insufficient light for photosynthesis, insufficient nutrients, exposure to toxic substances, infection by fungi, viruses and bacteria, and predation (Reynolds 1984). Susceptibility to these effects varies with algal species. The rate of mortality is a function of temperature, exponentially increasing with increasing temperature. Furthermore, when the algal cell dies, intracellular nutrients in excess of the minimum nutrient concentration[2] are released into the water by autolysis (Jørgensen 1980).

Predation by certain zooplankton species causes a further decrease in algal concentration. Many of the zooplankton are filter-feeders, i.e. by beating the water they

---

[2]Algae need a certain minimum intracellular concentration of nutrients before algal growth can occur - see discussion in paragraph 3.4.4.2

generate a current from which the algal particles are filtered out and ingested. The size of the particles that can be filtered varies among zooplankton species, and depends on the size of the zooplankton species. Some blue-green algae such as *Anabaena* and *Microcystis* are too big to be grazed by zooplankton; this may give them a competitive advantage over smaller algae such as *Chlorella*, a green algae, that are grazed by zooplankton (Reynolds 1984).

Respiration can be regarded as a loss process also, as a significant amount of the organic material produced by photosynthesis is used in respiration (James 1993). Oxygen is consumed during respiration, which can occur in the light as well as in the dark. As a consequence, respiratory oxygen consumption by algal cells sinking out of the euphotic zone into the hypolimnion can contribute significantly to oxygen depletion in the hypolimnion. The rate of respiration increases with increasing temperature, similar to photosynthesis (Reynolds 1984, Henderson-Sellers 1984).

The net algal concentration in a reservoir will depend on the balance between these loss processes and the process of algal growth. The processes contributing to loss and growth occur simultaneously during the entire course of an algal population, and the net algal concentration will increase as long as the rates of the loss processes are less than the rate of growth. The magnitude of the loss processes does not only vary seasonally (due to the dependence of the loss processes on temperature), it also varies between reservoirs, due to the influence of reservoir characteristics such as basin morphometry, hydrology, and trophic status. The ability of algae to withstand these loss processes, and hence increase their concentration, depends on their potential for growth (Reynolds 1984). The main factors determining algal growth potential are availability of nutrients and light, thus processes affecting these are the next point of discussion.

3.4.5 Processes affecting availability of nutrients

The most important nutrients for algal growth are inorganic carbon, phosphorus, nitrogen and, in the case of diatoms, silica (Thornton 1986). Nutrients entering a lake are derived from two sources (Thornton 1986):

- Allochtonous, i.e. deriving from geological, biological and atmospheric sources outside the lake basin
- Autochtonous, i.e. originating within the lake itself.

The availability of inorganic carbon has been dealt with in the discussion on photosynthesis in paragraph 3.4.4.1.

3.4.5.1 Processes affecting availability of phosphorus:

Phosphorus is essential to the function and growth of all plants, because it is a component of nucleic acids and ATP, a chemical compound that participates in intracellular energy transfer and anabolic processes (Henderson-Sellers 1984, Reynolds 1984). As a consequence, algal growth will be limited if there is an insufficient supply of phosphorus relative to the growth requirements of the algae. In natural waters, phosphorus concentrations are low relative to the demand for algal growth, therefore phosphorus often is the limiting nutrient in these waters (Ruttner 1952, Twinch and Breen 1980, Henderson-Sellers 1984). However, in waters that act as receiving waters for industrial, agricultural, and sewage effluents, the phosphorus concentration is much higher than in natural waters, and often the excessive algal growth that occurs in these water bodies is a direct consequence of elevated phosphorus concentrations. Removal of phosphorus is a popular method of combatting excessive algal growth - although algae can obtain nitrogen and carbon dioxide from the atmosphere through processes such as nitrogen fixation and dissolution of carbon dioxide, they cannot obtain phosphorus from the atmosphere, thus input of phosphorus into a water body is easier to control than that of carbon dioxide and nitrogen (Jørgensen 1980, Le Cren *et al* 1980).

Phosphorus occurs in several forms in the ecosystem. The different forms may be identified according to a chemical or a biological notation (Henderson-Sellers 1984):

Chemical notation: This is based on analytical separation methods. Phosphorus is divided into total phosphorus (TP), particulate phosphorus (also referred to as suspended phosphorus, or sestonic phosphorus), soluble reactive phosphorus (SRP), and soluble unreactive phosphorus (SUP).

Biological notation: This notation is most commonly used in water quality models, and therefore is the notation that will be used in this study. It is based on the location of phosphorus in the food chain, and phosphorus can be identified as orthophosphate (dissolved phosphate), dissolved organic phosphorus, bacterial phosphorus, detrital phosphorus, phytoplankton phosphorus, zooplankton phosphorus and fish phosphorus.

In eutrophication studies dissolved phosphate (PO_4-P) is of particular importance, as it is the only form of phosphorus that can be readily assimilated by algae (Twinch and Breen 1980, Henderson-Sellers 1984). Dissolved phosphate is not distributed homogeneously throughout the water body, as the result of various physical, biological, and chemical processes, it is in a dynamic state in the aquatic environment. For instance, eddy diffusion is the main physical process whereby dissolved phosphate is distributed throughout the reservoir. However, when the reservoir is stratified, the metalimnion forms such an effective barrier between the epilimnion and the hypolimnion that transport of phosphate between the epilimnion and hypolimnion is prevented.

Regarding biological processes that affect the availability of dissolved phosphate, the main process is uptake by algae. Some algae have the ability to store phosphate in excess of their immediate needs, upon algal death this excess phosphate is released into the water. During subsequent microbial decay of the dead algal cell organically bound phosphorus is broken down and becomes available as dissolved phosphate. Also, phosphate is excreted during respiration by algae and zooplankton during respiration (Canale 1973, Orlob 1983).

Regarding the effect of chemical processes, interaction between water and the bottom sediment is of great importance in phosphate dynamics, as phosphate bound to these sediments represents a vast potential nutrient pool (Kamp-Nielsen 1975, Sly 1986, Baudo *et al* 1990). In fact, in some cases phosphorus recycling from the bottom sediment may exceed external phosphorus loading, therefore it is possible for a reservoir to remain eutrophic even when external phosphorus loading becomes negligible (Stefan and Hanson 1981, Henderson-Sellers 1984, Jones and Welch 1990).

Apart from interaction between the bottom sediments and water, interaction between suspended sediment and water may be of importance also, especially because many South African reservoirs are subject to silt-laden inflows, resulting in high levels of turbidity due to inorganic suspended sediment (Twinch and Breen 1980).

Processes such as settling and resuspension of sediment are discussed in paragraph 3.4.6, therefore only the exchange of phosphate between the bottom sediments and water, and between suspended sediments and water are discussed here.

Regarding the bottom sediments, traditionally, aerobic sediments have been considered a sink for phosphates, whereas anaerobic sediments have been regarded as a source (Sly 1986). In reality the situation is much more complex - a variety of processes, such as adsorption-desorption of dissolved phosphate, diffusion, and degradation of organic matter occur in the bottom sediment.

Adsorption-desorption of phosphate by the bottom sediment is due to physical adsorption by sediment particles, as well as chemisorption and coprecipitation due to the presence of iron oxides and calcites in the bottom sediment. Physical adsorption is a function of the size and the surface structure of the sediment particles, as well as phosphate concentration of the overlying water. Regarding the size of sediment particles - the finer the sediment, the larger the surface area, therefore the larger is the adsorption capacity (per unit weight) of the sediments (Sly 1986, Kufel 1991). Generally lake sediments consist mostly of sand, silt, and clay particles. The diameters of these particles are indicated in Table 3.1. It has been found that pollutants such as

phosphate adsorb mainly on clay and silt particles, i.e. on sediment particles with a diameter < 62 μm (Baudo *et al 1990*). However, because clay particles have a disc like structure and a much smaller size than silt particles, the surface area of clay particles are bigger, therefore clay is more important than silt in so as far as adsorption of phosphate is concerned. As a consequence, the larger the clay fraction of the bottom sediment, the larger the capacity for adsorbing phosphate (Twinch and Breen 1980, Sly 1986, Baudo *et al* 1990).

Table 3.1. Sediment particle diameters (Friedman and Sanders 1978).

SEDIMENT	DIAMETER (μm)
Sand	62 - 500
Silt	2 - 62
Clay	< 2

Regarding the effect of phosphate concentration; phosphate will be adsorbed by sediment when the phosphate concentration in the overlying and interstitial water exceeds a concentration known as the *equilibrium concentration*. Desorption from the sediment, and subsequent diffusion into the interstitial and overlying water occur when the phosphate concentration falls below the equilibrium concentration (Breen 1983). Once the phosphate has diffused into the overlying water, it is dispersed into the rest of the water body by molecular and eddy diffusion.

Apart from physical adsorption by sediment particles, dissolved phosphate is adsorbed chemically also, due to the presence of iron complexes in the sediment. This process is strongly affected by the aerobic/anaerobic state of the overlying and interstitial water - if the water is aerobic, the top 1-2 cm of bottom sediment becomes aerobic (Ruttner 1952), and a Fe(III) complex, FeO(OH) (ferric oxyhydroxide), which forms under aerobic conditions, may be present in this sediment layer. Ferric oxyhydroxide is insoluble and often appears as a coating on sediment particles. It has a large, gel-like surface area, enabling it to adsorb phosphates. If the water above the

sediment becomes anaerobic, the aerobic sediment layer also will become anaerobic. Under anaerobic conditions, ferric oxyhydroxide (Fe(III)) is reduced to soluble ferrous oxides (Fe(II)), thereby releasing phosphate adsorbed by Fe(III) into the interstitial and overlying water (Mortimer 1941, Freney and Galbally 1982, Shaw and Prepas 1990, De Groot 1991, Wiltshire 1991).

Usually reduction of Fe(III) is of a chemical nature, but it also can be reduced during the microbial decay of organic matter. It has been observed that nitrate-reducing bacteria will utilise Fe(III) as an electron acceptor when nitrate is present in insufficient quantities (Sly 1986) - see discussion on microbial decay of organic matter in paragraph 3.4.3.

Adsorption of phosphate by ferric complexes is a function of iron concentration, as well as pH. Regarding the effect of iron concentration, in a study of seven lakes in Canada, Shaw and Prepas (1990) found that if the molar ratio Fe:P < 1.8, release of phosphate from the sediment could not be prevented, but that such release was hindered if the molar ratio of Fe:P > 1.8. This finding is supported by Sly (1986).

Regarding the effect of pH, according to a laboratory study done by Boers (1991), the phosphate release rate from sediment increases significantly at high pH (> 9.0). The enhanced release rate is independent of the aerobic/anaerobic state of the overlying water, and is due to increased desorption of phosphate ions from ferric oxyhydroxide at high pH. This finding is supported by Jones and Welch (1990).

Phosphate ions are precipitated with calcium also. Many South African reservoirs have high concentrations of calcium and carbonate ions. With increasing pH, phosphate is coprecipitated when calcium carbonate precipitates as calcite - the interaction between phosphate and the calcite surface during crystal growth leads to some of the phosphate being incorporated into the bulk structure of the calcite as growth occurs (House 1990). However, the crystal growth of calcite is inhibited by high concentrations of dissolved phosphate, thus this reaction is not of importance in eutrophic systems.

Regarding the effect of microbial decay of organic matter in the bottom sediment on the concentration of phosphate in the water (as was discussed in paragraph 3.4.3), particulate organic matter, mainly originating from algal detritus, is broken down to dissolved organic matter through the action of enzymes. Dissolved organic matter can be utilized readily by bacteria as a source of food and energy. Hence, during bacterial decay of organic matter in the bottom sediment, phosphate bound in dissolved organic matter is released as dissolved phosphate. Once the phosphate has been released, it will undergo the same reactions as discussed in the previous paragraphs, i.e. physical and chemical adsorption/desorption, and diffusion into the interstitial and overlying water, depending on the equilibrium concentration.

Regarding interaction of phosphate with **suspended** sediment, many South African reservoirs are highly turbid due to a high concentration of inorganic suspended sediment (TSS). As with the bottom sediment, phosphate will be physically and chemically adsorbed/desorbed by sediment particles in suspension. The adsorption/desorption on suspended particles will be affected by the same parameters as in the bottom sediment, i.e. equilibrium phosphate concentration, iron concentration, pH, and sediment particle size. Due to the geology of the greater part of Southern Africa (Karoo mudstones and shales), suspended inorganic sediment particles in South African waters are mostly clay, or very fine silt (Hart and Allanson 1984). These particles have a great capacity for adsorption/desorption of phosphate, and may act as a direct source of phosphate to algae (Grobler and Davies 1981), therefore it is important to incorporate the concentration of inorganic suspended sediment in a model and formulate its concentration as realistically as possible. The factors that affect inorganic sediment concentration are discussed in paragraph 3.4.5.

3.4.5.2 Availability of nitrogen:

Nitrogen is an important structural element of amino acids and proteins in the algal cell, but, unlike phosphorus, it does not take part in the energy metabolism of the cells (Henderson-Sellers 1984, Reynolds 1984). The nitrogen cycle has not been studied as extensively as the phosphorus cycle, probably because generally phosphorus is the limiting nutrient in oligotrophic and warm temperate lakes in the northern

hemisphere where most of the studies have been done. However, eutrophic lakes are characterized often by a seasonal change from phosphorus to nitrogen limitation (Dudel and Kohl 1991), and in many tropical lakes nitrogen seems to be the major growth-limiting nutrient (Reynolds 1984).

In natural waters nitrogen can be present as ammonium (NH_4^+), nitrate (NO_3^-), and nitrite (NO_2^-) salts, organic-N, and nitrogen gas (N_2). In oligotrophic lakes and reservoirs nitrogen is almost exclusively in the form of nitrate, with trace amounts only of nitrite and ammonia (typically < 150 μg N l^{-1}) (Ruttner 1952, Reynolds 1984). In lakes and reservoirs that receive sewage and agricultural effluents, the much higher ammonia concentration (> 1 mg N l^{-1}) may cause excessive algal growth (Reynolds 1984). The various forms of nitrogen are affected by several reactions in both the water column and the bottom sediments.

Consider the nitrogen reactions that occur in the water column: In the top layer of the water column (in the euphotic zone), the nitrogen concentration will decrease due to uptake of nitrogen by algae. Algae can utilize nitrogen in the form of ammonium, nitrate, nitrite, and nitrogen gas (Henderson-Sellers 1984). Assimilation of nitrogen by algae involves a number of reactions, but the substrate for the initial reaction is always ammonium (Reynolds 1984). Nitrate and nitrite have to be reduced before it can be assimilated, thus energetically ammonium is the most favourable source of nitrogen. As a consequence it has been observed that algae will assimilate ammonium in preference to nitrate, provided the ammonium concentration exceeds 7-14 μg N l^{-1} (Bienfang 1975, Bingham *et al* 1984, Reynolds 1984). Nitrogen uptake will take place according to Michaelis-Menten kinetics (see discussion in paragraph 3.4.4.2). As with phosphorus, algae will take up and store nitrogen in excess of their immediate needs (luxury uptake), but not to the extent that phosphorus is stored (Reynolds 1984).

Some blue-green algae such as *Anabaena* (but not *Microcystis*) possess specialized cells called heterocysts, that give them the ability to assimilate nitrogen from the atmosphere when the concentration of combined nitrogen (ammonia plus nitrate) in

the water is depleted (< 300 μg N l^{-1}, Reynolds 1984). This phenomenon is known as *nitrogen fixation*, and may contribute up to 50% of the annual nitrogen input into a lake (Ashton 1981, Reynolds 1984). Although nitrogen fixation does not occur when the concentration of combined nitrogen is high, a high concentration of phosphorus seem to be necessary (Jørgensen 1980). Furthermore, nitrogen fixation requires ATP (adenosine triphosphate), that is formed during photosynthesis, thus nitrogen fixation is limited to the euphotic zone. Also, it has been observed that the process is inhibited by full sunlight, and that the maximum rate of fixation occurs at a certain depth below the surface (Ashton 1979, Jørgensen 1980).

The process of nitrogen fixation has practical implications for the management of eutrophic water. According to Ashton (1979), any treatment that results in a lowering of nitrogen concentration, without a simultaneous decrease in phosphorus concentration, will be negated by nitrogen fixation.

Another important process that affects the concentration of nitrogen in the water column as well as in the bottom sediment, is nitrification - the bacterial oxidation of ammonia to nitrate. The nitrification reaction is affected by temperature, and takes place in two steps (Jørgensen 1980):

$$NH_4^+ + \frac{3}{2}O_2 \leftrightharpoons 2H^+ + NO_2^- + H_2O \qquad (3.2)$$

$$NO_2^- + \frac{1}{2}O_2 \leftrightharpoons NO_3^- \qquad (3.3)$$

The overall reaction is:

$$NH_4^+ + 2O_2 \rightarrow NO_3^- + H_2O + 2H^+ \qquad (3.4)$$

Nitrification can take place under aerobic conditions only; during the nitrification process 64 g of oxygen is utilized per 14 g of ammonia.

Regarding the process of denitrification, during the bacterial degradation of organic matter bacteria in the water utilize organic material and inorganic ions as a source of new cell material, as well as energy for growth (Tchobanoglous and Schroeder 1985). In lakes and reservoirs the main source of organic matter often is particulate organic matter originating from algal detritus. Particulate organic matter cannot be readily utilized by the bacteria, but has to be broken down enzymatically into a variety of dissolved organic compounds such as organic nitrogen in the amino form, i.e. $R\text{-}NH_2$ (with R representing methyl groups), and various other dissolved organic carbon compounds. The latter can be readily utilized by bacteria. Bacteria decompose part of the dissolved organic carbon compound to give hydrogen ions, carbon dioxide molecules, and electrons, i.e. the organic carbon compound acts as an electron donor that is oxidized upon release of electrons. The released electrons are transferred to a molecule that has the capacity to receive electrons, i.e. an electron acceptor, that is reduced upon receiving electrons. During the oxidation-reduction (redox) reaction free energy is released, which is utilized by bacteria to synthesize new cell material from the remainder of the dissolved organic matter (Tchobanoglous and Schroeder 1985). In natural waters, several compounds can act as electron acceptors (see discussion in paragraph 3.4.3). If nitrate acts as an electron acceptor, the process is known as *denitrification*. During the denitrification process, depending on the denitrifying organism, nitrate is reduced to nitrite only (by organisms known as *nitrate reducers*), or nitrate is reduced to dinitrogen gas via nitrite, nitric oxide, and nitrous oxide by organisms known as *denitrifiers* (Casey *et al* 1993), i.e.

$$NO_3^- \rightarrow NO_2^- \rightarrow NO \rightarrow N_2O \rightarrow N_2 \qquad (3.5)$$

If certain key bacteria are not present in sufficient concentrations, the process may stop at nitrous oxide (N_2O) (Ashton 1994). However, both nitrous oxide and nitrogen gas (N_2) will diffuse out of the water into the atmosphere, therefore denitrification constitutes a loss of nitrogen from the system - up to 30% or more of the total nitrogen input into the lake may be removed by denitrification (Jørgensen 1980, Seitzinger 1988). Consequently the denitrification process is of great significance in the

nitrogen budget of a reservoir (Toms *et al* 1975, Schroeder *et al* 1991). According to Seitzinger (1988) the loss of nitrogen via denitrification may cause algal growth to become nitrogen limited.

Denitrification can take place only if oxygen is not present. The specific rate of denitrification decreases with decreasing temperature, and is a function of the concentrations of nitrate and organic matter (Toms *et al* 1975, Jørgensen 1980, Seitzinger 1988).

Regarding the process of ammonification: when particulate organic matter is broken down through the action of enzymes, organic compounds containing nitrogen in the amino (NH_2) form are released. In further bacterial action, the amino acids are used either for the synthesis of new bacterial cell material, or are deaminized with the liberation of ammonia. The latter process is known as ammonification (Rheinheimer 1971).

Most of the nitrogen processes that occur in the water column, occur in the bottom sediments as well, eg. ammonification, nitrification and denitrification (Fig 3.10, after Sly 1986, and Schroeder *et al* 1991). In fact, in eutrophic reservoirs, where the concentration of particulate organic matter in the bottom sediment is much higher than in oligotrophic reservoirs (Nedwell and Brown 1982, Baudo *et al* 1990), the nitrogen processes that take place in the bottom sediment may have more significant effect on the nitrogen budget of the reservoir than the processes that occur in the water column.

The processes that take place in the bottom sediments will depend on whether the water above the bottom sediment is aerobic or anaerobic[3]. When the water is aerobic, the following will occur:

---

[3] In this study, the term *aerobic* denotes presence of oxygen, the term *anoxic* denotes absence of oxygen, but presence of nitrate, and the term *anaerobic* denotes absence of both oxygen and nitrate

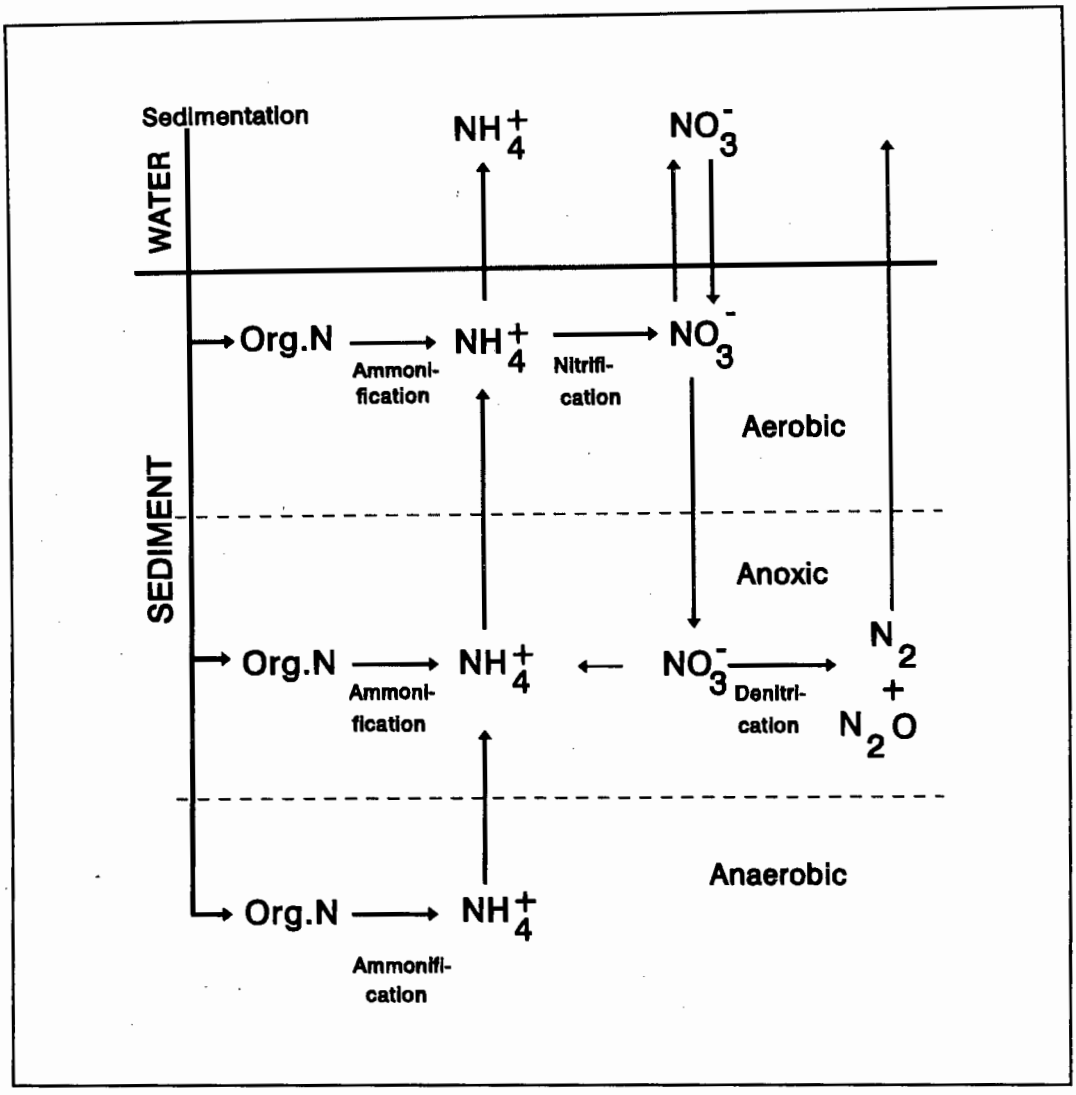

Figure 3.10
Nitrogen processes occurring in the bottom sediment of a reservoir

- Oxygen will diffuse into the bottom sediment and the top layer of the sediment will become aerobic. The thickness of the aerobic layer will depend on the oxygen concentration of the overlaying water to a certain extent, but due to the rate of oxygen consumption by respiration and nitrification, this layer usually is < 1 cm, and almost always < 2 cm (Mortimer 1941, Ruttner 1952, Kessel 1977, Baudo *et al* 1990, Ashton 1994). Below the aerobic layer will be an anoxic layer (i.e. it will contain nitrate, but no oxygen), and below the anoxic layer will be an anaerobic layer (i.e. it is devoid of both nitrate and oxygen).

- In the top, aerobic layer of sediment, organic nitrogen is ammonified to ammonium (see Fig 3.9). The ammonium that is formed will diffuse out of the sediments into the interstitial and overlaying water. As the ammonia is diffusing out, it is being nitrified to nitrate. If the diffusion rate is higher than the nitrification rate, some of the ammonium will diffuse into the overlaying water (Ashton 1994), where it will be nitrified rapidly due to the aerobic state of the overlaying water. The nitrate that is formed in the top layer of sediment will diffuse upwards into the water column. At the same time, nitrate from the water column will diffuse into the sediment. If the nitrate concentration in the overlying water is higher than the nitrate concentration in the sediment, the net effect will be an increase of nitrate in the sediment, and *vice versa*. However, it has been found that the major source of nitrate in the sediment is that produced in the sediment via nitrification (Seitzinger 1988). Some of the nitrate in the aerobic layer will diffuse downward into the anoxic sediment also (Van Kessel 1978).

  In the anoxic sediment layer, ammonium is generated by ammonification of organic nitrogen, and by reduction of nitrate, but the latter is a minor source of ammonium, as the majority of nitrate is denitrified to nitrous oxide and nitrogen gas. Both nitrogen gas and nitrous oxide will diffuse into the overlying water, from where it will be lost to the atmosphere. Denitrification in the sediment may constitute an important loss of nitrogen from the system, and as such may be a contributing factor in nitrogen growth limitation of algae (Seitzinger 1988).

- In the anaerobic sediment layer, where neither oxygen nor nitrate is present, the only nitrogen reaction that can occur is ammonification, i.e. amino acids (from dissolved organic matter) are deaminized, releasing ammonia in the process (Rheinheimer 1971). The ammonium thus formed, will diffuse into the layers above.

When the water above the bottom sediment is anaerobic, as is often the case in South African reservoirs during the period of stratification, the scenario is as follows:

As the water above the bottom sediment becomes depleted of oxygen, the top, aerobic layer of sediment rapidly becomes anaerobic, and nitrification stops completely. Under these circumstances, any residual nitrate is quickly denitrified to nitrogen gas or nitrous oxide; often this is lost from the system (Ashton 1994). Of the three sediment layers only the third anaerobic layer will remain. If the ammonium concentration in the overlying water is less than that in the bottom sediment, there will be a net diffusion of ammonium from the bottom sediment into the water above, from where it will be transported to the rest of the water column via molecular and eddy diffusion.

The aerobic/anaerobic state of the water above the sediments has several implications regarding the nitrogen budget of a reservoir. For instance, consider a reservoir where the water above the sediment always is aerobic. In the top, aerobic layer of sediment, amino acids in organic matter is deaminized to ammonia, which is nitrified to nitrate. As was stated earlier, most of the nitrate formed in the aerobic sediment layer is denitrified in the anoxic sediment layer below, and lost from the system. Under these circumstances, denitrification in the bottom sediment is much higher than that in the water column (usually greater than 70% of the total, Toms *et al* 1975, Seitzinger 1988, Ashton 1994). On the other hand, in highly eutrophic systems such as Hartbeespoort Dam Reservoir in South Africa, where the water above the bottom sediment becomes anaerobic for significant periods, usually denitrification in the water column is far greater than that in the bottom sediments, for the following reason: denitrification is a function of the concentrations of organic matter as well as nitrate. If the water above the bottom sediment becomes anaerobic for significant periods, the top layer of sediment will be anaerobic also. As a consequence no nitrate can be formed in the sediment, and thus no denitrification can take place in the sediment. However, in Hartbeespoort Dam Reservoir, the high incoming load of nitrate (>75% of the total incoming load) provides a continuous source of nitrate for denitrification in the water column, and, because of the high algal concentration, there is an abundance of dissolved organic carbon in the water column, often > 12 mg l^{-1} (Ashton 1994).

A further consequence of the aerobic/anaerobic state of the water above the sediments is that in reservoirs where the water is anaerobic for long periods, ammonium that is released from the bottom sediments may greatly exceed ammonium in the inflow (Baudo *et al* 1990). This has practical implications for management of an eutrophic water body - reducing the ammonia concentration in the inflow may not lead immediately to a significant decrease in ammonium concentration within the reservoir, because of the high load of ammonium from the bottom sediments.

3.4.6 Factors affecting availability of light

Even in a homogeneous water body, light is not uniformly distributed. It is absorbed exponentially with depth, thus photosynthesis will occur only in the upper part of the water body where there is sufficient light, in the region known as the *euphotic zone*. The *euphotic depth* is defined as that depth where photosynthetically active irradiance (PAR) is 1% of the value at the surface (Kirk 1983, Reynolds 1984, De Wet 1986). Four components are responsible for the absorption of PAR - the water itself, dissolved yellow pigments, inanimate particular matter, and photosynthetic biota.

Pure water absorbs light quanta very weakly in the blue and green regions of the spectrum. Absorption increases above 550 nm and is quite significant in the red part of the spectrum, at a wavelength of 680 nm. Absorption of light can be expressed in terms of an absorption coefficient, and the absorption coefficients for pure water for wavelengths ranging from 310 -800 nm is given in Table 3.2.

Table 3.2. Absorption coefficients for pure water (Kirk 1983).

λ (nm)	a (m^{-1})	λ (nm)	a (m^{-1})
310	0.105	560	0.0708
320	0.0844	570	0.0799
330	0.0678	580	0.108
340	0.0561	590	0.157
350	0.463	600	0.244
360	0.349	610	0.289
370	0.0300	620	0.309
380	0.0220	630	0.319
390	0.0191	640	0.329
400	0.0171	650	0.349
410	0.0162	660	0.400
420	0.0153	670	0.430
430	0.0144	680	0.450
440	0.0145	690	0.500
450	0.0145	700	0.650
460	0.0156	710	0.839
470	0.0156	720	1.169
480	0.0176	730	1.799
490	0.0196	740	2.38
500	0.0257	750	2.47
510	0.0357	760	2.55
520	0.0477	770	2.51
530	0.0507	780	2.36
540	0.0558	790	2.16
550	0.0638	800	2.07

Regarding dissolved yellow substances, during microbial decomposition of organic matter in soil and water, a complex group of substances, called *humic substances*, is formed. Water draining through the soil into rivers and lakes extract some of the water-soluble humic substances from the soil. These substances gives a yellow colour to water, referred to as *gelbstoff/gilvin.* Yellow coloured water absorbs PAR weakly at the red end of the visible spectrum, but absorption increases towards the blue end of the spectrum (Kirk 1983).

The concentration of gilvin, and thus light absorption due to gilvin, varies markedly between waters. Generally, the concentration of gilvin in a given water body is indicated by the absorption coefficient at 440 nm, as this wavelength corresponds most closely to the midpoint of the blue waveband, which forms part of the absorption spectrum of most algae.

Regarding inanimate particular matter, many South African reservoirs are subject to a high silt load from inflowing rivers, for instance, 33 of the 60 largest reservoirs in South Africa have been classified as highly turbid (Walmsley *et al* 1980, Grobler and Davies 1981). Inorganic suspended sediment (TSS) indirectly affects algal concentration through its significant contribution to absorption and scattering of photosynthetically active radiation (PAR) (Ritchie *et al* 1978, Walmsley *et al* 1980, Kirk 1983). Highly turbid waters will show increased absorption of PAR at the blue end of the visible spectrum (Kirk 1983).

It is not only the concentration of inorganic suspended sediment that is of importance, but its distribution also. When inorganic sediment enters a reservoir some of the particles will remain in suspension, or settle and remain settled, or settle and be resuspended (Rodney and Stefan 1984). Factors such as sediment particle diameter and viscosity of the water will determine whether inorganic sediment particles will remain suspended or settle down at the bottom of the reservoir. The settling velocity of those particles that do settle also will be a function of sediment particle diameter, water temperature (viscosity) and the hydrodynamics of the medium. Turbulence created by flood events or strong river inflow will counteract the effect of gravitational

settling, but under quiescent conditions most particles greater than 1 μm settle within about an hour (DWAF 1981, Hart and Allanson 1984, Grobler *et al* 1987).

The high TSS concentration in many South African reservoirs and the influence it has on light penetration necessitate that cognisance be taken of TSS concentration, and the processes that would affect it, else it is doubtful whether correct simulation of algal growth, for instance, would be possible.

Resuspension of the sediment at the bottom of the reservoir will occur when a sufficiently strong motion and shear is present near the bottom (Rodney and Stefan 1984). Wind-induced wave action is the primary cause of resuspension in reservoirs - wave action causes circular movement of the water particles, and these movements generate shear stress at the sediment water interface. When the shear stress exceeds a critical value, the top layer of sediment is set into motion and eventually may be resuspended. Ultimately, resuspension is a function of wind speed, fetch length, duration of wind, and water depth (DWAF 1981, Blom *et al,* 1994). Many South African reservoirs may be sufficiently shallow for resuspension to be significant (Grobler *et al* 1987), but no resuspension has been observed in deeper reservoirs such as Hartbeespoort during stratified periods (Cochrane *et al* 1987). As this study is limited to stratified reservoirs, the process of resuspension will not be addressed in this study.

The significance of the different wavelengths where pure water, gilvin, and sediment absorb PAR, becomes clear when the absorption of PAR by **photosynthetic pigments** is considered - different algae have different pigment compositions, which absorb PAR at different wavelengths. For instance, blue-green algae with substantial level of a biliprotein called phycocyanin, absorb light strongly in the green, blue, and red regions of the spectrum, whereas green algal cells absorb light strongly in the blue part of the spectrum only (Kirk 1983). This may give blue-green algae a competitive edge over green algae in highly turbid waters - highly turbid waters strongly absorb light in the blue part of the spectrum, which means that there may be a paucity of light that can be utilized by the green algae. The blue-green algae, that can utilize light in the green and red parts of the spectrum also, may not be affected

to the same degree. However, although certain light spectra may favour the growth of certain algae, insufficient light will limit the growth of all algae, and it must be kept in mind that algal growth can be limited by a multitude of other factors also.

3.4.7 Concepts describing algal growth limitation

Algae need sufficient quantities of nutrients and light to grow, but the quantities of utrients and light available for algal growth vary widely in space and time, and may differ from the requirements of the algal cell (Reynolds 1984). Algal growth rate will be affected by water temperature also. The fact that algal growth rate will be limited under certain conditions can be used advantageously by the water manager - if the conditions whereunder algal growth rate will be limited can be identified, and if these conditions are generally applicable to any water body, the water manager can strive to manipulate the dam such that limiting conditions will prevail in the dam. As a consequence, a number of concepts that attempt to relate limitation of algal growth rate to certain factors such as nutrients, light, and/or water temperature, have been developed.

The earliest concept is that expressed by Justus Liebig in 1840, relating growth rate to nutrient availability. *Liebig's Law of the Minimum* states that the yield of a plant is determined by the nutrient that is present in the least amount relative to the need of the plant (Odum 1971, Jørgensen 1978, Rossouw 1986a). According to Liebig's Law only one nutrient can limit algal growth at any particular time, and, if a particular nutrient is growth-limiting, an increase in any of the other essential nutrients will not result in increased growth. If the concentration of the limiting nutrient is increased, growth will increase until another nutrient becomes limiting.

The Law of the Minimum has found practical application in, for instance, a study by Lee and Jones (1980), who stated that algal growth is unlikely to occur below certain minimum concentrations of dissolved phosphate and/or nitrogen, and that an assessment of these nutrients during the period of peak algal biomass would indicate whether they are growth-limiting - an environmental (external) concentration of 0.01

mg l^{-1} PO_4-P and/or 0.02 mg l^{-1} nitrogen would inhibit growth. Similar results are cited by Rosssouw (1986a), Reynolds (1984), and Weiss (1969). However, the authors emphasize the main deficiency of the Liebig's Law, namely that it provides information on possible nutrient limitation only, and does not take cognisance of the fact that algal growth can be limited by factors other than nutrients, eg. light, or that algal growth may be negatively affected if some factor is present in excess, eg temperature and/or light. In fact, even regarding nutrient limitation, Rossouw (1986a) warns that this method of identifying minimum environmental N and P concentrations required for algal growth at best gives a rough estimate of the growth-limiting nutrient, and recommends strongly that this method should not be used on its own to determine nutrient limitation. A possible reason why this method fails to identify the growth-limiting nutrient conclusively, is because it is based on external nutrient concentrations, whereas algal growth rate is a function mainly of internal nutrient concentration (see discussion in paragraph 3.4.4.2).

Another concept of Liebig's Law of the Minimum, namely that a single nutrient is growth-limiting, has been challenged frequently by the concept that more than one nutrient can limit algal growth simultaneously (Lehman *et al* 1975, Jørgensen 1976, Ahlgren 1980, Jørgensen 1980). A final conclusion as to which concept is correct has not been reached as yet - on the basis of experimental studies, Droop (1983), as well as Rhee (1978) maintained that the single limitation concept is valid, but Kunikane *et al* (1981) maintained that multiple limitation occurs in natural waters.

A further deficiency of Liebig's Law of the Minimum is that it is applicable under steady state conditions only. However, due to water movement, steady state conditions do not prevail in lakes and rivers. Also, because fluctuations in irradiance and nutrient availability occur at the same time scale as algal response, there will always be a significant lag between external change and the internal response of the algal cell (Harris 1984, Reynolds 1984).

Another popular concept, also taking account of nutrient limitation only, is that of using the *Redfield Ratio* to predict whether phosphorus or nitrogen potentially is the limiting nutrient. This concept, developed by Redfield in 1958, is based on the observation that the typical N:P ratio of phytoplankton cells is 7:1 by mass, similar to the N:P ratio in the natural aquatic environment, and thus it is postulated that any deviation from this ratio would indicate possible nutrient limitation (Lee and Jones 1980, Rossouw 1986a).

This concept became very popular and was used in various forms in attempts to identify whether nitrogen or phosphorus potentially is the limiting nutrient, for instance:

- environmental N:P ratio (Chiaudani and Vighi 1974, Schindler 1978, Ashton 1979, Lee and Jones 1980, Chiaudani and Vighi 1982, Rossouw 1986a, Rossouw and Grobler 1988, Allanson *et al* 1990, Suttle *et al* 1991)
- TN:TP ratio (total nitrogen : total phosphorus)(Faafeng and Hessen 1993)
- cellular N:P ratio (Rhee 1978, Lean and Pick 1981, Rossouw 1986a).

Rossouw (1986a) did an in-depth laboratory study where different methods to determine nutrient limitation in impoundments were compared. Based on experimental evidence, she recommended that the environmental N:P ratio method should not be used on its own, as it does not always identify the growth-limiting nutrient clearly. This observation is supported by Lee and Jones (1980), Rhee (1980), and Placke (1983). A possible reason for the inadequacy of this method is the fact that it is based on external nutrient concentration only, whereas algal growth rate is a function of internal nutrient concentration, and only is affected indirectly by the external nutrient concentration (see discussion in paragraph 3.4.4.2).

Regarding the TN:TP ratio, according to Lee and Jones (1980), this approach is technically invalid, because part of the total nitrogen and total phosphorus content of water in reservoirs may be associated with inorganic particulate matter, i.e. appreciable changes in the total concentration of the limiting nutrient can occur without affecting algal concentration.

Regarding cellular N:P ratios, this method was found to be a better indicator of nutrient limitation than environmental N:P ratios, or environmental concentrations of nitrogen and phosphorus (Rhee 1978, Rossouw 1986a), possibly because algal growth rate mainly is a function of internal nutrient concentration (see discussion in paragraph 3.4.4.2). However, contrary to the Redfield Ratio concept that the optimal N:P ratio of phytoplankton cells is 7:1 by mass, it has been found that each algal species has its own specific optimal cellular N:P ratio (Rhee 1978, Rossouw 1986a, Galvez *et al* 1993), and thus the use of cellular N:P ratios to identify the growth-limiting nutrient should be used with the utmost care.

From the discussion in the previous paragraphs it would seem that the concept that nutrient limitation is dependant on environmental N and P concentrations, as well as the concept that the growth-limiting nutrient can be identified from N:P ratios (whether environmental, cellular, or TN:TP) at best is inconclusive as to what nutrient limits algal growth, and therefore it is not necessary to take cognisance of these concepts in the conceptualization of the model.

A further shortcoming of these concepts is that they take account of nutrient limitation only, whereas algal growth rate can be limited by light also, and will be affected by temperature. Furthermore, complex interactions between various physical, chemical and biological processes, as well as the influence of reservoir morphology and climate, cause the thermal structure, the underwater light field, and the pools of biologically available nutrients to change on an hourly, or at least, on a daily basis (Reynolds 1984). Therefore, in practice it may be difficult to identify unconditionally the factors that limit algal growth at different moments in time. However, by simulating the behaviour of the reservoir with the aid of a mathematical model, it is possible to identify exclusively the growth-limiting factors at different moments in time.

3.4.8 Concepts describing algal succession

Certain algae have a greater nuisance value than others, for instance, blue-green algae are more likely to cause taste and odours problems than green algae. Some blue-green algae such as *Nodularia* are highly toxic. Certain conditions favour growth of certain algae, as is evident in the seasonal succession that is found in natural waters - usually diatoms are the dominant algal group during spring, whereafter they are succeeded by green algae and flagellates. Later on in summer dinoflagellates are the most prominent algal species, and in late summer/autumn blue-green algae dominate (Barnes and Mann 1980). Although this pattern of succession may show some variation in detail, usually the general pattern tends to be the same for all water bodies. It would be to the advantage of the water manager if conditions that favour growth of, say, blue-green algae, could be identified, as this would allow him to manipulate the reservoir in such a way as to minimize conditions that would favour growth of blue-green algae. As with algal growth limitation, a number of concepts have been developed that try to identify conditions that would favour growth of green algae over those of blue-green algae.

One of the most popular concepts is the N:P ratio concept developed by Smith (1983). Following studies done by Tilman *et al* (1982), Flett *et al* (1980), Schindler (1977), and his own analysis of data from 17 lakes world-wide (of which 15 are situated in the cold temperate climate of the northern hemisphere), Smith postulated that blue-green algae will dominate if the epilimnetic TN:TP ratio < 29 by weight, and that blue-green algae will be rare if the epilimnetic TN:TP ratio > 29 by weight (Smith 1983). Although he acknowledged that many lakes that have a TN:TP ratio < 29 were not dominated by blue-green algae, Smith nevertheless concluded that the TN:TP ratio concept may have practical significance and suggested that TN:TP ratios be manipulated by, for instance, nitrogen fertilization of the lake, to ensure a TN:TP ratio > 29 by weight, as this would be unfavourable for blue-green algal growth. The idea of combatting blue-green algal growth by manipulating N:P ratios attracted great attention (Trimbee and Harris 1984, NIWR 1985, Stockner and Shortreed 1988, Chutter 1989, Chutter and Rossouw 1991, Suttle *et al* 1991). This concept is extremely

popular and is widely believed to be valid. However, although Smith's observation is supported by studies done by Schindler (1977), Barica *et al* (1980), and Stockner and Hyatt (1984), it is not supported in studies done by Hutchinson (1944), and Faafeng and Hessen (1993). It was refuted finally in a review by Shapiro (1990), citing several studies that did not conform to Smith's concept that the proportion of blue-green algae is related to the TN:TP ratio (Smith 1987, Reynolds 1986, Lathrop 1988, Suttle and Harrison 1988).

Several other concepts have been developed to predict the annual algal succession, specially the dominance of blue-green algae in late summer. These concepts are based on environmental conditions that favour growth of blue-green algae, for instance, elevated temperature, low light conditions, low free CO_2 concentration, stability of the water column (i.e. absence of wind mixing), and grazing (Shapiro 1990). However, several studies (Reynolds 1986, Shapiro 1990.) have come to the conclusion that none of these factors can be used on their own to predict algal succession and/or dominance of blue-green algae in late summer, because of the interrelations between the various factors. All these factors play a role in algal succession, although their relative importance may vary (Ashton 1985, Viner 1985, Shapiro 1990). Also, local climatic conditions such as floods or severe wind mixing may impose a disturbance of the sequence generally observed globally (Trimbee and Harris 1984, Ashton 1985, Reynolds 1986). Effectively, this means that although the global trend of algal succession may be observed generally, there will always be some reservoirs that do not conform to the generalized pattern, due to local climatic conditions (Schindler 1978). Seasonal variations in the conditions that govern algal succession are characteristic of each reservoir (Pollingher 1986), thus, to a certain extent, the behaviour of each reservoir will be unique with regard to the conditions that govern algal succession. If the water manager wants to foresee the effect of certain water treatment options, he must be able to assess the relative importance of various environmental factors, as well as local climatic conditions, on algal succession in the specific reservoir. Also, he needs to understand why a certain treatment had a desired/undesired affect (Shapiro 1990). Mathematical modelling of the behaviour of the reservoir could be an invaluable aid in resolving the problem - a mathematical

model takes cognisance of the interrelationships between the various factors that play a role in algal succession, as well as the effect of local climatic conditions. Furthermore, by modelling the behaviour of a reservoir it may be possible to ascertain the relative importance of various environmental factors on algal growth and succession in that particular reservoir.

CHAPTER 4

GENERAL FORMULATION OF AN EUTROPHICATION MODEL

4.1 BACKGROUND

During formulation of a model the behaviour of a reservoir must be expressed in some formal mathematical or statistical way (James 1993). Using the conceptual representation as a basis (Chapter 3), a set of equations must be chosen to simulate the various processes that occur in a reservoir, as well as the interactions between these processes. However, due to the complexity of the system, often processes have several alternative mathematical formulations, which may vary in complexity. It is virtually impossible to select a single correct formulation for a specific process (Orlob 1983), at best one can select a formulation that is most suitable to the objectives of the study. Also, increasing the complexity of the model does not necessarily result in a model that simulates the real system more accurately - a more complex model would contain more parameters, and as parameter estimations are never error-free, errors of measurement will contribute to the uncertainty of model predictions (Jørgensen 1980, Jørgensen *et al* 1982). It is therefore recommended that formulation (as well as conceptualization) of a model be as simple as possible, without compromising the objectives of the study.

The objectives of this study is to simulate the phenomenon of eutrophication in stratified reservoirs of small to medium size[1] in a warm temperate climate. By putting a limitation on the reservoir size, the influences of the earth's rotation, basin-scale wind-driven circulation, and horizontal advection due to inflow and outflow can be neglected, because in medium-sized reservoirs these are very small in comparison to

---

[1] A reservoir of small to medium size is defined as one with the major axis < 50 km (Orlob 1983, Tchobanoglous *et al* 1985).

the influence of stratification (Patterson *et al* 1984). Furthermore, in stratified reservoirs horizontal dispersion of, for instance, heat by internal currents is so rapid that horizontal gradients are smoothed in less than a day. Vertical gradients, however, vary according to an annual cycle, and thus, if simulations are done over a period of a few years, with a basic time-step of one day, variation in the horizontal direction can be neglected (Henderson-Sellers 1984, Patterson *et al* 1984), i.e. the model can be formulated as a one-dimensional model. Accordingly, the one-dimensional approach will be followed in this study.

This chapter is a review of possible formulations (as reported in the literature) of the processes that have been conceptualised in Chapter 3. In the next chapter, specific formulation of the processes in the original MINLAKE model is evaluated against the formulations reported in this chapter.

4.2 FORMULATION OF THE CRITERIA FOR ONE-DIMENSIONALITY

A number of criteria has been developed to ascertain whether a reservoir is suitable for one dimensional modelling. These criteria take into account the stability of the system, the effect of wind, and the advective effect of inflows and outflows:

4.2.1 Stability of a reservoir as criterium for one dimensional modelling

One dimensional models are most suitable for application to deep, highly stratified reservoirs (Orlob 1983). The densimetric Froude number can be used as an indication of the densimetric stability of the system, thereby providing a measure of the degree of stratification (Orlob 1983, Henderson-Sellers 1984, Tchobanoglous *et al* 1985):

$$F_D = \frac{LQ}{zV}\sqrt{\frac{\rho_0}{g\beta}} \quad (4.1)$$

F_D = densimetric Froude number
L = length of reservoir (m)
Q = volumetric discharge ($m^3 s^{-1}$)
z = average depth (m)
V = volume (m^3)
ρ_o = reference density (= 1000 kg m^{-3})
g = acceleration due to gravity (m s^{-2})
ß = average density gradient in reservoir (10^{-3}kg m^{-4}).

For deep, well stratified reservoirs, $F_D << 1/\pi$. For weakly stratified reservoirs (which will be described better by a two dimensional model), $0.1 < F_D < 1.0$. For fully mixed systems, $F_D > 1.0$ (Orlob 1983, Henderson-Sellers 1984, Tchobanoglous *et al* 1985).

4.2.2 The effect of wind as criterium for one dimensional modelling

Very strong winds may impart a sufficient amount of turbulent kinetic energy to destroy the stratification in a water body, thereby making one dimensional modelling unnecessary. The following formula gives an indication on the strength of wind speed that will destroy stratification in a particular reservoir (Henderson-Sellers 1984):

$$z_e > \frac{4 * 10^{-7} W^2}{h} \frac{\rho}{\Delta\rho} \frac{L_T}{2} \quad (4.2)$$

z_e = depth of epilimnion in mid-summer (m)
W = mean maximum wind speed (m^3s^{-1})
h = depth of the reservoir (m)
ρ = density of water (kg m^{-3})
$\Delta\rho$ = density difference between epilimnion and hypolimnion (kg m^{-3})
L_T = average length of reservoir in thermocline region (m).

Wind speeds that are so high that it causes the right hand side of Eq 4.2 to be greater than the left hand side, will destroy stratification, and hence the one dimensional character of the reservoir (Henderson-Sellers 1984).

4.2.3 The effect of inflow and outflow as criterium for one dimensional modelling

In most one dimensional models, inflows and outflows are assumed to be instantaneous events (Jokela and Patterson 1985). This assumption can be made because in deep, well stratified reservoirs the hydraulic currents induced by inflows and outflows are very small, and thus shear induced mixing can be taken as negligible. (Henderson-Sellers 1984). However, in reservoirs where the volume of the reservoir is relatively small compared with the peak rate of inflow, or in reservoirs situated on rivers, the hydraulic currents induced by inflows, or by through flow of the river, may be large enough to cause significant mixing in the hypolimnion, well in excess of the turbulent mixing caused by wind (Orlob 1983, Henderson-Sellers 1984). One dimensional models will not be suitable for simulation of these systems. To evaluate the relative importance of advection on the vertical distribution of heat (and hence the thermal stability of the reservoir), the following ratio must be determined (Henderson-Sellers 1984):

$$\frac{A_d K_H}{Qd} \qquad (4.3)$$

A_d = cross-sectional area at depth d (m^2)
d = depth of inflow or outflow (m)
K_H = vertical eddy diffusion coefficient of heat ($m^2 s^{-1}$)
Q = rate of inflow/outflow ($m^3 s^{-1}$).

If this ratio is much less than unity, advection will cause significant mixing, rendering the reservoir unsuitable for one dimensional modelling (Henderson-Sellers 1984).

To summarize: one dimensional models have found wide application, and the behaviour of most reservoirs can be described by a one dimensional model. However, the capabilities and limitations of any modelling approach should always be kept in mind (Henderson-Sellers 1984), therefore, before applying a one dimensional model to a reservoir, care should be taken that the reservoir satisfies the criteria for one dimensional modelling as set out in the preceding paragraphs.

4.2.4 The structure of a one-dimensional model

In one dimensional models the water body is divided into a number of horizontal layers. The division can be done either according to the *Eularian* approach, or according to the *Langrangian* approach (see discussion in Chapter 3). With both the Eularian and the Langrangian approach, uniform homogeneous distribution of a substance, and thus uniform density, is assumed within each layer. Provision is made for transport between layers by advection and diffusion, i.e. the concentration of a substance can change in the vertical direction, but not in a horizontal direction. The change in concentration of a substance (suspended as well as dissolved) between layers is described by the one-dimensional advection-diffusion equation (Orlob 1983, Henderson-Sellers 1984):

$$A_z\left[\frac{\partial C}{\partial t} + v\frac{\partial C}{\partial z}\right] = \frac{\partial}{\partial z}\left[A_z(K + \alpha)\frac{\partial C}{\partial z}\right] \pm \text{sources/sinks} \quad (4.4)$$

z	=	depth from the surface (m)
A_z	=	cross-sectional area at depth z (m^2)
C	=	concentration or intrinsic property of the fluid such as temperature (mg l^{-1} or °C)
t	=	time (day^{-1})
v	=	vertical velocity of a suspended substance (m day^{-1})
	=	0 for dissolved substances and temperature
K	=	vertical turbulent diffusion coefficient (m^2 day^{-1})
α	=	molecular diffusion coefficient (m^2 day^{-1}).

According to Henderson-Sellers (1984) models differ in the neglect/inclusion of the terms in Eq 4.4, and in the way the variables are parameterized. For instance, in some studies (Sundaram and Rehm 1971) the vertical advection term is neglected, making the formulation applicable only to lakes with no inflows and outflows. However, virtually all South African reservoirs have multiple inflows and therefore the vertical advection term would have to be included in the formulation.

Models also vary in the way the cross-sectional area, A_z, is specified. If the reservoir is deep and steep sided, the cross-sectional area can be taken as constant. For reservoirs with sloping sides, a cross-sectional area that varies with depth must be specified (Bedford and Babajimopoulos 1977, Henderson-Sellers 1984). In models that use a constant area the total depth is equal to the mean depth, whereas in models with a variable area the total depth is equal to the lake maximum depth (Henderson-Sellers 1984). It is therefore very important to specify whether Eq 4.4 relates to a constant or variable area, and to link subsequent formulations to a the mean/maximum depth. As South African reservoirs usually have sloping sides, the variable area approach will be followed in this study, i.e. formulations should be based on maximum depth.

The relevant hydrodynamic and water quality processes that act as sources/sinks of substances and heat, as well as the dispersive role of eddy diffusion have been discussed in Chapter 3. To facilitate understanding, formulation of the processes will be done in the same sequence as in Chapter 3.

4.3 FORMULATION OF THE HYDRODYNAMIC PROCESSES

The major hydrodynamic processes that take place in a reservoir have been identified as (*cf* Chapter 3):

- exchange of heat energy
- convective mixing
- advective mixing
- mixing due to wind action.

The annual cycle of stratification/overturn that is the result of the interaction between the processes listed above has been identified as the most important phenomenon in a reservoir, as it determines the physical, chemical and biological behaviour of the reservoir (Henderson-Sellers 1984). Summer stratification is characterized by the thermocline that forms a physical barrier between the epilimnion and the hypolimnion (*cf* Chapter 3), thus thermocline formation needs to be formulated also.

4.3.1 Exchange of heat energy

There is some exchange of thermal energy at the sides and bottom of a reservoir, but usually the effect of this exchange on the vertical temperature structure is negligible compared to the effect of the major thermal energy exchange that occurs at the water surface (Henderson-Sellers 1984). Surface thermal energy exchange can be formulated according to either of two theories, i.e. the *surface energy balance theory* or the *equilibrium temperature theory*. In principle the two concepts should give the same results (Henderson-Sellers 1984).

4.3.1.1 Surface energy balance theory:

According to this theory, the surface water temperature can be calculated from the balance between incoming heat from net solar and long wave radiation, and the loss of heat from back radiation, as well as the loss from convective and evaporative heat transfer (Dake and Harleman 1969, Henderson-Sellers 1984, Stefan and Ford 1975):

$$\Delta H = H_{sn} - H_e - H_c - H_b + H_a \qquad (4.5)$$

ΔH = surface heat flux (kcal m^{-2} d^{-1})
H_{sn} = net solar radiation (kcal m^{-2} d^{-1})
H_e = evaporative loss (kcal m^{-2} d^{-1})
H_c = convective heat transfer (kcal m^{-2} d^{-1})
H_b = back radiation (kcal m^{-2} d^{-1})
H_a = atmospheric long wave radiation (kcal m^{-2} d^{-1}).

If $\Delta H > 0$, the surface water temperature will increase, if $\Delta H < 0$, the surface water temperature will decrease.

Regarding *net solar radiation*, this is defined as incident shortwave radiation minus certain losses (Dake and Harleman 1969, Henderson-Sellers 1984). For instance, some of the incident solar radiation is reflected at the water surface, while the remainder penetrates deeper into the reservoir, where it is absorbed by the water.

The reflected fraction (also called albedo or solar reflectivity) is a function of solar zenith angle, the roughness of the surface (which will be determined by, for instance, wave height), and the concentration of inorganic suspended sediment. A general expression for solar reflectivity of clear water in the absence of high concentrations of inorganic suspended sediment is (Stefan *et al* 1982, Henderson-Sellers 1984):

$$r = 0.108 - 0.000139H_s \quad (4.6)$$

r = solar reflectivity (W m^{-2}) [2]
H_s = incident solar radiation (W m^{-2}).

If the effect of inorganic suspended sediment is incorporated, the above expression becomes (Stefan *et al* 1982, Henderson-Sellers 1984):

$$r = (0.108 + 0.36S_q) - 0.000139H_s \quad (4.7)$$

r = solar reflectivity (W m^{-2})
S_q = sediment concentration (mg l^{-1})
H_s = incident solar radiation (W m^{-2}).

Thus a fraction of the incident solar radiation is reflected at the water surface, whereas the remainder penetrates deeper into the reservoir. It is exponentially absorbed by water, according to Beer's Law (Henderson-Sellers 1984):

$$H(z) = (1-r)H_s e^{-\eta z} \quad (4.8)$$

$H(z)$ = solar radiation at depth z (kcal m^{-2} d^{-1})
r = reflected fraction (kcal m^{-2} d^{-1})
H_s = incident solar radiation (kcal m^{-2} d^{-1})
η = total extinction coefficient (m^{-1}).

[2] For a formulation expressing the solar reflectivity **r** in units of kcal m^{-2} d^{-1}, see Eq 5.3.

The total extinction coefficient is a function of extinction due to pure water, extinction due to the presence of inorganic suspended sediment, and extinction due to chlorophyll-a (Kirk 1983, Orlob 1983):

$$\eta = k_w + 0.043SS + k_2Chla \quad (4.9)$$

η	=	total extinction coefficient (m^{-1})
k_w	=	extinction coefficient of pure water (m^{-1}) (*cf* Table 3.3)
SS	=	inorganic suspended sediment concentration (mg l^{-1})
k_2	=	extinction coefficient due to chlorophyll-a (m^2 (g chla)$^{-1}$)
Chla	=	chlorophyll-a concentration (mg l^{-1}).

Thus, after some of the incoming solar radiation has been reflected at the water surface, the remainder is absorbed by water according to Beer's Law (Eq 4.8). However, it has been observed that the absorption of solar radiation by water in the surface layer deviates from Beer's Law - the fraction that is absorbed in the surface layer is greater than the absorption predicted by Beer's Law (Dake and Harleman 1969, Henderson-Sellers 1984). If the fraction of the incoming radiation that is absorbed in the surface is called ß, than the remaining fraction that will penetrate into the rest of the water body can be denoted by (1-ß). Thus, taking the reflected fraction, as well as the extra absorption in the surface into account, the net solar radiation (*cf* Eq 4.5) in the surface layer can be expressed by (Henderson-Sellers 1984):

$$H_{sn} = (1 - r)\ \beta H_s \quad (4.10)$$

H_{sn}	=	net solar radiation (W m^{-2})
r	=	solar reflectivity (W m^{-2}) (Eq 4.7)
ß	=	fraction of incoming solar radiation (H_s) absorbed in the surface layer.

The net solar radiation just below the surface layer, i.e. the net solar radiation that will penetrate deeper into the water body, can be formulated as (Henderson-Sellers 1984):

$$H_{sn} = (1 - r)(1 - \beta)H_s \qquad (4.11)$$

H_{sn} = net solar radiation (W m^{-2})
r = solar reflectivity (W m^{-2}) (Eq 4.8)
(1-ß) = fraction of incoming solar radiation (H_s) not absorbed in the surface layer.

This fraction, ß, is an indication of the long wave (infrared) content of solar radiation, since shorter wavelengths penetrate more readily into the water (Dake and Harleman 1969). Often constant values of 0.4 and 0.5 are ascribed to ß, but because ß is a function of water turbidity it would be more correct to express it as a function of the total extinction coefficient (Henderson-Sellers 1984):

$$\beta = 0.265 \ln \eta + 0.614 \qquad (4.12)$$

ß = fraction of the incident solar radiation absorbed in the surface layer
n = total extinction coefficient (m^{-1}).

To summarize: A fraction, r, of the incident solar radiation is reflected at the water surface, and a fraction, ß, is absorbed in the surface layer. The remainder of the solar radiation penetrates deeper into the water body where it is absorbed according to Beer's Law. Taking these factors into account, the net shortwave radiation at a given depth below the surface layer can be expressed by (Dake and Harleman 1969, Henderson-Sellers 1984):

$$H(z) = (1-r)(1-\beta)H_s e^{-\eta z} \quad (4.13)$$

$H(z)$ = net solar radiation at depth z (kcal m^{-2} d^{-1})
r = fraction reflected at the surface
β = fraction absorbed in the surface layer
H_s = incident solar radiation (kcal m^{-2} d^{-1})
n = total extinction coefficient (m^{-1}).

Regarding the second term on the right hand side of Eq 4.5, *evaporative heat transfer*, H_e: Numerous studies have been done to determine evaporative heat loss (Ryan *et al* 1974, Henderson-Sellers 1984). Evaporation increases with increased wind speed, and with decreasing vapour pressure of the air, therefore evaporative heat loss can be expressed as (Dake 1972, Henderson-Sellers 1984):

$$H_e = \rho L E \quad (4.14)$$

H_e = evaporative heat loss (kcal m^{-2} d^{-1})
ρ = density of water (g m^{-3})
L = latent heat of vaporization (kcal m^{-3})
E = mass flux of water (m d^{-1}).

For surface water temperatures between 0 and 35°C, the latent heat of vaporization can be approximated by (Dake 1972):

$$L = 597.31 - 0.5631 T_w \quad (4.15)$$

L = latent heat of vaporization (kcal m^{-3})
T_w = surface water temperature (°C).

The mass flux of water, i.e. the evaporation rate, E, in Eq 4.14, is a function of wind speed, the saturated vapour pressure at surface water temperature, and vapour pressure at air temperature (Henderson-Sellers 1984)

$$E = f(W_z)(e_s - e_a) \quad (4.16)$$

E = mass flux of water (evaporation rate) (cm s^{-1})
$f(W_z)$ = wind function
W_z = wind speed [3] at height z (m s^{-1})
e_s = saturated vapour pressure at the water surface (mbar)
e_a = saturated vapour pressure of the air (mbar).

Two formulations exist for the wind function, $f(W_z)$ - in the United Kingdom, usually $f(W_z)$ is formulated as follows (Shaw 1994):

$$f(W_z) = a(b + W_z) \quad (4.17)$$

$f(W_z)$ = wind function
W_z = wind speed at height z (m s^{-1})
a,b = empirical constants.

When the wind function is formulated according to Eq 4.17, Eq 4.16 is commonly known as *Stelling's Equation* - an equation that is widely used in engineering practice (Brutsaert 1982).

---

[3] **IMPORTANT**: If the observed wind speed was not measured at the height required by the model, the observed wind speed should be converted to wind speed at the required height (see Appendix A2). Also, if the observed wind speed was measured over land, some models may require conversion to wind speed over water (see Appendix A2)

In the USA and Australia, the following formulation of the wind function is used more frequently (Shaw 1994):

$$f(W_z) = NW_z \qquad (4.18)$$

$f(W_z)$ = wind function
W_z = wind speed at height z ($m\ s^{-1}$)
N = empirical mass transfer coefficient (wind function coefficient).

The mass transfer coefficient, N, is a function of the terrain roughness and atmospheric stability, and therefore varies between water bodies (Harbeck and Meyers 1970, Weisman 1975, Brutsaert 1982). It can be estimated for a specific reservoir by determining the product $W_z(e_s - e_a)$ from measurements of wind speed and vapour pressure, and measuring the evaporation rate, E. The wind function coefficient **N** is given by the slope of a plot of evaporation rate E, against $W_z(e_s - e_a)$.

This method was used by Harbeck and Meyers (1970) to determine the mass transfer coefficient for three lakes in the USA (*cf* Table 4.1). If these values are to be compared to values determined for a specific reservoir, it is important to ensure that the units of measurement are the same, and that the wind speeds are quoted at the same height.

Table 4.1. Mass transfer coefficient for different lakes*

LAKE	WIND COEFFICIENT
Falcon Dam	0.0105
Lake Hefner	0.0120
Lake Mead	0.0118

* Units of measurement: Evaporation rate: cm day^{-1}.
Vapour pressure: mbar.
Wind speed : m s^{-1} at 2 m height

Regarding the third term on the right hand side of Eq 4.5, *convective heat loss* H_c, (also known as sensible heat loss): This term accounts for the heat that is conducted away from the surface of the water by the atmosphere (*cf* paragraph 3.3.2.1). The ratio between convective heat loss and evaporative heat loss is given by Bowen's Ratio (Humphreys 1940, Harbeck and Meyers 1970, Weisman 1975, Henderson-Sellers 1984):

$$R = \frac{\gamma P}{1000}\left(\frac{T_s - T_a}{e_s - e_a}\right) \qquad (4.19)$$

R	=	Bowen's ratio
	=	H_c/H_e
H_c	=	convective heat loss (cal cm^{-2} d^{-1})
H_e	=	evaporative heat loss (cal cm^{-2} d^{-1})
γ	=	Bowen coefficient
P	=	atmospheric pressure (mbars)
T_s	=	surface water temperature (°C)
T_a	=	air temperature (°C)
e_s	=	saturated vapour pressure at water surface (mbar)
e_a	=	vapour pressure of the air (mbar).

The value of the Bowen coefficient ranges between 0.58 and 0.66 (Harbeck and Meyers 1970), with a most probable value of 0.66 (Humphreys 1940, Harbeck and Meyers 1970, Ryan *et al* 1974, Henderson-Sellers 1984).

From the Bowen ratio (Eq 4.19) and the expression for evaporative heat loss (Eq 4.16), the convective heat loss can be written as:

$$H_c = \frac{\gamma P}{1000} f(W_z)(T_s - T_a) \quad (4.20)$$

H_c = convective heat loss (cal cm^{-2} d^{-1})
γ = Bowen coefficient
= 0.66
P = atmospheric pressure (mbars)
$f(W_z)$ = wind function (*cf* Eq 4.18)
= cW_z
c = wind coefficient
W_z = wind speed at height z (m s^{-1})
T_s = surface water temperature (°C)
T_a = air temperature (°C).

The Bowen ratio had been developed on the assumption that the eddy diffusivity of heat and water vapour are equal. This assumption is valid for reservoirs where the water surface temperature is within approximately two degrees of the air temperature, but becomes questionable when the difference between surface water temperature and air temperature is large (Harbeck and Meyers 1970).

Regarding the fourth term on the right hand side of Eq 4.5, *back radiation* H_b: all material with a temperature greater than absolute zero emits radiation according to the Stefan-Boltzmann Law (Henderson-Sellers 1984), thus the water surface of a reservoir will emit a certain amount of long wave radiation, leading to a reduction in the surface energy budget (*cf* Eq 4.5):

$$H_b = \varepsilon_w \sigma T^4_w \quad (4.21)$$

H_b = back radiation (kcal m^{-2} d^{-1})
ε_w = emissivity of water ($\approx$ 0.97)
σ = Stefan-Boltzman constant
= 1.171 * 10^{-6} kcal m^{-2} $°K^{-4}$
T_w = water surface temperature (°K).

Regarding the last term on the right hand side of Eq 4.5, i.e. *atmospheric long wave radiation* H_a: some of the long wave radiation emitted by the water body and the surrounding area is absorbed by the atmosphere and clouds and emitted back towards the water body, thereby adding energy to the surface energy budget (Dake and Harleman 1969, Henderson-Sellers 1984):

$$H_a = \varepsilon_a \sigma T^4_a \quad (4.22)$$

H_a = atmospheric radiation (kcal m^{-2} d^{-1})
ε_a = emissivity of the atmosphere
σ = Stefan-Boltzman constant
= 1.171 * 10^{-6} kcal m^{-2} $°K^{-4}$
T_a = air temperature (°K).

Essentially, this formulation is the same as the formulation for back radiation (*cf* Eq 4.21). However, contrary to the emissivity of water, which has a constant value of 0.97, the emissivity of the atmosphere, being a function of cloud cover, is more variable. Even so, most of formulations for atmospheric emissivity (as represented in Table 4.2) have been developed for cloudless conditions (Henderson-Sellers 1984):

Table 4.2. Formulae for atmospheric conditions under cloudless conditions

(from Henderson-Sellers 1984)

AUTHOR	FORMULA (cloudless conditions)
Swinbank	$0.937 * 10^{-5} T_a^2$
Idso and Jackson	$1.0 - 0.26 \exp\{-7.77 * 10^{-5}(T_a-273)^2\}$
Bruetsaert	$0.642 (e_a/T_a)^{1/7}$
Idso	$0.70 + 5.95 * 10^{-7} e_a \exp(1500/T_a)$

T_a = air temperature (°K)

e_a = vapour pressure of air (mbar).

These formulae can be modified for cloudy skies by the following factor (Henderson-Sellers 1984):

$$FC = 1 + k_1 C^2 \qquad (4.23)$$

FC = modifying factor for cloud cover

k_1 = cloud height coefficient

C = cloud cover ratio.

The cloud height coefficient varies between 0.04 and 0.25, with a recommended value of 0.17 (Henderson-Sellers 1984).

4.3.1.2 Equilibrium temperature theory of surface heat exchange:

According to Noble (1981), in the mathematical modelling of water temperature it has been observed that it is not always possible to obtain an analytical solution for surface water temperature, because some of the terms in the expression for net heat exchange at the air-water interface are non-linear. The concept of equilibrium temperature was developed to linearize the net heat flux expression.

Equilibrium temperature is defined as the surface water temperature where no net heat would be exchanged across the air-water interface (Noble 1981, Henderson-Sellers 1984):

$$H_N = k_E(T_E - T_S) = 0 \qquad (4.24)$$

H_N = net surface heat exchange (kcal m^{-2} d^{-1})
k_E = surface exchange coefficient
T_E = equilibrium temperature (°K)
T_S = temperature at the water surface (°K).

In terms of the equilibrium concept, if $T_S > T_E$, heat will be lost from the water body and the surface water temperature will decrease. If $T_S < T_E$, the surface water temperature will increase.

The effects of atmospheric long wave radiation, evaporation, and convective heat loss are all incorporated into a single coefficient, the surface exchange coefficient. This coefficient is reservoir specific, and must be calculated for each reservoir being studied (Henderson-Sellers 1984):

$$k_E = 4\varepsilon\sigma(273)^3 + L\rho(\gamma + \frac{\partial e_s}{\partial T_s})\, f(W) \qquad (4.25)$$

k_E	=	surface exchange coefficient
ε	=	emissivity of the atmosphere (= 0.97)
σ	=	Stefan-Boltzman constant
	=	$1.171 * 10^{-6}$ kcal m^{-2} $°K^{-4}$
L	=	latent heat of vaporization (kcal m^{-3})
ρ	=	density of water (g m^{-3})
γ	=	wet and dry bulb hygrometric constant (Penman 1948)
e_s	=	saturated vapour pressure at the water surface (mbar)
f(W)	=	horizontal wind velocity function
	=	cW
c	=	wind function coefficient (as in Eq (4.18))
W	=	wind speed over water surface [4] (m s^{-1}).

4.3.2 Convective mixing

Imberger and Patterson (1981) formulated convective mixing as part of the turbulent kinetic energy budget during calculation of the mixed layer depth (see paragraph 4.3.4.2). No other specific formulation for convective mixing could be found, in some models (Riley 1988) calculation of convective mixing is simply based on density differences - the density in each layer is compared with the density of the layer immediately below, taking into account temperature, as well the concentration of inorganic suspended sediment and dissolved salts. If the density of the upper layer is higher than the density of the lower layer, the density of the two layers are

[4] If the observed wind speed was not measured at the height required by the model, the observed wind speed should be converted to wind speed at the required height. Also, if the observed wind speed was measured over land, it should be converted to wind speed over water (see Appendix A2).

averaged. This procedure is repeated until the density of the upper layer is equal or less than that of the layer below.

4.3.3 Advective mixing

Normally the density of water flowing into a reservoir differs from that at the surface of the reservoir, due to differences in water temperature and in concentrations of dissolved salts and inorganic suspended sediment (TSS). If the inflowing water is lighter, it will overflow on top of the surface water of the reservoir, if it is of the same density as the reservoir surface water, it will disperse into the surface water. When heavier water enters the reservoir it pushes the reservoir water ahead of itself back into the reservoir, until buoyancy forces due to the density difference at the interface between reservoir and river water balances the inertial force of the incoming water. At this point (called the *plunge point* or *plunge line*) the incoming water plunges and flows underneath along the submerged river bed, entraining reservoir water in the process. The inflow can be divided into three distinct mixing regimes (Fischer *et al* 1979):

- Mixing associated with the plunge point
- In the case of plunging inflow where river water underflows reservoir water, bottom roughness often leads to mixing (entrainment) at the interface between river and reservoir water
- When the density of the inflowing water equals that of the reservoir water, the inflowing water will leave the bottom and flow horizontally into the reservoir.

The inflowing water transport a number of constituents into various portions of a stratified reservoir. From a modelling point of view, to determine the layers that are affected by the inflow, the depth of the reservoir at the plunge point has to be formulated, as well as the amount of entrainment.

4.3.3.1 Formulation of reservoir depth at the plunge point:

If the river bed has a mild slope, mixing at the plunge point is very small (Fischer *et al* 1979), and the plunge depth is a function of bed friction and the balance between inertial and buoyancy forces [5]. However, if the river bed is steep, the flow depth will change abruptly at the plunge point, causing significant mixing at the plunge point. In this case plunging depth is a function of entrance mixing and the densimetric Froude number (Akiyama and Stefan 1984).

Several formulations of plunging depth have been proposed for mild slopes. These formulations are based on laboratory, field, or theoretical studies (Table 4.3)

[5] Generally, the balance between inertial and buoyancy forces is expressed by the densimetric Froude number F_p (Henderson-Sellers 1984), i.e.
F_p = inertial force/buoyancy force.

Table 4.3 Summary of equations for calculation of plunge depth for mild slopes (Akiyama and Stefan 1984)

Investigator	Plunge depth h_p
Jain (1980)	$1.6\left(\frac{\alpha_i}{1+\alpha_i}\right)^{0.126}\left(\frac{8S}{f_t}\right)^{0.008}\left(\frac{q^2}{\epsilon_0 g}\right)^{1/3}$ (4.26)
Hebbert *et al* (1979)	$1.16\left(\frac{Q^2}{\epsilon_0 g}\right)^{\frac{1}{5}}$ for Wellington Reservoir (4.27)
Savage and Brimberg (1975)	$\left(\frac{\left(2.05\ \frac{S}{f}\right)^{0.478}}{(i+\alpha)}\right)^{\frac{-2}{3}} \cdot \left(\frac{q^2}{\epsilon_0 g}\right)^{\frac{1}{3}}$ (4.28)
Wunderlich and Elder (1973)	$\left(\frac{1}{0.5}\right)^{\frac{2}{3}} \cdot \left(\frac{q^2}{\epsilon_0 g}\right)^{\frac{1}{3}}$ (4.29)
Singh and Shah (1971)	$1.85 + 1.3\left(\frac{q^2}{\epsilon_0 g}\right)^{\frac{1}{3}}$ (4.30)

h_p = plunge depth (m)

α_i = ratio of interfacial to bed shear stress

S = bed slope

f_t = total friction coefficient

q = inflow flux per unit span

ϵ_0 = relative density difference between inflow and ambient water

= $\Delta\rho_0/\rho_a$

g = gravitational acceleration

Q = river inflow discharge

f = bed friction coefficient.

Most of the formulations in Table 4.3 have the general format:

$$h_p = \left(\frac{1}{F_p^2}\right)\left(\frac{q_0^2}{\epsilon_0 g}\right)^{\frac{1}{3}} \qquad (4.31)$$

h_p = plunge depth (m)

F_p = densimetric Froude number at plunge point

q_0 = inflow flux per unit span

ϵ_0 = relative density difference between inflow and ambient water

= $\Delta\rho_0/\rho_a$

$\Delta\rho_0$ = excess density of inflow relative to ρ_a (g m^{-3})

ρ_a = ambient water density (g m^{-3}).

The formulation of Hebbert *et al* (1979) differs slightly from the general format, because a triangular instead of a rectangular cross section was used (Hebbert *et al* 1979, Akiyama and Stefan 1984). However, since the cross section of South African rivers are mostly rectangular, the general formulation as given in Eq 4.31 is preferred.

The above formulations, with the general format of Eq 4.31, is not suitable for steep slopes where significant mixing occurs at the plunge point (Fischer *et al* 1979,

Akiyama and Stefan 1984). Taking cognisance of this, Akiyama and Stefan (1984) formulated h_p (plunge point depth) for either a mild or a steep slope, defining a mild slope as S < 1/150 (0.0066), a steep slope as S > 1/150, and a critical slope as S = 1/150

Formulation for a mild slope (S < 1/150):

$$h_{ps} = \frac{1}{2}\left(\frac{2+\gamma}{2} + \frac{S_2 S}{f_t} + \sqrt{\left[\frac{2+\gamma}{2}+\frac{S_2 S}{f_t}\right]^2 - 4\frac{(S_2\, S/f_t)}{(1+\gamma)}}\right)\left(\frac{f_t}{S_2\, S}\right)^{\frac{1}{3}}\left(\frac{q_0^2}{\epsilon_0 g}\right)^{\frac{1}{3}} \quad (4.32)$$

Formulation for a steep slope (S > 150):

$$h_{pm} = \frac{1}{2}\left(\frac{2+\gamma}{2} + S_1 + \sqrt{\left[\frac{2+\gamma}{2} + S_1\right]^2 - 4\frac{(S_1)}{(1+\gamma)}}\right)\left(\frac{1}{S_1}\right)^{\frac{1}{3}}\left(\frac{q_0^2}{\epsilon_0 g}\right)^{\frac{1}{3}} \quad (4.33)$$

If the slope is critical, S = 1/150 ($h_{pm} = h_{ps}$).

h_{ps} = plunge depth for mild slope (m)

h_{pm} = plunge depth for steep slope (m)

γ = rate of initial mixing

= q_a/q_0

q_a = inflow rate of ambient water per unit span into plunge region

q_0 = flow rate per unit span downstream of plunge point (underflow)

S_1 = coefficient (= 0.2 ~ 0.3)

S_2 = coefficient (= 0.6 ~ 0.9)

f_t = total friction coefficient

= $f_b + f_i$

f_b = bed friction coefficient

f_i = friction coefficient for interface

S = bed slope

ϵ_0 = initial density difference relative to ambient density

= $\Delta\rho_0/\rho_a$

$\rho_a+\rho_0$ = density of inflow water (g m^{-3})

ρ_a = density of ambient water (g m^{-3})

g = gravitational acceleration (m s^{-2}).

4.3.3.2 Formulation of entrainment due to advection:

When the inflowing water plunges and flows underneath the reservoir water, bottom roughness often leads to entrainment at the interface between river and reservoir water. Based on the pioneering work of Ellison and Turner (1959), the rate of entrainment can be expressed as (Fischer *et al* 1979, Akiyama and Stefan, 1984):

$$\frac{dh}{dt} = Eu_d \qquad (4.34)$$

dh/dt = rate of entrainment (m s^{-1})

u_d = mean velocity of the underflowing water (m s^{-1})

E = entrainment coefficient.

Based on experimental studies done by Ellison and Turner (1959), the entrainment coefficient, E, can given by the following[6] (Akiyama and Stefan 1984):

[6] This formulation is applicable to inflow from rivers with a rectangular cross-section. Fischer *et al* (1979) give a more complicated formulation applicable to rivers with a triangular cross-section. However, since most South African rivers tend to have a more rectangular cross-section, the formulation for a triangular cross-section will not be considered here.

$$E = \frac{\beta}{Ri^n} \qquad (4.35)$$

E = entrainment coefficient
Ri = Richardson number
n, ß = constants.

For stratified reservoirs the values of the constants n and ß have been established as (Akiyama and Stefan 1984):

$n = 1; \qquad \beta = 0.0015$

The Richardson number, (Ri in Eq 5.35) is given by (Ellison and Turner 1959, Imberger *et al* 1978, Akiyama and Stefan 1984):

$$Ri = \frac{\epsilon_d g h_d \cos\theta}{u_d^2} \qquad (4.36)$$

ϵ_d = density difference downstream of plunge point (underflow) relative to ambient water density (g m^{-3})
= $\Delta\rho_0/\rho_a$
$\Delta\rho_0$ = excess density of underflow relative to ρ_a (g m^{-3})
ρ_a = ambient water density (g m^{-3})
g = acceleration due to gravity (m s^{-2})
h_d = underflow depth (m)
θ = angle of the bed slope
u_d = underflow velocity (m s^{-1}).

4.3.4 Formulation of mixing due to wind action

As was discussed in paragraph 3.3.2.4, first attempts at describing the effect of mixing due to wind action was based on the concept of turbulent diffusion.

4.3.4.1 Formulation of the vertical transport of heat and mass by turbulent diffusion:

The diffusion concept of vertical heat transport and thermocline formation requires specification of the vertical eddy diffusion coefficient indicated in Eq 4.4. Vertical transport of heat and mass due to turbulence created by internal currents, wind effects, and inflows, can be parameterized as a turbulent (eddy) diffusion coefficient, analogous to the molecular diffusion coefficient in molecular (Fickian) diffusion. Most formulations of the eddy diffusion coefficient do not take turbulence generated by inflows into account. This approach may be acceptable for lakes with no inflows, or even for reservoirs under conditions of 'normal flow', as the incoming water will disperse into the reservoir at a point of similar temperature/density, and dispersion by advective turbulence can be neglected under these conditions (Jassby and Powell 1975). However, usually South African reservoirs have multiple inflows, and regularly are subject to high inflows from storm events, thus the effect of advective turbulence must be taken into account. If it is not included in the formulation of the eddy diffusion coefficient, it should be formulated separately (see paragraph 4.3.3).

Regarding formulation of the eddy diffusion coefficient, during overturn the eddy diffusion coefficient is a function of wind stirring only, and is constant with depth. However, under stratified conditions the eddy diffusion is a function of wind stirring only in the epilimnion, and therefore it is not constant with depth (Sundaram and Rehm 1973). Its value is greatest near the surface, and declines with depth towards the thermocline, where it reaches a minimum value. In the hypolimnion the eddy diffusion coefficient increases slightly with depth, reaching a maximum hypolimnetic value at about mid depth in the hypolimnion (Orlob and Selna 1970). The value of the eddy diffusion coefficient in the epilimnion is comparable to the value during overturn; these values are several hundred times greater than the value in the hypolimnion.

Formulation of the epilimnetic eddy diffusion coefficient:

The epilimnetic eddy diffusion coefficient also is called the *surface eddy diffusion coefficient*. The term *neutral value of the eddy diffusion coefficient* refers to the value of the epilimnetic eddy diffusion coefficient during overturn (Henderson-Sellers 1984). Although the eddy diffusion coefficient is not constant in the epilimnion, for modelling purposes it often is formulated as being constant (Henderson-Sellers 1984). Wind blowing over the surface of the lake generates shear which causes turbulence and hence, mixing. Sundaram and Rehm (1973) and McCormick and Scavia (1981) therefore formulate the epilimnetic eddy diffusion coefficient as a function of surface shear velocity:

$$K_{H_o} = cu_{*s} \qquad (4.37)$$

K_{Ho} = epilimnetic eddy diffusion coefficient ($m^2\ s^{-1}$)
c = empirical constant
u_{*s} = surface shear velocity ($m\ s^{-1}$).

From the study by Sundaram and Rehm (1973), it appears that the value of c should be determined for each reservoir. For Cayuga Lake in the USA, they determined the value of c as equal to 0.0282.

The surface shear velocity, u_{*s}, is related to wind speed by the following formulation (Henderson-Sellers 1984):

$$u_{*s}^2 = \frac{\rho_a}{\rho_w} C_D U_{10}^2 \qquad (4.38)$$

ρ_a = density of air ($g\ m^{-3}$)
ρ_w = density of water ($g\ m^{-3}$)
C_D = drag coefficient
U_{10} = wind speed measured at 10 metre height ($m\ s^{-1}$).

Various formulations for is given for C_D, for instance (Henderson-Sellers 1984):

(Van Dorn 1953)

$$C_D = \left[1.0 + 1.9\left(\frac{1 - 5.6}{U_{10}}\right)^2\right]10^{-3} \qquad U_{10} > 5.6 \text{ m s}^{-1}$$
$$C_D = 1.0 * 10^{-3} \qquad U_{10} \leq 5.6 \text{ m s}^{-1} \qquad (4.39)$$

C_D = drag coefficient
U_{10} = wind speed measured at 10 metre height (m s^{-1}).

Wu (1969) developed a formulation that was meant for oceans, but it is used for lakes as well (Henderson-Sellers 1984):

$$C_D = 1.25U_{10}^{-0.5} * 10^{-3} \qquad U_{10} \leq 1 \text{ m s}^{-1}$$
$$= 0.5U_{10} * 10^{-3} \qquad 1 < U_{10} < 15 \text{ m s}^{-1} \qquad (4.40)$$
$$= 2.6 * 10^{-3} \qquad U_{10} \geq 15 \text{ m s}^{-1}$$

C_D = drag coefficient
U_{10} = wind speed measured at 10 metre height (m s^{-1}).

Apart from Eq 4.37, several other formulations of the epilimnetic eddy diffusion coefficient are reviewed by Henderson-Sellers (1984). The simplest formulation relates the epilimnetic eddy diffusion coefficient to wind speed:

$$K_{H_o} = 4.5 * 10^{-5}U \qquad (4.41)$$

K_{Ho} = epilimnetic eddy diffusion coefficient (m^2 s^{-1})
U = wind speed (m s^{-1}).

Henderson-Sellers (1984) also quotes several more complex formulations that relate the epilimnetic eddy diffusion coefficient to wind shear velocity. These formulations are variations of the following general format:

$$K_{H_o} = \frac{1}{P_o} u_* kz \qquad (4.42)$$

K_{Ho} = epilimnetic eddy diffusion coefficient ($m^2\ s^{-1}$)
P_o = turbulent Prandtl number (≈ 1)
u_* = shear velocity ($m\ s^{-1}$)
k = Von Karman's constant (≈ 0.40)
z = depth from the surface (m).

Formulation of the hypolimnetic eddy diffusion coefficient:
In the hypolimnion, the eddy diffusion coefficient is a function of both water movement and thermal stability, and therefore must be determined for each reservoir (see discussion in paragraph 3.3.2.5). For a particular reservoir, the hypolimnetic eddy diffusion coefficient increases with depth, reaching a maximum at about mid-depth in the hypolimnion.

Turbulent (eddy) diffusion is the main mechanism for dispersion of heat and mass in the hypolimnion and therefore correct formulation of this coefficient is important. The importance of hypolimnetic eddy diffusion is evident in the numerous methods of formulation for the hypolimnetic eddy diffusion coefficient - formulation of heat transfer coefficients from vertical temperature gradients in lakes was first attempted by McEwen (1929), and later by Hutchinson (1957). However, Powell and Jassby (1974) identified some inconsistencies in the formulation of McEwen, and subsequently developed a method of formulation that is based on temperature gradients as well as heat fluxes. The flux gradient method of Powell and Jassby (1974) has generally superseded the temperature gradient method of McEwen and Hutchinson (Henderson-Sellers 1984), and thus the temperature gradient method will not be

discussed here. Other methods for formulating the hypolimnetic eddy diffusion coefficient are the functional method, and formulations relating the hypolimnetic eddy diffusion coefficient to eddy viscosity or reservoir surface area.

Formulation of the eddy diffusion coefficient by the flux gradient method:
The flux gradient method is widely used for calculation of the eddy diffusion coefficient (Powell and Jassby 1974, Henderson-Sellers 1984). It is based on simultaneous calculation of heat fluxes and thermal gradients, using the Fickian diffusion equation as a starting point (Powell and Jassby 1974):

$$J_{sz} = -K_{sz} \frac{\partial s}{\partial z} \qquad (4.43)$$

J_{sz} = mean flux of substance s in the z (vertical) direction due to turbulent mixing
K_{sz} = eddy transport coefficient of substance s in the z direction ($cm^2\ s^{-1}$)
$\partial s/\partial z$ = concentration gradient of substance s in the z direction.

In terms of the above equation, the vertical flux of thermal energy in water can be related to the temperature gradient by the following (Powell and Jassby 1974):

$$H_w = \rho c K_H \frac{\partial \theta}{\partial z} \qquad (4.44)$$

H_w = thermal energy flux ($cal\ m^{-2}\ d^{-1}$)
ρ = water density ($g\ m^{-3}$)
c = specific heat capacity of water ($cal\ g^{-1}\ °C^{-1}$)
K_H = eddy diffusion coefficient ($cm^2\ s^{-1}$)
$\partial\Theta/\partial z$ = temperature gradient ($°C\ m^{-1}$).

If it is assumed that horizontal transport of heat is negligible, and that there is no back radiation of heat from the sediments, the thermal energy flux, H_w, can be estimated using the first law of thermodynamics, which states that an energy change occurring in a system can be deduced from the conservation of energy principle (Barrow 1973, Powell and Jassby 1974, Bruetsaert 1982):

$$\rho c \frac{\partial \theta_z}{\partial t} = -\frac{\partial}{\partial z}(H_w) - \frac{\partial R}{\partial z} \qquad (4.45)$$

ρ = water density (g cm^{-3})
c = specific heat capacity of water (cal g^{-1} °C^{-1})
$\partial\theta/\partial t$ = change in temperature with time t (°C s^{-1})
H_w = thermal energy flux (cal cm^{-2} s^{-1})
R = net incoming solar radiation (cal cm^{-2} s^{-1})
z = depth from the surface (cm).

Assuming that the heat flux, H_w, as well as the net solar radiation, R, is zero at the bottom of the reservoir, and integrating the above equation from depth z to the bottom of the reservoir at depth h, the vertical eddy diffusion coefficient can be expressed as (Powell and Jassby 1974):

$$K_H = -\frac{1}{\partial\theta_z/\partial z}\left(\int_z^h \frac{\partial \theta_z}{\partial t} dz - \frac{1}{\rho c} R\right) \qquad (4.46)$$

K_H = vertical eddy diffusion coefficient (cm^2 s^{-1})
$\partial\theta/\partial z$ = vertical temperature gradient (°C m^{-1})
$\partial\theta/\partial t$ = change in temperature with time, t (°C s^{-1})
ρ = water density (g cm^{-3})
c = specific heat capacity of water (cal g^{-1} °C^{-1})
R = net incoming solar radiation (cal cm^{-2} s^{-1})
z = depth from the surface (cm)
h = *mean* depth of the reservoir (cm).

However, the above equation assumes that the reservoir area does not change with depth (Bedford and Babajimopoulos 1977), and therefore is applicable only to steep sided reservoirs. For reservoirs with sloping sides, i.e. where the area changes with depth, Eq. 4.46 should be changed to (Powell and Jassby 1974, Jassby and Powell 1975):

$$K_z = -\frac{1}{\partial\theta_z/\partial z}\left(\frac{S_z}{A_z} - \frac{R_z}{\rho c}\right) \qquad (4.47)$$

with

$$S_z = \frac{d}{dt}\int_z^h A_z\theta_z dz \qquad (4.48)$$

K_z	=	eddy diffusion coefficient at depth z ($cm^2\ s^{-1}$)
$\partial\theta_z/\partial z$	=	vertical temperature gradient (°C cm^{-1})
A_z	=	reservoir cross-sectional area at depth z (cm^2)
ρ	=	water density (g cm^{-3})
c	=	specific heat capacity of water (cal g^{-1} °C^{-1})
R_z	=	solar radiation flux at depth z (cal $cm^{-2}\ s^{-1}$)
z	=	depth from the surface (cm)
h	=	depth at the bottom of the reservoir (cm)
t	=	time (s)
θ_z	=	temperature at depth z (°C).

It is important to note that in Eq 4.46 (constant area) h denotes the mean depth of the reservoir, whereas in Eq 4.47 (variable area), h denotes the depth at the bottom of the reservoir. Also, both equations take the stabilizing effect of heat gained via solar radiation into account, but assume that vertical transport of heat via convection, and horizontal transport via advection are negligible (Jassby and Powell 1975). Thus this formulation is valid under stratified conditions only, and not during overturn when convection overwhelms wind-induced turbulence (Henderson-Sellers 1984). Also,

dispersion due to turbulence generated by inflows must be calculated separately (see paragraph 4.3.3).

Formulation of the eddy diffusion coefficient by the functional method:

Many of the models based on the diffusion concept of heat dispersion and thermocline formation (paragraph 3.3.2.5) formulated the eddy diffusion coefficient by means of the functional method (Henderson-Sellers 1984). The basis of the functional method is the hypothesis that, under stratified conditions, eddy diffusion can be expressed as the product of the neutral value of the eddy diffusion coefficient (i.e. the value in the absence of stratification), and a function of a stability parameter (Sundaram and Rehm 1971, Henderson-Sellers 1984):

$$K_H = K_{H_o} f(S') \qquad (4.49)$$

K_H = hypolimnetic eddy diffusion coefficient ($cm^2\ s^{-1}$)

K_{Ho} = neutral value of the eddy diffusion coefficient ($cm^2\ s^{-1}$)

S' = stability parameter.

Theoretical and laboratory studies suggest that the eddy diffusion coefficient in a stratified fluid may be a function of the gradient Richardson number, R_i (the ratio between buoyancy forces and shear stress). Many empirical formulations have been developed that express K_H as a function of R_i. Two typical examples are the following (Sundaram and Rehm 1971, Henderson-Sellers 1984):

$$K_H = K_{Ho}(1 + \sigma_1 R_i)^{-1} \quad (4.50)$$

$$K_H = K_{Ho}(1 - \sigma_2 R_i) \quad (4.51)$$

K_H = hypolimnetic eddy diffusion coefficient ($cm^2\ s^{-1}$)
K_{Ho} = neutral value of the eddy diffusion coefficient ($cm^2\ s^{-1}$)
σ_1, σ_2 = empirical constants
R_i = gradient Richardson number.

The gradient Richardson number is formulated as (Sundaram and Rehm 1971, Jassby and Powell 1975, Henderson-Sellers 1984):

$$R_i = \frac{N^2}{(\partial u/\partial z)^2} \quad (4.52)$$

R_i = gradient Richardson number
N = Brunt-Väisälä frequency (buoyancy frequency) (s)
$\partial u/\partial z$ = horizontal velocity shear ($m\ s^{-1}$).

The Brunt-Väisälä frequency, N, is given by (Henderson-Sellers 1984):

$$N^2 = \frac{g}{\rho}\frac{\partial \rho}{\partial z} \quad (4.53)$$

g = acceleration due to gravity ($m\ s^{-1}$)
ρ = density of water ($g\ m^{-3}$)
z = depth from the surface (m).

In practice it is difficult to establish a realistic value for $\partial u/\partial z$, the horizontal velocity shear (Eq 4.52). However, theoretical studies done by Welander (1968) indicated that under certain circumstances the eddy diffusion coefficient may be a function of the buoyancy frequency, N, only - when turbulence is generated by a local vertical shear process, as would be the case in lakes and reservoirs, the following formulation applies (Jassby and Powell 1975, Henderson-Sellers 1984):

$$K_H \propto (N^2)^{-\frac{1}{2}} \tag{4.54}$$

When turbulence is generated by a cascade process (i.e. turbulent energy enters the system at large scales and cascades down to smaller scales as would be the case in oceans), the formulation is as follows:

$$K_H \propto (N^2)^{-1} \tag{4.55}$$

Formulation of the hypolimnetic eddy diffusion coefficient by relating it to eddy viscosity:

When a force is applied to a liquid, the liquid will start to flow. If the resultant flow is turbulent, the shear stress associated with the velocity gradient is given by (Smith 1975):

$$\tau = \epsilon \frac{dU}{dz} \tag{4.56}$$

τ = shear stress per unit area (kg m^{-2} s^{-1})

ϵ = coefficient of eddy viscosity (g s^{-1} cm^{-1})

dU/dz = velocity gradient.

It is important to note that the eddy viscosity coefficient is a property of the motion within the fluid, and not of the fluid itself (Reynolds 1974, Smith 1975), and therefore it is unique to a particular reservoir. Viscosity tends to dampen turbulence (Smith 1975). Also, both turbulent transport and viscosity are affected by buoyancy, thus Ozmidov (1965) postulated that turbulent transport is proportional to dissipation of energy by viscosity, and to buoyancy:

$$K_H \propto \frac{\varepsilon}{N^2} \qquad (4.57)$$

K_H = vertical turbulent diffusion coefficient ($cm^2 s^{-1}$)
ε = internal energy dissipation rate
N = buoyancy frequency (Brunt-Väisälä frequency) (s).

The buoyancy frequency (also known as the Brunt-Väisälä frequency) is given by (Patterson *et al* 1984):

$$N^2 = \frac{g}{\rho}\frac{\partial \rho}{\partial z} \qquad (4.58)$$

N = buoyancy frequency (s)
g = acceleration due to gravity ($m\ s^{-1}$)
ρ = density of water ($kg\ m^{-3}$)
$d\rho/dz$ = change of density with depth.

The internal energy dissipation rate, ε, may be estimated by the following (Fischer *et al* 1979):

$$\varepsilon = \frac{(P_w A_s + P_s)}{P} \qquad (4.59)$$

P_w = energy introduced by wind at the surface of the lake
A_s = lake surface area (m^2)
P_s = energy introduced by inflowing streams
P = potential energy of column of water.

The energy introduced by wind at the surface of the lake, P_w, is given by the following (Fischer *et al* 1979):

$$P_w = \tau u_w \qquad (4.60)$$

P_w = rate of working by the wind on the lake surface (kg m^{-1} s^{-2})
τ = shear stress (kg m^{-2} s^{-1})
= $C_D \rho_a U^2$
C_D = drag coefficient
ρ_a = density of air (kg m^{-3})
U = wind speed at 10 metre height (m s^{-1})
u_w = surface drift velocity (m s^{-1}).

Under steady state conditions the surface drift velocity, $u_w \approx u_{*s}$ (the surface shear velocity) (Fischer *et al* 1979, Imberger and Hamblin 1982). The surface shear velocity is given by equation 4.48.

The energy introduced by inflowing streams is given by (Fischer *et al* 1979, Imberger and Patterson 1981):

$$P_s = g\Delta\rho DQ \qquad (4.61)$$

P_s = energy introduced by inflowing streams
g = acceleration due to gravity (m s^{-1})
$\Delta\rho$ = density difference between reservoir and river water (kg m^{-3})
D = depth of neutral buoyancy (m)
Q = river inflow rate (m^3s^{-1}).

Analogous to Eq 4.55, if it is assumed that the reservoir is in 'equilibrium' with the external energy inputs, the eddy diffusion coefficient can be formulated as a function of energy dissipation, as well as buoyancy frequency (Imberger *et al* 1978, Fischer *et al* 1979, Imberger and Hamblin 1982):

$$K_H = \frac{cH^2}{T_m S} \qquad (4.62)$$

K_H = eddy diffusion coefficient (m^2 s^{-1})
c = ź/H
ź = height of the effective centre of volume (m)
H = total depth of the reservoir (m)
T_m = characteristic mixing time scale (s)
S = stability (Eq 4.65).

Regarding the value of the coefficient c (= ź/H), according to Fischer *et al* (1979), for all practical purposes this coefficient should be constant, even for reservoirs with widely different geometries. They recommend a value of 0.048 for c, based on results obtained from four different reservoirs.

The characteristic mixing time scale, T_m, is given by (Imberger *et al* 1978, Fischer *et al* 1979, Imberger and Hamblin 1982):

$$T_m = \frac{P}{(P_w A_s + P_s)} \qquad (4.63)$$

P_w = energy introduced by wind at the surface of the lake
A_s = lake surface area (m^2)
P_s = energy introduced by inflowing streams
P = potential energy of column of water.

The potential energy of the water column is given by (Fischer *et al* 1979):

$$P = \Delta\rho g V \bar{z} \qquad (4.64)$$

P = potential energy of the water column
$\Delta\rho$ = density difference between surface and bottom layers (kg m^{-3})
g = acceleration due to gravity (m s^{-2})
V = lake volume (m^3)
$\acute{z}$ = height of the centre of volume (m).

The stability, S, in Eq 4.62 is given by (Fischer *et al* 1979, Imberger and Hamblin 1982):

$$S = \frac{HN_2}{g\Delta\rho} \qquad (4.65)$$

H = total depth of the reservoir (m)
N = buoyancy frequency (Eq 4.58)
g = acceleration due to gravity (m s^{-2})
$\Delta\rho$ = density difference between surface and bottom waters (kg m^{-3}).

The formulation for the hypolimnetic eddy diffusion coefficient given in Eq 4.62 makes provision for turbulence generated by wind at the surface of the reservoir, as well as turbulence generated by inflows. Furthermore, according to Patterson *et al* (1984), for all practical purposes, under conditions of strong stratification (large values of N^2), the value of the turbulent diffusion coefficient will be virtually equal to that of the molecular diffusion. Under conditions of weak stratification (small values of N^2), the value of the hypolimnetic eddy diffusion coefficient K_H, as formulated in Eq 4.62 will be limited by some prescribed maximum value of K_H. Imberger and Patterson (1981) set this maximum value at $10^{-4}m^2s^{-1}$, i.e. for $K_H < 10^{-4}m^2s^{-1}$, K_H is calculated according to Eq 4.62, and for values greater than $10^{-4}m^2s^{-1}$, K_H is taken as equal to $10^{-4}m^2s^{-1}$.

Formulation of the hypolimnetic eddy diffusion coefficient as a function of reservoir surface area:

The data required to calculate the eddy diffusion coefficient according to the methods described in the preceding paragraphs are not always available. However, turbulent mixing in the hypolimnion is due to internal currents that are an indirect response to surface wind stress and advection, and, because surface wind stress is a function of wind fetch length, it should be possible to establish a link between the hypolimnetic eddy diffusion coefficient and reservoir surface area. For instance, Mortimer (1942) observed that the mean[7] hypolimnetic eddy diffusion coefficient increases with reservoir surface area (Table 4.4, Figure 4.1).

[7]The value of the eddy diffusion coefficient is not constant in the hypolimnion, but increases with increasing depth below the thermocline. The mean value would be the mean of these increasing values.

TABLE 4.4 Hypolimnetic eddy diffusion coefficient as a function of lake area (Mortimer, 1942).

Lake	Area (km^2)	**Mean** hypolimnetic eddy diffusion coefficient ($cm^2\ s^{-1}$)
Holsfjord	121	3.1
Geneva	503	1.9
Lomond	71	0.53
Windermere (north basin)	8.2	0.39
Windermere (south basin)	6.7	0.09
Maxinkuckee	7.5	0.07
Kizakiko	1.4	0.05
Lunz	0.68	0.05
Esthwaite Water	1.0	0.03
Schleinsee	0.15	0.02

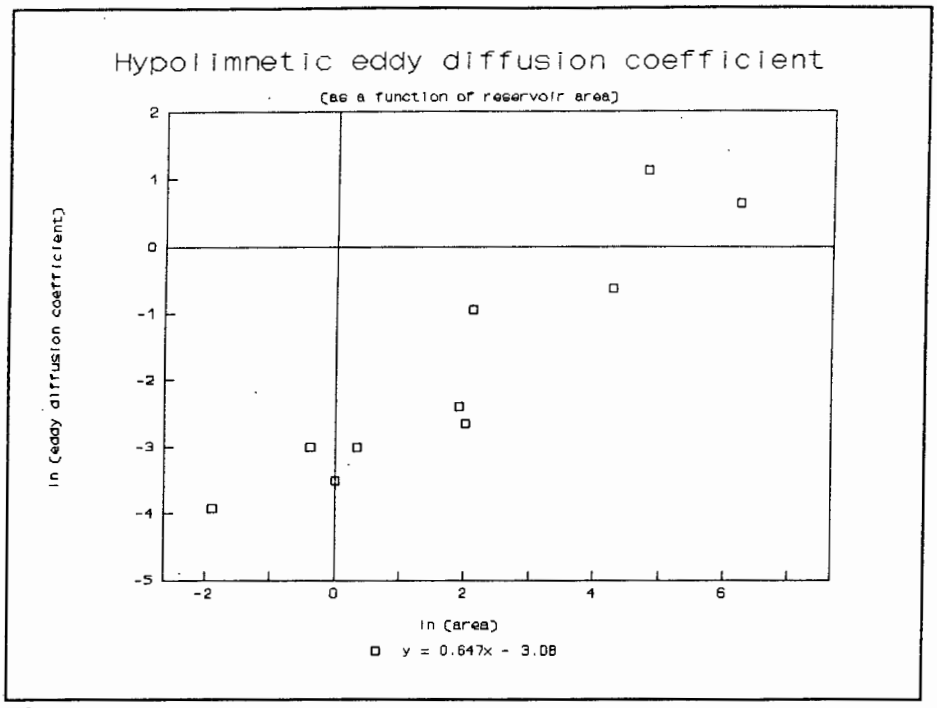

Figure 4.1
Mean hypolimnetic eddy diffusion coefficient as a function of reservoir surface area (After Mortimer 1942)

The *mean* value of the hypolimnetic eddy diffusion coefficient, as determined with the above method, can merely serve as an estimate of the hypolimnetic eddy diffusion coefficient, as it does not take the effect of thermal stability on eddy diffusion into account (see paragraph 3.3.2.5).

The formulation of Stefan and Fang (1994) also utilises the surface area of the lake, but care is taken of the effect of thermal stability by formulating the hypolimnetic eddy diffusion coefficient as a function of both reservoir surface area and the Brunt-Väsäilä frequency:

$$K_z = 8.17 * 10^{-4} * A_s^{0.56} * (N^2)^{-0.43} \qquad (4.66)$$

K_z = hypolimnetic eddy diffusion coefficient in a particular layer (m_2s^{-1})
A_s = lake surface area (km^2)
N = Brunt-Väsäilä frequency (s).

Formulations of the hypolimnetic eddy diffusion coefficient that is based on lake surface area only take turbulence generated by wind stirring into account, and do not take turbulence generated by inflowing water into account. Turbulence generated by inflows therefore has to be formulated separately (see paragraph 4.3.3)

The need to formulate the eddy diffusion coefficient originated with models based on the diffusion concept (see paragraph 3.3.2.5). However, these models were inadequate for simulation of thermocline formation, consequently the *integral energy concept* was developed to simulate formation of the thermocline.

4.3.4.2 Formulation of the integral energy concept of thermocline formation:

The integral energy concept was pioneered by Turner and Kraus (1967) on the basis of experimental results. Models based on the integral energy concept provide a better simulation of mixed layer depth than models based on the diffusion concept. However, integral energy models still employ eddy diffusion as the main mode of heat and mass dispersion, especially in the hypolimnion, and therefore integral energy models should be seen as a refinement of the diffusion concept, rather than being competitive (Stefan and Ford 1975).

As was discussed in paragraph 3.3.2.6, the integral energy concept postulates that deepening of the epilimnion is a function of both wind-induced turbulent kinetic energy, and the stability of the system. This concept has been formulated in varying degrees of complexity - the formulation of Imberger and co-workers (Imberger and Patterson 1981) is very detailed and complex, verging on the two-dimensional. Firstly, they calculate the amount of turbulent kinetic energy that would be required to lift (entrain) colder, denser hypolimnetic water into the epilimnion, thereby causing the epilimnion to deepen. Thereafter the turbulent kinetic energy available to the system is calculated in four distinct sections, starting with calculation of kinetic energy available from convective overturn. If it is more than the turbulent kinetic energy required for deepening of the epilimnion, deepening occurs. If it is less, the 'residual' available energy is carried over to the next calculation, which is the contribution of

wind stirring to the available turbulent kinetic energy budget. Again, if the available energy (including the residual) is larger than the required energy, deepening will occur, with the residual available energy from this calculation carried over to next step. The procedure is repeated for calculation of deepening by shear production at the thermocline, and deepening by billowing. If, at the end of the calculation, the available energy is less than the required energy, the available energy is dissipated in overcoming viscosity, and no deepening occurs.

The approach of Stefan and co-workers is slightly different, but much less complex (Stefan and Ford 1975, Ford and Stefan 1980). They postulate that the work required to lift a layer of colder, denser water immediately below the mixed layer into the mixed layer is equal to the rate of change of potential energy. The potential energy of the system is changed also by heat input. By formulating the work required as the rate of change in potential energy, formulation of complex processes such as deepening of the thermocline by shear production, billowing, Langmuir circulation, etc., is circumvented (Stefan and Ford 1975). The available potential energy is compared to the kinetic (mechanical) energy input from wind. Based on experimental work done by Linden (1973), Stefan and Ford (1975) postulate that deepening of the mixed layer depends on a certain critical ratio of kinetic to potential energy. This ratio is estimated to be close to unity. Wind shear stress is assumed to be the major source of kinetic energy, and thus turbulent kinetic energy is formulated as (Ford and Stefan 1980):

$$TKE = \int_{A_s} C u_{*w} dA \qquad (4.67)$$

TKE	=	wind-induced turbulent kinetic energy
A_s	=	surface area (km^2)
C	=	empirical coefficient for wind sheltering
u_{*w}	=	water shear velocity ($m\ s^{-1}$)
τ	=	shear stress at the air-water interface ($kg\ m^{-2}\ s^{-1}$).

The rate of change of potential energy, i.e. the work required to lift the mass of water $\Delta\rho\ \Delta V$, from immediately below the mixed layer into the mixed layer, is given by (Ford and Stefan 1980):

$$W_L = \Delta\rho\Delta V g(D - Z_g) \tag{4.68}$$

W_L = work required (rate of change of potential energy)
$\Delta\rho$ = density difference between mixed layer and underlying layer (kg m^{-3})
ΔV = incremental volume (m^3)
g = acceleration due to gravity (m s^{-2})
D = depth of mixed layer (m)
Z_g = depth of centre of gravity of mixed layer (m).

Eq 4.67 and 4.68 are combined to obtain σ, the critical ratio for deepening of the mixed layer (Ford and Stefan 1980):

$$\sigma = \frac{\int_{As} u_{*w}\tau dA\Delta t}{\Delta\rho\Delta V g(D - Z_g)} \tag{4.69}$$

σ = critical ratio for deepening of the mixed layer
Δt = time step.

The rest of the symbols are as per Eq 4.67 and 4.68 above. The wind sheltering coefficient has been moved over to the left hand side of the equation and incorporated into σ. If $\sigma > 1$, i.e. if the amount of turbulent kinetic energy in the mixed layer is greater than the amount of potential energy in the system, vertical entrainment and mixing will take place, if it is less ($\sigma < 1$), the kinetic energy is dissipated in overcoming viscosity, and no deepening occurs.

In calculating the kinetic energy budget, neither formulation takes the contribution of inflows (advective kinetic energy) into account. For lakes, and even for reservoirs under 'normal' flow conditions, this approach may be sufficient. However, advective kinetic energy due to storm events may be large enough to cause disruption of the thermocline. Stefan and co-workers take care of this by separately formulating mixing due to advection (see paragraph 4.3.3), whereas Imberger and co-workers formulate the mixing effect of inflowing streams as part of a global vertical diffusion coefficient (Imberger and Patterson 1981).

The difference in the formulations of Imberger and co-workers, and Stefan and co-workers, is based on a very subtle difference in interpretation of the integral energy concept (see paragraph 3.3.2.6). Though the formulation of Stefan and co-workers is considerably less complex, it appears to be adequate for simulation of temperature distribution with depth and formation of the thermocline in a typical South African reservoir. For instance, when both the MINLAKE model (based on the formulation of Stefan and co-workers), and the DYRESM model (based on the formulation of Imberger and co-workers), were applied to Roodeplaat Dam in South Africa, using the same data bases, there was virtually no difference in simulated temperature and mixed layer depth (Görgens *et al* 1993).

4.4 FORMULATION OF WATER QUALITY PROCESSES.

The specific water quality problem that is addressed in this study is that of eutrophication. In Chapter 3 (paragraph 3.4) the processes that should be considered in the conceptualisation of an eutrophication model have been identified as:

- Processes affecting dissolved oxygen concentration
- Microbial decomposition of organic matter
- Processes affecting algal concentration (including algal photosynthesis, respiration, mortality, and the availability of nutrients and light).

To facilitate understanding, formulation of these processes will follow the same sequence as in Chapter 3.

4.4.1 Formulation of processes affecting oxygen concentration.

The amount of dissolved oxygen in water can be expressed as a concentration in mg l^{-1} (or kg m^{-3}), or as a percentage saturation (see discussion in paragraph 3.4.2). In this study, oxygen is expressed as a concentration in mg l^{-1}.

4.4.1.1 Formulation of saturated oxygen concentration:

The maximum concentration of oxygen that can dissolve in water under normal atmospheric conditions is known as the saturated concentration, which is a function of temperature as well as pressure, and thus altitude. The change in saturated dissolved oxygen concentration with temperature can be formulated as (Henderson-Sellers 1984):

$$C_s = [14.652 - 4.1022 * 10^{-1}(T-273) + 7.991 * 10^{-3}(T-273)^2 - 7.77774 * 10^{-5}(T-273)^3]10^{-3} \quad (4.70)$$

C_s = saturated dissolved oxygen concentration at 0°C and 1 atmosphere pressure (kg m^{-3})

T = surface water temperature (°K).

However, the above formulation does not make provision for the effect of altitude on saturated dissolved oxygen concentration. As many South African reservoirs are situated at an altitude > 1000 m above mean sea level, the effect of altitude would have to be taken into account. Bratby (1977) formulates saturated dissolved oxygen concentration as a function of both water temperature and altitude:

$$C_s = C_{s20} * \frac{51.6}{(31.6 + T)} * \frac{P_s - e_s}{P_0 - P_w} \quad (4.71)$$

C_s = saturated dissolved oxygen concentration at 0°C and 1 atmosphere pressure (mg l^{-1})

C_{s20} = saturated dissolved oxygen concentration at 20°C and 1 atmosphere pressure (kg m^{-3})

= 9.07 (mg l^{-1})

51.6 = universal constant

31.6 = universal constant

T = surface water temperature (°C)

P_s = atmospheric pressure at the site (mbar)

e_s = saturated water vapour pressure at surface water temperature (mbar)

P_0 = atmospheric pressure at sea level

= 1013 mbar

P_w = saturated water vapour pressure at 20°C

= 23.35 mbar.

The saturated vapour pressure at a particular temperature can be calculated from the classical Clausius-Clapeyron formulation (Barrow 1973, Henderson-Sellers 1984):

$$\frac{1}{e_s}\frac{de_s(T)}{dT} = \frac{M_v}{R}\frac{L_v}{T^2} \qquad (4.72)$$

e_s = saturated water vapour pressure (N m^{-2})

T = air temperature (°K)

M_v = molecular weight of water vapour

= $18 * 10^{-3}$ kg mol^{-1}

R = gas constant

= 8.314 J $°K^{-1}$ mol^{-1}

L_v = latent heat of vaporization (J kg^{-1})

with

$$L_v = [2500.9 - 2.365(T_w - 273)] * 10^{-3} \qquad (4.73)$$

T_w = water temperature (°K).

Henderson-Sellers (1984) also gives an alternative, empirical formulation for saturated water vapour pressure:

$$e_s(T) = 2.171 * 10^{10}\, e^{\left(\frac{-4157}{T - 33.91}\right)} \qquad (4.74)$$

e_s = saturated water vapour pressure (N m^{-2})

T = air temperature (°K).

4.4.1.2 Formulation of sources of oxygen:

There are two major sources of dissolved oxygen in a reservoir:

- Transfer of atmospheric oxygen to the water
- Oxygen produced during algal photosynthesis.

Transfer of atmospheric oxygen to the water takes place at the water surface until an equilibrium is reached between the oxygen concentration in air and that dissolved in water. Generally, the transfer of oxygen between the atmosphere and the reservoir can be formulated as (James 1993):

$$V\frac{dc}{dt} = K_L A(c_s - c) \qquad (4.75)$$

V	=	reservoir volume (l)
dc/dt	=	change in dissolved oxygen concentration with time
K_L	=	mass transfer coefficient ($time^{-1}$)
A	=	reservoir surface area (m)
c_s	=	saturation concentration of oxygen in water (mg l^{-1})
c	=	dissolved oxygen concentration (mg l^{-1}).

The saturation concentration of oxygen in water must be corrected for the effect of temperature and altitude, as described in paragraph 4.4.1.1.

The mass transfer coefficient, K_L, incorporates the effects of turbulence, layer thickness, and the resistance these layers offer to the transfer of oxygen from the atmosphere (see discussion in paragraph 3.4.2.1). The mass-transfer coefficient is affected by wind speed - at wind speeds $\geq$ 3 m s^{-1} air flow over the water surface changes from aerodynamically smooth to turbulent. At wind speeds less than 2 - 3 m s^{-1} (aerodynamically smooth flow) the transfer of atmospheric oxygen into the water

body is a function of molecular diffusion only, and the transfer coefficient can be formulated as (Lewis and Whitman 1924, O'Connor 1983):

$$K_L = \frac{D}{\delta} \qquad (4.76)$$

K_L = oxygen transfer coefficient ($m\ s^{-1}$)
D = molecular diffusivity ($m^2 s^{-1}$)
= $6.92 * 10^{-15}\ T_K/\mu$ (Riley 1988)
T_K = water temperature (°K)
μ = absolute viscosity (Nsm^{-2})
δ = thickness of the diffusional layer (m).

At wind speeds $\geq$ 2 m s^{-1} the renewal rate of the sublayer at the water surface varies non-linearly with wind speed (see paragraph 3.4.2.1), and hence the transfer of atmospheric oxygen into the water body becomes a function of both diffusion and the renewal rate of the sublayer at the water surface (Cohen 1983, O'Connor 1983):

$$K_L = \sqrt{Dr} \qquad (4.77)$$

K_L = oxygen transfer coefficient ($m\ s^{-1}$)
D = molecular diffusivity ($m^2 s^{-1}$)
r = rate of surface renewal.

The surface renewal rate can be formulated as (O'Connor 1983):

$$r = \frac{u_{*w}}{\kappa z_{ew}} \tag{4.78}$$

r = rate of surface renewal

u_{*w} = water shear velocity (m s^{-1})

κ = Von Karman constant (= 0.4)

z_{ew} = equilibrium surface roughness height

$\approx$ 0.25 cm.

O'Connor (1983) expresses the water shear velocity in terms of the air shear velocity by means of the following:

$$u_{*w} = u_{*a}\left[\frac{\rho_a}{\rho_w}\right]^{\frac{1}{2}} \tag{4.79}$$

u_{*w} = water shear velocity (m s^{-1})

u_{*a} = shear velocity of air (m s^{-1})

ρ_a/ρ_w = density of air/density of water

= 0.0012.

Using the above expression for surface renewal rate, O'Connor (1983) formulates the oxygen transfer coefficient for wind speeds $\geq$ 3 m s^{-1} as a function of shear velocity, and the roughness, of air:

$$K_L = \left[\frac{Du_{*a}}{\kappa z_e} \cdot \frac{\rho_a \nu_a}{\rho_w \nu_w}\right]^{\frac{1}{2}} \quad (4.80)$$

K_L = oxygen mass transfer coefficient (m s^{-1})
D = molecular diffusivity (m^2 s^{-1})
u_{*a} = shear velocity of the air (m s^{-1})
κ = Von Karman constant (= 0.4)
z_e = equilibrium surface roughness height
≈ 0.25 cm
ρ_a/ρ_w = density of air/density of water
= 0.0012
υ_a/υ_w = viscosity of air/viscosity of water
= 15.

The shear velocity of air can be expressed in terms of wind speed (O'Connor 1983):

$$u_{*a} = \sqrt{C_d} U_{10} \quad (4.81)$$

u_{*a} = shear velocity of the air (m s^{-1})
C_d = drag coefficient at 10 metre height (*cf* Eq 4.37 and 4.38)
U_{10} = wind speed at 10 metre height (m s^{-1}).

Thus the oxygen mass transfer coefficient can be formulated also in terms of wind speed (O'Connor 1983):

$$K_L = \left[\frac{D}{\kappa z_e} \cdot \frac{\rho_a \nu_a}{\rho_w \nu_w}\sqrt{C_d} U_w\right]^{\frac{1}{2}} \quad (4.82)$$

K_L	=	oxygen mass transfer coefficient (m s^{-1})
D	=	molecular diffusivity (m^2 s^{-1})
u_{*a}	=	shear velocity of the air (m s^{-1})
κ	=	Von Karman constant (= 0.4)
z_e	=	equilibrium surface roughness height
	$\approx$	0.25 cm
ρ_a/ρ_w	=	density of air/density of water
	=	0.0012
υ_a/υ_w	=	viscosity of air/viscosity of water
	=	15.

The relationship between viscosity and molecular diffusivity is given by the Schmidt number (Reynolds 1974). Cohen (1983) expresses the oxygen mass transfer coefficient in terms of the Schmidt number, and water shear velocity:

$$K_L Sc^{\frac{1}{2}} = A_0 + 0.048\ (u_{*w})^{1.015} \quad (4.83)$$

K_L	=	oxygen mass transfer coefficient (cm s^{-1})
Sc	=	Schmidt number
	=	υ/D
υ	=	kinematic viscosity ($cm^2 s^{-1}$)
D	=	molecular diffusivity (cm^2 s^{-1})
A_0	=	0.0029 for $U_{*w} \leq 2$ cm s^{-1}
	=	0.0148 for $U_{*w} > 2$ cm s^{-1}
u_{*w}	=	water shear velocity (cm s^{-1}).

Equation 4.83 is formulated in terms of water shear velocity. It can be formulated in terms of wind speed by using the following relationship between water shear velocity and wind speed (Henderson-Sellers 1984):

$$u_{*w} = \frac{\rho_a}{\rho_w} C_D U_{10}^2 \qquad (4.84)$$

u_{*w} = water shear velocity (m s^{-1})
ρ_a/ρ_w = density of air/density of water (0.0012)
C_d = drag coefficient at 10 metre height (*cf* Eq 4.37 and 4.38)
U_{10} = wind speed at 10 metre height (m s^{-1}).

Another source of oxygen is the oxygen produced during photosynthesis. According to Henderson-Sellers (1984) the photosynthetic production of oxygen at depth *z* and time *t* can be formulated as:

$$p(z,t) = p_m(t)\exp\left(\frac{-\tau^2}{2\sigma^2}\right) \qquad (4.85)$$

p(z,t) = photosynthetic production of oxygen at depth *z* and time *t* (mg O_2 h^{-1})
$p_m(t)$ = maximum oxygen production occurring at or just below the surface at time *t* (mg O_2 h^{-1})
τ = optical depth (m)
= $nz/\ln 2$
n = extinction coefficient (m^{-1})
z = depth (m)

$$\sigma = \frac{\log I_o - \log 0.5\, I_k}{\log 2}\sqrt{\left(\frac{2}{\pi}\right)}$$

I_o = subsurface light intensity (W m^{-2}).

Stefan and Fang (1994) formulate the oxygen produced during photosynthesis as follows:

$$P = P_{max} Min[L] Chla \quad (4.87)$$

P = oxygen produced during photosynthesis (mg O_2 (mg Chla)$^{-1}$ h^{-1})

P_{max} = maximum specific photosynthetic oxygen production rate at light saturating conditions (mg O_2 (mg Chla)$^{-1}$ h^{-1})

Min[L] = light limitation function on algal growth as a function of depth and time

Chla = chlorophyll-*a* concentration (μg l^{-1}).

P_{max}, the maximum specific photosynthetic oxygen production rate, is temperature dependent and is specified as (Stefan and Fang 1994):

$$P_{max} = 9.6 * 1.036^{(T-20)} \quad (4.88)$$

P_{max} = maximum specific photosynthetic oxygen production rate at light saturating conditions (mg O_2 (mg Chla)$^{-1}$ h^{-1})

T = water temperature (°C).

The light limitation function, Min[L] in Eq 4.87, is given by the following (Megard *et al* 1984, Stefan and Fang 1994):

$$\text{Min}[L] = \frac{I\left(1 + 2\sqrt{\frac{K_1}{K_2}}\right)}{I + K_1 + \frac{I^2}{K_2}} \qquad (4.89)$$

I = photosynthetically active radiation (PAR) (Einstein m^{-2} h^{-1})
K_1 = light limitation coefficient
K_2 = light inhibition coefficient.

4.4.1.3 Formulation of processes that decrease oxygen concentration (oxygen sinks):

According to Klapper (1991), sinks of oxygen arise mainly from biological and chemical oxidation processes. In paragraph 3.4.2 microbial decay of organic matter was identified as one of the major sinks of oxygen in eutrophic reservoirs. Microbial decay in the water column is discussed in the next section. Oxygen consumption due to microbial decay of organic matter in the bottom sediments contributes to the sediment oxygen demand (SOD) as specified in paragraph 3.4.2.3. The most simplistic way of modelling SOD is to formulate it as a constant rate per cross-sectional area (EPA 1985, Cole 1991):

$$\frac{dO}{dt} = \frac{K_b A_z}{V} \qquad (4.90)$$

dO/dt = change in oxygen concentration
K_b = sediment oxygen demand (g O_2 m^{-2} day^{-1})
A_z = sediment cross-sectional area at depth z (m^2)
V = volume of water layer (m^3).

The oxygen demand of the sediments will be affected by the oxygen concentration of the overlying water (paragraph 3.4.2.3). This resulted in the following formulation (EPA 1985):

$$SOD = a\ DO^{b} \qquad (4.91)$$

SOD	=	sediment oxygen demand (g O_2 m^{-2} day^{-1})
DO	=	concentration of dissolved oxygen in the overlying water (mg l^{-1})
a,b	=	empirical constants.

The effect of oxygen concentration on sediment oxygen demand can be expressed by a Michaelis-Menten type function also (EPA 1985). This type of formulation is discussed in more detail in paragraph 4.4.1.4.

Regarding the effect of temperature on sediment oxygen demand, usually this is formulated in terms of the van't Hoff form of the Arrhenius relationship (EPA 1985):

$$k_T = k_{Tr}\ \theta^{(T-20)} \qquad (4.92)$$

k_T	=	rate at ambient temperature (°C)
k_{Tr}	=	rate at reference temperature (usually 20°C)
θ	=	Arrhenius temperature coefficient.

Processes such as nitrification will contribute to a decrease in dissolved oxygen concentration. Formulation of nitrification is discussed in paragraph 4.4.4.2.

4.4.1.4 Formulation of the effect of the aerobic/anaerobic state of the water on process rates:

Some processes such as, for instance, sediment release/adsorption of phosphate, and detrital decay, have different reaction rates under aerobic and anaerobic conditions. Also, processes such as nitrification occur under aerobic conditions only, whereas denitrification and release of ammonia from the bottom sediment take place under anaerobic conditions only. Many South African dams experience anaerobic conditions during stratification - in a survey of 21 South African dams (Walmsley and Butty 1980a), 14 became anaerobic during some part of the year, therefore the effect of the aerobic/anaerobic state of the water on process rates must be taken into account when modelling the water quality behaviour of South African dams. This means that aerobic processes must be formulated such that the aerobic process rate approaches zero as the dissolved oxygen concentration approaches zero. Similarly, anaerobic processes should be formulated such that the process rate increases as the dissolved oxygen concentration approaches zero. The simplest way of achieving this is by specifying a limiting oxygen concentration - aerobic processes take place at oxygen concentrations greater than the limit, and anaerobic processes at oxygen concentrations smaller than the limit (Cole 1991). The main problem with this method is a technical one - in models using this technique, the discontinuous "on" and "off" switching of process rates may result in numerical instabilities, causing the model to "hang", i.e. cease calculating (Dold *et al* 1991).

The problem of numerical instability can be overcome by multiplying the process rate with a *switching function* in the form of a Monod Equation (*cf* Eq 4.101), instead of specifying a limiting oxygen concentration. A typical formulation for an aerobic reaction would be (Sykes *et al* 1978, Bedford *et al* 1983, Dold *et al* 1991):

$$\rho = \rho_{(aerobic)} \frac{O}{O + K_o} \qquad (4.93)$$

ρ = reaction rate

$\rho_{(aerobic)}$ = reaction rate under fully aerobic conditions

O = oxygen concentration (mg l^{-1})

K_o = aerobic switching constant (mg l^{-1}).

The aerobic switching constant, K_o, is similar to the Monod half-saturation coefficient (Eq 4.101), i.e. it is the oxygen concentration where the aerobic reaction rate is equal to half the reaction rate under fully aerobic conditions.

Similarly, a typical formulation of an anaerobic reaction would be (Sykes *et al* 1978, Dold *et al* 1991):

$$\rho = \rho_{(anaerobic)} \frac{K_o}{K_o + O} \qquad (4.94)$$

ρ = reaction rate

$\rho_{(anaerobic)}$ = reaction rate under fully anaerobic conditions

O = oxygen concentration (mg l^{-1})

K_o = anaerobic switching constant (mg l^{-1}).

In this case, K_o is the oxygen concentration where the anaerobic reaction rate is equal to half the reaction rate under fully anaerobic conditions.

By linking the reaction rate to an aerobic/anaerobic switching function, a mathematically continuous function is obtained, which should eliminate problems with numerical instability as discussed above. Although the switching function method requires specification of extra coefficients (aerobic/anaerobic K_o), this appears to be

the best method to account for the effect of the aerobic/anaerobic state of the water on reaction rates.

4.4.2 Formulation of microbial decay of organic matter

Microbial decay of organic matter has been formulated in two ways, simple first-order decay, and simultaneous first-order decay (EPA 1985).

A simple first-order formulation is as follows (Jørgensen 1980):

$$r_{bio} = r_{bio,max} \cdot CD \cdot f(t) \qquad (4.95)$$

r_{bio} = rate of decay (mg l^{-1} $24h^{-1}$)
$r_{bio,max}$ = maximum specific rate of decay (mg l^{-1} $24h^{-1}$)
CD = concentration of detritus carbon (mg l^{-1})
f(T) = temperature function.

In formulating microbial decay of organic matter as simultaneous first-order decay, cognisance is given to the fact that decay takes place in two steps (Jørgensen 1980, Mann 1988). Organic matter is divided into a particulate and dissolved fraction, with each fraction being degraded at a specific rate according to first-order kinetics (EPA 1985). A typical two-step formulation, distinguishing between particulate and dissolved BOD[8], is (EPA 1985):

[8] Many formulations express detritus concentration as a biological oxygen demand (BOD), which means that a change in detrital concentration will be reflected as a change in dissolved oxygen concentration (see discussion in paragraph 3.4.3).

$$dDO/dt = k_1 L_{sol} + k_2 L_{det} \quad (4.96)$$

dDO/dt	=	change in dissolved oxygen concentration due to microbial decay of organic matter (mg l^{-1})
k_1, k_2	=	decay rates for BOD fractions
L_{sol}	=	soluble BOD (mg l^{-1})
L_{det}	=	particulate BOD (mg l^{-1}).

The effect of temperature on the rate of BOD decay can be expressed by a temperature function as given in Eq 4.92. Also, the rate of decay is much faster under aerobic than under anoxic conditions (see paragraph 3.4.3)[9], thus the rate of decay should be linked to an aerobic switching function (*cf* Eq 4.93).

Conflicting statements are given in the literature regarding the effectiveness of formulations describing detrital decay. According to some authors (Jørgensen 1976, Jørgensen 1980, Orlob 1983) a simple first-order formulation of detrital decay appears to be sufficient in most cases. However, Martone (1976) did a study of BOD kinetic models and found that simple first-order kinetics did not universally describe observed BOD data. Although two-step formulations of detrital decay provided a better statistical fit in some cases, they have a certain measure of empiricism and have not been shown to be universally applicable (EPA 1985).

In literature on lakes and reservoirs, no formulations could be found that take the regeneration of particulate BOD during the decay of dissolved BOD into account.

In paragraph 3.4.3 an analogy was drawn between the death-regeneration concept used in modelling of the activated sludge process, and Mann's concept of regeneration of particulate BOD during microbial decay of dissolved organic matter

[9] In the absence of oxygen, nitrate can be used as an electron acceptor, but the rate of the nitrogen redox reaction is much slower.

in lakes and reservoirs. In Section 5.3.3.2 this analogy is used in formulating microbial decay in lakes and reservoirs.

4.4.3 Formulation of the processes that affect algal concentration.

Algal concentration is the sum of processes leading to algal growth, and processes leading to algal loss. Algal growth is dependant on light (i.e. the process of photosynthesis) and nutrients (i.e. the process of nutrient uptake), with temperature having a modifying effect (James 1993). Processes that will contribute to a decrease in algal concentration are hydraulic washout, sedimentation, mortality, respiration, and predation.

4.4.3.1 Formulation of the process of photosynthesis:

Formulation of the process of growth due to photosynthesis is one of the most complex aspects of lake modelling, as the rate of photosynthesis depends on the underwater light intensity, which is controlled by a number of factors such depth, water colour, turbidity and length of day (James 1993). This paragraph deals only with the formulation of the process of photosynthesis as a function of light intensity; formulation of the factors that affect light intensity is discussed in paragraph 4.4.5.

Generally, photosynthesis can be related to light intensity by the following basic equation (James 1993):

$$P = P_{max}\frac{I}{I_k}\exp\left(1 - \frac{I}{I_k}\right) \qquad (4.97)$$

P = rate of photosynthesis (g m^{-3} d^{-1})

P_{max} = maximum rate of photosynthesis (g m^{-3} d^{-1})

I = light intensity (μE m^{-2} s^{-1})

I_k = optimum light intensity corresponding to P_{max} (μE m^{-2} s^{-1}) (see Fig 3.6).

Orlob (1983) quotes a number of formulations for photosynthesis that range from very simple (Shelef *et al* 1972) to more complex (Jørgensen 1976):

Shelef *et al* 1972:

$$f(I) = 1 - \exp\left(\frac{I}{IK}\right) \qquad (4.98)$$

f(I) = rate of photosynthesis (g m^{-3} d^{-1})
I = irradiance*
I_k = light saturation parameter*[10].

Jørgensen (1976) incorporates the effect of depth and phytoplankton concentration on light intensity in the formulation for photosynthesis. (It is also possible to formulate these effects separately (see paragraph 4.4.5)).

$$Light = \frac{S}{(\alpha + \beta \cdot CA)V} \ln\left(\frac{I_0 + KI}{I_0 \cdot e^{((-\alpha - \beta \cdot CA)(\frac{V}{S}))} + KI}\right) \qquad (4.99)$$

Light = effect of light on algal growth rate (photosynthesis)
S = surface area of the lake (m^2)
α = extinction coefficient of water (m^{-1})
ß = specific extinction coefficient of phytoplankton (m^2 g^{-1})
CA = phytoplankton concentration (mg l^{-1})
V = volume of lake (m^3)
I_0 = light intensity at the lake surface (kcal m^{-2} 24 h^{-1})
KI = Michaelis constant for light intensity (kcal m^{-2} 24 h^{-1}).

[10] * denotes that various units have been given for the variable indicated.

Several of the formulations quoted by Orlob (1983), as well as the formulation by Megard *et al* (1984) make provision for the effect of photo inhibition on photosynthesis at high irradiances:

Megard *et al* (1984):

$$P(I) = \frac{\upsilon I}{K_1 + I + \frac{I^2}{K_2}} \qquad (4.100)$$

$P(I)$	=	specific rate of photosynthesis (mmol O_2 mg $chla^{-1}$ h^{-1})
υ	=	theoretical maximum rate of photosynthesis (mmol O_2 mg $chla^{-1}$ h^{-1})
I	=	photosynthetically active irradiance (Einstein m^{-2} h^{-1})
K_1	=	Michaelis constant for light limited growth (Einstein m^{-2} h^{-1})
K_2	=	light inhibition coefficient (Einstein m^{-2} h^{-1}).

4.4.3.2 Formulation of nutrient uptake and algal growth rate:

The two concepts describing nutrient uptake and algal growth rate have been identified as the *Monod* concept, and the *Droop* concept (See paragraph 3.4.4.2). The Monod concept treats nutrient uptake and algal growth as a single process under steady state conditions and has been widely used for many years (Orlob 1983, see discussion in paragraph 3.4.4.2). The equation that describes the Monod process was derived from the Michaelis-Menten formulation of biochemical enzyme kinetics, and is commonly known as the *Monod Equation* (Orlob 1983, Reynolds 1984, James 1993):

$$\mu = \mu_{max} \frac{S}{K_s + S} \qquad (4.101)$$

μ = rate of growth with nutrients limitation i.e. specific growth rate (day^{-1})

μ_{max} = rate of growth in absence of nutrients limitation, i.e. maximum growth rate (day^{-1})

S = dissolvevd nutrient concentration (mg l^{-1})

K_s = half-saturation constant (mg l^{-1}).

The half-saturation constant K_s is the nutrient concentration where the specific growth rate equals half the maximum growth rate (Fig 3.9), i.e. when

$$\mu = 1/2\ \mu_{max},$$

then

$$K_s = S$$

A disadvantage of the Monod concept is that it does not make provision for the ability of algae to store nutrients in excess of their immediate needs (luxury uptake), and therefore it tends to predict the end of an algal bloom prematurely.

This shortcoming can be rectified by formulating nutrient uptake and algal growth in two steps (Droop 1983, James 1993). Using phosphorus uptake as an example of nutrient uptake; the kinetics of phosphorus uptake rate has been the subject of numerous laboratory studies (Reynolds 1984), and the available data indicate that, generally, phosphorus uptake can be formulated by a Monod type equation (*cf* Eq 4.101):

$$U = U_{max} \frac{Q_m - Q}{Q_m - K_Q}\left(\frac{S}{K_s + S}\right) \quad (4.102)$$

U = specific uptake rate (day^{-1})

U_{max} = maximum specific uptake rate (day^{-1})

Q_m = maximum nutrient concentration that can be stored in the algal cell (mg nutrient (mg chla)$^{-1}$)

Q = nutrient concentration in the algal cell (mg l^{-1})

K_Q = minimum nutrient concentration in algal cell required for algal growth (mg nutrient (mg chla)$^{-1}$)

S = nutrient concentration in reservoir water (mg l^{-1})

K_s = half-saturation coefficient for nutrient uptake (mg l^{-1}).

Incorporation of a maximum intracellular nutrient concentration in the above equation for nutrient uptake means that the rate of nutrient uptake depends on both external and internal nutrient concentrations, with the uptake rate being greatest when intracellular nutrient concentration Q equals the minimum intracellular nutrient concentration K_Q. The uptake rate decreases as the intracellular concentration approaches Q_m, the maximum intracellular nutrient concentration (Lehman *et al* 1975).

Growth rate is formulated as a function of intracellular nutrient concentration (Droop 1973):

$$\mu = \mu_{max}\left(\frac{Q - K_Q}{Q}\right) \quad (4.103)$$

μ = specific growth rate (day^{-1})

μ_{max} = maximum specific growth rate (day^{-1})

Q = intracellular nutrient concentration (mg l^{-1})

K_Q = minimum nutrient concentration in algal cell required for algal growth (mg nutrient (mg chla)$^{-1}$).

Jørgensen (1976) tested two models, one based on Monod kinetics, and the other based on the Droop concept, and also found that the model based on the Monod concept tend to underpredict algal concentration. Simulations obtained with the model based on the Droop concept were in better agreement with the observed, probably because the Droop concept is more in accordance with the actual physiology of phytoplankton (Jørgensen 1980).

4.4.3.3 Formulation of the temperature effect on algal growth rate:

According to Orlob (1983), the effect of temperature on algal growth rate should be modelled realistically, else large discrepancies can arise between simulated and observed algal concentrations. Orlob (1983) gives a comprehensive list of equations relating the effect of temperature to algal growth rate. Most of these incorporate an optimum temperature for algal growth. A few of the equations that are considered most representative are given below, the reader is referred to Orlob (1983), as well as Jørgensen (1980) for a more complete list of temperature equations.

The formulation of Lehman *et al* (1975) considers an optimum, maximum, and minimum temperature for algal growth:

$$K(T) = K_{opt}\exp\left[-2.3\,\frac{(T - T_{opt})^2}{(T_{max} - T_{opt})^2}\right] \quad \text{for} \quad T > T_{opt} \qquad (4.104)$$

and

$$K(T) = K_{opt}\exp\left[-2.3\,\frac{(T_{opt} - T)^2}{(T_{opt} - T_{min})^2}\right] \quad \text{for} \quad T \leq T_{opt} \tag{4.105}$$

$K(T)$ = temperature coefficient at ambient temperature

K_{opt} = temperature coefficient at optimum temperature

T_{opt} = optimum temperature for algal growth (°C)

T = ambient water temperature (°C)

T_{max} = upper temperature for where algal growth rate has declined to 10% of the maximum growth rate (°C)

T_{min} = lower temperature where algal growth rate has declined to 10% of the maximum growth rate (°C).

The formulation of Jørgensen (1976) does not consider a maximum or minimum temperature explicitly:

$$K(T) = K_{opt}\exp\left(-2.3\left|\frac{T - T_{opt}}{K_T}\right|\right) \tag{4.106}$$

$K(T)$ = temperature coefficient at ambient temperature

K_T = constant

T_{opt} = optimum temperature for algal growth (°C)

T = ambient water temperature (°C).

The formulation of Straškraba (1976) provides for the eventuality that the optimum temperature for growth will change under slowly-changing ambient water temperature changes:

$$K(T) = K(T_{opt}).\ exp[-K(T_{opt} - T)^2] \quad (4.107)$$

$$T_{opt} = T + 28\ exp(-0.115T) \quad (4.108)$$

$K(T)$ = temperature coefficient at ambient temperature
T_{opt} = optimum temperature for algal growth (°C)
T = ambient water temperature (°C).

4.4.3.4 Formulation of the processes that decrease algal concentration:

In paragraph 3.4.4.4 the most important processes that lead to a decrease in algal concentration were identified as hydraulic washout, sedimentation, mortality, respiration, and predation.

Regarding hydraulic washout, no specific formulation for hydraulic washout could be found. Apparently it is usually modelled as part of the entrainment that occurs when water is discharged from the reservoir.

Regarding sedimentation, sinking of algal cells is a function of shape, size, specific gravity, and the viscosity and turbulence of the surrounding water (Orlob 1983). Formulation of the sinking rate is complicated by the irregular shape and size of algal cells, and the fact that some algae can control their buoyancy. Even though it may be an over-simplification, most models formulate sinking rate as a first-order reaction (Orlob 1983, James 1993):

$$S = K_{sed}N \quad (4.109)$$

S = rate of sedimentation (m day^{-1})
K_{sed} = sedimentation coefficient
N = algal concentration (mg l^{-1}).

Regarding loss of algae through mortality, the rate of mortality may be temperature dependant (Jørgensen 1980). Usually it is sufficient to approximate mortality by a first-order reaction (Orlob 1983):

$$M = K_m N \qquad (4.110)$$

M = mortality rate (mg l^{-1} day^{-1})
K_m = mortality coefficient (day^{-1}).

If the effect of temperature on mortality is taken into account, the above expression becomes:

$$M = K_m f(t) N \qquad (4.111)$$

$f(T)$ = temperature function (*cf* Eq 4.92)
N = algal concentration (mg l^{-1}).

Similar to mortality, the rate of respiration rate can be formulated as a first-order reaction that increases with temperature (Jørgensen 1980, Orlob 1983, EPA 1985):

$$R = K_r f(T) \qquad (4.112)$$

R = respiration rate (mg l^{-1} day^{-1})
K_r = respiration coefficient (day^{-1})
$f(T)$ = temperature function (same as in Eq 4.111 above).

A more complicated formulation of respiration rate is given by Lehman *et al* (1975), taking into account the effect of temperature, as well as the effect of varying intracellular nutrient levels, on respiration rate:

$$R = R_{max}\left(\frac{C}{C_m N}\right) N\, f(T) \qquad (4.113)$$

R	=	respiration rate (mg l^{-1} day^{-1})
R_{max}	=	maximum respiration rate at optimum temperature (mg l^{-1} day^{-1})
C	=	intracellular carbon concentration (μmoles C $cell^{-1}$)
C_m	=	maximum intracellular carbon concentration (μmoles C $cell^{-1}$)
N	=	algal concentration (mg l^{-1})
f(T)	=	temperature function (Eq 4.92).

Regarding decrease of algal concentration by predation, in lakes and reservoirs zooplankton grazing may have a limiting effect on algal blooms (Orlob 1983). Both Orlob (1983) and Jørgensen (1980) quote a number of formulations for zooplankton grazing. The formulation that seems to be most in accordance with observed behaviour is that of Steele (1974), since it specifies a threshold algal concentration below which zooplankton grazing ceases:

$$Chla_t = GRZ + MYZ\frac{PHYT - KTR}{KZ + PHYT}ZOO \qquad (4.114)$$

$Chla_t$	=	threshold concentration (g m^{-3} day^{-1})
GRZ	=	zooplankton grazing rate (g m^{-3} day^{-1})
MYZ	=	growth rate of zooplankton (day^{-1})
	=	MYZMAX.f(T)
MYZMAX	=	maximum growth rate of zooplankton (day^{-1})
f(T)	=	temperature function
PHYT	=	algal concentration (g m^{-3})
KTR	=	threshold concentration for grazing (g m^{-3})
ZOO	=	zooplankton concentration (g m^{-3}).

4.4.4. Formulation of the processes that affect availability of nutrients.

The processes that affect nutrient availability have been identified in paragraph 3.4.5. Vertical transport of nutrients in a lake is described by the one-dimensional advection-diffusion equation (Eq 4.4), which requires that the processes affecting nutrient availability be formulated in terms of nutrient sources or sinks. Phosphorus and nitrogen have been identified as the most important nutrients for algal growth (see Chapter 3).

4.4.4.1 Formulating the availability of phosphorus:

Phosphorus occurs in several forms in the ecosystem (see paragraph 3.4.5.1). Dissolved phosphate (PO_4-P) is the only form of phosphorus that can be readily assimilated by algae, and as the aim of this study is to address the problem of eutrophication, formulation of the availability of phosphorus will be done in terms of dissolved phosphate.

The concentration of phosphate in water will be decreased by uptake of phosphate by algae, and zooplankton grazing. It will be increased by release of phosphate into the water via processes such as algal mortality and respiration, and detrital decay. Also, interaction at the sediment-water interface may cause phosphate to be either released or adsorbed by the sediments.

The effect of uptake by algae:

The decrease in phosphate concentration due to uptake of phosphate by algae is expressed by Eq 4.102, except that in this case it should be regarded as a loss term:

$$U = U_{max} \frac{Q_m - Q}{Q_m - K_Q}\left(\frac{S}{K_s + S}\right) \qquad (4.115)$$

U	=	specific phosphate uptake rate (day^{-1})
U_{max}	=	maximum specific phosphate uptake rate (day^{-1})
Q_m	=	maximum phosphate concentration that can be stored in the algal cell (mg P (mg chla)$^{-1}$)
Q	=	intracellular phosphate concentration (mg l^{-1})
K_Q	=	minimum intracellular phosphate concentration required for algal growth (mg P (mg chla)$^{-1}$)
S	=	phosphate concentration in reservoir water (mg l^{-1})
K_s	=	half-saturation coefficient for phosphate uptake (mg l^{-1}).

The effect of algal mortality:

This constitutes a source of phosphate - when algal cells die, excess nutrients that have been stored in the cell during luxury uptake, are released. (Organically bound phosphorus, i.e. the phosphorus corresponding to the minimum intracellular concentration, is released during detrital decay (Jørgensen 1980)). The only formulation of phosphate release via algal mortality that could be found is that of Riley and Stefan (1988):

$$\frac{\partial P}{\partial t} = K_m \theta^{(T-20)}(Q - K_Q CHLa) \quad (4.116)$$

$\partial P/\partial t$ = increase in phosphorus concentration with time
K_m = mortality coefficient (day^{-1})
θ = Arrhenius temperature coefficient
T = ambient water temperature (°C)
Q = intracellular phosphorus concentration (mg P (mg chla)$^{-1}$)
K_Q = minimum intracellular phosphorus concentration required for growth (mg P (mg chla)$^{-1}$).

The effect of excretion:

Excretion of phosphorus by phytoplankton will cause an increase in phosphorus concentration also. Generally, excretion and respiration are combined and modelled as a single term (EPA 1985), therefore phosphorus excretion can be formulated as follows (Riley and Stefan 1988):

$$\frac{\partial P}{\partial t} = K_r \theta^{(T-20)} Q \quad (4.117)$$

$\partial P/\partial t$ = increase in phosphorus concentration with time
K_r = respiration coefficient (day^{-1})
θ = Arrhenius temperature coefficient
T = ambient water temperature (°C)
Q = intracellular phosphorus concentration (mg P (mg chla)$^{-1}$).

Detrital decay:

During detrital decay organically bound phosphorus, i.e. the phosphorus corresponding to the minimum intracellular concentration, is released (Jørgensen 1980). A typical formulation of detrital decay as a source of dissolved phosphate is as follows (Jørgensen 1976):

$$\frac{dPs}{dt} = K4\ DP\ K6^{(T-20)} \qquad (4.118)$$

dPS/dt	=	change in dissolved phosphate concentration due to detrital decay
K4	=	biodegradation rate of detritus (h^{-1})
DP	=	detritus phosphorus (intracellular phosphorus) (mg l^{-1})
K6	=	Arrhenius temperature coefficient for detrital decay
T	=	water temperature (°C).

However, as was discussed in paragraph 3.4.3, the rate of detrital decay is much faster under aerobic than under anoxic conditions, and therefore Eq 4.118 would have to multiplied by an aerobic switching function also (*cf* Eq 4.93).

The role of the bottom sediments:

Regarding the role of the bottom sediments in the availability of dissolved phosphate, as was discussed in paragraph 3.4.5.1, traditionally, aerobic sediments have been considered a sink for phosphates, whereas anaerobic sediments have been considered a source of phosphate (Sly 1986). The actual situation is much more complex, but often the complexity of sediment modelling has to be limited due to lack of sediment data for calibration, spatial inhomogeneity of sediments, or uncertainty in determining sedimentation (Van der Molen 1991). Thus, according to Jørgensen (1980), Jørgensen *et al* (1982), Orlob (1983), and James (1993) most models formulate nutrient exchange with bottom sediment as a constant release rate, or as a simple first-order reaction:

Constant release rate (Riley 1988):

$$\Delta P = \pm PR * A \qquad (4.118)$$

ΔP = change in phosphate concentration due to sediment exchange of phosphate (mg l^{-1})
$+PR$ = sediment release rate of phosphate (g m^{-2} d^{-1})
$-PR$ = sediment adsorption rate of phosphate (g m^{-2} d^{-1})
A = sediment interface (m^2).

First-order reaction (Orlob 1983):

$$REL = RELK \cdot SETTL \qquad (4.120)$$

REL = sediment release rate of phosphate (g m^{-2} d^{-1})
RELK = sediment release coefficient
SETTL = rate of removal of phosphate by settling (g m^{-3} d^{-1}).

The release of phosphates from the bottom sediment is much slower under aerobic than under anaerobic conditions, and in some cases, phosphate is adsorbed by the bottom sediment under aerobic conditions (*cf* paragraph 3.4.5.1). As many South African dams experience anaerobic conditions during the stratified period, the above formulations for sediment release of phosphate would have to be linked to an aerobic/anaerobic switching function (*cf* Eq 4.93 and 4.94) to simulate sediment phosphate release/adsorption in South African dams.

Kamp-Nielsen (1980, 1981) tested the effect of eight sediment submodels of different complexity on overall model performance. He concluded that, for hydraulic retention times of less than one year, overall model performance is independent of the complexity of the sediment submodel, except for the submodel using a constant release rate, which he rejects as too simple.

Jørgensen *et al* (1982) agree with Kamp-Nielsen's finding that a constant release rate model is too simple. They also tested two sediment submodels of varying complexity and came to the conclusion that the more complex submodel did not improve overall model performance, unless grazing in the sediment during a certain period in spring is included. They recommend that, for lakes with a retention time greater than one year, the minimum requirement would be the submodel shown schematically in Figure 4.2.

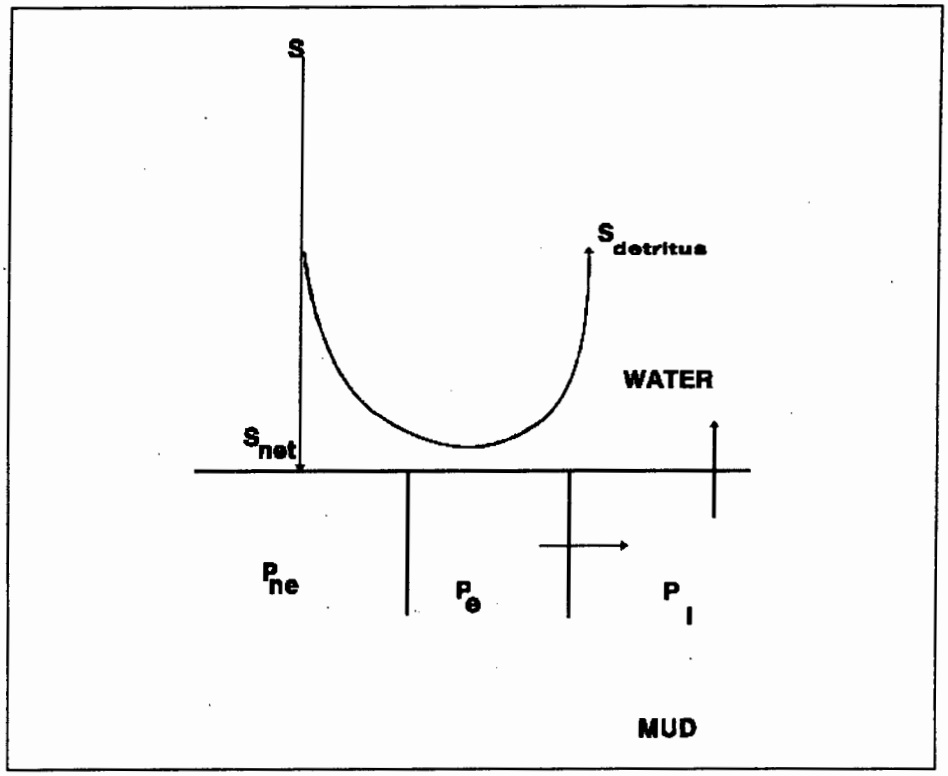

Figure 4.2
Interaction of phosphate with the bottom sediment (Jørgensen *et al* 1982).

The key to the symbols in Fig 4.2 is as follows:

S = sedimentation, S_{net} = net sedimentation, $S_{detritus}$ = sedimentation of detritus, P_{ne} = non-exchangeable phosphate in the bottom sediment, P_e = exchangeable phosphate in the bottom sediment, P_i = phosphate in the interstitial water, P_s = dissolved phosphate in water.

According to the submodel shown in Figure 4.2 the rate of nutrient exchange decreases with decreasing nutrient concentration in the sediment, and a distinction is made between exchangeable and unexchangeable nutrients in the bottom sediment. Thus the contribution of phosphorus exchange at the sediment-water interface to the concentration of soluble phosphorus in the overlying water is formulated as follows (Jørgensen 1976):

$$\frac{dPSS}{dt} = \frac{1.2(Plw - PS) - 1.7}{1000} \cdot \frac{T + 273}{280} \cdot \frac{S}{V} \qquad (4.121)$$

dPS/dt = change in soluble phosphorus concentration in lake water (mg l^{-1})
Plw = phosphorus in the interstitial water in the sediment (mg l^{-1})
T = temperature (°C)
S = surface area of the lake (m^2)
V = volume of the lake (m^3).

The phosphorus in the interstitial water in the sediment, Plw, is given by the following (Jørgensen 1976):

$$\frac{dPlw}{dt} = \frac{K5 \cdot PE \cdot K6^{(T-20)}}{1 - DMU} - \frac{1.2(Plw - PS) - 1.7}{LUL(1 - DMU)} \cdot \frac{T + 273}{280} \qquad (4.122)$$

Plw = phosphorus in the interstitial water in the sediment (mg l^{-1})
K5 = biodegradation rate of organic phosphorus in the sediment
= 0.0018 per 24 h
PE = exchangeable phosphorus in upper layer of sediment (mg l^{-1})
K6 = Arrhenius temperature coefficient for biodegradation
DMU = dry matter in upper layer of sediment (kg kg^{-1})
PS = soluble phosphorus in lake water (mg l^{-1})
LUL = upper unstabilized layer (100 mm)
T = temperature (°C).

Exchangeable phosphorus in the upper layer of sediment (PE in Eq 4.122 above) is formulated as (Jørgensen 1976):

$$\frac{dPE}{dt} = \frac{SA \cdot CA \cdot V \cdot 10^3}{f \cdot PP \cdot LUL \cdot S} - K5 \cdot PE \cdot K6^{(T-20)} + \frac{SA \cdot DP \cdot V \cdot 10^3}{f \cdot LUL \cdot S} \quad (4.123)$$

PE	=	exchangeable phosphorus in upper layer of sediment (mg l^{-1})
SA	=	phytoplankton settling rate (h^{-1})
CA	=	phytoplankton concentration (mg l^{-1})
V	=	volume of the lake (m^3)
f	=	ratio of total phosphorus to exchangeable phosphorus in the sediment
PP	=	phosphorus content in phytoplankton
LUL	=	upper unstabilized layer (100 mm)
S	=	surface area of the lake (m^2)
K5	=	biodegradation rate of organic phosphorus in the sediment
	=	0.0018 per 24 h
K6	=	temperature coefficient for biodegradation.

Although some of the parameters in the sediment submodel represented in Eq 4.121 to 4.123 need to be measured by means of field examinations, these measurements are relatively easy. Also, the amount of data required is limited, which means that this submodel should be suitable for most lake/reservoir studies (Jørgensen *et al* 1982). However, the biodegradation rate of organic phosphorus in the sediment possibly will depend on the aerobic/anaerobic state of the sediment, and therefore the biodegradation rate may have to be linked to an aerobic/anaerobic switching function (*cf* Eq 4.93 and 4.94).

4.4.4.2 Formulating the availability of nitrogen:

Nitrogen concentration in water will be affected by processes such as uptake of nitrogen by algae, nitrogen fixation, nitrification, denitrification, ammonification, as well as the processes that occur at the sediment water interface (*cf* paragraph 3.4.5.2).

The effect of uptake by algae:

In natural waters nitrogen can be present in many forms (*cf* paragraph 3.4.5.2), but algal uptake of nitrogen occurs almost exclusively from the nitrate-nitrite and ammonium fraction. Nitrate and nitrite have to be reduced before it can be assimilated, thus, energetically, ammonium is the most favourable source of nitrogen. For instance, it has been observed that algae will assimilate ammonium in preference to nitrate, provided the ambient ammonium concentration exceeds 7-14 μg l^{-1} (Bienfang 1975, Bingham *et al* 1984, Reynolds 1984). Jørgensen (1980) quotes several formulations for nitrate uptake that make provision for the preferential uptake of ammonia:

Conway (1974)

$$UN(NIT) = UNMAX(NIT) - 0.009 \cdot (NH_4) \qquad (4.124)$$

Dugdale *et al* (1971)

$$UN(NIT) = UNMAX(NIT) - 0.0106(NH_4) + 0.000714(NIT) \qquad (4.125)$$

Najarian *et al* (1975)

$$UN(NIT) = UNMIN(NIT) + \left(1 - \frac{NIT}{NH_4L}\right) \cdot UNMAX(NIT) - UNMIN(NIT) \qquad (4.126)$$

$UN(NIT)$ = uptake rate of nitrate (day^{-1})

(NH_4) = ammonium-N concentration (mg l^{-1})

(NIT) = nitrate-N concentration (mg l^{-1})

NH_4L = threshold limit concentration of ammonium (mg l^{-1}).

UNMAX(NIT) and UNMIN(NIT) are unspecified, but possibly refers to maximum and minimum uptake rates of nitrate.

The formulation of Scavia (1980), as well as Riley and Stefan (1988), for nitrate uptake is in the form of a Michaelis-Menten equation, with the preferential uptake of ammonium reflected in the half-saturation constant:

$$U_{NO} = U' \left(1 - \frac{NH}{HSCNH + NH}\right) \tag{4.127}$$

with

$$U' = U_{max} \left(\frac{CHLa\ N_{max} - N_c}{CHLa\ (N_{max} - N_{min})}\right) \left(\frac{NH + NO}{HSCN + NH + NO}\right) \tag{4.128}$$

U_{NO} = nitrate uptake rate (day^{-1})
U' = nitrogen uptake rate (day^{-1})
NH = ammonium concentration ($mg\ l^{-1}$)
HSCNH = ammonium preference constant ($mg\ l^{-1}$)
U_{max} = maximum nitrogen uptake rate (day^{-1})
CHLa = chlorophyll-a concentration ($mg\ l^{-1}$)
N_{max} = maximum intracellular nitrogen concentration (mg N (mg chla)$^{-1}$)
N_{min} = minimum intracellular nitrogen concentration required for algal growth (mg N (mg chla)$^{-1}$)
NO = nitrate concentration ($mg\ l^{-1}$)
HSCN = half saturation constant for nitrogen uptake ($mg\ l^{-1}$).

Riley and Stefan (1988) then formulate ammonium uptake rate as:

$$U_{NH} = U' \left(\frac{NH}{HSCNH + NH}\right) \tag{4.129}$$

The notation of the symbols is as specified above.

Some blue-green algae such as *Anabaena* have the ability to fix atmospheric nitrogen when nitrogen in the water becomes depleted. The rate of nitrogen fixation therefore increases with decreasing inorganic nitrogen concentration. Also, a high concentration of total phosphorus seems to be necessary (Jørgensen 1980).

Gargas (1976) formulated nitrogen fixation as a Michaelis-Menten type equation:

$$NFIX = KNFIX \cdot \left(1 - \frac{NS}{KN + NS}\right) \cdot PHYT(N) \qquad (4.130)$$

NFIX	=	rate of nitrogen fixation (g m^{-3} day^{-1})
KNFIX	=	nitrogen fixation coefficient (day^{-1})
NS	=	concentration of soluble inorganic nitrogen (g m^{-3})
KN	=	half-saturation constant for uptake of soluble inorganic nitrogen (g m^{-3})
PHYTN	=	concentration of nitrogen fixing algae (g m^{-3}).

The formulation of Jørgensen (1980) is more empirical, as it requires measurement of the concentration of nitrogen fixing algae, but it does make provision for the effect of phosphorus on nitrogen fixation:

$$NFIX = KNF(5 \cdot PS - NS)\, NPHYT \qquad (4.131)$$

for $5PS > NS$, and

$$NFIX = 0 \qquad (4.132)$$

for $5PS \leq NS$

NFIX	=	rate of nitrogen fixation (g m^{-3} day^{-1})
KNF	=	temperature dependent rate constant
PS	=	soluble phosphorus concentration (g m^{-3})
NS	=	soluble inorganic nitrogen concentration (g m^{-3})
NPHYT	=	observed concentration of nitrogen fixing algae (g m^{-3}).

The contribution of algal mortality:

When algal cells die, excess nutrients that have been stored in the cell during luxury uptake are released. In the cell, nitrogen is stored as ammonia. The release of ammonia upon algal mortality can be formulated in the same way as phosphate release (Eq 4.117):

$$\frac{\partial N}{\partial t} = K_m \theta^{(T - 20)}(Q - K_Q CHLa) \qquad (4.133)$$

$\partial N/\partial t$	=	increase in nitrogen concentration with time
K_m	=	mortality coefficient (day^{-1})
θ	=	Arrhenius temperature coefficient
T	=	ambient water temperature (°C)
Q	=	intracellular ammonium concentration (mg N (mg chla)$^{-1}$)
K_Q	=	minimum intracellular ammonium concentration required for growth (mg P (mg chla)$^{-1}$).

The contribution of excretion:

The nitrogen concentration in a layer will be increased also by excretion of ammonia by algae during respiration. Again, this can be formulated similar to release of phosphate by excretion:

$$\frac{\partial N}{\partial t} = K_r \theta^{(T-20)} Q \qquad (4.134)$$

$\partial N/\partial t$ = increase in nitrogen concentration with time

K_r = respiration coefficient (day^{-1})

θ = Arrhenius temperature coefficient

T = ambient water temperature (°C)

Q = intracellular ammonium concentration (mg N (mg chla)$^{-1}$).

Detrital decay:

During detrital decay organically bound ammonium, i.e. the ammonium corresponding to the minimum intracellular concentration, is released. This can be formulated analogous to phosphate release during detrital decay:

$$\frac{dN}{dt} = K4 \; DN \; K6^{(T-20)} \qquad (4.135)$$

dN/dt = change in ammonium concentration due to detrital decay (mg l^{-1})

K4 = biodegradation rate of detritus (h^{-1})

DP = detritus nitrogen (intracellular ammonium)(mg l^{-1})

K6 = Arrhenius temperature coefficient for detrital decay

T = water temperature (°C).

The rate of detrital decay is much faster under aerobic than under anoxic conditions, and therefore Eq 4.135 would have to multiplied by an aerobic switching function also (*cf* Eq 4.93).

The role of the bottom sediments:

The nitrogen processes that occur in the bottom sediments are quite complex (see discussion in paragraph 3.4.5.2), but, as with phosphorus, most models simulate the exchange of nitrogen at the sediment-water interface as a constant release rate, or as a simple first-order reaction.

Jacobsen *et al* (1975) do not formulate the sediment release of ammonia and nitrate separately, but give an empirical equation for the sediment release of nitrogen, taking aerobic as well as anaerobic conditions into account, as well as the effect of temperature:

$$\begin{aligned} N_r &= (3.9 \cdot S_N + 0.13)e^{0.134t} \quad \text{(aerobic)} \\ &= (4.0 \cdot S_N + 0.08)e^{0.151t} \quad \text{(anaerobic)} \end{aligned} \tag{4.136}$$

N_r = nitrogen released from sediment

S_N = nitrogen in upper layer of sediment (g l^{-1})

t = temperature in °C.

Jørgensen (1976) used the above empirical formulation for nitrogen release under anaerobic conditions to develop a more detailed submodel for nitrogen release from the sediment:

$$N_r = \frac{4.0 \cdot S_N + 0.08}{1000} \cdot \frac{S}{V} \cdot e^{0.151T} \quad (4.137)$$

$$\frac{dS_N}{dt} = \frac{SA \cdot CA \cdot V}{S \cdot PN \cdot LUL} - \frac{4.0 \cdot S_N + 0.08}{1000 \cdot LUL} \cdot e^{(0.151T)} + \frac{SA \cdot DN \cdot V}{LUL \cdot S} \quad (4.138)$$

S_N = nitrogen in upper layer of sediment (g l^{-1})
S = surface area of the lake (m^2)
V = volume of the lake (m^3)
T = water temperature (°C)
SA = phytoplankton settling rate (h^{-1})
CA = phytoplankton concentration mg l^{-1}
PN = nitrogen content in phytoplankton (mg l^{-1})
LUL = upper unstabilized layer of sediment (100 mm)
DN = detritus nitrogen in lake water (mg l^{-1}).

The above formulation refers to the sediment release of nitrogen under anaerobic conditions and therefore can be used to describe sediment release of ammonia, as only ammonia is released from the sediment under anaerobic conditions. However, due to the empirical nature of Eq 4.137 and 4.138, these should be used with caution.

Nitrification and denitrification:

If ammonia and nitrate are to be modelled as two separate compounds, processes such as nitrification and denitrification must be formulated also. During the process of nitrification, ammonia is nitrified to nitrate (Jørgensen 1980):

$$NH_4^+ + \frac{3}{2}O_2 \leftrightharpoons 2H^+ + NO_2^- + H_2O \qquad (4.139)$$

$$NO_2^- + \frac{1}{2}O_2 \leftrightharpoons NO_3^- \qquad (4.140)$$

The overall reaction is:

$$NH_4^+ + 2O_2 \rightarrow NO_3^- + H_2O + 2H^+ \qquad (4.141)$$

According to Orlob (1983), the most generally applied formulation for nitrification is a first-order kinetic equation, even though nitrification takes place in two steps:

$$NITR = NITRIK \cdot NH_4 \qquad (4.142)$$

NITR = nitrification rate (g m^{-3} day^{-1})
NITRK = nitrification rate coefficient (day^{-1})
NH_4 = concentration of ammonia nitrogen (g m^{-3}).

However, because nitrification is a bacterial reaction, it will be affected by temperature, and therefore the above equation should make provision for the temperature effect. This can be done by multiplying Eq 4.142 with a temperature function (eg Eq 4.92). Also, oxygen is utilized during the nitrification process, i.e. nitrification can take place under aerobic conditions only, therefore Eq 4.142 should be multiplied by an aerobic switching function as well (Eq 4.93).

Regarding the process of denitrification, this is the biochemical reduction of nitrate (or nitrite) to nitrous oxide, and then to nitrogen gas (Jørgensen 1980):

$$NO_3^- \rightarrow NO_2^- \rightarrow N_2O \rightarrow N_2 \qquad (3.143)$$

Jørgensen (1980) and Orlob (1983) quote a detailed Michaelis-Menten type formulation for denitrification. Though the Michaelis-Menten formulation is a more accurate description of the process kinetics, it requires specification of the concentration of denitrifying bacteria (which is generally not known in reservoirs), as well as specification of a greater number of coefficients than would be required for a first-order formulation (Jørgensen 1980, Orlob 1983). A first-order formulation should give a satisfactory description of the process (Jørgensen 1980), though the temperature dependency of the process should be taken into account, as well as the fact that denitrification can take place under anaerobic conditions only. The latter effect can be incorporated into the formulation by means of an anaerobic switching function (*cf* Eq 4.94). A possible formulation for denitrification would be of the following format:

$$\mathrm{DENIT} = \mathrm{DENITK} \cdot \mathrm{NIT}\ f(T) \frac{K_o}{K_o + O} \qquad (4.144)$$

DENIT	=	denitrification rate (g m^{-3} day^{-1})
DENITK	=	denitrification rate constant at 20°C (day^{-1})
NIT	=	nitrate-N concentration (g m^{-3})
f(T)	=	temperature function (Eq 4.110)
K_o	=	switching constant for denitrification
O	=	ambient dissolved oxygen concentration (g m^{-3}).

The switching constant for denitrification depicts the oxygen concentration where the rate of denitrification is equal to half the maximum rate of denitrification, i.e. the rate of denitrification under fully anaerobic conditions.

4.4.5 Formulation of the availability of light.

Even in a homogeneous water body, light is not uniformly distributed, but is absorbed exponentially with depth (see discussion in paragraph 3.4.6). The rate of absorption depends on the turbidity of the water, and can be expressed in terms of an extinction coefficient by means of Beer's Law (Kirk 1983, Henderson-Sellers 1984):

$$I(z) = I_0 e^{(-\eta z)} \qquad (4.145)$$

$I(z)$ = light intensity at depth z
I_0 = incident light intensity
η = total extinction coefficient (m^{-1}).

As the absorption of light is a function of the turbidity of the water, the value of the extinction coefficient will vary between reservoirs and must be determined for each reservoir. The extinction coefficient can be formulated as a simple function of total turbidity, or it can be formulated as a function of the different components that contribute to turbidity and absorption of light in water.

The most elementary formulation of the extinction coefficient is obtained by linking it to Secchi disc depth (which is also is a measure of turbidity). Henderson-Sellers (1984) gives a few expressions of η as a function of Secchi disc depth, for instance:

$$\eta = \frac{1.7}{d} \qquad (4.146)$$

η = extinction coefficient (m^{-1})
d = Secchi disc depth (m).

However, according to Kirk (1983), in waters where a high concentration of particles causes increased light scattering, use of the Secchi disc sometimes gives highly inaccurate values for the total extinction coefficient. The extinction coefficient can be calculated more accurately by taking into account the four components that are responsible for absorption of light in water, i.e. pure water, dissolved yellow pigments, inanimate particular matter and photosynthetic biota. Kirk (1983) gives the following formulation:

$$k_d = k_w + k_g + k_{tr} + k_{ph} \qquad (4.147)$$

k_d = total extinction coefficient (m^{-1})
k_w = contribution of pure water (m^{-1})
k_g = contribution of gilvin (gelbstoff) (m^{-1})
k_{tr} = contribution of tripton (m^{-1})
k_{ph} = contribution of phytoplankton (m^{-1}).

The contribution of phytoplankton, k_{ph}, is given by:

$$k_{ph} = B_c k_c \qquad (4.148)$$

B_c = chlorophyll-a concentration (mg m^{-3})
k_c = specific extinction coefficient per unit phytoplankton concentration (m^2 mg $Chla^{-1}$).

The specific extinction coefficient, k_c, is algal species dependant, and thus will be unique for each reservoir, depending on the composition of algae in the reservoir.

The contribution of tripton, k_{tr}, refers to the contribution of inanimate particulate matter, and thus includes the contribution of total inorganic suspended sediment. The following formulation is given for k_{tr} (Stefan *et al* 1982, Henderson-Sellers 1984):

$$k_{tr} = 0.52\ TSS^{0.63} \quad (4.149)$$

k_{tr} = extinction due to suspended sediment concentration (m^{-1})
TSS = concentration of inorganic suspended sediment (mg l^{-1}).

The concentration of inorganic suspended sediment in a layer can be calculated by Eq 4.4, the one-dimensional advection diffusion equation. Application of this equation requires calculation of the sediment fall velocity. According to Rooseboom (1992) a general equation for sediment fall velocity is:

$$V_{ss} \propto \sqrt{\frac{(\rho_s - \rho)gd}{\rho\ C_D}} \quad (4.150)$$

V_{ss} = sediment fall velocity (m s^{-1})
ρ_s = sediment density (g cm^{-3})
ρ = fluid density (g cm^{-3})
g = gravitational acceleration (cm s^{-2})
d = particle diameter (cm)
C_D = drag coefficient.

In view of the high concentration of inorganic suspended sediment in many South African reservoirs, particular attention should be paid to formulation of sediment fall velocity and the resultant calculation of TSS concentration in a model.

In the next chapter the specific formulation of processes in the original MINLAKE model is compared and evaluated against the general formulations in this chapter.

CHAPTER 5

FORMULATION AND MODIFICATION OF THE MINLAKE MODEL.

5.1 INTRODUCTION.

The problem being addressed in this study is simulation of the eutrophic behaviour of stratified reservoirs in South Africa, i.e in a warm temperate/subtropical climate. To develop a new model from first principles would be a tremendous task, therefore it was decided to assess an eutrophication model called MINLAKE (Minnesota Lake Water Quality Model) as to its applicability to South African reservoirs.

The MINLAKE model was developed by St Anthony Falls Hydraulic Laboratory at the University of Minnesota, USA. It is a one-dimensional model that simulates the following variables on a daily basis:

Water temperature
Mixed layer depth

Concentrations of:

Chlorophyll-a
Total phosphorus
Dissolved phosphate
Detritus as BOD
Inorganic suspended sediment (TSS)
Total dissolved salts (TDS)
Ammonia
Nitrate
Zooplankton.

In this chapter the formulation of the MINLAKE model is compared to, and critically evaluated against, the general formulation of eutrophication models as discussed in Chapter 4. Formulation of the modifications that had to be made to the MINLAKE to enable simulation of the hydrodynamic and water quality behaviour of a typical South African reservoir are discussed also - even before the start of the project it was envisaged that the MINLAKE model may have to be modified, because of climatic differences between South Africa and Minnesota. The climate in the greater part of South Africa can be specified as warm temperate, or even subtropical, whereas the climate in Minnesota is cold temperate.

5.1.2 The structure of the MINLAKE model.

The MINLAKE model is a one-dimensional model and thus it treats the reservoir as being divided into a maximum of 40 horizontal slices. The division is done according to the Eularian approach, i.e. all the slices, except the top slice, are of equal thickness, but varying area. The thickness of the top layer varies to accommodate the change reservoir depth with changing volume (paragraph 3.2.3). Within each layer, dispersion of substances is assumed to be horizontally homogeneous. The area of each layer can vary with depth. Vertical transport of a substance is calculated with the one-dimensional advection-diffusion equation (*cf* Eq 4.4):

$$A_z\left[\frac{\partial C}{\partial t} + v\frac{\partial C}{\partial z}\right] = \frac{\partial}{\partial z}\left[A_z(K + \alpha)\frac{\partial C}{\partial z}\right] \pm \text{sources/sinks} \qquad (5.1)$$

z	=	depth from the surface (m)
A_z	=	cross-sectional area at depth z (m^2)
C	=	concentration or intrinsic property of the fluid such as temperature (mg l^{-1} or °C)
v	=	vertical velocity of a suspended substance (m day^{-1})
	=	0 for dissolved substances and temperature
K	=	vertical turbulent diffusion coefficient (m^2 day^{-1})
α	=	molecular diffusion coefficient (m^2 day^{-1}).

The MINLAKE model is a lake-averaged model, i.e. the simulated value at any depth is taken to be the average of all the observed values taken at different points on the same horizontal plane.

The model can be divided into two parts, hydrodynamic and water quality, and it is possible to simulate only the hydrodynamic behaviour of a reservoir, without taking the water quality response into account. This is possible because the hydrodynamic response has a dominating influence on the water quality behaviour, whereas the effect of the water quality response on the hydrodynamic behaviour is relatively minor. Due to the dominating influence of the hydrodynamics, simulation of the hydrodynamic behaviour must be resolved before the water quality response can be simulated.

5.2 HYDRODYNAMIC FORMULATION OF THE MINLAKE MODEL.

In Chapter 3, the major hydrodynamic processes that take place in a reservoir have been identified as :

- Exchange of heat energy
- Convective mixing
- Advective mixing
- Mixing due to wind action

5.2.1 MINLAKE formulation of exchange of heat energy.

The MINLAKE model formulates the exchange of heat energy according to the surface energy balance theory (*cf* paragraph 4.3.1.1), i.e. the depth profile of temperature is computed from the balance between incoming heat from solar and long-wave radiation, and the outflow of heat through convection, evaporation, and back radiation (Riley 1988):

$$\Delta H = H_{sn} - H_e - H_c - H_b + H_a \quad (5.2)$$

ΔH = surface heat flux (kcal m^{-2} d^{-1})
H_{sn} = net solar radiation (kcal m^{-2} d^{-1})
H_e = evaporative loss (kcal m^{-2} d^{-1})
H_c = convective heat transfer (kcal m^{-2} d^{-1})
H_b = back radiation (kcal m^{-2} d^{-1})
H_a = atmospheric long wave radiation (kcal m^{-2} d^{-1}).

The MINLAKE model does not simulate any heat flux from the water to the bottom sediment. Regarding incoming solar radiation, the model takes cognisance of the fact that some of the incoming solar radiation is reflected at the water surface. The reflected fraction is formulated as follows:

$$r = 0.087 - 6.76 * 10^{-5} H_s + 0.11[1 - \exp(-0.01SS)] \quad (5.3)$$

r = reflected fraction (kcal m^{-2} day^{-1})
H_s = incoming solar radiation (kcal m^{-2} day^{-1})
SS = concentration of inorganic suspended sediment (TSS) in the first layer (mg l^{-1}).

Though Eq 5.3 differs slightly from the formulation found in the literature (Eq 4.7), taking into account the different units of measurement (kcal m^{-2} day^{-1} instead of W m^{-2}), the reflected fraction as calculated with Eq 5.3 is the same as that calculated with Eq 4.7, therefore the above formulation of the reflected fraction was accepted as correct.

Apart from the reflected fraction, the remainder of the incoming solar radiation penetrates deeper into the reservoir, where it is absorbed by water. The MINLAKE model formulates the exponential absorption of radiation according to Beer's Law (Eq 4.8):

$$H(z) = H_{sn} e^{-\eta z} \qquad (5.4)$$

$H(z)$	=	solar radiation at depth z (kcal m^{-2} d^{-1})
H_{sn}	=	net solar radiation (kcal m^{-2} d^{-1})
	=	$(1-r)H_s$
r	=	reflected fraction (kcal m^{-2} d^{-1})
H_s	=	incident solar radiation (kcal m^{-2} d^{-1})
n	=	total extinction coefficient (m^{-1}).

The effect of inorganic suspended sediment (TSS) and algal concentration on light penetration is taken into account by formulating the total extinction coefficient as a function of extinction due to pure water, as well as extinction due to the concentrations of TSS and chlorophyll-a. This is in accordance with the approach found in the literature (*cf* Eq 4.9):

$$\eta = k_w + 0.043SS + k_2 Chla \qquad (5.5)$$

n	=	total extinction coefficient (m^{-1})
k_w	=	extinction coefficient of pure water (m^{-1}) (*cf* Table 3.3)
SS	=	inorganic suspended sediment concentration (mg l^{-1})
k_2	=	extinction coefficient due to chlorophyll-a (m^2 (g chla)$^{-1}$)
Chla	=	chlorophyll-a concentration (mg l^{-1}).

In the model, the extinction coefficient of pure water, k_w, as well as the extinction coefficient due to chlorophyll-a, k_2, must be specified by the user. The concentration of inorganic suspended sediment (TSS) is calculated by the model.

As was discussed in paragraph 4.3.1.1, it has been observed that the fraction of incident radiation absorbed in the surface layer, ß, is greater than that predicted by Beer's Law. The MINLAKE model takes cognisance of this by formulating the net solar

radiation in the surface layer according to Eq 4.10, and the net solar radiation below the surface layer according to Eq 4.11. However, in the original MINLAKE model, ß was given a constant value of 0.4. This value was "hard-wired" into the model, i.e. it could not be changed by the user. As it would be more correct to express ß as a function of the total extinction coefficient (see paragraph 4.3.1.1), the hard-wired value of ß in the original MINLAKE formulation was replaced by the following formulation (cf Eq 4.12):

$$\beta = 0.265 \ln \eta + 0.614 \qquad (5.6)$$

ß = *fraction of the incident solar radiation absorbed in the surface layer*

η = *total extinction coefficient (m^{-1}).*

In the original MINLAKE model the remaining fraction of incident solar radiation after reflection and surface absorption, was hard-wired into model at a constant value of 0.6. This value was replaced by (1-ß) (cf paragraph 4.3.1.1)

The net solar radiation at a given depth below the surface layer is formulated according to Eq 4.13:

$$H(z) = (1-r)(1-\beta)H_s e^{-\eta z} \qquad (5.7)$$

H(z) = net solar radiation at depth z (kcal m^{-2} d^{-1})

r = fraction reflected at the surface

ß = fraction absorbed in the surface layer

H_s = incident solar radiation (kcal m^{-2} d^{-1})

η = total extinction coefficient (m^{-1}).

Regarding the second term on the right hand side of Eq 5.2, *evaporative heat loss*: In the original MINLAKE model it is formulated as follows (Riley 1988):

$$H_e = Lf(W)(e_s - e_a) \qquad (5.8)$$

L	=	latent heat of vaporisation
	=	$597.31 - 0.5631T_w$ (kcal m^{-3})
T_w	=	water temperature (°C)
f(W)	=	wind function
e_s	=	saturated vapour pressure at the water surface
e_a	=	vapour pressure of the air.

Essentially, this formulation is the same as depicted in Chapter 4, Eq 4.14 to 4.16. Formulation of the wind function, f(W), is similar to Eq 4.18:

$$f(W) = cW \qquad (5.9)$$

f(W)	=	wind function
c	=	wind coefficient
W	=	average wind speed *at 10 meter height* (m s^{-1}).

The wind coefficient, c, is analogous to the mass transfer coefficient, N, in Eq 4.18, and must be specified by the user. Also, it is very important to note that the MINLAKE model requires the average wind speed to be measured at 10 meter height, thus the value of the wind coefficient, c, should also be determined at 10 meter height.[1] If the observed wind speed is not measured at 10 meter height, it should be converted to

---

[1] The values of the mass transfer coefficient, N, in Table 4.1 was determined at 2 meter height. If any of these values are be used for the wind coefficient, c, in the MINLAKE model, they should be converted to values at 10 meter height (see Appendix A2)

wind speed at 10 meter height. The way in which this can be accomplished is set out in detail in Appendix A2.

Usually, the saturated vapour pressure at the water surface, e_s, and, the vapour pressure of the air, e_a, are determined by measurement, but based on work done by Murray (1967), in the MINLAKE model the saturated vapour pressure at the water surface is calculated by substituting the water surface temperature in the Magnus-Tetons formula:

$$e_s = 6.1078 \exp\left[\frac{17.27 * T_s}{T_{sk} - 35.86}\right] \qquad (5.10)$$

e_s = saturated vapour pressure at the water surface (mbar)
T_s = surface water temperature (°C)
T_{sk} = surface water temperature (°K).

No other reference could be found in the literature to substantiate this method of calculation. However, when values of the saturated vapour pressure at the water surface, e_s, were calculated according to Eq 5.10 for a range of surface water temperatures, the values were in accordance with measured values as tabulated by Brutsaert (1982), therefore Eq 5.10 was accepted as correct.

The vapour pressure of the air, e_a, is calculated from the dew point temperature (Riley 1988):

$$e_a = \left[4.528 * 10^{(7.45T_d/(235+T_d))}\right]\left(\frac{1013}{760}\right) \qquad (5.11)$$

e_a = vapour pressure of air (mbar)
T_d = dew point temperature (°C).

Again, no other reference could be found in the literature to substantiate this method of calculation, but values calculated according to Eq 5.11 for a range of dew point temperatures were in accordance with measured values (CRC 1978), and therefore Eq 5.11 was accepted as correct.

Regarding the third term on the right hand side of Eq 5.2, *convective heat loss, H_c:* in the MINLAKE model this is formulated as follows:

$$H_c = 0.618\ f(W)\ (T_s - T_a) \qquad (5.12)$$

H_c = convective heat loss (kcal m^{-2} day^{-1})
f(W) = wind function (Eq 5.9)
T_s = water surface temperature (°C)
T_a = air temperature (°C).

This formulation is the same as in the literature (Henderson-Sellers 1984, also Eq 4.20).

Regarding the third term on the right hand side of Eq 5.2, *back radiation:* in the MINLAKE model this has been formulated according to Eq 4.21:

$$H_b = \varepsilon_w \sigma T^4_w \qquad (5.13)$$

H_b = back radiation (kcal m^{-2} d^{-1})
ε_w = emissivity of water ($\approx$ 0.97)
σ = Stefan-Boltzman constant
= 1.171 * 10^{-6} kcal m^{-2} $°K^{-4}$
T_w = water surface temperature (°K).

Regarding the last term on the right hand side of Eq 5.2, *atmospheric long wave radiation*, this is formulated in the MINLAKE model according to Eq 4.22:

$$H_a = \varepsilon_a \sigma T^4_a \qquad (5.14)$$

H_a = atmospheric radiation (kcal m^{-2} d^{-1})
ε_a = emissivity of the atmosphere
σ = Stefan-Boltzman constant
= 1.171 * 10^{-6} kcal m^{-2} $°K^{-4}$
T_a = air temperature (°K).

The emissivity of the atmosphere, ε_a, is calculated according to the formulation of Idso and Jackson (Table 4.2), with a correction for cloudy skies (*cf* Eq 4.23)

$$\epsilon_a = \left[1 - 0.261 \exp(-6.77 * 10^{-4} T_a^2)\right] (1 + kC^2) \qquad (5.15)$$

ε_a = emissivity of the atmosphere
T_a = air temperature (°C)
k = cloud height coefficient
= 0.17
C = cloud cover ratio.

The cloud cover ratio, C, is calculated from the daily percentage sunshine, which is part of the daily data input into the model.

5.2.2 MINLAKE formulation of convective mixing.

The MINLAKE model does not have a specific formulation for calculation of convective mixing - calculation of convective mixing is based on density differences. The density in each layer is compared with the density of the layer immediately below, taking into account temperature, as well the concentration of inorganic suspended sediment and dissolved salts. If the density of the upper layer is higher than the density of the lower layer, the two layers are mixed, thereby averaging the density, and temperature, of the two layers, as well as the concentration of nutrients, etc. This procedure is repeated until the density of the upper layer is equal or less than that of the layer below.

5.2.3 MINLAKE formulation of advective mixing.

Depending on the densities of the inflowing and the reservoir water, water flowing into a reservoir will plunge beneath the reservoir at a certain point (the plunge point) and flow along the submerged river bed. In the process, reservoir water is entrained into the current of inflowing water. The following needs to be formulated:

- Reservoir depth, and mixing, at the plunge point.
- Entrainment into the underflowing water below the plunge point.

5.2.3.1 MINLAKE formulation of reservoir depth, and mixing, at the plunge point: The MINLAKE model has a rather sophisticated formulation of plunge point depth, based on the work done by Ellison and Turner (1959), and Akiyama and Stefan (1984). If the river bed slope is steep, significant mixing may occur at the plunge point, thus, in the MINLAKE model, the plunge point depth is formulated separately for mild slopes and steep slopes (*cf* Eqs 4.32 and 4.33), and provision is made for greater mixing at the plunge point in the case of steep slopes.

For a mild slope ($S \leq 0.00666$), the depth at the plunge point is formulated as:

$$h_{ps} = \frac{1}{2}\left(\frac{2+\gamma}{2} + \frac{S_2 S}{f_t} + \sqrt{\left[\frac{2+\gamma}{2} + \frac{S_2 S}{f_t}\right]^2 - 4\frac{(S_2\, S/f_t)}{(1+\gamma)}} \right) \left(\frac{f_t}{S_2\, S}\right)^{\frac{1}{3}} \left(\frac{q_0^2}{\epsilon_0 g}\right)^{\frac{1}{3}}$$

(5.16)

For a steep slope ($S > 0.00666$), the formulation is:

$$h_{pm} = \frac{1}{2}\left(\frac{2+\gamma}{2} + S_1 + \sqrt{\left[\frac{2+\gamma}{2} + S_1\right]^2 - 4\frac{(S_1)}{(1+\gamma)}} \right) \left(\frac{1}{S_1}\right)^{\frac{1}{3}} \left(\frac{q_0^2}{\epsilon_0 g}\right)^{\frac{1}{3}}$$

(5.17)

h_{ps} = plunge depth for mild slope

h_{pm} = plunge depth for steep slope

γ = rate of initial mixing

= q_a/q_0

q_a = inflow rate of ambient water per unit span into plunge region

q_0 = flow rate per unit span downstream of plunge point (underflow)

S_1 = coefficient (= 0.2 ~ 0.3)

S_2 = coefficient (= 0.6 ~ 0.9)

f_t = total friction coefficient

= $f_b + f_i$

f_b = bed friction coefficient

f_i = friction coefficient for interface

S = bed slope

ϵ_0 = initial density difference relative to ambient density

= $\Delta\rho_0/\rho_a$

$\rho_a+\rho_0$ = density of inflow water (g m^{-3})

ρ_a = density of ambient water (g m^{-3})

g = gravitational acceleration (m s^{-2}).

The value of the rate of initial mixing, γ, has been hard-wired into the original model to a value of 0.15 for mild slopes, and 1.8 for steep slopes. In the absence of evidence to the contrary, it was assumed that these values are representative of typical values of the rate of initial mixing. The total friction coefficient, (also known as Manning's friction factor), as well as the bed slope for each river, must be specified by the user as part of the input data.

5.2.3.2 MINLAKE formulation of entrainment due to inflow:

Once the river water plunges beneath the reservoir water at the plunge point, it flows along the submerged river bed. Reservoir water will be entrained into the underflowing water, the amount of water entrained depends on the roughness and slope of the submerged river bed (*cf* paragraph 3.3.2.3 and 4.3.3.2). The MINLAKE model formulates the rate of entrainment of reservoir water into the underflowing water according to the formulation of Akiyama and Stefan (1984) (*cf* Eq 4.34):

$$\frac{dh}{dt} = Eu_d \qquad (5.18)$$

dh/dt = rate of entrainment (m s^{-1})

u_d = mean velocity of the underflowing water (m s^{-1})

E = entrainment coefficient.

The entrainment coefficient is formulated for a rectangular river cross-section (*cf* Eq 4.35):

$$E = \frac{\beta}{Ri^n} \qquad (5.19)$$

E = entrainment coefficient

Ri = Richardson number

n = 1

β = 0.0015.

The values of n, as ß, were obtained from Akiyama and Stefan (1984) (*cf* Eq 4.35), and were hard-wired into the original model. As these values seem to be generally representative, no changes were made.

The Richardson number, Ri, also is formulated for a rectangular river cross-section, according to Eq 4.36:

$$Ri = \frac{\epsilon_d g h_d \cos\theta}{u_d^2} \qquad (5.20)$$

ϵ_d = density difference downstream of plunge point (underflow) relative to ambient water density (g m^{-3})

= $\Delta\rho_0/\rho_a$

$\Delta\rho_0$ = excess density of underflow relative to ρ_a (g m^{-3})

ρ_a = ambient water density (g m^{-3})

g = acceleration due to gravity (m s^{-2})

h_d = underflow depth (m)

Θ = angle of the bed slope

u_d = underflow velocity (m s^{-1}).

South African rivers are more likely to have a rectangular than triangular cross-section, and therefore the MINLAKE formulations for the entrainment coefficient and the Richardson number were accepted as suitable for simulation of advective mixing in South African reservoirs. For formulation of the entrainment coefficient and the Richardson number for triangular river cross-sections, the reader is referred to Imberger *et al* (1978), and Fischer *et al* (1979).

5.2.4 MINLAKE formulation of thermocline depth and mixing due to wind action.

In the MINLAKE model, formation of the thermocline is formulated according to the integral energy concept (See paragraph 4.3.4.2). Care is taken of mixing due to wind action by formulation of an epilimnetic, as well as an hypolimnetic eddy diffusion coefficient.

5.2.4.1 MINLAKE formulation of thermocline formation:

The integral energy concept of thermocline formation was pioneered by two groups of researchers, Imberger and co-workers, the developers of the DYRESM model, and by Stefan and Ford, the developers of the MINLAKE model. As was discussed in paragraph 4.3.4.2, the formulation of Stefan and Ford is less complex (without being less effective) than that of Imberger and co-workers, and hence is to be preferred.

According to Stefan and Ford (and thus the MINLAKE model), deepening of the mixed layer, i.e formation of the thermocline, depends on a certain critical ratio of kinetic to potential energy. The major source of kinetic energy is wind shear stress - turbulent kinetic energy generated by advection is formulated separately (paragraph 5.2.3). Thus, in the MINLAKE model, turbulent kinetic energy is formulated as:

$$TKE = \int_{As} Cu_{*w}\tau \, dA \qquad (5.21)$$

TKE	=	wind-induced turbulent kinetic energy
A_s	=	surface area (km^2)
C	=	empirical coefficient for wind sheltering
u_{*w}	=	water shear velocity ($m\ s^{-1}$)
τ	=	shear stress at the air-water interface ($kg\ m^{-2}\ s^{-1}$).

The rate of change of potential energy of the system is seen to be equal to the work required to lift a mass of water $_{\Delta}\rho_{\Delta}V$, from the layer of colder, denser water

immediately below the mixed layer into the mixed layer, with heat input having a modifying effect (Ford and Stefan 1980):

$$W_L = \Delta\rho\Delta V g\ (D - Z_g) \qquad (5.22)$$

W_L = work required (rate of change of potential energy)

$\Delta\rho$ = density difference between mixed layer and underlying layer (kg m^{-3})

ΔV = incremental volume (m^3)

g = acceleration due to gravity (m s^{-2})

D = depth of mixed layer (m)

Z_g = depth of centre of gravity of mixed layer (m).

As the work required is formulated as a function of the density difference between the mixed layer and the layer immediately underneath, the work required will be affected by the temperature of these layers, because of the density properties of water at different temperatures - the rate of change of water density is not constant with increasing temperature; the higher the temperature, the greater the change in density per degree change in temperature, and the greater the resistance to mixing (see paragraph 3.3.1).

Eq 5.21 and 5.22 are combined to obtain σ, the critical ratio for deepening of the mixed layer (Ford and Stefan 1980):

$$\sigma = \frac{\int_{As} u_{*w}\tau dA\Delta t}{\Delta\rho\Delta V g(D - Z_g)} \qquad (5.23)$$

σ = critical ratio for deepening of the mixed layer

Δt = time step.

The rest of the symbols are as per Eq 5.21 and 5.22 above.

The wind sheltering coefficient has been moved over to the left hand side of the equation and incorporated into σ. If $\sigma > 1$, i.e. if the amount of turbulent kinetic energy in the mixed layer is greater than the amount of potential energy in the system, vertical entrainment and mixing will take place, if it is less ($\sigma < 1$), the kinetic energy is dissipated in overcoming viscosity, and no deepening occurs.

In the MINLAKE model, only formation of the thermocline is described by calculating the balance between kinetic and potential energy - mixing due to wind action is formulated as epilimnetic and hypolimnetic turbulent diffusion coefficients.

5.2.4.2 MINLAKE formulation of mixing due to wind action:

Models based on the integral energy concept still employ eddy diffusion as the main mode of heat and mass dispersion (paragraph 4.3.4.2). In both the original and the modified MINLAKE model, eddy diffusion is formulated separately for the epilimnion and the hypolimnion by use of an epilimnetic and hypolimnetic eddy diffusion coefficient.

MINLAKE formulation of the epilimnetic eddy diffusion coefficient:

The epilimnetic eddy diffusion coefficient is formulated as a function of wind speed only, and is taken to be constant with depth. The formulation is as follows:

$$K = 28W^{1.3} \qquad (5.24)$$

K = epilimnetic eddy diffusion coefficient ($m^2\ day^{-1}$)

W = wind speed (mph).

This formulation is analogous to the formulation of Sundaram and Rehm (1973), and McCormick and Scavia (1981) as given in Eq 4.37. The main difference is that, in the MINLAKE model, the epilimnetic diffusion coefficient is formulated as a function of wind speed, whereas in Eq 4.37 it is formulated as a function of surface shear velocity. This

difference is not significant, as surface shear velocity can be related to wind speed (and *vice versa*) by Eq 4.38.

Of greater concern was the origin and general validity of the constant value of 28 in Eq 5.24 - this value was hard-wired into the model, which implies that there is no need for the user to change it. By comparing Eq 4.37 and 5.24, it would seem that this is the value ascribed to the constant c in Eq 4.37. However, according to Sundaram and Rehm (1973) the value of c is not universal, but should be determined for each lake. Also, the reason for using a value of 28 in Eq 5.24 could not be established (see discussion in paragraph 6.3.4.2). Consequently, in accordance with Eq 4.37, the hard-wired value of 28 was removed from Eq 5.24 and replaced with a constant, c, which has to be specified by the user.

MINLAKE formulation of the hypolimnetic eddy diffusion coefficient:
Formulation of the hypolimnetic eddy diffusion coefficient in the MINLAKE model is in correspondence with Eq 4.55, i.e. the hypolimnetic eddy diffusion coefficient, K_H, is related to the Brunt-Väisälä frequency, N. However, the MINLAKE model recognises that the hypolimnetic eddy diffusion coefficient increases with depth, (reaching a maximum at about mid-depth in the hypolimnion), and thus the value of the hypolimnetic eddy diffusion coefficient is taken to be either that given by Eq 5.25, or equal to the maximum hypolimnetic eddy diffusion coefficient, whichever yields the lesser value.

$$K_H = K_{max} C N^{-1} \qquad (5.25)$$

K_H = hypolimnetic eddy diffusion coefficient ($m^2\ day^{-1}$)
K_{max} = maximum hypolimnetic eddy diffusion coefficient ($m^2\ day^{-1}$)
C = minimum value of N at which the maximum hypolimnetic diffusion rate occurs (s)
N = Brunt-Väisälä frequency - Eq 4.53 (s).

The maximum hypolimnetic eddy diffusion coefficient, K_{max}, has to be specified by the user, as it is dam-specific. The MINLAKE manual indicates that K_{max} should be estimated from the reservoir surface area (but also see discussion in paragraph 6.3.4).

In so far as the value of C is concerned (the minimum value of N at which the maximum hypolimnetic eddy diffusion rate occurs), this value has been hard-wired into the model as 8.66×10^{-3}. According to the manual, this value was obtained from the study of Jassby and Powell (1975). Although this value is not quoted explicitly in the study of Jassby and Powell (1975), it appears to have been inferred from Fig 3 in the study. In the absence of evidence to the contrary, this value was accepted as generally applicable.

Regarding the relationship between the hypolimnetic eddy diffusion coefficient, K_H, and the Brunt-Väisälä frequency, N; in the MINLAKE model K_H is related to $(N^2)^{-1}$, whereas, according to Eq 4.54, it is more appropriate to relate K_H to $(N^2)^{-0.5}$. However, changing the relationship from $(N^2)^{-1}$ to $(N^2)^{-0.5}$ during calibration of the model did not bring about any change in the calibration results, therefore the original relationship ($K_H \propto (N^2)^{-1}$) was retained.

The MINLAKE formulation of the eddy diffusion coefficient (epilimnetic and hypolimnetic) does not include the effect of turbulence generated by inflows - this is formulated separately (see paragraph 5.2.3.2). Furthermore, to prevent numerical instabilities in the change-over between epilimnetic and hypolimnetic diffusion coefficient, a *mean* turbulent diffusion coefficient is calculated for each layer. Firstly, the turbulent diffusion coefficient, AMK, is calculated for each layer according to Eq 5.24 or 5.25, depending on whether the layer is in the epilimnion or in the hypolimnion. Thereafter the diffusion coefficient between layers is calculated as the harmonic mean of the diffusion coefficients in adjacent layers:

$$HMK = \frac{2 * AMK(I) * AMK(I-1)}{AMK(I) + AMK(I-1)} \qquad (5.26)$$

HMK = mean turbulent diffusion coefficient in layer (I) (m day^{-1})

AMK(I) = turbulent diffusion coefficient in layer (I) (m day^{-1})

AMK(I-1) = turbulent diffusion coefficient in previous layer (m day^{-1}).

This approach prevents numerical instabilities due to a sudden change in diffusion coefficient between layers, as may be the case when changing from the epilimnion to the hypolimnion.

5.3 MINLAKE FORMULATION OF THE WATER QUALITY PROCESSES.

The MINLAKE model has a sophisticated representation of water quality/eutrophication processes. For instance, it can simulate up to three different algal classes, which means that the model can be used to simulate algal succession. More important though, once the model has been calibrated to a particular reservoir, it can be used to assess whether application of certain management options will be effective in changing algal growth from blue-green to green algae.

The processes that should be considered in the water quality part of an eutrophication model have been identified in Chapter 3 as:

- Processes affecting dissolved oxygen concentration
- Microbial decay of organic matter
- Processes affecting algal concentration (including photosynthesis, respiration, mortality, and the availability of nutrients and light).

5.3.1 MINLAKE formulation of processes affecting dissolved oxygen concentration.

In the MINLAKE model dissolved oxygen is expressed as a concentration in mg l^{-1}.

5.3.1.1 MINLAKE formulation of saturated oxygen concentration:

Saturated dissolved oxygen concentration, i.e. the maximum amount of oxygen that can dissolve in water at a given time, is a function of both temperature and pressure, and thus altitude. However, in the original MINLAKE model, it is formulated as a function of temperature only:

$$OSAT = (14.652 - T_s (0.41022 - T_s * ((7.991 * 10^{-3}) - 7.7774 * 10^{-5} * T_s))) \quad (5.27)$$

OSAT	=	saturated dissolved oxygen concentration (mg l^{-1})
T_s	=	surface water temperature (°C).

Basically, the above formulation is equivalent to Eq 4.70. However, these formulations do not provide for the effect of altitude on saturated dissolved oxygen concentration. As many South African reservoirs are situated at an altitude > 1000 m above mean sea level, the original MINLAKE model was modified to take the effect of altitude on saturated dissolved oxygen concentration into account. This was done according to the formulation of Bratby (Eq 4.71). Thus, instead of Eq 5.27, the saturated dissolved oxygen concentration is formulated as follows:

$$OSAT = OSAT20 \left(\frac{51.6}{31.6 + T_s}\right) \left(\frac{ATPS - ESA}{1013 - 23.35}\right) \quad (5.28)$$

OSAT	=	*saturated dissolved oxygen concentration (mg l^{-1})*
OSAT20	=	*saturated dissolved oxygen concentration at 20°C*
	=	*9.07 mg l^{-1}*
51.6	=	*universal constant*
31.6	=	*universal constant*
T_s	=	*surface water temperature (°C)*
ATPS	=	*atmospheric pressure at the site (mbar)*
ESA	=	*saturated water vapour pressure at surface water temperature (mbar)*
1013	=	*atmospheric pressure at sea level (mbar)*
23.35	=	*saturated water vapour pressure at 20°C (mbar).*

The atmospheric pressure at the site is formulated as (CRC 1978, Henderson-Sellers 1984):

$$ATPS = 1005 - 0.102 * ST \quad (5.29)$$

ATPS = *atmospheric pressure at the site (mbar)*

ST = *altitude at level of the water surface (meter above sea level).*

The altitude at the level of the water surface (ST) is part of the original model input.

In the original MINLAKE model, ESA, the saturated water vapour pressure at surface water temperature, has already been formulated as part of the evaporative heat loss in the energy budget. The same formulation for ESA was used, i.e.

$$ESA = 6.1078 * \exp\left(\frac{17.2693882 * T_s}{(T_s + 273) - 35.86}\right) \quad (5.30)$$

ESA = *saturated water vapour pressure at surface water temperature (mbar)*

T_s = *surface water temperature (°C).*

This change in formulation does not require specification of any additional coefficients - the only coefficient that has to be specified is ST, the altitude at the level of the water surface, which is part of the original model input.

5.3.1.2 MINLAKE formulation of sources of oxygen:

The MINLAKE model includes the two major sources of oxygen - atmospheric transfer and oxygen produced during photosynthesis.

Formulation of the atmospheric exchange of oxygen is in accordance with the general formulation in Eq 4.75:

$$dO/dT = \frac{K_L}{dz} (O_{2_{sat}} - O_2) \qquad (3.31)$$

dO/dt	=	change in dissolved oxygen concentration (mg l^{-1} day^{-1})
K_L	=	transfer velocity (m day^{-1})
dz	=	a characteristic depth
	=	thickness of the first layer (m)
O_{2sat}	=	saturated dissolved oxygen concentration (mg l^{-1})
O_2	=	dissolved oxygen concentration in the first layer (mg l^{-1}).

The transfer velocity, K_L, is a function of wind speed (see paragraph 4.4.1.2). At wind speeds less than 2-3 m s^{-1} (aerodynamically smooth flow) the transfer of oxygen is a function of molecular diffusion only, and thus can be formulated as a constant rate. According to the MINLAKE manual (Riley 1988), for modelling purposes the minimum transfer rate for wind speeds < 2 m s^{-1} was set at 0.25 m day^{-1}, from observing data presented by Cohen (1983) and O'Connor (1983).

The MINLAKE formulation of K_L for wind speeds > 2 m s^{-1} (aerodynamically turbulent flow) is an approximation of several formulations (Riley 1988):

$$K_L = 1.1 * 10^6 * u_*^2 * S_c^{-0.5} \qquad (5.32)$$

u.	=	water shear velocity induced by wind (m s^{-1})
Sc	=	Schmidt number
	=	ν/D
ν	=	kinematic viscosity (m^2 s^{-1})
D	=	molecular diffusivity (m^2 s^{-1}).

The Schmidt Number, Sc, is formulated as:

$$Sc = \frac{\nu}{D} = \frac{1.45 * 10^5}{T_K} * \left[\frac{1.79}{1 + 0.03368T_c + 0.000221T_c^2}\right]^2 \quad (5.33)$$

Sc = Schmidt number

T_K = water temperature (°K)

T_c = water temperature (°C).

The molecular diffusivity, D, is formulated as:

$$D = 6.92 * 10^{-15} \frac{T_K}{\mu} \quad (5.34)$$

D = molecular diffusivity ($m^2\ s^{-1}$)

T_K = water temperature (°K)

μ = absolute viscosity (Nsm^{-2}).

The basic formulation of atmospheric transfer in the MINLAKE model agrees with the general formulation (Eq 4.75). Formulation of the transfer rate for wind speeds > 2 m s^{-1} (Eq 5.32) appears to be an approximation of Eq 4.83, and thus was accepted as adequate, i.e no changes were made to the MINLAKE formulation of transfer velocity. However, the program code relating to calculation of the transfer velocity contained some coding errors. These were corrected, and part of the code was rewritten to make it more user-friendly. (For a full discussion, see paragraph 7.7.1.1).

Regarding the production of oxygen via photosynthesis, the formulation in the original MINLAKE model is based on the approach by Stumm and Morgan (1970). According to this approach, the net oxygen resulting from photosynthesis is the balance of oxygen produced during photosynthesis, and oxygen consumed during heterotrophic respiration. In the original MINLAKE model, this is formulated as follows:

$$dO/dT = \frac{P * Chla - R * Chla}{YCHO_2} \qquad (5.35)$$

dO/dt = change in dissolved oxygen concentration (mg l^{-1})
P = rate of photosynthesis
R = algal respiration rate
Chla = chlorophyll-a concentration (mg l^{-1})
$YCHO_2$ = mass ration of dissolved oxygen produced from chlorophyll in photosynthesis, and oxygen utilized in respiration (mg Chla mg O_2^{-1}).

The coefficient $YCHO_2$ has to be specified by the user, and requires assumption of chlorophyll-a to dry weight, and of the photosynthetic/respiration reaction. A value of 0.0083 is suggested.

This formulation of oxygen produced during photosynthesis seemed to be fundamentally correct, and therefore no changes/modifications were made.

5.3.1.3 MINLAKE formulation of sinks of oxygen:

The main sinks of oxygen are microbial decay of organic matter, and the oxygen demand of the sediments. Further sinks of oxygen are nitrification and algal respiration, though these are minor compared to the oxygen utilised during microbial decay of organic matter and sediment oxygen demand.

In the original MINLAKE model, microbial decay of organic matter is simulated as a function of the organic mass, which is expressed in oxygen equivalents. Thus the oxygen utilized during microbial decay is equivalent the change in detritus concentration:

$$\Delta O = \Delta BOD \qquad (5.36)$$

In the original MINLAKE model microbial decay of organic matter was represented as follows:

$$dO/dt = BODK20 * 1.055^{(T - 20)} * BOD \qquad (5.37)$$

dO/dt	=	change in dissolved oxygen concentration (mg l^{-1})
BODK20	=	microbial decay rate of organic matter at 20°C (day^{-1})
1.055	=	Arrhenius temperature coefficient
T	=	water temperature in a layer (°C)
BOD	=	concentration of organic matter in a layer (mg l^{-1}).

Eq 5.37 presents several difficulties, however, these relate to the manner the rate of microbial decay is represented, and thus the way in which these are addressed are discussed in the next section (paragraph 5.3.2). Basically, in the modified MINLAKE model two formulations of the decay of organic matter were tested - the first formulation is a simple first-order formulation that makes no distinction between particulate and dissolved BOD. In this case, the oxygen utilized during microbial decay of detritus is formulated as:

$$dO/dt = dBOD/dt$$

$$= (BODK\ \theta^{(T-20)}) \left(\frac{DSO}{DSO+BODOK}\right) + (DNK\ \theta_N^{(T-20)}) \left(\frac{KONO}{KONO+DSO}\right) \left(\frac{NO}{NO+KNNO}\right) BOD \qquad (5.38)$$

dO/dt = *change in dissolved oxygen concentration due to detrital decay (mg l^{-1})*

dBOD/dt = *change in detrital concentration due to decay (mg l^{-1})*

BODK = *detrital decay rate at 20 °C (day^{-1})*

θ = *Arrhenius temperature coefficient for detrital decay (cf Eq 4.92).*

BODOK = *aerobic switching constant for detrital decay (mg O_2 l^{-1})*

DSO = *dissolved oxygen concentration (mg l^{-1})*

DNK = *denitrification rate at 20 °C (day^{-1})*

θ_N = *Arrhenius temperature coefficient for denitrification*

KONO = *anaerobic switching constant for denitrification (mg $O_2 l^{-1}$)*

NO = *nitrate concentration (mg l^{-1})*

KNNO = *nitrate switching constant for denitrification (mg NO_3 l^{-1})*

BOD = *concentration of BOD (mg l^{-1}).*

For a discussion of the derivation of the above equation, the reader is referred to Eq 5.47.

In the second formulation of detrital decay in the modified MINLAKE model a distinction is made between particulate and dissolved organic matter. No oxygen is consumed during decomposition of particulate matter to dissolved organic matter. During the utilization of dissolved organic matter by bacteria (i.e. decay), two-thirds of the dissolved organic matter is reconstituted as particulate organic matter (synthesis), and oxygen is consumed only during decay of the remaining one-third when energy for synthesis is generated. Thus, the oxygen utilised is represented by:

$$dO/dt = dBODS/dt$$

$$= (BODSK\ \theta^{(T-20)}) \left(\frac{DSO}{DSO+BODSOK}\right) + (DNK\ \theta_N^{(T-20)}) \left(\frac{KONO}{KONO+DSO}\right) \left(\frac{NO}{NO+KNNO}\right) 0.333\ BODS \quad (5.39)$$

dO/dt = *change in dissolved oxygen concentration due to decay of organic matter (mg l^{-1})*

dBODS/dt = *change in dissolved BOD concentration due to decay (mg l^{-1})*

BODSK = *dissolved BOD decay rate at 20 °C (day^{-1})*

θ = *Arrhenius temperature coefficient for detrital decay (cf Eq 4.92).*

BODSOK = *aerobic switching constant for decay of dissolved BOD (mg O_2 l^{-1})*

DSO = *dissolved oxygen concentration (mg l^{-1})*

DNK = *denitrification rate at 20 °C (day^{-1})*

θ_N = *Arrhenius temperature coefficient for denitrification*

KONO = *anaerobic switching constant for denitrification (mg $O_2 l^{-1}$)*

NO = *nitrate concentration (mg l^{-1})*

KNNO = *nitrate switching constant for denitrification (mg NO_3 l^{-1})*

BODS = *concentration of dissolved BOD (mg l^{-1}).*

The reader is referred to Eq 5.48 for an explanation of the terms in Eq 5.39.

Regarding the oxygen demand of the sediment as a sink of oxygen; several chemical and biological reactions that utilise oxygen take place in the bottom sediments. In the original MINLAKE model the general approach usually followed in eutrophication models is observed (*cf* paragraph 4.4.1.3), i.e. the consumption of oxygen due to processes in the bottom sediment is parameterized as an *sediment oxygen demand (SOD)*, and formulated as a constant rate per cross-sectional area:

$$dO/dt = SB20 * 1.055^{(T-20)} * \frac{AREA}{V} \quad (5.40)$$

dO/dt	=	change in dissolved oxygen concentration in a layer (mg l^{-1})
SB20	=	sediment oxygen demand at 20°C
1.055	=	Arrhenius temperature coefficient
T	=	water temperature in a layer (°C)
AREA	=	area of bottom sediment in a layer (m^2)
V	=	volume of layer (m).

The oxygen utilising processes that take place in the bottom sediment can occur in the presence of oxygen only, i.e. when the overlying water is aerobic. The original MINLAKE model does not distinguish between aerobic/anaerobic conditions and their effect on sediment oxygen demand, therefore the original model was modified by multiplying the sediment oxygen demand at 20°C with an aerobic switching function (cf Eq 4.93). Also, in the original model the Arrhenius temperature coefficient was hard-wired into the model to a value of 1.055 for all reactions, which is not realistic. This was changed to allow the user to specify a temperature coefficient for sediment oxygen demand in the input file. Furthermore, formulation of the sediment oxygen demand will be affected by the modified formulation of decay of organic matter - see paragraph 5.3.2.1. and 5.3.2.2. If microbial decay of organic matter is represented by a simple first-order formulation, sediment oxygen demand is formulated as:

$$dO/dt = SB20 \left(\frac{DSO}{DSO + SBOK} \right) \theta_{SOD}^{(T - 20)} \frac{AREA}{V} \qquad (5.41)$$

dO/dt	=	*change in dissolved oxygen concentration in a layer (mg l^{-1})*
SB20	=	*sediment oxygen demand at 20°C*
DSO	=	*dissolved oxygen concentration in a layer (mg l^{-1})*
SBOK	=	*switching constant for sediment oxygen demand (mg l^{-1})*
θ_{SOD}	=	*Arrhenius temperature coefficient for sediment oxygen demand*
T	=	*water temperature in a layer (°C)*
AREA	=	*area of bottom sediment in a layer (m^2)*
V	=	*volume of layer (litre).*

*If decay of organic matter is represented by a more complex formulation (*cf *paragraph 5.4.2.2.) where a distinction is made between particulate and dissolved organic matter, then formulation of the sediment oxygen demand must provide for the fact that decay of dissolved organic matter in the sediment will exert an oxygen demand under aerobic conditions only - under anaerobic conditions dissolved BOD in the bottom sediments cannot decay, and it diffuses back into the water column (*cf *Eq 5.52). Thus, in this case, sediment oxygen demand is formulated as follows:*

$$dO/dt = (SB20+BBOT)\left(\frac{DSO}{DSO + SBOK}\right)\theta_{SOD}^{(T-20)}\frac{AREA}{V} \quad (5.42)$$

dO/dt = *change in dissolved oxygen concentration in a layer (mg l^{-1})*

SB20 = *sediment oxygen demand exerted by chemical reactions taking place in the bottom sediment (mg m^{-2} day^{-1})*

BBOT = *sediment oxygen demand due to decay of dissolved organic matter in the bottom sediment (mg m^{-2} day^{-1})*

DSO = *dissolved oxygen concentration in a layer (mg l^{-1})*

SBOK = *switching constant for sediment oxygen demand (mg l^{-1})*

θ_{SOD} = *Arrhenius temperature coefficient for sediment oxygen demand*

T = *water temperature in a layer (°C)*

AREA = *area of bottom sediment in a layer (m^2)*

V = *volume of layer (litre).*

The distinction between chemical oxygen demand (SB20) and the demand due to decay of dissolved organic matter is necessary to enable simulation of the diffusion of dissolved organic matter back into the water column under anaerobic conditions (see paragraph 5.4.2.2).

Depending on the formulation used for decay of organic matter, formulation of sediment oxygen demand in the modified MINLAKE model results in specification of two, or at the most, three additional coefficients (the Arrhenius coefficient for sediment oxygen demand; SBOK, the aerobic switching constant for sediment oxygen demand; and BBOT, the oxygen demand due to decay of organic matter in the bottom sediment).

Although the Arrhenius temperature coefficient must now be specified by the user, this approach should provide a more accurate result than that obtained with the one hard-

wired value that was taken as valid for all reactions. Addition of the other two calibration coefficients is justified in view of the fact that in eutrophic dams the sediment oxygen demand due to biological decay of organic matter may be considerable, especially under the climatic conditions experienced in Southern Africa. Very likely sediment oxygen demand plays an important role in the anaerobic conditions that are regularly observed in South African dams, and therefore this reaction must be represented as accurately as possible.

Regarding nitrification as a sink of oxygen, during nitrification 4.57 gram of oxygen is utilised for every gram of nitrogen that is oxidized, thus, in the original MINLAKE model the oxygen utilised during nitrification is represented as follows:

$$dO/dt = XKNNH * 1.055^{(T-20)} * XNHD * 4.57 \qquad (5.43)$$

dO/dt	=	change in dissolved oxygen concentration in a layer (mg l^{-1})
XKNNH	=	nitrification rate (day^{-1})
1.055	=	Arrhenius temperature coefficient
T	=	water temperature in a layer (°C)
XNHD	=	ammonia concentration in a layer (mg l^{-1})
4.57	=	grams of oxygen utilised per gram of nitrogen.

Modifications made to the above formulation relate to the nitrification rate, and not to the utilization of oxygen during nitrification, and thus these changes are discussed in detail in paragraph 5.3.4.2. Basically, because nitrification can take place under aerobic conditions only, the nitrification rate was multiplied by an aerobic switching function. Also, it has been found (see paragraph 3.4.4.2), that nitrification is inhibited under low ammonia concentrations, and thus a further factor was brought in to account for this. The resultant formula describing oxygen utilised during nitrification in the modified MINLAKE model is as follows:

$$dO/dt = XKNH \left(\frac{DSO}{DSO + KONH}\right) \theta_{NNH}^{(T - 20)} \left(\frac{NH}{NH + XNH}\right) 4.57 \qquad (5.44)$$

dO/dt = *change in dissolved oxygen concentration in a layer (mg l^{-1})*

XKNH = *nitrification rate (day^{-1})*

KONH = *switching constant for nitrification (day^{-1})*

DSO = *dissolved oxygen concentration in a layer (mg l^{-1})*

θ_{NNH} = *Arrhenius temperature coefficient*

T = *water temperature in a layer (°C)*

NH = *ammonia concentration in a layer (mg l^{-1})*

XNH = *ammonia concentration where nitrification rate has been reduced to half the maximum rate (mg l^{-1})*

4.57 = *grams of oxygen utilised per gram of nitrogen.*

Regarding algal respiration as a sink of oxygen, in the original MINLAKE model oxygen utilised during respiration is formulated as follows:

$$dO/dt = \frac{RM * CHLA}{YCHO_2} \qquad (5.45)$$

dO/dt = change in dissolved oxygen concentration in a layer (mg l^{-1})

RM = algal respiration rate (day^{-1})

CHLA = concentration of chlorophyll-a (mg l^{-1})

$YCHO_2$ = mass ration of dissolved oxygen produced from chlorophyll in photosynthesis, and oxygen utilized in respiration (mg Chla mg O_2^{-1}).

The algal respiration rate must be specified by the user for each algal group. The coefficient $YCHO_2$ has the same meaning and value as specified for oxygen produced during algal photosynthesis. The fundamental concept of oxygen utilised during algal respiration appeared to be correct, and therefore no changes were made.

5.3.2 MINLAKE formulation of microbial decay of organic matter

In both the original and the modified MINLAKE model, detrital mass is expressed in oxygen equivalents (BOD). This is done by means of a BOD coefficient - because the oxygen demand of organic matter depends on the composition of the organic matter (biodegradable vs unbiodegradable), it will be unique for each reservoir. The BOD coefficient affords the user the opportunity to specify the amount of detritus (as BOD) produced by the algae (as chlorophyll-a) for a specific reservoir.

No distinction is made between particulate and dissolved BOD in the original MINLAKE model (see paragraph 4.4.2). The main source of BOD is algal mortality:

$$dBOD/dt = MR * 1.055^{(T-20)} * \frac{CHLa}{YCBOD} \qquad (5.46)$$

dBOD/dt	=	increase in BOD concentration (mg l^{-1})
MR	=	algal mortality rate at 20°C (day^{-1})
1.055	=	Arrhenius temperature coefficient (*cf* Eq 4.92).
T	=	water temperature (°C)
CHLa	=	chlorophyll-a concentration (mg l^{-1})
YCBOD	=	BOD coefficient
	=	mass ratio of biodegradable detritus produced from chlorophyll-a (mg Chla (mg Bod)$^{-1}$).

The main sinks of detritus in the original MINLAKE model are settling and bacterial decay. The same formulation is used to calculate the settling of detrital particles and the settling of algal cells, i.e. settling is regarded as a loss process in each layer. The net settling velocity in a layer is calculated as the difference in settling velocity between the top and the bottom of the layer, taking the effect of turbulence on settling into account. This formulation is discussed in detail in paragraph 5.3.3.4, Eq 5.64 - 5.66.

In the original model, bacterial decay of organic matter is represented as a simple first-order reaction (see discussion in paragraph 4.4.2):

$$\Delta O = \Delta BOD = k_{BOD}\, 1.055^{(T-20)} (BOD) \qquad (5.47)$$

ΔO = change in dissolved oxygen concentration due to bacterial decay of detritus (mg l^{-1})

ΔBOD = change in detritus concentration (mg l^{-1})

k_{BOD} = first order decay coefficient (day^{-1})

1.055 = Arrhenius temperature coefficient

BOD = BOD concentration (mg l^{-1}).

Several deficiencies were identified in the above formulation:

- No provision is made for the fact that microbial decay of organic matter is much faster under aerobic than anaerobic conditions (see paragraph 3.4.2)
- Once all the oxygen has been utilized, nitrate will be utilized as an electron acceptor (denitrification), but the process of denitrification is not included in the above formulation (see paragraph 3.4.5.2).
- No distinction is made between particulate and dissolved organic matter.
- The Arrhenius temperature coefficient has been hard-wired into the model to a value of 1.055 for all reactions.

In an attempt to rectify these shortcomings, two different formulations of microbial decay of organic matter were tested. The first formulation is a simple first-order formulation, treating organic matter in the particulate form only. The second formulation is more complex - organic matter is divided into a particulate and dissolved fraction, incorporating the concept of Mann (1988), and Dold (1991), that particulate organic matter is regenerated during decay of dissolved organic matter (paragraph 3.4.2).

5.3.2.1 First formulation of microbial decay of organic matter in the modified MINLAKE model:

This formulation is a simple first-order formulation, making no distinction between the particulate and dissolved forms of organic matter. It is advisable to keep formulation as simple as possible, and there is some evidence that the decay of organic matter can be adequately described by a simple first-order formulation, even though the actual process is much more complex (see discussion in paragraph 4.4.2). Thus, the basic formulation in the original MINLAKE model was retained, and it was modified only by:

- *multiplying it with an aerobic switching function (cf Eq 4.93) to account for the fact that oxygen is utilised during decay under aerobic conditions only,*
- *the process of denitrification was incorporated*
- *instead of a single, hard-wired value of the Arrhenius temperature coefficient, the model was modified to allow the user to specify the value in the input file.*

Thus the simple, first-order formulation in the modified MINLAKE model is as follows:

$$dBOD/dt = (BODK * QBOD^{(T-20)}) * \left(\frac{DSO}{DSO+BODOK}\right) + (DNK * \Theta_N^{(T-20)}) * \left(\frac{KONO}{KONO+DSO}\right) * \left(\frac{NO}{NO+EDNK}\right) * BOD \quad (5.48)$$

dBOD/dt = *change in detrital concentration due to decay (mg l^{-1})*

BODK = *detrital decay rate at 20 °C (day^{-1})*

QBOD = *Arrhenius temperature coefficient for detrital decay (cf Eq 4.92).*

BODOK = *aerobic switching constant for detrital decay (mg O_2 l^{-1})*

DSO = *dissolved oxygen concentration (mg l^{-1})*

DNK = *denitrification rate at 20 °C (day^{-1})*

Θ_N = *Arrhenius temperature coefficient for denitrification*

KONO = *anaerobic switching constant for denitrification (mg $O_2 l^{-1}$)*

NO = *nitrate concentration (mg l^{-1})*

EDNK = *nitrate switching constant for denitrification (mg NO_3 l^{-1})*

BOD = *concentration of BOD (mg l^{-1}).*

The terms on the right hand side of Eq 5.48 are as follows:

First term: *detrital decay rate, corrected for the effect of temperature.*

Second term: *aerobic switching constant to affect oxygen utilization under aerobic conditions only.*

Third term: *denitrification rate, corrected for the effect of temperature.*

Fourth term: *anaerobic switching function, because denitrification can take place under anaerobic conditions only.*

Fifth term: *Michaelis-Menten type switching function to allow for the fact that denitrification can take place only when nitrate is present.*

Regarding settling of detritus and the sources of detritus - no distinction is made between particulate and dissolved BOD in formulating detrital decay, and thus the formulation for settling in the original MINLAKE was retained. Similarly, algal mortality

is formulated as the only source of detritus (Eq 5.46) - the only change to Eq 5.46 was to remove the hard-wired value of the Arrhenius temperature coefficient, and to allow the user to specify the coefficient.

The results obtained with decay formulated according to Eq 5.48 are discussed in paragraphs 7.6.1 and 8.2.6.

5.3.2.2 Second formulation of microbial decay of organic matter in the modified MINLAKE model:

A second, more complex formulation was tested also. In this formulation, a distinction is made between particulate and dissolved forms of organic matter, and the regeneration of particulate organic matter from dissolved organic matter is taken into account. The reasons for the more complex formulation were as follows:

- *Microbial decay of organic matter is one of the greatest oxygen sinks in eutrophic reservoirs, leading to anaerobic conditions, and thus decay of organic matter should be formulated as realistically as possible.*

- *Although it seems that a simple first-order formulation of detrital decay is sufficient in many cases, it does not describe observed BOD data universally. Two-step formulations of detrital decay are not universally applicable either, but it does provide a better statistical fit in some cases (see paragraph 4.4.2).*

- *Basically the simple first-order, as well as the two-step formulation of detrital decay are equivalent to the classical synthesis-endogenous respiration approach in modelling of micro-organism metabolism in the activated sludge process. However, Dold et al (1981) found that this approach was not successful when anaerobic states occur during the process. A growth-death-regeneration concept was necessary (paragraph 3.4.3), in which it is assumed that death due to predation and other causes occurs continuously, giving rise to generation of biodegradable (and unbiodegradable) organic solid material. The biodegradable solids are solubilized, and the soluble material is utilized*

as substrate for synthesis of bacterial solids. During the synthesis process a part of the soluble BOD (≈ ⅓) is used to generate energy (by taking O_2 or nitrate as electron acceptors) to synthesize the balance (⅔) of BOD to organisms. Whereas BOD is generated continuously under aerobic and anaerobic conditions, BODS is used for synthesis only if O_2 or nitrate is present, i.e. during O_2 and nitrate deficient conditions there is a continuous accumulation of BOD, which is reduced as soon as O_2 or nitrate becomes available.

One consequence of this approach is that endogenous respiration per se no longer is present, the oxygen utilized in synthesis or regeneration of new mass now takes the place of endogenous respiration in the classical synthesis/endogenous respiration approach. The two approaches give equivalent results if the system remains aerobic, but the death/regeneration approach gives superior and more realistic results if sequences of aerobic/anoxic/anaerobic states are encountered (Dold et al 1981).

This approach is equivalent to Mann's concept that particulate organic matter is regenerated from dissolved organic matter, thus it is possible that a formulation that makes provision for regeneration of particulate organic matter from dissolved organic matter may give a better result under anaerobic conditions - many South African dams turn anaerobic during part of the hydrological cycle, and thus simulation under anaerobic conditions is important. Therefore, as shown diagrammatically in Fig 5.1, it is postulated that upon death of algae (mortality), particulate BOD is formed, which is decomposed to dissolved BOD through the action of enzymes (paragraph 3.4.3). No oxygen is utilized during this step. Based on the work of death/regeneration approach of Dold et al (1981), during the subsequent decay of dissolved BOD, only one third of the decaying dissolved BOD utilizes oxygen/nitrate as an electron acceptor, and releases intracellular ammonia and phosphate. The other two-thirds form particulate BOD again.

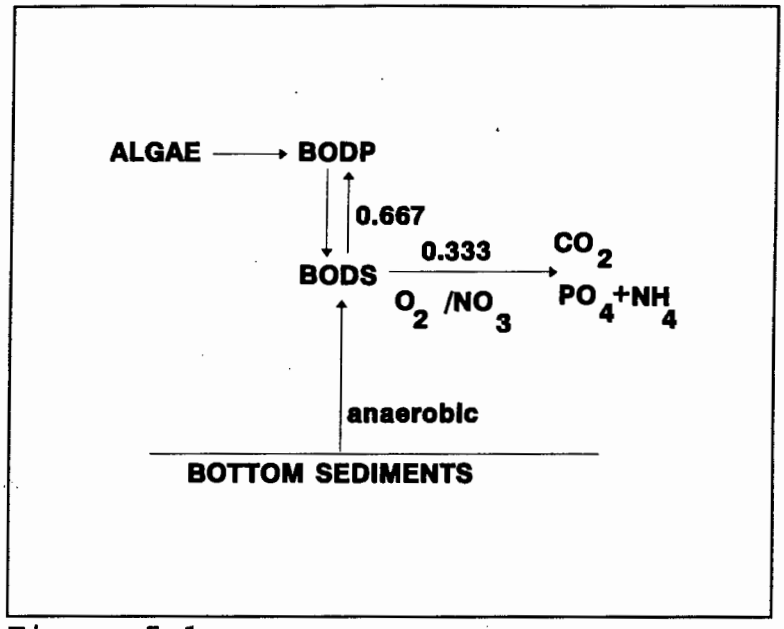

Figure 5.1
Diagram of detrital decay, accounting for regeneration of particulate BOD from dissolved BOD during decay of the latter.

Formulation of the scheme in Fig 5.1 is as follows:

Sources of particulate BOD:

- *Algal mortality - cf Eq 5.46.*
- *Regeneration from dissolved BOD - two-thirds of the decaying dissolved BOD forms particulate BOD again.*

Thus the sources of particulate BOD were formulated as:

$$dBODP/dt = \left(\frac{XKM*CHLa}{YCBOD}\ QCHLa^{(T-20)}\right)+(0.666\ BODS*BODSK\ \theta^{(T-20)})\left(\frac{DSO}{DSO+BODSOK}\right)+\left(DNK\ \theta_N^{(T-20)}\right)\left(\frac{KONO}{KONO+DSO}\right)\left(\frac{NO}{NO+EDNK}\right) \quad (5.49)$$

dBODP/dt = *increase in particulate BOD concentration (mg l^{-1})*

XKM = *algal mortality rate at 20°C (day^{-1})*

CHLa = *chlorophyll-a concentration (mg l^{-1})*

YCBOD = *BOD coefficient (cf Eq 5.46)*

= *mass ratio of biodegradable detritus produced from chlorophyll-a (mg chla (mg Bod)$^{-1}$)*

QCHLa = *Arrhenius temperature coefficient for algal mortality (cf Eq 4.92)*

T = *water temperature in the layer (°C)*

BODS = *concentration of dissolved BOD (mg l^{-1})*

BODSK = *decay rate dissolved BOD at 20 °C (day^{-1})*

θ = *Arrhenius temperature coefficient for detrital decay*

BODSOK = *aerobic switching constant for dissolved BOD decay (mg O_2 l^{-1})*

DSO = *dissolved oxygen concentration (mg l^{-1})*

DNK = *denitrification rate at 20 °C (day^{-1})*

θ_N = *Arrhenius temperature coefficient for denitrification*

KONO = *anaerobic switching constant for denitrification (mg $O_2 l^{-1}$)*

NO = *nitrate concentration (mg l^{-1})*

EDNK = *nitrate switching constant for denitrification (mg NO_3 l^{-1}).*

Basically, Eq 5.49 is equivalent to Eq 5.48, except for addition of the mortality term. The explanation for rest of the terms is as for Eq 5.48.

Decomposition of particulate BOD:

(This formulation serves as a sink of particulate BOD, and as a source of dissolved BOD)

$$dBOD/dt = BODPK * \theta^{(T-20)} * BODP \qquad (5.50)$$

dBOD/dt = *decrease in particulate BOD (increase in dissolved BOD) (mg l^{-1})*

BODPK = *decomposition rate of particulate BOD at 20°C (day^{-1})*

θ = *Arrhenius temperature coefficient*

BODP = *concentration of particulate BOD (mg l^{-1}).*

Dissolved BOD:

During microbial decay of dissolved BOD (i.e utilization of dissolved BOD as substrate), oxygen, and thereafter nitrate, serves as an electron acceptor, thus this reaction constitutes a sink of dissolved BOD:

$$dBODS/dt = (BODSK\ \theta^{(T-20)}) \left(\frac{DSO}{DSO+BODSOK}\right) + (DNK\ \theta_N^{(T-20)}) \left(\frac{KONO}{KONO+DSO}\right) \left(\frac{NO}{NO+EDNK}\right) BODS \qquad (5.51)$$

dBODS/dt = *change in dissolved BOD concentration due to decay (mg l^{-1})*

BODSK = *dissolved BOD decay rate at 20 °C (day^{-1})*

θ = *Arrhenius temperature coefficient for detrital decay (cf Eq 4.92).*

BODSOK = *aerobic switching constant for decay of dissolved BOD (mg O_2 l^{-1})*

DSO = *dissolved oxygen concentration (mg l^{-1})*

DNK = *denitrification rate at 20 °C (day^{-1})*

θ_N = *Arrhenius temperature coefficient for denitrification*

KONO = *anaerobic switching constant for denitrification (mg $O_2 l^{-1}$)*

NO = *nitrate concentration (mg l^{-1})*

EDNK = *nitrate switching constant for denitrification (mg NO_3 l^{-1})*

BODS = *concentration of dissolved BOD (mg l^{-1}).*

Basically, Eq 5.51 is the same as Eq 5.48, except that Eq 5.51 describes the decay of dissolved BOD, whereas no distinction is made between dissolved and particulate BOD in eq 5.48. Therefore, the terms in Eq 5.51 has the same basis as in Eq 5.48.

Regarding settling of detritus - because a distinction is made between particulate and dissolved detritus, settling, as formulated in the original MINLAKE model, applies to particulate BOD only. Dispersion of dissolved BOD will be similar to that of other dissolved substances such as dissolved phosphate, and thus the formulation used to describe the turbulent diffusion of dissolved phosphate (Eq 5.71) was used to describe dispersion of dissolved BOD also.

Regarding decay of organic matter in the bottom sediments - if no distinction is made between particulate and dissolved BOD, decay of organic matter in the bottom sediments can be described as part of the sediment oxygen demand (SOD) as formulated in Eq 5.38. However, if organic matter is simulated as particulate and dissolved BOD, provision must be made for the fact that, under anaerobic conditions, when no decay can take place in the bottom sediments, dissolved BOD will diffuse out of the bottom sediments back into the water column, thereby constituting a source of dissolved BOD. In the modified MINLAKE model, this was formulated as follows:

$$dBODS/dt = BBOT \frac{A}{V} \theta^{(T-20)} \left(\frac{BBOTOK}{BBOTOK + DSO} \right) \qquad (5.52)$$

dBODS/dt	=	*increase in dissolved BOD concentration in a layer (mg l^{-1})*
BBOT	=	*dissolved BOD released from bottom sediment (mg l^{-1})*
A	=	*area of bottom sediment in a layer (m^2)*
V	=	*volume of layer (m^3)*
θ	=	*Arrhenius temperature coefficient for BODS release from the bottom sediment*
T	=	*water temperature of the layer (°C)*
BBOTOK	=	*anaerobic switching constant for BODS release (mg O_2 l^{-1})*
DSO	=	*dissolved oxygen concentration in the layer (mg l^{-1}).*

Under aerobic conditions, decay of dissolved BOD in the bottom sediments is modelled as part of the sediment oxygen demand (cf Eq 5.39).

The results that were obtained with the two different formulations (i.e. formulating BOD decay as a one step process, and the more complex two-step formulation that distinguishes between particulate and dissolved BOD), are discussed in paragraphs 7.6 and 8.2.6.

5.3.3 MINLAKE formulation of the processes that affect algal concentration

The MINLAKE model has been formulated such that up to three algal classes can be simulated simultaneously. Each algal class is simulated separately, whereafter the concentrations are added together to give the total algal concentration. Total algal concentration, as well as algal concentration for each class, are represented as chlorophyll-a. For each algal class, the process of algal growth contributes to an increase in chlorophyll-a concentration, whereas processes such as hydraulic washout, diffusion, sedimentation, algal respiration and mortality, and zooplankton grazing contribute to a decrease in chlorophyll-a concentration.

Algal growth is considered to be independent of external nutrient levels. Thus algal growth rate is limited by either internal phosphorus, or internal nitrogen, or light. In each layer the growth limitation by internal nutrients or light is given by:

$$\mu = \mu_{max} [L_P : L_I]_{min} f(T) \qquad (5.53)$$

μ = specific algal growth rate (day^{-1})
μ_{max} = nutrient saturated growth rate (day^{-1})
L_P = nutrient limited growth ratio (between 0 and 1)
L_I = light limited growth ratio (between 0 and 1)
f(T) = temperature effect on algal growth rate.

Formulation of the light limited growth ratio, the nutrient limited growth ratio, and the temperature effect on algal growth rate is discussed in the next paragraphs.

5.3.3.1 MINLAKE formulation of the process of photosynthesis:

The process of photosynthesis is formulated as a light limited growth ratio (*cf* Eq 5.53):

$$L_I = \frac{I_{ave}\left(1 + 2\left(\frac{K_1}{K_2}\right)^{0.5}\right)}{I_{ave} + K_1 + \frac{I^2}{K_2}} \qquad (5.54)$$

L_P = nutrient limited growth ratio (between 0 and 1)
I_{ave} = average photosynthetically active irradiance (μE m^{-2} s^{-1})
K_1 = light limitation coefficient (μE m^{-2} s^{-1})
K_2 = light inhibition coefficient (μE m^{-2} s^{-1}).

The above formulation is based on the formulation of Megard *et al* (1984) (*cf* Eq 4.100). The light limitation coefficient, K_1 is analogous to a Michaelis-Menten type half-saturation coefficient for light limited growth. Incorporation of a light inhibition coefficient, K_2, provides for the effect of photo inhibition on photosynthesis at high irradiances.

Regarding average photosynthetically active irradiance; firstly, photosynthetically active irradiance (PAR) in the top of the first layer is calculated from incoming solar radiation, whereafter it is considered to be attenuated in the same way as solar radiation. *Average* PAR in a layer is calculated from the attenuated fraction. In the original MINLAKE model, calculation of PAR from incoming solar radiation in the top of the first layer has been formulated as follows:

$$I = \frac{27.25}{TD} RAD(1 - Albedo) \quad (5.55)$$

I	=	photosynthetically active irradiance over the daylight period (μE m^{-2} s^{-1})
27.25	=	constant
TD	=	daylight period (hr)
RAD	=	solar radiation (cal cm^{-2} day^{-1})[2]
Albedo	=	solar radiation reflected at the water surface as formulated in Eq 5.3.

Photosynthetically active radiation is assumed to be distributed symmetrically about a midday maximum. Average photosynthetically active radiation in a layer is found by integrating the light attenuation function over the thickness of the layer, divided by the thickness of the layer:

$$I_{ave} = \frac{I_i[1 - \exp(-kDz_i)]}{kDz_i} \quad (5.56)$$

I_{ave}	=	average photosynthetically active irradiance in a layer (μE m^{-2} s^{-1})
I_i	=	PAR reaching the top of the layer (μE m^{-2} s^{-1})
k	=	total extinction coefficient (Eq 5.5)
Dz_i	=	thickness of layer i (m).

The daylight period, TD, in Eq 5.55 warrants some discussion. The daylight period, (length of day) is a function of latitude, as well as the angle of sun (solar declination), but in the original MINLAKE model the daylight period was given by the following:

---

[2]In the MINLAKE manual the units 'cal cm^{-2} day^{-1}' are referred to also as 'Langley day^{-1}'

$$TD = 12.16 + 2.36*\cos(0.0172*(172 - DY)) \quad (5.57)$$

DY = Julian day.

This expression was hard-wired into the model. No explanation as to the origin of the constants in the formulation was given. However, according to Kirk (1983), the length of day at any given latitude can be formulated as:

$$N = 0.133 \cos^{-1}(-\tan\gamma \tan\delta) \quad (5.58)$$

N = day length (hr)
γ = latitude (degrees)
δ = angle of the sun (solar declination).

Solar declination can be formulated as (Kirk 1983):

$$\delta = 0.39637 - 22.9133 \cos\psi + 4.02543 \sin\psi - 0.3872 \cos 2\psi + 0.052 \sin 2\psi \quad (5.59)$$

δ = angle of the sun (solar declination)
ψ = date expressed as an angle
= 360°d/365
d = Julian day.

NB: On any given date the solar declination for the Southern hemisphere has the same numerical value as for the Northern hemisphere, but opposite sign.

It would seem that the expression in the MINLAKE model has been hard-wired to the latitude of the Minnesota Lakes, and that the solar declination is calculated from the Julian day, but for the Northern hemisphere, which means that Eq 5.57 is totally unsuitable for South African conditions. In the modified MINLAKE model, daylight period is formulated according to Eq 5.58 and 5.59, and the user must specify the latitude and whether the calculation is done for the Northern or the Southern hemisphere.

5.3.3.2 MINLAKE formulation of nutrient uptake and algal growth rate:

Nutrient uptake and algal growth rate is formulated as a two-step process, in accordance with the Droop concept (*cf* paragraph 4.4.3.2). The formulation for algal growth rate is as given in Eq 5.53. The nutrient limited growth ratio in Eq 5.53 is formulated as:

$$L_P = \frac{N_c - Chla(N_{min})}{N_c} \qquad (5.60)$$

L_P = nutrient limited growth ratio (between 0 and 1)

N_c = intracellular nutrient concentration (mg l^{-1})

Chla = chlorophyll-a concentration (mg l^{-1})

N_{min} = Minimum cell quota of nutrient to chlorophyll-a required for growth (mg nutrient mg $Chla^{-1}$).

Nutrient uptake rate is formulated according the Michaelis-Menten concept:

$$U = U_{max} \frac{(Chla)\ (N_{max}) - N_c}{(Chla)\ (N_{max} - N_{min})} \left(\frac{S}{K_s + S} \right) Chla \qquad (5.61)$$

U	=	specific uptake rate (day^{-1})
U_{max}	=	maximum specific uptake rate (day^{-1})
Chla	=	chlorophyll-a concentration in a layer ($mg\ l^{-1}$)
N_{max}	=	maximum nutrient concentration that can be stored in the algal cell (mg nutrient (mg chla)$^{-1}$)
N_c	=	nutrient concentration in the algal cell ($mg\ l^{-1}$)
N_{min}	=	minimum nutrient concentration in algal cell required for algal growth (mg nutrient (mg chla)$^{-1}$)
S	=	nutrient concentration in a layer ($mg\ l^{-1}$)
K_s	=	half-saturation coefficient for nutrient uptake ($mg\ l^{-1}$).

As was discussed in paragraph 4.4.3.2, models that formulate nutrient uptake and algal growth as a two-step process according to the Droop concept simulate algal growth more accurately than those formulated according to the Monod concept, and thus no changes were made to the MINLAKE formulation of nutrient uptake and algal growth.

5.3.3.3 MINLAKE formulation of the effect of temperature on algal growth rate:

The temperature effect is calculated separately for each algal class. According to the MINLAKE manual, the formulation in the original MINLAKE model is based on the formulation of Lehman (1975) (paragraph 4.4.3.3):

$$XT = \exp\left(-2.3\left(\frac{T - T_{opt}}{T_{opt}}\right)^2\right) \quad for\ T < T_{opt} \qquad (5.62)$$

XT	=	temperature function for particular algal class
T_{opt}	=	optimum temperature for algal growth (°C)
T	=	ambient water temperature in a layer (°C)
T_{min}	=	lower temperature where algal growth rate has declined to 10% of the maximum growth rate (°C).

If the above formulation is compared to that of Lehman (Eq 4.102 and 4.103), it seems that T_{min} has been omitted from the expression below the line. This is equivalent to hard-wiring the value of T_{min} to 0°C, i.e. the minimum temperature for algal growth to occur is set at 0°C. Such an approach may be appropriate for a cold temperate climate, but not for the warm temperate/subtropical climate of Southern Africa, where it has been observed, for instance, that growth of blue-green algae does not occur below 17 - 18°C (Krüger and Eloff 1978). Thus the above formulation was changed by re-incorporating T_{min} into the formulation according to the formulation of Lehman (1975). T_{min} can be specified by the user. Furthermore, though of lesser importance, in the original MINLAKE formulation the expression above the line is $(T - T_{opt})$, instead of $(T_{opt} - T)$ as in Lehman's formulation. As the expression is squared this difference is not really of any significance, but it was corrected nevertheless to $(T_{opt} - T)$ as in Lehman's formulation.

If the ambient water temperature is greater than the optimum temperature for algal growth, the original MINLAKE formulation of the temperature effect is as follows:

$$XT = \exp\left(-2.3\left(\frac{T - T_{opt}}{T_{max} - T_{opt}}\right)^2\right) \qquad (5.63)$$

XT	=	temperature function for particular algal class
T_{opt}	=	optimum temperature for algal growth (°C)
T	=	ambient water temperature (°C)
T_{max}	=	upper temperature for where algal growth rate has declined to 10% of the maximum growth rate (°C).

Basically, Eq 5.63 is in accordance with Lehman's formulation and therefore no changes were made to this equation.

5.3.3.4 MINLAKE formulation of the processes that decrease algal concentration: In the original MINLAKE model, processes such as settling, hydraulic washout, algal respiration and mortality, and zooplankton grazing contribute to a decrease in chlorophyll-a concentration.

Settling are regarded as a loss process in each layer. Net settling velocity in a layer is calculated as the difference between the settling velocity at the top and the bottom of a layer. The effect of turbulence on settling is taken into account by use of a Peclet number. [3]

[3]The Peclet number relates the effect of flow on transfer by turbulent diffusion (Reynolds 1974)

$$CC(I) = \left[1+\left(\frac{ATOP(I+1)*FV}{V(I)}\right)(1+PE(I+1))\right] * Chla(I) + \left[\left(\frac{ATOP(I)*FV}{V(I)}\right)*PE(I)\right] * Chla(I) - \left[\left(\frac{FV}{V(I)}\right)*(ATOP(I+1)-ATOP(I))\right] * Chla(I) \quad (5.64)$$

CC(I)	=	change in Chla concentration in layer I (mg l^{-1})
ATOP(I)	=	surface area at the top of layer I (m^2)
ATOP(I+1)	=	surface area at the top of the layer below layer I (m^2)
	=	surface area at the bottom of layer I
V(I)	=	volume of layer I (m^3)
PE(I)	=	Peclet number of layer I (Eq 5.65)
PE(I+1)	=	Peclet number of the layer below layer I
FV	=	settling velocity (m day^{-1})
Chla (I)	=	chlorophyll-a concentration in layer I (mg l^{-1}).

The settling velocity must be specified by the user for each algal group. The Peclet number is formulated as follows:

$$PE = \frac{1.0 - 0.1\ ABS(X)^5}{X} \quad (5.65)$$

with

$$x = \frac{FV * (DZ(I-1)+DZ(I)*0.5}{HMK(I)} \quad (5.66)$$

FV	=	algal settling velocity (m day^{-1})
HMK(I)	=	mean turbulent diffusion coefficient in layer I (m day^{-1}) (*cf* Eq 5.26)
HMK(I+1)	=	mean turbulent diffusion coefficient in the layer below layer I (m day^{-1})
DZ(I)	=	thickness of layer I (m)
DZ(I-1)	=	thickness of the layer above layer I (m).

No changes were deemed necessary to the above formulation of the effect of settling velocity on algal concentration.

Regarding hydraulic washout, there is no specific formulation for hydraulic washout - the MINLAKE model follows the general trend and calculate losses during hydraulic washout as part of the entrainment that occur during discharge.

Regarding algal respiration, in the original MINLAKE model it is formulated as a first-order reaction, taking account of the effect of temperature on respiration:

$$R = k_r \, \theta^{(T - 20)} (Chla) \qquad (5.67)$$

R	=	algal respiration rate (mg l^{-1} day^{-1})
k_r	=	respiration coefficient (day^{-1})
θ	=	Arrhenius temperature coefficient
T	=	ambient water temperature in a layer (°C)
Chla	=	chlorophyll-a concentration (mg l^{-1}).

No changes were made to this formulation.

Algal mortality is formulated in the same way as respiration:

$$M = k_m \, \theta^{(T - 20)} (Chla) \qquad (5.68)$$

M	=	mortality rate (mg l^{-1} day^{-1})
k_m	=	mortality coefficient (day^{-1})
θ	=	Arrhenius temperature coefficient
T	=	ambient water temperature in a layer (°C)
Chla	=	chlorophyll-a concentration (mg l^{-1}).

No changes were made to this formulation.

Algal concentration is decreased further by zooplankton grazing. In the original MINLAKE model, the grazing term for each algal class is given by:

$$G = G_{max}\left(\frac{Chla-Chla_{min}}{Chla-Chla_{min}+HSC_G}\right)\theta_G^{T-20}\,ZP\Delta t\frac{V(IZ)}{V}(CF) \qquad (5.69)$$

G	=	grazing in a layer (mg Chla l^{-1})
G_{max}	=	maximum grazing rate (mg Chla day^{-1})
$Chla_{min}$	=	minimum chlorophyll-a concentration for grazing to occur (mg l^{-1})
HSC_G	=	half saturation constant for grazing (mg Chla l^{-1})
θ_G	=	Arrhenius temperature coefficient for zooplankton grazing
T	=	temperature in a layer (°C)
ZP	=	zooplankton concentration at day depth layer (# m^{-3})
Δt	=	time spent in a layer (day)
V(IZ)	=	volume of day depth layer (m^3)
V	=	volume of layer (m^3)
CF	=	conversion factor for m^3 to litre.

This formulation corresponds to the formulation of Steele (1974). In paragraph 4.4.3.4 it was concluded that the formulation of Steele appears to be most in accordance with observed behaviour, and therefore no changes were made to the formulation in the original MINLAKE model.

5.3.4. MINLAKE formulation of the processes that affect the availability of nutrients.

In the original MINLAKE model, only phosphorus and nitrogen are formulated as nutrients. Although the model will be improved by formulation of silica as a nutrient[4], unfortunately the necessary data were not available.

5.3.4.1 MINLAKE formulation of the availability of phosphorus:

In the original MINLAKE model, phosphorus is simulated as total phosphorus, and as dissolved phosphate. Total phosphorus is calculated simply as the sum of dissolved phosphate, and internal and detrital phosphorus.

The concentration of dissolved phosphate in a layer is affected by algal uptake, diffusion, algal mortality and respiration, zooplankton grazing, inflow, and sediment phosphorus release.

The effect of uptake by algae:

The decrease in the concentration of dissolved phosphate in a layer is equivalent to Eq 5.61, except that in this case it is regarded as a loss term. At the same time, the internal phosphate concentration is increased by the uptake of phosphate from the water:

---

[4] The growth of diatoms may be limited by low silica concentration. Although diatoms occur in South African reservoirs, they are not dominant in eutrophic South African reservoirs.

$$U = U_{max} \frac{(Chla)\ (P_{max}) - P_c}{(Chla)\ (P_{max} - P_{min})} \left(\frac{P}{K_p + P} \right) \qquad (5.70)$$

U	=	specific uptake rate (day^{-1})
U_{max}	=	maximum specific uptake rate (day^{-1})
Chla	=	chlorophyll-a concentration (mg l^{-1})
P_{max}	=	maximum phosphate concentration that can be stored in the algal cell (mg phosphate (mg chla)$^{-1}$)
P_c	=	phosphate concentration in the algal cell (mg l^{-1})
P_{min}	=	minimum phosphate concentration in algal cell required for algal growth (mg nutrient (mg chla)$^{-1}$)
P	=	concentration of dissolved phosphate in reservoir water (mg l^{-1})
K_p	=	half-saturation coefficient for phosphate uptake (mg l^{-1}).

As discussed in paragraph 5.3.3.3, no changes were made to this formulation

The effect of turbulent diffusion:

Turbulent diffusion is one of the main transport mechanisms of nutrients, specially in the hypolimnion (see discussion in paragraph 3.4.2.5). In the original MINLAKE model, the net effect of turbulent diffusion on the concentration of dissolved phosphate in a layer is formulated as the difference between phosphate transported into the layer, and that transported out of the layer by means of turbulent diffusion:

$$dP/dT = 1 + \frac{ATOP(I)}{V(I)} * \frac{HMK(I)}{DZ(I) + DZ(I-1)} + \frac{ATOP(I+1)}{V(I)} * \frac{HMK(I+1)}{DZ(I) + DZ(I+1)} \quad (5.71)$$

ATOP(I)	=	Surface area at the top of layer I ($m^{2)}$
ATOP(I+1)	=	surface area at the top of the layer below layer I ($m^{2)}$
	=	surface area at the bottom of layer I
V(I)	=	volume of layer I (m^3)
HMK(I)	=	mean turbulent diffusion coefficient in layer I (m day^{-1}) (*cf* Eq 5.26)
HMK(I+1)	=	mean turbulent diffusion coefficient in the layer below layer I (m day^{-1})
DZ(I)	=	thickness if layer I (m)
DZ(I+1)	=	thickness of the layer below layer I (m)
DZ(I-1)	=	thickness of the layer above layer I (m).

No changes were made to this formulation.

The contribution of algal mortality:

Owing to the phenomenon of luxury uptake, phosphate is released into the water during algal mortality. Only excess phosphorus stored in the cell is released into the surrounding water, organically bound phosphate is released during detrital decay.

Formulation of phosphate release during mortality in the original MINLAKE model is equivalent to the formulation by Riley and Stefan (1988):

$$\frac{\partial P}{\partial t} = k_m \theta^{(T-20)} (P_c - P_{min} CHLa) \qquad (5.72)$$

$\partial P/\partial t$ = increase in phosphorus concentration with time

k_m = mortality coefficient (day^{-1})

θ = Arrhenius temperature coefficient for mortality

T = ambient water temperature in a layer(°C)

P_c = intracellular phosphorus concentration (mg P (mg chla)$^{-1}$)

P_{min} = minimum intracellular phosphorus concentration required for growth (mg P (mg chla)$^{-1}$).

Dissolved phosphate concentration in a layer is taken to be increased in a similar way by zooplankton grazing. No changes were made to the original MINLAKE formulation of phosphate released by algal mortality and zooplankton grazing.

The contribution of excretion and respiration:

According to the MINLAKE manual, intracellular phosphorus concentration is decreased by excretion of phosphorus from the cell. Simultaneously, the concentration of dissolved phosphate in a layer is increased by the excreted phosphorus. The excretion loss/increase is taken as equal to the respiration rate. The resultant increase in dissolved phosphate concentration is formulated as follows:

$$dP/dt = k_r \theta^{(T-20)} P_c \qquad (5.73)$$

dP/dt = change in dissolved phosphate concentration in the layer (mg l^{-1})

k_r = respiration coefficient

θ = Arrhenius temperature coefficient for respiration

T = water temperature in the layer

P_c = intracellular phosphorus concentration (mg l^{-1}).

No changes were made to this formulation.

Detrital decay:

During detrital decay intracellular phosphorus (i.e. the phosphorus corresponding to the minimum intracellular concentration) is released. In the original MINLAKE model, this was formulated as follows:

$$dP/dt = BODK\ 1.055^{(T-20)}\ BOD\ YPBOD \qquad (5.74)$$

dP/dt = increase in dissolved phosphate concentration due to detrital decay (mg l^{-1})

BODK = detrital decay rate at 20°C (day^{-1})

1.055 = Arrhenius temperature coefficient

BOD = concentration of detritus (mg l^{-1})

YPBOD = phosphate yield coefficient (mg P mg BOD^{-1}).

The changes made to the formulation of detrital decay, as discussed in paragraphs 5.3.2.1 and 5.3.2.2, also will affect release of phosphate during detrital decay. In the modified MINLAKE model two possible formulations of detrital decay were tested, and thus formulation of phosphate release depends on formulation of detrital decay. If detrital decay is formulated as a simple first-order reaction, phosphate release can be formulated as:

$$dP/dt = (BODK * \theta^{(T-20)}) \left(\frac{DSO}{DSO+BODOK}\right) + (DNK\ \theta_N^{(T-20)}) \left(\frac{KONO}{KONO+DSO}\right) \left(\frac{NO}{NO+EDNK}\right) BOD \cdot YPBOD \quad (5.75)$$

dP/dt = *change in dissolved phosphate concentration due to detrital decay (mg l^{-1})*

BODK = *detrital decay rate at 20 °C (day^{-1})*

θ = *Arrhenius temperature coefficient for detrital decay (cf Eq 4.92).*

BODOK = *aerobic switching constant for detrital decay (mg O_2 l^{-1})*

DSO = *dissolved oxygen concentration (mg l^{-1})*

DNK = *denitrification rate at 20 °C (day^{-1})*

θ_N = *Arrhenius temperature coefficient for denitrification*

KONO = *anaerobic switching constant for denitrification (mg $O_2 l^{-1}$)*

NO = *nitrate concentration (mg l^{-1})*

EDNK = *nitrate switching constant for denitrification (mg NO_3 l^{-1})*

BOD = *concentration of BOD (mg l^{-1})*

YPBOD = *phosphate yield coefficient (mg P mg BOD^{-1}).*

(For an explanation of the terms in the above equation, see Eq 5.48).

In the second formulation of detrital decay in the modified MINLAKE model, a distinction is made between particulate and dissolved BOD, and the regeneration of particulate BOD during decay of dissolved BOD is taken into account (cf paragraph 5.3.2.2) - during decay of dissolved BOD, two-thirds form particulate BOD, and only one-third decays by utilising oxygen/nitrate, and releasing intracellular phosphorus. In this case, phosphate release can be formulated as:

$$dP/dt = (BODSK * \theta^{(T-20)}) \left(\frac{DSO}{DSO+BODSOK}\right) + (DNK\ \theta_N^{(T-20)}) \cdot \left(\frac{KONO}{KONO+DSO}\right)\left(\frac{NO}{NO+EDNK}\right) 0.333\ BODS \cdot YPBOD \qquad (5.76)$$

dP/dt = *change in dissolved phosphate concentration due to decay of dissolved BOD (mg l^{-1})*

BODSK = *dissolved BOD decay rate at 20 °C (day^{-1})*

θ = *Arrhenius temperature coefficient for detrital decay (cf Eq 4.92).*

BODOK = *aerobic switching constant for detrital decay (mg O_2 l^{-1})*

DSO = *dissolved oxygen concentration (mg l^{-1})*

DNK = *denitrification rate at 20 °C (day^{-1})*

θ_N = *Arrhenius temperature coefficient for denitrification*

KONO = *anaerobic switching constant for denitrification (mg $O_2 l^{-1}$)*

NO = *nitrate concentration (mg l^{-1})*

EDNK = *nitrate switching constant for denitrification (mg NO_3 l^{-1})*

BODS = *concentration of dissolved BOD (mg l^{-1})*

YPBOD = *phosphate yield coefficient (mg P mg BOD^{-1}).*

The role of the bottom sediments:

In the original MINLAKE model, release/adsorption of phosphate by the bottom sediments is formulated as a constant rate:

$$dP/dt = \frac{BRR}{V} A \qquad (5.77)$$

dP/dt = change in dissolved phosphate concentration (mg l^{-1})

BRR = sediment phosphorus release/adsorption rate (g m^{-2} day^{-1})

A = bottom sediment area in a layer (m^2)

V = volume of a layer (m^3).

The value of BRR has to be specified by the user, and by specifying a positive or a negative value either release or adsorption can be simulated during a run. Both cannot be simulated during the same run. During calibration of the model on Roodeplaat Dam this formulation was found to be totally inadequate - under anaerobic conditions phosphate is released by the bottom sediments in Roodeplaat Dam, but under aerobic conditions phosphate is adsorbed. As the reservoir regularly turns anaerobic during the stratified period, there is definite need to simulate both release and adsorption of phosphate by the bottom sediments during the same run. According to the discussion in paragraph 4.4.4.1 on the role of bottom sediments, as some South African reservoirs have retention times greater than one year (Walmsley and Butty 1980a), the best way of simulating phosphate adsorption release probably would be to utilize the sediment submodel developed by Jørgensen et al (1982). However, the necessary data to calibrate such a submodel are not available for South African reservoirs. The best that could be done with the available data was to modify the formulation in the original MINLAKE model so the user can specify both a release and adsorption rate. By linking these rates to the anaerobic/aerobic state of the water by means of a switching function (Eq 4.93 and 4.94), it is possible to simulate both sediment phosphate release and adsorption during the same run, depending on the anaerobic/aerobic state of the overlying water. Also, according to Henderson-Sellers (1984), it has been found that phosphate will be released from sediments at a steady rate until a certain equilibrium concentration is reached, whereafter release is inhibited. This was confirmed by a study done on Roodeplaat Dam (DWAF 1981), thus this behaviour was incorporated into the program by linking BRR (the sediment phosphorus release rate) to a phosphate switching function, EBRR. Furthermore, both sediment phosphate release and adsorption are affected by temperature (Jørgensen 1980), thus both the adsorption and release rate was linked to an Arrhenius-type temperature function. The resultant formulation for sediment phosphate release in the modified MINLAKE model is as follows:

$$dP/dt = \left[BRR\left(\frac{BRPK + DSO}{BRPK}\right)\left(\frac{EBRR}{EBRR+P}\right) - BAA\frac{DSO}{DSO + BRPK}\right] * QBRR^{(T-20)}\frac{A}{V}$$

(5.78)

dP/dt = *change in dissolved phosphate concentration in a layer (mg l^{-1})*

BRR = *sediment phosphate release rate (g m^{-2} day^{-1})*

BAA = *sediment phosphate adsorption rate (g m^{-2} day^{-1})*

BRPK = *switching constant for sediment phosphate release/adsorption (mg l^{-1}) (Eq 4.93 and 4.94)*

EBRR = *phosphate switching function (mg l^{-1})*

= *1/2 equilibrium concentration for sediment phosphate release*

P = *dissolved phosphate concentration in a layer (mg l^{-1})*

DSO = *dissolved oxygen concentration in a layer (mg l^{-1})*

QBRR = *Arrhenius temperature coefficient for sediment phosphate release/adsorption*

T = *water temperature in a layer (°C)*

A = *bottom sediment area in a layer (m^2)*

V = *volume of a layer (m^3).*

Although the above formulation requires specification of four extra coefficients (BRPK, BAA, EBRR and QBRR), this is the minimum formulation for simulating the role of the bottom sediments in a typical South African reservoir such as Roodeplaat Dam.

5.3.4.2 MINLAKE formulation of the availability of nitrogen:

In both the original and the modified MINLAKE model, ammonia and nitrate are simulated separately. This allows for the effect of processes such as nitrification to be simulated.

In the original MINLAKE model the concentrations of ammonia and nitrate are affected by turbulent diffusion, algal uptake, respiration, detrital decay, nitrification, inflow, and sediment release.

The effect of turbulent diffusion:

Turbulent diffusion is one of the most important mechanisms for transporting nutrients, specially in the hypolimnion. To simulate the effect of turbulent diffusion on the concentrations of ammonia and nitrate, the same formulation is used as with dissolved phosphate, i.e. Eq 5.71. No changes were made to this formulation.

The effect of uptake by algae:

In the original MINLAKE model, formulation of nitrogen uptake by algae makes provision for the preferential uptake of ammonia over nitrate (see discussion in paragraph 4.4.4.2). The formulation in the original MINLAKE model is based on the formulation by Scavia (1980):

$$U_{NO} = U' \left(1 - \frac{NH}{HSCNH + NH}\right) \qquad (5.79)$$

and

$$U_{NH} = U' \left(\frac{NH}{HSCNH + NH}\right) \qquad (5.80)$$

with

$$U' = U_{max}\left(\frac{CHLa\ N_{max} - N_c}{CHLa\ (N_{max} - N_{min})}\right)\left(\frac{NH + NO}{HSCN + NH + NO}\right) \qquad (5.81)$$

U_{NO} = nitrate uptake rate (day^{-1})

U_{NH} = ammonium uptake rate (day^{-1})

U' = nitrogen uptake rate (day^{-1})

NH = ammonium concentration (mg l^{-1})

HSCNH = ammonium preference constant (mg l^{-1})

U_{max} = maximum nitrogen uptake rate (day^{-1})

CHLa = chlorophyll-a concentration (mg l^{-1})

N_{max} = maximum intracellular nitrogen concentration (mg N (mg Chla)$^{-1}$)

N_{min} = minimum intracellular nitrogen concentration required for algal growth (mg N (mg Chla)$^{-1}$)

NO = nitrate concentration (mg l^{-1})

HSCN = half saturation constant for nitrogen uptake (mg l^{-1}).

No changes were made to formulation of nitrogen uptake by algae. In both the original and the modified MINLAKE models, algal uptake of ammonia and nitrate decreases concentration of these nutrients in a layer, whereas it increases the internal concentration of nitrogen.

The effect of mortality:

In both the original and the modified MINLAKE model, mortality affects the concentration of ammonium only. When the algal cell dies, excess ammonium stored in the cell is released into the surrounding water. The formulation is the same as for phosphate release during mortality (Eq 5.72):

Detrital decay:

Ammonia released during detrital decay is similar to phosphate release during detrital decay, and thus formulation, and changes made to the formulation in the original MINLAKe model, is the same as for phosphate (*cf* Eq 5.75 to 5.76), except that a nitrogen yield coefficient (YNBOD) is utilised instead of a phosphate yield coefficient (YPBOD).

The role of the bottom sediments:

Ammonium is released from the bottom sediments if the overlying water is anaerobic, whereas nitrate is released when the overlying water is aerobic. In the original MINLAKE model, sediment release of ammonia and nitrate is formulated as a constant rate, similar to the formulation for sediment phosphate release:

$$dNH/dt = \frac{BRNH}{V} A \qquad (5.84)$$

dNH/dt	=	change in ammonium concentration in a layer (mg l^{-1})
BRNH	=	sediment ammonium release rate (g m^{-2} day^{-1})
V	=	volume of the layer (m^3)
A	=	bottom sediment area in a layer (m^2).

The formulation for sediment nitrate release is the same, except that a sediment nitrate release rate, BRNO, is utilised instead of the sediment ammonia release rate, BRNH.

In the original MINLAKE model, the effect of the aerobic/anaerobic state of the water on sediment ammonia/nitrate release was not taken into account. To ensure that ammonium is released under anaerobic conditions only, the formula for sediment ammonium release was linked to an anaerobic switching function, whereas the formula for sediment nitrate release was linked to an aerobic switching function to ensure sediment nitrate release under aerobic conditions only. The effect of temperature on the release rates were taken into account by linking the release rates to an Arrhenius-type temperature function. The modified formulation for sediment ammonium release is as follows:

$$\frac{dNH}{dt} = k_m \theta^{(T-20)} (N_c - N_{min} Chla) \quad (5.82)$$

dNH/dt = increase in ammonia concentration in a layer (mg l^{-1})
k_m = mortality coefficient (day^{-1})
θ = Arrhenius temperature coefficient for mortality
T = ambient water temperature in a layer(°C)
N_c = intracellular nitrogen (ammonium) concentration (mg N (mg chla)$^{-1}$)
N_{min} = minimum intracellular nitrogen concentration required for growth (mg N (mg chla)$^{-1}$).

The increase in ammonium concentration in a layer due to zooplankton grazing is formulated in a similar way. No changes were made to the MINLAKE formulation of ammonium released during mortality and zooplankton grazing.

The contribution of excretion and respiration:

According to the MINLAKE manual, excretion and respiration affect the concentration of ammonium only. The intracellular concentration is decreased by excretion of ammonium, whereas the ammonium concentration in a layer is increased by the excreted ammonium. The excretion loss/increase is taken as equal to the respiration rate. The resultant increase in ammonium concentration is formulated as follows:

$$dNH/dt = k_r \theta^{(T-20)} N_c \quad (5,83)$$

dNH/dt = change in ammonium concentration in the layer (mg l^{-1})
k_r = respiration coefficient
θ = Arrhenius temperature coefficient for respiration
T = ambient water temperature in a layer(°C).

No changes were made to this formulation.

$$dNH/dt = BRNH \frac{A}{V} \left(\frac{BRNHK}{BRNHK+DSO} \right) QBRNH^{(T-20)} \quad (5.85)$$

dNH/dt = *change in ammonium concentration in a layer (mg l^{-1})*
BRNH = *sediment ammonium release rate (g m^{-2} day^{-1})*
V = *volume of the layer (m^3)*
A = *bottom sediment area in a layer (m^2).*
BRNHK = *switching constant for ammonium sediment release (mg l^{-1})*
DSO = *dissolved oxygen concentration in the layer (mg l^{-1})*
QBRNH = *Arrhenius temperature coefficient for sediment ammonium release*
T = *ambient water temperature in a layer (°C).*

Similarly, the modified formulation for sediment nitrate release is as follows:

$$dNO/dt = BRNO \frac{A}{V} \left(\frac{DSO}{DSO+BRNOK} \right) QBRNO^{(T-20)} \quad (5.86)$$

dNO/dt = *change in nitrate concentration in a layer (mg l^{-1})*
BRNO = *sediment nitrate release rate (g m^{-2} day^{-1})*
V = *volume of the layer (m^3)*
A = *bottom sediment area in a layer (m^2).*
BRNOK = *switching constant for nitrate sediment release (mg l^{-1})*
DSO = *dissolved oxygen concentration in the layer (mg l^{-1})*
QBRNO = *Arrhenius temperature coefficient for sediment nitrate release*
T = *ambient water temperature in a layer (°C).*

In both the original and the modified MINLAKE models the user has to specify the ammonium and nitrate release rate. As discussed in the formulation of sediment phosphate release, most likely sediment nutrient release is inadequately represented

by a constant release rate, but this is the best representation that can be calibrated with the available data.

Nitrification:

Nitrification leads to a decrease in ammonium concentration, and an increase in nitrate concentration. Thus, in the original MINLAKE model, nitrification is formulated as a loss term when calculating ammonium concentration, and as a source term when calculating nitrate concentration. The formulation is as follows:

$$dN/dt = XKNH * \theta_{NNH}^{(T-20)} * NH \qquad (5.87)$$

dN/dt	=	change in ammonia/nitrate concentration in a layer (mg l^{-1})
XKNH	=	nitrification rate (day^{-1})
θ_{NNH}	=	Arrhenius temperature coefficient for nitrification
T	=	ambient water temperature in a layer(°C)
NH	=	ammonium concentration in the layer (mg l^{-1}).

The original MINLAKE model does not provide for the fact that nitrification can take place under aerobic conditions only. Also, it has been observed (NIWR 1985) that nitrification is inhibited by high ammonium concentrations. Therefore, Eq 5.87 was linked to an aerobic switching function to ensure that nitrification takes place under aerobic conditions only. The inhibiting effect of high ammonium concentrations is provided for by incorporation of a Michaelis-Menten type expression, where the user can specify an inhibition coefficient, i.e the ammonium concentration where the nitrification rate is equal to half the maximum rate. The modified formulation is as follows:

$$dN/dt = XKNH \left(\frac{DSO}{DSO+KONH}\right) \theta_{NNH}^{(T-20)} \left(\frac{NH}{NH+XNH}\right) NH \qquad (5.88)$$

dN/dt = *change in ammonia/nitrate concentration in a layer (mg l^{-1})*

XKNH = *nitrification rate (day^{-1})*

DSO = *dissolved oxygen concentration in a layer (mg l^{-1})*

KONH = *switching constant for nitrification*

θ_{NNH} = *Arrhenius temperature coefficient for nitrification*

T = *ambient water temperature in a layer(°C)*

NH = *ammonium concentration in the layer (mg l^{-1})*

KNH = *inhibition coefficient for nitrification (mg l^{-1}).*

The modified formulation requires specification of two extra coefficients, i.e. the switching constant for nitrification, and the inhibition coefficient for nitrification. However, because many South African reservoirs turn anaerobic during stratification, and also because of the high ammonium concentrations present in some reservoirs, these modifications are regarded as essential.

Denitrification:

The original MINLAKE model does not include the process of denitrification. This process can take place under anaerobic conditions only, and as the model was developed on lakes in the cold temperate region of the northern hemisphere, where anaerobic conditions are less likely to develop than in a warm temperate/subtropical climate, the developers probably did not regard inclusion of the process of denitrification as essential. However, anaerobic conditions develop regularly in the majority of South African dams (Walmsley and Butty 1980a), and denitrification plays a very important part in the nitrogen budget (see paragraph 3.4.4.2). Therefore the original model was changed to include the process of denitrification via a simple first order reaction. Also, the change was affected in such a way that denitrification takes place under anaerobic conditions only. This was done by multiplying the denitrification rate with an anaerobic switching function (*cf* Eq 4.94).

Denitrification is a bacterial process that utilises detritus as substrate. Thus, formulation of denitrification would depend on formulation of detrital decay (paragraph 5.3.2). If detrital decay is formulated as a simple first-order reaction (Eq 5.48), denitrification can be formulated as:

$$dNO/dt = \left(DNK\ \Theta_N^{(T-20)}\right)\left(\frac{KONO}{KONO+DSO}\right)\left(\frac{NO}{NO+EDNK}\right)\frac{BOD}{2.86} \qquad (5.89)$$

dNO/dt	=	change in nitrate concentration in a layer due to denitrification (mg l^{-1})
DNK	=	denitrification rate at 20°C (day^{-1})
Θ_N	=	Arrhenius temperature coefficient for denitrification
T	=	water temperature in a layer (°C)
KONO	=	anaerobic switching constant for denitrification (mg O_2 l^{-1})
DSO	=	dissolved oxygen concentration in a layer (mg l^{-1})
NO	=	nitrate concentration in a layer (mg l^{-1})
EDNK	=	nitrate switching constant for denitrification (mg NO_3 l^{-1})
BOD	=	concentration of detritus as BOD (mg l^{-1}).

The constant 2.86 in the above equation originates from the fact that, during detrital decay via denitrification, each electron utilises 2.86 mg of nitrate.

If detrital decay is formulated as a two-step process, distinguishing between particulate and dissolved BOD, only one third of the dissolved BOD disappears by utilising oxygen/nitrate as an electron acceptor. (The other two-thirds form particulate BOD again). In this case, denitrification is formulated as follows:

$$dNO/dt = \left(DNK\ \theta_N^{(T-20)}\right)\left(\frac{KONO}{KONO+DSO}\right)\left(\frac{NO}{NO+EDNK}\right)\frac{0.333\ BODS}{2.86} \quad (5.90)$$

BODS = concentration of dissolved BOD (mg l^{-1}).

The rest of the symbols are as per Eq 5.89 above.

Inclusion of the denitrification process requires specification of four extra coefficients, i.e the denitrification rate, Arrhenius temperature coefficient for denitrification, an anaerobic switching function, and a nitrate switching function. However, the necessity of including this process was proved during calibration of the MINLAKE model on Roodeplaat Dam - calibration of the nitrate concentration was possible only once the process of denitrification was included; without denitrification there is a steady increase in nitrate concentration during the stratified period that does not correlate with the observed nitrate concentration (see discussion in paragraph 7.3.3).

5.3.5 MINLAKE formulation of the availability of light

The light that is available in a layer is a function of the amount of light extinction. In the original MINLAKE model, the extinction of light is taken to be equal to the extinction of solar radiation, which is formulated according to Beer's Law (Eq 5.4):

$$H(z) = H_{sn}e^{-\eta z} \quad (5.91)$$

H(z) = solar radiation at depth z (kcal m^{-2} d^{-1})
H_{sn} = net solar radiation (kcal m^{-2} d^{-1})
= $(1-r)H_s$
r = reflected fraction (kcal m^{-2} d^{-1})
H_s = incident solar radiation (kcal m^{-2} d^{-1})
n = total extinction coefficient (m^{-1}).

In both the original and the modified MINLAKE models, the total extinction coefficient is formulated as:

$$\eta = k_w + 0.043SS + k_2Chla \qquad (5.92)$$

η	=	total extinction coefficient (m^{-1})
k_w	=	extinction coefficient of pure water (m^{-1}) (*cf* Table 3.3)
SS	=	inorganic suspended sediment concentration (mg l^{-1})
k_2	=	extinction coefficient due to chlorophyll-a (m^2 (g chla)$^{-1}$)
Chla	=	chlorophyll-a concentration (mg l^{-1}).

From Eq 5.92 above, it is evident that the availability of light in a layer is affected by the concentration of algae and total inorganic suspended sediment (TSS). Formulation of the processes that contribute to algal concentration in a layer has been discussed in paragraph 5.3.3, thus only formulation of processes that contribute to TSS concentration will be discussed here.

In the original MINLAKE model, the concentration of TSS in a layer is calculated using the one-dimensional advection-diffusion equation (Eq 5.1). TSS is a conservative substance, and thus the only sources of TSS in a layer is inflow and resuspension. As discussed in paragraph 3.4.5, resuspension will not be addressed in this study, as the amount of resuspension in stratified reservoirs is negligible. The main sink of TSS in a layer is settling. In the original MINLAKE model, the settling velocity of TSS particles is calculated from the formulation given by Gibbs *et al* (1971):

$$v = \frac{-3\mu + \left[9\mu d^2 + g r_s^2 \rho_f (\rho_s - \rho_f)(0.015476 + 0.19841 r_s)\right]^{0.5}}{\rho_f (0.011607 + 0.14881 r_s)} \; 864 \qquad (5.93)$$

v	=	TSS settling velocity (m day^{-1})
μ	=	dynamic viscosity (poises) (Eq 5.94)
r_s	=	sediment particle radius (cm)
ρ_f	=	density of fluid (g cm^{-3})
ρ_s	=	density of sediment particle (g cm^{-3})
g	=	gravitational acceleration (cm s^{-2}).

The dynamic viscosity, μ, is formulated as:

$$\mu = \frac{1.79 * 10^{-2} \; \rho_f}{1 + 0.03368T + 0.000221T^2} \qquad (5.94)$$

μ	=	dynamic viscosity (poises)
ρ_f	=	density of fluid (g cm^{-3})
T	=	water temperature.

The effect of turbulence on sediment fall velocity is expressed by means of a Peclet number, similar to that for algal settling velocity (Eq 5).

It seems that Eq 5.93 is based on the general formulation for sediment fall velocity (Eq 4.151), and thus no changes were made to the basic formulation. However, in the original MINLAKE model, the sediment particle radius is hard-wired to a value of 0.5 μm, which corresponds to the radius of clay particles. In South African reservoirs silt particles often constitute the greater part of the sediment under dry flow conditions. Under storm flow conditions sand particles may form a significant part of the sediment composition. Therefore, the model was modified to allow the user to specify a sediment particle radius under both dry flow and storm flow conditions. The user must specify the flow rate that would constitute a change from dry flow to storm flow conditions.

In the following two chapters calibration of the MINLAKE model to a typical South African reservoir (Roodeplaat Dam near Pretoria), as well as the changes to the original model that were necessary to enable calibration, are discussed. Calibration of the hydrodynamic part of the model is reported in Chapter 6, and the water quality part in Chapter 7.

CHAPTER 6

CALIBRATION OF THE HYDRODYNAMIC PART OF THE MINLAKE MODEL TO A SOUTH AFRICAN RESERVOIR

6.1 INTRODUCTION

The South African reservoir chosen for calibration of the MINLAKE model is Roodeplaat Dam, north of Pretoria. The reasons for choosing Roodeplaat Dam were the following:

- it has been classified as a highly eutrophic impoundment (Toerien *et al* 1976)
- it has a one of the best data bases in the country
- it is an important recreational site, as well as a potential source of potable and irrigation water.

Roodeplaat Dam can be classified as a warm monomictic reservoir, with the stratified period lasting from about late September to April. During stratification the difference between epilimnetic and hypolimnetic water temperature can be as much as 13°C. Roodeplaat Dam has a surface area of 400 ha, and a maximum depth of 43 metres. The hypolimnion regularly becomes anoxic during the stratified period, and blue-green algae are the dominant algal group. A more detailed description of the physical and chemical characteristics of Roodeplaat Dam is given in Appendix A1.

To ensure that Roodeplaat Dam is suitable for one-dimensional modelling, it was tested against the criteria for one-dimensionality taking into account stability, the effect of wind, and the advective effect of inflows and outflows, as given in paragraph 4.2. It was found that Roodeplaat Dam is suitable for one-dimensional modelling.

Regarding the MINLAKE model, a few technical modifications were necessary to enable running of the model on Roodeplaat Dam:

- The MINLAKE model, as supplied, made provision for a single inflow or outflow only. The level of outflow, and the discharge rate, must be specified by the user. As Roodeplaat Dam receives inflow from three rivers, and both overflow and draw-off can take place, the original MINLAKE program was changed (in consultation with the developers of the program) to incorporate a total of 5 in/outflows.

- The original program could be run for one year only. The run period was extended to 3 years to enable establishment of trends and simulate algal succession.

Once these technical changes were incorporated into the model, attention could be focused on establishing the data bases required to run the model. According to the structure of the MINLAKE model, the data are separated into three files; a meteorological file, inflow water quality file, and an input file. Construction of the meteorological and inflow water quality data files for Roodeplaat Dam are discussed in Appendix A1. The input file contains certain constants relating to the physical characteristics of the reservoir, as well as the calibration coefficients.

Determining the optimum value of each calibration coefficient for a particular reservoir constitutes calibration of a model. However, when calibrating a model, it is impractical to attempt to calibrate the model in its entirety - it is necessary to identify the dominant processes and to get an indication of the degree in which the dominant processes are affected by interaction with the lesser dominant, i.e. there is a sequence of calibration in which the dominant processes are calibrated first, and then the lesser dominant ones. However, the interaction of the lesser dominant processes on the dominant ones must be taken into account, thus calibration becomes an iterative process.

In reservoirs, the hydrodynamic behaviour has a dominating influence on the water quality behaviour, whereas the water quality has a relatively weaker effect on the hydrodynamics (Henderson-Sellers 1984, Orlob 1983). Regarding the hydrodynamic response, water temperature, especially the distribution of water temperature with depth, forms the principal outcome against which the hydrodynamic response can be evaluated (Henderson-Sellers 1984). The vertical temperature gradient affects the thermal stability of the water column, which plays a part in the amount of turbulent mixing and vertical exchanges of energy and nutrients such as dissolved oxygen and phosphate. It is therefore essential that the simulated water temperature corresponds reasonably well with the observed water temperature before attempting to optimise the simulated values of the other variables. The MINLAKE model takes cognizance of this effect by structuring the model in such a way that it is possible to calibrate the water temperature separately from the water quality variables. Once good correspondence between simulated and observed water temperature is obtained, calibration of the water quality variables can be attempted, using the simulated water temperature as a basis. In this chapter, calibration results of the hydrodynamic part of the MINLAKE model, as manifested by water temperature, are reported. Calibration of the water quality part of the model is reported in Chapter 7, and the results are discussed in Chapter 8.

In the MINLAKE model mathematical descriptions of the processes range from ones that are empirically formulated from experimental results to ones that have fundamental physical and biological bases. Even with the latter group usually it is not possible to formulate the processes mathematically exact. Formulation of processes often is approximated by the use of calibration coefficients. It is virtually impossible to assign values to these coefficients *ab initio*, the values must be optimized by calibration against experimental data on the system. Where experimental data on the system are not available, values must be derived from experimental work on other, similar systems.

In finding values for the coefficients, the approach generally should be to obtain an estimate of each coefficient on as independent base as possible. Hydrodynamic

coefficients usually are site specific, but coefficients relating to the water quality processes often are climate specific, so that calibration of a model for a particular system usually can provide coefficients that apply to other systems in the same climatic region (Henderson-Sellers 1984).

Once appropriate values have been established for the coefficients, the model can be calibrated, provided that all the important processes have been included and formulated correctly in the model. In contrast, if important processes have been omitted or incorrectly formulated, then it is most unlikely that the model can be calibrated, even though appropriate values for the coefficients have been established.

Calibration of the original MINLAKE model requires specification of a large number of coefficients - 10 reservoir specific physical coefficients, 5 hydrodynamic coefficients, and 21 water quality coefficients (of which 17 must be specified separately for each algal class). The coefficients for the original MINLAKE model are listed in Table 6.1.

Table 6.1. Coefficients to be specified by the user in the original MINLAKE model.

CALIBRATION COEFFICIENT	SYMBOL	UNITS
PHYSICAL RESERVOIR CONSTANTS		
Minimum layer thickness	DZLL	m
Maximum layer thickness	DZUL	m
Width of inflowing river (must be specified for each inflowing river)	WCHAN	m
Altitude of reservoir bottom	DBL	metres above sea level
Stage (reservoir water level)	ST	metres above sea level
Downstream slope of inflowing river (must be specified for each river)	S	
Manning's friction factor	FT	English units
Height of reservoir wall	ELCB	metres above sea level
Side slope of outflow channel	ALPHA	
Bottom width of outflow channel	BW	m

(continued...)

HYDRODYNAMIC COEFFICIENTS	SYMBOL	UNITS
Extinction coefficient of water	XK1	m^{-1}
Extinction coefficient due to chlorophyll-a	XK2	$m^2\ g^{-1}$ Chla
Wind function coefficient	WCOEFF	none
Wind sheltering coefficient	WSTR	none
Maximum eddy diffusion coefficient	HKMAX	$m^2\ day^{-1}$
WATER QUALITY COEFFICIENTS	**SYMBOL**	**Units**
Sediment oxygen depletion rate	SB20	$g\ m^2\ day^{-1}$
Sediment phosphorus release coefficient	BRR	$g\ m^2\ day^{-1}$
Detrital decay rate	BODK20	day^{-1}
Detrital settling rate	FVBOD	$m\ day^{-1}$
Algal respiration rate*	XKR1	day^{-1}
Algal mortality rate*	XKM	day^{-1}
Algal settling rate*	FVCHLA	$m\ day^{-1}$
Maximum phosphorus uptake rate*	UPMAX	day^{-1}
Half saturation coefficient for phosphorus uptake*	HSCPA	$mg\ l^{-1}$
Minimum intracellular phosphorus concentration needed for growth*	PMIN	mg P mg^{-1}Chla
Maximum intracellular phosphorus storage capacity*	PMAX	mg P mg^{-1}Chla
Maximum nitrogen uptake rate*	UNMAX	day^{-1}
Half saturation coefficient for nitrogen uptake*	HSCN	$mg\ l^{-1}$
Minimum intracellular nitrogen concentration needed for growth*	XNMIN	mg N mg^{-1}Chla
Maximum intracellular nitrogen storage capacity*	XNMAX	mg N mg^{-1}Chla
Half saturation coefficient for preferential ammonium uptake *	HSCNH	$mg\ l^{-1}$
Maximum nutrient saturated growth rate*	GROMAX	day^{-1}
Upper temperature at which algal growth is reduced 90%*	TMAX	°C
Optimum algal growth temperature*	TOPT	°C
Half saturation coefficient for light limited growth*	HSC1	$\mu E\ m^{-2}\ s^{-1}$
Light inhibition coefficient*	HSC2	$\mu E\ m^{-2}\ s^{-1}$

* Indicate those water quality coefficients that have to specified for each algal class

6.2 ESTABLISHING VALUES FOR THE RESERVOIR SPECIFIC PHYSICAL CONSTANTS.

6.2.1 DZLL and DZUL - Minimum and maximum layer thickness.

The MINLAKE model is a one-dimensional model and thus the reservoir is divided into a number of horizontal layers (*cf* Chapter 3). The model establishes the initial thickness of each layer as follows: the user must specify a set of initial conditions on the first day of simulation i.e. measurements of water temperature and water quality variables must be given at certain depths in the reservoir. In establishing the initial layer thicknesses, the model uses the depths specified in the initial conditions as the midpoints of the layers, and then calculates the thickness of each layer from these midpoints. The calculation is done from the bottom to the surface of the reservoir. The thickness of each layer will vary from day to day, due to various factors such as, for instance, water level, entrainment due to inflow and outflow, and turbulent mixing. The user must specify a minimum layer thickness, DZLL - if the thickness of a layer becomes less than DZLL, the layer is mixed with an adjacent layer. The MINLAKE manual indicated a minimum layer thickness of 0.5 m for Lake Riley in the USA. After repeated runs, it was found that a minimum layer thickness, DZLL, of 0.2 m gave the best results for Roodeplaat Dam Reservoir.

The user must also specify a maximum layer thickness, DZUL - if the thickness of a layer becomes greater than DZUL, the layer is divided into two layers of equal thickness. The value of DZUL must therefore be greater than twice the value of DZLL. The MINLAKE manual indicated a value of 1.2 m for Lake Riley in the USA. For Roodeplaat Dam, the best results were obtained with a value of 1.5 for DZUL. The model became numerically unstable at DZUL values greater or equal to 2 metre.

6.2.2 WCHAN - width of inflowing channel.

The width in metres of each inflowing river must be specified by the user. These data are used to calculate the velocity of the river as it enters the reservoir, which in turn is used to calculate plunging depth, as well as the amount of entrainment between layers due to inflow. The data for the three rivers flowing into Roodeplaat Dam Reservoir (as obtained from the Department of Water Affairs and Forestry) are summarized in Table 6.2:

TABLE 6.2. Widths of the rivers flowing into Roodeplaat Dam Reservoir.

RIVER	BOTTOM WIDTH (m)	TOP WIDTH (m)	AVERAGE WIDTH (m)
Pienaars River	34	58	46
Hartbeesspruit	42	44	43
Edenvalespruit	16	36	26

The value of WCHAN for each river was taken as the average width of each river, i.e. WCHAN for Pienaars River was taken as 46 m, for Hartbeesspruit as 43 m, and for Edenvalespruit as 26 m. The model response is not very sensitive to the value of WCHAN.

6.2.3 ST - stage (reservoir water level).

The reservoir water level has to be given in metres above sea level. Data received from The Department of Water Affairs and Forestry indicated that the full supply level of Roodeplaat Dam Reservoir is at 1214 metres above sea level. This was confirmed by consulting an 1:10 000 orthographic map of the area surrounding Roodeplaat Dam Reservoir. It must be noted that Walmsley and Butty (1980a) erroneously gave the full supply level as 1314 metre above sea level. The study by Walmsley and Butty has become a standard reference work on Roodeplaat Dam Reservoir, and therefore the full supply level is quite often mistakenly quoted as 1314 metre above sea level in a number of studies on Roodeplaat Dam Reservoir.

6.2.4 DBL - altitude of reservoir bottom.

According to the literature (Walmsley and Butty, 1980a, Pieterse and Röhrbeck 1990) the maximum depth of Roodeplaat Dam Reservoir is 43 m. The full supply level of the reservoir is 1214 m above sea level, therefore the reservoir bottom is at an altitude of 1171 m.

6.2.5 S - downstream slope (bed slope) of each inflowing river.

Data on the bedslope are needed to calculate the velocity of the river as it enters the river, which is then used to calculate the depth of the plunge point and the amount of mixing at the plunge point. According to data received from the Department of Water Affairs and Forestry, the downstream slope of Pienaars River is 0.006, Hartbeesspruit 0.006, and Edenvalespruit 0.013.

6.2.6 FT - Manning's friction factor

Manning's friction factor is used to calculate the velocity of each river as it enters the reservoir. This information is required to calculate the plunging depth, and the amount of entrainment due to inflow from each river. Different values of Manning's friction factor are indicated in Table 6.3 (Perry and Chilton, 1973).

Table 6.3 Average values of Manning's friction factor, n.

SURFACE	n
Natural stream channels	
Clean straight bank, full stage	0.03
Winding, some pools and shoals	0.04
Same, but with stony sections	0.055
Sluggish reaches, very deep pools, rather weedy	0.070

The MINLAKE manual indicates a range of 0.035 to 0.05. After repeated runs a value of 0.035 was taken as the most appropriate value of FT for each of the rivers. The model is not very sensitive to the value of FT.

6.2.7 ELCB - height of reservoir wall

This information is needed to calculate overflow. The height of the reservoir wall is equivalent to the full supply level, i.e. 1214 m above sea level.

6.2.8 BW - diameter of outflow pipe

In the original model the outflow channel is assumed to have a trapezoidal shape, and the user must specify the side slope and bottom width of the outflow channel. However, many South African reservoirs have circular outflow channels. The model was changed accordingly, with BW representing the diameter of the outflow pipe. Bw must be specified by the user to enable calculation of the layers that are affected by outflow. According to data received from the Department of Water Affairs and Forestry, the diameter of the outflow pipes in Roodeplaat Dam Reservoir is 0.6 meter.

6.3 ESTABLISHING VALUES FOR THE HYDRODYNAMIC COEFFICIENTS.

To establish appropriate values for the hydrodynamic coefficients for Roodeplaat Dam Reservoir, and to ensure that the processes affecting simulation of water temperature are adequately formulated, a critical study of these coefficients and the associated processes was undertaken.

6.3.1 Attenuation of solar radiation by water and the coefficients XK1 and XK2.

In the original MINLAKE model, the attenuation of solar radiation by water is described by Beer's Law (*cf* Eq 5.4 and 5.5):

$$H_{s(i)} = H_{s(i-1)} * \exp(-k\Delta z) \quad (6.1)$$

$H_{s(i-1)}$ = solar radiation at the top of the layer (kcal m^{-2} day^{-1})
$H_{s(i)}$ = solar radiation at the bottom of the layer (kcal m^{-2} day^{-1})
k = total extinction coefficient (m^{-1})
Δz = thickness of layer (m).

with

$$k = XK1 + 0.043\ TSS + XK2\ CHLa \quad (6.2)$$

k = total extinction coefficient (m^{-1})
XK1 = extinction coefficient of pure water (m^{-1})
TSS = simulated Total Inorganic Suspended Sediment (TSS) concentration in each layer (mg l^{-1})
XK2 = extinction coefficient due to chlorophyll-a (m^2 g^{-1} Chla)
Chla = chlorophyll-a concentration in layer (mg l^{-1}).

6.3.1.1 Extinction coefficient of pure water - XK1:

The extinction coefficient of pure water, XK1, is one of the coefficients that must be specified by the user. This value can range from 0.02 - 0.2 m^{-1}, depending on the colour of the water (Orlob 1983). Pure water may be coloured due to the presence of, for instance, peat or gilvin. For Roodeplaat Dam the value for XK1 had been determined for as 0.39 m^{-1} (De Wet, 1986).

6.3.1.2 XK2 - the extinction coefficient due to chlorophyll-a:

No specific value for the extinction coefficient due to chlorophyll-a, XK2, could be found for Roodeplaat Dam Reservoir, but the value of XK2 for Hartbeespoort Dam Reservoir had been determined as 12 m^2 g^{-1} Chla (NIWR 1985). For Roodeplaat Dam, the best simulation results were obtained with a value of 16 m^2 g^{-1} Chla.

6.3.1.3 The effect of TSS concentration:

Regarding the effect of TSS concentration on the total extinction coefficient - in each layer, this effect is calculated by the model from the simulated daily TSS concentration. No user interaction is required in the calculation. However, if TSS concentrations were incorrectly simulated, it may affect calculation of the extinction coefficient in Eq 6.2, and hence the distribution of water temperature with depth. Unfortunately TSS concentrations were not measured in Roodeplaat Dam Reservoir, and therefore it was difficult to assess simulated TSS concentrations. This problem was alleviated to some extend by calculating TSS concentrations from Secchi disc depth measurements in Roodeplaat Dam Reservoir (*cf* Appendix A1) but this method provided a measure of TSS concentrations in the upper layers of the reservoir only, it did not give any indication of the observed TSS concentration in the hypolimnion.

To get an indication of the effect of TSS concentration on the extinction coefficient, runs were done no TSS and arbitrarily high TSS concentrations. Simulation of mixing depth was affected slightly, but no significant change in the temperature simulation could be discerned. It was concluded that simulated TSS concentration has little effect on calculation of the extinction coefficient and hence on the simulation of water temperature. However, at a later stage it was found that TSS concentration has a very

definite effect on simulated algal concentration, because of its effect on underwater light intensity (see paragraph 7.5).

Once values for the different components of the total extinction coefficient (*cf* Eq 6.2) had been established for Roodeplaat Dam Reservoir, the process of attenuation of radiation through absorption by water was checked to ensure that it was adequately formulated in the model (*cf* Chapter 4 and 5).

6.3.1.4 Formulation of the attenuation process:

The attenuation of radiation through absorption by water can be described by Beer's Law (Eq 6.1). However, in the surface layer of a reservoir absorption of radiation deviates from Beer's Law (Henderson-Sellers 1984). A fraction, ß, of the nett solar radiation that enters the water body, is absorbed in the surface layer, while the remainder, (1-ß), penetrates deeper into the water body (and is attenuated according to Beer's Law - see discussion in Chapter 4). The fraction ß that is absorbed in the surface layer originally was 'hard-wired' in the model to a value of 0.4, but, according to Henderson-Sellers (1984), ß is a function of the water turbidity and therefore ß should be expressed in terms of the total extinction coefficient (*cf* Eq 5.6):

$$\beta = 0.265 \ln \eta + 0.614 \qquad (6.3)$$

ß = fraction of the incident solar radiation absorbed in the surface layer

η = total extinction coefficient (m^{-1})

This expression for ß was incorporated into the model, but it resulted in no change in the water temperature simulation results. However, the expression was retained in the model, as it is considered to have more generality than the original hard-wired value.

6.3.2 Evaporative and convective heat loss and the coefficient WCOEFF

The wind function coefficient is a component of the formulas used to calculate evaporative heat loss, as well as convective heat loss. A literature study indicated that these processes were adequately formulated in the model (see discussion in Chapters 4 and 5).

6.3.2.1 WCOEFF - wind function coefficient:

No specific value of WCOEFF has been determined for Roodeplaat Dam Reservoir. The MINLAKE manual indicated a value of 25.67 for Lake Riley in the USA (MINLAKE 1988). After an extensive literature survey it was concluded that the wind coefficient should be determined for each location, but that the value of 25.62 for Lake Riley, as indicated in the MINLAKE manual, is a fairly average value (Harbeck 1970, Henderson-Sellers 1984). After running the model a number of times with different arbitrary chosen values of the wind coefficient, it was concluded that the model response is moderately sensitive to the value of the wind coefficient, and that the value of 25.67 for Lake Riley is appropriate for Roodeplaat Dam Reservoir as well.

6.3.3 Calculation of kinetic energy and the coefficient WSTR

In the model the coefficient WSTR is associated with calculation of the kinetic energy supplied to the reservoir by the wind. This process appeared to be adequately formulated in the model (see paragraph 5.2.4.1).

6.3.3.1 WSTR (wind sheltering coefficient):

The effect of wind may be influenced by the surrounding topography. The model takes cognisance of this effect by the use of a wind sheltering coefficient, WSTR, which may vary from zero to 1, with zero indicating severe wind sheltering, and 1 indicating no wind sheltering. No specific value of WSTR had been determined for Roodeplaat Dam Reservoir. To estimate the sensitivity of the model to the wind sheltering coefficient, the model was run with a coefficient of 0.10 and 0.90. Although these different values did not affect the simulated water temperature significantly, later simulations indicated

that it did have a marked effect on simulation of the mixed layer depth. After repeated runs a wind sheltering coefficient of 0.90 was found to be the optimum value for Roodeplaat Dam Reservoir.

6.3.4 Eddy diffusivity and the coefficient HKMAX.

In the original MINLAKE model, eddy diffusivity is calculated separately in hypolimnion and in the epilimnion. An eddy diffusion coefficient is associated with this process. This coefficient has different values in the hypolimnion and the epilimnion. In the original MINLAKE model, only the maximum value of the eddy diffusion coefficient in the hypolimnion (HKMAX), had to be specified by the user (*cf* paragraph 5.2.4.2).

No specific value of HKMAX had been determined for Roodeplaat Dam Reservoir, but the MINLAKE manual indicated that this value is a function of reservoir area, and gave a value of 0.08 for a 12 ha lake, and 0.12 for a 120 ha lake (Riley 1988). Roodeplaat Dam Reservoir has a surface area of ≈ 400 ha. To get an indication of the model sensitivity to HKMAX, the model was run with different (arbitrary) values of HKMAX. The simulated water temperature in the hypolimnion was extremely sensitive to different values of HKMAX, therefore an in-depth study of eddy diffusivity in both the epilimnion and the hypolimnion was undertaken to ensure that the process was correctly and adequately formulated, and to establish the optimum value of HKMAX for Roodeplaat Dam Reservoir. (Also see discussion in Chapters 4 and 5).

6.3.4.1 Hypolimnetic eddy diffusivity (incorporating HKMAX):

In the original MINLAKE model eddy diffusivity in the hypolimnion is calculated as follows (*cf* Eq 5.25):

$$K_H = HKMAX \qquad (6.4)$$

or

$$K_H = HKMAX\ CN^{-1} \qquad (6.5)$$

(which ever yields the lesser value)

K_H = hypolimnetic eddy diffusivity (m^2d^{-1})
HKMAX = maximum eddy diffusion coefficient (m^2d^{-1})
C = minimum value of N at which maximum eddy diffusivity occurs)
N = Brünt-Våisala frequency

The Brünt-Våisala frequency, N, is calculated by the model (for a discussion of the Brünt-Våisala frequency see Chapter 4). In a study by Jassby and Powell (1975), the value of C in the above equation had been determined as 0.0086. This value does not appear to be reservoir specific, and therefore the same value of C was used for Roodeplaat Dam Reservoir.

The maximum eddy diffusion coefficient, HKMAX, is derived from the eddy diffusion coefficient - the value of the eddy diffusion coefficient increases with depth from the surface, reaching a maximum, HKMAX, at about mid depth in the hypolimnion. In the original MINLAKE model, HKMAX has to be specified by the user. The hypolimnetic eddy diffusion coefficient can be calculated by various methods (*cf* Chapter 4), for Roodeplaat Dam HKMAX was estimated roughly from the reservoir surface area (based on the study done by Mortimer, 1942). A more exact value was calculated utilising the formulation of Jassby and Powell (1975, *cf* Chapter 4).

Estimation of the maximum eddy diffusion coefficient HKMAX from the reservoir area: The value of HKMAX can be estimated from the reservoir surface area as follows: In a study by Mortimer (1942) the **mean** value of the eddy diffusion coefficient as a function of reservoir surface area has been determined for a number of lakes. From these mean values (Table 6.4) the **mean** eddy diffusion coefficient for a particular reservoir can be obtained by interpolation, provided the surface area of the reservoir is known. The mean value can serve as a rough estimate for HKMAX.

TABLE 6.4 Eddy diffusion coefficient as a function of lake area only (Mortimer, 1942)

Lake	Area (km^2)	**Mean** hypolimnetic eddy diffusion coefficient (cm^2s^{-1})
Holsfjord	121	3.10
Geneva	503	1.90
Maxinkuckee	7.5	0.07
Lomond	71.0	0.53
Windermere (North basin)	8.2	0.39
Windermere (South basin)	6.7	0.09
Kizakiko	1.4	0.05
Lunz	0.68	0.05
Esthwaite Water	1.0	0.03
Schleinsee	0.15	0.02

From Table 6.4 the mean hypolimnetic eddy diffusion coefficient (in cm^2s^{-1}) for a particular reservoir can be calculated as a function of reservoir surface area (in km^2) with the following formula:

$$\ln K_H = 0.647(\ln A) - 3.08 \quad (6.6)$$

K_H = mean hypolimnetic eddy diffusion coefficient (cm^2s^{-1})
A = reservoir surface area (km^2).

Roodeplaat Dam has an area of 4.0 km^2. From Eq 6.6 the **mean** hypolimnetic eddy diffusion coefficient for Roodeplaat Dam was calculated as 0.113 cm^2s^{-1}, or 0.97 m^2d^{-1}, i.e. HKMAX for Roodeplaat Dam must be greater than 0.97 m^2d^{-1}.

Calculation of the maximum eddy diffusion coefficient, HKMAX from the depth and reservoir surface area:

HKMAX can be determined also by calculating the value of the eddy diffusion coefficient in each layer; the value of the eddy diffusion coefficient in each layer increases with increasing depth from the surface, reaching a maximum, HKMAX, at about mid depth in the hypolimnion. In each layer, the eddy diffusion coefficient is calculated from the bathometry of the reservoir, the water temperature and the incoming solar radiation, and it is assumed that there is no heat exchange with the bottom sediments (Jassby and Powell 1975, Henderson-Sellers, 1984). As the MINLAKE model is a variable area model (paragraph 5.2), the eddy diffusion coefficient was calculated using Eq 4.47 and 4.48:

$$K = -\frac{1}{\frac{\partial\theta}{\partial z}}\left(\frac{S}{A_z} - \frac{R}{C_p}\right) - \alpha \qquad (6.7)$$

where

$$S = \frac{d}{dt}\int_z^{z_b} A\theta dz \qquad (6.8)$$

K	=	eddy diffusion coefficient ($cm^2\ s^{-1}$)
θ	=	water temperature (°C)
z	=	depth of layer (cm)
z_b	=	depth of bottom layer (cm)
A	=	area of the reservoir at depth z (cm^2)
R	=	net incoming solar radiation ($cal\ cm^{-2}s^{-1}$)
C_p	=	specific heat of water ($cal\ g^{-1}°C^{-1}$)
α	=	molecular diffusion coefficient
	=	$0.12 \times 10^{-2} cm^2 s^{-1}$
u	=	horizontal component of vertical advection.

This derivation is valid only for the period when the reservoir is stratified i.e when convective transport of heat is negligible (Henderson-Sellers, 1984).

To determine HKMAX for Roodeplaat Dam Reservoir, the values of the eddy diffusion coefficient in each layer of the hypolimnion was calculated according to Eq (6.7 and 6.8) from data observed for Roodeplaat Dam Reservoir on 8 October, 21 October, and 29 November (for details of calculation see Appendix A3). The calculation was complicated by lack of observed water temperature data in the hypolimnion during stratification - water temperature measurements were never done down to the bottom of the reservoir during the stratified period. The above dates were chosen because the water temperature was measured down to 32 m on these days (total depth of Roodeplaat Dam Reservoir is 43 m). For each day, the measured water temperature had to be extrapolated to obtain the maximum eddy diffusion coefficient, HKMAX. The

values thus obtained, are plotted against depth from surface in Fig 6.1. Because these values were obtained by extrapolation, they are at best an approximation of HKMAX - from the plots in Fig 6.1 it was concluded that HKMAX for Roodeplaat Dam Reservoir should be approximately 1.8 m^2day^{-1}. After repeated runs the optimum value of HKMAX was established as 1.7 m^2day^{-1}.

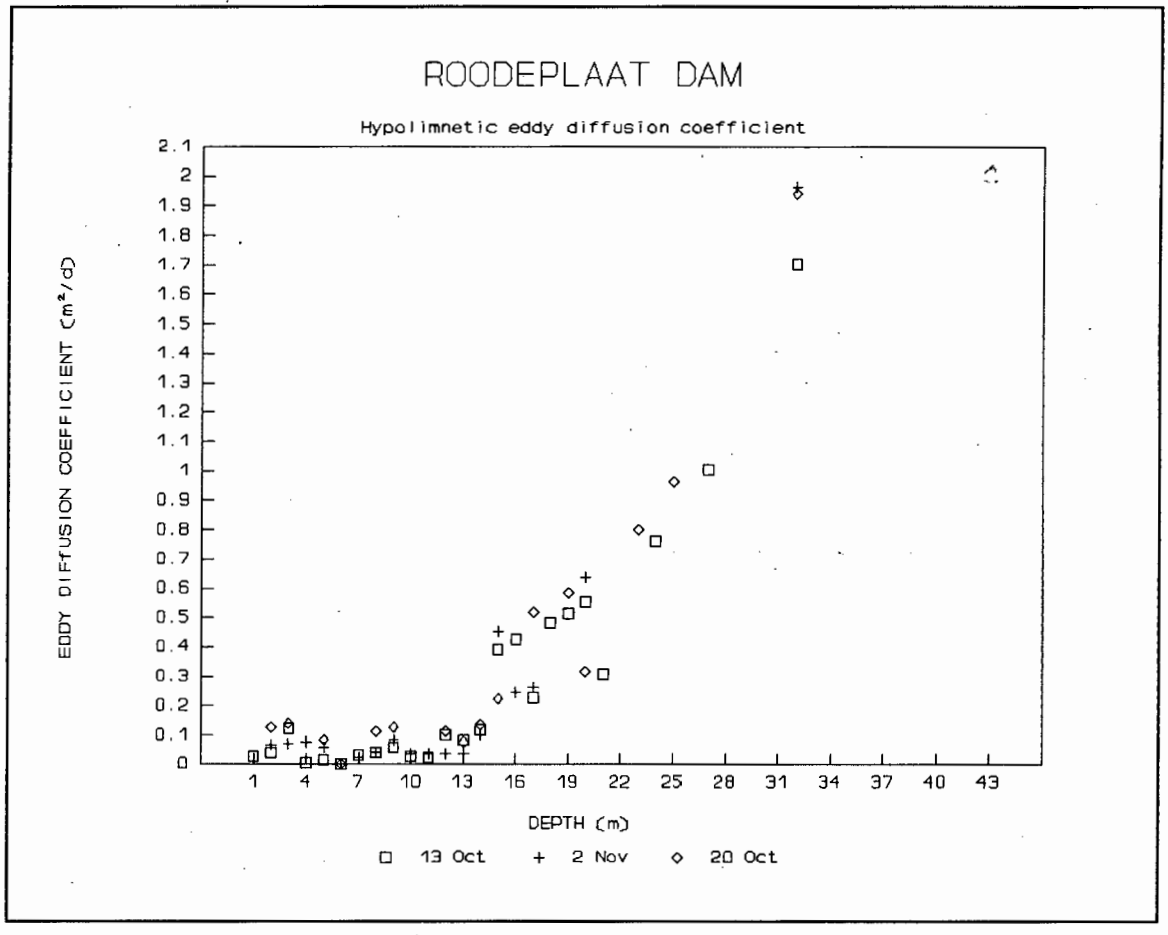

Figure 6.1.
Determination of maximum eddy diffusion coefficient in Roodeplaat Dam Reservoir.

6.3.4.2 Epilimnetic eddy diffusivity:

In the MINLAKE model eddy diffusivity in the epilimnion is assumed to be constant. It is calculated by the model as a function of wind speed (Eq 5.24):

$$K_{Ho} = c\ W^{1.3} \qquad (6.9)$$

K_{Ho} = epilimnetic eddy diffusivity (m^2d^{-1})
c = epilimnetic eddy diffusion coefficient
W = daily wind speed at 10 m above the water surface ($m\ s^{-1}$).

As was discussed in paragraph 4.3.4.1, the value of c, the epilimnetic diffusion coefficient, is reservoir specific, therefore it should be specified by the user. No specific value had been determined for Roodeplaat Dam Reservoir. In the original MINLAKE model, the value of c had been hard-wired to a value of 28.0. The origin of this value could not be established from the references available.

An intensive literature survey revealed that a detailed study on eddy diffusivity had been done by Sundaram *et al* (1973). In this study the epilimnetic diffusivity was calculated for a specific lake i.e. Cayuga Lake in New York. The depth of this lake is about 60 m and the minimum temperature during spring homothermy is 2.9 °C (Sundaram and Rehm 1973). The epilimnetic diffusivity for this lake is expressed as:

$$K_{Ho} = 0.0282\ w^* \qquad (6.10)$$

K_{Ho} = epilimnetic diffusivity ($cm^2\ s^{-1}$)
0.0282 = epilimnetic diffusion coefficient for Cayuga Lake
w^* = friction velocity ($cm^2\ s^{-1}$).

However, in Eq 6.10, epilimnetic eddy diffusivity is calculated as a function of friction velocity, and not as a function of wind speed, as was done in the original MINLAKE model (Eq 6.9). Also, in Eq 6.10 the diffusivity is expressed in $cm^2\ s^{-1}$, whereas the units required by the MINLAKE model is $m^2 day^{-1}$. To compare the two formulations, Eq 6.10 was rewritten as a function of wind speed and in units of $m^2 day^{-1}$:

The relationship between friction velocity w^*, and wind speed W, is expressed by (Henderson-Sellers, 1984):

$$w^* = \sqrt{\frac{\sigma_a}{\sigma_w} C_D W} \qquad (6.11)$$

w^* = friction velocity ($m\ s^{-1}$)
σ_w = density of the water ($mg\ m^{-3}$)
σ_a = density of the air ($mg\ m^{-3}$)
C_D = drag coefficient
W = wind speed ($m\ s^{-1}$).

Also, according to Henderson-Sellers (1984), for $W < 15\ m\ s^{-1}$:

$$C_D = \sqrt{0.0005\ W^{0.5}} \qquad (6.12)$$

W = daily average wind speed at 10 m above the water surface ($m\ s^{-1}$).

The average annual wind speed at Roodeplaat Dam Reservoir is ≈ 4.5 m s^{-1}. Substitution of the density of air (1.117 mg m^{-3}), density of water (1000 mg m^{-3}), and C_D (Eq 6.12) in Eq 6.11 gives the following:

$$w^* = 0.00076 * W^{1.25} \quad (6.13)$$

Substituting w^* from Eq 6.13 into Eq 6.10, and expressing the epilimnetic eddy diffusivity K_{Ho}, in m^2 day^{-1} as required by the model, instead of cm^2 s^{-1}, Eq 6.10 gives:

$$K_{Ho} = 1.85\ W^{1.25} \quad (6.14)$$

K_{Ho} = epilimnetic eddy diffusivity ($m^2 day^{-1}$)
1.85 = epilimnetic eddy diffusion coefficient for Cayuga Lake
W = daily average wind speed at 10 m above the water surface (m s^{-1}).

Thus Eq 6.10 and Eq 6.14 both express the epilimnetic eddy diffusivity for Cayuga Lake; in Eq 6.10 epilimnetic eddy diffusivity is expressed as a function of friction velocity, w^*, and in units of cm^2 s^{-1}, whereas in Eq 6.14 it is expressed as a function of wind speed and in units of m^2 day^{-1}. Eq 6.14 has the same format as the formulation on the original MINLAKE model (Eq 6.9), and therefore the formulation in the model was accepted as adequate.

Regarding the epilimnetic diffusion coefficient, according to Eq 6.14, the epilimnetic diffusion coefficient for Cayuga Lake (expressed as a function of wind speed, and in $m^2 day^{-1}$), was 1.85. To get an indication of the value of the epilimnetic diffusion coefficient for Roodeplaat Dam Reservoir, the value of 1.85 for Cayuga Lake was used as a starting point for Roodeplaat Dam Reservoir. Although the value of the epilimnetic diffusion coefficient is reservoir specific, after repeated runs the value of 1.85 was

established as the optimum value for Roodeplaat Dam Reservoir also[1]. Changing the value of the epilimnetic diffusion coefficient, c, did not affect the simulated water temperature significantly, but during subsequent calibration of simulated dissolved oxygen concentration, it was found that the value of c has a profound effect on the simulated distribution of dissolved oxygen with depth during overturn. In fact, the optimum value of 1.85 for c for Roodeplaat Dam Reservoir was established only after calibration of dissolved oxygen concentration.

The value of 1.85 is significantly different from the value of 28.0 that was hard-wired into the original MINLAKE model. As the value of the epilimnetic eddy diffusion coefficient is reservoir specific, the original model was modified so that this value could be specified by the user.

6.4 HYDRODYNAMIC SIMULATION RESULTS

The values of the physical reservoir constants for Roodeplaat Dam Reservoir, as well as the optimum values of the hydrodynamic coefficients required by the modified model for Roodeplaat Dam Reservoir, as discussed in the previous paragraphs, are indicated in Table 6.5.

---

[1] It is important to note that the value of the epilimnetic eddy diffusion coefficient is reservoir specific, thus the fact that a value of 1.85 for the epilimnetic diffusion coefficient gave good results for both Cayuga Lake and Roodeplaat Dam should be regarded as fortuitous; it does not mean that this value is universally applicable to all reservoirs.

Table 6.5 Optimum values of the physical reservoir constants and hydrodynamic coefficients, as required by the modified MINLAKE model, for Roodeplaat Dam Reservoir.

CALIBRATION COEFFICIENT	SYMBOL	OPTIMUM VALUE FOR ROODEPLAAT DAM RESERVOIR	UNIT
PHYSICAL RESERVOIR CONSTANTS			
Minimum layer thickness	DZLL	0.5	m
Maximum layer thickness	DZUL	1.2	m
Width of inflowing river (must be specified for each inflowing river)	WCHAN		m
Altitude of reservoir bottom	DBL	1168	meters above sea level
Stage (reservoir water level)	ST	1214	meters above sea level
Downstream slope of inflowing river (must be specified for each river)	S	0.006 0.006 0.013	
Manning's friction factor	FT	0.035	English units
Height of reservoir wall	ELCB	1214	meters above sea level
Diameter of outflow pipe	BW	0.6	m
HYDRODYNAMIC COEFFICIENTS			
Light extinction coefficient of pure water	XK1	0.99	m^{-1}
Light extinction coefficient due to chlorophyll-a	XK2	12	$m^2\ g^{-1}$ Chla
Wind function coefficient	WCOEFF	25.6	
Wind sheltering coefficient	WSTR	0.95	
Epilimnetic diffusion coefficient	c	1.85	
Maximum hypolimnetic diffusion coefficient	HKMAX	1.7	m^2day^{-1}

Using a two year time-series inflow and meteorological data (see Appendix A1), and values for the coefficients as listed in Table 6.5, the model was run for Roodeplaat Dam Reservoir. The structure of the MINLAKE model is such that water temperature simulations can be done without taking the water quality behaviour of the reservoir into account, and, as a starting point, only water temperature was simulated.

Regarding the simulation period, the data required to calibrate the model (*cf* Appendix A1) for Roodeplaat Dam Reservoir were available as from 16 April 1980, consequently, as a starting point, the model was run from April 1980 to April 1982. However, in Roodeplaat Dam Reservoir turnover occurs roundabout April. Turnover constitutes a period of great instability in a reservoir (Henderson-Sellers 1984). During the initial hydrodynamic calibration it seemed as if the correspondence between simulated and observed hydrodynamic variables (water temperature and mixing depth) was adequate, but when calibration of the water quality part of the model was attempted, there was a significant deviation between simulated and observed nutrient concentrations during the first 7 months of the simulation period. Thereafter the deviance decreased, but good correspondence between simulated and observed concentrations never was obtained, because of the initial deviance. A likely cause for the deviance was the unstable conditions in the reservoir during turn-over at the start of the simulation period. To remedy the situation, the program was run with the starting date in October, i.e. the beginning of the period of stratification. As a consequence, results from the early part of the study are reported for the period April 1980 - April 1982, whereas final results are reported for the period October 1980 - October 1982.

6.4.1 Water temperature.

The temperature profiles are ***the*** basic response against which the hydrodynamic response can be evaluated. It was essential that the simulated water temperature corresponds reasonably with the observed water temperature before attempting to optimise the simulated values of the other variables.

Figure 6.2 is a time-series graph of simulated and observed water temperature at 1 and 16 m depths[2], and in Figure 6.3 the distribution with depth of simulated and observed water temperature is shown. At both 1 and 16 m depth below the surface,

[2] Results are reported at depths of 1 and 16 meters, as these depths reflect epilimnetic and hypolimnetic conditions respectively.

the correspondence between simulated and observed water temperature is very good for the first 19 months of the 2 year simulation period. Thereafter the simulated temperature is slightly too high. In spite of repeated efforts, the reason for this deviant behaviour could not be ascertained.

NOTE: The simulated water temperature was affected most by:

- The value of maximum hypolimnetic diffusion coefficient for Roodeplaat Dam reservoir
- Adapting the wind speed measured at 1.8 m, to wind speed at 10 m, as required by the model (see Appendix A1)

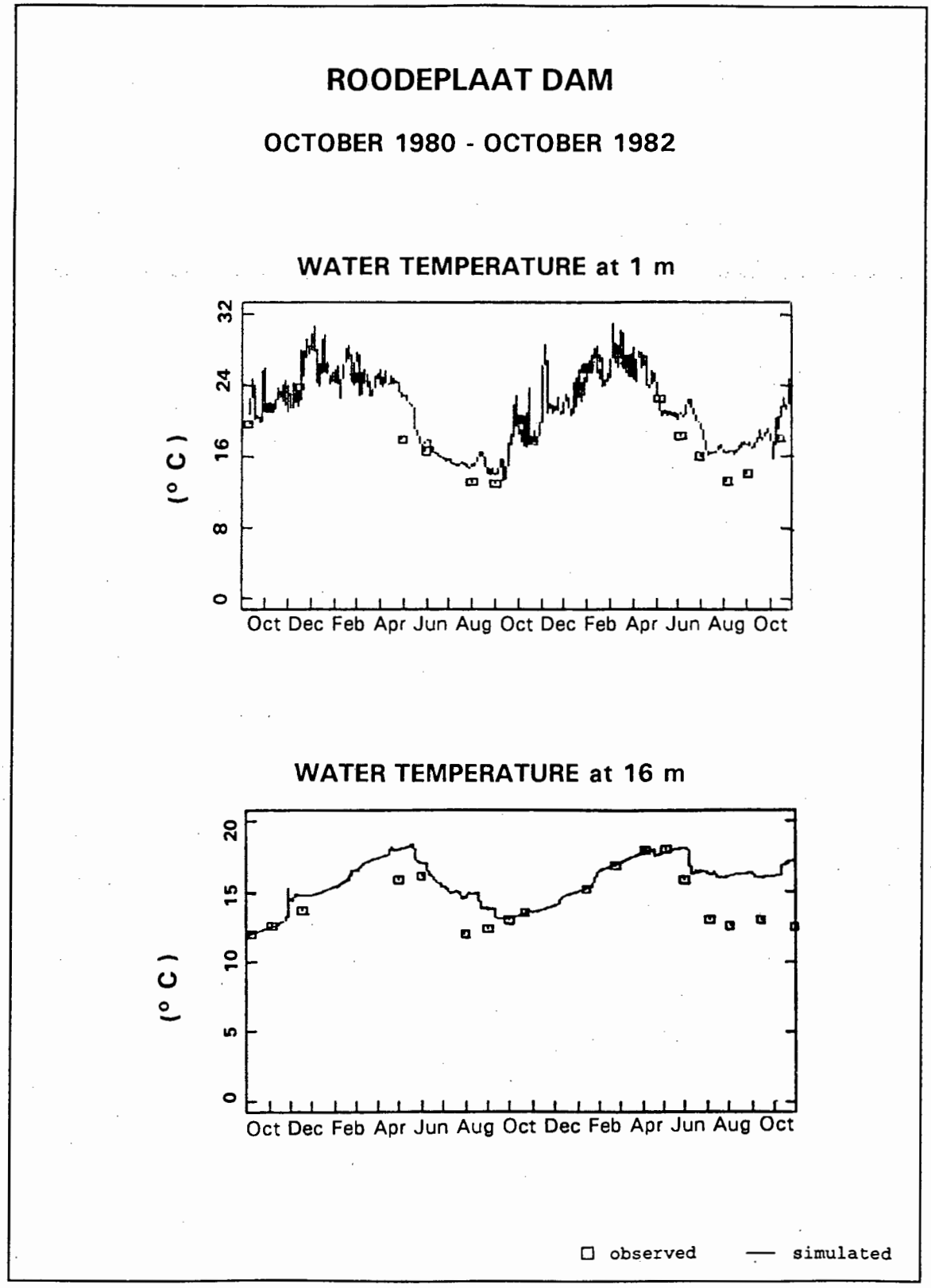

Figure 6.2
Time-series graphs of simulated and observed water temperature as obtained with the modified MINLAKE model on Roodeplaat Dam.

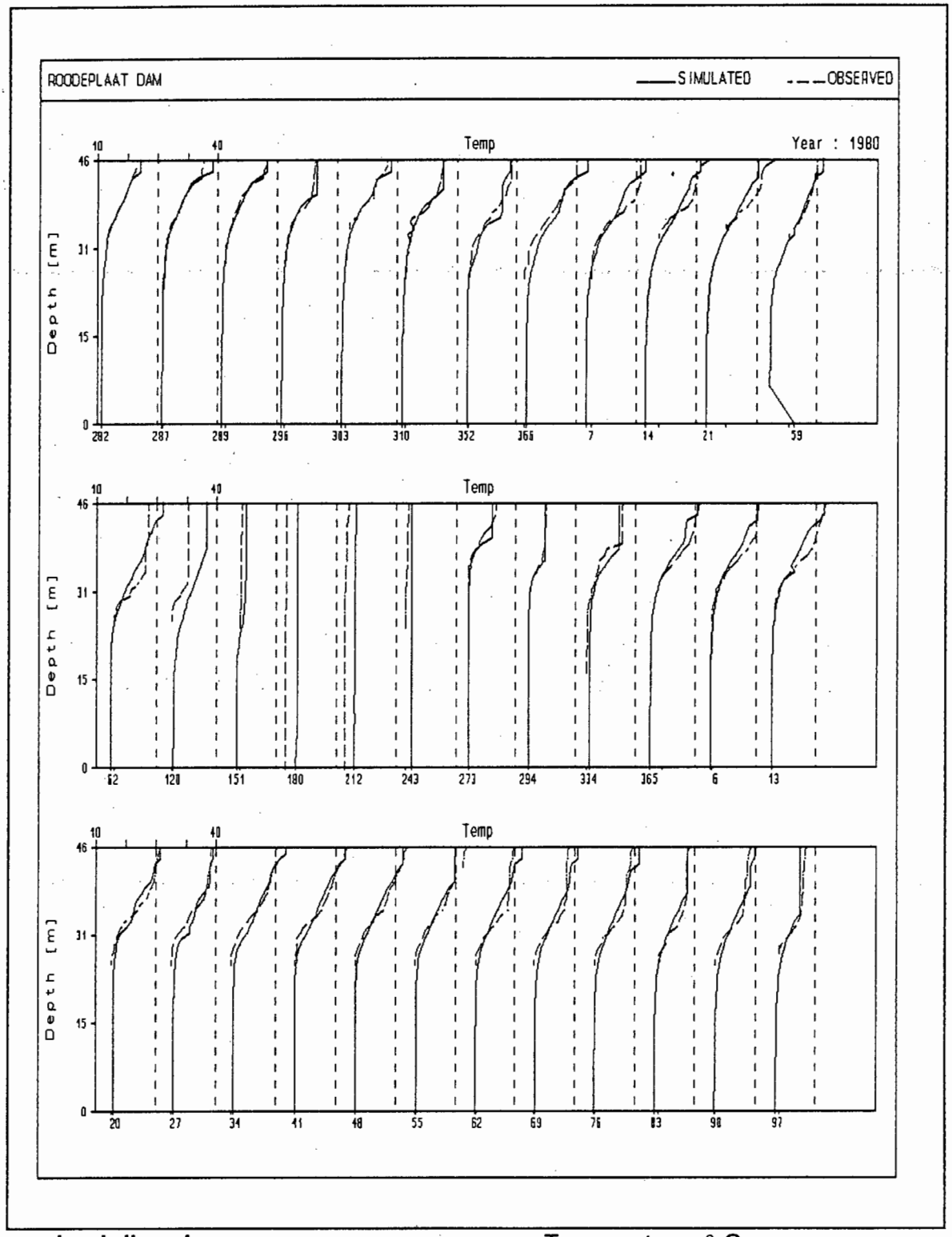

Figure 6.3
Depth profiles of simulated and observed water temperature as obtained with the modified MINLAKE model on Roodeplaat Dam.

6.4.2 Mixed layer depth

Hydrodynamic mixing (depicted as mixing depth in the MINLAKE model) significantly affects the concentration of nutrients, as well as the concentration of TSS and water temperature. Time-series plots of simulated and observed mixing depth are shown in Figure 6.4.

Note: The simulated mixing depth was affected most by:

- Adapting the wind speed measured at 1.8 m to wind speed at 10 m as required by the model.
- Choosing an appropriate value for the epilimnetic eddy diffusion coefficient **c**, when calculating the epilimnetic eddy diffusivity (*cf* discussion in previous paragraph).

Once the hydrodynamic part of the model has been calibrated successfully on Roodeplaat Dam, the water quality part of the model could be calibrated. Results of the water quality calibration are reported in the next chapter.

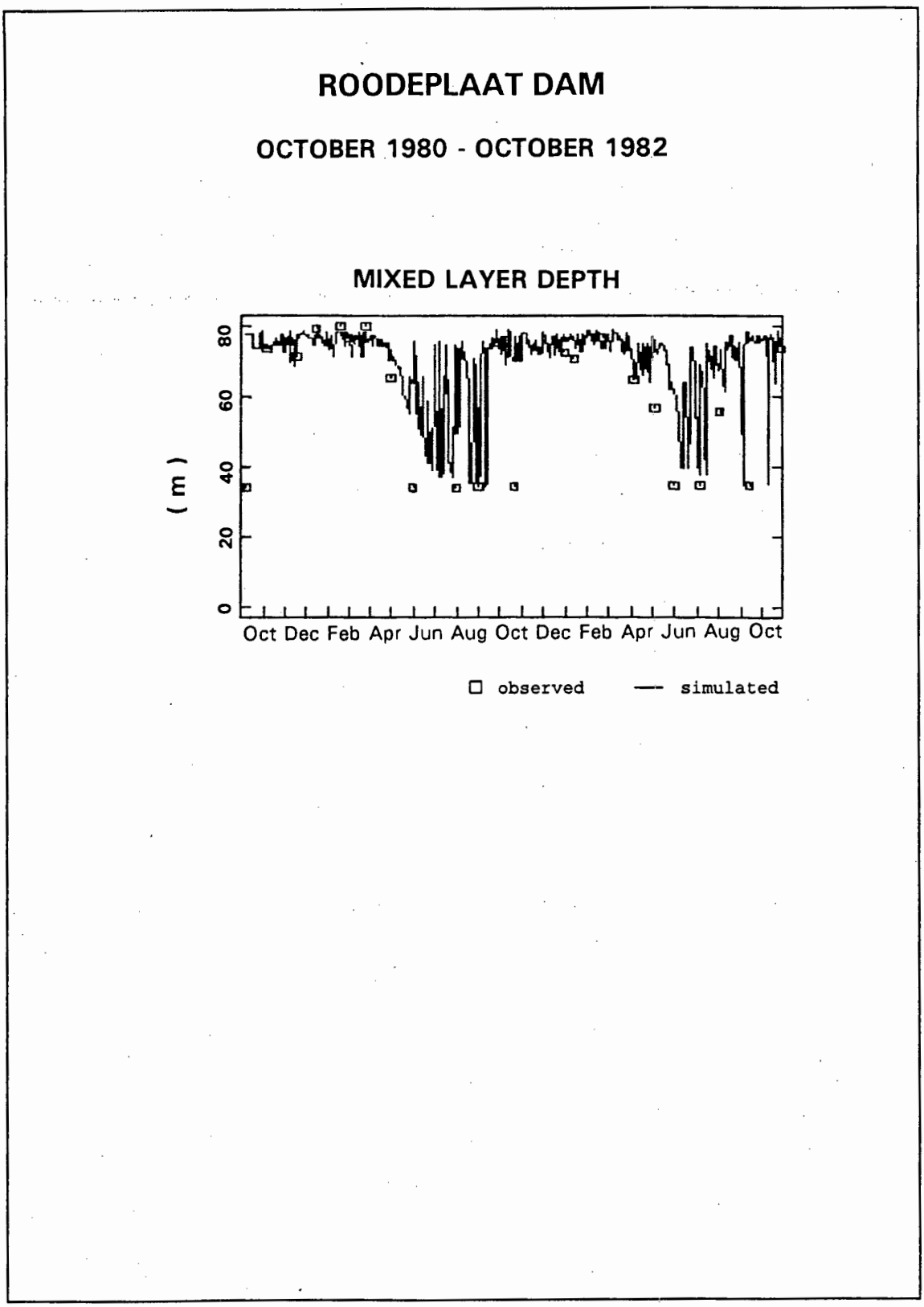

Figure 6.4
Time-series graph of simulated and observed mixed layer depth as obtained with the modified MINLAKE model on Roodeplaat Dam.

CHAPTER 7

CALIBRATION OF THE WATER QUALITY PART OF THE MINLAKE MODEL TO A SOUTH AFRICAN RESERVOIR

7.1 INTRODUCTION

The hydrodynamic processes in a reservoir affect the water quality response significantly, whereas the effect of water quality processes on the hydrodynamic response is much smaller, therefore the hydrodynamic part of the model had to be calibrated first. Once the hydrodynamic calibration had been done (see Chapter 6) attention could be focused on calibration of the water quality part of the model. The procedure recommended by the developers of the original MINLAKE model for calibration of the water quality variables is to start with the variables that are least affected by other variables, progress to variables with strong interactions, and finish with variables that are more affected by other variables but do not strongly interact with these other variables. Accordingly, the water quality variables were calibrated in the following order:

Dissolved phosphate
Nitrogen (ammonia and nitrate)
Chlorophyll-a
TSS
Detritus
Oxygen
TDS

Because of the inter-dependence between nutrients and chlorophyll-a, calibration of these variables is an iterative process, necessitating the model to be run a number of times. The major part of calibration time was spend in calibration of nutrient-chlorophyll-a interactions.

NOTE: ***Simulation period:***

For Roodeplaat Dam Reservoir, the data required to calibrate the model (*cf* Appendix A1) were available as from 16 April 1980, consequently, as a starting point, the model was run from April 1980 to April 1982. However, in Roodeplaat Dam Reservoir turnover occurs roundabout April. Turnover constitutes a period of great instability in a reservoir (Henderson-Sellers 1984). During the initial hydrodynamic calibration, it seemed as if the correspondence between simulated and observed hydrodynamic variables (water temperature and mixing depth) was adequate, but when calibration of the water quality part of the model was attempted, there was a significant deviation between simulated and observed nutrient concentrations during the first 7 months of the simulation period. Thereafter the deviance decreased, but good correspondence between simulated and observed concentrations never was obtained, because of the initial deviance. A likely cause for the deviance was the unstable conditions in the reservoir during turn-over at the start of the simulation period. To remedy the situation, the program was run with the starting date in October, i.e. the beginning of the period of stratification. Thus simulation results obtained during the initial calibration period are reported for the period April 1980 - April 1982, whereas the final results are reported for the period October 1980 - October 1982.

As was discussed in Chapter 6, running of the MINLAKE model requires specification of several calibration coefficients by the user. The coefficients required by the original MINLAKE model are listed in Table 7.1.

Table 7.1. Coefficients to be specified by the user in the original MINLAKE model

CALIBRATION COEFFICIENT	SYMBOL	UNITS
PHYSICAL RESERVOIR CONSTANTS		
Minimum layer thickness	DZLL	m
Maximum layer thickness	DZUL	m
Width of inflowing river (must be specified for each inflowing river)	WCHAN	m
Altitude of reservoir bottom	DBL	metres above sea level
Stage (reservoir water level)	ST	metres above sea level
Downstream slope of inflowing river (must be specified for each river)	S	
Manning's friction factor	FT	English units
Height of reservoir wall	ELCB	metres above sea level
Side slope of outflow channel	ALPHA	
Bottom width of outflow channel	BW	m
HYDRODYNAMIC COEFFICIENTS		
Extinction coefficient of water	XK1	m^{-1}
Extinction coefficient due to chlorophyll-a	XK2	$m^2\ g^{-1}$ Chla
Wind function coefficient	WCOEFF	none
Wind sheltering coefficient	WSTR	none
Maximum eddy diffusion coefficient	HKMAX	$m^2\ day^{-1}$

continued....

WATER QUALITY COEFFICIENTS		
Sediment oxygen depletion rate	SB20	g m^2 day^{-1}
Sediment phosphorus release coefficient	BRR	g m^2 day^{-1}
Detrital decay rate	BODK20	day^{-1}
Detrital settling rate	FVBOD	m day^{-1}
Algal respiration rate*	XKR1	day^{-1}
Algal mortality rate*	XKM	day^{-1}
Algal settling rate*	FVCHLA	m day^{-1}
Maximum phosphorus uptake rate*	UPMAX	day^{-1}
Half saturation coefficient for phosphorus uptake*	HSCPA	mg l^{-1}
Minimum intracellular phosphorus concentration needed for growth*	PMIN	mg P mg^{-1}Chla
Maximum intracellular phosphorus storage capacity*	PMAX	mg P mg^{-1}Chla
Maximum nitrogen uptake rate*	UNMAX	day^{-1}
Half saturation coefficient for nitrogen uptake*	HSCN	mg l^{-1}
Minimum intracellular nitrogen concentration needed for growth*	XNMIN	mg N mg^{-1}Chla
Maximum intracellular nitrogen storage capacity*	XNMAX	mg N mg^{-1}Chla
Half saturation coefficient for preferential uptake of ammonium over nitrate*	HSCNH	mg l^{-1}
Maximum nutrient saturated growth rate*	GROMAX	day^{-1}
Upper temperature at which algal growth is reduced 90%*	TMAX	°C
Optimum temperature for algal growth*	TOPT	°C
Half saturation coefficient for light limited growth*	HSC1	µE m^{-2} s^{-1}
Light inhibition coefficient*	HSC2	µE m^{-2} s^{-1}

* Indicate those water quality coefficients that have to specified for each algal class

7.2 ESTABLISHING VALUES FOR THE COEFFICIENTS ASSOCIATED WITH DISSOLVED PHOSPHATE CONCENTRATION

The calibration coefficients pertaining to simulation of dissolved phosphate concentration are indicated in Table 7.2. Values for some of the coefficients could be established from work that has been done on Roodeplaat Dam (DWAF 1981, Rossouw 1986), else, as a first approximation, the default values indicated in the MINLAKE manual were used. (In the original MINLAKE manual, the default values are the values used for Lake Riley in the USA).

Table 7.2. Kinetic coefficients pertaining to phosphorus simulation in the original MINLAKE model, and values used to obtain the first Roodeplaat simulations with the original MINLAKE model.

COEFFICIENT	VALUE	UNIT
BRR - sediment phosphorus release/adsorption coefficient	0.001	g m^{-2} day^{-1}
UPMAX - maximum uptake rate of PO_4 by Chla	6.0*	mg P mg^{-1} Chla d^{-1}
PMIN - minimum intracellular phosphorus concentration required for growth	1.0*	mg P mg^{-1} Chla
PMAX - maximum capacity of cell to store phosphorus	10.9*	mg P mg^{-1} Chla
YPBOD - mass ration of phosphorus produced from detrital decay	0.0091	mg P mg^{-1} Chla

* Default values as per MINLAKE manual.

Using the values for the phosphate kinetic coefficients as listed in Table 7.2, and incorporating the modifications in the hydrodynamic part of the model, the model was run for a period of two years, initially from April 1980 - April 1982. In Fig 7.1 time-series graphs of the simulated and observed phosphate concentrations are shown: Contrary to observations, the simulated phosphate concentration showed a steady increase with time.

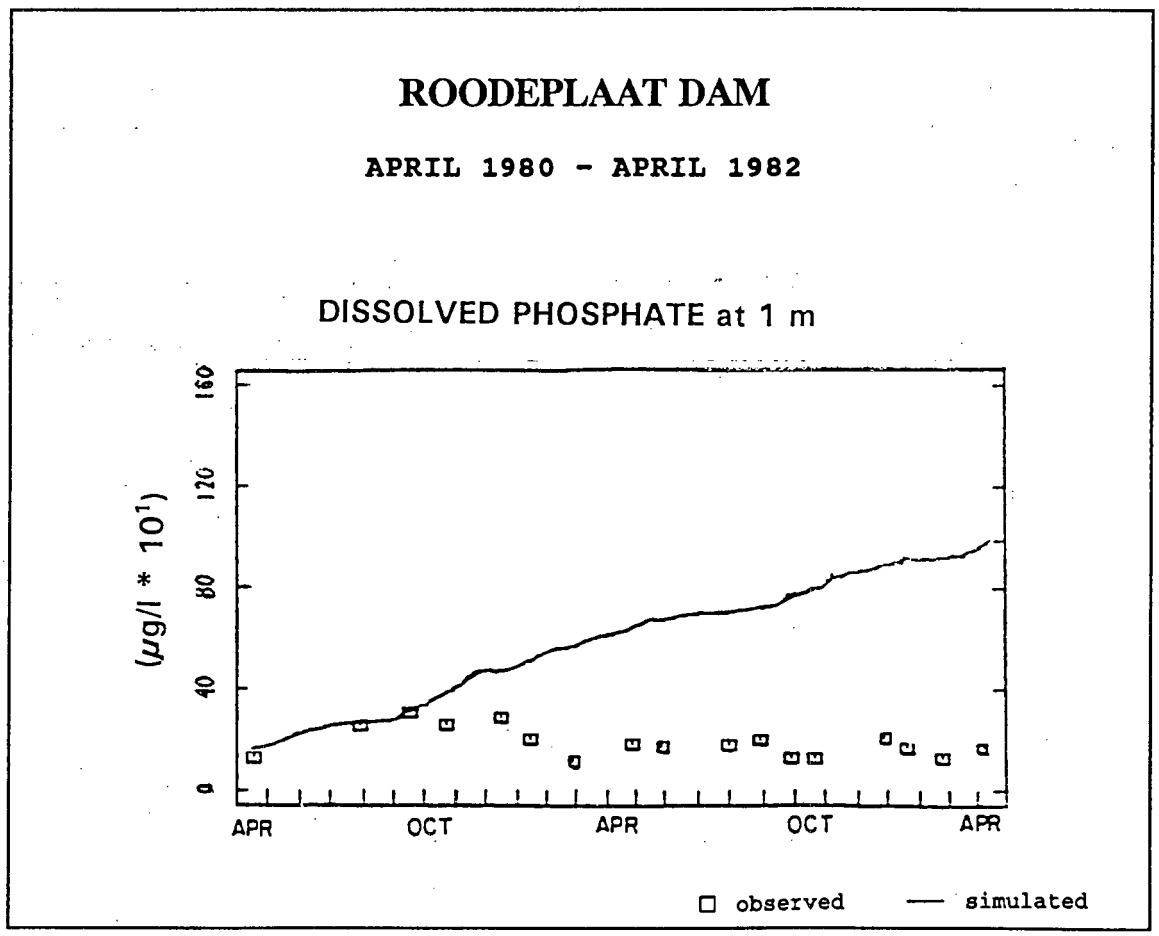

Fig 7.1

Time-series graph of observed and simulated dissolved phosphate concentrations in Roodeplaat Dam as obtained with the original MINLAKE model and default values for the calibration coefficients.

Possible reasons for this deviant behaviour were:

- Inadequate formulation of the processes governing the concentration of dissolved phosphate
- The values chosen for the phosphate kinetic coefficients were not optimal for Roodeplaat Dam Reservoir.

To establish the exact cause of the deviant behaviour, a detailed study had to be made of the various processes pertaining to dissolved phosphate, their formulations, and the associated kinetic coefficients.

7.2.1 Release/adsorption rate of dissolved phosphate from the bottom sediments - BRR

In the original MINLAKE model, sediment phosphate release/adsorption is represented as a constant rate, utilizing a sediment phosphate release/adsorption coefficient BRR, that has to be specified by the user (Eq 5.77):

$$PRA = BRR * \frac{Area}{volume} \qquad (7.1)$$

PRA = sediment phosphate release/adsorption (g m^{-3})
BRR = sediment phosphate release/adsorption coefficient (g $m^{-2}d^{-1}$)
Area = area of bottom sediment in particular layer (m^2)
Vol = volume of a particular layer (m^3).

A positive value for BRR would indicate sediment phosphate release, while a negative value would indicate sediment phosphate adsorption. This means that sediment release and adsorption of phosphate could not occur during the same run. From the study that has been done on Roodeplaat Dam Reservoir (DWAF 1981), it is known that phosphate is released under anaerobic conditions and adsorbed under aerobic

conditions. As a first approximation, because only one of the processes could be represented, BRR was treated as a release coefficient by setting the value of BRR at 0.001 mg m^{-2} d^{-1} (DWAF 1981). However, the original MINLAKE model does not make provision for linking BRR to the aerobic state of the water, thus treating BRR as a release coefficient effectively meant that there was a constant release of simulated phosphate from the sediment, regardless of whether the overlying water was anaerobic or not. This may be a reason for the steady increase in the simulated dissolved phosphate concentration depicted in Fig 7.1. Clearly the model had to be modified to simulate the dissolved phosphate behaviour in Roodeplaat Dam Reservoir. Accordingly, the following changes were incorporated into the model (also see paragraph 5.3.4.1):

- *Sediment phosphate release:*

  The sediment phosphorus release coefficient, BRR, was linked to the aerobic state of the water by incorporating an anaerobic switching function. The associated switching constant is called BRPK (*cf* Eq 5.78). The user has the option of changing the value of BRPK. For Roodeplaat Dam Reservoir BRPK was set empirically at 0.02 mg O_2/l. The phosphorus release coefficient, BRR, was set as before, i.e. at 0.001 g m^{-2} d^{-1} (DWAF, 1981).

  Also, the study on Roodeplaat Dam Reservoir (DWAF 1981) indicated that phosphate release from the sediment under anaerobic conditions will continue at a steady rate until an equilibrium phosphate concentration in the overlying water is reached, whereafter the release effectively is zero. For Roodeplaat Dam Reservoir, laboratory studies indicated that the equilibrium phosphate concentration is 0.15 mg P l^{-1} (DWAF 1981). This behaviour was incorporated into the program by linking BRR (the sediment phosphorus release rate) to a phosphate switching function with the following format (*cf* Eq 5.78):

$$SF = \frac{EBRR}{(EBRR + P)} \qquad (7.2)$$

SF = switching function

EBRR = phosphate switching constant (mg P l^{-1})

P = phosphate concentration in the overlying water (mg P l^{-1}).

The user has the option of changing the value of EBRR. For Roodeplaat Dam Reservoir, EBRR was set at 0.075 mg P l^{-1} (DWAF 1981).

- *Sediment phosphate adsorption:*
  A sediment phosphate adsorption process was added to the program by incorporating a sediment phosphorus adsorption coefficient, called BAA, into the program (*cf* Eq 5.78). To ensure sediment phosphate adsorption during aerobic conditions only, BAA was linked to an aerobic switching function. The switching constant for aerobic phosphate adsorption was the same as that for the anaerobic release of phosphate (BRPK; 0.02 mg O_2/l), i.e. when release of dissolved phosphate by the bottom sediments was switched off, adsorption was switched on. There is no indication in the literature as to the amount of dissolved phosphate adsorbed by the bottom sediments of Roodeplaat Dam Reservoir, by iteration the best value was found to be 0.01 g m^{-2} d^{-1}.

- *Effect of temperature on sediment phosphate adsorption/release:*
  Both sediment adsorption and release are affected by temperature (Jørgensen 1980). This behaviour was incorporated into the program by linking both BAA and BRR to an Arrhenius temperature coefficient called QBRR. The user has the option of changing the value of QBRR. For Roodeplaat Dam the value of QBRR was found by calibration and set at 1.088.

Regarding the changes to formulation of sediment phosphate release/adsorption, according to Kamp-Nielsen (1980, 1981), for hydraulic retention times of less than one

year overall model performance is independent of the complexity of the sediment submodel, except for submodels utilising a constant release rate, which he rejects as being too simple. The retention time of Roodeplaat Dam is 0.7 - 1.5 years (Walmsley and Butty 1980a). It is realised that, in spite of the modifications as discussed in the previous paragraphs, the formulation as given in Eq 5.78 probably is an over-simplification of the real process, but this formulation is the best possible with the available data.

7.2.2 Interaction between algae and dissolved phosphate.

The coefficients of interest are: UPMAX, - maximum uptake rate of PO_4 by Chla; PMIN - minimum concentration of intracellular phosphorus required for growth; PMAX - maximum capacity of cell to store phosphorus; and HSCPA - half saturation coefficient for dissolved phosphate uptake (Table 7.2). These coefficients have more bearing on simulation of chlorophyll-a concentration than on simulation of dissolved phosphate concentration, and are therefore discussed with chlorophyll-a simulation results.

7.2.3 Phosphorus produced from detrital decay - YPBOD.

During detrital decay intracellular phosphorus is released into the water (see discussion paragraph 4.4.4.1) In the original MINLAKE model the detrital decay process is modelled in such a way that there is a constant release of intracellular phosphorus. In the modified model, detrital decay, and thus intracellular release is terminated under anaerobic conditions by use of a switching function (*cf* Eq 5.75 and Eq 5.76). The original MINLAKE model made provision for intracellular phosphorus release by utilizing a coefficient called YPBOD. This coefficient was retained, and set at 0.00091 mg P mg^{-1} Chla for Roodeplaat Dam Reservoir (Rossouw 1986a). The simulated dissolved phosphate concentration is not very sensitive to this coefficient.

7.2.4 Final dissolved phosphate simulation results.

The changes that had to be incorporated into the original MINLAKE model to allow simulation of dissolved phosphate concentration in Roodeplaat Dam are indicated in Table 7.3.

Table 7.3 A comparison of phosphorus processes in the original and modified MINLAKE model

ORIGINAL MINLAKE MODEL	MODIFIED MINLAKE MODEL
■ In the same run, either release only, or adsorption only, of dissolved phosphate by bottom sediment	■ In the same run, release or adsorption of dissolved phosphate by bottom sediment
■ Sediment phosphate release rate not sensitive to oxygen or phosphate concentration in overlying water, nor to temperature.	■ Release rate of dissolved phosphate from the bottom sediment: - Only under anaerobic conditions. - Inhibited by steady state dissolved phosphate concentration in the overlying water. - Affected by water temperature.
■ Sediment phosphate adsorption rate not sensitive to aerobic/anaerobic state of the water	■ Adsorption rate of dissolved phosphate by the bottom sediment: - Only under aerobic conditions.
■ Constant release of intracellular phosphorus	■ Release of intracellular phosphorus under aerobic conditions only.

After all the changes, as indicated in Table 7.3, were incorporated into the program, the modified model was run for a period of two years, from October 1980 - October 1982. The values of kinetic coefficients pertaining to dissolved phosphate simulation in the modified model were as indicated in Table 7.4. Time-series graphs of simulated and observed dissolved phosphate concentrations at a depth of 1 and 16 metres are

shown in Fig 7.2, while depth profiles are shown in Fig 7.3. Generally, the correspondence between simulated and observed dissolved phosphate concentration is good.

Table 7.4 Kinetic coefficients pertaining to phosphorus simulation in the modified MINLAKE model, and values used to obtain the final simulation results.

KINETIC COEFFICIENT	VALUE	UNIT	REFERENCE
BRR - sediment phosphorus release coefficient	0.001	g m^{-2} day^{-1}	DWAF 1981
BRPK - switching constant for phosphorus adsorption/release	0.02	mg O_2 l^{-1}	Calibration
EBRR - equilibrium concentration for sediment phosphate release	0.075	mg P l^{-1}	DWAF 1981
QBRR - temperature coefficient for sediment phosphate release/adsorption	1.088		Calibration
UPMAX - maximum uptake rate of PO_4 by Chla	4.00 (Blue-green) 0.52 (Green)	mg P mg^{-1} Chla	Calibration Calibration
PMIN - minimum intracellular phosphorus concentration required for growth	0.49 (Blue-green) 1.23 (Green)	mg P mg^{-1} Chla	Reynolds 1984 Reynolds 1984
PMAX - maximum capacity of cell to store phosphorus	4.9 (Blue-green) 11.0 (Green)	mg P mg^{-1} Chla	Calibration Calibration
YPBOD - mass ratio of phosphorus produced from detrital decay	0.0091	mg P mg^{-1} Chla	DWAF 1981

Note: Satisfactory simulation of dissolved phosphate concentration was possible only once the sediment phosphorus kinetics of Roodeplaat Dam Reservoir had been adequately simulated, i.e. recognising that phosphate is released from the bottom sediments under anaerobic conditions and adsorbed under aerobic conditions.

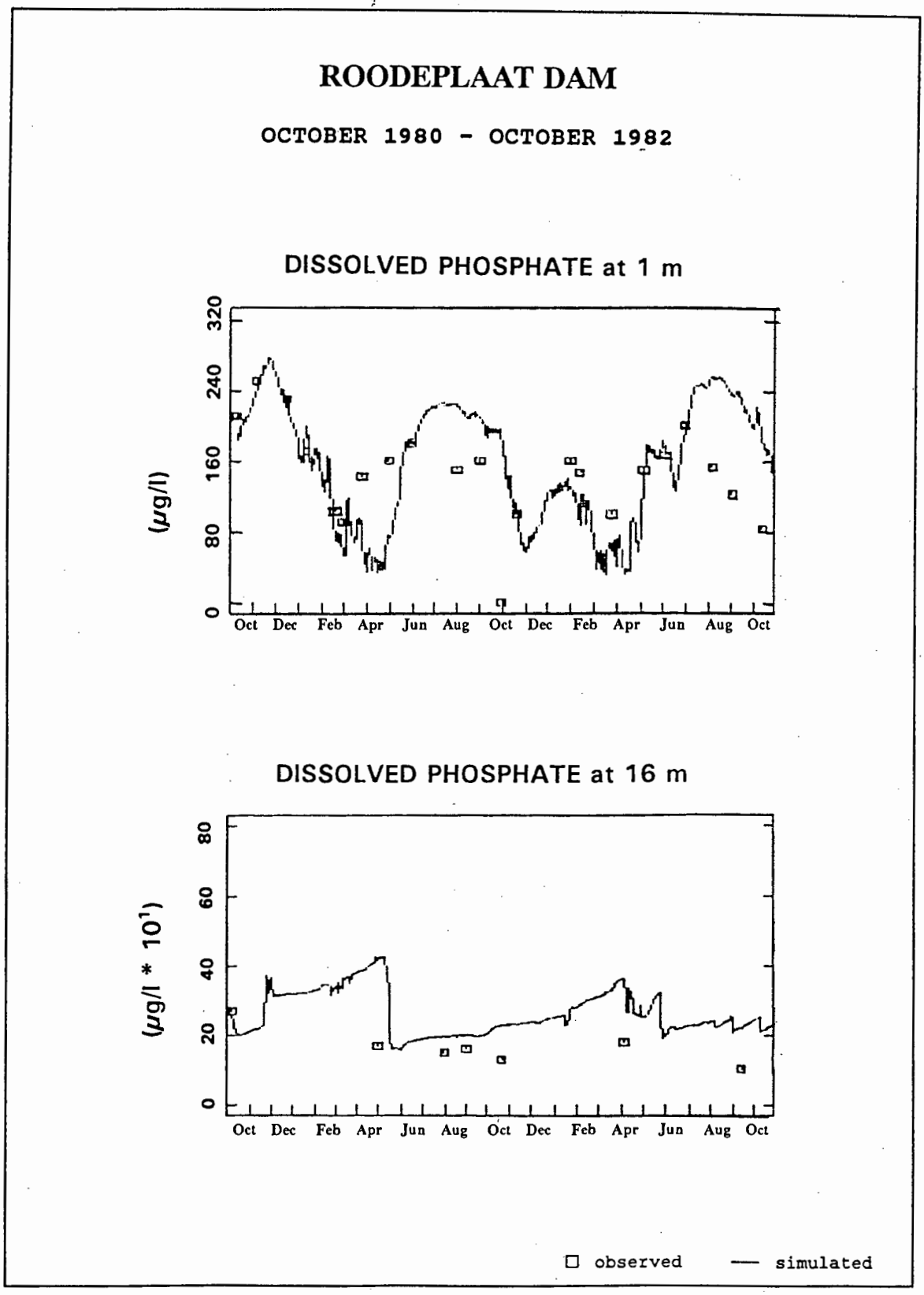

Fig 7.2
Time-series graph of observed and simulated dissolved phosphate concentration at 1 and 16 m depth in Roodeplaat Dam, as obtained with the modified MINLAKE model and optimum values for the calibration coefficients.

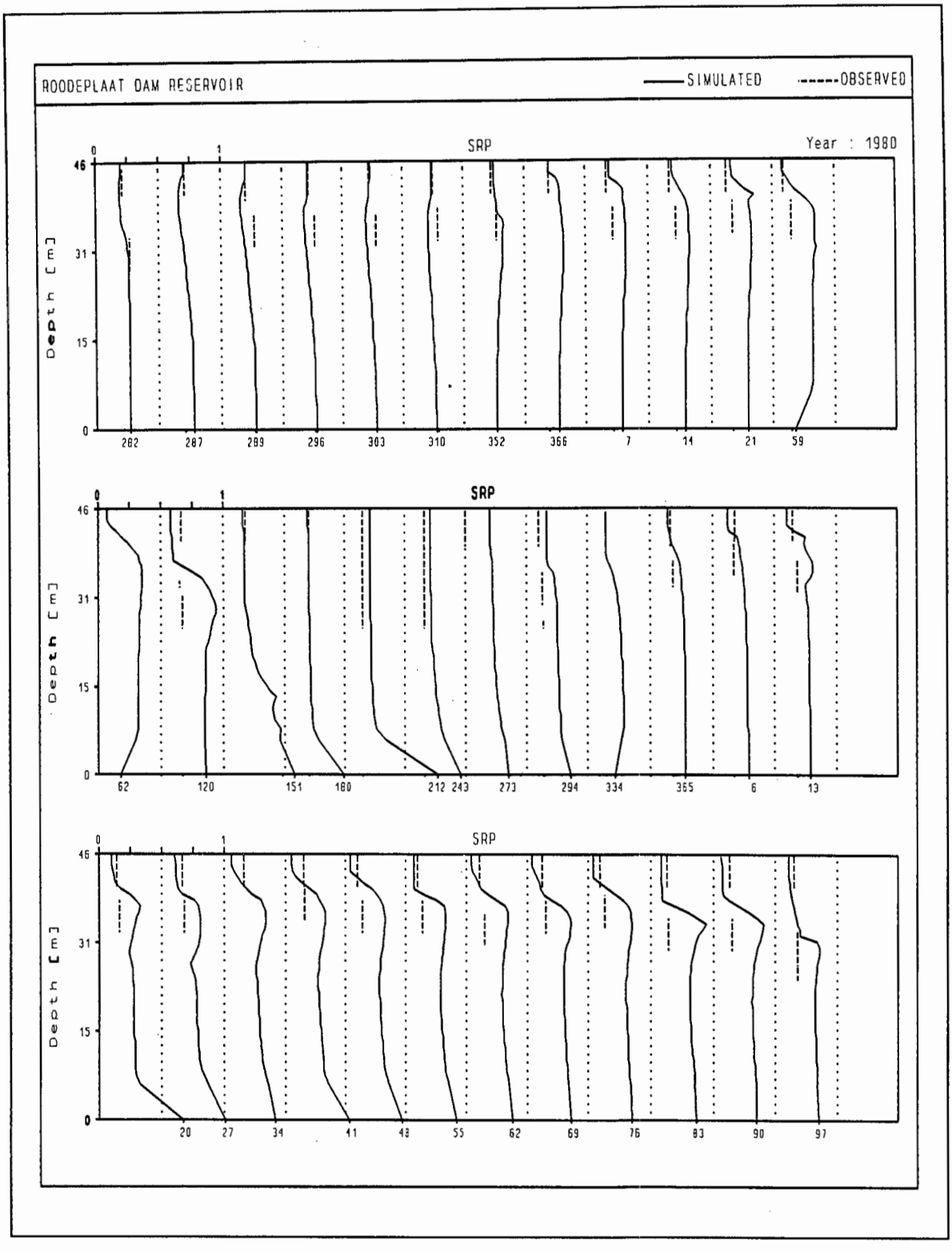

x-axis: Julian day Phosphate concentration: mg/l

Fig 7.3
Depth profiles of simulated and observed phosphate concentration as obtained with the modified MINLAKE model on Roodeplaat Dam for the period October 1980 to October 1982

7.3 ESTABLISHING VALUES FOR THE COEFFICIENTS ASSOCIATED WITH NITROGEN CONCENTRATION.

The structure of the original MINLAKE model is such that nitrogen (ammonia and nitrate) behaviour can be simulated only if two or more algal classes are being simulated. Even if two (or more) algal classes are simulated, the user still has the option as to whether nitrogen behaviour should be simulated. Thus it is possible to simulate two algal classes without taking nitrogen into account, i.e. it can be assumed that both algal classes are phosphorus limited.

Studies that had been done on Roodeplaat Dam indicated that blue-green algae were the more dominant group during the study period (DWAF (HRI) 1984, Pieterse and Röhrbeck 1990), but there was no clear evidence as to the growth limiting nutrient (also see discussion in paragraph 7.4). As a starting point only one algal class (blue-green algae) was simulated in Roodeplaat Dam, with the assumption that algal growth was phosphate limited only. However, it soon became clear that at least two algal classes had to be simulated, and that nitrogen limited growth should be taken into account also (see discussion below in paragraph 7.4), but when the original MINLAKE model was run with the nitrogen option, the program became numerically unstable. The reason for this was not clear, but, because the MINLAKE manual gives conflicting instructions as to how the nitrogen option should be chosen, it was possible that the nitrogen option was chosen incorrectly. Though the manual gives a step-by-step example of how the model should be run, the nitrogen option is not covered in this example.

To assist the user in learning the program, data bases (including nitrogen data) for Lake Riley in the USA are provided with the model. As a test, the original MINLAKE model was run with the Lake Riley data bases. Again the program became numerically unstable, indicating that the numerical instability was not due to erroneous data input - it was probably caused by a coding/formulation error in the program. After an intensive investigation, it was found that the numerical instability was caused by two coding errors.

Regarding the kinetic coefficients pertaining to ammonia and nitrate simulation: a range of possible values was indicated for most of the nitrogen coefficients. A warning is given that nitrogen coefficients have been less well investigated and that less information was available in the literature on these coefficients (Riley 1988). (A later literature study to obtain optimum values for the nitrogen coefficients proved this statement, i.e. though abundant information on coefficients pertaining to phosphorus behaviour can be found in the literature, far less information is available on nitrogen coefficients.) Though several studies have been done on Roodeplaat Dam Reservoir (DWAF 1981, Pieterse *et al* 1990, Toerien *et al* 1976, Walmsley *et al* 1980) none of the values for the nitrogen coefficients could be established from these studies. As a starting point for simulating ammonia and nitrate behaviour in Roodeplaat Dam Reservoir, values for the nitrogen coefficients had to be chosen from the ranges indicated in the MINLAKE manual. These values, and the coefficients they relate to, are indicated in Table 7.5.

Table 7.5. Kinetic coefficients pertaining to nitrogen simulation in the original MINLAKE model, and values used to obtain the first Roodeplaat simulations with the original MINLAKE model.

KINETIC COEFFICIENT	VALUE	UNIT
UNMAX - maximum uptake rate of nitrogen by Chla	2.0 (blue-green) 2.0 (green)	mg N mg $Chla^{-1}$ d^{-1}
XNMIN- minimum intracellular nitrogen concentration required for growth	1.53 (blue-green) 2.73 (green)	mg N mg $Chla^{-1}$
XNMAX - maximum capacity of cell to store nitrogen	7.5 (blue-green) 8.5 (green)	mg N mg $Chla^{-1}$
HSCN - Half saturation constant for nitrogen uptake	0.014 (blue-green) 0.034 (green)	mg l^{-1}
HSCNH - Half saturation constant for preferential uptake of ammonium over nitrate	0.01 (blue-green) 0.025 (green)	mg l^{-1}
XKNNH - nitrification rate	0.05	day^{-1}
BRNO - Sediment nitrate release/adsorption rate	0.99	g NO_3 m^{-2} d^{-1}
BRNH - sediment ammonium release/adsorption rate	0.05	g NHO_4 m^{-2} d^{-1}
YNHBOD - mass ratio of ammonium nitrogen released per dissolved oxygen utilized in detrital decay	0.05	mg NH_4 mg BOD^{-1}

Time-series graphs of the simulated ammonia concentration obtained with these values for the nitrogen coefficients, as well as the observed ammonia concentration in Roodeplaat Dam Reservoir, are indicated in Fig 7.4. Simulated and observed nitrate concentrations for Roodeplaat Dam Reservoir are indicated in Fig 7.5.

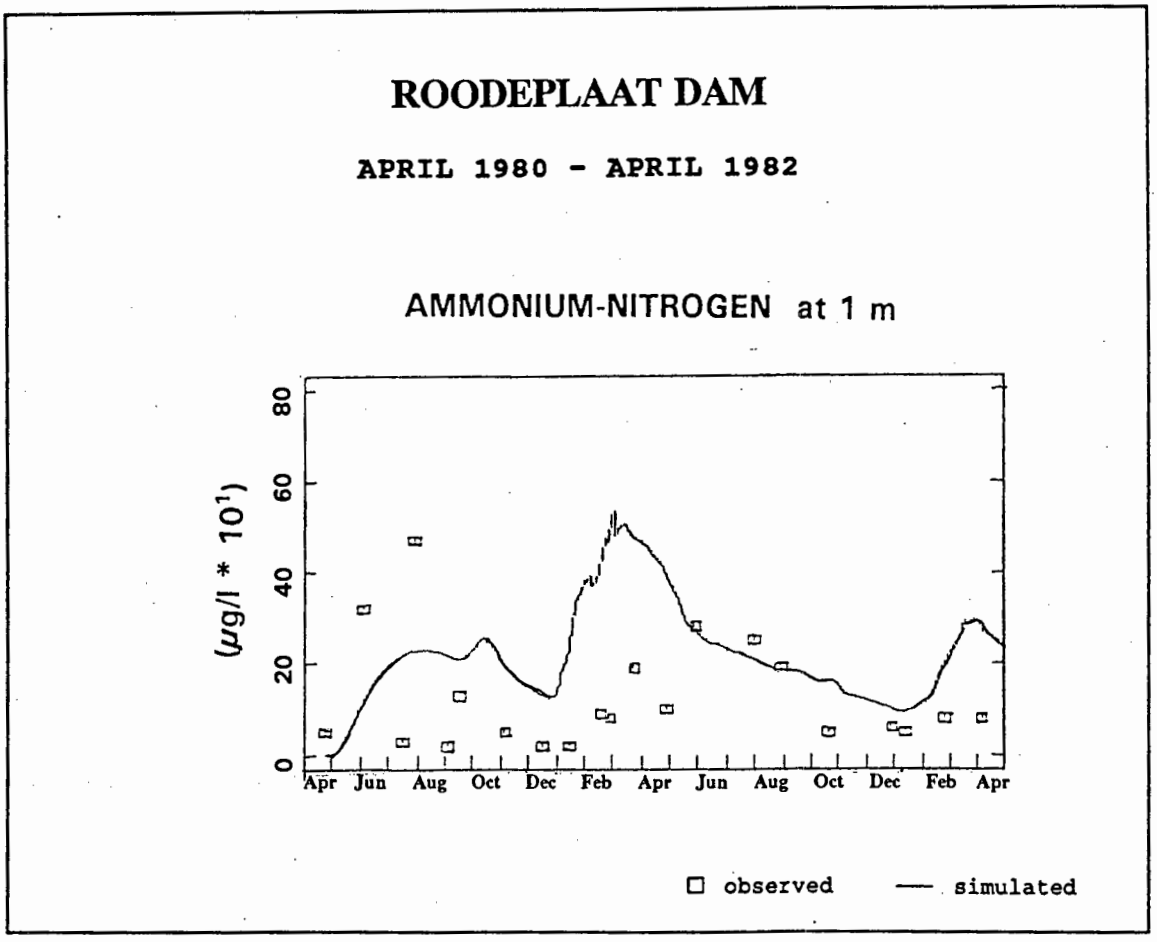

Fig 7.4
Time-series graph of observed and simulated ammonia concentration in Roodeplaat Dam, as obtained with the original MINLAKE model and default values for the calibration coefficients.

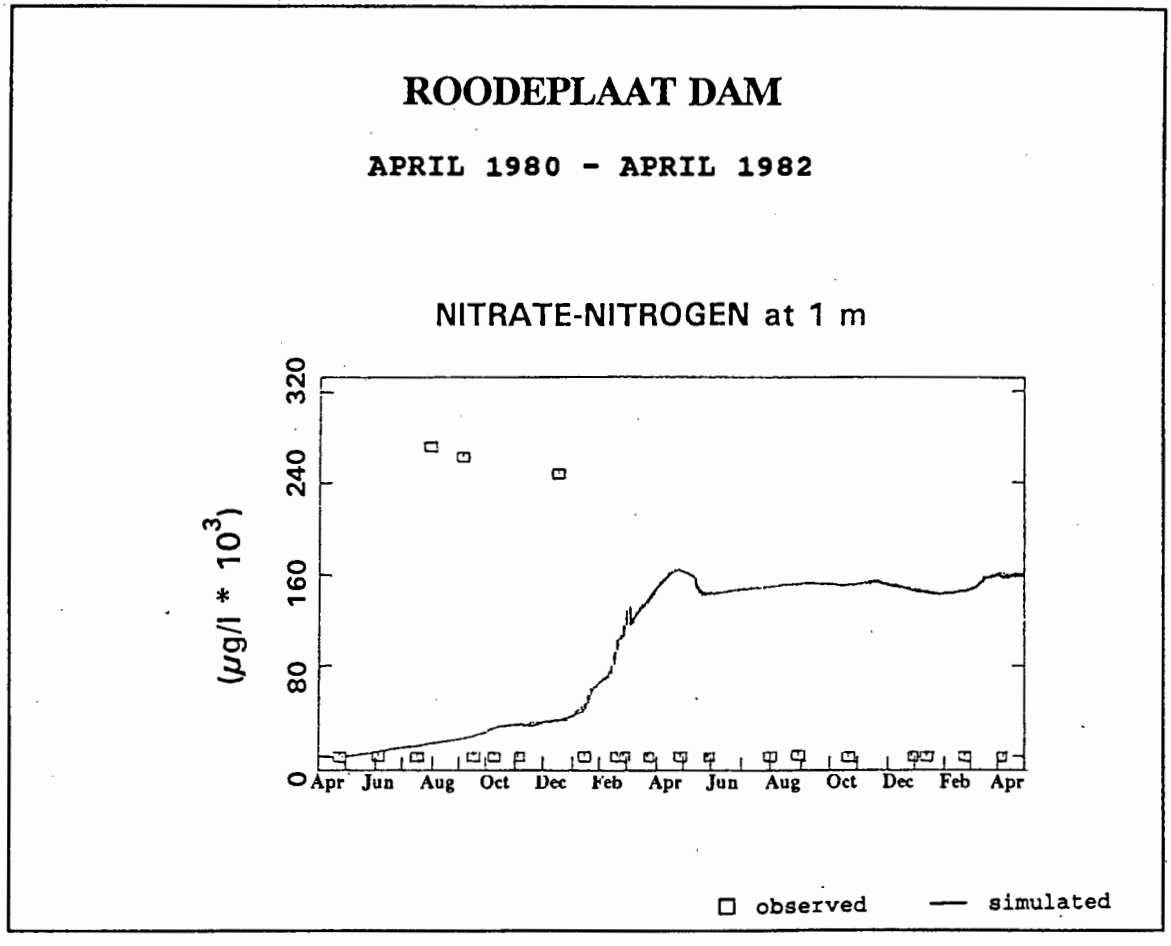

Fig 7.5
Time-series graph of observed and simulated nitrate concentration in Roodeplaat Dam, as obtained with the original MINLAKE model and default values for the calibration coefficients.

Correspondence between simulated and observed concentrations for both ammonia and nitrate is poor. Possible reasons for the poor result are the following:

- Formulations of the nitrogen processes in the original MINLAKE model are incorrect or inadequate.
- The values chosen for the nitrogen coefficients are not the optimum values for Roodeplaat Dam Reservoir.

This led to an intensive literature study of the nitrogen coefficients and the processes they relate to; these were studied interactively.

7.3.1 Nitrogen and algal growth

The coefficients of interest are: UNMAX - maximum uptake rate of nitrogen by Chla; XNMIN - minimum intracellular nitrogen concentration required for growth; XNMAX - maximum capacity of cell to store nitrogen; HSCN - half saturation constant for nitrogen uptake; and HSCNH - half saturation constant for preferential uptake of ammonium over nitrate.

As with the dissolved phosphate - chlorophyll-a kinetics, and the related coefficients UPMAX, PMIN, PMAX and HSCPA, the nitrogen coefficients UNMAX, XNMIN, XNMAX, HSCN and HSCNH have more bearing on simulation of chlorophyll-a concentration than on simulation of nutrient (nitrogen) concentration, and, therefore are discussed with the chlorophyll-a simulation results. These coefficients are a good example of the interaction between processes.

7.3.2 Nitrification - XKNH

In the original MINLAKE model, the process of nitrification is represented by (*cf* Eq 5.87):

$$dN/dt = XKNH\ \theta^{(T-20)}\ NH \qquad (7.3)$$

dN/dt	=	change in ammonia/nitrate concentration in a layer (mg l^{-1})
XKNH	=	nitrification rate (day^{-1})
θ	=	Arrhenius temperature coefficient for nitrification
T	=	ambient water temperature in a layer(°C)
NH	=	ammonium concentration in the layer (mg l^{-1}).

The user has the option of choosing an appropriate value for the nitrification rate coefficient, XKNH, but the MINLAKE manual gives no default value for the nitrification rate coefficient, nor a range of possible values. Values in the literature ranged from 0.005 to 0.8, with 0.02 to 0.03 the most typical values (James 1993, Orlob 1983, Cole 1991). For Roodeplaat Dam Reservoir, a value of 0.02 for XKNH gave the best result.

Furthermore, during the nitrification process 64 g of oxygen per 14 g of ammonia-N is consumed, therefore nitrification can occur under aerobic conditions only, though, according to the literature nitrification will take place at dissolved oxygen concentrations as low as 0.3 mg l^{-1} (Jørgensen 1980). In Hartbeespoort Dam Reservoir, the rate of nitrification rose rapidly as soon as the dissolved oxygen concentration exceeded 1.0 mg l^{-1} (NIWR 1985). The formulation in the original MINLAKE model did not provide for nitrification under aerobic conditions only, i.e. the rate of nitrification is not affected by the aerobic/anaerobic state of the water. This omission was rectified by linking the rate of nitrification to an aerobic switching function (*cf* Eq 4.91). The user has the option of choosing an appropriate value for the switching constant, called KONH. For Roodeplaat Dam Reservoir, the best result was obtained with a switching constant of 0.3 mg O_2 l^{-1}.

The rate of nitrification is inhibited by high substrate concentrations (Jørgensen 1980, Vincent *et al* 1981). In Hartbeespoort Dam Reservoir nitrification rates increased with increasing ammonia concentration up to 2 mg NH_4 l^{-1}, and then levelled off (NIWR 1985). The original MINLAKE model does not recognise this behaviour, therefore the program was modified by linking the nitrification rate coefficient to an ammonia switching function (called XNH), similar to an aerobic switching function. The user has the option of choosing an appropriate switching constant. No specific data were recorded for Roodeplaat Dam Reservoir, therefore the ammonia switching constant was set at 1 mg NH_4 l^{-1}, analogous to the situation in Hartbeespoort Dam reservoir.

Furthermore, because nitrification is a bacterial reaction, the reaction rate will be temperature dependant (Cole 1991, Jørgensen 1980, James, 1993). In the original MINLAKE model, the temperature dependence was expressed by means of an Arrhenius temperature coefficient, but the coefficient was hard-wired into the model to a value of 1.055. This value cannot be regarded as generally valid, for instance, in Hartbeespoort Dam Reservoir the Q_{10} value for nitrification has been determined as 1.83 , i.e an Arrhenius temperature coefficient of 1.063. The model was modified to allow the user to specify the value of the Arrhenius temperature coefficient for nitrification. In absence of data on Roodeplaat Dam Reservoir, a temperature coefficient of 1.063, similar to that of Hartbeespoort Dam Reservoir, was chosen.

The final formulation for nitrification in the modified MINLAKE model is as follows (Eq 5.88):

$$dN/dt = XKNH \left(\frac{DSO}{DSO+KONH}\right) \theta^{(T-20)} \left(\frac{NH}{NH+XNH}\right) NH \quad (7.4)$$

dN/dt	=	change in ammonia/nitrate concentration in a layer (mg l^{-1})
XKNH	=	nitrification rate (day^{-1})
DSO	=	dissolved oxygen concentration in a layer (mg l^{-1})
KONH	=	switching constant for nitrification
θ	=	Arrhenius temperature coefficient for nitrification
T	=	ambient water temperature in a layer(°C)
NH	=	ammonium concentration in the layer (mg l^{-1})
XNH	=	inhibition coefficient for nitrification (mg l^{-1}).

7.3.3 Denitrification

The original MINLAKE model did not make provision for the process of denitrification - a process that can be of great significance in eutrophic and hypertrophic reservoirs - as much as 30 - 80% of the total annual nitrogen load may be lost through denitrification (NIWR 1985, Jørgensen 1983, Seitzinger 1988). The simulated nitrate concentration in Roodeplaat Dam obtained with the original MINLAKE model (Fig 7.5) showed a steady increase in concentration, with the simulated concentration during the latter half of the simulation period much higher than the observed nitrate concentration. The deviant simulated behaviour was attributed to omission of the denitrification process, thus the process of denitrification was added to the program. Denitrification is a bacterial process that utilizes biodegradable detritus as substrate, thus formulation of denitrification will depend on formulation of detrital decay. In the modified MINLAKE model, detrital decay is formulated in two ways (see discussion in paragraph 5.3.2). If detrital decay is formulated as a simple first-order reaction (Eq 5.48), denitrification can be formulated as (Eq 5.89):

$$dNO/dt = (DNK \cdot QDNK^{(T-20)}) \left(\frac{KONO}{KONO+DSO}\right)\left(\frac{NO}{NO+EDNK}\right)\frac{BOD}{2.86} \quad (7.5)$$

If detrital decay is formulated as a two-step process, denitrification is formulated as (Eq 5.90):

$$dNO/dt = (DNK \cdot QDNK^{(T-20)})\left(\frac{KONO}{KONO+DSO}\right)\left(\frac{NO}{NO+EDNK}\right)\frac{0.333\ BODS}{2.86} \quad (7.6)$$

dNO/dt	=	change in nitrate concentration in a layer due to denitrification (mg l^{-1})
DNK	=	denitrification rate at 20°C (day^{-1})
QDNK	=	Arrhenius temperature coefficient for denitrification
T	=	water temperature in a layer (°C)
KONO	=	anaerobic switching constant for denitrification (mg O_2 l^{-1})
DSO	=	dissolved oxygen concentration in a layer (mg l^{-1})
NO	=	nitrate concentration in a layer (mg l^{-1})
EDNK	=	nitrate switching constant for denitrification (mg NO_3 l^{-1})
BOD	=	concentration of detritus as BOD (mg l^{-1}).
BODS	=	concentration of detritus as soluble BOD (mg l^{-1}).

Both formulations require the same calibration coefficients, i.e. a denitrification rate, DNK; an anaerobic switching constant KONO, a temperature coefficient QDNK; and a denitrification inhibition coefficient, EDNK:

7.3.3.1 Denitrification rate coefficient DNK:

Literature values for the denitrification rate coefficient, DNK, varied from 0.002 to 0.15 d^{-1} (Orlob 1983, Cole, 1991). No information regarding the denitrification rate coefficient could be found for Roodeplaat Dam Reservoir, nor for Hartbeespoort Dam Reservoir, consequently, for Roodeplaat Dam Reservoir, the value of DNK was set empirically at 0.03 d^{-1}. (The process was formulated in such a way that the user has the option of choosing an appropriate value for the denitrification rate coefficient, DNK.)

7.3.3.2 Anaerobic switching constant KONO:

Normally denitrification occurs under anaerobic conditions only (Le Cren *et al* 1980, Jørgensen 1980, Orlob 1983, Klapper 1991), but it has been found that, in natural waters, denitrification may occur at appreciable concentrations of dissolved oxygen (Toms, 1975). In Hartbeespoort Dam Reservoir, for instance, denitrification occurred up to a dissolved oxygen concentration of 6 mg l^{-1} (NIWR 1985). To enable simulation of this behaviour, the denitrification rate coefficient, DNK, was linked to an anaerobic switching function. The user has the option of choosing an appropriate value for the switching constant, called KONO. For Roodeplaat Dam Reservoir, the switching constant was set at 3.3 mg $_2$ l^{-1}, analogous to the situation in Hartbeespoort Dam Reservoir.

7.3.3.3 Temperature coefficient QDNK:

Because denitrification is a bacterial reaction, the reaction rate is affected by temperature and substrate concentration (Toms 1975, Seitzinger 1988, Jørgensen 1980). To provide for the temperature effect, the denitrification rate coefficient, XDNK, was linked to an Arrhenius temperature coefficient. The user has the option of choosing an appropriate value for this coefficient, called QDNK. No specific data could be found for Roodeplaat Dam Reservoir, but from the literature a value of 1.032 (i.e. a Q_{10} value of 1.37) seemed to be the most appropriate value (NIWR 1985).

7.3.3.4 Denitrification inhibition coefficient, EDNK:

To simulate the inhibition of denitrification by high substrate concentrations, the denitrification rate coefficient was linked to a nitrate switching function, similar to an aerobic switching function. The user has the option of choosing an appropriate value for the switching constant, called EDNK. No specific data were recorded for Roodeplaat Dam Reservoir, but in Hartbeespoort Dam Reservoir maximum denitrification rates were recorded at a NO_3-N concentration of 3.0 mg l^{-1} (NIWR 1985). The switching constant for Roodeplaat Dam Reservoir was therefore set at 1.5 mg NO_3-N l^{-1}.

7.3.4 Sediment nitrate release rate - BRNO

Under aerobic conditions, nitrate will be released from the bottom sediments (see paragraph 3.4.4.2). In the original MINLAKE model release of nitrate from the bottom sediment is formulated as a first-order reaction by utilizing a sediment nitrate release rate, BRNO (*cf* eq 5.84), but no provision was made for the fact that nitrate will be released from the bottom sediment under aerobic conditions only. This meant that simulated nitrate is released from the bottom sediment continuously, which probably contributed to the inordinately high simulated nitrate concentration obtained with the original MINLAKE model on Roodeplaat Dam (Fig 7.5). To ensure that nitrate will be released from the bottom sediment under aerobic conditions only, the sediment nitrate release rate was linked to an aerobic switching function. Furthermore, the release rate is affected by temperature (EPA 1985), therefore it was linked to a temperature function (*cf* Eq 4.94). The resulting formulation in the modified model is as follows (Eq 5.86):

$$\mathrm{dNO/dt} = \mathrm{BRNO}\ \frac{A}{V}\left(\frac{\mathrm{DSO}}{\mathrm{DSO}+\mathrm{BRNOK}}\right)\mathrm{QBNO}^{(T-20)} \qquad (7.7)$$

dNO/dt	=	change in nitrate concentration in a layer (mg l^{-1})
BRNO	=	sediment nitrate release rate (g m^{-2} day^{-1})
V	=	volume of the layer (m^3)
A	=	bottom sediment area in a layer (m^2).
BRNOK	=	switching constant for nitrate sediment release (mg l^{-1})
DSO	=	dissolved oxygen concentration in the layer (mg l^{-1})
QBNO	=	Arrhenius temperature coefficient for sediment nitrate release
T	=	water temperature in the layer (°C)

The sediment nitrate release rate, BRNO, must be specified by the user. No value could be found for Roodeplaat Dam, but according to the literature, 0.1083 g N m^{-2} d^{-1} will be released from the bottom sediments under aerobic conditions (EPA 1985). For Roodeplaat Dam Reservoir, the value of BRNO was set empirically at 0.075 g NO_3-N m^{-2} d^{-1}.

In the modified MINLAKE model, the user has the option of specifying an appropriate value for the aerobic switching constant, called BRNOK. For Roodeplaat Dam Reservoir, this value was set empirically at 1.0 mg O_2 l^{-1}. The user has the option also of specifying a value for the Arrhenius temperature coefficient. No specific value could be obtained for Roodeplaat Dam, but the best result was obtained with a value of 1.088.

7.3.5 Sediment ammonium release rate - BRNH

Ammonium will be released from the bottom sediment under anaerobic conditions only (see discussion in paragraph 3.4.4.2). As with sediment nitrate release, in the original MINLAKE model sediment ammonium release was formulated as a first-order reaction through utilization of a sediment ammonium release rate, BRNH, which has to be specified by the user (Eq 5.84). The original MINLAKE model does not recognise that sediment ammonium release will be affected by the aerobic state of the water. This omission was rectified by linking the sediment ammonium release rate to an anaerobic switching function. Also, the release rate is affected by temperature (Jørgensen 1980). As this is not provided for in the original MINLAKE model, the sediment ammonia release rate was multiplied by a temperature function (Eq 4.94). The user has the option of specifying the value of the Arrhenius temperature coefficient. Thus formulation of sediment ammonia release rate in the modified model is as follows (Eq 5.85):

$$dNH/dt = BRNH \cdot QRNH^{(T-20)} \frac{A}{V} \left(\frac{BRNHK}{BRNHK+DSO} \right) \qquad (7.8)$$

dNH/dt	=	change in ammonium concentration in a layer (mg l^{-1})
BRNH	=	sediment ammonium release rate (g m^{-2} day^{-1})
QRNH	=	Arrhenius temperature coefficient for sediment ammonium release
T	=	water temperature in the layer (°C)
V	=	volume of the layer (m^3)
A	=	bottom sediment area in a layer (m^2).
BRNHK	=	switching constant for ammonium sediment release (mg l^{-1})
DSO	=	dissolved oxygen concentration in the layer (mg l^{-1}).

No value for the sediment ammonium release rate, BRNH, could be found for Roodeplaat Dam Reservoir. According to the literature (EPA 1985) 0.3125 g N m^{-2} d^{-1} could be released from the bottom sediment under anaerobic conditions. For Roodeplaat Dam Reservoir BRNH was set empirically at 0.2 g NH_4-N m^{-2} d^{-1}. Also, no specific value of the Arrhenius temperature coefficient could be found for Roodeplaat Dam, but the best results were obtained with a value of 1.088. Regarding the value of the anaerobic switching constant, BRNHK, in the modified model the user has the option of choosing an appropriate value for BRNHK. For Roodeplaat Dam Reservoir, the value of BRNHK was set empirically at 0.001 mg O_2 l^{-1}.

7.3.6 Ammonium nitrogen released during detrital decay - YNHBOD

During detrital decay intracelluiar nitrogen in the form of ammonia is released into the water (*cf* paragraph 4.4.4.2). As with release of intracellular phosphate (paragraph 7.2.3), in the original MINLAKE model detrital decay is modelled in such a way that there is a constant release of intracellular ammonia. In the modified MINLAKE model, detrital decay, and thus intracellular release, can take place under aerobic conditions only. The original MINLAKE model made provision for intracellular ammonium release by utilizing a coefficient called YNHBOD. This coefficient was retained in the modified model. In the MINLAKE manual the recommended value for YNBOD is 0.05 mg NH_4 mg BOD^{-1}. The value of YNHBOD did not effect the ammonia concentration significantly, and therefore the recommended value of 0.05 mg NH_4 mg BOD^{-1} was retained for Roodeplaat Dam Reservoir.

7.3.7 Final nitrogen simulation results

The changes that had to be made to the original MINLAKE model to enable simulation of ammonia and nitrate concentrations in Roodeplaat Dam are indicated in Table 7.6.

Table 7.6 A comparison of nitrogen processes in the original and modified MINLAKE model.

ORIGINAL MINLAKE MODEL	MODIFIED MINLAKE MODEL
■ Constant, continuous release of ammonia from the bottom sediment	■ Constant release of ammonia from the bottom sediment under anaerobic conditions only
■ Effect of temperature on sediment ammonia release not taken into account	■ Effect of temperature on sediment ammonia release taken into account
■ Constant, continuous release of nitrate from the bottom sediment	■ Constant release of nitrate from the bottom sediment under aerobic conditions only.
■ Effect of temperature on sediment nitrate release not taken into account	■ Effect of temperature on sediment nitrate release taken into account
■ Continuous nitrification Value of Arrhenius temperature coefficient for nitrification hard-wired into the model	■ Nitrification: - Under aerobic conditions only - Inhibited by high ammonia concentration - User can choose value for Arrhenius temperature coefficient
■ No denitrification	■ Denitrification: - Under anaerobic conditions only - Inhibited by high substrate concentration - Effect of temperature is incorporated
■ Constant release of intracellular ammonia	■ Release of intracellular ammonia under aerobic conditions only.

After all the changes, as indicated in Table 7.6, were incorporated into the program, the modified model was run for a period of two years, from October 1980 - October 1982. The values of the kinetic coefficients associated with the simulation of nitrogen in the modified model were as indicated in Table 7.7.

Table 7.7 Kinetic coefficients associated with nitrogen simulation in the modified MINLAKE model, and values used to obtain the final simulation results.*

KINETIC COEFFICIENT	VALUE	UNIT	REFERENCE
XKNNH - nitrification rate	0.02	day^{-1}	calibration
DNK - denitrification rate	0.03	day^{-1}	calibration
XKONH - aerobic switching constant for nitrification	0.3	mg O_2 l^{-1}	NIWR 1985, calibration
KONO - anaerobic switching constant for denitrification	3.0	mg O_2 l^{-1}	NIWR 1985, calibration
QNNH - Arrhenius temperature coefficient for nitrification	1.063		NIWR 1985
QDNK - Arrhenius temperature coefficient for denitrification	1.032		NIWR 1985
XNH - nitrification inhibition constant	1.0	mg NH_4-N l^{-1}	NIWR 1985
EDNK - denitrification inhibition constant	1.5	mg NO_3-N l^{-1}	NIWR 1985
BRNOK - aerobic switching function for sediment nitrate release	1.00	mg O_2 l^{-1}	calibration
BRNHK - anaerobic switching function for sediment ammonia release	0.001	mg O_2 l^{-1}	calibration
BRNO - Sediment nitrate release rate	0.075	g NO_3 m^{-2} d^{-1}	calibration
BRNH - sediment ammonia release rate	0.20	g NH_4 m^{-2} d^{-1}	calibration
QBNO - Arrhenius temperature coefficient for sediment nitrate release	1.088		calibration
QBNH - Arrhenius temperature coefficient for sediment ammonia release	1.088		calibration
YNHBOD - mass ratio of ammonium nitrogen released per dissolved oxygen utilized in detrital decay	0.02	mg NH_4 mg BOD^{-1}	Riley 1988

* Values for nitrogen coefficients associated with algal growth is given in Table 7.10.

Time-series graphs of simulated and observed dissolved ammonia concentrations at a depth of 1 and 16 metres are shown in Fig 7.6, while depth profiles are shown in Fig 7.7. Generally, correspondence between simulated and observed dissolved ammonia concentration is good. Time-series graphs of simulated and observed dissolved nitrate concentrations at a depth of 1 and 16 metres are shown in Fig 7.8. Depth profiles of nitrate concentrations are shown in Fig 7.9. Correspondence between observed and simulated nitrate concentrations is satisfactory.

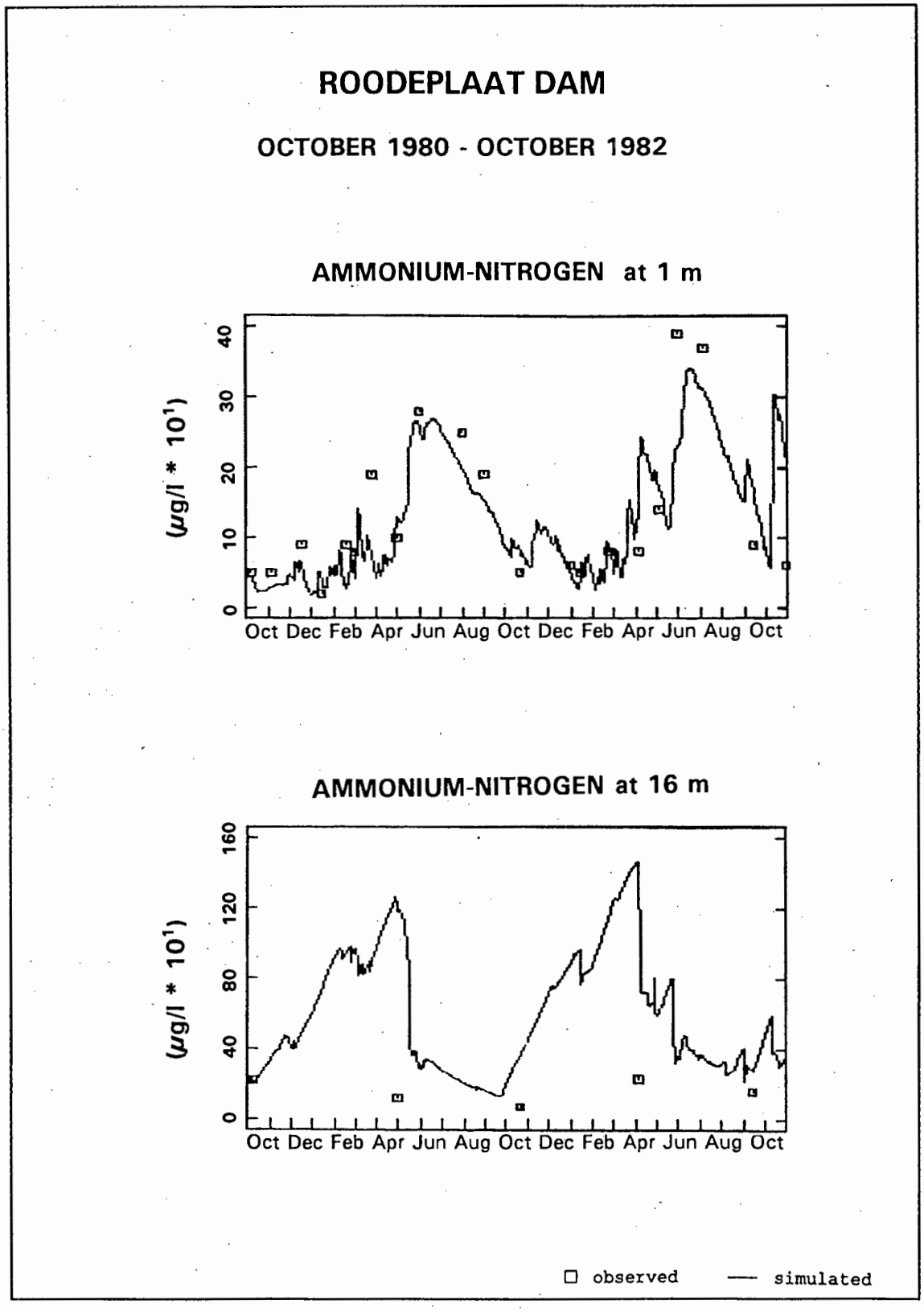

Fig 7.6
Time-series graphs of observed and simulated ammonia concentration at 1 and 16 m depth in Roodeplaat Dam, as obtained with the modified MINLAKE model and optimum values for the calibration coefficients.

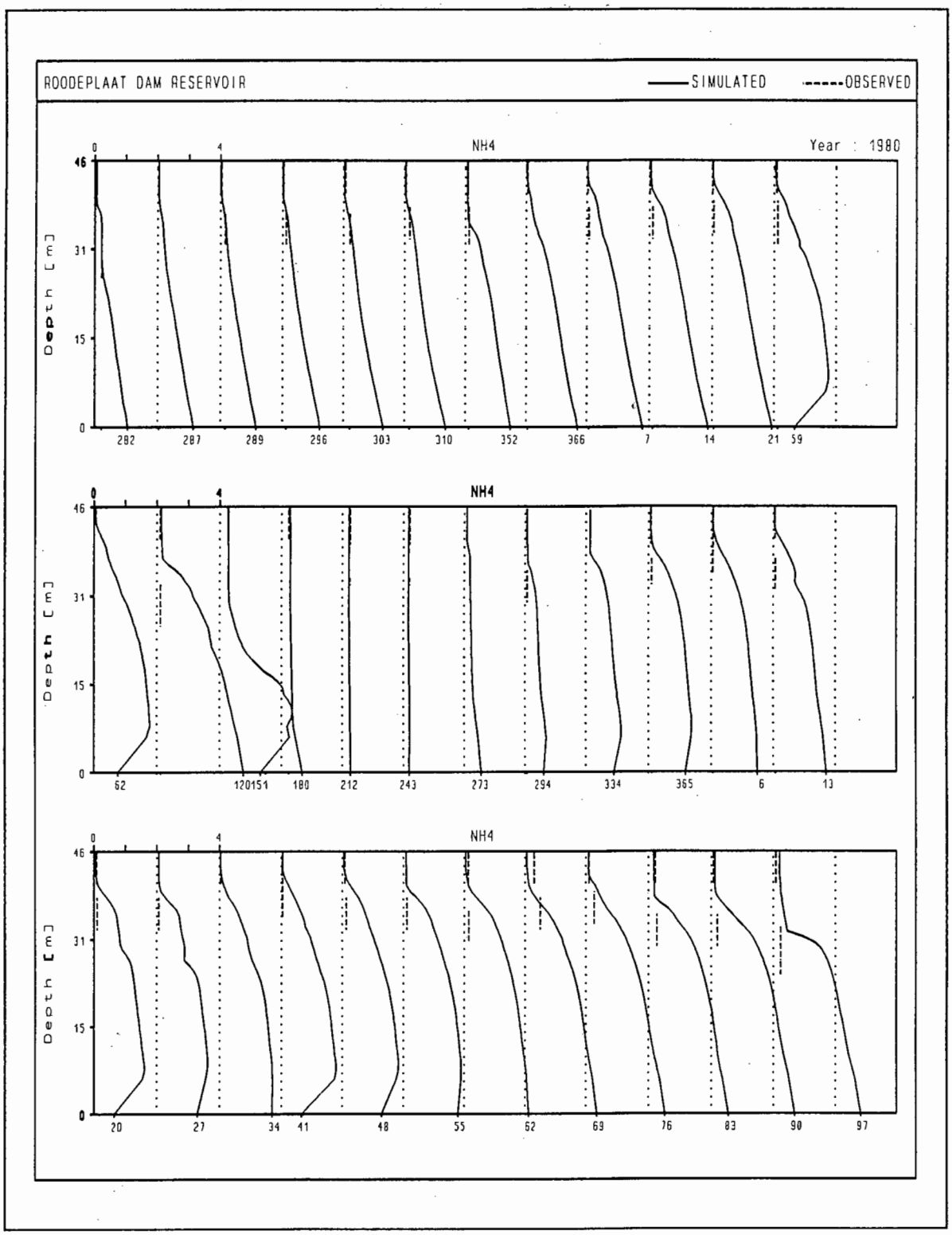

x-axis: Julian day

Ammonia concentration: mg/l

Figure 7.7
Depth profiles of simulated and observed ammonia concentration obtained with the modified MINLAKE model on Roodeplaat Dam for the period October 1980 to October 1982.

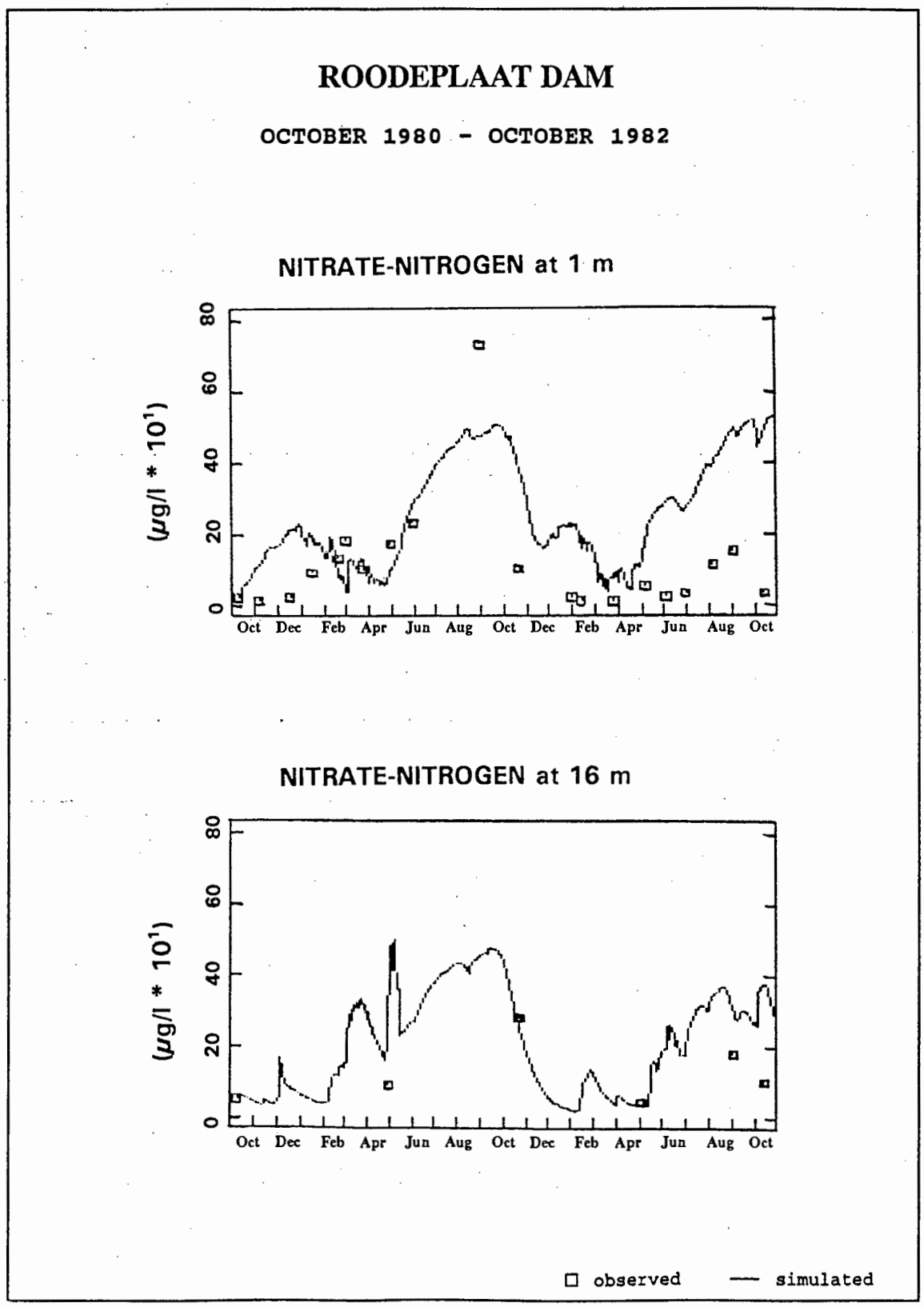

Fig 7.8
Time-series graphs of observed and simulated nitrate concentration in Roodeplaat Dam, as obtained with the modified MINLAKE model and optimum values for the calibration coefficients

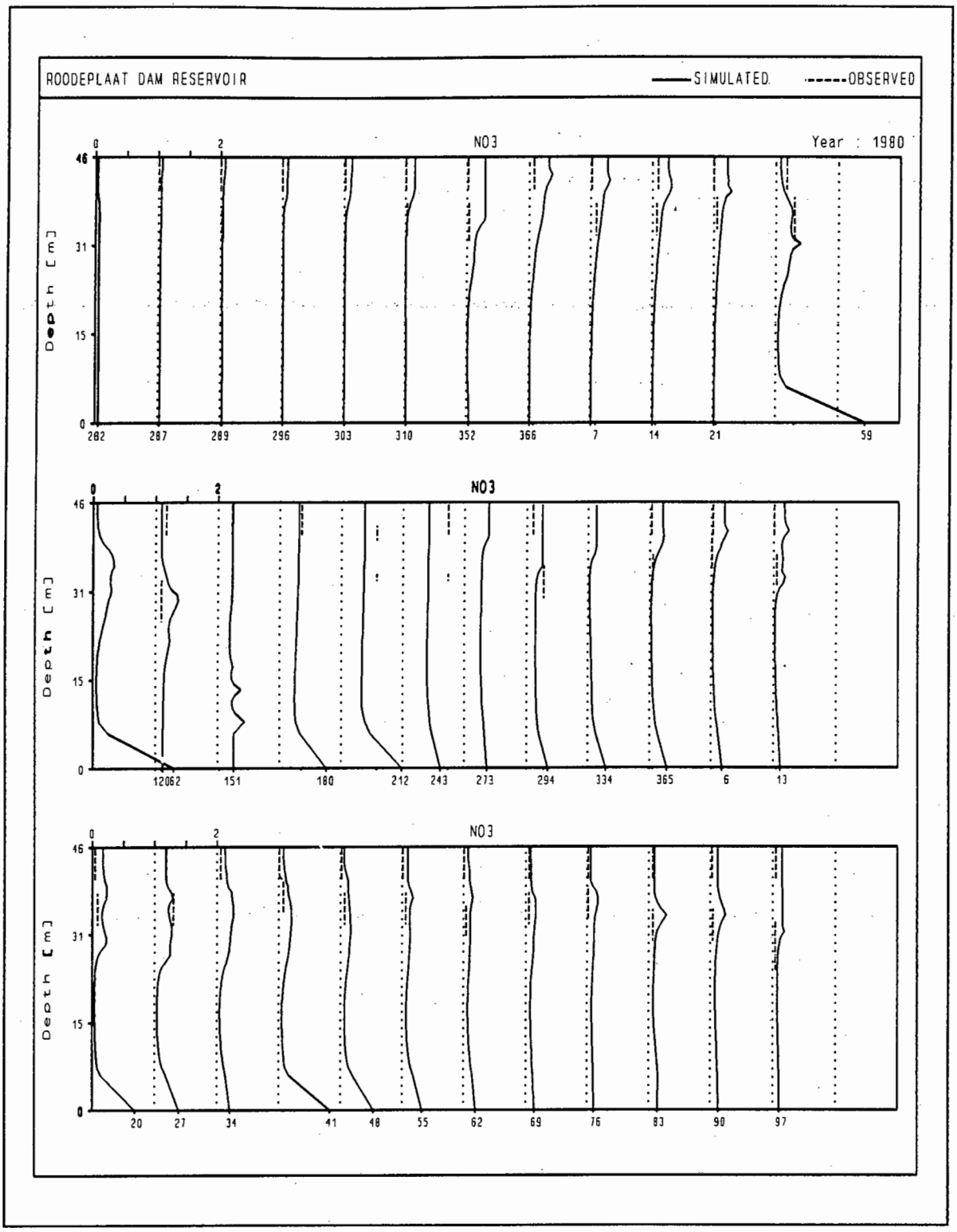

x-axis: Julian day

Nitrate concentration: mg/l

Figure 7.9
Depth profiles of simulated and observed nitrate concentration obtained with the modified MINLAKE model on Roodeplaat Dam for the period October 1980 to October 1982.

7.4 CHLOROPHYLL-a SIMULATION RESULTS

The original MINLAKE model simulates algal growth rate as a change in chlorophyll-a concentration. Provision is made to simulate up to three algal classes. If only one algal class is simulated, algal growth is either light or phosphorus limited. If more than one algal class is simulated, the last algal class is either light or phosphorus limited, while the other class(es) can be either light, phosphorus or nitrogen limited. Thus simulation of nitrogen limited growth is possible only if two or more algal classes are simulated. The user has the option of choosing whether nitrogen limited growth should be simulated or not, i.e. it is possible to simulate two or more algal classes assuming light or phosphorus to be the only limiting factors.

Studies on Roodeplaat Dam indicated a seasonal dominance by different algal groups during the study period (October 1980 to October 1982). Between January and May blue-green algae were dominant, but between September and November green algae were dominant (DWAF-HRI 1984, Pieterse and Röhrbeck 1990). However, the concentration of blue-green algae were much higher than that of green algae (DWAF-HRI 1984), and therefore, as a starting point, only one algal group, the blue-greens, was simulated.

Regarding the growth-limiting nutrient, studies done on Roodeplaat Dam differ as to what nutrient is growth-limiting; according to Steyn and Toerien (1976), during 1972 phosphate was the primary growth limiting nutrient in Roodeplaat Dam, but it was evident that nitrogen would soon become the limiting nutrient because the secondary effluents being discharged into Pienaars River contained more phosphate than nitrogen. According to Toerien *et al* (1975), bio-assay studies done during October 1973 indicated that algal growth in Roodeplaat Dam was nitrogen limited. According to Pieterse and Toerien (1978), phosphate was the growth limiting nutrient during the period January 1976 to December 1977, but a later study by Pieterse and Röhrbeck (1990) indicated that, although phosphate was the limiting nutrient for the period 1976 to 1978, there was evidence that the growth limiting role of inorganic nitrogen was being extended. Therefore, there is no clear evidence as to whether phosphorus or

nitrogen was the growth limiting nutrient during the study period. However, the structure of the model is such that, if only one algal group is simulated, phosphorus is the only growth limiting nutrient that is taken into account, and thus, as a starting point, light and phosphorus were the only growth limiting factors being simulated; nitrogen limitation was not included.

In spite of a fair amount of literature on Roodeplaat Dam Reservoir (Toerien *et al* 1975, Steyn and Toerien 1976, Toerien *et al* 1976, Pieterse and Toerien 1978, Walmsley and Butty 1980a, DWAF-Hri 1984, Pieterse and Röhrbeck 1990), no specific values could be obtained for the kinetic coefficients pertaining to algal growth, therefore values had to be obtained from the literature. Where possible, values for *Microcystis aeruginosa* were used, as it is one of the dominant blue-green algae in Roodeplaat Dam Reservoir (DWAF-HRI 1984). The kinetic coefficients pertaining to algal growth, and the values used as a first approximation, are indicated in Table 7.8.

Table 7.8. List of kinetic coefficients associated with algal growth, as required by the original MINLAKE model.

KINETIC COEFFICIENT	VALUE	UNIT	REFERENCE
Pmin - minimum intracellular ratio of phosphorus to Chla for growth to occur	0.034	mg P mg^{-1} Chla	
Pmax - maximum intracellular ratio of phosphorus to Chla	0.15	mg P mg^{-1} Chla	Orlob 1983
HSCPA - half saturation coefficient for phosphate uptake	0.0025	mg l^{-1}	EPA 1985
Upmax - maximum phosphate uptake rate	2.0	mg P mg^{-1} Chla day^{-1}	
Xnmin - minimum intracellular ratio of nitrogen to Chla for growth to occur	-	mg N mg $Chla^{-1}$	
Xnmax - maximum intracellular ratio of nitrogen to Chla	-	mg N mg $Chla^{-1}$	
UNMAX - maximum nitrogen uptake rate	-	mg N mg $Chla^{-1}$ day^{-1}	
HSCN - half saturation coefficient for nitrogen uptake	-	mg l^{-1}	
HSCNH - half saturation coefficient for the preferential uptake of ammonium over nitrate	-	mg l^{-1}	
Gromax - maximum nutrient saturated growth rate	0.08	day^{-1}	
Tmax - upper temperature where growth is reduced 90%	45	°C	Orlob 1983
Topt - optimal temperature for algal growth	35	°C	Orlob 1983
XKR1 - algal respiration rate	0.08	day^{-1}	Canale 1976
XKM - algal mortality rate	0.07	day^{-1}	EPA 1985
FVCHLA - settling rate of algae	0.002	m day^{-1}	Orlob 1983
HSC1 - half saturation coefficient for light limited algal growth	250	$\mu E\ m^{-2}\ s^{-1}$	Megard 1984
HSC2 - light inhibition coefficient	1900	$\mu E\ m^{-2}\ s^{-1}$	Megard 1984
XK2 - light extinction coefficient for chlorophyll-a	12	m^2 g $Chla^{-1}$	NIWR 1985
XK1 - light extinction coefficient for pure water	0.39	m^{-1}	De Wet 1986

The original MINLAKE model was run with the values for the algae coefficients as indicated in Table 7.9, incorporating the hydrodynamic modifications as indicated in Chapter 6. The simulated algal concentrations obtained with the very first run were contrary to the observed algal concentrations (Fig 7.10) - simulated algal concentrations were high during the winter period (April - September), and low during the summer period (January to April).

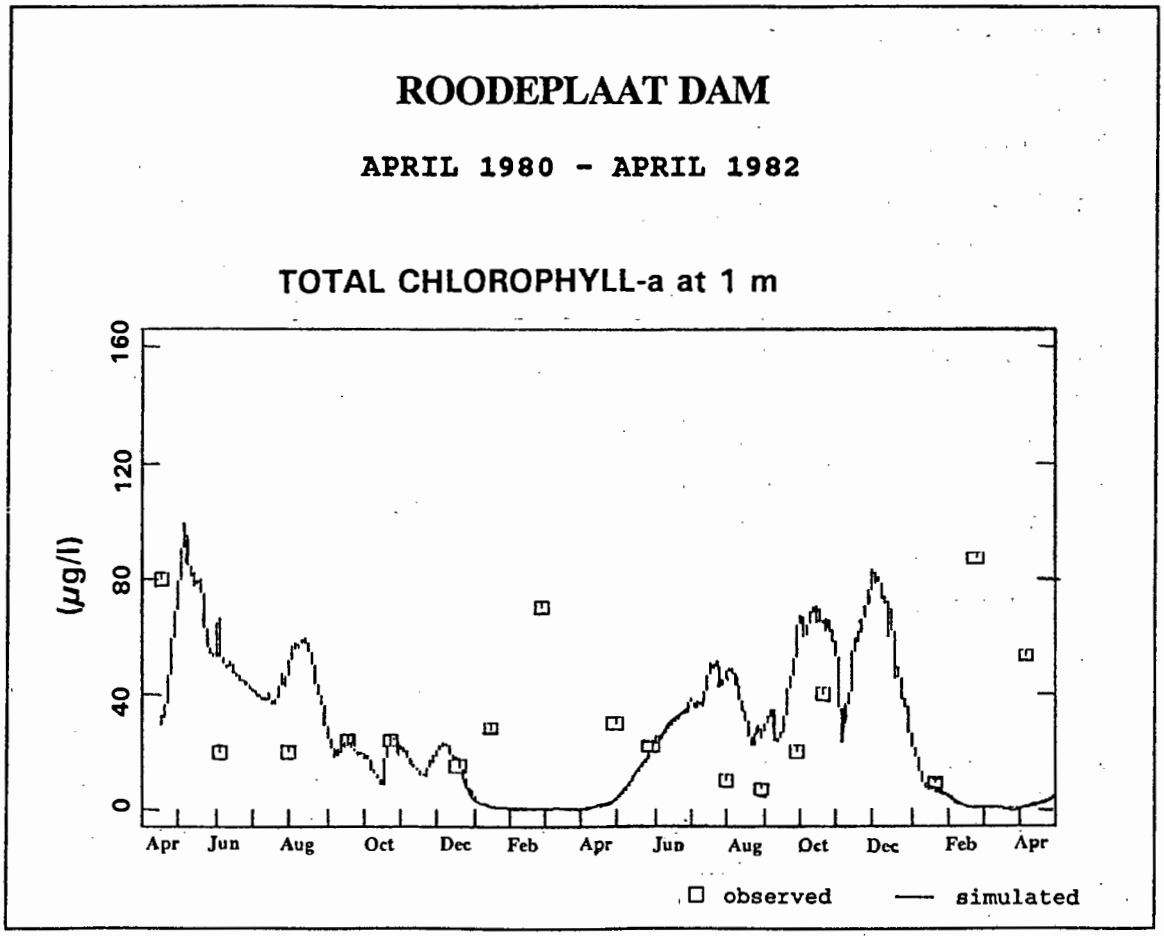

Fig 7.10
Time-series graph of observed vs simulated chlorophyll-a concentration in Roodeplaat Dam, as obtained from the first run with the original MINLAKE model.

Eventually, this anomalous behaviour was traced to a coding error in the program - light intensity is an important factor in algal growth in the program, but calculation of the available light in a layer requires calculation of the daylight period (*cf* Eq 5.55). Daylight period is a function of latitude and hemisphere, but in the original MINLAKE model calculation of the daylight period has been hard-wired to the latitude of the Minnesota Lakes, and to the northern hemisphere. Thus, when the original model was applied to Roodeplaat Dam in the southern hemisphere, the hard-wired expression resulted in the model calculating the maximum daylight period during April to September, which corresponds to the northern hemisphere summer, but to the southern hemisphere winter. Similarly, the model calculated the minimum daylight period during December to April, which corresponds to southern hemisphere summer. This 'miscalculation' of daylight period caused the anomalous simulated algal concentrations seen in Fig 7.10.

The hardwired expression for calculation of daylight period was changed to allow the user to enter the appropriate latitude and hemisphere (see discussion in paragraph 5.3.3.2). Thereafter the model was run again, with the values of the calibration coefficients as indicated in Table 7.9.

The observed chlorophyll-a concentration, and the simulated chlorophyll-a concentration obtained after correction of the daylight period, using the coefficients as indicated in Table 7.9, are shown in Fig 7.11. Correspondence between simulated and observed concentrations during the first summer-period is satisfactory, but during the second summer period the simulated concentration is too low. Also, the simulated concentration does not reflect the increase in observed concentration during the period September - October 1981.

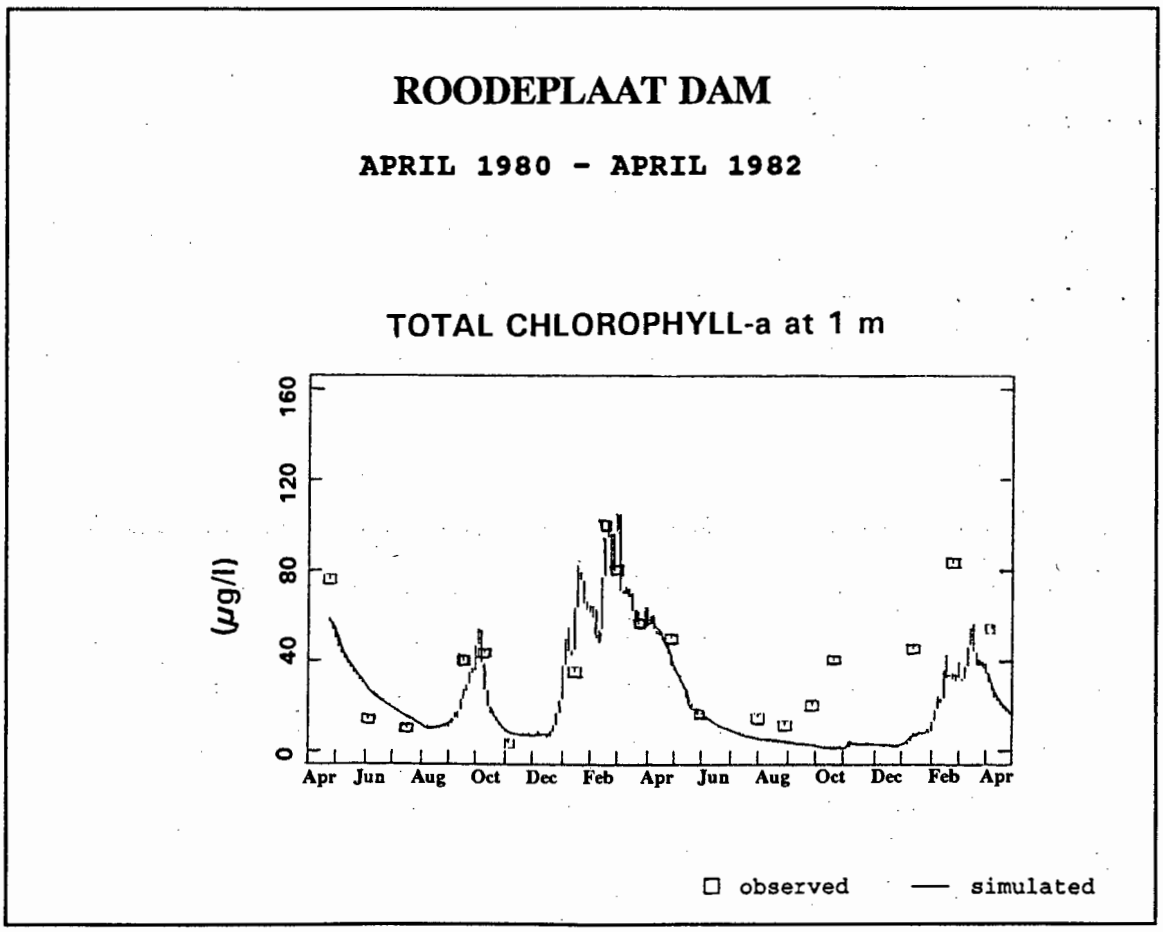

Fig 7.11
Time-series graph of observed vs simulated chlorophyll-a concentration in Roodeplaat Dam as obtained with the original MINLAKE model, after correction of daylight period calculation to Southern hemisphere conditions.

The reason for the difference between simulated and observed behaviour could be attributed to the following:

- Only blue-green algae were simulated
- Nitrogen limited growth was not simulated
- Algal growth processes were inadequately formulated
- The values chosen for the kinetic coefficients are not the optimal values for Roodeplaat Dam Reservoir.

An attempt was made to simulate two algal classes, including the nitrogen option. Blue-green algae were chosen as the first class, because, according to the structure of the model, growth of the first algal class can be either light, phosphorus or nitrogen limited (if the nitrogen option is chosen), while the last class can only be light or phosphorus limited. However, when the model was run with two algal classes, including the nitrogen option for the first class, the program became numerically unstable. Eventually this instability was traced to two coding errors in the ammonium subroutine in the program - see discussion in paragraph 7.3.

Once these technical problems were solved, attention was focused on evaluating the various processes relating to algal growth kinetics, and the kinetic coefficients associated with these processes.

7.4.1 Processes pertaining to algal growth and the associated kinetic coefficients.

In the original MINLAKE model, nutrient uptake and algal growth rate are formulated as a two-step process. Provision is made for light as a growth-limiting factor, and the effect of temperature is taken into account (see discussion in paragraphs 5.3.3.2 to 5.3.3.4). As was discussed in paragraph 4.4.3.2, models that formulate nutrient uptake and algal growth rate as a two-step process (i.e. the Droop concept, see Chapter 3) simulate algal growth more accurately than those formulated according to the Monod concept. It was concluded that algal growth kinetics were adequately formulated in the original MINLAKE model, and that none of the processes relating to algal growth kinetics had to be modified. Attention was therefore focused on obtaining optimum

values for the kinetic coefficients pertaining to the growth of green and blue-green algae, and to nitrogen limited algal growth. Values of the latter differ for green and blue-green algae. Though a range of possible values is indicated in the MINLAKE manual for most of the coefficients, information on values for the nitrogen coefficients is rather vague. A warning is given in the manual that nitrogen coefficients have been less well investigated, and that less information was available in the literature on these coefficients - a statement that proved to be only too true. Furthermore, the values of many of the coefficients related to nutrient uptake and algal growth are temperature sensitive. Most of the values have been determined in studies done in a cold temperate climate in the northern hemisphere, whereas Roodeplaat Dam is situated in a warm temperate/subtropical climate. As a result, often the water temperature in Roodeplaat Dam was outside the temperature range where a coefficient had been determined.

The coefficients associated with algal growth kinetics, and the values finally chosen for Roodeplaat Dam Reservoir, are discussed below. To facilitate the discussion, the formulations pertaining to algal growth kinetics are repeated briefly.

In the original MINLAKE model, phosphate uptake is expressed by (Eq 5.61):

$$U = U_{max} \frac{(Chla)\ (P_{max}) - P_c}{(Chla)\ (P_{max} - P_{min})} \frac{S}{K + S} \qquad (7.9)$$

U	=	specific phosphate uptake rate (mg P mg^{-1} Chla day^{-1})
U_{max}	=	maximum uptake rate (mg P mg^{-1} Chla day^{-1})
P_c	=	internal P concentration (mg l^{-1})
P_{max}	=	capacity of cell to store P (maximum intracellular ratio of phosphate to chlorophyll-a) (mg P mg^{-1} Chla)
P_{min}	=	minimum intracellular ratio of phosphate to chlorophyll-a for growth to occur (mg P mg^{-1} Chla)
Chla	=	chlorophyll-a concentration (mg l^{-1})
S	=	dissolved phosphate concentration in water (mg l^{-1})
K	=	half saturation coefficient for phosphate uptake (mg l^{-1}).

Nitrate and ammonium uptake are modelled in a manner similar to phosphate uptake; provision is made for the preferential uptake of ammonia over nitrate (Eqs 5.79 to 5.81).

Nitrate uptake:

$$U_{NO} = \left[\frac{Chla(N_{max}) - N_c}{Chla(N_{max} - N_{min})}\right]\left[\frac{NH + NO}{HSCN + NH + NO}\right]\left[1 - \frac{NH}{HSCNH + NH}\right] \quad (7.10)$$

Ammonium uptake:

$$U_{NH} = \left[\frac{Chla(N_{max}) - N_c}{Chla(N_{max} - N_{min})}\right]\left[\frac{NH + NO}{HSCN + NH + NO}\right]\left[\frac{NH}{HSCNH + NH}\right] \quad (7.11)$$

U_{NO} = specific nitrate uptake rate (mg NO_3 mg $Chla^{-1}$ day^{-1})

U_{NH} = specific ammonium uptake rate (mg NH_4 mg $Chla^{-1}$ day^{-1})

Chla = chlorophyll-a concentration (mg l^{-1})

N_{max} = capacity of cell to store nitrogen (maximum intracellular ratio of nitrogen to chlorophyll-a) (mg N mg $Chla^{-1}$)

N_{min} = minimum intracellular ratio of nitrogen to chlorophyll-a for growth to occur (mg N mg $Chla^{-1}$)

N_c = internal nitrogen concentration (mg l^{-1})

NH = ammonium concentration in water (mg l^{-1})

NO = nitrate-nitrite concentration in water (mg l^{-1})

HSCN = half saturation coefficient for nitrogen uptake (mg l^{-1})

HSCNH = ammonium preference constant (mg l^{-1}).

Algal growth rate is given by (Eq 5.53):

$$\mu = \mu_{max}[L_P : L_I]_{min}\, f(T) \quad (7.12)$$

μ = specific growth rate (day^{-1})

μ_{max} = nutrient saturated growth rate (day^{-1})

L_P = nutrient limited growth ratio (between 0 and 1)

L_I = light limited growth ratio (between 0 and 1)

f(T) = temperature effect on growth.

Nutrient limited growth ratio (Eq 5.60):

$$L_P = \frac{N_c - Chla(N_{min})}{N_c} \qquad (7.13)$$

L_P = nutrient limited growth ratio (between 0 and 1)
N_c = internal nutrient concentration (mg l^{-1})
Chla = chlorophyll-a concentration (mg l^{-1})
N_{min} = minimum intracellular ratio of nutrient to chlorophyll-a for growth to occur (mg nutrient mg $Chla^{-1}$).

Light limited growth ratio (Eq 5.54):

$$L_I = \frac{I\left(1 + 2\left(\frac{K_1}{K_2}\right)^{0.5}\right)}{I + K_1 + \frac{I^2}{K_2}} \qquad (7.14)$$

L_I = light limited growth ratio (between 0 and 1)
I = photosynthetically active irradiance - PAR ($\mu E\ m^{-2}\ s^{-1}$)
K_1 = half saturation coefficient for light limited growth ($\mu E\ m^{-2}\ s^{-1}$)
K_2 = light inhibition coefficient ($\mu E\ m^{-2}\ s^{-1}$).

Photosynthetically active irradiance is calculated from the incoming solar radiation. The model requires solar radiation to be measured in Langleys (cal cm^{-2} day^{-1}). These energy units need to be converted to quantum units:

$$I_s = \frac{27.25}{TD} RAD \qquad (7.15)$$

I_s = average incident photosynthetically active radiation (PAR) over the daylight period ($\mu E\ m^{-2}\ s^{-1}$)

TD = photo period, also known as astronomical day length or theoretical day length (hr)

RAD = incident solar radiation (cal $cm^{-2}\ day^{-1}$).

In the surface layer I_s is obtained from incoming solar radiation, thereafter PAR is taken to be attenuated in the same way as solar radiation, i.e. it can be described by Beer's Law:

$$I_{ave} = \frac{I_i\ [1 - exp(-kDz_i)]}{kDz} \qquad (7.16)$$

I_{ave} = average PAR in a layer ($\mu E\ m^{-2}\ s^{-1}$)

I_i = PAR reaching the top of the layer ($\mu E\ m^{-2}\ s^{-1}$)

k = light extinction coefficient

DZ_i = thickness of layer i (m)

The temperature effect on algal growth rate is given by (Eqs 5.62 and 5.63):

If $T < T_{opt}$

$$f(T) = \exp\left[-2.3\left[\frac{T - T_{opt}}{T_{opt} - T_{min}}\right]^2\right] \quad (7.17)$$

If $T > T_{opt}$

$$f(T) = \exp\left[-2.3\left[\frac{T - T_{opt}}{T_{max} - T_{opt}}\right]^2\right] \quad (7.18)$$

$f(T)$	=	temperature effect on growth
T	=	water temperature in layer (°C)
T_{opt}	=	optimum temperature for nutrient saturated growth (°C)
T_{min}	=	lower temperature where growth is reduced 90%
T_{max}	=	higher temperature where growth is reduced 90%.

The kinetic coefficients associated with the above formulas, as required by the original MINLAKE model, have been listed in Table 7.9.

The values of the above coefficients differ for green and blue-green algae, except for the light extinction coefficient.

7.4.1.1 Pmin - minimum intracellular ratio of phosphorus to Chla for growth to occur:

A warning is given in the MINLAKE manual that the model is very sensitive to any coefficient that is multiplied by chlorophyll-a concentration, and particularly sensitive to the coefficient Pmin (Eqs.7.9 and 7.13). The manual also states that literature values for Pmin range from 0.06 to 3.3 mg P mg^{-1} Chla, and recommends a value of approximately 1 for Pmin.

The original (and modified) MINLAKE model was indeed found to be extremely sensitive to the value of Pmin. As to the value of Pmin for Roodeplaat Dam Reservoir, no specific value could be found from work that has been done on the reservoir, and an appropriate value had to be established from the literature. Various values for Pmin for nitrogen-fixing and non nitrogen-fixing blue-green algae, as well as for green algae, were found in the literature (Bierman 1977, Canale 1976, Orlob 1983), but Pmin was expressed in moles P $cell^{-1}$, whereas the MINLAKE model requires Pmin to be in mg P mg^{-1} Chla. To convert from moles P $cell^{-1}$ to mg P mg^{-1} Chla, data on the amount of chlorophyll-a per cell for the specific algae are required. These could not be found for any of the algal groups in Roodeplaat Dam Reservoir, and therefore these values of Pmin could not be utilized.

After a further intensive literature search a reference was found where the values of Pmin for some algae/algal classes are given as a percentage of the algal dry weight (Reynolds 1984). To convert these values to mg P mg^{-1} Chla as required by the model, information on the Chla/dry weight ratio is required. For Roodeplaat Dam Reservoir, this ratio could be established from limnological data on the dam for both blue-green and green algae (DWAF (HRI) 1984).

Regarding blue-green algae, because *Microcystis* was the more dominant blue-green algae in Roodeplaat Dam Reservoir during the simulation period (DWAF (HRI) 1984), as a starting point, the Pmin value for *Microcystis* was chosen as the Pmin value for the first algal group being simulated (i.e. the blue-green algae). According to Reynolds (1984) the Pmin value for *Microcystis* is 0.34% of algal dry weight. The Chla/dry weight ratio for *Microcystis* in Roodeplaat Dam was calculated as 0.0065 (calculated from measurements at the dam wall - DWAF (HRI) 1984). A Pmin value of 0.34% of algal dry weight therefore converts to 0.52 mg P mg^{-1} Chla. After repeated runs it was established that the best results are obtained with a Pmin value of 0.49 mg P mg^{-1} Chla for the first algal group (blue-green algae). This value is well within the range of 0.06 - 3.3 mg P mg^{-1} Chla indicated in the MINLAKE manual (MINLAKE 1988), but it does not agree with the statement in the manual that the value of Pmin can usually be assumed to be approximately one.

Regarding green algae, the only Pmin values quoted are for *Scenedesmus* (Reynolds 1984), an algae that appeared only once in Roodeplaat Dam Reservoir during the simulation period (DWAF (HRI) 1984). However, in absence of more reliable data, the values for *Scenedesmus* had to be used. Two values were quoted, 0.10% and 0.59% of algal dry weight. From the limnological data on Roodeplaat Dam Reservoir, the Chla/dry weight ratio for green algae was calculated as 0.0048 (from measurements at the dam wall). A Pmin value of 0.10% of algal dry weight therefore converts to 0.21 mg P mg^{-1} Chla, while a Pmin value of 0.59% of algal dry weight converts to 1.23 mg P mg^{-1} Chla. After repeated runs, taking the effect of Pmin on the other kinetic coefficients into account, a value of 1,23 mg P mg^{-1} Chla was established as the best value of Pmin for the second algal group being simulated, i.e. the green algae. Again this value is well within the range of 0.06 - 3.3 mg P mg^{-1} Chla indicated in the MINLAKE manual (Riley 1988), and it agrees fairly well with the statement in the manual that the value of Pmin can usually be assumed to be approximately one.

7.4.1.2 Pmax - maximum intracellular ratio of phosphorus to Chla:

This coefficient reflects the capacity of certain algae to take up and store nutrients in excess of what is needed for growth - a phenomenon known as luxury uptake of nutrients (*cf* Eq 7.9). According to the MINLAKE manual, little information on values for Pmax is available in the literature (Riley 1988), but a value of ten times Pmin is recommended.

Very little information on the value of Pmax could indeed be obtained from the literature. As a starting point, as recommended by the MINLAKE manual, the value of Pmax was set at ten times the value of Pmin, i.e Pmax was set at 4.9 mg P mg^{-1} Chla for blue-green algae, and at 12.3 mg P mg^{-1} Chla for green algae. After repeated runs these values were found to be the best values for Pmax for Roodeplaat Dam Reservoir.

General remarks on the value of Pmax:

The model is moderately sensitive to the value of Pmax. In both the original and modified MINLAKE models, the value of Pmax affects the intracellular phosphate concentration as calculated by the model - if Pmax is set too high, the capacity of the cell to store phosphate is too high, which means that the calculated intracellular phosphate concentration may be too high. This may lead to the following:

- Because algal growth is modelled as a function of the intracellular phosphate concentration, excessive algal growth may occur if the intracellular phosphate concentration is too high, i.e. simulated algal concentration will be higher than the observed, or simulated algal growth may occur during periods when no observed algal growth occurs.
- The dissolved phosphate concentration in the layers where algal growth, and therefore nutrient uptake, occurs, will be too low - because the capacity of the cell to store phosphate is too high, uptake of dissolved phosphate will also be too high.

If Pmax is set too low, the capacity of the cell to store phosphate is minimized, which means that the intracellular phosphate concentration will be too low. This may lead to the following:

- Simulated algal growth will be inhibited, i.e. simulated algal concentration will be lower than the observed.
- External dissolved phosphate concentration in the layers where algal growth occurs will be too high, because of the diminished capacity of the cell to take up and store dissolved phosphate.

7.4.1.3 HSCPA - half saturation coefficient for dissolved phosphate uptake:

In the original (and modified) MINLAKE model phosphate uptake is expressed by Eq 7.9. The half saturation coefficient for phosphate uptake in Eq 7.9 has to be specified by the user. The MINLAKE manual indicates that values in the range 0.02 to 0.04

mg l^{-1} are commonly used in models (Riley 1988). Literature values varied from 0.0025 to 0.06 mg l^{-1} for blue-green algae (Orlob 1983, EPA 1985) and from 0.0025 to 0.47 for green algae (EPA 1985). From a study that was done on Hartbeespoort Dam Reservoir (Cochrane *et al* 1987), the value of HSCPA for blue-green algae in Roodeplaat Dam Reservoir was set at 0.020 mg l^{-1}. For green algae, after repeated runs the optimum value was established as 0.025 mg l^{-1}. The model was not very sensitive to the value of HSCPA.

7.4.1.4 Upmax - maximum phosphate uptake rate:

No specific value for Upmax could be found for Roodeplaat Dam Reservoir. Although various values for Upmax were found in the literature (Orlob 1983, Canale 1976, Bierman 1977), these values were not in the units required by the model (day^{-1} instead of the required mg P mg^{-1} Chla day^{-1}). The MINLAKE manual indicates that calibrated values for Pmax range from 4 to 10 mg P mg^{-1} Chla day^{-1}, and that the value for blue-green algae should be higher than that of green algae (Riley 1988).

Considerable time was spent on finding the optimum value of Upmax, especially for green algae. After repeated runs, the optimum value for blue-green algae was established as 4.0 mg P mg^{-1} Chla day^{-1} (the lower limit recommended in the MINLAKE manual), and for green algae as 0.52 mg P mg^{-1} Chla day^{-1}. Although the latter value is lower than the recommended range of 4.0 - 10 mg P mg^{-1} Chla day^{-1}, higher values resulted in a sharp peak of excessive simulated growth of green algae during July - August 1981, contrary to the observed. All efforts to minimize this peak by specifying a higher value for Upmax and changing the other coefficients for green algae were unsuccessful. For instance, specifying a value of 4 mg P mg^{-1} Chla day^{-1} for Upmax (the lower end of the range suggested in the MINLAKE manual), and trying a range of values, as well as different combinations of values for each of the other coefficients in Table 7.9, either resulted in no change to the unwanted peak, or else the correctly simulated green algal growth during October 1981 disappeared first before the unwanted peak in July - August 1981 disappeared. The unwanted peak could only be controlled by specifying a low value for Upmax - the peak starts appearing at an Upmax value for green algae of 0.54 mg P mg^{-1} Chla day^{-1}, hence Upmax was set at 0.52 mg P mg^{-1} Chla day^{-1}.

7.4.1.5 XNMIN - minimum intracellular ratio of nitrogen to Chla for growth to occur (Eqs 7.10, 7.11, and 7.13):

No specific value for Xnmin could be found for Roodeplaat Dam Reservoir, therefore the values for both blue-green and green algae had to be established from the literature. According to the MINLAKE manual (Riley 1988), the value of Xnmin should be approximately 1.5 mg N mg $Chla^{-1}$. As a starting point, this value was used for both blue-green and green algae, but the results obtained for blue-green algae with this value were unsatisfactory. A literature study resulted in several values of Xnmin for both green and blue-green algae, (Bierman 1977, Canale 1976, Orlob 1983), but the units were usually in moles $cell^{-1}$ instead of mg N mg $Chla^{-1}$ as required by MINLAKE. The only values that could be utilized were those given by Reynolds (1984); for *Microcystis aeruginosa* the value of XNMIN is indicated as 3.8% of algal dry weight. From limnological data on Roodeplaat Dam Reservoir (DWAF (HRI) 1984) the Chla/dry weight ratio for *Microcystis* was calculated as 0.0065 (from measurements at the dam wall). A Xnmin value of 3.8% of algal dry weight therefore converts to 5.85 mg N mg $Chla^{-1}$. After repeated runs it was established that, for blue-green algae, the best results are obtained with a Xnmin value of 5.5 mg N mg $Chla^{-1}$. This value is significantly different from the value recommended by the MINLAKE manual (1.5 mg N mg $Chla^{-1}$).

No value for Xnmin for green algae is given in Reynolds (1984), therefore the value of 1.5 mg N mg $Chla^{-1}$ as recommended in the MINLAKE manual was used for green algae. Good results were obtained with this value for green algae and therefore all simulations was done with a XNMIN value of 1.5 mg N mg $Chla^{-1}$ for green algae.

General remarks on the value of Xnmin:

The model is rather sensitive to the value of Xnmin for blue-green algae; simultaneous successful simulation of algal growth, dissolved phosphate concentration and ammonia/nitrate concentration was possible only once Xnmin for blue-green algae was specified correctly.

7.4.1.6 XNMAX - maximum intracellular ratio of nitrogen to chlorophyll-a (Eqs 7.10 and 7.11):

As with PMAX, the coefficient XNMAX reflects the capacity of certain algae to take up and store nutrients in excess of what is needed for immediate growth, i.e. luxury uptake. No specific values for XNMAX could be found for Roodeplaat Dam Reservoir. The MINLAKE manual (Riley 1988) recommends a value of approximately five times Xnmin, therefore as a starting point, a XNMAX value of 22.5 mg N mg $Chla^{-1}$ was specified for blue-green algae, and 7.5 mg N mg $Chla^{-1}$ for green algae. Good results were obtained with these values, and thus these values were retained for all subsequent simulations. The model is not very sensitive to the value of XNMAX.

7.4.1.7 UNMAX - maximum nitrogen uptake rate:

The maximum nitrogen uptake rate must be specified in units of mg N mg $Chla^{-1}$ day^{-1} for each algal group. The MINLAKE manual quite rightly states that most literature values of UNMAX are given either in terms of moles per cell, or independent of nitrogen mass or chlorophyll-a, and thus cannot be used in the MINLAKE model. It is suggested that trial values similar to the maximum phosphate uptake rate should be used. After repeated runs, taking into account the interaction between UNMAX and other coefficients, and the effect of various values of UNMAX on simulated concentration of chlorophyll-a, ammonia and nitrate, it was found that a value of 0.65 mg N mg $Chla^{-1}$ day^{-1} gave the best result for blue-green algae. A value of 0.55 mg N mg $Chla^{-1}$ day^{-1} gave the best results for green algae.

7.4.1.8 HSCN - half saturation coefficient for nitrogen uptake (Eq 7.10 and 7.11):

No specific value for Roodeplaat Dam Reservoir has been determined. According to the MINLAKE manual values for HSCN may vary widely in the literature from approximately 0.014 to 0.073 mg l^{-1}. In fact, values in the literature (EPA 1985, Orlob 1983, Reynolds 1984) ranged from 0.001 - 4.34 for blue-green algae, and from 0.001 - 1.236 for green algae. No specific value could be found for *Microcystis aeruginosa*, the dominant blue-green algae in Roodeplaat Dam Reservoir, but Reynolds (1984) indicated that the HSCN value for blue-green algae is higher than that of green algae. After repeated runs, taking into account the interaction between HSCN and the other

coefficients, the optimum HSCN value for blue-green algae was established as 0.06 mg l^{-1}, and for green algae as 0.034 mg l^{-1}. The model is moderately sensitive to the value of HSCN.

7.4.1.9 HSCNH - half saturation coefficient for the preferential uptake of ammonia over nitrate (Eqs 7.10 and 7.11):

Nitrate and nitrite have to be reduced to ammonium prior to assimilation by algae (Reynolds 1984, see also discussion in Chapter 3), therefore algae will show a preference for ammonium uptake to nitrate/nitrite uptake. The degree of preference varies with algal class, for instance, blue-green algae take up ammonium almost exclusively, i.e. nitrate uptake during blue-green algal growth is very low, while green algae take up approximately equal amounts of ammonium and nitrate (Ashton 1992). The original (and modified) MINLAKE model makes provision for the preferential uptake of ammonia via the coefficient HSCNH. No specific value could be found for Roodeplaat Dam Reservoir, but the MINLAKE manual (Riley 1988) indicates a value of 0.025 mg l^{-1} as an average value. According to Reynolds (1984) preferential uptake of ammonia will occur provided the ammonia concentration in the surrounding water exceeds 7 - 14 μg l^{-1}. This implies that the value of HSCNH should not be lower than 7 - 14 μg l^{-1}. After repeated runs, the optimum value of HSCNH for blue-green algae in Roodeplaat Dam Reservoir was determined as 0.025 mg l^{-1}, and for green algae as 0.015 mg l^{-1}.

General remarks on the value of HSCNH:

The model is quite sensitive to the value of HSCNH - though the value of HSCNH did not have a very significant effect on the simulated concentration of blue-green algae, it did have a marked effect on simulated ammonium and nitrate concentrations in the epilimnion. The observed ammonium concentration in the epilimnion increases sharply with overturn, followed by a sharp decrease due to nitrification (Fig 7.6). During this period (April to October), the simulated ammonia concentration is very sensitive to the value of HSCNH for blue-green algae. Regarding the observed epilimnetic nitrate concentration: nitrification leads to an increase in nitrate concentration from the end of April onwards, the observed nitrate concentration reaches a peak in late

August/early September, whereafter it decreases due to the occurrence of denitrification with the onset of stratification. The simulated nitrate concentration during the period May to October was very sensitive to the value of HSCNH for green algae.

7.4.1.10 Gromax - maximum specific nutrient saturated growth rate (Eq 7.12):
The MINLAKE manual indicates that the value of GROMAX, along with the value of UPMAX, will primarily dictate the rate of increase in chlorophyll-a concentration, and that the value of GROMAX will be affected by the value of PMIN.

In a laboratory study that has been done on a fresh sample of *Microcystis aeruginosa* from Hartebeespoort Dam Reservoir, the maximum specific nutrient saturated growth rate was determined as 0.30 day^{-1} (Kruger and Eloff 1978). *Microcystis aeruginosa* is the dominant blue-green algae in Roodeplaat Dam Reservoir and, after repeated runs it was established that a value of 0.25 day^{-1} gave the best results for Roodeplaat Dam also.

Regarding the specific growth rate of green algae, in a study conducted on the Vaal River (Cloot *et al* 1992), the maximum specific nutrient saturated growth rate for green algae was indicated as 1.45 day^{-1}. After repeated runs this value was found to apply to Roodeplaat Dam Reservoir as well.

NB: Though the model is moderately sensitive to the value of GROMAX for both blue-green and green algae, the user should always be aware of the interdependence of the coefficients GROMAX, UPMAX, PMIN, UNMAX and XNMIN. A change in any one of these coefficients may necessitate a change in one of the other coefficients, which may lead to, for instance, a change in the simulated concentration of both chlorophyll-a and dissolved phosphate. It is therefore essential that simulated concentrations of dissolved phosphate, ammonia, and nitrate, be checked regularly during calibration of chlorophyll-a concentrations and *vice versa*.

7.4.1.11 TMAX - upper temperature where growth is reduced 90% (Eqs 7.17 and 7.18):

According to the MINLAKE manual, values for TMAX are typically in the range 32 - 42°C, with the value for blue-green algae higher than that for green algae.

No specific TMAX-value for blue-green algae could be found for Roodeplaat Dam Reservoir, but in a laboratory study that has been done on a fresh sample of *Microcystis aeruginosa* from Hartbeespoort Dam Reservoir (Kruger *et al* 1978), it has been observed that no growth occurs above 40°C. After a few runs, the value of TMAX for Roodeplaat Dam Reservoir was set at 40°C. Changing the value of TMAX to, for instance, 45°C, did not have a significant effect on the simulated concentration of blue-green algae.

Regarding green algae, no specific TMAX-value could be found for Roodeplaat Dam Reservoir, nor for any other water body in the same climatic region in South Africa. After repeated runs the optimum value of TMAX for green algae for Roodeplaat Dam Reservoir was set at 20°C.

7.4.1.12 TOPT - optimum temperature for algal growth (Eqs 7.17 and 7.18):

According to the MINLAKE manual, TOPT is typically in the range 20 - 30°C. As with TMAX, no specific value of TOPT could be found for Roodeplaat Dam Reservoir for either blue-green or green algae. Regarding blue-green algae, in the laboratory study that has been done on *Microcystis aeruginosa* from Hartbeespoort Dam Reservoir (Kruger and Eloff 1978), the optimum temperature was established as ranging from 24 - 35°C. After repeated runs, the value of TOPT for blue-green algae in Roodeplaat Dam Reservoir was set at 35°C. The model was moderately sensitive to the value of TOPT for blue-green algae in simulating blue-green algal concentration, and not sensitive at all to this value in simulating algal succession.

Regarding green algae, in a study that conducted on the Vaal River (Cloot *et al* 1992), TOPT for green algae is indicated as 13°C. After repeated runs TOPT for green algae in Roodeplaat Dam Reservoir was set at 14°C. The model is quite sensitive to the

value of Topt for green algae. If TOPT is set incorrectly, unwanted simulated green algal growth will occur during months when no observed green algal growth occurs. As with the value of TMAX for green algae, specifying the value of TOPT correctly did not have a significant effect on simulated green algal concentration, but it did have a significant effect on simulation of algal succession. Once again this is in accordance with the statement by Reynolds (1984) that, in the presence of high nutrient concentrations, temperature is one of the principal factors determining algal succession.

7.4.1.13 TMIN - minimum temperature at which growth is reduced 90% (Eq 7.17 and 7.18):

In the original MINLAKE model TMIN was hardwired to a constant value of 0°C. To ensure greater flexibility, the model was modified such that the user has the option of choosing an appropriate value of TMIN.

Regarding the value of TMIN for blue-green algae in Roodeplaat Dam Reservoir, it has been observed that, in Hartbeespoort Dam Reservoir, natural blooms of *Microcystis aeruginosa* only start to form once the water temperature is above 17-18°C, below this there is a drastic decrease in the growth rate of *Microcystis* (Kruger and Eloff 1978). After repeated runs a value of 18.5°C was found to be the optimum value of TMIN for blue-green algae in Roodeplaat Dam Reservoir.

The MINLAKE model is moderately sensitive to the value of TMIN for blue-green algae in simulating the concentration of blue-green algae. However, the value of TMIN for blue-green algae is extremely important in simulation of algal succession. Simulation of algal succession was possible only once the TMIN-value for blue-green algae was set correctly. If TMIN for blue-green algae is set too low (as was the case when TMIN was hard-wired into the original MINLAKE program to a value of 0°C), simulated algal growth occurs during the winter months, contrary to the observed.

Regarding the value of TMIN for green algae; in a study conducted on the Vaal River the value of TMIN for green algae is indicated as 5°C (Cloot *et al* 1992). After repeated

runs the optimum value of TMIN for green algae in Roodeplaat Dam Reservoir was found to be 8°C. The model was not very sensitive to the TMIN-value for green algae - there was a marginal difference between results obtained with a TMIN value of 8°C, and 5°C.

7.4.1.14 XKR1 - algal respiration rate:

Algal respiration rate affects simulated algal concentration, as well as simulated dissolved oxygen concentration. The MINLAKE manual indicates that values for XKR1 vary from 0.05 to 0.15 day^{-1}. According to the literature (Reynolds 1984, Henderson-Sellers 1984, Jørgensen 1980), generally, algal respiration rate is 5-20% of the rate of photosynthesis.

No algal respiration rates have been reported for Roodeplaat Dam Reservoir, therefore, after repeated runs, the optimum value of XKR1 for blue-green algae in Roodeplaat Dam Reservoir was established as 0.028 day^{-1} (11% of the photosynthesis rate of blue-green algae), and for green algae as 0.14 day^{-1} (10% of the photosynthesis rate of green algae).

7.4.1.15 XKM - algal mortality rate:

According to the MINLAKE manual, the rate of decline in algal populations will be affected strongly by XKM, the algal mortality rate, which typically ranges between 0.05 to 0.1 day^{-1} (Riley 1988). Literature values varied from 0.001 - 0.17 day^{-1} (EPA 1985, Orlob 1983, Reynolds 1984), as well as a value of 10% of the algal photosynthesis rate (Cole 1991).

No specific data on algal mortality rate for the algae in Roodeplaat Dam Reservoir could be obtained. After repeated runs, the optimum value of XKM for blue-green algae in Roodeplaat Dam Reservoir was accepted as 0.025 day^{-1} (10% of blue-green algal photosynthesis rate), and for green algae as 0.14 day^{-1} (10% of green algal photosynthesis rate).

7.4.1.16 FVCHLA - settling rate of algae:

The MINLAKE manual indicates that the settling rate varies widely with algal species, typically the settling rate for blue-green algae is less than 0.1 m day^{-1}, while the settling rate for green algae varies between 0.1 and 0.5 m day^{-1} (Riley 1988). The MINLAKE manual states further that the model is quite sensitive to the value of FVCHLA.

Again no data on algal settling rates were available for Roodeplaat Dam Reservoir. Regarding blue-green algae, because of the positive buoyancy of these algae, their settling rate generally may even be negative, or at best, very low (Reynolds 1984). After repeated runs the optimum value of FVCHLA for blue-green algae in Roodeplaat Dam Reservoir was established as 0.002 m day^{-1}. Regarding green algae, no specific value for the settling rate of green algae could be obtained from the literature, therefore, after repeated runs the optimum value of FVCHLA for green algae in Roodeplaat Dam Reservoir was established as 0.050 m day^{-1}.

7.4.1.17 XK1 and XK2 - light extinction coefficients:

The values that were chosen for XK1 (extinction coefficient for pure water) and XK2 (extinction coefficient due to chlorophyll-a) were discussed in paragraphs 6.3.1.1 and 6.3.1.2 with the hydrodynamic simulation results.

7.4.1.18 HSC1 - half saturation coefficient for light limited growth, and HSC2 - light inhibition coefficient:

In both the original and modified MINLAKE models, light limited algal growth rate is formulated according to the formulation by Megard *et al* (1984). This formulation requires specification of HSC1 and HSC2 for each algal species. A range of values is suggested in the publication by Megard *et al* (1984), but a warning is given that these are at best crude estimates of the values, as they are affected by temperature and irradiance. This is supported by Davison (1991) who states that the response of photosynthesis to temperature at subsaturating light levels is very different from that at saturating light levels. The range of values given by Megard has been determined in a temperate climate (Minnesota, USA), where irradiance at maximum full sunlight is approximately 1944 $\mu E\ m^{-2}\ s^{-1}$. The highest temperature quoted in the study is 22°C.

In contrast, at Hartbeespoort Dam, situated in the same climatic region as Roodeplaat Dam, irradiance at full sunlight during summer is > 2000 $\mu E\ m^{-2}\ s^{-1}$ (Zohary and Breen 1989). Regarding temperature, during the study period the surface water temperature in Roodeplaat Dam sometimes was as high as 26°C. As a result, the values given by Megard *et al* (1984) could not be used for Roodeplaat Dam. Based on work done by Zohary and co-workers on *Microcystis Aeruginosa* in Hartbeespoort Dam (Robarts and Zohary 1984, Zohary and Breen 1989, Zohary and Madeira 1990) as well as Robarts (1984) and Cloot *et al* (1993), HSC1 values of 1200 $\mu E\ m^{-2}\ s^{-1}$ for blue-green algae, and 140 $\mu E\ m^{-2}\ s^{-1}$ for green algae were found to give the best results for Roodeplaat Dam. Similarly, the value of HSC2 for blue-green algae was established as 2000 $\mu E\ m^{-2}\ s^{-1}$, and for green algae as 900 $\mu E\ m^{-2}\ s^{-1}$.

It must be stressed that, in view of the later finding that algal growth in Roodeplaat Dam is light limited for part of the year, much time was spent in determining optimum values for HSC1 and HSC2 for Roodeplaat Dam. The values as quoted above were accepted as the optimum only after intensive study of the references quoted above, and testing the interactive effect of different values of HSC1 and HSC2 on values of the other coefficients relating to algal growth and nutrient concentration.

7.4.1.19 Qchla - Arrhenius temperature coefficient for processes related to simulation of algal concentration:

The rates of many processes related to simulation of algal concentration are affected by temperature, eg the rates of algal respiration and mortality. Usually the effect of temperature is formulated according to Eq 4.94, requiring specification of an Arrhenius temperature coefficient. This coefficient is algal species dependent, but in the original MINLAKE model it was hard-wired to a single value of 1.055. The model was changed to allow the user to choose a value for each algal species being simulated. No specific values have been determined for the algal species in Roodeplaat Dam, but according to the literature (Orlob 1983, Reynolds 1984) a value of 1.088 can be taken as representative for blue-green algae, and 1.055 for green algae.

7.4.2 Final chlorophyll-a simulation results

No changes had to be made to the processes relating to nutrient uptake and algal growth rate in the original MINLAKE model, however, two hard-wired values (for daylight period and minimum temperature for algal growth) were changed to allow the user to enter appropriate values. After these hard-wired values were changed, the model was run for a period of two years, from October 1980 to October 1982, using values for the kinetic coefficients as indicated in Table 7.9.

Time-series graphs of simulated and observed chlorophyll-a concentration at 1 and 16 metres are shown in Figure 7.12 and Fig 7.13. Depth profiles of chlorophyll-a concentrations are shown in Fig 7.14. Correspondence between simulated and observed algal concentration is good, and the simulation indicates the observed seasonal succession from blue-green to green to blue-green algae clearly.

Table 7.9 Kinetic coefficients associated with simulation of chlorophyll-a concentration in the modified MINLAKE model, and values used to obtain the final simulation results.

KINETIC COEFFICIENT	VALUE	UNIT	REFERENCE
Pmin - minimum intracellular ratio of phosphorus to Chla for growth to occur	0.49 (blue-greens) 1.23 (greens)	mg P mg^{-1} Chla	Reynolds 1984
Pmax - maximum intracellular ratio of phosphorus to Chla	4.90 (blue-greens) 11.0 (greens)	mg P mg^{-1} Chla	MINLAKE manual
HSCPA - half saturation coefficient for phosphate uptake	0.020 (blue-greens) 0.025 (greens)	mg l^{-1}	NIWR 1985 EPA 1985
Upmax - maximum phosphate uptake rate	4.0 (blue-greens) 0.52 (greens)	mg P mg^{-1} Chla day^{-1}	MINLAKE manual, calibration
Xnmin - minimum intracellular ratio of nitrogen to Chla for growth to occur	5.5 (blue-greens) 1.5 (greens)	mg N mg $Chla^{-1}$	Reynolds 1984 MINLAKE manual
Xnmax - maximum intracellular ratio of nitrogen to Chla	22.25 (blue-greens) 7.5 (greens)	mg N mg $Chla^{-1}$	MINLAKE manual
UNMAX - maximum nitrogen uptake rate	0.65 (blue-greens) 0.55 (greens)	mg N mg $Chla^{-1}$ day^{-1}	MINLAKE manual
HSCN - half saturation coefficient for nitrogen uptake	0.06 (blue-greens) 0.034 (greens)	mg l^{-1}	Calibration
HSCNH - half saturation coefficient for the preferential uptake of ammonium over nitrate	0.025 (blue-greens) 0.015 (greens)	mg l^{-1}	MINLAKE manual, Reynolds 1984

(Continued....)

KINETIC COEFFICIENT	VALUE	UNIT	REFERENCE
Gromax - maximum nutrient saturated growth rate	0.25 (blue-greens) 1.45 (greens)	day^{-1}	Kruger and Eloff 1978 Cloot *et al* 1992
Tmax - upper temperature where growth is reduced 90%	40 (blue-greens) 20 (greens)	°C	Kruger *et al* 1978, calibration
Topt - optimal temperature for algal growth	35 (blue-greens 14 (greens)	°C	Kruger *et al* 1978, Cloot *et al* 1992
Tmin - lower temperature where algal growth is reduced 90%	18.5 (blue-greens) 8.0 (greens)	°C	Kruger *et al* 1978, calibration
Qchla - Arrhenius temperature coefficient for processes relating to algal concentration, eg respiration	1.088 (blue-greens) 1.055 (greens)		
XKR1 - algal respiration rate	0.028 (blue-greens) 0.14 (greens)	day^{-1}	Reynolds 1984
XKM - algal mortality rate	0.025 (blue-greens) 0.14 (greens)	day^{-1}	Cole 1991
FVCHLA - settling rate of algae	0.002 (blue-greens) 0.05 (greens)	m day^{-1}	Calibration
HSC1 - half saturation coefficient for light limited algal growth	1200 (blue-greens) 140 (greens)	$\mu E\ m^{-2}\ s^{-1}$	Megard 1984, calibration
HSC2 - light inhibition coefficient	2000 (blue-greens) 900 (greens)	$\mu E\ m^{-2}\ s^{-1}$	Megard 1984, calibration
XK2 - light extinction coefficient for chlorophyll-a	16	m^2 g $Chla^{-1}$	NIWR 1985
XK1 - light extinction coefficient for pure water	0.39	m^{-1}	De Wet 1986

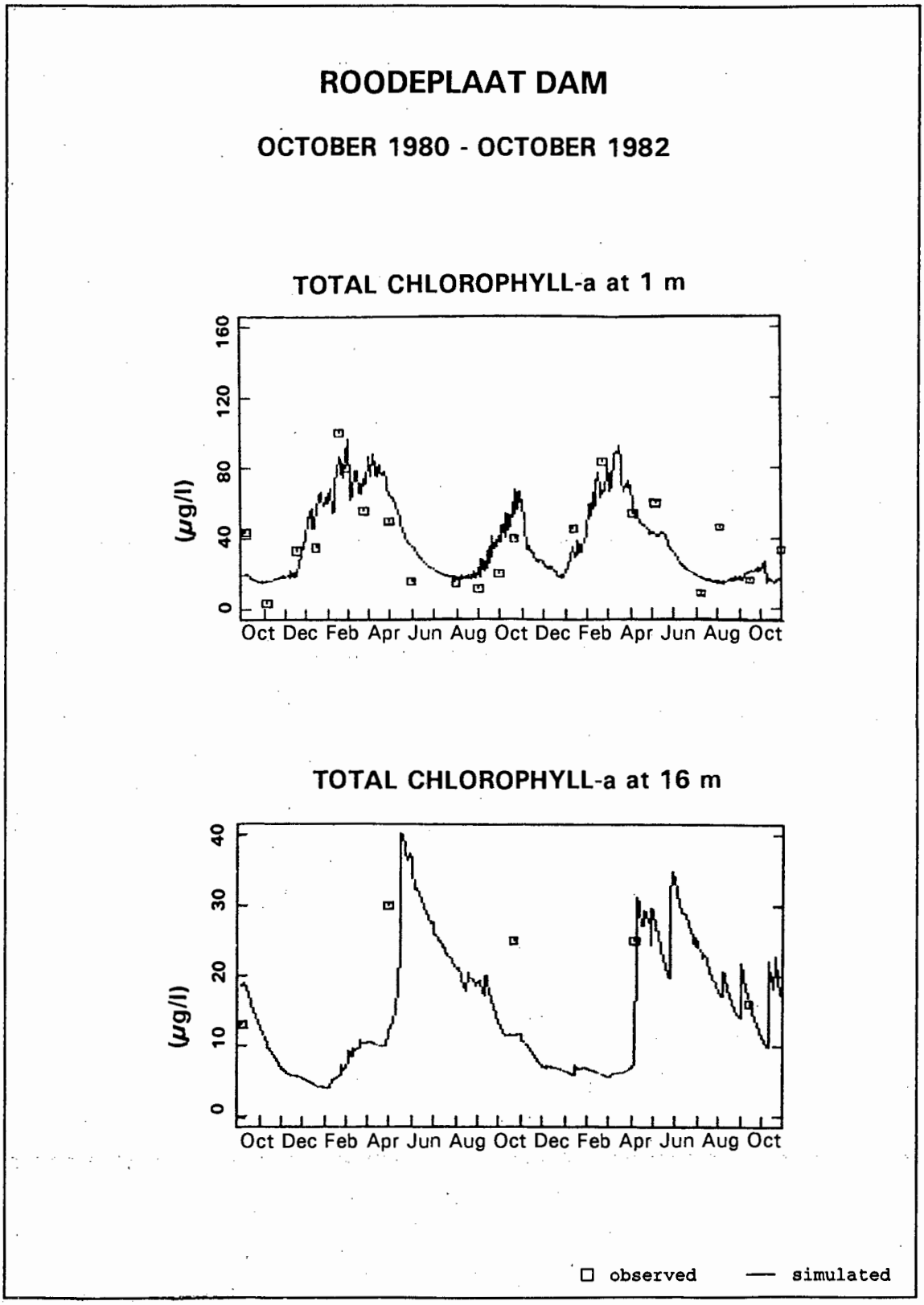

Fig 7.12
Time-series graphs of observed vs simulated chlorophyll-a concentration in Roodeplaat Dam obtained with the modified MINLAKE model and optimum values for the calibration coefficients

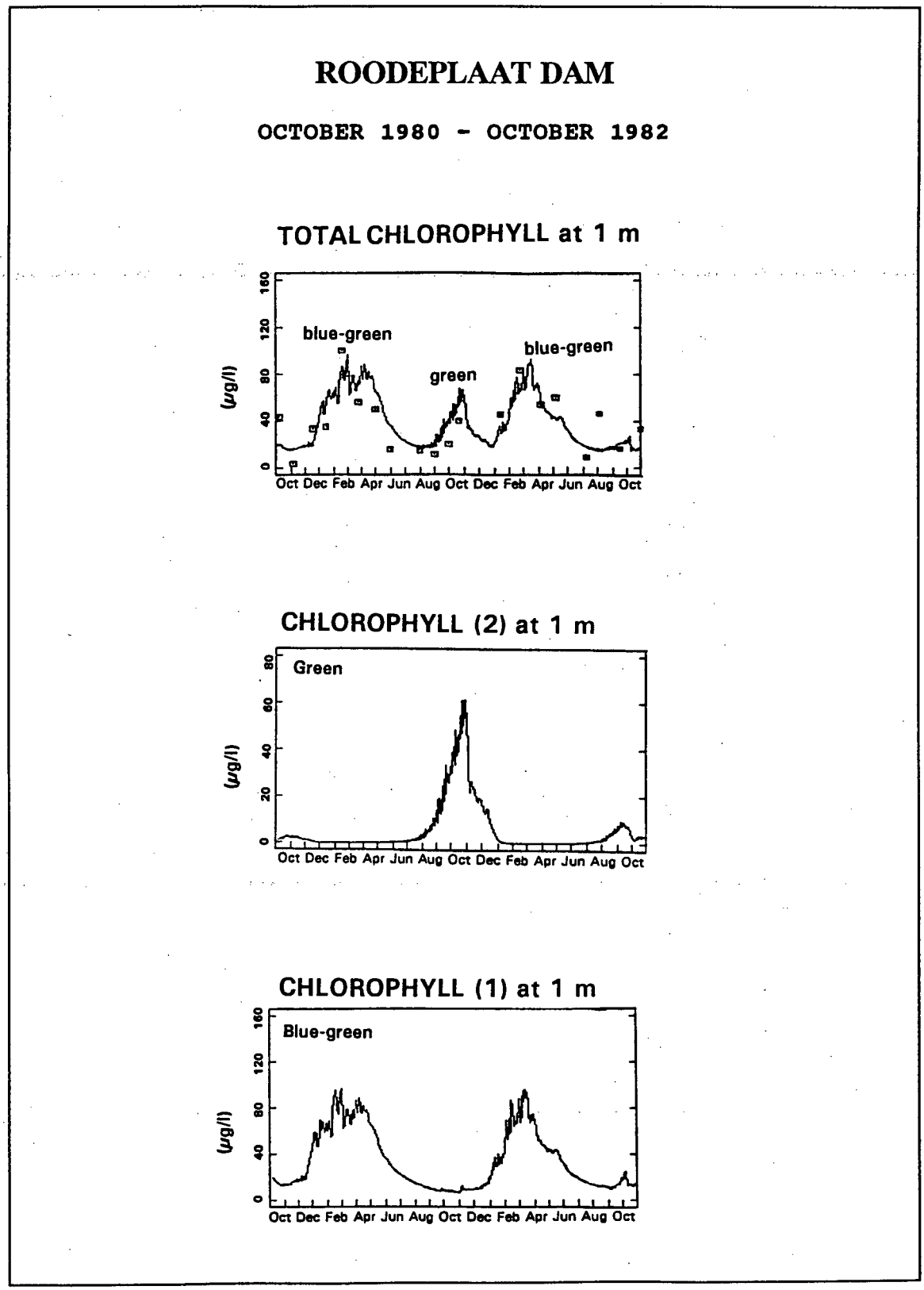

Fig 7.13
Time-series graph of observed vs simulated chlorophyll-a concentration in Roodeplaat Dam, as obtained with the modified MINLAKE model and indicating algal succession.

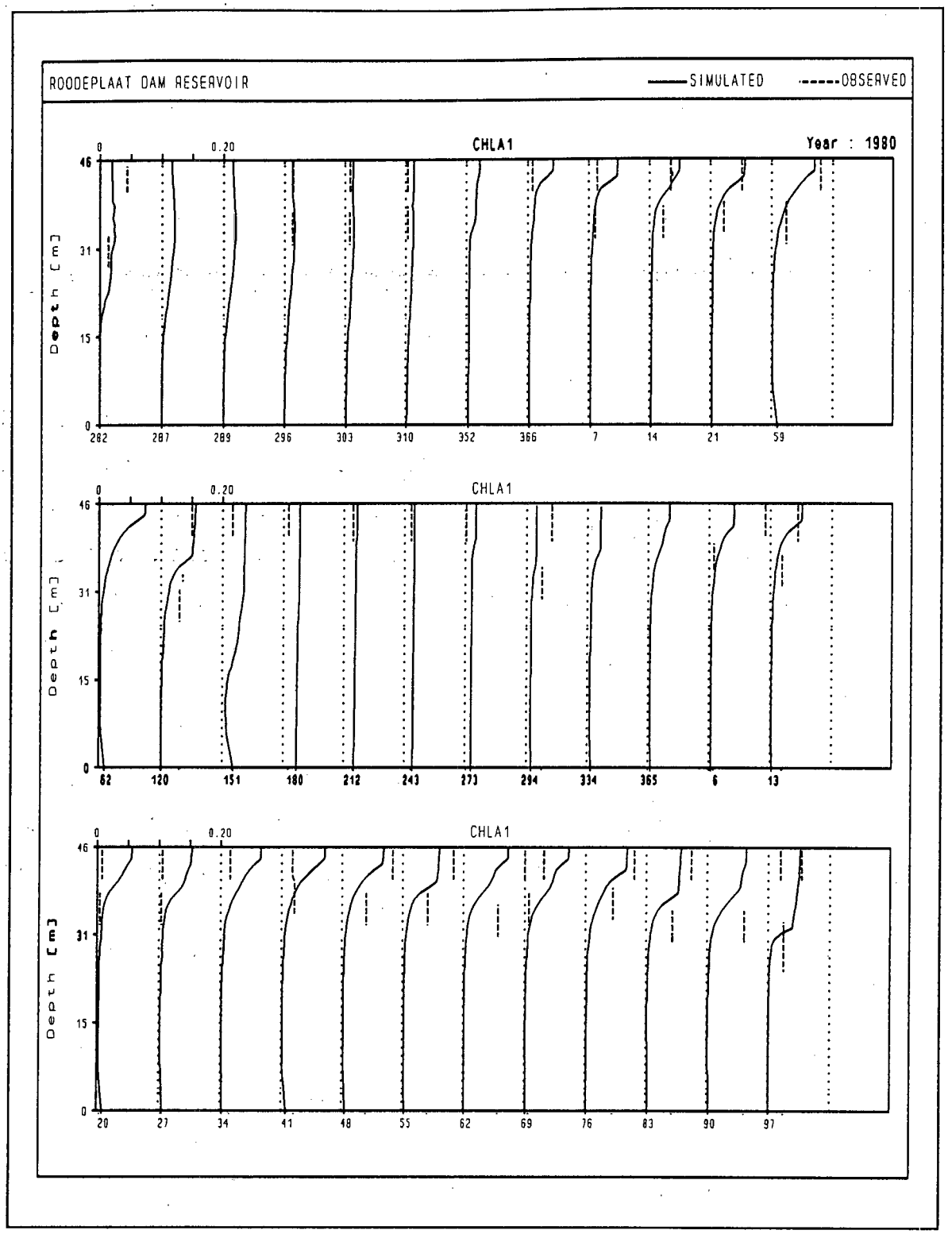

x-axis: Julian day Chlorophyll-a concentration: mg/l

Fig 7.14
Depth profiles of observed and simulated chlorophyll-a concentrations in Roodeplaat Dam, as obtained with the modified MINLAKE model and optimum values for the calibration coefficients.

7.5 SIMULATION OF TOTAL INORGANIC SUSPENDED SEDIMENT (TSS) CONCENTRATION

Concentration of total inorganic suspended sediment (TSS) is modeled as an implicit part of the processes that govern water quality and temperature distribution in a reservoir. South African reservoirs tend to be highly turbid due to the TSS load received from incoming rivers. Therefore it did not come as a surprise when, during calibration of the MINLAKE model on Roodeplaat Dam, it was found that TSS concentration has a definite effect on simulation of algal growth. Consequently it is important to simulate TSS concentration in Roodeplaat Dam as accurately as possible. However, simulation of TSS concentration in the reservoir was hampered by the fact that no measurements of TSS concentration in Roodeplaat Dam reservoir have been reported, nor in the three inflowing rivers. This problem was solved by synthesizing daily TSS concentrations for the three rivers from river flow rate. TSS concentrations in the reservoir were approximated from secchi disc depth data - see discussion in Appendix A1.

In both the original and the modified MINLAKE model, during simulation of TSS concentration in the reservoir sediment settling velocity in each layer is calculated as a function of temperature, sediment particle radius, and sediment particle density (*cf* Eq 5.93):

$$v = \frac{-3\mu + \left[9\mu d^2 + g r_s^2 \rho_f (\rho_s - \rho_f)(0.015476 + 0.19841 r_s)\right]^{0.5}}{\rho_f (0.011607 + 0.14881 r_s)} 864 \qquad (7.19)$$

v	=	TSS settling velocity (m day^{-1})
μ	=	dynamic viscosity (poises) (Eq 5.94)
r_s	=	sediment particle radius (cm)
ρ_f	=	density of fluid (g cm^{-3})
ρ_s	=	density of sediment particle (g cm^{-3})
g	=	gravitational acceleration (cm s^{-2}).

In the original MINLAKE model, the sediment particle radius is hard-wired to a value of 0.5 μm, and the sediment particle density to a value of 2.65 g cm^{-3}. Because no sediment particle analysis had been done for Roodeplaat Dam, the default radius of 0.5 μm and specific weight of 2.65 mg l^{-1} specified in the model were used as a first estimate.

In Fig 7.15 the simulated TSS concentration in the dam for a particle radius of 0.5 μm is shown. The field data points were calculated from secchi disc depths, as discussed in Appendix A1. Correspondence between simulated and calculated TSS data is poor, with the simulated TSS concentration far too high. Furthermore, because the only source of TSS in the dam is that entering the dam from the three inflowing rivers, it was expected that TSS concentration in the Dam would follow the same trend as the total TSS concentration entering the Dam from the three rivers. The total TSS concentration entering the Dam is shown in Fig 7.16 - clearly the simulated TSS concentration in Fig 7.15 does not follow the same trend as the total TSS concentration entering the Dam, especially during the winter months, and therefore simulation of TSS concentration had to be reassessed.

In the original MINLAKE model, the value for the sediment particle radius was hard-wired into the model as 0.5 μm, and the density as 2.65 g cm^{-3}. In reassessing the simulation of TSS concentration, the validity of these values to Roodeplaat Dam was investigated.

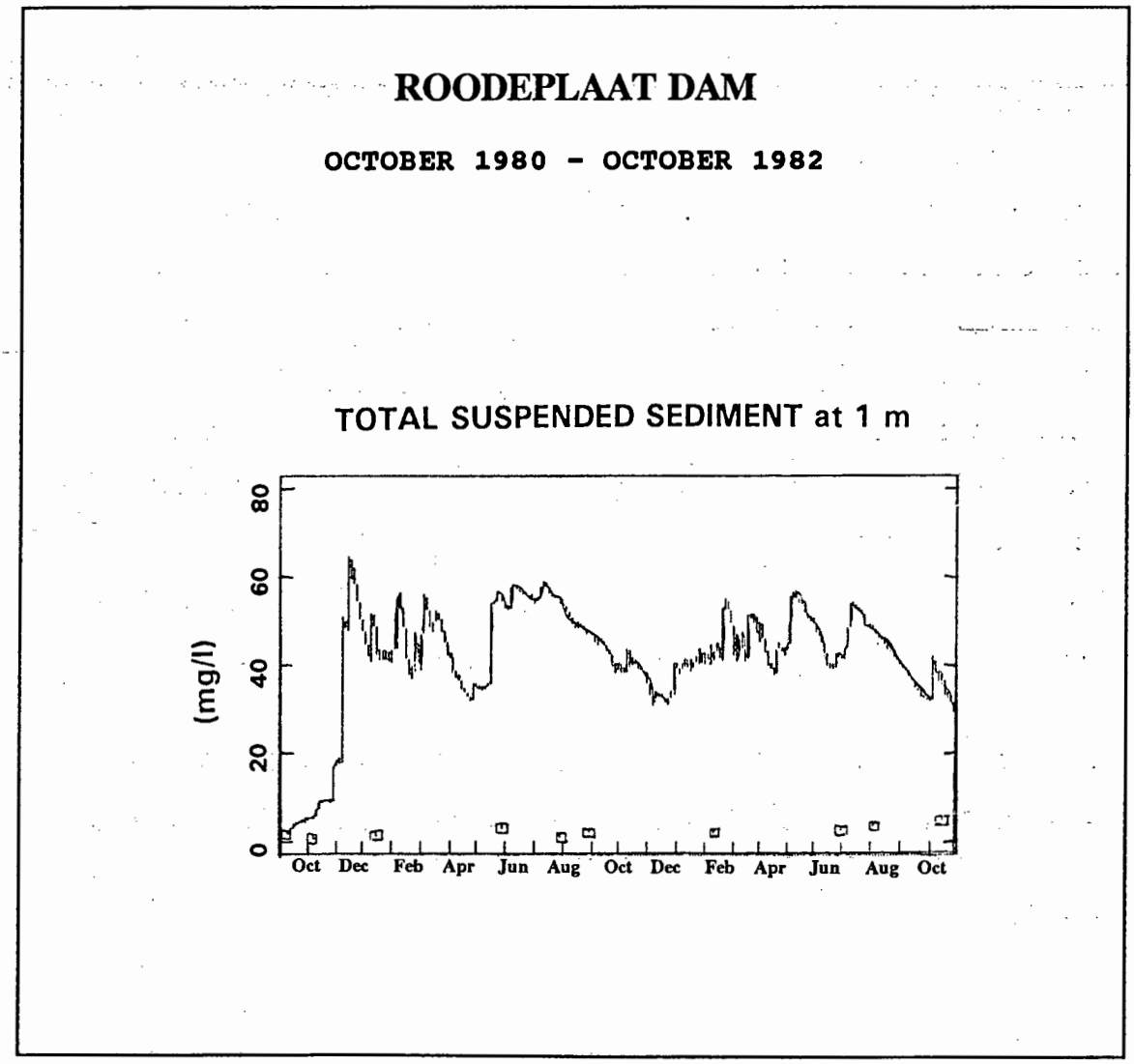

Fig 7.15
Time-series graph of calculated and simulated TSS concentration in Roodeplaat Dam, as obtained with the original MINLAKE model, utilising a particle radius of 0.5 μm.

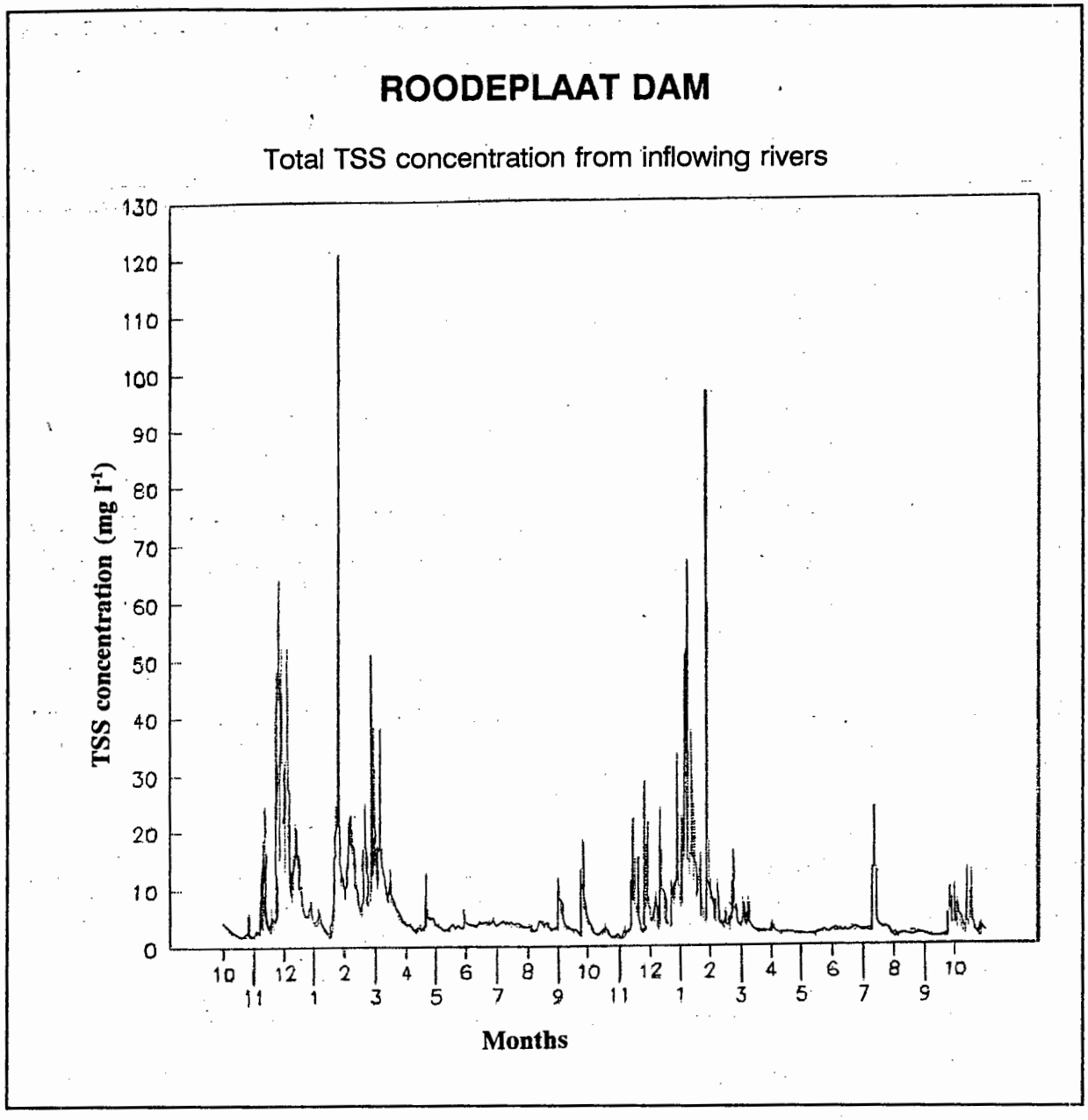

Figure 7.16
Time-series graph of TSS concentration entering Roodeplaat Dam for the period October 1980 to October 1982.

7.5.1 The effect of sediment particle radius on simulation of TSS concentration.

No sediment analysis for Roodeplaat Dam could be found, thus the following information was used as a basis for reassessing simulated TSS concentration:

- A sediment analysis for Hartebeespoort Dam gave the following (NIWR 1985):

Sand	45%
Silt	46%
Clay	9%

  It was assumed that Roodeplaat Dam would have the same sediment analysis.

- The sediment entering Roodeplaat Dam consists mostly of a fine silt, except during storm events, when a heavier, more sandy sediment is found (G Quibell 1993).

Diameters for different sediment particles are given in Table 7.10 (Friedman, 1978, Lindholm, 1987).

Table 7.10 Sediment particle diameters.

SEDIMENT	DIAMETER (μm)	RADIUS (μm)
Sand	62 - 500	32 - 250
Silt	2 - 62	1 - 31
Clay	< 2	< 1

From Table 7.10 it was concluded that a radius of 0.5 μm corresponds more to clay particles, whereas the sediment entering Roodeplaat Dam would appear to be mostly fine silt, therefore a sediment particle radius of 1 μm (corresponding to the bottom range of silt particle radii) would be more appropriate for Roodeplaat Dam.

Furthermore, generally the sediment particles entering the dam during the summer storm events are larger (G Quibell 1993) i.e, during storm events a different sediment particle radius should be specified. After repeated simulations the model was adapted as follows: From an analysis of the flow data from the three rivers entering the dam, it was decided that a total flow (entering the dam from all three rivers) greater than 20 cfs constitutes a storm event. Thus, for total flows greater than 20 cfs the particle radius is specified as 2 μm (corresponding to bigger silt particles). For total flows less than 20 cfs the particle radius is specified as 1 μm (corresponding to the lower end of silt particle radii). These particle radii were considered to be appropriate for the following reasons:

- For the surface layer of the reservoir, the simulated TSS concentration modelled with these radii, and the calculated data are shown in Fig 7.17. Not only does the simulated TSS concentration follow the same trend as the total TSS concentration entering the Dam (*cf* Fig 7.16), but the simulated and calculated data correspond very well during both the summer period (i.e during storm events) and the first winter period. The correspondence during the second winter period is not very good, but, as discussed in the hydrodynamic simulation results, during this period the simulated water temperature is too high, and very likely this causes the simulated TSS concentration to be too low.

- Depth profiles of simulated TSS concentration for Roodeplaat Dam Reservoir are shown in Fig 7.18. Although no observed data are available with depth, the depth profiles follow the same trend as observed by Ritchie *et al* (Ritchie 1978) in reservoirs in northern Mississippi, i.e. during overturn the concentration of suspended sediment was nearly homogeneous with depth, but as the thermocline developed with the onset of stratification, a gradient in the distribution of TSS developed also. TSS concentration remained nearly homogeneous in the epilimnion, but increased with depth in the hypolimnion. The same trend is obvious in the depth profiles of Roodeplaat Dam reservoir.

- The effect of different sediment particle radii on simulation of algal growth is shown in Fig 7.19. With the default particle radius of 0.5 μm, the simulated algal growth is too low when compared to observed algal concentration - probably because the simulated TSS concentration is too high, causing simulated underwater light intensity to be too low. With a particle radius of 1 μm, simulated and observed algal concentrations correspond very well. A particle radius of 1.5 μm instead of 1 μm gives rise to a slight difference in simulated algal concentration the during summer periods. A further increase in particle radius did not result in any change in the simulated algal concentration. Therefore, the particle radius of 2 μm chosen for storm events on the basis of TSS simulations, will be acceptable also for the simulation of algal growth.

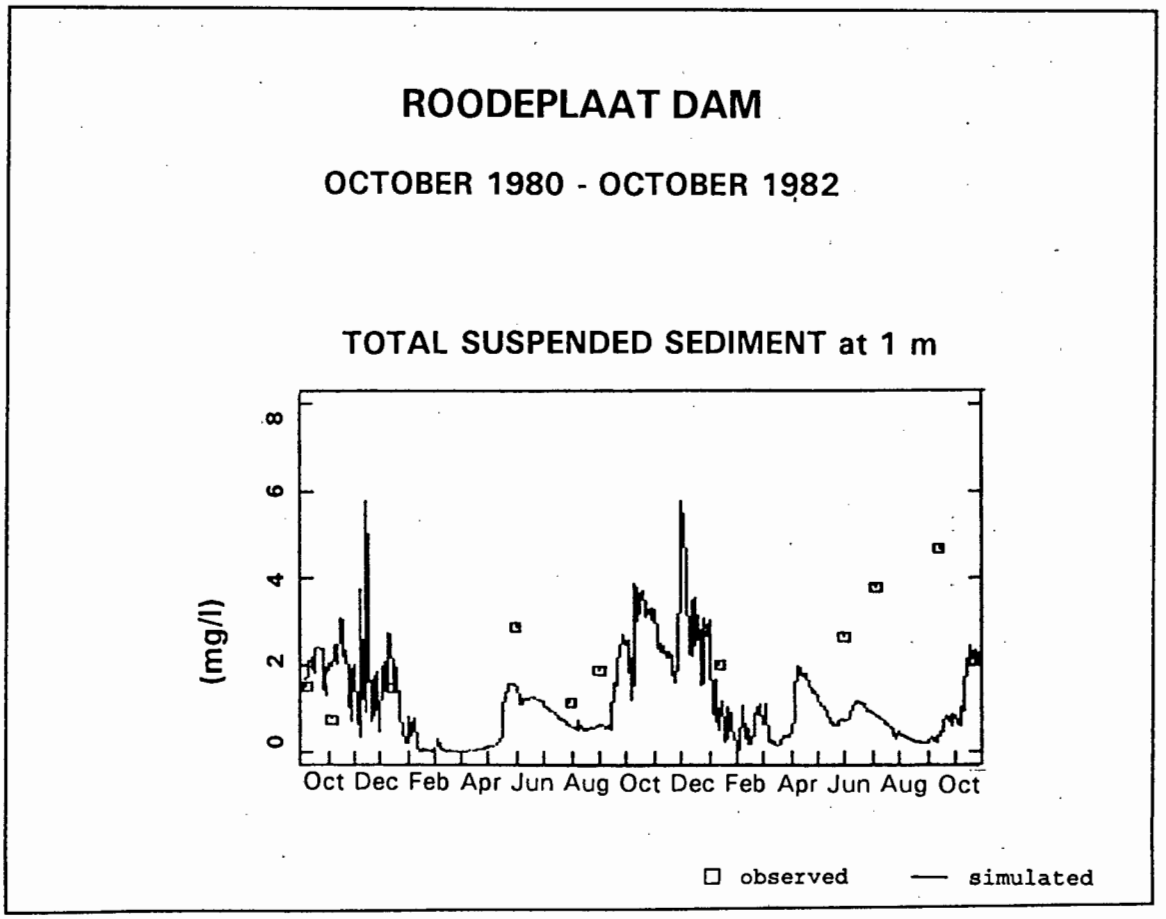

Fig 7.17
Time-series graph of calculated and simulated TSS concentration in Roodeplaat Dam as obtained with the modified MINLAKE model utilising particle radii of 1 μm (non-storm events) and 2 μm (storm events).

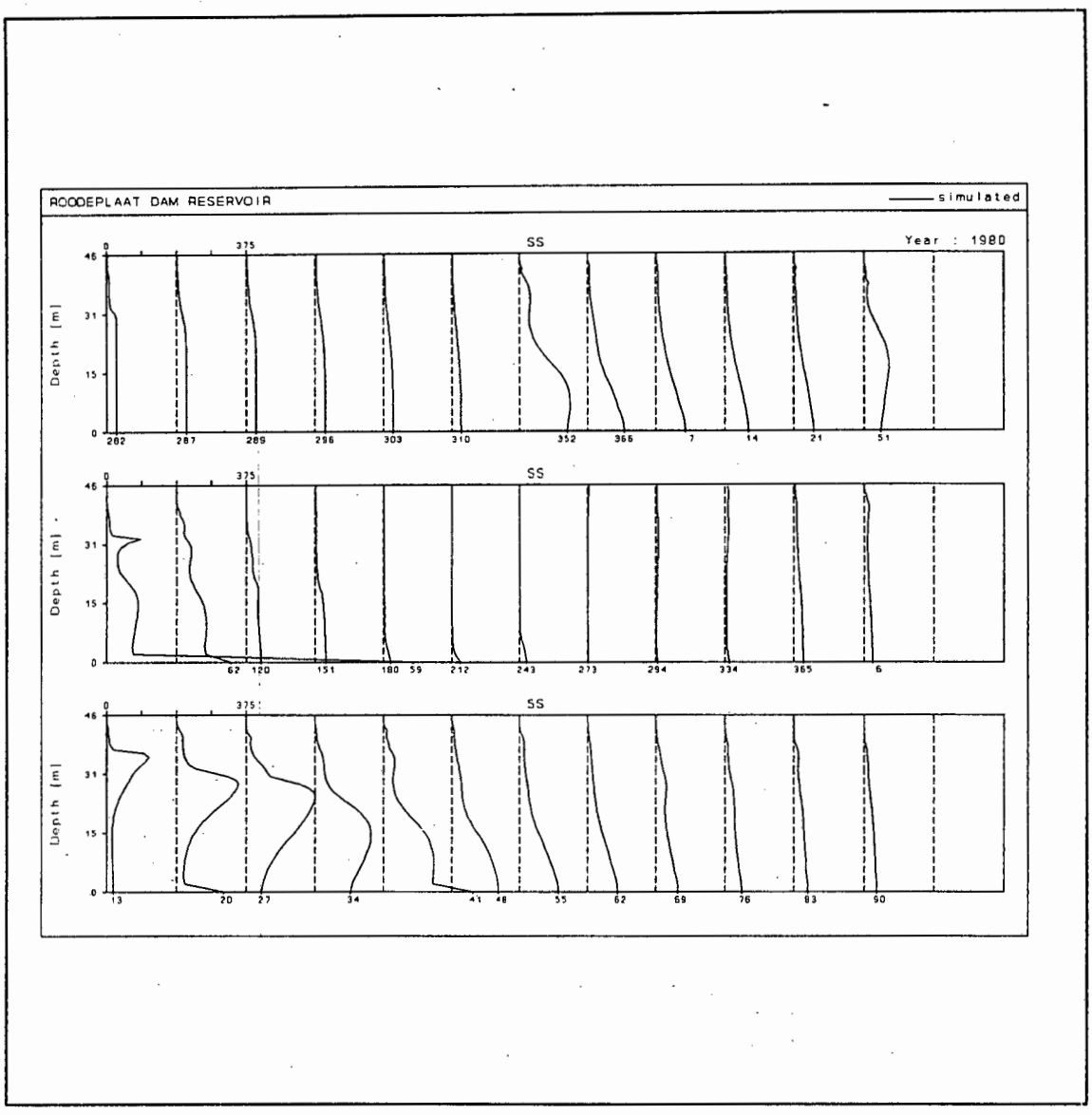

x-axis: Julian Day

TSS concentration: mg l^{-1}

Fig 7.18
Depth profiles of simulated TSS concentration as obtained with the modified MINLAKE model on Roodeplaat Dam.

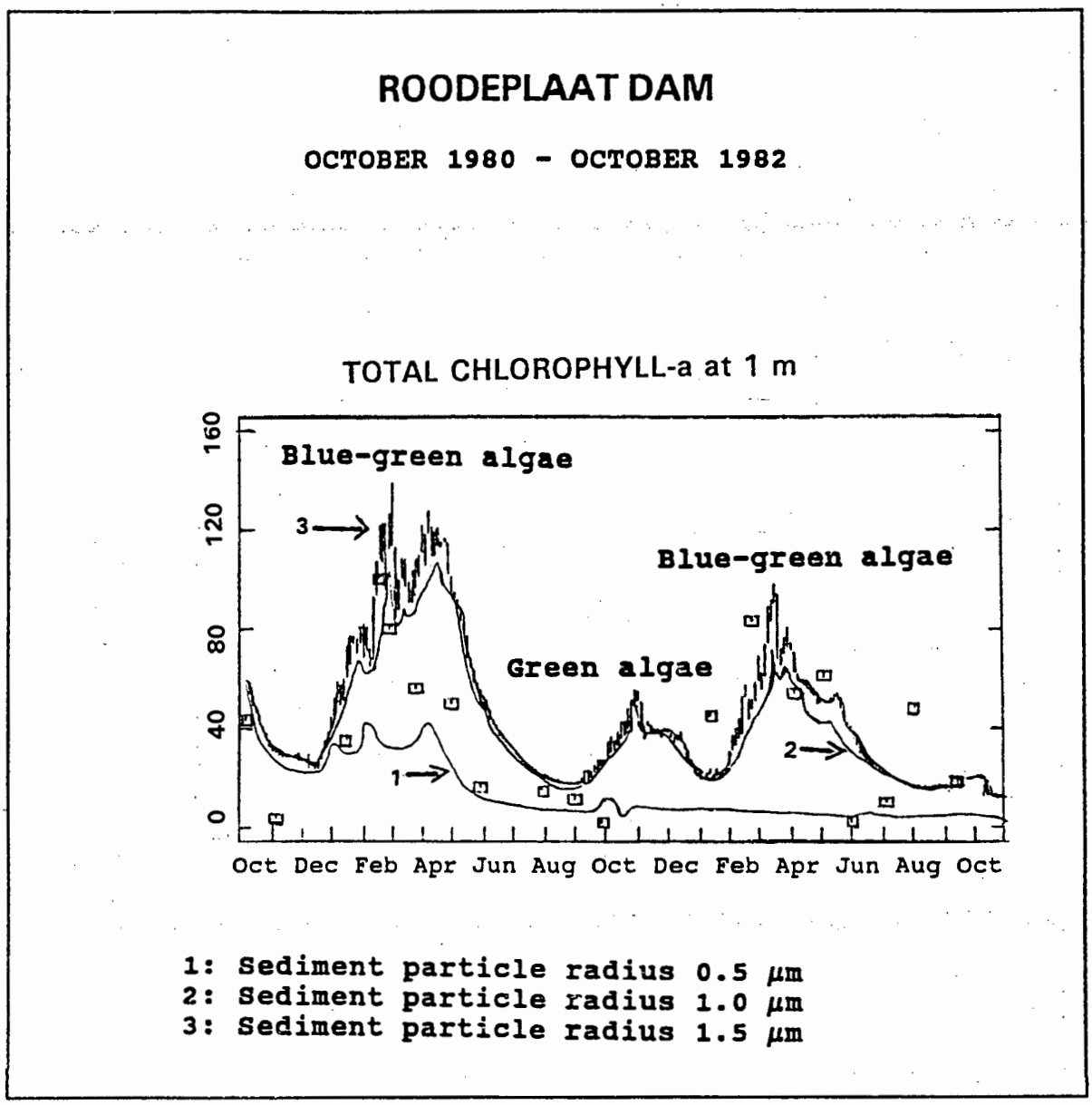

Fig 7.19
Time-series graph of simulated chlorophyll-a concentration obtained with the modified MINLAKE model on Roodeplaat Dam, utilising different sediment particle radii.

7.5.2 The effect of sediment particle density on simulation of TSS concentration

No specific data were available on sediment particle density for Roodeplaat Dam. A few runs were done with values of 3.65 and 1.65 g cm^{-3} for the sediment particle density, but the best results were obtained with a the default value of 2.65 g cm^{-3}.

7.6 DETRITUS SIMULATION RESULTS

During calibration of the dissolved oxygen part of the model, it became evident that detrital decay is one of the main sinks of dissolved oxygen in both the epilimnion and the hypolimnion. In fact, in highly eutrophic dams such as Roodeplaat Dam the anaerobic conditions that develop regularly during the stratified period probably can be attributed mainly to detrital decay. As the aerobic/anaerobic state of the water affects the reaction rates of a multitude of processes, it is important to simulate detrital decay as accurately as possible.

In the original MINLAKE model, algal mortality serves as a source of detritus. The detrital mass that is produced upon algal mortality is expressed in oxygen equivalents, i.e. only the biodegradable part of the detritus is taken into account. However, the composition of detritus (biodegradable vs unbiodegradable) is unique for each reservoir. In the original MINLAKE model, the user must specify the amount of biodegradable detritus produced upon algal mortality by means of a coefficient called YCBOD (see paragraph 5.3.2). No specific value has been determined for Roodeplaat Dam, therefore, as a first approximation, the default value of 0.0083 mg Chla mg^{-1} BOD was used. Eventually, a value of 0.0073 mg Chla mg^{-1} BOD was found to most appropriate.

Regarding detrital decay, in the original MINLAKE model it is represented as a simple first-order reaction (Eq 5.47):

$$\Delta O = \Delta BOD = BODK * 1.055^{(T-20)}(BOD) \quad (7.20)$$

ΔO	=	change in dissolved oxygen concentration due to bacterial decay of detritus (mg l^{-1})
ΔBOD	=	change in detritus concentration (mg l^{-1})
BODK	=	first order decay coefficient (day^{-1})
1.055	=	Arrhenius temperature coefficient
BOD	=	BOD concentration (mg l^{-1}).

The first-order decay coefficient, BODK, must be specified by the user. No specific value has been determined for Roodeplaat Dam, therefore the default value of 0.07 day^{-1} recommended in the MINLAKE manual was used. The simulated BOD concentration obtained when the original MINLAKE model was run on Roodeplaat Dam, is shown in Fig 7.20.

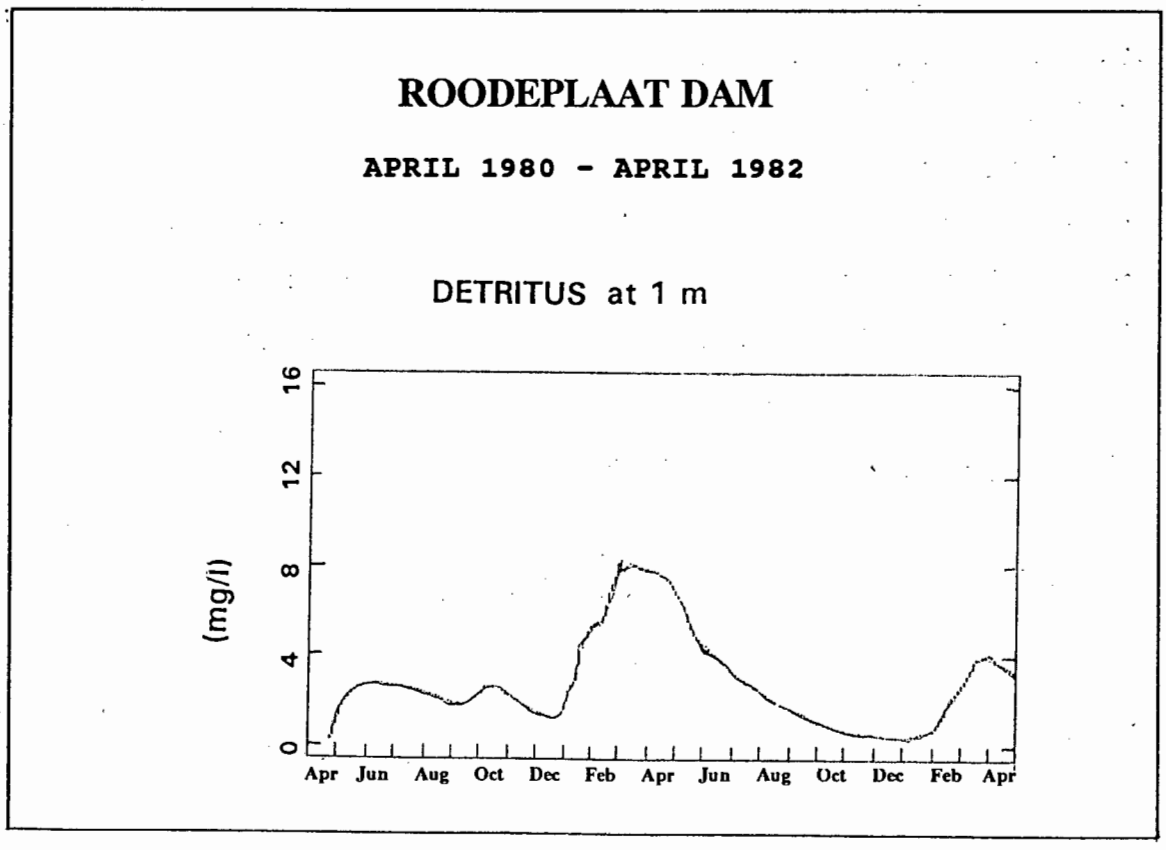

Fig 7.20
Time-series graph of simulated BOD concentration obtained with the original MINLAKE model on Roodeplaat Dam.

Unfortunately no observed BOD data are available for Roodeplaat Dam, and therefore it is difficult to assess the validity of the simulated BOD results. However, as was discussed in paragraph 5.3.2, a number of deficiencies were identified in Eq 7.19:

- No provision is made for the fact that microbial decay of organic matter is much faster under aerobic than anaerobic conditions (see paragraph 3.4.2)
- Once all the oxygen has been utilized, nitrate will be utilized as an electron acceptor (denitrification), but the process of denitrification is not included in the above formulation (see paragraph 3.4.5.2).
- No distinction is made between particulate and dissolved organic matter.
- The Arrhenius temperature coefficient has been hard-wired into the model to a value of 1.055 for all reactions.

In an attempt to rectify these shortcomings, two different formulations of microbial decay of organic matter were tested. The first formulation is a simple first-order formulation, making no distinction between particulate and dissolved forms of BOD. In the second formulation organic matter is divided into a particulate and dissolved part, taking into account the concept of Mann (1988) and Dold (1981) that particulate organic matter is regenerated during decay of dissolved organic matter (paragraphs 3.4.3, 5.3.2.1 and 5.3.2.2).

7.6.1 Detrital simulation results obtained with the first modified formulation

Basically, this formulation is equivalent to the formulation for detrital decay in the original MINLAKE model, except that provision has been made for the fact that microbial decay is much faster under aerobic than anaerobic conditions, and the process of denitrification has been incorporated. The formulation is as follows (Eq 5.48):

$$dBOD/dt = (BODK * QBOD^{(T-20)}) \left(\frac{DSO}{DSO+BODOK}\right) + (DNK \cdot QDNK^{(T-20)}) \cdot \left(\frac{KONO}{KONO+DSO}\right)\left(\frac{NO}{NO+EDNK}\right) BOD \quad (7.21)$$

dBOD/dt	=	change in detrital concentration due to decay (mg l^{-1})
BODK	=	detrital decay rate at 20 °C (day^{-1})
QBOD	=	Arrhenius temperature coefficient for detrital decay (cf Eq 4.92).
BODOK	=	aerobic switching constant for detrital decay (mg O_2 l^{-1})
DSO	=	dissolved oxygen concentration (mg l^{-1})
DNK	=	denitrification rate at 20 °C (day^{-1})
QDNK	=	Arrhenius temperature coefficient for denitrification
XKONO	=	anaerobic switching constant for denitrification (mg $O_2 l^{-1}$)
NO	=	nitrate concentration (mg l^{-1})
EDNK	=	denitrification inhibition factor (mg NO_3 l^{-1})
BOD	=	concentration of BOD (mg l^{-1}).

BODK - detrital decay rate at 20 °C:

As mentioned previously, no specific value for BODK had been determined for Roodeplaat Dam. However, after repeated runs, taking the effect of different values of BODK on other variables such as concentration of dissolved oxygen into account, the optimum value for BODK for Roodeplaat Dam was determined as 0.13 day^{-1}.

QBOD - Arrhenius temperature coefficient for detrital decay:

Again, no specific value had been determined for Roodeplaat Dam, but according to the literature (EPA 1987, Orlob 1983) a value of 1.049 is a fairly representative value.

BODOK - aerobic switching constant for detrital decay:

The rate of detrital decay is much faster under aerobic than under anaerobic conditions (paragraph 3.4.2). The constant BODOK is similar to the Monod half-saturation coefficient for nutrient uptake, and represents the dissolved oxygen

concentration where the decay rate is equal to half the maximum decay rate. No specific value has been determined for Roodeplaat Dam, but after repeated runs, taking the interactive effect of detrital decay on other processes into account, it was established that the best results are obtained with a value of 0.01 mg O_2 l^{-1} for BODOK.

The values of the other coefficients - DNK, QDNK, XKONO, and EDNK have been discussed in paragraph 7.3.3 as part of the nitrogen simulation results. A time-series graph of the simulated detritus concentration obtained with the above formulation of detrital decay is shown in Fig 7.21. Unfortunately detritus concentrations in Roodeplaat Dam are not measured and therefore a comparison between observed and simulated data is not possible. This result is discussed further in Chapter 8.

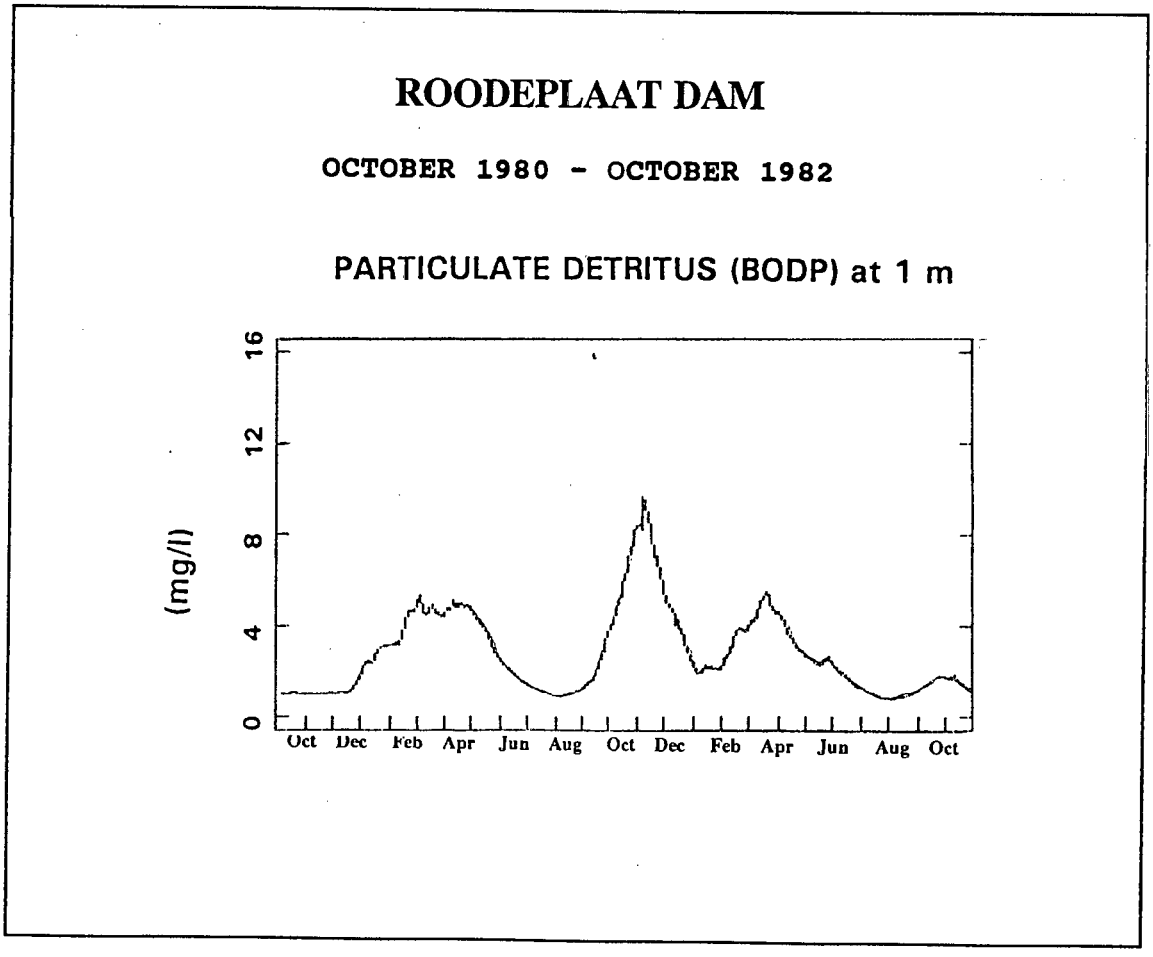

Fig 7.21
Time-series graph of simulated BOD as obtained with the modified MINLAKE model on Roodeplaat Dam, utilising the first formula (Eq 7.21) for detrital decay.

7.6.2 Detritus simulation results obtained with the second modified formulation.

The second modified formulation is more complex (paragraph 5.3.2.2). A distinction is made between dissolved and particulate BOD, and provision is made for regeneration of particulate BOD during decay of dissolved organic matter (see paragraph 5.3.2.2). Upon death of algae (mortality), particulate BOD is formed, which is decomposed to dissolved BOD through the action of enzymes (paragraph 3.4.3). This is not a microbial process and thus no oxygen is utilised. During the subsequent decay of dissolved BOD, only one third of the decaying dissolved BOD utilizes oxygen/nitrate as an electron acceptor, and releases intracellular ammonia and phosphate. The other two-thirds form particulate BOD again. The formulations incorporated into the modified MINLAKE model to affect these changes have been discussed in paragraph 5.3.2.2, but to facilitate discussion of the values of the calibration coefficients associated with these formulations, the formulations are repeated briefly:

The sources of particulate BOD was formulated as (Eq 5.49):

$$dBODP/dt = \left(\frac{XKM*CHLa}{YCBOD}\ QCHLa^{(T-20)}\right) + (0.666\ BODS*BODSK\ QBOD^{(T-20)})\left(\frac{DSO}{DSO+BODSOK}\right) + (DNK\ QDNK^{(T-20)})\left(\frac{KONO}{KONO+DSO}\right)\left(\frac{NO}{NO+EDNK}\right) \quad (7.22)$$

dBODP/dt	=	increase in particulate BOD concentration (mg l^{-1})
XKM	=	algal mortality rate at 20°C (day^{-1})
CHLa	=	chlorophyll-a concentration (mg l^{-1})
YCBOD	=	BOD coefficient (cf Eq 5.46)
	=	mass ratio of biodegradable detritus produced from chlorophyll-a (mg chla (mg BOD)$^{-1}$)
QCHLa	=	Arrhenius temperature coefficient for algal mortality (cf Eq 4.92)
T	=	water temperature in the layer (°C)
BODS	=	concentration of dissolved BOD (mg l^{-1})
BODSK	=	decay rate dissolved BOD at 20 °C (day^{-1})
QBOD	=	Arrhenius temperature coefficient for detrital decay
BODSOK	=	aerobic switching constant for dissolved BOD decay (mg O_2 l^{-1})
DSO	=	dissolved oxygen concentration (mg l^{-1})
DNK	=	denitrification rate at 20 °C (day^{-1})
QDNK	=	Arrhenius temperature coefficient for denitrification
KONO	=	anaerobic switching constant for denitrification (mg $O_2 l^{-1}$)
NO	=	nitrate concentration (mg l^{-1})
EDNK	=	denitrification inhibition constant (mg NO_3 l^{-1}).

Decomposition of particulate BOD was formulated as (Eq 5.50):
(This formulation serves as a sink of particulate BOD and as a source of dissolved BOD)

$$dBOD/dt = BODPK * QBOD^{(T-20)} * BODP \quad (7.23)$$

dBOD/dt	=	decrease in particulate BOD (increase in dissolved BOD) (mg l^{-1})
BODPK	=	decomposition rate of particulate BOD at 20°C (day^{-1})
QBOD	=	Arrhenius temperature coefficient
BODP	=	concentration of particulate BOD (mg l^{-1}).

Decay of dissolved BOD was formulated as (Eq 5.51)

$$dBODS/dt = (BODSK\ QBOD^{(T-20)}) \left(\frac{DSO}{DSO+BODSOK}\right) + (DNK\ QDNK^{(T-20)}) \left(\frac{KONO}{KONO+DSO}\right)\left(\frac{NO}{NO+EDNK}\right) BODS \quad (7.24)$$

dBODS/dt	=	change in dissolved BOD concentration due to decay (mg l^{-1})
BODSK	=	dissolved BOD decay rate at 20 °C (day^{-1})
QBOD	=	Arrhenius temperature coefficient for detrital decay (cf Eq 4.92).
BODSOK	=	aerobic switching constant for decay of dissolved BOD (mg O_2 l^{-1})
DSO	=	dissolved oxygen concentration (mg l^{-1})
DNK	=	denitrification rate at 20 °C (day^{-1})
QDNK	=	Arrhenius temperature coefficient for denitrification
KONO	=	anaerobic switching constant for denitrification (mg $O_2 l^{-1}$)
NO	=	nitrate concentration (mg l^{-1})
EDNK	=	denitrification inhibition constant (mg NO_3 l^{-1})
BODS	=	concentration of dissolved BOD (mg l^{-1}).

Values of the coefficients XKM (algal mortality rate) and Qchla (Arrhenius temperature coefficient for algal mortality) have been discussed with the algal simulation results in paragraph 7.4.1, and values of the coefficients DNK, QDNK, KONO, and EDNK have been discussed with the nitrogen simulation results in paragraph 7.3.

The optimum value of the coefficient YCBOD is as before, i.e. 0.0073 mg Chla mg^{-1} BOD. Regarding the value of the BODSK, the decay rate of dissolved BOD at 20°C, no specific value has been determined for Roodeplaat Dam, but after repeated runs the optimum value was established as 0.09 day^{-1}. The value of QBOD, the Arrhenius temperature coefficient, is as before (1.049), as well as the value of BODSOK, the aerobic switching constant for detrital decay, i.e. 0.01 mg O_2 l^{-1}. No specific value could be found for the decomposition rate of particulate BOD (BODPK) for Roodeplaat Dam, but after repeated runs the optimum value was established as 0.08 day^{-1}.

Time-series graphs of simulated dissolved and particulate BOD concentrations obtained with detrital decay formulated as in Eq 7.21 - 7.23, are given in Fig 7.22 and Fig 7.23. As was stated previously, unfortunately a comparison between simulated and observed concentrations is not possible, as detritus concentration is not measured in Roodeplaat Dam. A discussion of the results obtained with the more complex formulation of detrital decay, as well as a comparison of the results obtained with the two formulations for detrital decay are given in Chapter 8.

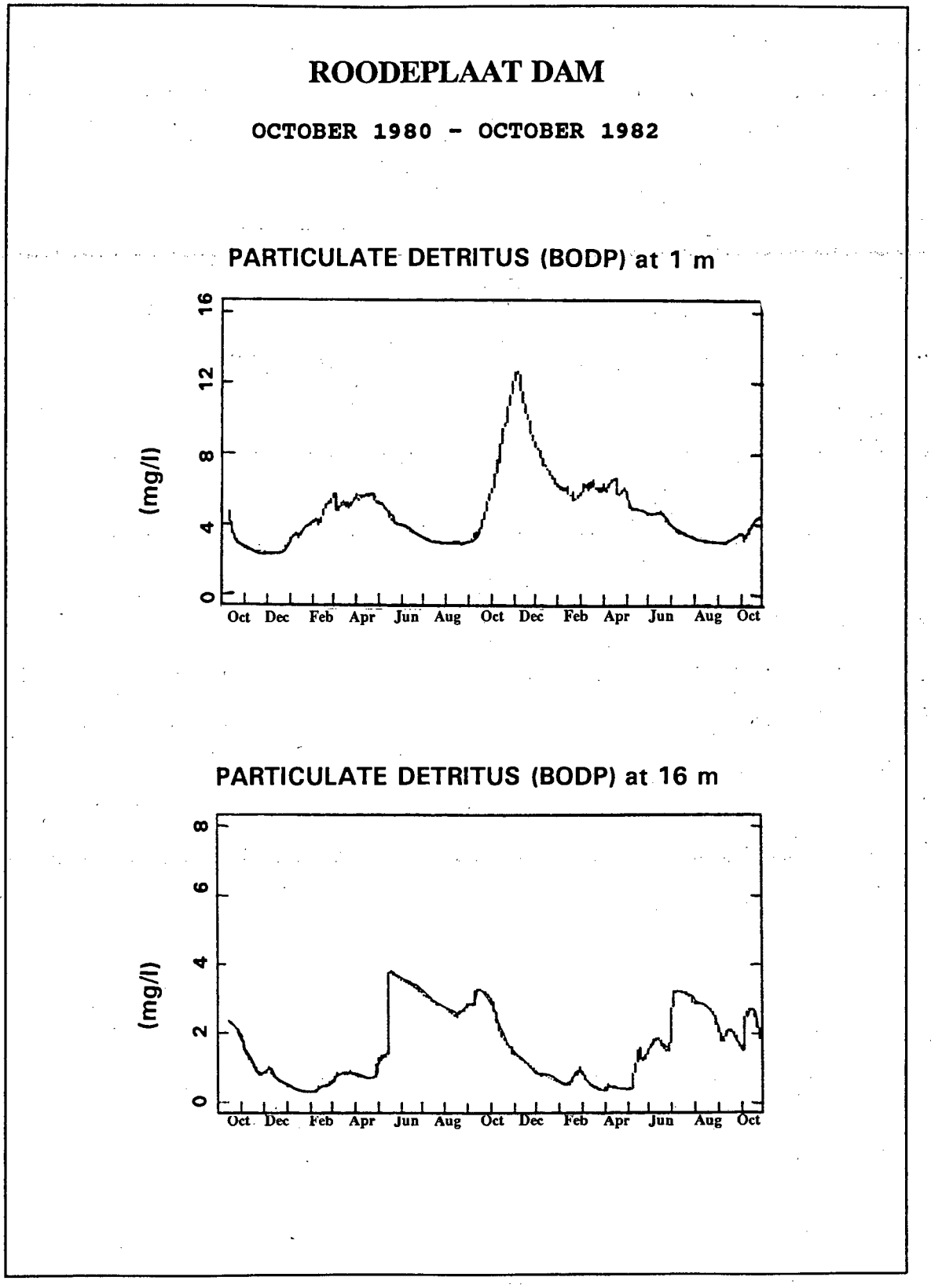

Fig 7.21
Time-series graph of simulated particulate BOD concentration as obtained with the modified MINLAKE model on Roodeplaat Dam

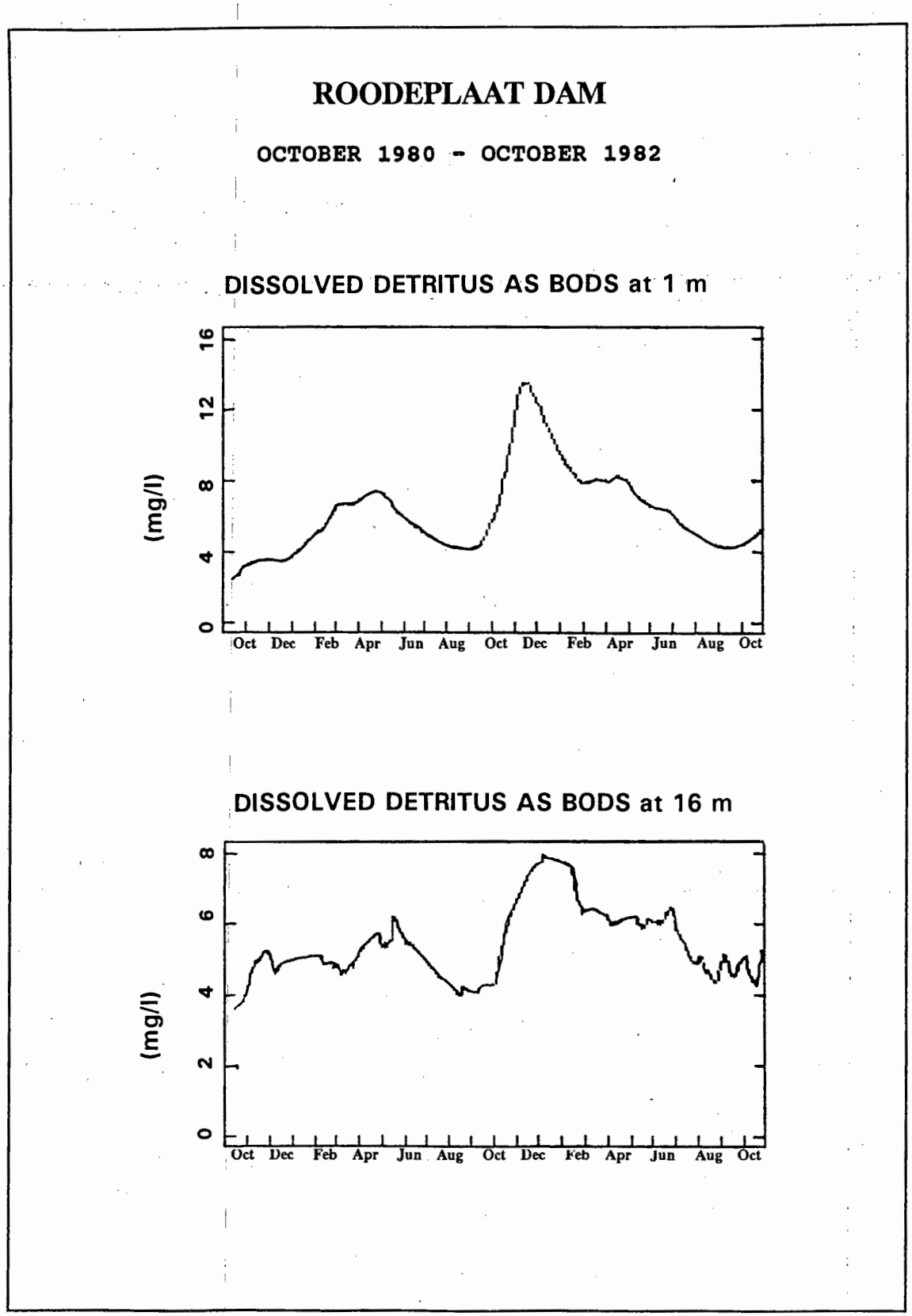

Fig 7.22
Time-series graph of simulated dissolved BOD concentration as obtained with the modified MINLAKE model on Roodeplaat Dam

7.6.3 Comparison of detrital decay processes in the original and modified MINLAKE model.

Several deficiencies were identified in the formulation for detrital decay in the original MINLAKE model. Two different formulations for detrital decay were tested in the modified model, one more complex than the other. A comparison of the processes associated with formulation of detrital decay in the original and the modified MINLAKE model is given in Table 7.11.

Table 7.11. Comparison of detrital decay processes in the original and modified MINLAKE model.

ORIGINAL MINLAKE MODEL	MODIFIED MINLAKE MODEL	
	First formulation	**Second formulation**
■ Only particulate BOD simulated.	■ Only particulate BOD simulated.	■ Both particulate and dissolved BOD simulated. Regeneration of particulate BOD during decay of dissolved BOD.
■ Decay rate: - Not affected by aerobic/ anaerobic state of the water. - Arrhenius temperature coefficient hard-wired into the model.	■ Decay rate: - Under aerobic conditions only. - User can choose value of Arrhenius temperature coefficient.	■ Decomposition rate (particulate BOD): - Not affected by aerobic/ anaerobic state of the water. - User can choose value of Arrhenius temperature coefficient. ■ Decay rate (dissolved BOD): - Under aerobic conditions only. - User can choose value of Arrhenius temperature coefficient.
■ No denitrification.	■ Denitrification: - Under anaerobic conditions only. - User can choose value of Arrhenius temperature coefficient. - Inhibited by high nitrate concentration.	■ Denitrification: - Under anaerobic conditions only. - User can choose value of Arrhenius temperature coefficient. - Inhibited by high nitrate concentration.
■ Sources of BOD: - Algal mortality.	■ Sources of BOD: - Algal mortality.	■ Sources of BOD: - Particulate: Algal mortality. Regeneration during decay of dissolved BOD. - Dissolved: Decomposition of particulate BOD. Release from bottom sediment under anaerobic conditions.

7.7 OXYGEN SIMULATION RESULTS

Dissolved oxygen concentration is one of the more difficult variables to calibrate, because so many processes contribute to the oxygen budget. However, it is essential that the concentration of dissolved oxygen be simulated as correctly as possible, as the reaction rates of a multitude of processes differ under aerobic and anaerobic conditions. This is of special importance in South Africa, as many of our dams turn anaerobic during part of the hydrological cycle.

In the original MINLAKE model, the concentration of dissolved oxygen is increased by:

- reaeration
- algal photosynthesis.

The concentration of dissolved oxygen is decreased by:

- respiration
- detrital decay
- nitrification
- sediment oxygen demand.

The dissolved oxygen concentration in a layer will be further affected by turbulent diffusion - in the MINLAKE model this effect is simulated by use of a epilimnetic diffusion coefficient that is calculated by the model, and by use of a maximum hypolimnetic diffusion coefficient that must be specified by the user.

Regarding the coefficients associated with simulation of dissolved oxygen concentration, the coefficients associated with algal photosynthesis and respiration, detrital decay and nitrification will affect simulation of dissolved oxygen concentration also, but these coefficients have been discussed in paragraphs 7.4.1 and 7.3.2. Again, these coefficients are a good example of the interaction between processes. The only coefficient that has not been discussed previously, is the coefficient YCHO2 - the ratio

of oxygen produced by photosynthesis to oxygen utilized in respiration. No specific value for YCHO2 has been determined for Roodeplaat Dam. The default value of 0.0083 indicated in the MINLAKE manual (Riley 1988) was used as a starting point, but a value of 0.0075 gave the best results. Regarding the initial values of the other, interactive coefficients, these are discussed in paragraphs 7.4.1 and 7.3.2.

The result of the first run that was obtained when the original MINLAKE program was run with default values for the coefficients pertaining to simulation of dissolved oxygen concentration is shown in Fig 7.23. Simulated oxygen concentrations in both the epilimnion and the hypolimnion were far too low in comparison with the observed. The discrepancy between observed and simulated concentrations could have been caused by the following:

- the kinetic coefficients pertaining to the processes that contribute to the oxygen budget, were inadequately specified
- the processes that contribute to the oxygen budget were inadequately formulated and/or represented.

Clearly a detailed investigation of these processes, and the related kinetic coefficients, was necessary.

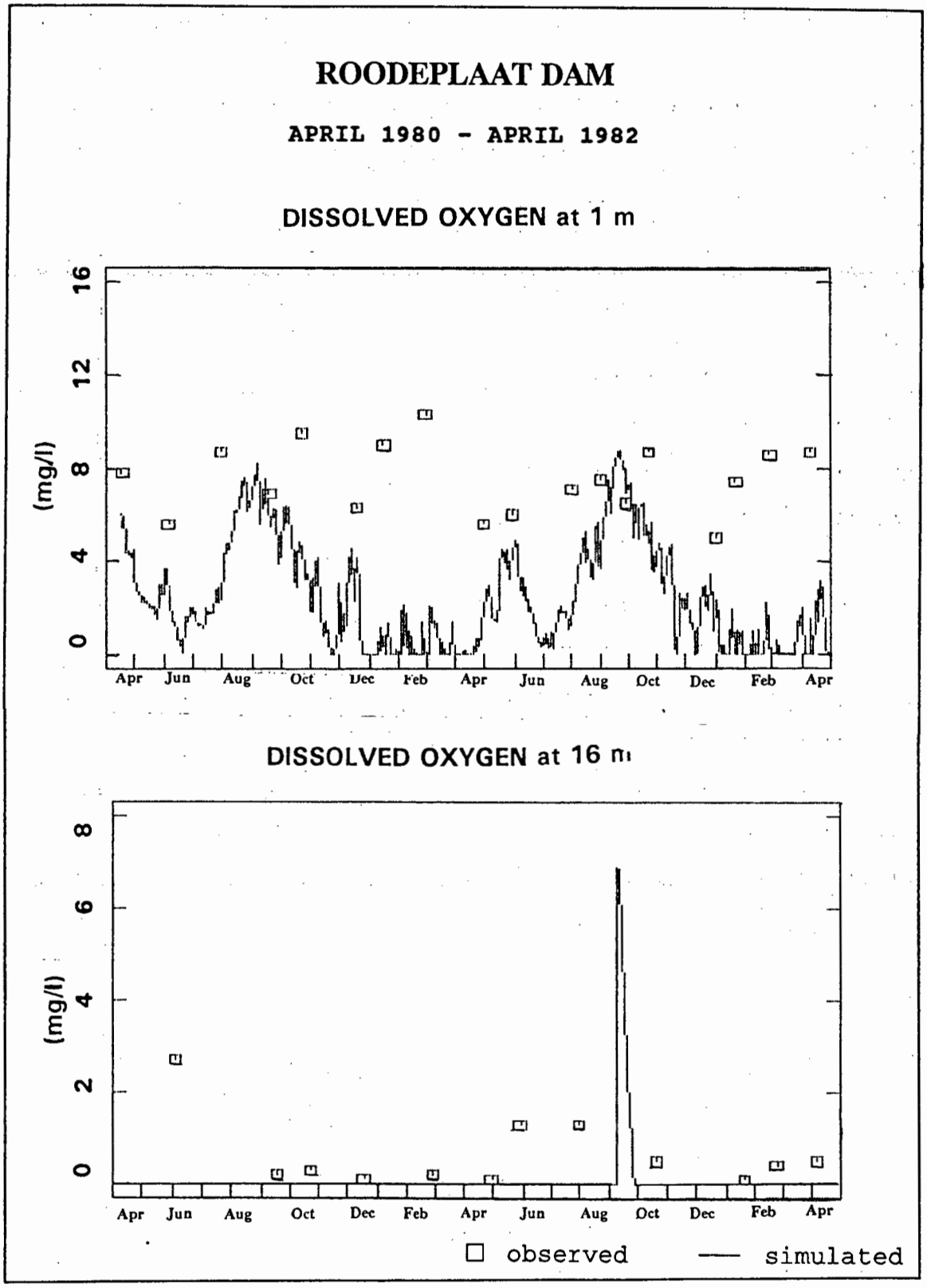

Fig 7.23
Time-series graphs of observed and simulated dissolved oxygen concentration at 1 and 16 m depth as obtained with the original MINLAKE model on Roodeplaat Dam.

7.7.1 Reaeration

Reaeration only takes place in the surface layer (see theoretical discussion in paragraph 3.4.2.1). Generally, reaeration is formulated as follows (Eq 4.75):

$$dO/dt = K_L A (C_s - C) \quad (7.25)$$

dO/dt	=	change in oxygen concentration with time
K_L	=	transfer velocity (m day^{-1})
A	=	reservoir surface area (m)
C_s	=	saturated dissolved oxygen concentration (mg.l^{-1})
C	=	actual dissolved oxygen concentration in surface layer (mg l^{-1})

In the MINLAKE source code, problems were encountered with the coding and formulation of the transfer velocity, K_L, as well as with the formulation of the saturated dissolved oxygen concentration, C_s.

7.7.1.1 Transfer velocity:

According to the MINLAKE manual, most researchers agree that wind does have an effect on the oxygen transfer velocity, although there is a disagreement on the exact mechanism. However, for the purposes of modelling, the effect is more critical than the specific, small scale mechanism involved, and therefore the formulation for K_L is an approximation of several formulations (Eq 5.32):

$$K_L = \frac{1.1 * 10^6 u_*^2}{S_c^{0.5}} \quad (7.26)$$

K_L	=	transfer velocity (mass transfer coefficient)	(m day^{-1})
u_*	=	water shear velocity induced by wind (m s^{-1})	
S_c	=	Schmidt number, ν/D	

that is

$$S_c = \frac{1.45 * 10^5}{T_K}\left[\frac{1.79}{1 + 0.03368T_c + 0.000221T_c^2}\right]^2 \quad (7.27)$$

v	=	kinematic viscosity ($m^2\ s^{-1}$)
D	=	molecular diffusivity ($m^2\ s^{-1}$)
	=	$6.92 * 10^{-15}\ T_K/\mu$ ($m^2\ s^{-1}$)
T_K	=	temperature (K)
μ	=	absolute viscosity (Nsm^{-2})
T_c	=	temperature (°C).

Two problems were encountered with the above formulation:

1. Formulation of K_L:

Apparently the formulation of K_L in MINLAKE is based mainly on the formulation of Cohen (1983):

$$K_L S_c^{0.5} = A_o + A(U_w^*)^{1.015} \quad (7.28)$$

K_L	=	mass transfer coefficient ($cm\ s^{-1}$)
S_c	=	Schmidt number as above
A_o	=	empirical constant
	=	0.0148 $cm\ s^{-1}$ for a well-mixed water body
A	=	empirical constant
	=	0.048 $cm\ s^{-1}$
U_w^*	=	water shear velocity ($cm\ s^{-1}$).

In MINLAKE, K_L is in $m\ day^{-1}$. If the above formulation of Cohen is rewritten in terms of $m\ d^{-1}$ instead of $cm\ s^{-1}$, the following is obtained:

$$K_L S_c^{(0.5)} = 12.78 + (3.58 * 10^6)\ U_w^{*1.015} \quad (7.29)$$

The value of A_o, 12.78, is very small in comparison with the rest, and can be neglected. Eq 7.29 then becomes:

$$K_L S_c^{(0.5)} = (3.58 * 10^6) U_w^{*1.015} \quad (7.30)$$

When the model was run with the value for K_L as per Eq 7.30 instead of Eq 7.26, the correspondence between simulated and observed dissolved oxygen concentration in the upper layers improved significantly. It would therefore seem that the expression for K_L in Eq 7.25 is not correct - in fact, if Eq 7.26 and 7.30 are compared, the following deduction can be made: it would seem that, when rewriting Eq 7.28 from cm s^{-1} to m d^{-1} to obtain Eq 7.26, **A** was inadvertently assigned the value of 0.0148, (i.e. the value of A_o) instead of a value of 0.048. To counteract this mistake, the term $(U_w^*)^{1.015}$ in Eq 7.28 probably had to be replaced by the term $(U_w^*)^2$ in Eq 7.26.

2. Coding of the Schmidt number:

The formulation of the Schmidt number is given in Eq 7.27 above. In the source code of the original MINLAKE model the value for T_k (surface water temperature in Kelvin) was hard-wired to a constant value of 289 K (16°C). In Roodeplaat Dam reservoir the temperature of the surface layer vary between 15 and 28 °C, therefore the source code was changed to read the actual temperature of the surface layer instead of the constant value of 289 K. This change did not result in a significant change in the simulated dissolved oxygen concentration, but the changed formulation is considered to be more correct than the formulation with a constant temperature.

7.7.1.2 Saturated dissolved oxygen concentration:

The saturated dissolved oxygen concentration in the surface layer is a function of water temperature and altitude (see theoretical discussion in paragraph 3.4.2). In the MINLAKE model, the saturated dissolved oxygen concentration in the surface layer is expressed only as a function of water temperature, and not as a function of altitude:

$$C_s = 14.652 - T2(1)(0.41022 - T2(1)(7.991 * 10^{-3} - 7.7774 * 10^{-5}\ T2(1))) \quad (7.31)$$

C_s = saturated dissolved oxygen concentration in surface layer (mg l^{-1})

14.652= value of C_s at 0°C and 1000 mbar

T2(1) = water temperature of the surface layer (°C)

Roodeplaat Dam reservoir is situated at an altitude of 1214 m. The atmospheric pressure at this altitude is 860 mbar, therefore it was considered more correct to express the saturated dissolved oxygen concentration as a function of both temperature and altitude, instead of correcting for temperature only and assuming standard atmospheric pressure of 1013 mbar, as was done in the original MINLAKE model. Eq 7.32 was therefore replaced with the following formulation by Bratby (1977):

$$C_s = C_{s20}\left(\frac{51.6}{(31.6 + T2(1))}\right)\left(\frac{P_s - ESA}{(1013-23.35)}\right) \quad (7.32)$$

C_s = saturated dissolved oxygen concentration in surface layer (mg l^{-1})

C_{s20} = saturated dissolved oxygen concentration in surface layer at 20 °C and 100 mbar (mg l^{-1})

= 9.07 mg l^{-1}

51.6 = constant

31.6 = constant

T2(1) = water temperature of the surface layer (°C)

P_s = atmospheric pressure at the site (mbar) (calculated in the model from altitude)

ESA = saturated water vapour pressure at surface layer water temperature (mbar)[1]

1013 = 1 atmosphere (mbar)

23.35 = saturated water vapour pressure at 20 °C (mbar).

The last term in Eq 7.32 refers to the effect of temperature on the saturated dissolved oxygen concentration, while the second term in Eq 7.32 refers to the effect of altitude. Although the temperature effect has been correctly formulated in MINLAKE (Eq 7.32), it was easier to replace the entire MINLAKE formulation with that of Bratby, instead of trying to adapt the MINLAKE formulation for the effect of altitude. Fig 7.24 shows the difference in saturated dissolved oxygen concentration calculated with the MINLAKE formulation and with the Bratby formulation. Although there is not much difference in the saturated oxygen concentration calculated with the two formulations, the formulation of Bratby is considered more correct, and consequently this formulation was coded into the MINLAKE model. The use of the Bratby formula instead of the original MINLAKE formula did not cause any significant change in the simulated oxygen concentration.

[1] In the model, ESA has been calculated already as part of the heat budget.

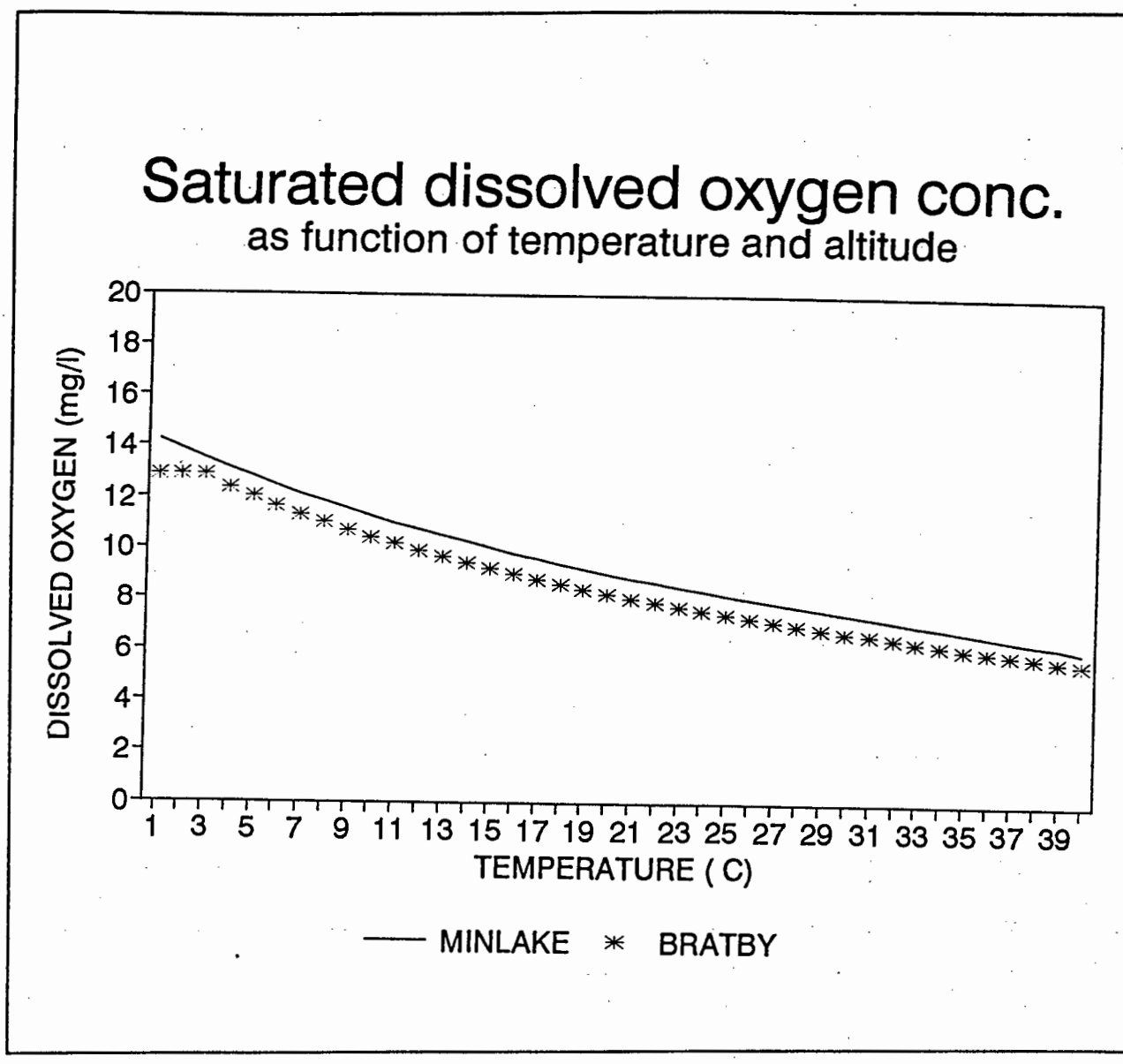

Fig 7.24
Graph of dissolved oxygen concentration as a function of temperature and altitude, as calculated with a) the MINLAKE formulation, and b) Bratby's formulation.

7.7.2 Algal photosynthesis/respiration.

In the MINLAKE model, the processes of oxygen production by algal photosynthesis and oxygen consumption by algal respiration are formulated together:

$$\frac{\text{Prodsum} - \text{Resp}}{\text{YCHO2}} \qquad (7.33)$$

Prodsum	=	specific algal growth rate * Algal concentration
Resp	=	rate of respiration (day^{-1})
YCHO2	=	ratio of oxygen produced by photosynthesis to oxygen utilized in respiration.

Values chosen for the specific algal growth rate and the respiration rate have been discussed in paragraph 7.4.1.9 and 7.4.1.13. Regarding the kinetic constant YCHO2 - no specific value was available for Roodeplaat Dam, but the MINLAKE manual indicated a value of 0.0083. After repeated runs, it was found that a value of 0.0075 gave the best results for Roodeplaat Dam.

7.7.3 Detrital decay.

During calibration of the model it became evident that detrital decay is one of the main sinks of oxygen in both the epilimnion and the hypolimnion. However, in the epilimnion, oxygen consumption due to detrital decay is small when compared with the two main sources of oxygen, i.e. reaeration and photosynthesis, therefore the process of detrital decay does not affect the oxygen budget in the epilimnion significantly.

Since there are no sources of oxygen in the hypolimnion, the effect of detrital decay on the oxygen budget is more significant. Also, the importance of linking the detrital decay rate to the aerobic/anaerobic state of the water became evident during

calibration of the oxygen part of the model - good correspondence between simulated and observed oxygen concentration, especially at deeper depths during overturn, was possible only once the detrital decay rate was linked to the aerobic state of the water (*cf* paragraph 7.6).

The values of the coefficients relating to detrital decay will affect simulation of dissolved oxygen also, but the values of these coefficients have been discussed in paragraph 7.6.

7.7.4 Sediment oxygen demand.

In the original MINLAKE model, the user should specify a sediment oxygen demand (mg O_2 m^2 d^{-1}). A demand for oxygen exists in the sediment due to mineralization of organic matter (i.e. bacterial respiration), and chemical reactions (*cf* paragraph 3.4.2.3). In the modified MINLAKE model formulation of the sediment oxygen demand will depend on formulation of detrital decay (*cf* paragraph 5.3.1.3) - if decay of organic matter is represented by the more complex formulation where a distinction is made between particulate and dissolved organic matter (paragraph 5.3.2.2), then formulation of the sediment oxygen demand must provide for the fact that detrital decay will exert a sediment oxygen demand under aerobic conditions only. Under anaerobic conditions dissolved BOD in the bottom sediment cannot decay, and it diffuses back into the water column. Thus, if a distinction is made between dissolved and particulate BOD, sediment oxygen demand is formulated as follows (Eq 5.42):

$$dO/dt = (SB20+BBOT)\left(\frac{DSO}{DSO + SBOK}\right)\theta_{SOD}^{(T-20)}\frac{AREA}{V} \quad (7.34)$$

dO/dt	=	change in dissolved oxygen concentration in a layer (mg l^{-1})
SB20	=	sediment oxygen demand exerted by chemical reactions taking place in the bottom sediment (mg m^{-2} day^{-1})
BBOT	=	sediment oxygen demand due to decay of dissolved organic matter in the bottom sediment (mg m^{-2} day^{-1})
DSO	=	dissolved oxygen concentration in a layer (mg l^{-1})
SBOK	=	switching constant for sediment oxygen demand (mg l^{-1})
θ_{SOD}	=	Arrhenius temperature coefficient for sediment oxygen demand
T	=	water temperature in a layer (°C)
AREA	=	area of bottom sediment in a layer (m^2)
V	=	volume of layer (litre).

If no distinction is made between dissolved and particulate BOD, there is no need to distinguish between the sediment oxygen demand exerted by chemical reactions and that due to detrital decay. In this case, sediment oxygen demand is formulated as:

$$dO/dt = (SB20)\left(\frac{DSO}{DSO + SBOK}\right)\theta_{SOD}^{(T-20)}\frac{AREA}{V} \quad (7.35)$$

In the above equation, SB20 represents the sum of the oxygen demand due to chemical reactions and detrital decay. The rest of the symbols are as per Eq 7.34.

No specific data on sediment oxygen demand for Roodeplaat Dam reservoir could be found. The default value in MINLAKE was 1 mg O_2 m^{-2} d^{-1}, while Tomaszek (1991) found an average sediment oxygen demand of 2.35 mg O_2 m^{-2} d^{-1} for the highly

eutrophic reservoir at Rzeszow in Poland. After repeated runs, the following gave the best results for Roodeplaat Dam:

- If sediment oxygen demand is represented by Eq 7.34, after repeated runs, the optimum value of SB20 (the chemical oxygen demand) was established as 1.5 mg O_2 m^{-2} d^{-1} and that of BBOT as 3 mg O_2 m^{-2} d^{-1}.
- If sediment oxygen demand is represented by Eq 7.35, after repeated runs the optimum value of SB20 was established as 4.5 mg O_2 m^{-2} d^{-1}.

Regarding the dependence of sediment oxygen demand on the aerobic state of the water: According to Tomaszek (1991), at an oxygen concentration of 5-8 mg l^{-1}, oxygen consumption by the sediment is independent of initial oxygen concentration. However, below a concentration of 1.0-1.5 mg l^{-1} oxygen consumption by the sediment dropped considerably. Using the study by Tomaszek as a basis, the value of the aerobic switching constant SBOK in Eqs 7.34/7.35 was set at
0.75 mg O_2 l^{-1}. This value proved to be the optimum value for Roodeplaat Dam also.

Regarding the Arrhenius temperature function for sediment oxygen demand, according to the literature (EPA 1985), there still is some dispute over the value of the Arrhenius temperature coefficient. After repeated runs, a value of 1.026 was found to give the best results for Roodeplaat Dam.

7.7.5 Epilimnetic diffusion coefficient

After correction of coding errors, incorporation of the modifications relating to simulation of dissolved oxygen concentration in the original MINLAKE model, and (what was considered as) optimum values have been chosen for the relevant coefficients, correlation between simulated and observed oxygen concentration was reasonably good, except during the fully mixed period, when simulated dissolved oxygen concentrations at depths greater than about 5-8 metre were consistently too high in comparison with the observed. Eventually it was found that the erroneously high concentrations were due to incorrect coding of the epilimnetic diffusion coefficient

(also see discussion in paragraph 6.3.4.2). In both the original and the modified MINLAKE models, epilimnetic eddy diffusivity is taken to be constant with depth, and is calculated as a function of wind speed only. In the original MINLAKE model the epilimnetic eddy diffusion coefficient is formulated as (Eq 6.8):

$$K_{Ho} = c\,W^{1.3} \qquad (7.36)$$

K_{Ho} = epilimnetic eddy diffusivity (m^2d^{-1})
c = epilimnetic eddy diffusion coefficient
W = daily wind speed at 10 m above the water surface ($m\ s^{-1}$)

The value of **c**, the epilimnetic eddy diffusion coefficient, is reservoir specific, but in the original MINLAKE model **c** is hard-wired to a value of 28.0. The origin of this value could not be established from the available references. After an intensive study, the optimum value of c for Roodeplaat Dam was established as 1.87, a value significantly different from the hard-wired value in the original model (see discussion in paragraph 6.3.4.2).

The value of c has a profound effect on simulation of dissolved oxygen concentration during the fully mixed period. Good correlation between simulated and dissolved oxygen concentration was possible only once the optimum value of this coefficient has been found for Roodeplaat Dam. Time-series graphs of simulated and observed oxygen concentration in Roodeplaat Dam at depths of 1 and 16 m are shown in Fig 7.25. Depth profiles of simulated and observed dissolved oxygen concentration are shown in Fig 7.26. The depth profiles show good correspondence between simulated and observed concentration over the entire depth of the dam, with the biggest discrepancy usually near the surface layer, as is also indicated in the time-series graph in Fig 7.25. These results are discussed further in Chapter 8.

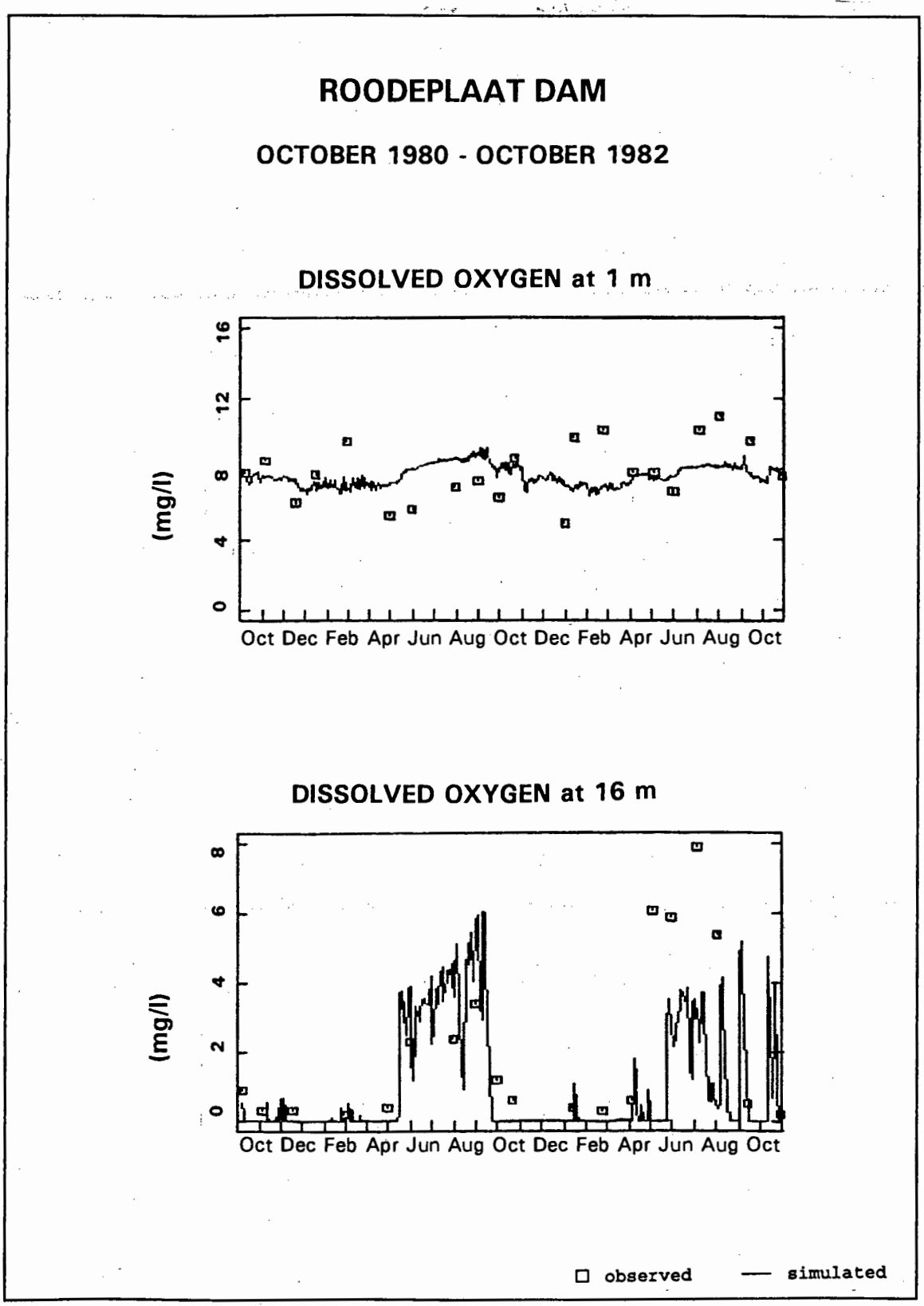

Fig 7.25
Time-series graphs of observed vs simulated dissolved oxygen concentration at 1 and 16 m depth obtained with the modified MINLAKE model on Roodeplaat Dam.

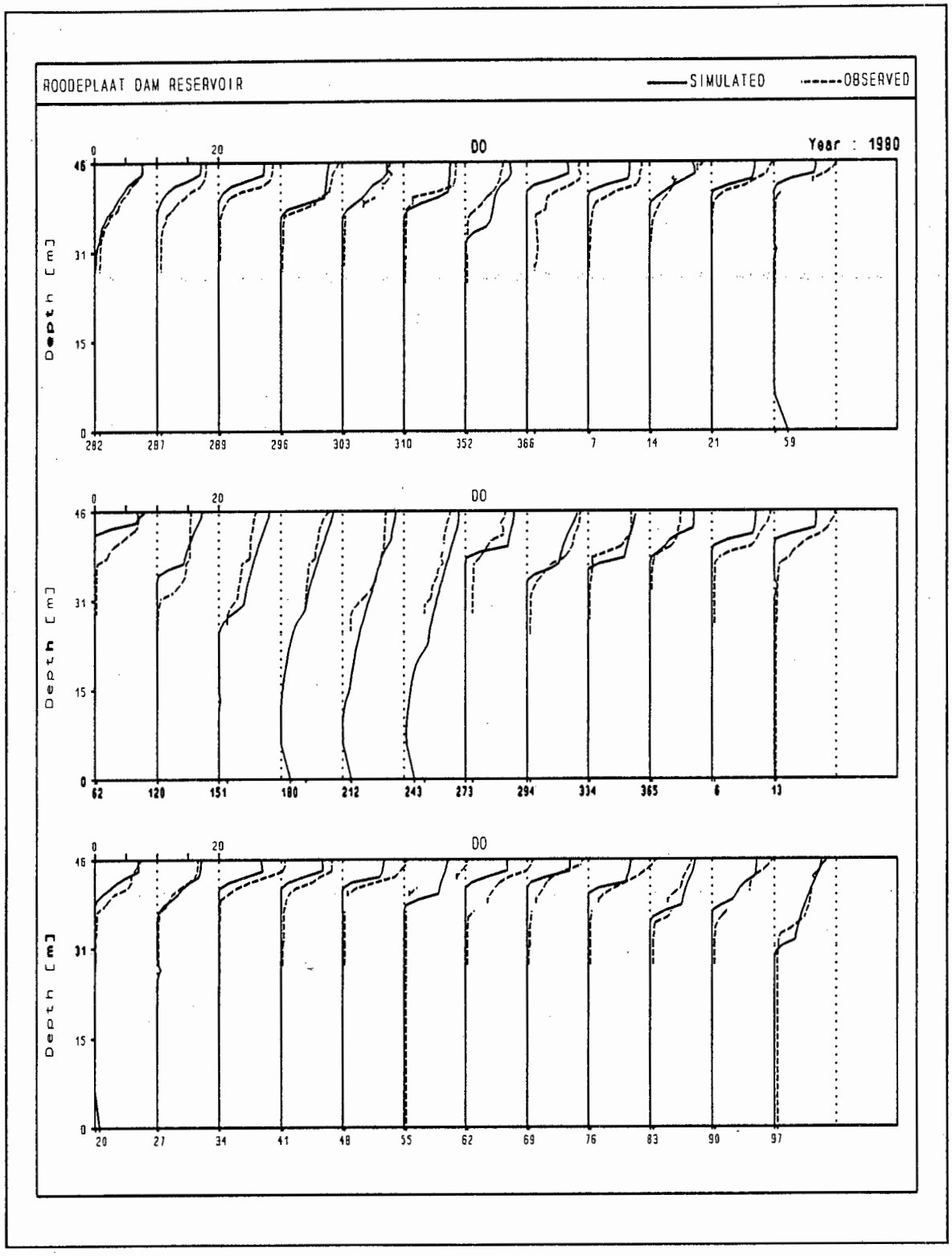

x-axis: Julian day

Oxygen concentration: mg/l

Figure 7.26
Depth profiles of observed and simulated dissolved oxygen concentration obtained with the modified MINLAKE model on Roodeplaat Dam.

7.8 SIMULATION OF TOTAL DISSOLVED SOLIDS (TDS)

In both the original and the modified MINLAKE model, distribution of total dissolved solids (TDS) through the depth of the reservoir is calculated by means of the one-dimensional advection-diffusion equation (Eq 5.1). The only source of TDS is that entering the reservoir from the inflowing rivers. In both the original and the modified MINLAKE model, the user can choose whether TDS sinks should be modelled; for Roodeplaat Dam no sinks of TDS were modelled. Time-series graphs of simulated and observed TDS concentrations at 1 and 16 metre depths are shown in Fig 7.27.

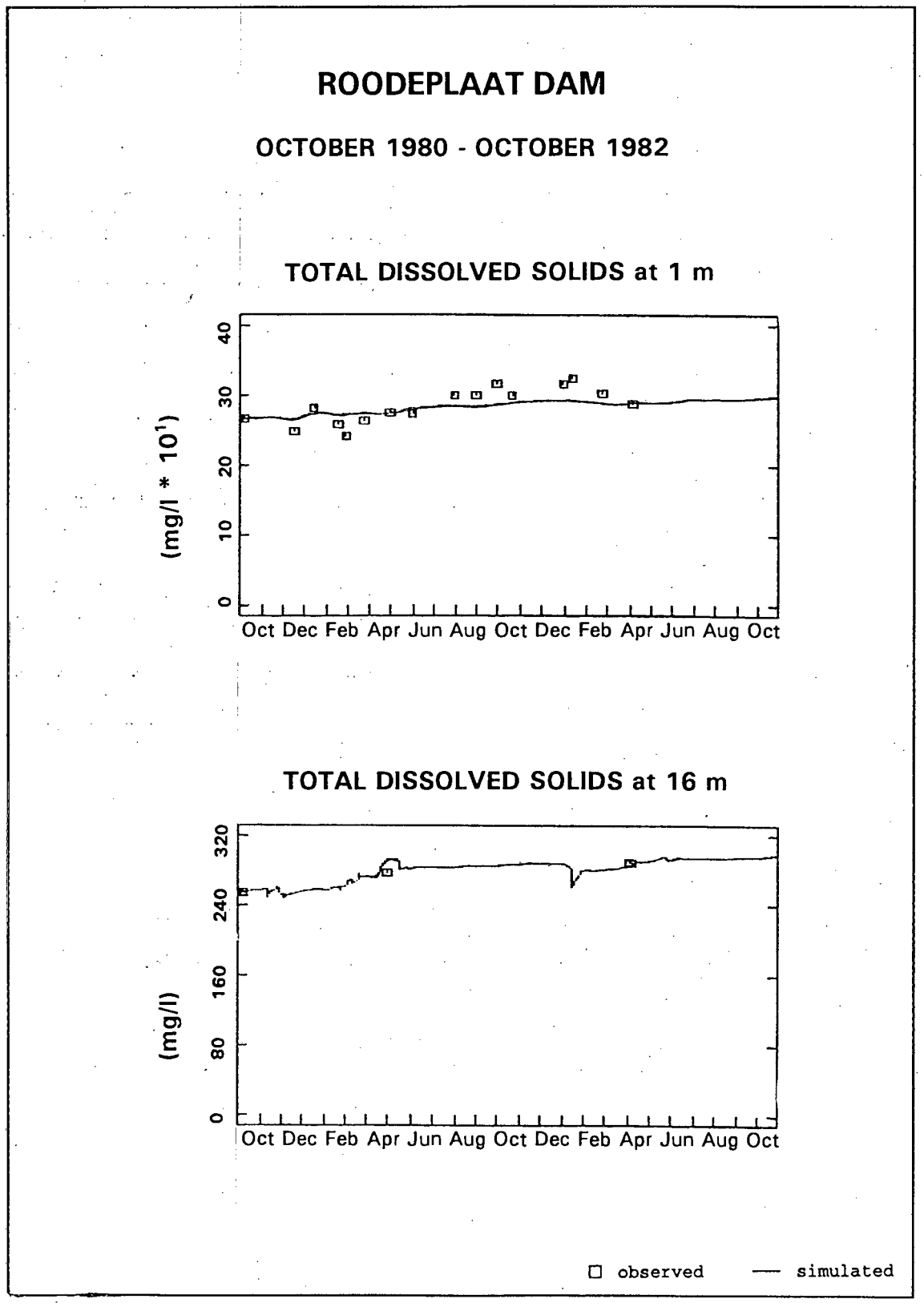

Fig 7.27
Time-series graphs of observed and simulated TDS concentration obtained with the modified MINLAKE model on Roodeplaat Dam.

7.9 FINAL VALUES OF THE WATER QUALITY CALIBRATION COEFFICIENTS AS ESTABLISHED FOR ROODEPLAAT DAM

Regarding the water quality calibration coefficients indicated in Table 7.1, very few of the default values indicated in the MINLAKE manual were found to be suitable for Roodeplaat Dam. Also, simulation of the water quality behaviour of Roodeplaat Dam required modification/addition of a number of processes, which necessitated incorporation of extra calibration coefficients. The water quality coefficients required by the modified MINLAKE model, and the values that gave optimum results for Roodeplaat Dam, are indicated in Table 7.13. The results reported in this chapter are discussed further in Chapter 8, and the merit of modifying/adding certain processes, with the associated increase in calibration coefficients, are discussed in Chapter 9.

Table 7.13 Water quality coefficients required by the modified MINLAKE model, with the values that gave optimum results for Roodeplaat Dam.

COEFFICIENT	VALUE	UNIT
BODPK - decomposition rate for particulate BOD (detritus)	0.08	day^{-1}
QBOD - Arrhenius temperature coefficient for detrital decay	1.047	
*BODSK - dissolved BOD decay rate	0.09	day^{-1}
BODSOK - aerobic switching constant for detrital decay	0.01	mg O_2 l^{-1}
*BBOT - dissolved BOD released from bottom sediment under anaerobic conditions	1.5	g m^2day^{-1}
SB20 - sediment oxygen demand	1.5	g m^2day^{-1}
*BBOTOK - anaerobic switching constant for release of dissolved BOD from bottom sediment (see BBOT)	0.75	mg O_2l^{-1}
FVBOD - fall velocity of particulate detritus	0.002	m^2day^{-1}
BRR - sediment phosphate release rate	0.001	g m^2day^{-1}
BRPK - switching constant for sediment phosphate release /adsorption	0.02	mg O_2l^{-1}
BAA - sediment phosphate adsorption rate	0.01	g m^2day^{-1}
EBRR - equilibrium concentration for sediment phosphate release	0.075	mg P l^{-1}

(continued...)

COEFFICIENT	VALUE	UNIT
QBRR - temperature coefficient for sediment phosphate release/adsorption	1.088	
UPMAX - maximum phosphate uptake rate	4.00 (blue-greens) 0.52 (greens)	mg P mg $Chla^{-1}$ day^{-1}
GROMAX - maximum nutrient saturated growth rate	0.25 (blue-greens) 1.45 (greens)	day^{-1}
TMAX - upper temperature at which algal growth rate is reduced 90%	45 (blue-greens) 20 (greens)	°C
TOPT - optimum temperature for algal growth	40 (blue-greens) 14 (greens)	°C
TMIN - minimum temperature where algal growth rate is reduced 90%	18.5 (blue-greens) 8.0 (greens)	°C
XKR1 - algal respiration rate	0.028 (blue-greens) 0.140 (greens)	day^{-1}
XKM - algal mortality rate	0.025 (blue-greens) 0.140 (greens)	day^{-1}
HSCPA - half saturation coefficient for phosphorus uptake	0.020 (blue-greens) 0.025 (greens)	mg l^{-1}
HSC1 - half saturation coefficient for light limited growth	1200 (blue-greens) 140 (greens)	$\mu E\ m^{-2}s^{-1}$
HSC2 - light inhibition coefficient	2000 (blue-greens) 900 (greens)	$\mu E\ m^{-2}s^{-1}$
XK2 - light extinction coefficient for chlorophyll-a	16	$m_2g\ Chla^{-1}$
XK1 - light extinction coefficient for pure water	0.39	m^{-1}
PMIN - minimum intracellular phosphorus concentration required for growth	0.49 (blue-greens) 1.23 (greens)	mg P mg^{-1} Chla
PMAX - maximum intracellular phosphorus storage capacity	4.90 (blue-greens) 1.23 (greens)	mg P mg^{-1} Chla

(continued...)

COEFFICIENT	VALUE	UNIT
FVCHLA - algal settling rate	0.002 (blue-greens) 0.050 (greens)	m day^{-1}
QCHLA - Arrhenius temperature coefficient for processes relating to algal concentration, eg respiration	1.088 (blue-greens) 1.055 (greens)	
UNMAX - maximum nitrogen uptake rate	0.65 (blue-greens) 0.55 (greens)	mg N mg $Chla^{-1}$ day^{-1}
XNMIN - minimum intracellular nitrogen concentration required for algal growth	5.5 (blue-greens) 1.5 (greens)	mg N mg^{-1}Chla
XNMAX - maximum intracellular nitrogen storage capacity	22.25 (blue-greens) 7.5 (greens)	mg N mg^{-1}Chla
HSCN - half saturation coefficient for nitrogen uptake	0.06 (blue-greens_ 0.034 (greens)	mg l^{-1}
HSCNH - half saturation coefficient for preferential uptake of ammonia over nitrate	0.025 (blue-greens) 0.015 (greens)	mg l^{-1}
XKNNH - nitrification rate	0.02	day^{-1}
XDNK - denitrification rate	0.03	day^{-1}
XKONH - aerobic switching constant for nitrification	0.3	mg $O_2 l^{-1}$
XKONO - anaerobic switching constant for denitrification	3.3	mg $O_2 l^{-1}$
QNNH - Arrhenius temperature coefficient for nitrification	1.063	
QDNK - Arrhenius temperature coefficient for denitrification	1.032	
XNH - nitrification inhibition constant	1.0	mg $NH_4 l^{-1}$
EDNK - denitrification inhibition constant	1.5	mg $NO_3 l^{-1}$
BRNOK - aerobic switching constant for sediment nitrate release	1.00	mg $O_2 l^{-1}$
BRNHK - anaerobic switching constant for sediment ammonium release	0.001	mg $O_2 l^{-1}$
BRNO - sediment nitrate release rate	0.075	mg NO_3 m^{-2} day^{-1}

(continued...)

COEFFICIENT	VALUE	UNIT
BRNH - sediment ammonia release rate	0.2	mg NH_4 m^{-2} day^{-1}
QBNO - Arrhenius temperature coefficient for sediment nitrate release	1.088	
QBRNH - Arrhenius temperature coefficient for sediment ammonia release	1.088	
YNHBOD - mass ratio of ammonia released per dissolved oxygen utilized during detrital decay	0.02	mg NH_4 mg BOD^{-1}
YPBOD - mass ratio of phosphorus produced from detrital decay	0.0009	mg P mg $^{-1}$Chla
YCHO2 - mass ratio of dissolved oxygen produced during photosynthesis, and oxygen utilized during respiration	0.0075	mg Chla $mg^{-1}O_2$
YCBOD - mass ratio of chlorophyll to detritus	0.0075	mg Chla mg BOD^{-1}

* These coefficients are needed only if detrital decay is simulated as a two-step process involving both particulate and dissolved detritus (see paragraph 7.6).

CHAPTER 8

DISCUSSION OF THE SIMULATION RESULTS OBTAINED WITH THE MODIFIED MINLAKE MODEL ON ROODEPLAAT DAM RESERVOIR

In this chapter, the results obtained with the MINLAKE model after incorporation of the modifications as indicated in Chapters 5, 6 and 7, and values for the calibration coefficients[1] as indicated in Table 7.13, are discussed.

8.1 DISCUSSION OF HYDRODYNAMIC SIMULATION RESULTS

The principal outcomes against which the hydrodynamic response can be evaluated are water temperature and mixed layer depth. The vertical distribution of temperature with depth determines the physical structure of the water column, affecting, for instance, transport of nutrients in the water column. Mixed layer depth is indicative of the degree of hydrodynamic mixing that takes place. Hydrodynamic mixing significantly affects the concentration of nutrients and TSS, as well as the distribution of water temperature.

8.1.1 Simulation of water temperature

Time-series graphs of observed and simulated water temperature at 1 and 16 m depth from the surface are shown in Fig 8.1. Depth profiles of observed and simulated water temperature are indicated in Fig 8.2. There is good correspondence between simulated and observed water temperature at all depths for the first 18 months of the simulation period. Thereafter the simulated temperature is higher than the observed.

---

[1] These values are regarded as the optimum values for Roodeplaat Dam.

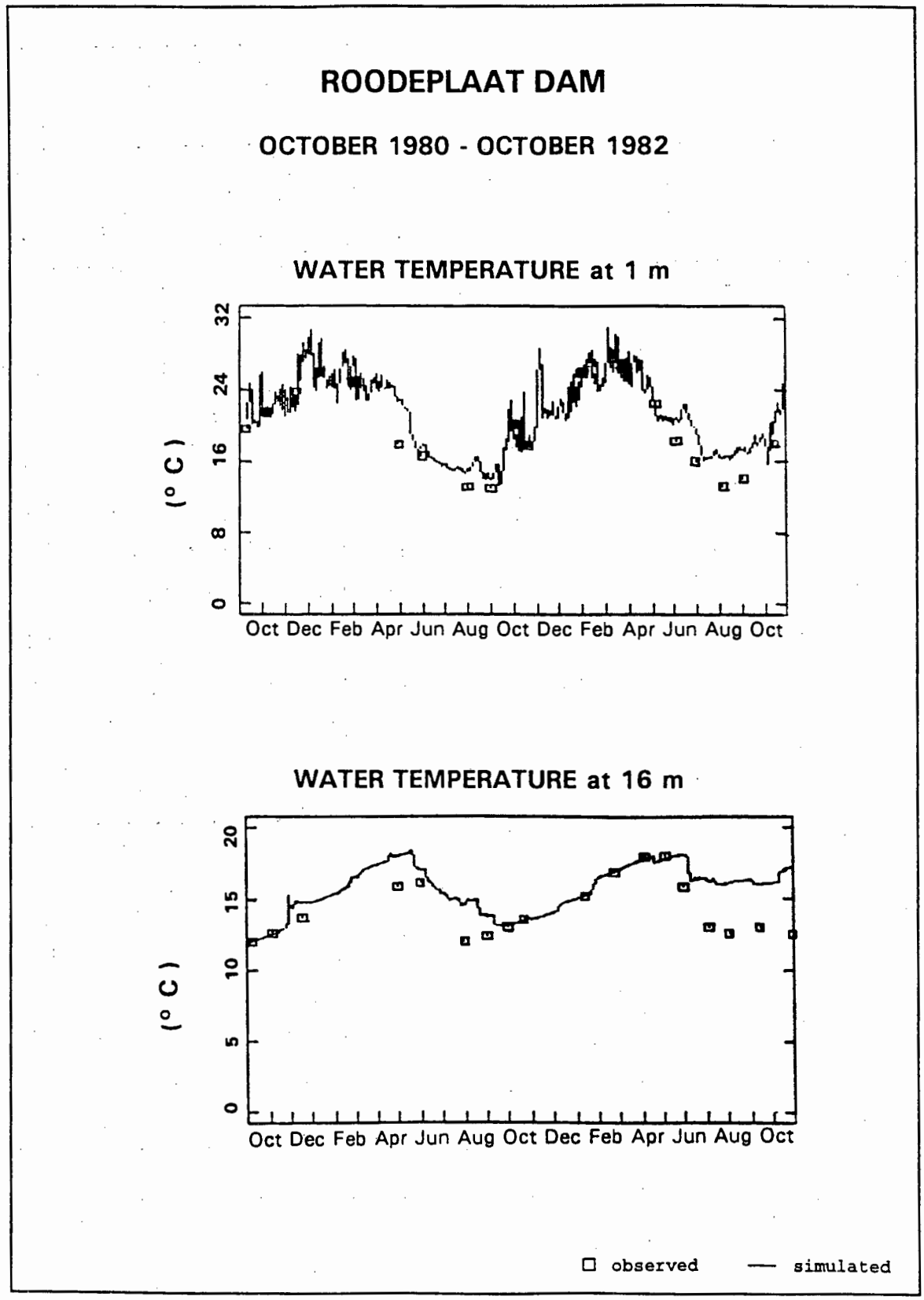

Figure 8.1
Time-series graphs of simulated and observed water temperature as obtained with the modified MINLAKE model on Roodeplaat Dam.

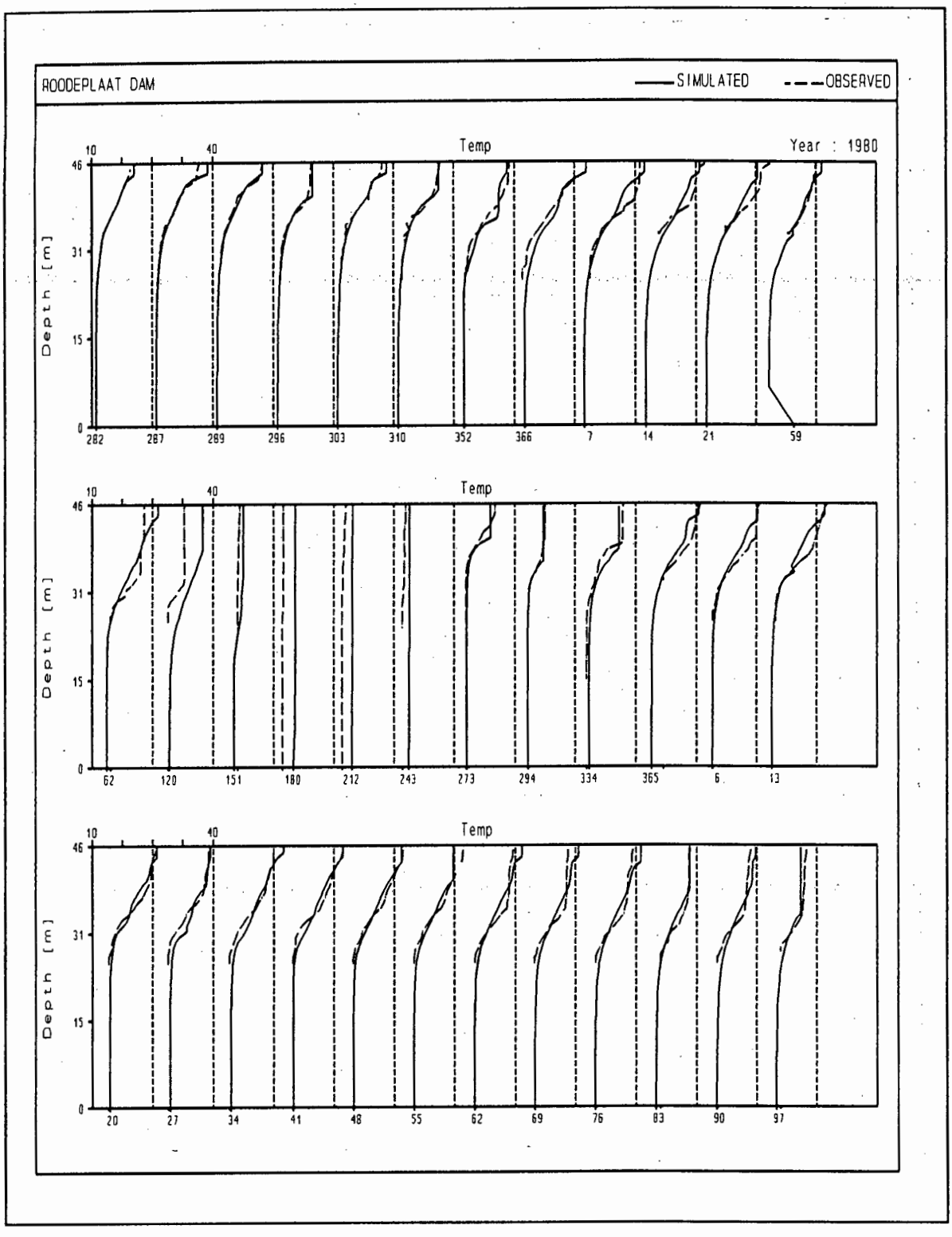

x-axis: Julian day

Temperature: ° C

Figure 8.2
Depth profiles of simulated and observed water temperature as obtained with the modified MINLAKE model on Roodeplaat Dam.

The deviance seems to increase with depth. In spite of an intensive investigation, the reason for this deviant behaviour could not be established. This anomalous behaviour of simulated water temperature is very unfortunate, as it probably will cause simulated concentrations of nutrients, chlorophyll-a and TSS to deviate from the observed also.

The good correspondence between simulated and observed water temperature obtained during the first 18 months of the simulation period is reflected in the depth profiles (Fig 8.2). Periods of stratification and complete mixing are shown clearly. Of interest is the profile for 28 February 1981 (Julian day 59 in the top row in Fig 8.2), indicating an increase in water temperature in the bottom layers. An investigation of the inflow data and the output file created by the model revealed that a storm event occurred in the catchment area of the Pienaars River (the major river entering Roodeplaat Dam) on that day, resulting in a high TSS concentration in the incoming water. Because of the high TSS concentration (and thus high density), the incoming water dispersed in the bottom layers of the reservoir, causing an increase in the temperature of these layers, due to the higher temperature of the inflowing water compared to that in the bottom layers. The effect of this increase in temperature (and dissolved oxygen concentration, see Fig 8.17) on, for instance, nutrient concentrations, is discussed at a later stage.

8.1.2 Simulation of mixed layer depth

Mixed layer depth is indicative of the hydrodynamic mixing that takes place in the reservoir. Simulation of mixed layer depth is depicted in Fig 8.3; periods of stratification and complete mixing are clearly indicated and correspond well with the observed.

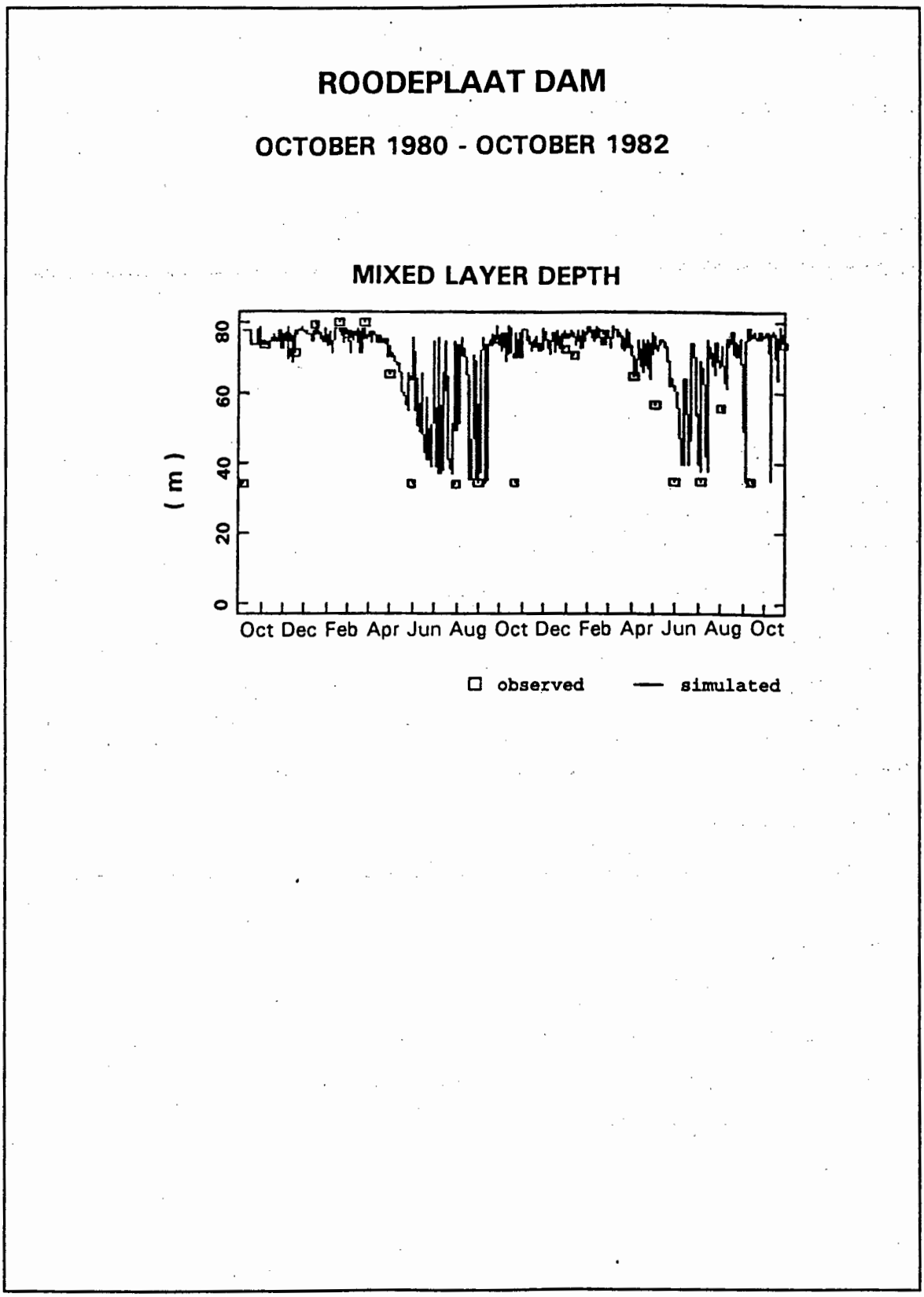

Figure 8.3
Time-series graph of simulated and observed mixed layer depth as obtained with the modified MINLAKE model on Roodeplaat Dam.

Regarding the deviance between simulated and observed water temperature during the last 6 months of the simulation period (see paragraph 8.1.1), initially it was thought that the deviant behaviour might be due to inadequate simulation of mixing depth during the second fully mixed period (Fig 8.3). However, any changes in the coefficients pertaining to simulation of mixed layer depth (eg the wind coefficient, WCOEF, the wind sheltering coefficient WSTR, and the epilimnetic diffusion coefficient, c) to increase correspondence between simulated and observed mixed layer depth during the second period of overturn only resulted in the simulated mixed layer depth during the first period of overturn being far too deep when compared with the observed, whereas no significant improvement in the deviance between simulated and observed temperature could be seen. Also, the changes caused the simulated concentrations of nutrients, chlorophyll-a and dissolved oxygen to deviate significantly from the observed, and, in spite of intensive effort (changing the coefficients relating to simulation of these concentrations) it was not possible to get the simulated and observed concentrations to correspond. Therefore, it was decided that the deviant behaviour of the simulated water temperature during the last six months of the simulation period could not be attributed to possible inadequate simulation of mixed layer depth.

8.1.3 General remarks on simulation of the hydrodynamic behaviour of Roodeplaat Dam.

No significant changes had to be made to the hydrodynamic processes in the original model to simulate the water quality behaviour of Roodeplaat Dam. Also, the hydrodynamic part required virtually no calibration - good correspondence between simulated and observed water temperature was obtained once the epilimnetic, and especially the hypolimnetic eddy diffusion coefficients were specified correctly. This means that it should be relatively easy to simulate the hydrodynamic behaviour,[2] as reflected in simulated water temperature, of any one-dimensional reservoir in South Africa by using the modified MINLAKE model.

---

[2] The structure of the model is such that the hydrodynamic behaviour can be simulated without taking the water quality behaviour into account.

8.2 DISCUSSION OF WATER QUALITY SIMULATION RESULTS

In contrast with calibration of the hydrodynamic part of the original MINLAKE model, several processes had to be modified before successful water quality calibration for Roodeplaat Dam could be obtained. Water quality calibration was complicated by the shortage of observed data in the hypolimnion; virtually no observations were conducted beyond a depth of 20 m. (Maximum depth of reservoir is 43 m).

8.2.1 Dissolved phosphate

Successful calibration of the phosphorus part of the model was possible only once the sediment phosphorus kinetics in Roodeplaat Dam were properly simulated, i.e recognising that phosphate is released from the bottom sediments under anaerobic conditions and adsorbed under aerobic conditions (*cf* paragraph 7.2.1). Time-series graphs of simulated and observed dissolved phosphate concentration at depths of 1 and 16 m are shown in Fig 8.4. Correspondence between simulated and observed data at 1 m depth is very good, and phosphate uptake at 1 m depth during periods of high algal growth is clearly indicated. With regard to dissolved phosphate in the hypolimnion, there are very few observed data points, but the simulated results correspond reasonably well with these isolated observed data points. Also, the simulated results reflect the expected observed behaviour of the reservoir, for instance, with overturn at the end of April 1981 the simulated phosphate concentration at 16 m depth reflects a sudden decrease due to the fact that, in Roodeplaat Dam, phosphate is adsorbed by the bottom sediment under aerobic conditions.

During the last few months of the simulation period the simulated dissolved phosphate concentrations at both 1 and 16 m depths are high in comparison with the observed, most probably this deviance is caused by the erroneously high simulated water temperature during this period (*cf* paragraph 8.1.1).

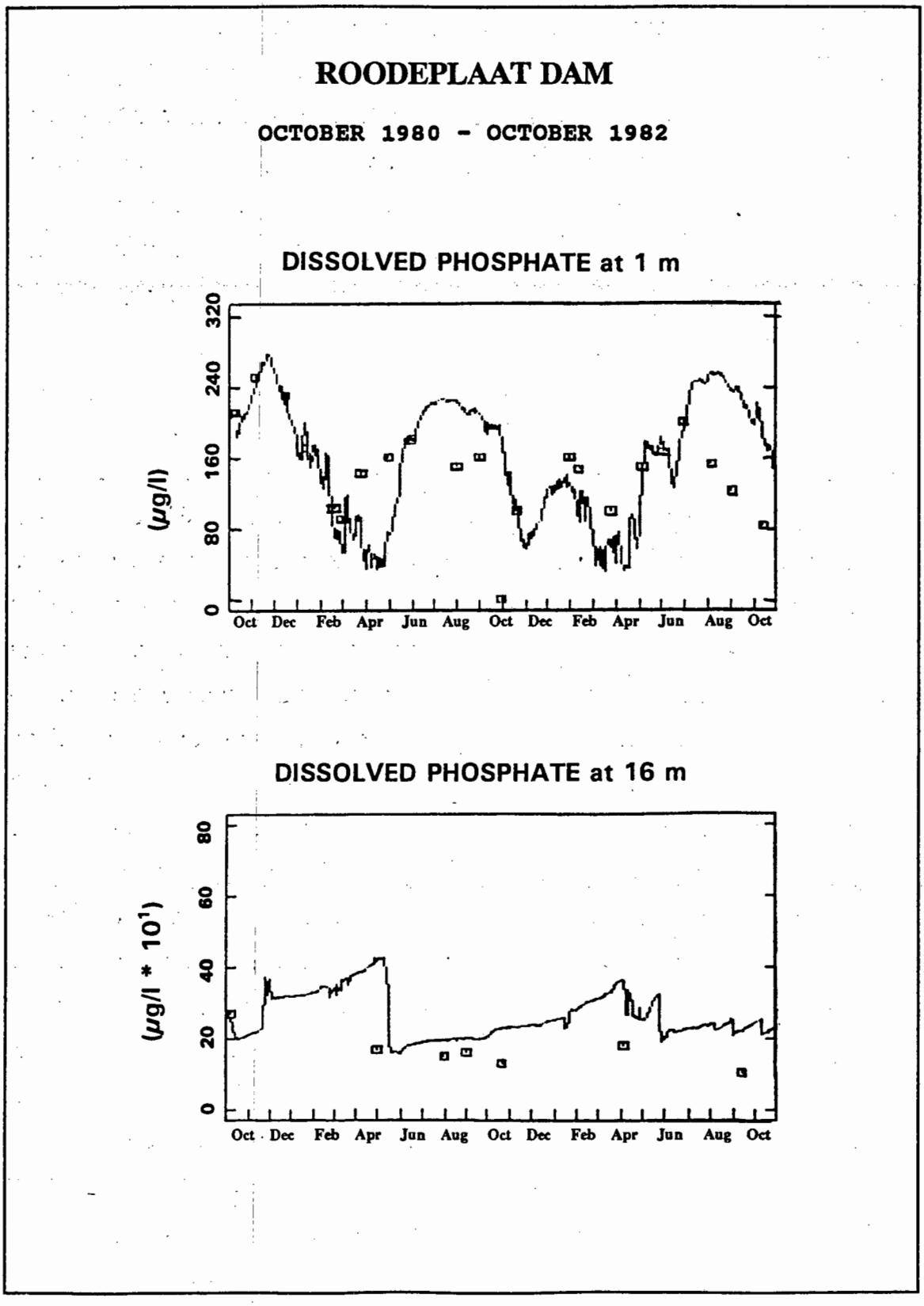

Fig 8.4
Time-series graph of observed and simulated dissolved phosphate concentration at 1 and 16 m depth in Roodeplaat Dam, as obtained with the modified MINLAKE model and optimum values for the calibration coefficients.

Depth profiles of simulated and observed dissolved phosphate concentration are shown in Fig 8.5. Though comparison of simulated and observed behaviour is impeded by the lack of observed data below the epilimnion, again the simulated depth profiles reflect the expected behaviour of the reservoir. For instance, one of the main sources of phosphate is that entering the reservoir via the three inflowing rivers. The depth profiles in Fig 8.5 clearly reflect the effect of inflowing phosphate concentrations, as well as the depth at which these concentrations enter the reservoir. Periods of stratification and turn-over can be identified also in the depth profiles.

The simulated depth profiles are a good indication of the complex interaction between reservoir processes, but care should be exercised when interpreting the results. For instance, as mentioned previously, on Julian day 59 (28 February 1981), a storm event took place, and, because of the resultant high TSS concentration in the Pienaars River (i.e. a density effect), the water from this river dispersed in the bottom layers of the dam, thereby increasing the temperature and dissolved oxygen concentration in these layers. As a result, the dissolved phosphate concentration in these layers decreased, because phosphate is adsorbed by the bottom sediment under aerobic conditions. The effect of the decrease in phosphate concentration in the bottom layers can still be seen three days later, on Julian day 62. The subsequent increase in dissolved phosphate concentration in the bottom layers on, for instance, Julian days 180 (29 June 1981) and 212 (31 July 1981) seem anomalous, as aerobic conditions existed in the bottom layers on these days, i.e. one would expect a decrease in dissolved phosphate concentration due to adsorption. Also, usually an increase in dissolved oxygen concentration in the bottom layers of the reservoir of the type reflected in the depth profile for Julian day 212 (Fig 8.17) is caused by inflowing river water dispersing in the bottom layers due to a high TSS concentration in the river after a storm event, as was the case with Julian day 59. However, an investigation of the river inflow data and the meteorological data did not indicate a storm event, nor abnormally high TSS concentrations on Julian days 180 and 212. Further investigation of the inflow data showed that dispersal of the inflowing water into the bottom layers of the reservoir probably was due to the low temperature of the inflowing water. For instance, on Julian day 180 the water temperature in the Pienaars River was 10°C.

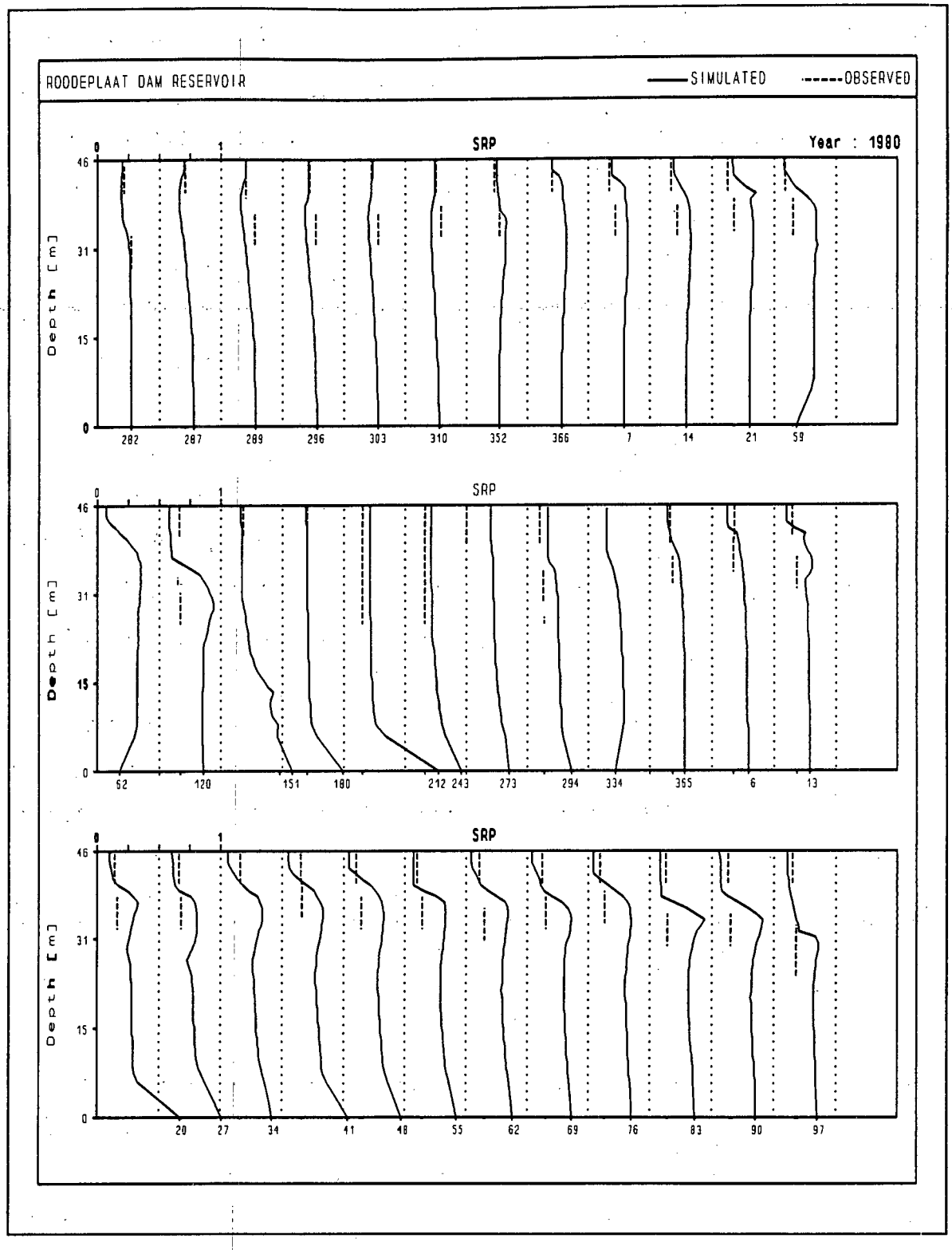

x-axis: Julian day

Phosphate concentration: mg/l

Fig 8.5
Depth profiles of simulated and observed phosphate concentration as obtained with the modified MINLAKE model on Roodeplaat Dam for the period October 1980 to October 1982.

Thus, on Julian day 59 the incoming water dispersed in the bottom layers of the dam due a storm event (density effect), whereas on Julian days 180 and 212 low flow conditions prevailed, and the incoming water dispersed in the bottom layers due to a temperature effect.

Regarding the dissolved phosphate concentration in the bottom layers, because of the storm event on Julian day 59, the phosphate concentration in the incoming rivers was quite low, eg in the Pienaars River it was 0.55 mg l^{-1}, compared to an average concentration in this river of 3.69 mg l^{-1} for the study period. Because the incoming phosphate concentration was so low, adsorption of phosphate by the sediment in the bottom layers (as a result of aerobic conditions caused by the oxygen in the incoming water) caused a decrease in dissolved phosphate concentration in the bottom layers of the reservoir, as explained previously. However, on Julian day 180 (29 June 1981) typical low flow conditions existed in the incoming rivers, as reflected in the dissolved phosphate concentration in the Pienaars River - 5.48 mg l^{-1} compared to the average of 3.68 mg l^{-1} for this river during the study period. The aerobic conditions that existed in the bottom layers on this day mean that phosphate must have been adsorbed by the bottom sediment in these layers. However, the phosphate concentration in the incoming rivers was so high that it caused a nett increase in dissolved phosphate concentration in the bottom layers where the cold incoming water dispersed.

8.2.2 Ammonia

The original model makes provision for the processes of nitrification, and ammonia release from the bottom sediments, but does not recognise that nitrification can occur under aerobic conditions only, and that ammonia is released at different rates from the bottom sediments under aerobic and anaerobic conditions (Jørgensen 1980). Incorporating this behaviour into the model by linking the rates of these two processes to the aerobic/anaerobic state of the water through use of switching functions played an important role in calibrating of the nitrogen part of the model (*cf* Chapter 5 and 7).

Time-series graphs of the ammonia concentration at depths of 1 and 16 m are shown in Fig 8.6. Depth profiles are shown in Fig 8.7.

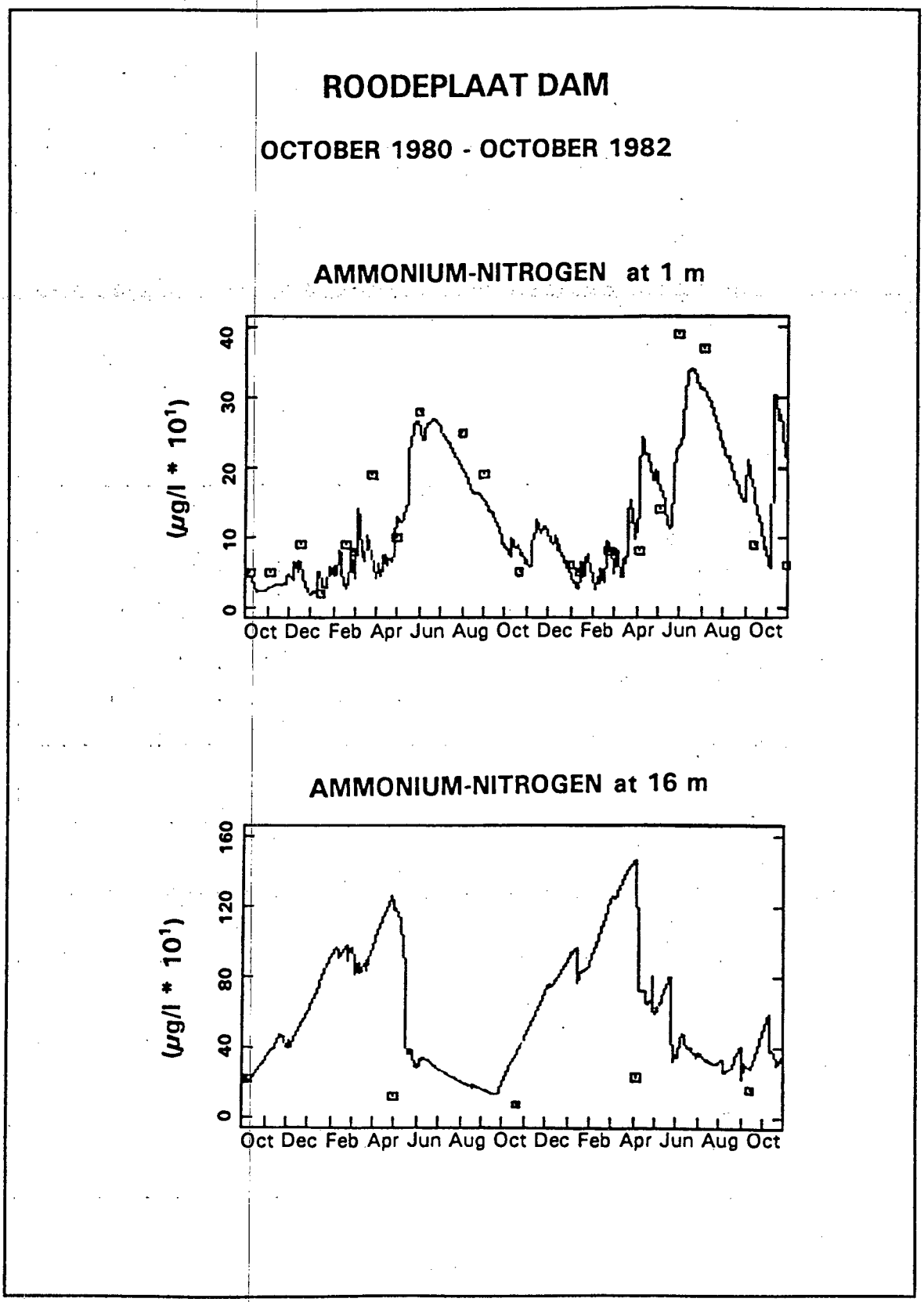

Fig 8.6
Time-series graphs of observed and simulated ammonia concentration at 1 and 16 m depth in Roodeplaat Dam, as obtained with the modified MINLAKE model and optimum values for the calibration coefficients.

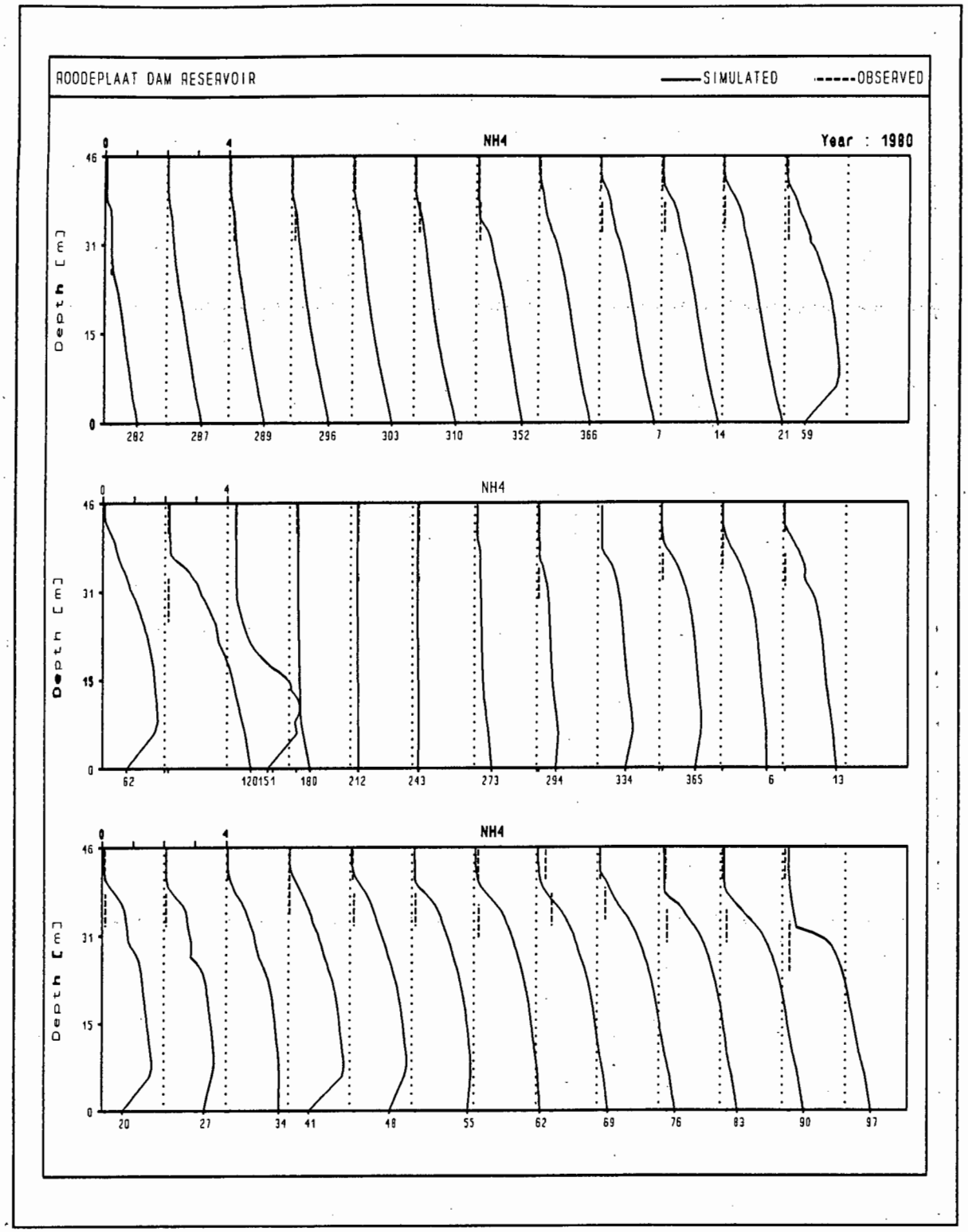

x-axis: Julian day

Ammonia concentration: mg/l

Figure 8.7
Depth profiles of simulated and observed ammonia concentration obtained with the modified MINLAKE model on Roodeplaat Dam for the period October 1980 to October 1982.

Correspondence between observed and simulated ammonia concentration at 1 m depth is very good. Due to a lack of data in the hypolimnion, it was not possible to come to a firm conclusion about the correspondence between observed and simulated ammonia concentration in the hypolimnion. However, the simulated behaviour at both 1 and 16 m depth seems to reflect the behaviour generally expected in reservoirs, for example Hartebeespoort Dam (Ashton 1994): during stratification there is a built-up of ammonia in the hypolimnion due to ammonia release from the sediments, but with the onset of overturn (April) this ammonia is mixed throughout the water body, causing a sudden increase in the epilimnetic concentration. This is reflected in the simulated concentration at 1 m depth. The elevated ammonia concentration in the hypolimnion soon decreases, this decrease being caused by nitrification that occurs from the surface to the bottom of the reservoir, due to the aerobic conditions that exist throughout the reservoir during overturn. This behaviour also is reflected in the simulated concentrations at 1 and 16 m depth.

With regard to the simulation of ammonia in the hypolimnion, the sediment in Roodeplaat Dam probably has a high nutrient load assimilation due to nutrient rich inflow and mineralization of detritus, therefore an important source of ammonia may be that released from the bottom sediments. Simulation of ammonia in the surface layer was successful only by assuming the sediment was a major source of ammonia. The simulated concentration in the hypolimnion may seem high (eg. Fig 8.7, Julian day 120 - 30 April 1991 - where the hypolimnetic ammonia concentration is > 2.0 mg l^{-1}), but in Hartbeespoort Dam, for instance, observed hypolimnetic ammonia concentrations are sometimes as high as 5 mg l^{-1} (NIWR 1985).

Furthermore, though the simulated ammonia concentrations do not seem to correspond well with the few observed values available for the hypolimnion in Roodeplaat Dam, it should be remebered that the observed values were obtained from an integrated sample taken over 5 meters. The depth profiles indicate that integrated samples were taken very close to, or in, the region of the metalimnion where rapid changes with depth usually occur - the integrated sample may not be representative of all the depths over the 5 m sampling interval.

8.2.3 Nitrate

The original MINLAKE model does not make provision for denitrification, a process that is important in virtually all South African reservoirs. Successful simulation of nitrate concentrations in Roodeplaat Dam was possible only once the process of denitrification was incorporated into the model, and the rates of denitrification and sediment nitrate release were linked to the aerobic/anaerobic state of the water by means of switching functions (*cf* Chapters 5 and 7).

In Fig 8.8 the correspondence between simulated and observed nitrate concentration at depths of 1 and 16 m is shown. Depth profiles are shown in Fig 8.9. The simulated results show good correspondence with the observed data. The simulated results are also in correspondence with nitrate behaviour generally observed in South African reservoirs; for instance, in Hartebeespoort Dam it has been observed (Ashton 1994) that there is a massive built-up of nitrate during overturn, i.e from April to September. This trend is reflected in the simulated data for Roodeplaat Dam. As soon as anaerobic conditions develop in the hypolimnion, denitrification occurs, which leads to a loss of nitrate from the system. Once again this trend is clearly reflected in both the time-series graphs and the depth profiles for Roodeplaat Dam (Fig 8.8 and 8.9).

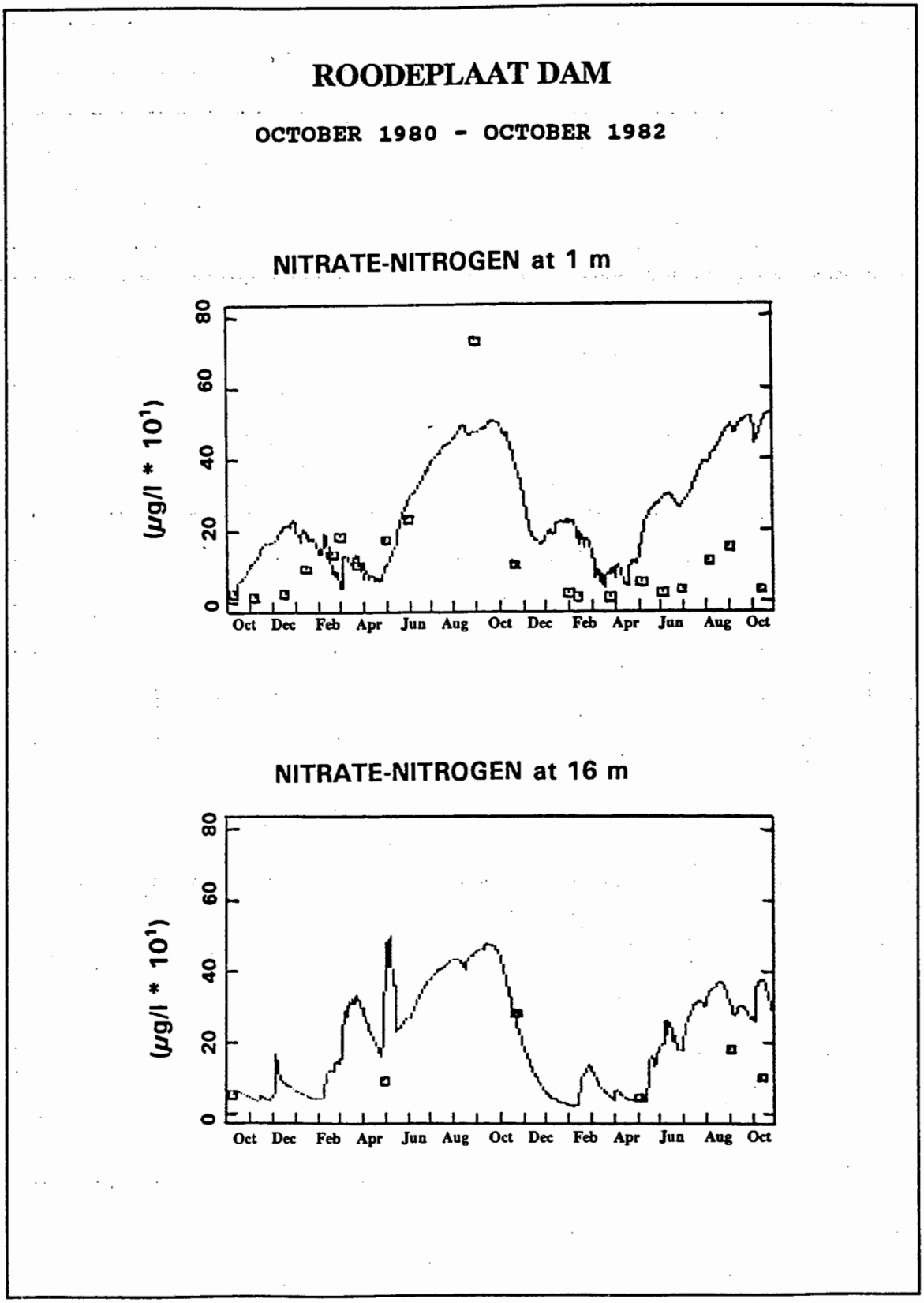

Fig 8.8
Time-series graphs of observed and simulated nitrate concentration in Roodeplaat Dam, as obtained with the modified MINLAKE model and optimum values for the calibration coefficients

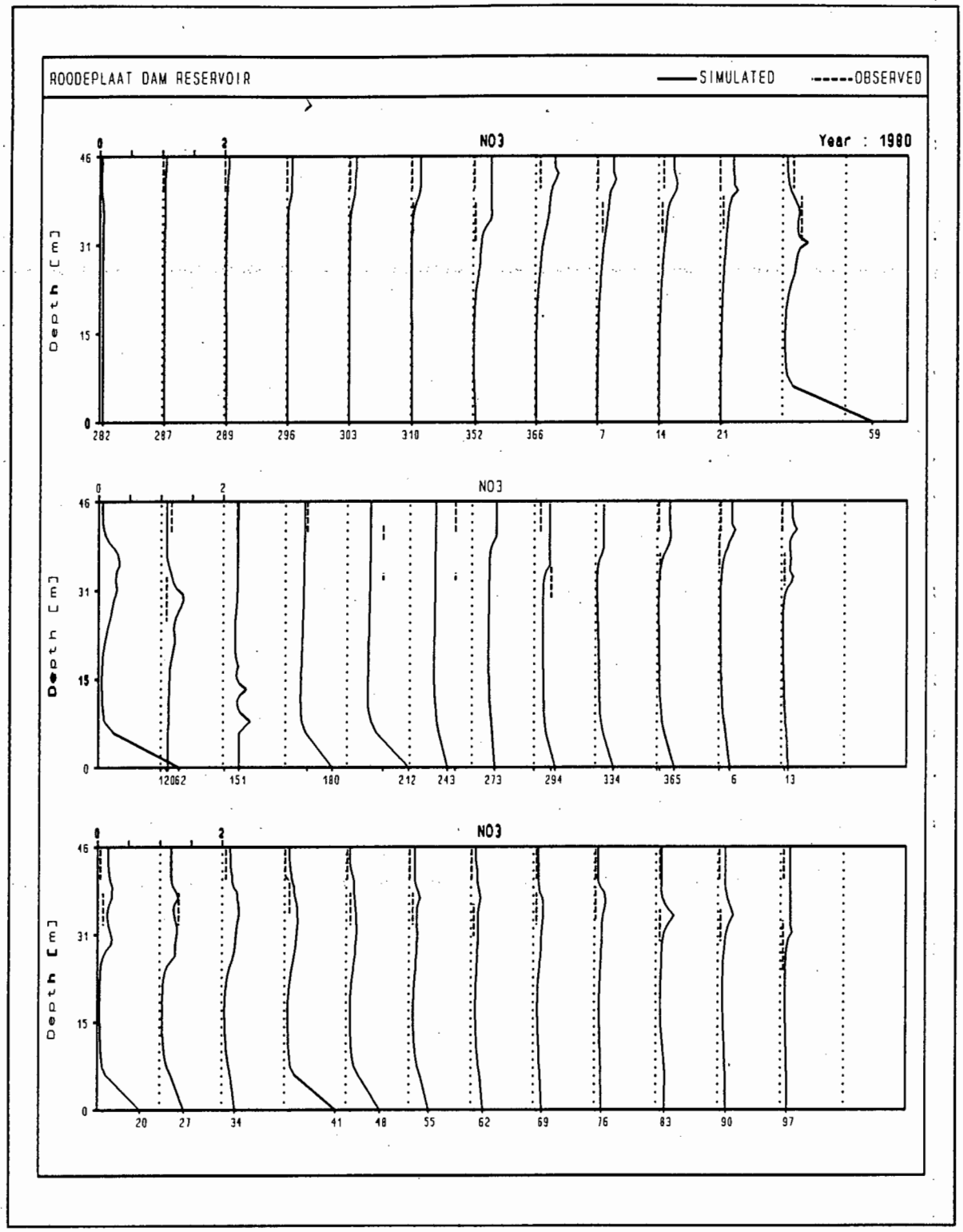

x-axis: Julian day

Nitrate concentration: mg/l

Figure 8.9
Depth profiles of simulated and observed nitrate concentration obtained with the modified MINLAKE model on Roodeplaat Dam for the period October 1980 to October 1982.

8.2.4 Algae

In both the original and modified MINLAKE model, algal growth rate is simulated as a change in chlorophyll-a concentration. Up to three algal classes can be simulated. No changes had to be made to the processes relating to algal growth rate in the original MINLAKE model to enable simulation of algal concentration in Roodeplaat Dam. However, simulation of the algal concentration in Roodeplaat Dam required simulation of at least two algal groups (blue-green and green algae), and simulation of both phosphorus and nitrogen as limiting nutrients.

Time-series graphs of simulated and observed chlorophyll-a concentrations at depths of 1 and 16 m from the surface are shown in Fig 8.10. Depth profiles are depicted in Fig 8.11). The correspondence between observed and simulated chlorophyll-a concentration is very good. Furthermore, the simulated concentration at 1 m depth clearly indicates algal succession from blue-green to green to blue-green algae over the two year simulation period (Fig 8.10a). The ability of the model to simulate algal succession successfully is particularly valuable, as the modified MINLAKE model is the only model calibrated for a South African reservoir capable of successfully simulating algal succession at present.

ROODEPLAAT DAM

OCTOBER 1980 - OCTOBER 1982

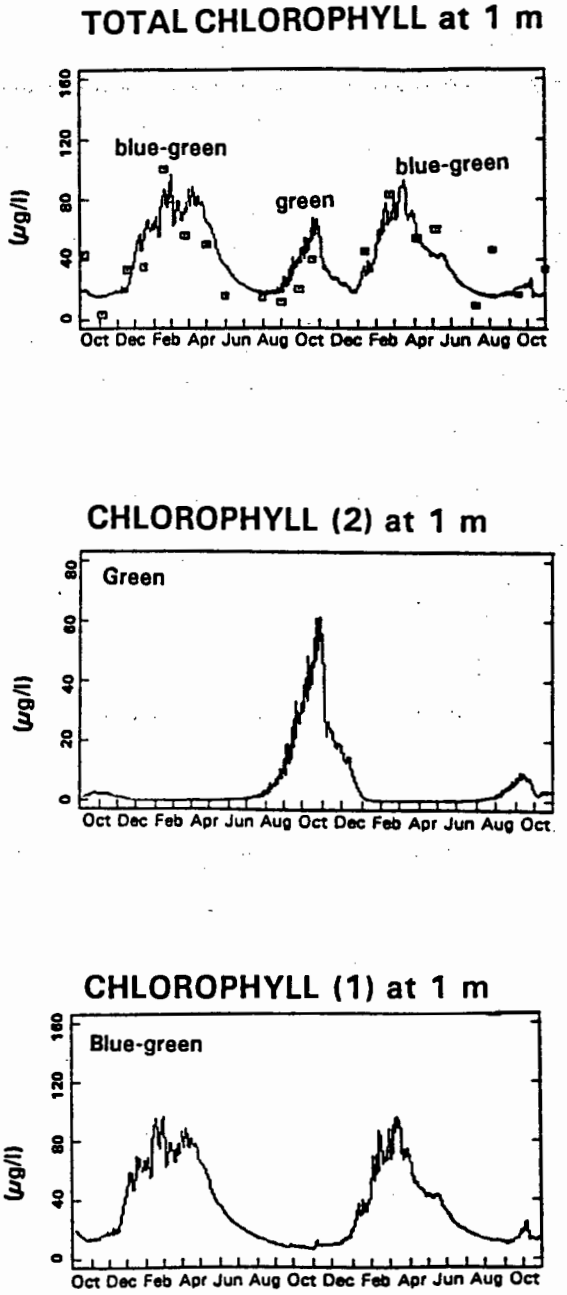

Fig 8.10
Time-series graphs of observed vs simulated chlorophyll-a concentration in Roodeplaat Dam obtained with the modified MINLAKE model and optimum values for the calibration coefficients

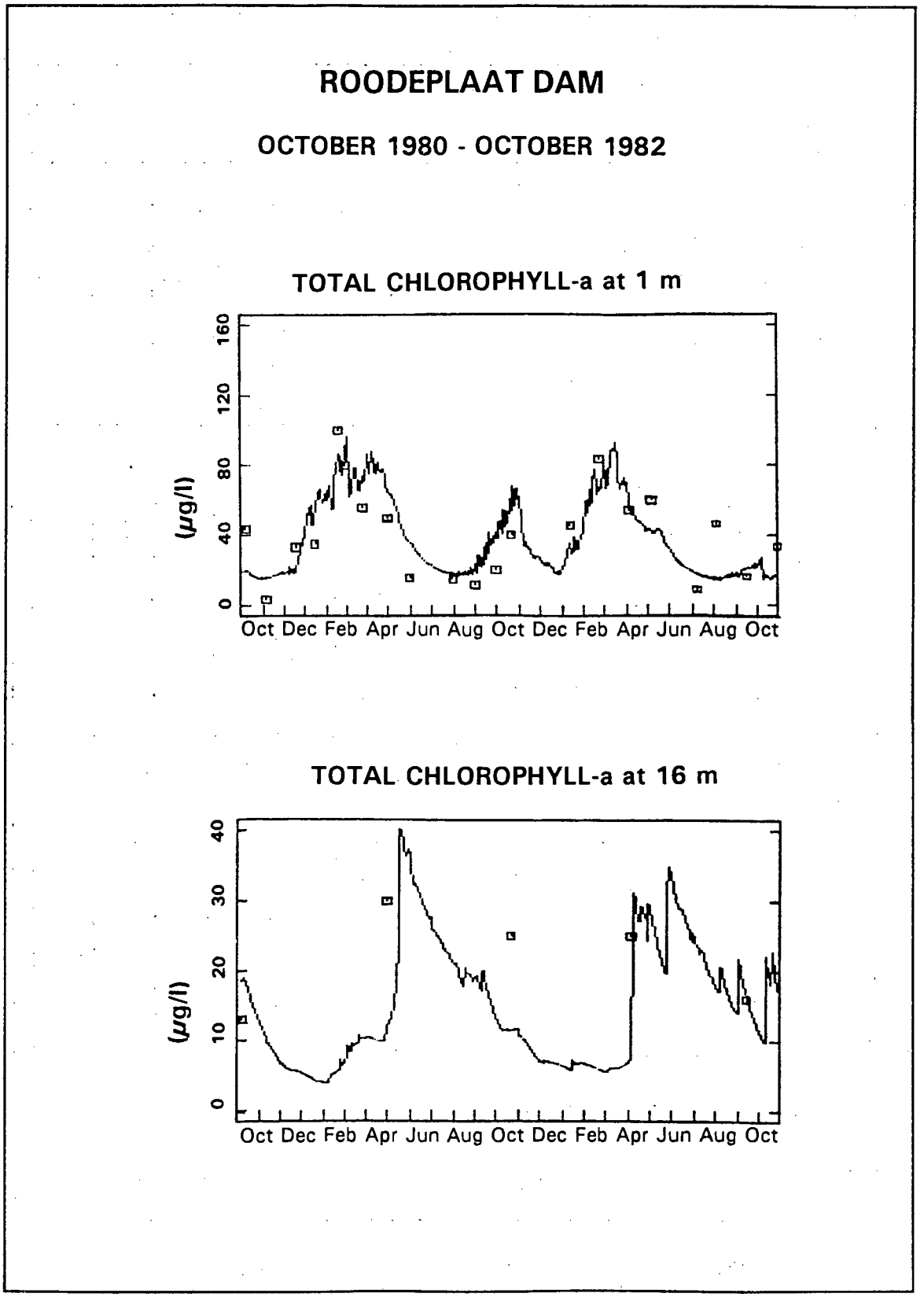

Fig 8.10a)
Time-series graph of observed vs simulated chlorophyll-a concentration in Roodeplaat Dam, as obtained with the modified MINLAKE model and indicating algal succession.

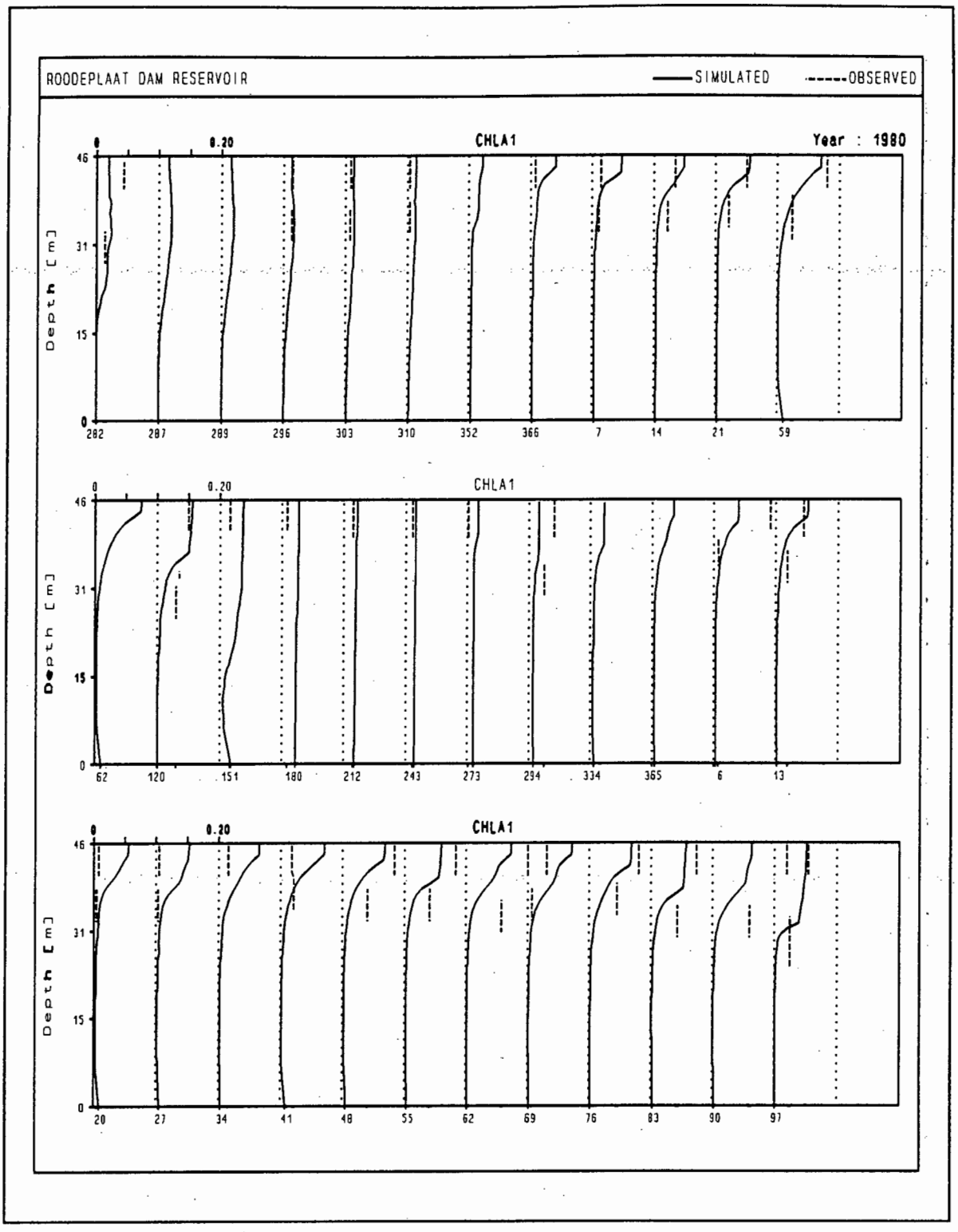

x-axis: Julian day Chlorophyll-a concentration: mg/l

Fig 8.11
Depth profiles of observed and simulated chlorophyll-a concentration in Roodeplaat Dam, as obtained with the modified MINLAKE model and optimum values for the calibration coefficients.

Regarding the factors that affect algal succession - during calibration of the model to Roodeplaat Dam simulation of algal succession was possible only once the coefficients relating to the effect of water temperature and light intensity on algal growth rate have been specified correctly. For instance, even though the MINLAKE manual indicates that the model is not very sensitive to the value of TMAX[3], the value of TMAX for green algae, and TMIN for blue-green algae, did have a profound effect on algal succession - in Roodeplaat Dam, observed green algal growth occurs mainly in late winter/spring, followed by blue-green algae during summer and early autumn. If TMAX for green algae is specified too high, unwanted simulated green algal growth occurs during November/December, contrary to the observed. The TMAX value for blue-green algae did not have any significant effect on algal succession. Similarly, if TMIN for blue-green algae is specified too low, unwanted simulated blue-green algal growth occurs during spring, contrary to the observed. TMIN for green algae did not have a significant effect on simulation of algal succession.

The finding that simulation of algal succession is sensitive to the values of TMAX for green algae, and TMIN for blue-green algae, is in accordance with studies that have been done on other South African dams. For instance, in a study done by Kruger *et al* (1978) on *Microcystis aeruginosa* from Hartbeespoort Dam, it was found that it is sensitive to low temperatures, (virtually no growth occurred below 17.5°C), but that it can adapt to temperatures as high as 45°C. Green algae do not have the same ability to adapt to high temperatures. Furthermore, according to Reynolds (1984), in the presence of high nutrient concentrations (as is the case in Roodeplaat Dam), usually temperature and light become the principal factors that determine algal succession.

Regarding the factor that limits algal growth rate, a popular method that is used widely in South Africa to predict whether phosphorus or nitrogen will potentially limit algal

---

[3] TMAX: upper temperature where algal growth rate is reduced 90%.
TMIN: lower temperature where algal growth rate is reduced 90%. In the original MINLAKE model, TMIN was hard-wired to a value of 0°C. In the modified model, the user can choose the value of TMIN.

growth rate, is to calculate the N:P ratio. However, as was discussed in paragraph 3.4.7, this method should be used with care - often the ratio is calculated using the external concentrations of phosphorus and nitrogen, or even the concentrations of total phosphorus and total nitrogen, whereas algal growth rate is a function of internal nutrient concentration. Also, the N:P ratio method does not take into account that light may be a limiting factor. In fact, light as a possible limiting factor seems to have been neglected in studies of South African impoundments during the last 12 years, possibly because of the wide use of the N:P ratio method to identify limiting conditions.

Another way of determining the limiting nutrient in a reservoir, is to conduct algal bio-assay studies. However, these studies indicate the limiting nutrient at the time of the study only, and also do not take light as a limiting factor into account.

In this study, a new approach has been developed wherein the MINLAKE model is used to determine, on a daily basis, the factor that limits algal growth rate in an impoundment, taking into account phosphorus, nitrogen and light as limiting factors. In calculating algal growth rate, the model expresses the effect of phosphorus, nitrogen, and light on the algal growth rate, each as a ratio between zero and one - the factor with the lowest value is regarded as the limiting factor (*cf* Chapter 4 and 5). However, because these values are not retained as output data in the model, it was not evident to the user which of the three factors are limiting at any given moment. In order to identify the limiting factors, the model was modified to retain these values by printing it to a separate file. From this file, the daily values of each of the limiting factors can be represented in graphic format - the graph of factors that limited growth rate of blue-green algae in Roodeplaat Dam, is shown in Fig 8.12.

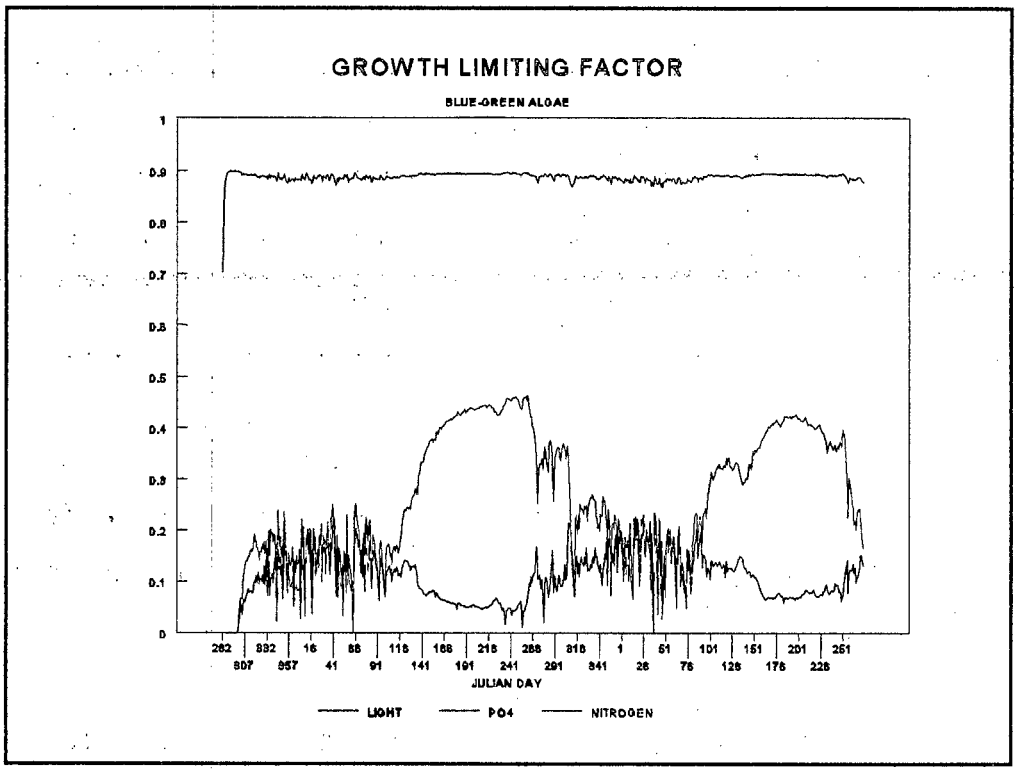

Figure 8.12
Factors limiting growth of blue-green algae in Roodeplaat Dam Reservoir.

From the graph it is evident that, during the study period, the dissolved phosphate concentration in Roodeplaat Dam was so high that it never was a limiting factor as far as blue-green algal growth rate is concerned, and that the growth rate of blue-green algae in Roodeplaat Dam was limited mostly by nitrogen concentration and/or light.

The ability of the model to simulate algal succession, and the fact that the model can give an indication of the factor that limits algal growth rate on a daily basis, indicates that the model can be a powerful aid in evaluating different management strategies to minimize eutrophication.

8.2.5 Total inorganic suspended sediment (TSS)

TSS concentration is modeled as an integral part of the processes that govern water quality and temperature distribution. During calibration of the model on Roodeplaat Dam, it was found that, although TSS concentration did not have a significant effect on simulation of water temperature, it did have a very definite effect on simulation of algal growth rate, because of its effect on the underwater light climate. Thus it was important to simulate TSS concentration as accurately as possible, but simulation was hampered severely by the fact that TSS concentrations are not measured in any of the rivers flowing into Roodeplaat Dam, nor in the dam itself. This problem was solved by synthesizing daily TSS concentrations for the three rivers from river flow rate. TSS concentrations in the reservoir were approximated from secchi disc depth data (see discussion in Appendix A1).

In Fig 8.13 time-series graphs of calculated and simulated TSS concentrations at 1 and 16 m depth from the surface are shown. The simulated concentration corresponds well with the data calculated from secchi disc depth measurements. Also, as expected, the simulated concentration follows the same trend as total TSS entering the reservoir (Fig 8.14).

Depth profiles of simulated TSS concentration in Roodeplaat Dam are shown in Fig 8.15. No observed data are available with depth, but if the simulated profiles are compared to that obtained by Ritchie *et al* (1978) during a study on reservoirs in northern Mississippi, the same trend is observed, i.e. during the fully mixed period TSS concentration is nearly homogeneous with depth, but as the thermocline develops with the onset of stratification, a gradient develops in the distribution of TSS also. TSS concentration in the epilimnion remains nearly homogeneous, but it increases with depth in the hypolimnion. The heavy TSS load that enters the dam via the inflowing rivers during storm events also is indicated clearly (*cf* Julian Day 59).

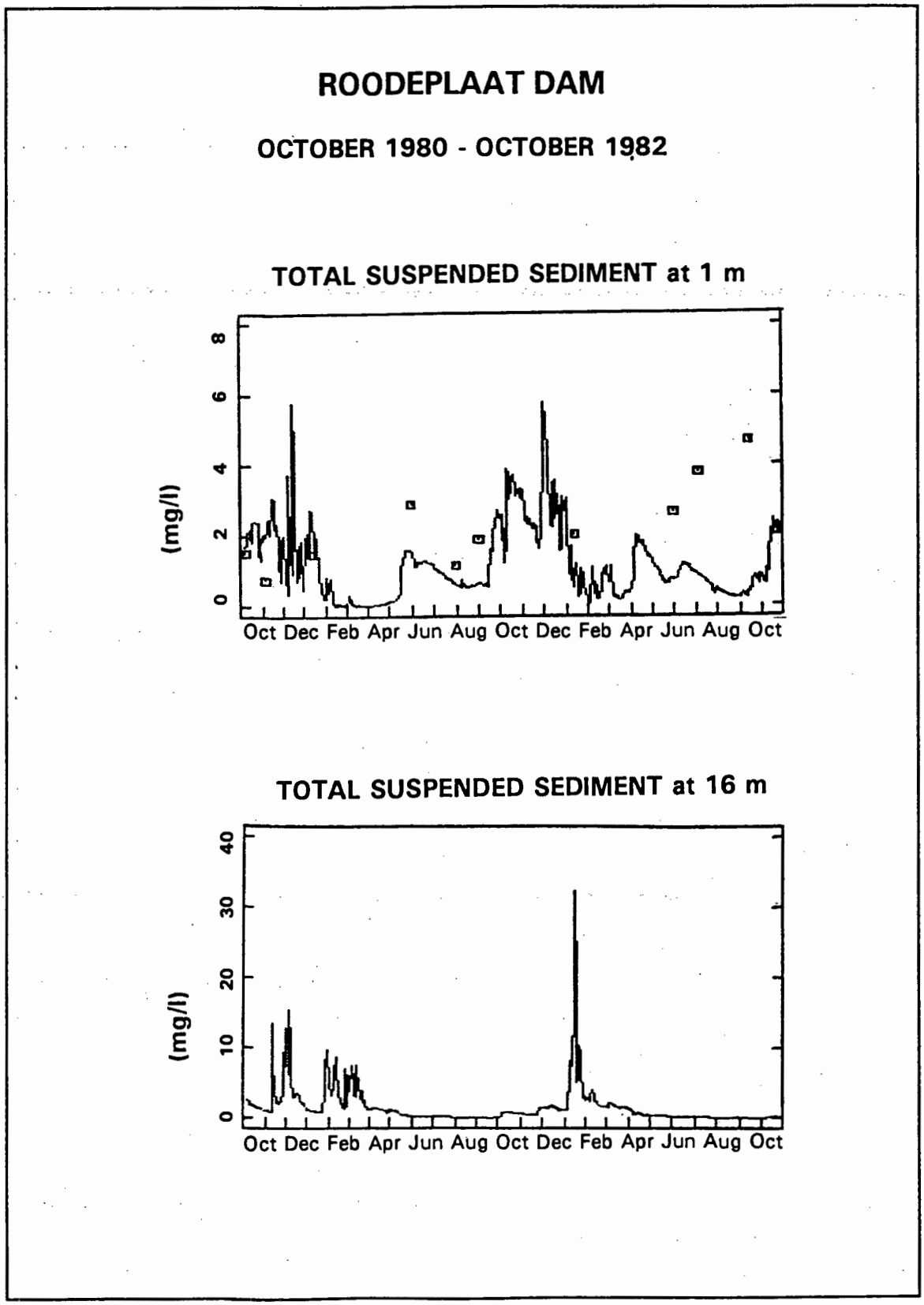

Fig 8.13
Time-series graph of calculated and simulated TSS concentration in Roodeplaat Dam as obtained with the modified MINLAKE model utilising particle radii of 1 μm (non-storm events) and 2 μm (storm events).

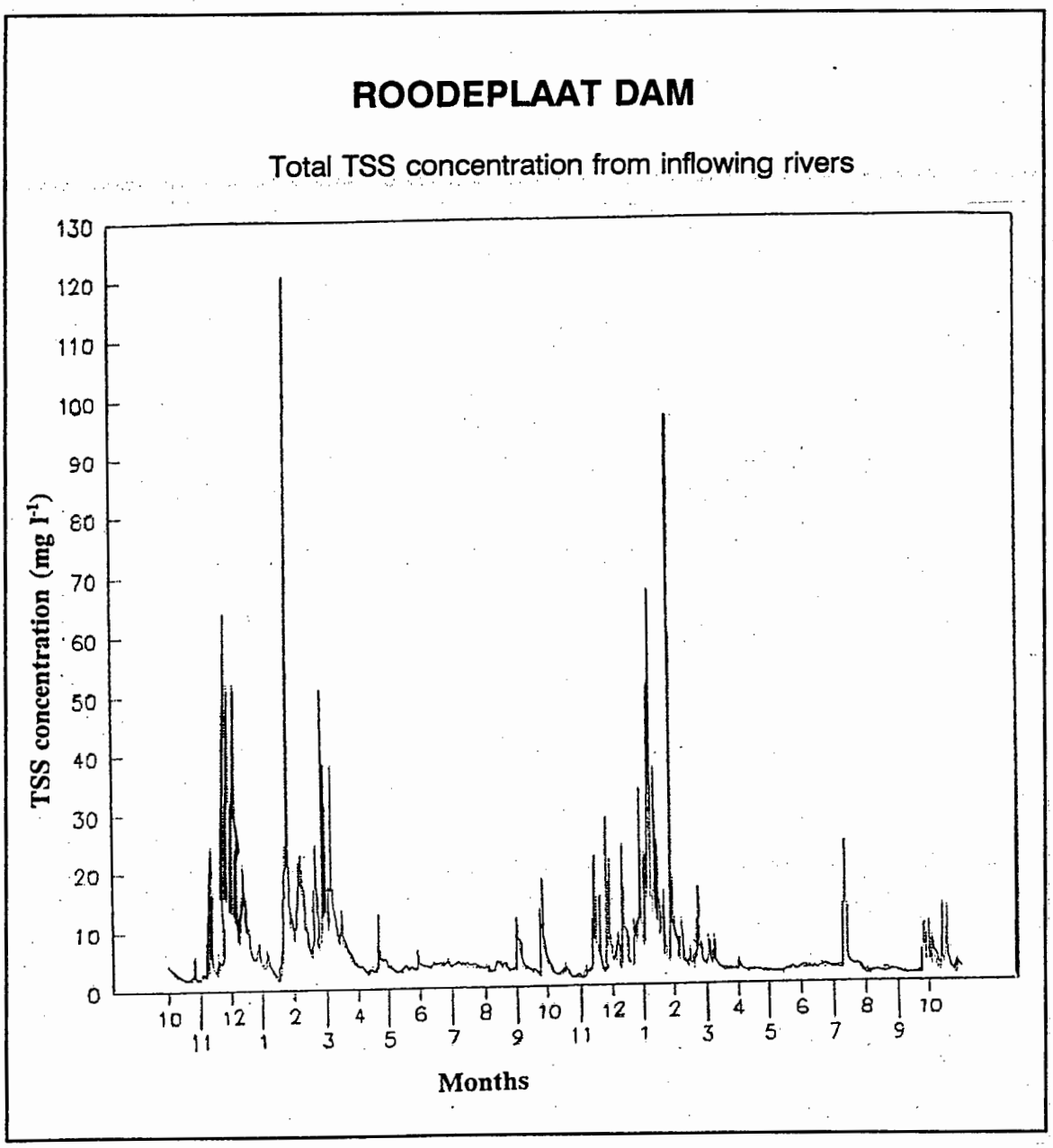

Figure 8.14
Time-series graph of TSS concentration entering Roodeplaat Dam for the period October 1980 to October 1982.

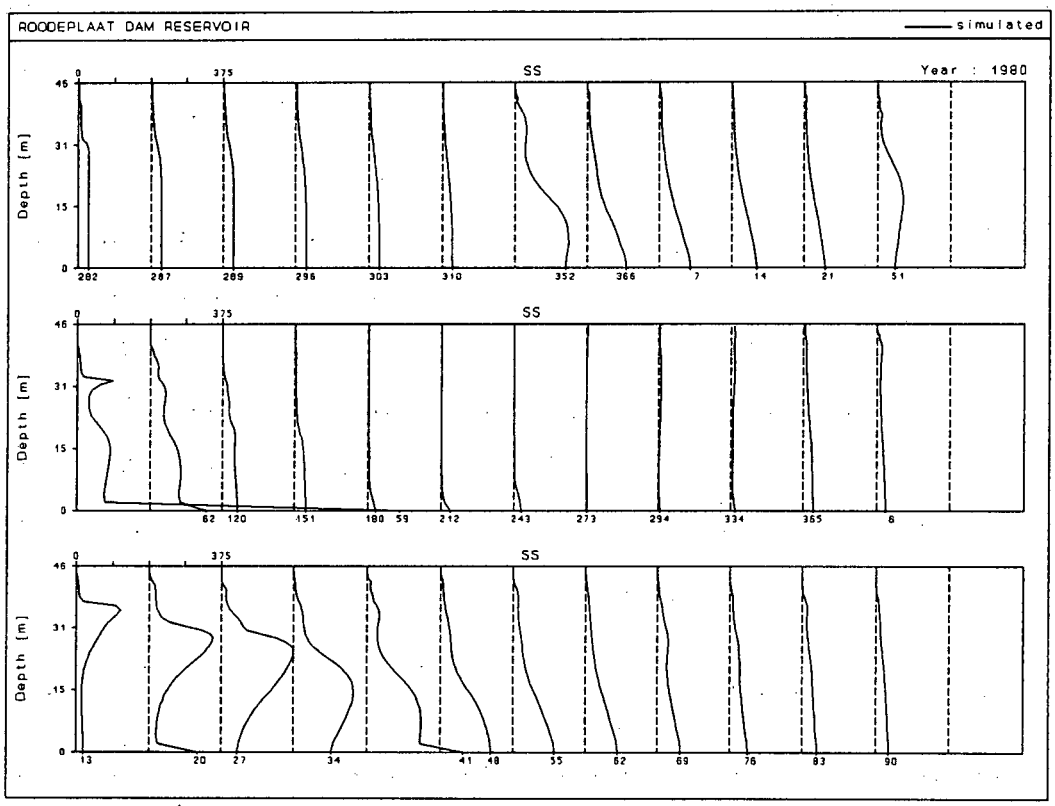

x-axis: Julian Day

TSS concentration: mg l^{-1}

Fig 8.15
Depth profiles of simulated TSS concentration as obtained with the modified MINLAKE model on Roodeplaat Dam.

8.2.6 Detritus

The concentration of detritus in a reservoir mainly affects concentrations of dissolved oxygen and nitrate, and to a lesser degree, concentrations of dissolved phosphate and ammonia. In the original MINLAKE model, detritus is simulated as biological oxygen demand (BOD). During calibration of the model on Roodeplaat Dam, it was found that oxygen utilized during detrital decay was a major cause of the anaerobic conditions that develop regularly in the dam during the stratified period. In view of the effect of the aerobic/anaerobic state of the water on a multitude of reaction rates, it was important to simulate detrital decay as accurately as possible.

The original MINLAKE mmodel does not recognise that detrital decay can take place under aerobic conditions only, and denitrification, an important process in the nitrogen budget of many South African dams, is not included. Furthermore, provision is made for simulation of detritus as BOD in particulate form (BODP) only, but indications from the literature (Mann 1988) are that the dissolved form of detritus (BODS) is much more important than previously realised, and that particulate detritus (BODP) is regenerated during decay of dissolved detritus (BODS) (Mann 1988, Dold *et al* 1980).

In the modified MINLAKE model, two formulations of detrital decay, one more complex than the other, were tested (see paragraph 5.3.2). In the first formulation, provision is made for the aerobic/anaerobic state of the water on the rate of detrital decay, and the process of denitrification is incorporated. The second formulation is a more complex refinement of the first, distinguishing between particulate and dissolved BOD, and simulating regeneration of particulate BOD during decay of soluble BOD.

The results obtained with these formulations are shown in Fig 8.14 to 8.16. The detritus concentration simulated by the more complex formulation did not differ significantly from that simulated by the less complex formulation. Unfortunately no observed data are available, but the MINLAKE manual indicates that BODP concentration should be between 0 - 10 mg/l. Simulated BOD concentrations obtained with both modified formulations are generally in this range.

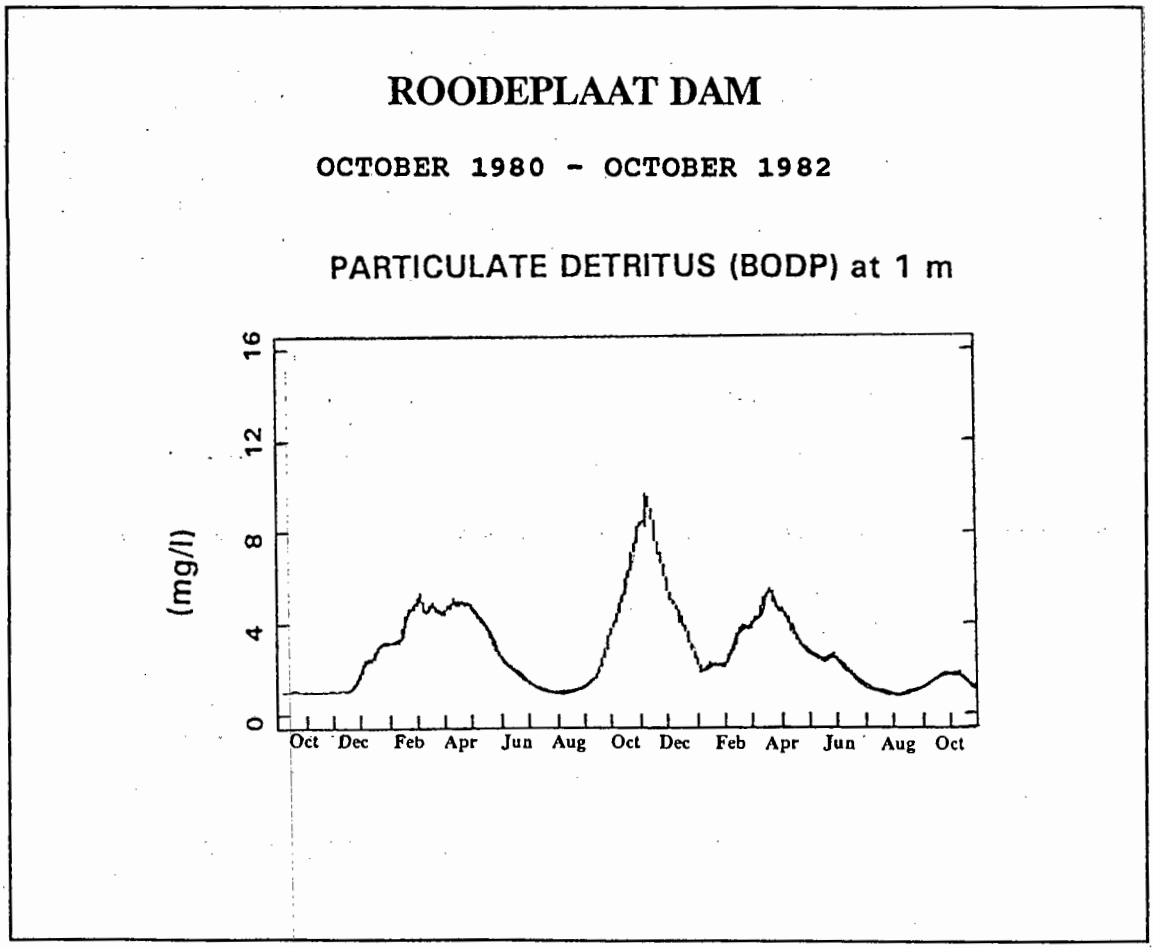

Fig 8.16
Time-series graph of simulated BOD as obtained with the modified MINLAKE model on Roodeplaat Dam, utilising the first formula (Eq 7.21) for detrital decay.

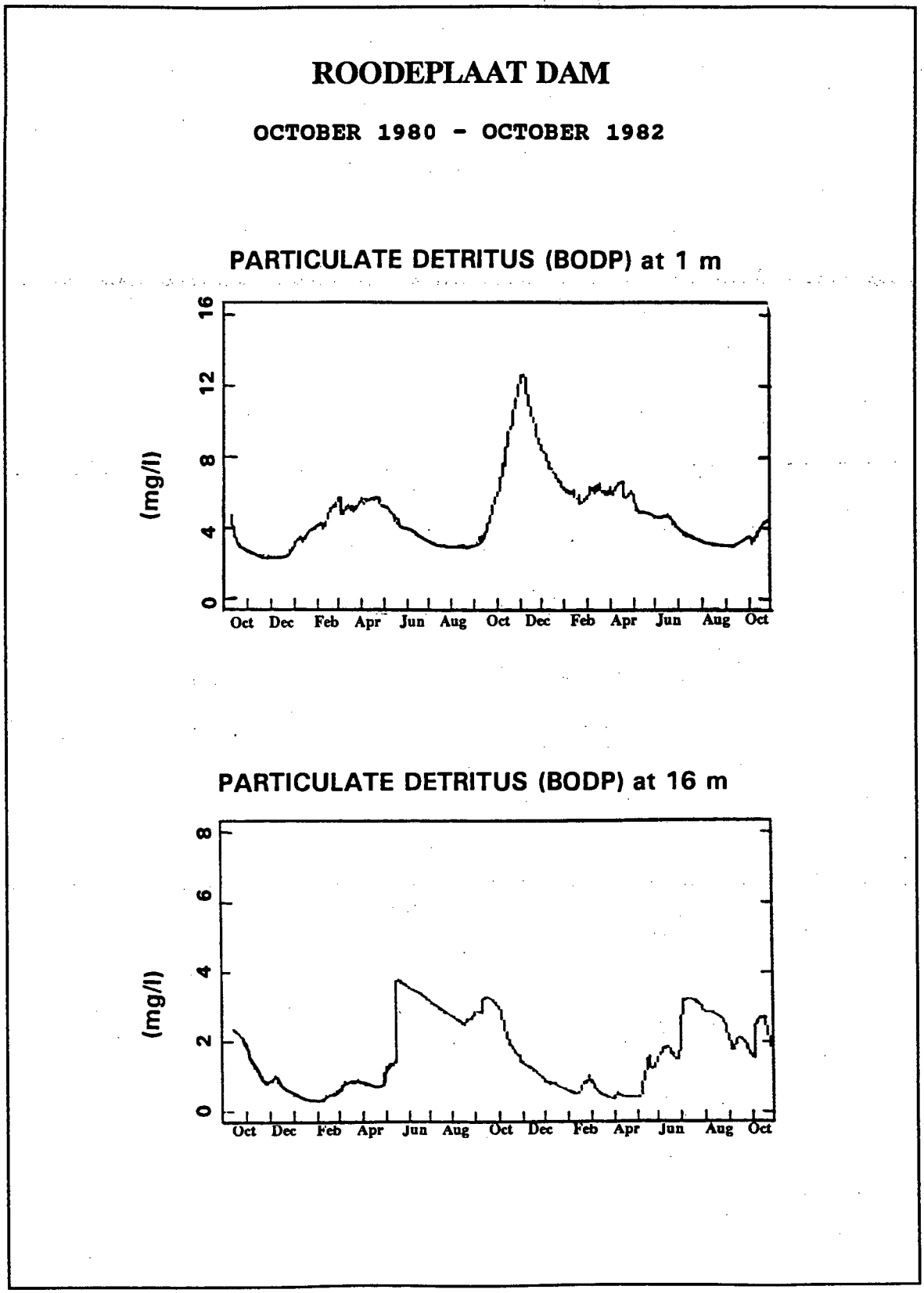

Fig 8.17
Time-series graph of simulated particulate BOD concentration as obtained with the modified MINLAKE model on Roodeplaat Dam

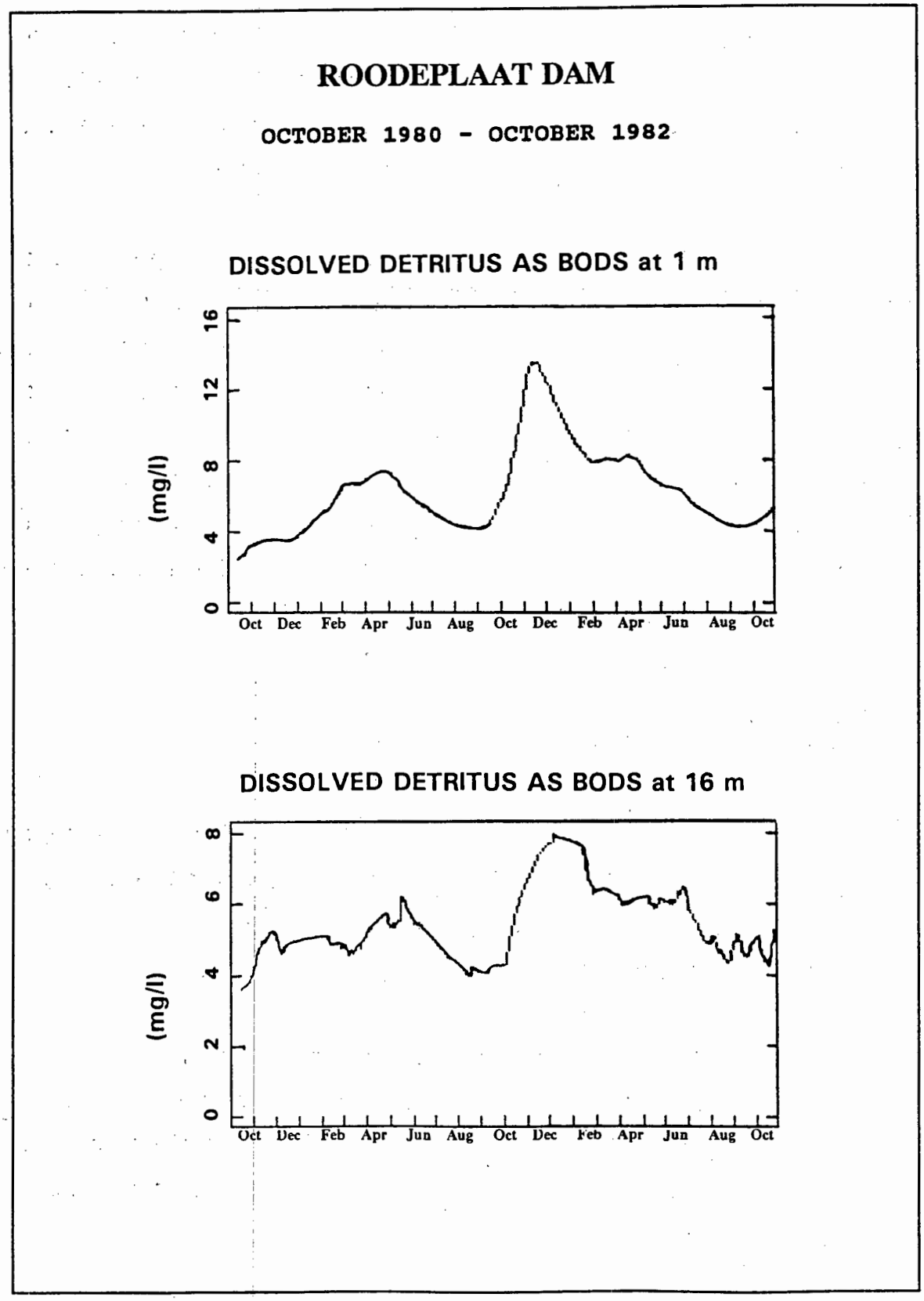

Fig 8.18
Time-series graph of simulated dissolved BOD concentration as obtained with the modified MINLAKE model on Roodeplaat Dam

As expected, the simulated BODP and BODS concentrations also follow the general trend of the chlorophyll-a simulations. Under the circumstances, the simulated detritus results obtained with both formulations are regarded as representative of the actual detritus concentrations in the dam during the hydrological cycle.

Without observed BOD data, it is not really possible to evaluate the two modified formulations properly, especially because there is no significant difference in BOD simulation results obtained with the two formulations. There was no significant difference in the effect on simulated oxygen concentration either, thus it was decided to release two versions of the model, one with the less complex BOD formulation, and one with the more complex formulation. (Unfortunately, due to the complex interactions between processes, as well as the structure of the model, it is not possible to have both formulations in the same version, with the user choosing the required option.)

Further reasons for releasing both formulations are as follows:

Regarding the less complex formulation:

- It requires fewer calibration coefficients than the more complex version, and should be adequate if the model is to be used for operational purposes.

Regarding the more complex formulation:

- Conceptually, it is more sound than the less complex formulation.
- It is more flexible for future expansion as more data become available.
- It is possible that conditions in Roodeplaat Dam are such that it causes the two formulations to give virtually the same results. However, this may not be the case in another dam.

8.2.7 Dissolved oxygen

In view of the effect of the aerobic/anaerobic state of the water on the rates of a multitude of processes, correct simulation of dissolved oxygen concentration is of the utmost importance, especially in South African reservoirs where anaerobic conditions occur regularly during the stratified period. No significant changes had to be made to the processes relating to dissolved oxygen concentration in the original MINLAKE model, however, a few coding errors had to be corrected (*cf* paragraph 7.7). Simulation of dissolved oxygen concentration was affected most by:

- simulation of detritus
- correct specification of the epilimnetic diffusion coefficient

Time-series graphs of simulated and observed dissolved oxygen concentrations at depths of 1 and 16 m from the surface are shown in Fig 8.19. Depth profiles are depicted in Fig 8.20. In view of the multitude of processes that affect dissolved oxygen concentration, and the complex interaction between these processes, correspondence between simulated and observed dissolved oxygen concentration is considered good. It must be kept in mind also that, because of processes such as algal photosynthesis and oxygen mass transfer (aeration) that occur in the surface layer, oxygen concentration in this layer will vary greatly during the day, and thus the observed concentration in the surface layer depends largely on the time of day that the measurements were made. Furthermore, the requirement for water quality management is not so much a knowledge of the exact dissolved oxygen concentration, it is considered more important to know when the hypolimnion will be aerobic/anaerobic. This is indicated clearly in both the time-series graph at 16 m, and the depth profiles.

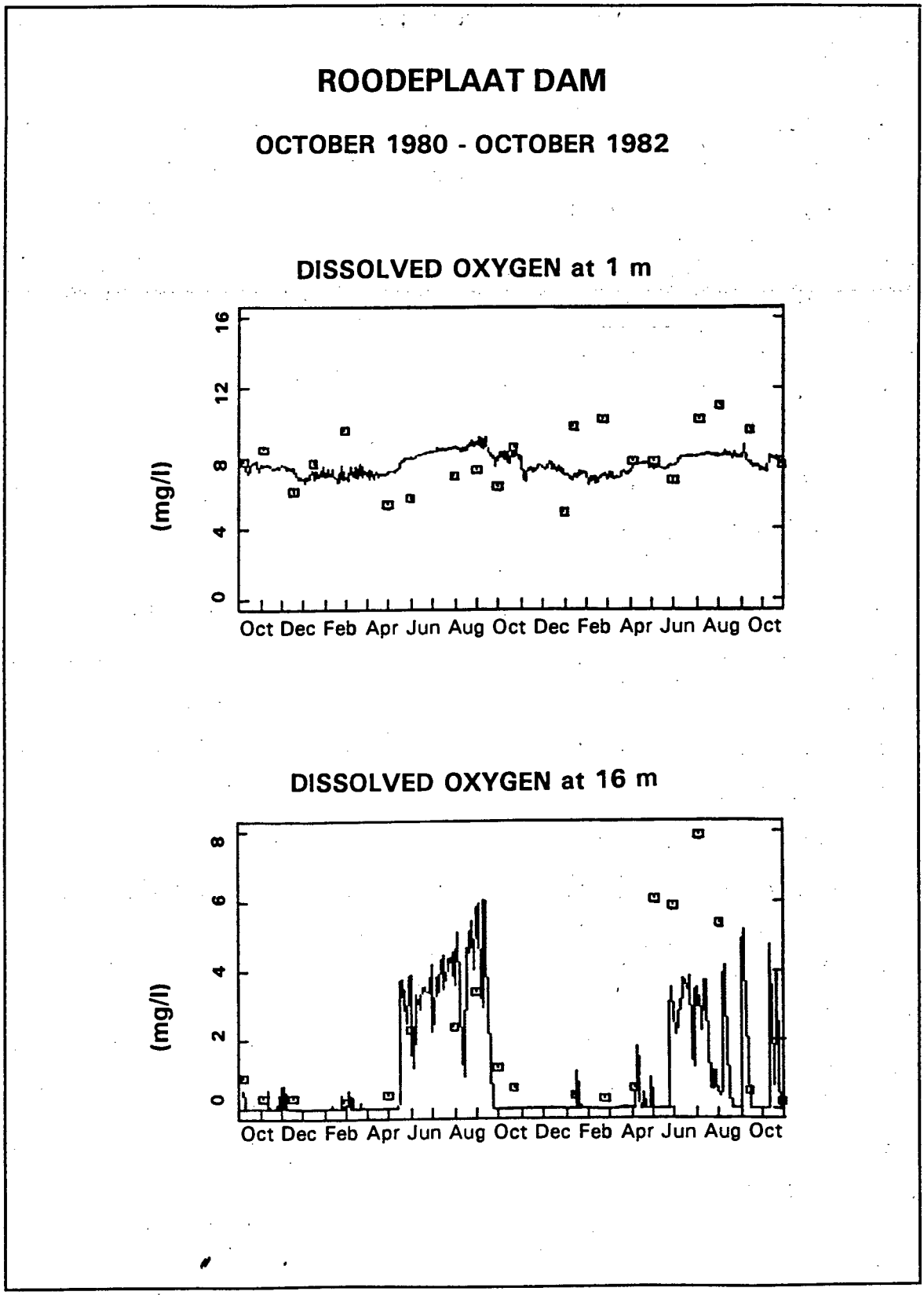

Fig 8.19
Time-series graphs of observed vs simulated dissolved oxygen concentration at 1 and 16 m depth obtained with the modified MINLAKE model on Roodeplaat Dam.

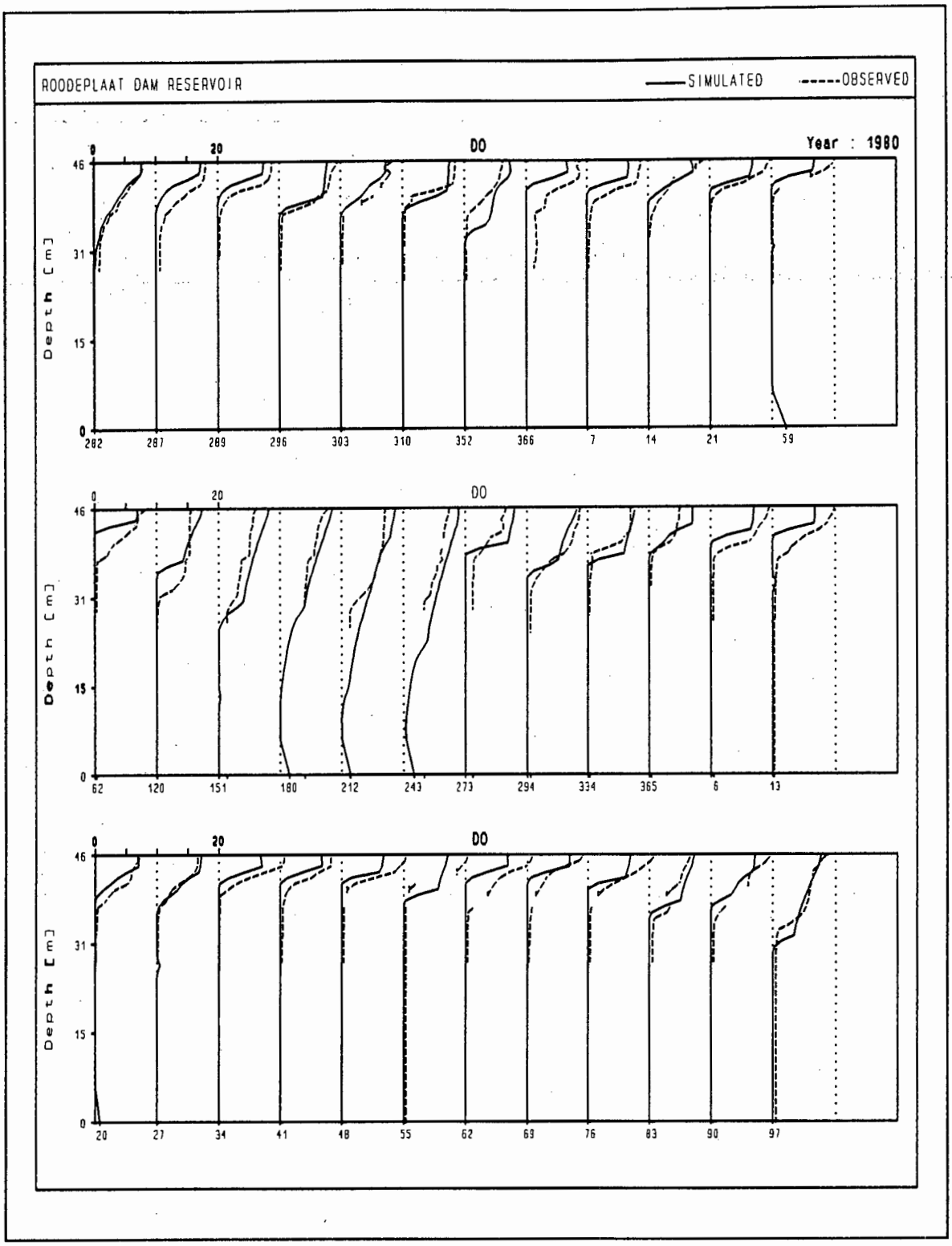

x-axis: Julian day

Oxygen concentration: mg/l

Figure 8.20
Depth profiles of observed and simulated dissolved oxygen concentration obtained with the modified MINLAKE model on Roodeplaat Dam.

8.2.8 Total dissolved salts (TDS)

Time series graphs of simulated and observed TDS concentrations are shown in Fig 8.21. TDS is a conservative substance, and correspondence between simulated and observed concentrations serves as a measure of the validity of the hydrodynamic simulation. As correspondence between simulated and observed TDS concentration is good, the ability of the MINLAKE model to simulate the hydrodynamic behaviour of Roodeplaat Dam is confirmed.

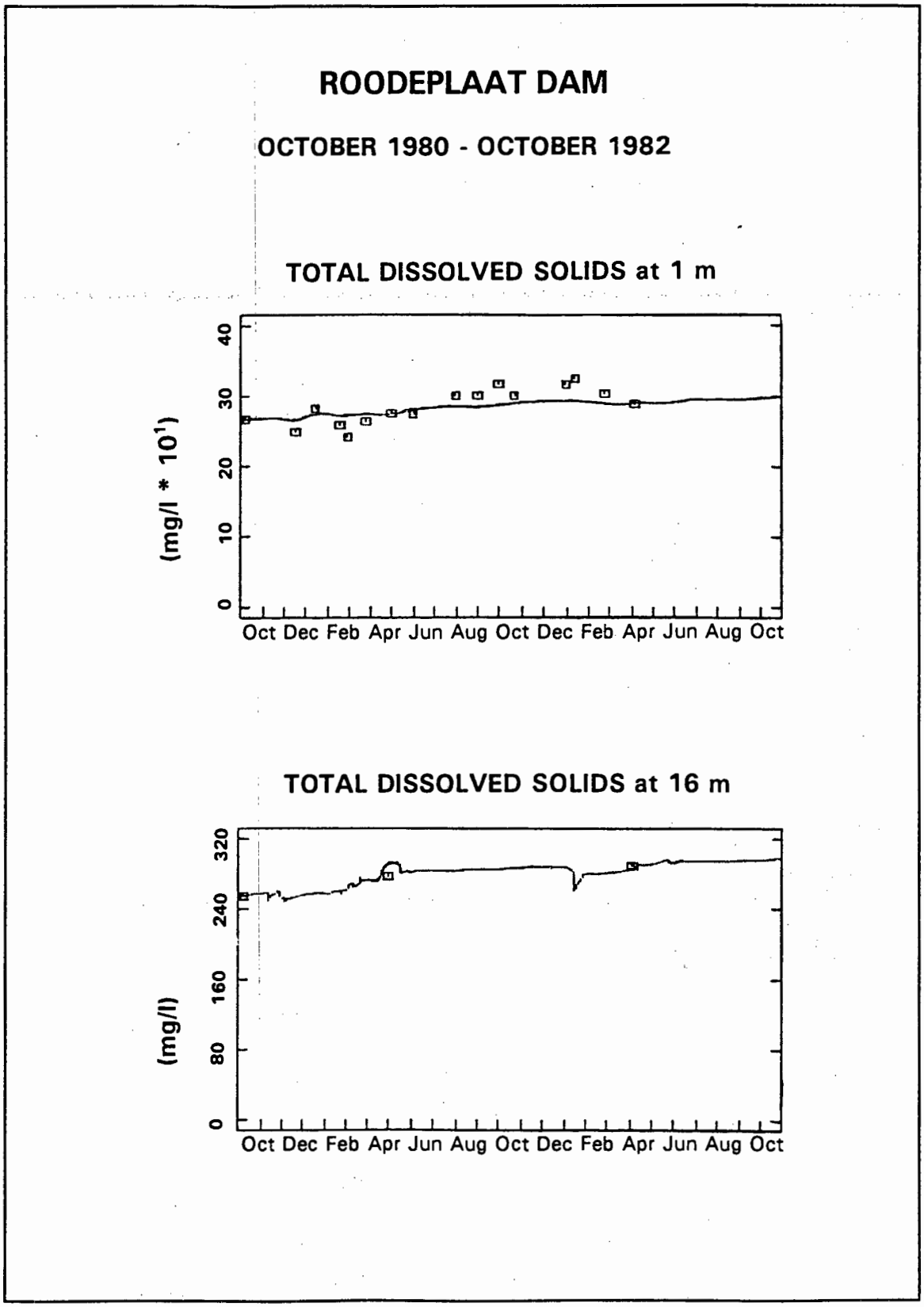

Fig 8.21
Time-series graphs of observed and simulated TDS concentration obtained with the modified MINLAKE model on Roodeplaat Dam.

CHAPTER 9

VERIFICATION OF THE MODIFIED MINLAKE MODEL

9.1 INTRODUCTION

When the original MINLAKE model was tested on Roodeplaat Dam, correspondence between simulated and observed water temperature was good, but correspondence between simulated and observed water quality response was very poor (*cf* Chapters 6 and 7). The poor correspondence could have been due to:

- Omission of important processes
- Inadequate process formulation
- Non-optimal kinetic coefficients

In the modified model, various processes were added, some reformulated, and optimum values for the kinetic coefficients under South African climatic conditions were established (see Chapters 5, 6, 7, and 8). The modified MINLAKE model simulates both the hydrodynamic and the water quality behaviour of Roodeplaat Dam remarkably well. However, because of the process modifications, the modified model requires an additional 19 calibration coefficients. Ideally, because of the inherent uncertainty associated with the values of these coefficients, the number of coefficients should be kept to a minimum, as additional coefficients increase the uncertainty of model predictions also.

The interactive nature of reservoir processes meant that process modifications and establishing of optimum values for the coefficients were done interactively also. It is thus difficult to say whether the improved results were due to the process

modifications, or due to the optimum values of the kinetic coefficients, or both. To resolve the question, the original MINLAKE model, without the process modifications, was run on Roodeplaat Dam, using optimum values for the kinetic coefficients under South African conditions (*cf* Table 7.13). The results are depicted in Fig 9.1 to 9.9. Clearly the correspondence between simulated and observed water quality results is poor. It was concluded that both process modifications and optimum values for the kinetic coefficients were essential for the successful calibration of the model to a South African reservoir.

The need to modify the original MINLAKE model arose mainly from climatic differences between South Africa and Minnesota, USA, where the model was developed. The greater part of South Africa has a warm temperate/subtropical climate, whereas the Minnesota Lakes are situated in a cold temperate climate. The warmer climate in South Africa results in a greater temperature difference between the epilimnion and the hypolimnion, i.e. a greater degree of stratification. More important though, the higher temperatures also cause an increase in the reaction rates of a multitude of processes, one of the most significant being detrital decay rate. Detrital decay is a major sink of oxygen in the hypolimnion, and thus, in eutrophic dams with a high concentration of detritus, anaerobic conditions may develop in the hypolimnion due to oxygen consumption during detrital decay. The higher the water temperature (i.e. higher reaction rate) the more likely the possibility of anaerobic conditions developing, given a sufficiently high detrital concentration. Thus, if two dams with the same (high) detrital concentration are considered, one situated in a warm climate, and the other situated in a cold climate, the dam situated in the warm climate will turn anaerobic sooner than the one situated in the colder climate, (even though the two dams have the same concentration of detritus), due to accelerated rate of detrital decay (and hence oxygen consumption).

According to Mortimer (1942), the water quality behaviour of dams where anaerobic conditions develop is fundamentally different from dams that stay aerobic. The original MINLAKE model did not make provision for the effect of the aerobic/anaerobic state of the water on the reaction rates. Many South African dams turn anaerobic during

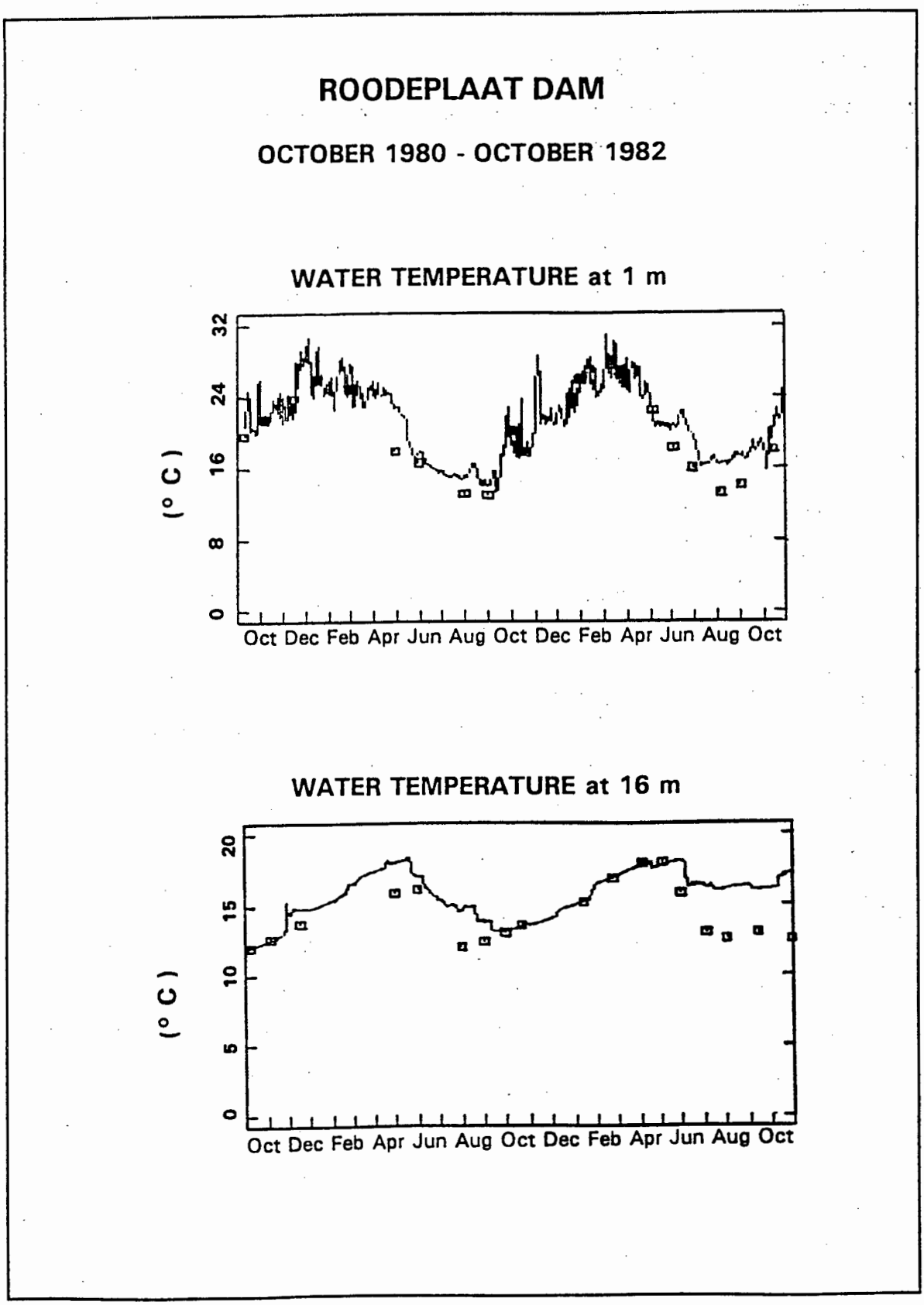

Figure 9.1
Plot of simulated vs observed temperature as obtained with the original model and optimum coefficients for Roodeplaat Dam.

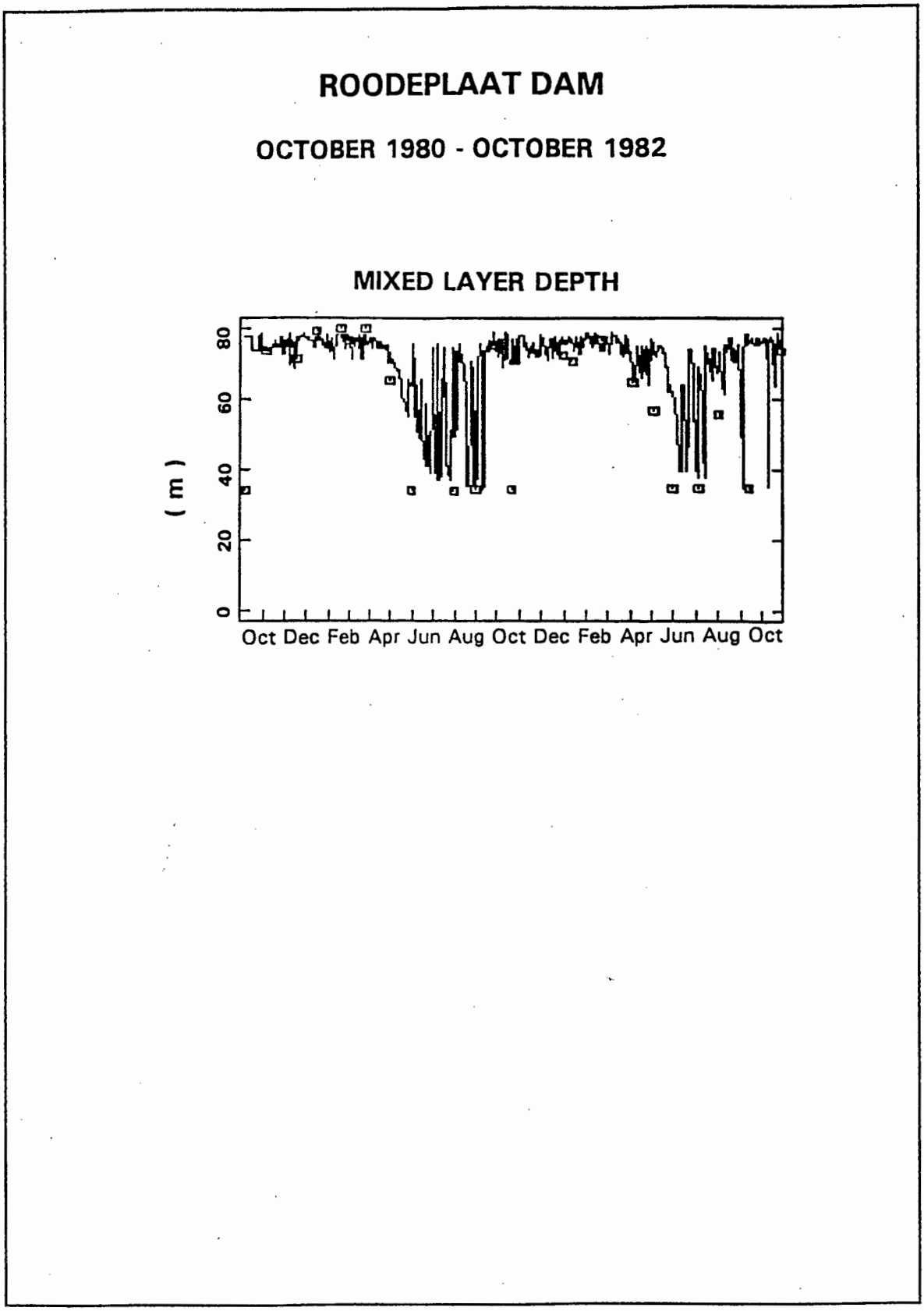

Figure 9.2
Plot of simulated vs observed mixed layer depth as obtained with the original model and optimum coefficients for Roodeplaat Dam.

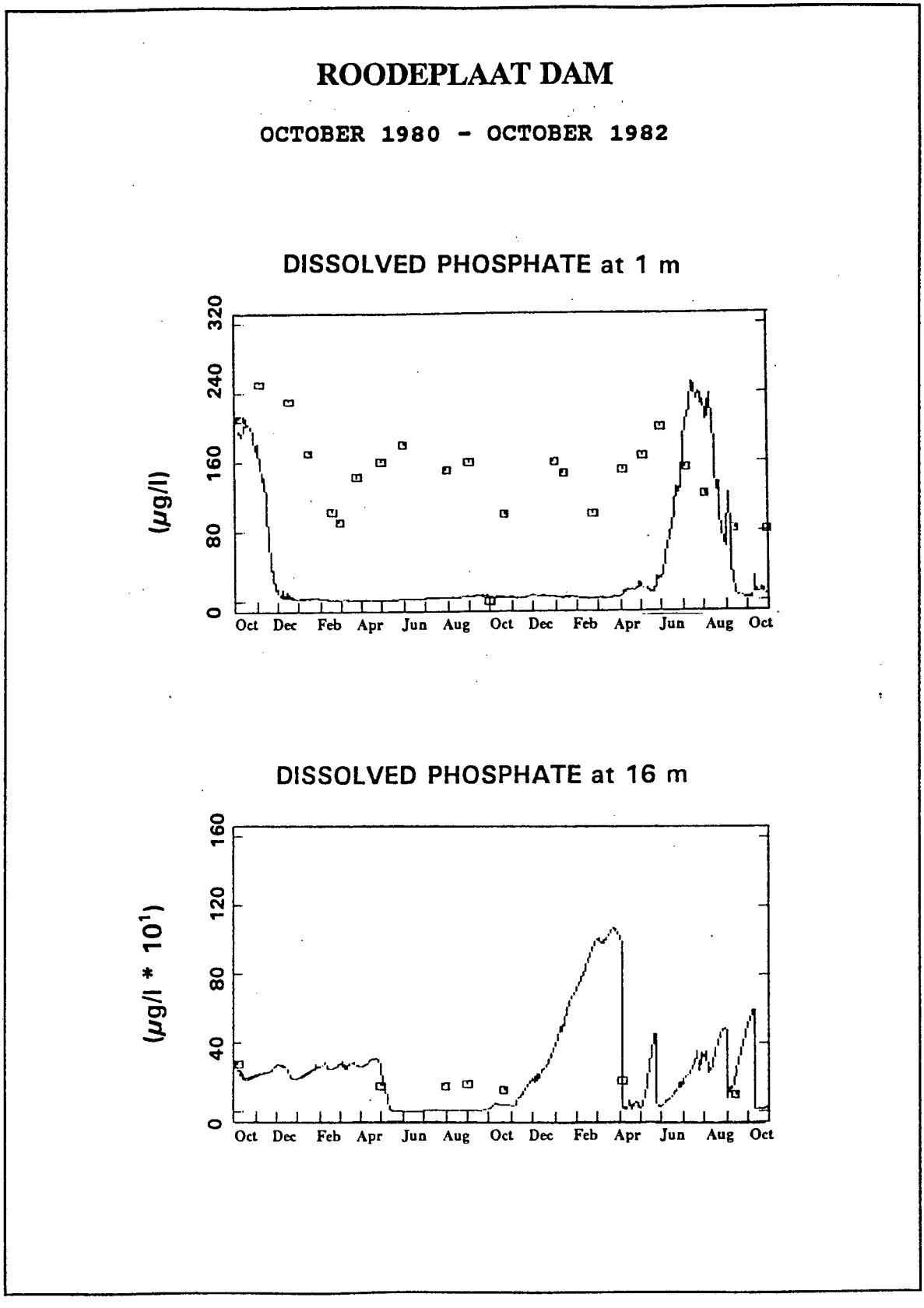

Figure 9.3
Plot of simulated vs observed dissolved phosphate concentration as obtained with the original model and optimum coefficients for Roodeplaat Dam.

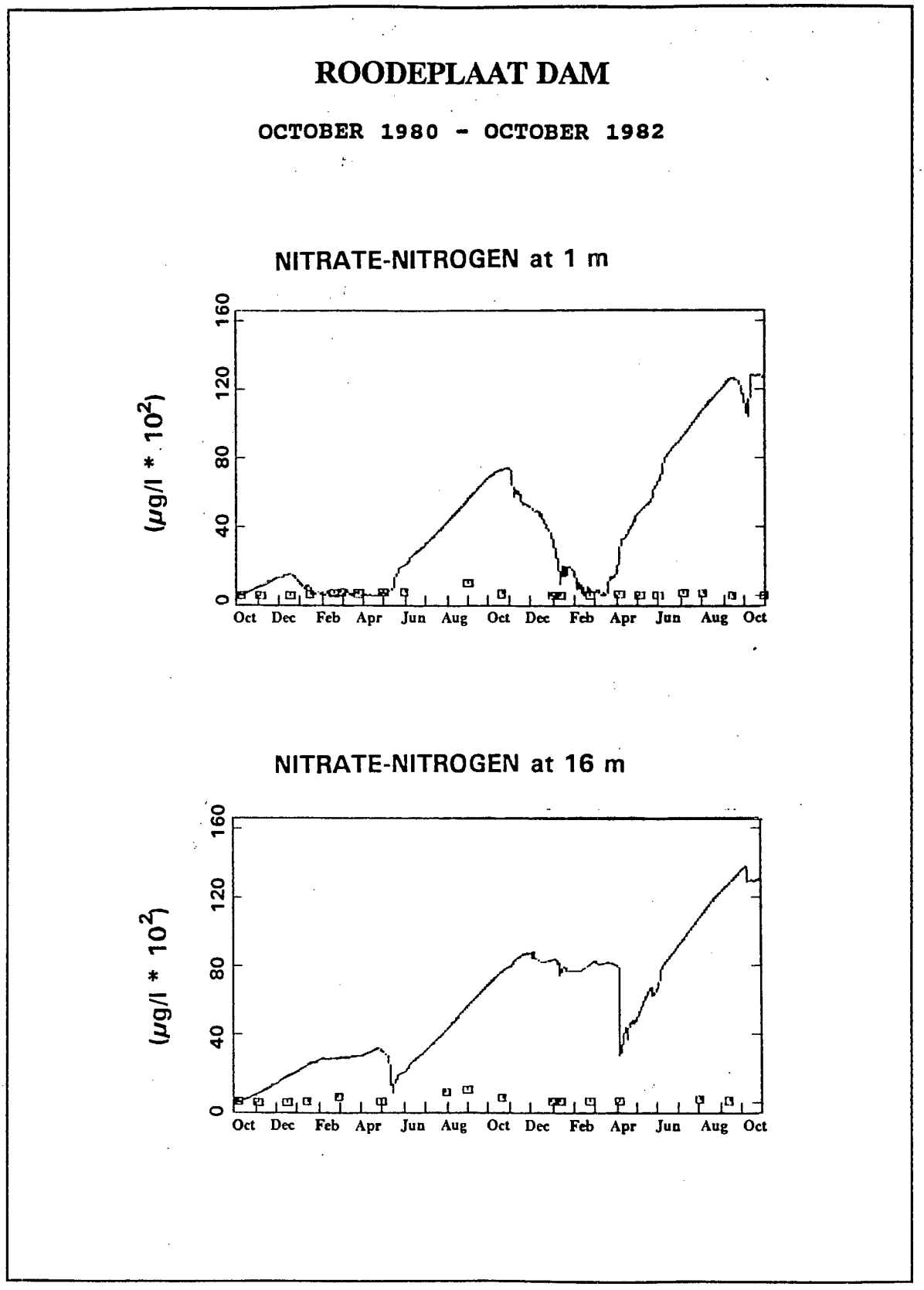

Figure 9.4
Plot of simulated vs observed nitrate concentration as obtained with the original model and optimum coefficients for Roodeplaat Dam.

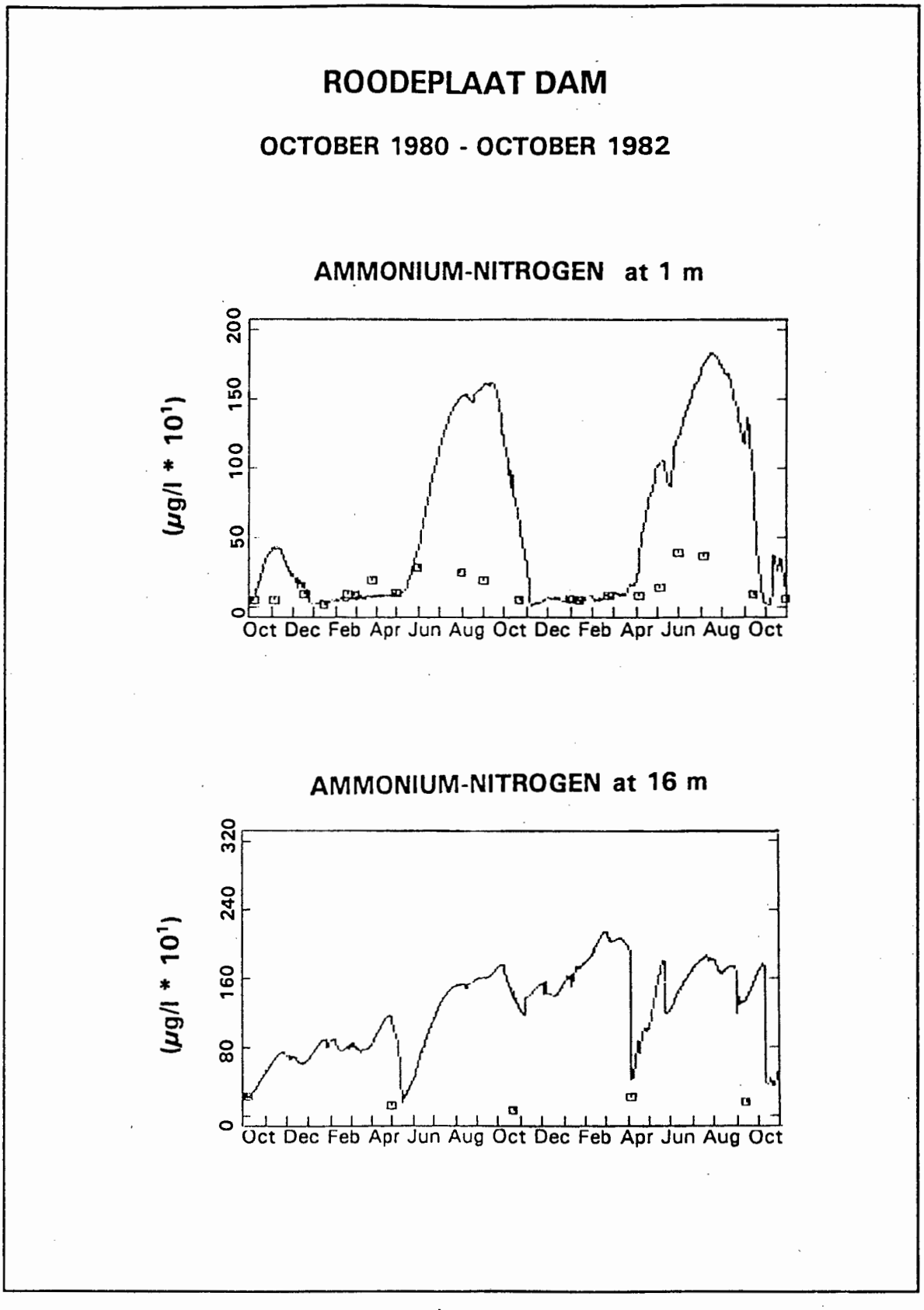

Figure 9.5
Plot of simulated vs obsered ammonia concentration as obtained with the original model and optimum coefficients for Roodeplaat Dam.

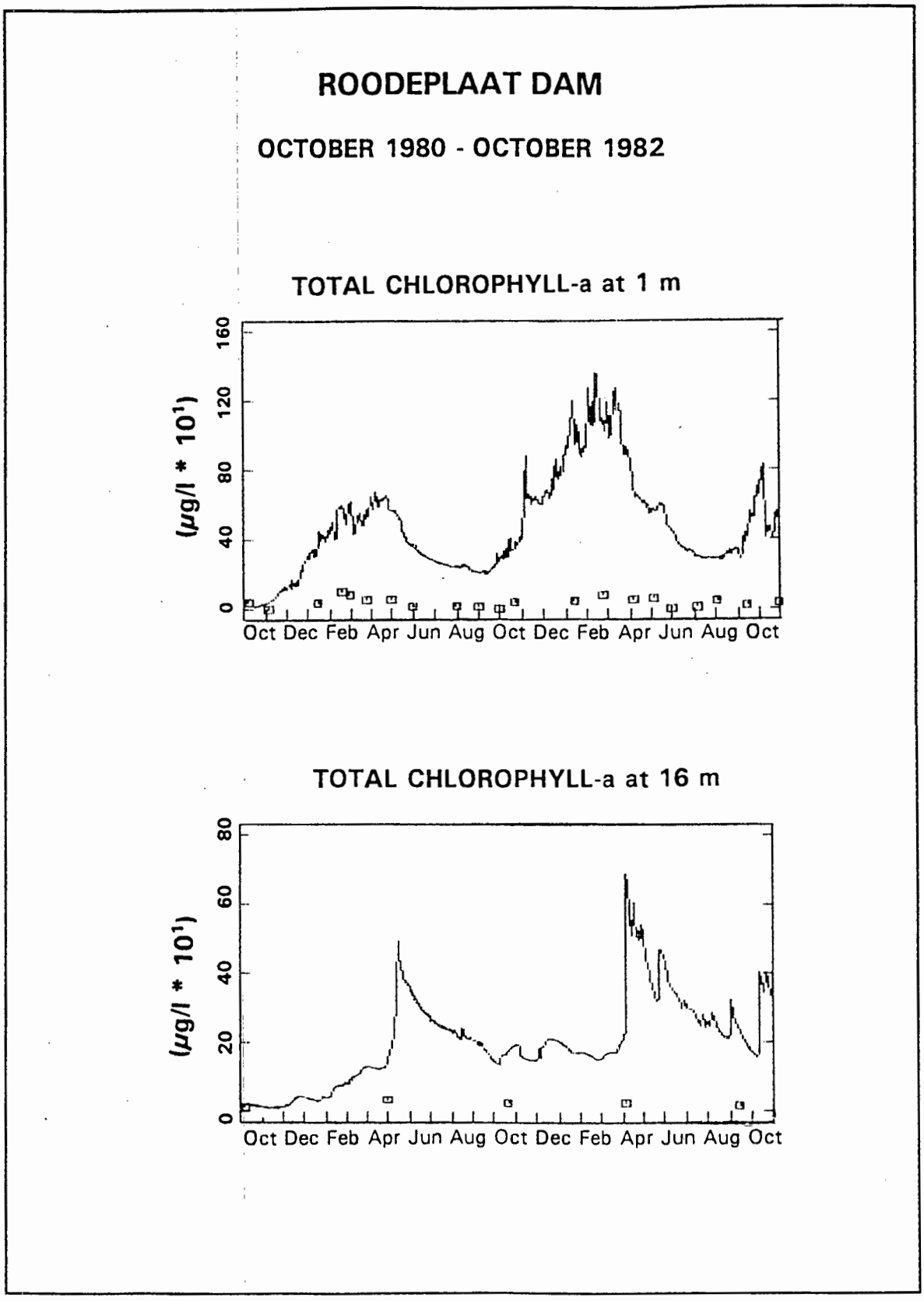

Figure 9.6
Plot of simulated vs observed chlorophyll-a concentration as obtained with the original model and optimum coefficients for Roodeplaat Dam.

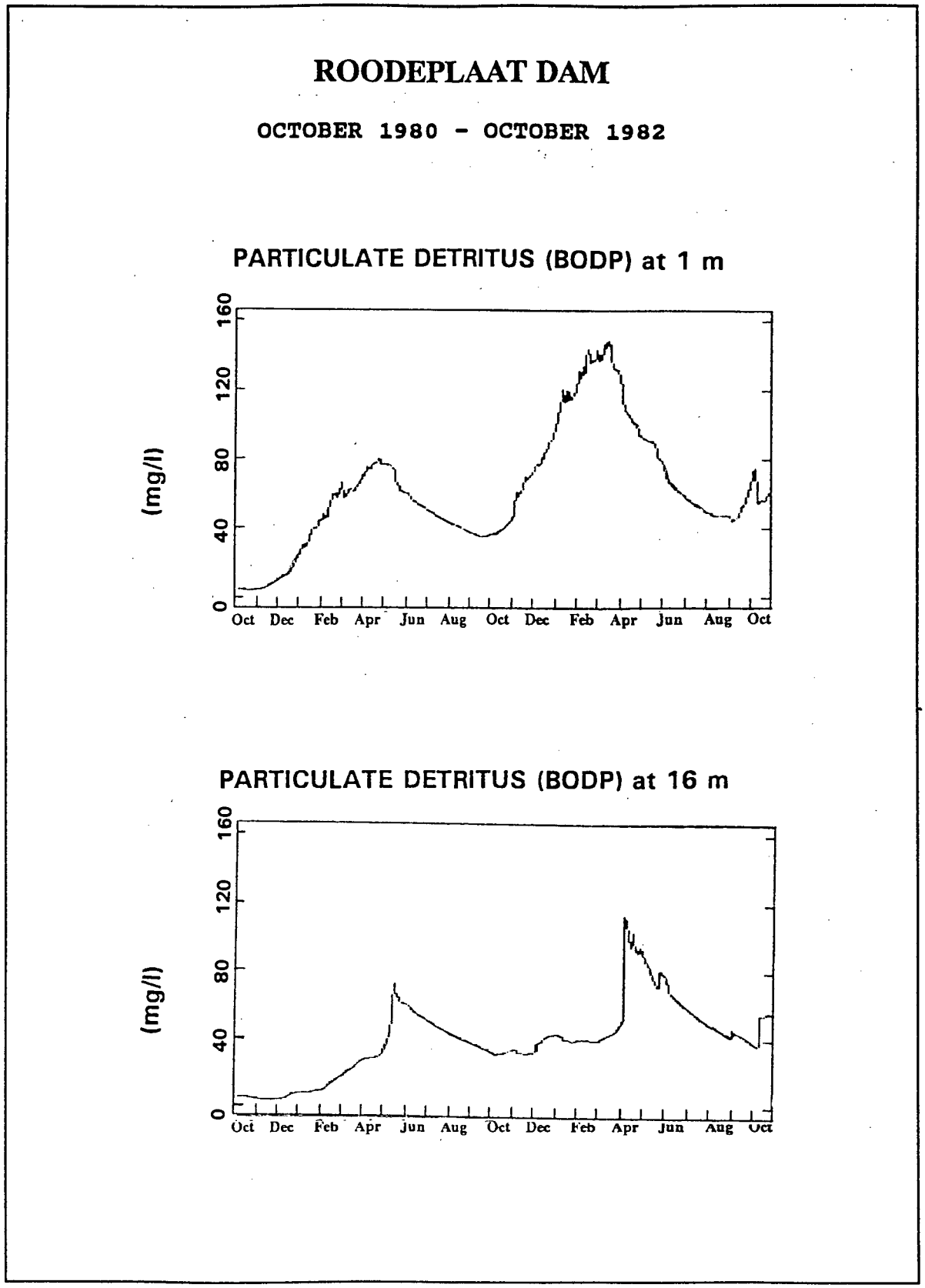

Figure 9.7
Plot of simulated vs observed particulated BOD concentration as obtained with the original model and optimum coefficients for Roodeplaat Dam.

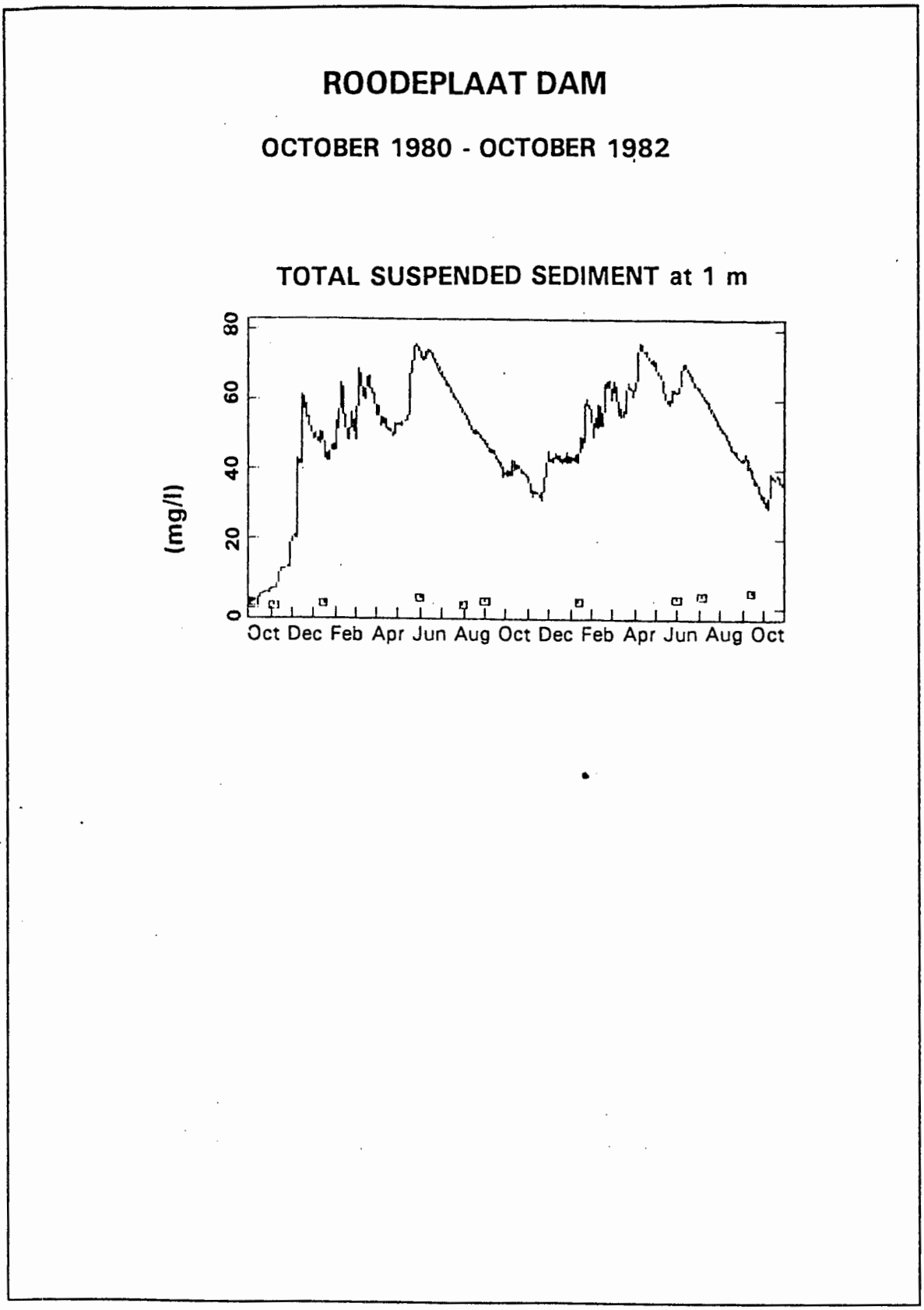

Figure 9.8
Plot of simulated vs observed TSS concentrations as obtained with the original model and optimum coefficients for Roodeplaat Dam.

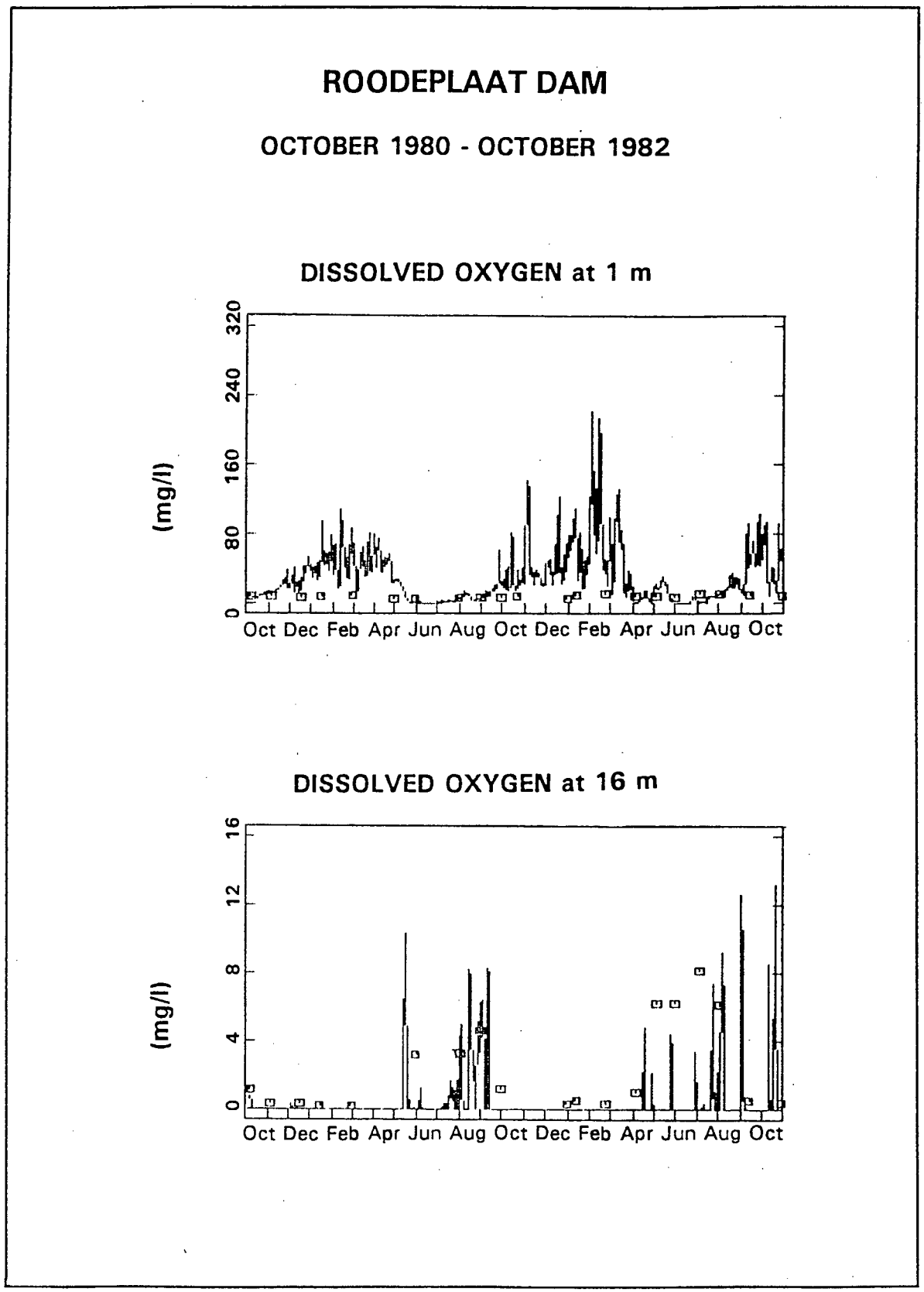

Figure 9.9
Plot of simulated vs observed dissolved oxygen concentrations as obtained with the original model and optimum coefficients for Roodeplaat Dam

part of the hydrological cycle (Walmsley and Butty 1980a), and thus it was essential that the model should be able to model the behaviour of dams under both aerobic and anaerobic conditions. Accordingly, the modifications that had to be made to the original MINLAKE model to enable simulation of the water quality behaviour of Roodeplaat Dam relate almost exclusively to either the effect of temperature and/or the aerobic/anaerobic state of the water on reaction rates (*cf* Chapter 5, 6, 7 and 8). Regarding the original model, because of the colder climate in Minnesota where the model was developed, most likely the effect of climate on reaction rates is not as evident as in the warmer climate of South Africa, thus it would have been difficult to incorporate these effects into the original model during development.

9.2 TESTING THE MODIFIED MINLAKE MODEL ON LAKE RILEY

It would seem that the modified MINLAKE model has greater generality than the original MINLAKE model, as it can simulate the behaviour of a dam under both aerobic and anaerobic conditions. However, to assess the generality of the modified model, the modified model should be applied to another reservoir. Unfortunately it has not yet been possible to establish the required data bases for another South African reservoir, but data bases for a period of 6 months for Lake Riley in the USA were supplied with the original model. It was decided to test the modified model on Lake Riley, as that would give an indication also as to whether the modified model is applicable to dams in all climates, as expected, or whether, for some reason, it is suitable to dams in a warm temperate/subtropical climate only. Accordingly, the modified model was applied to Lake Riley, utilizing the data bases supplied with the original model, and values for the algal and climate specific kinetic coefficients appropriate to Lake Riley (*cf* Riley 1988). The switching constants (used to link several process rates to the aerobic state of the water) as set for Roodeplaat Dam, had to be changed slightly to reflect conditions in Lake Riley. The results obtained for Lake Riley with the original MINLAKE model, as well as with the modified MINLAKE model, using appropriate switching constants/kinetic coefficients for Lake Riley, are shown in Fig 9.10 to 9.16. Correspondence between simulations obtained with the modified and the original model on Lake Riley is good.

9.3 CONCLUSIONS

The fact that the modified model gives good results for a reservoir in a warm temperate climate in the southern hemisphere, as well as for a reservoir in a cold temperate climate in the northern hemisphere, seems to indicate that the modified model has validity over a wide range of conditions. This implies also that no problems should be encountered in applying the model to other reservoirs in South Africa.

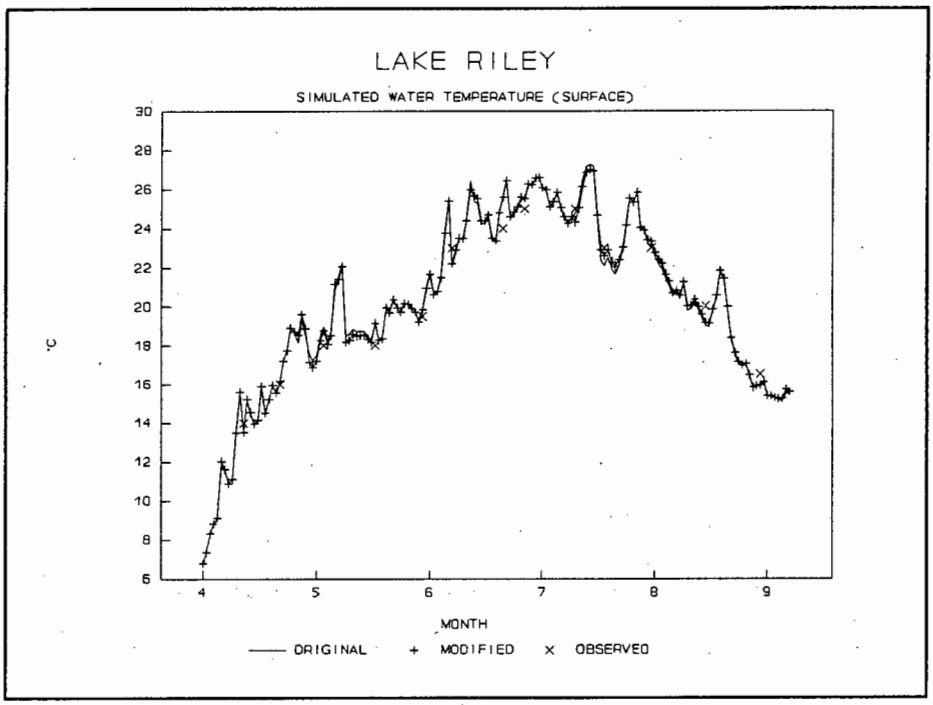

Figure 9.10
Simulated water temperature with original and modified MINLAKE models.

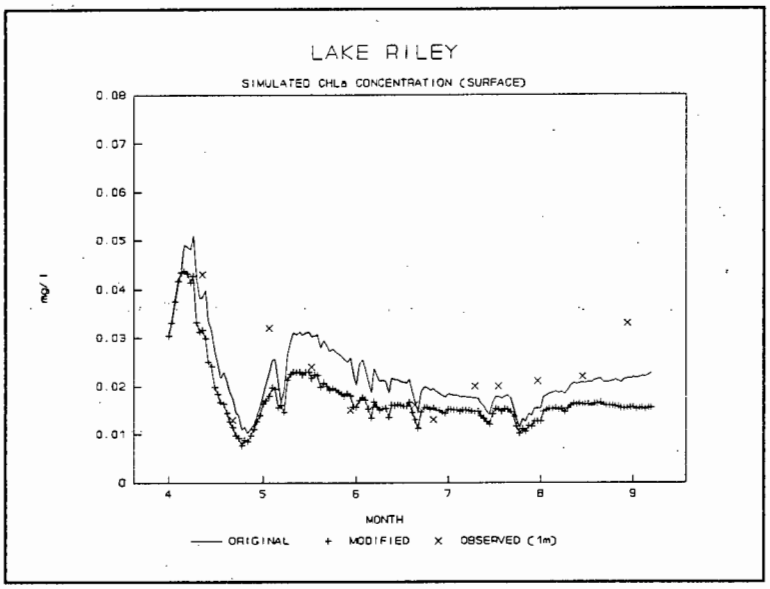

Figure 9.11
Simulated chlorophyll-a concentration obtained with the original and modified MINLAKE models.

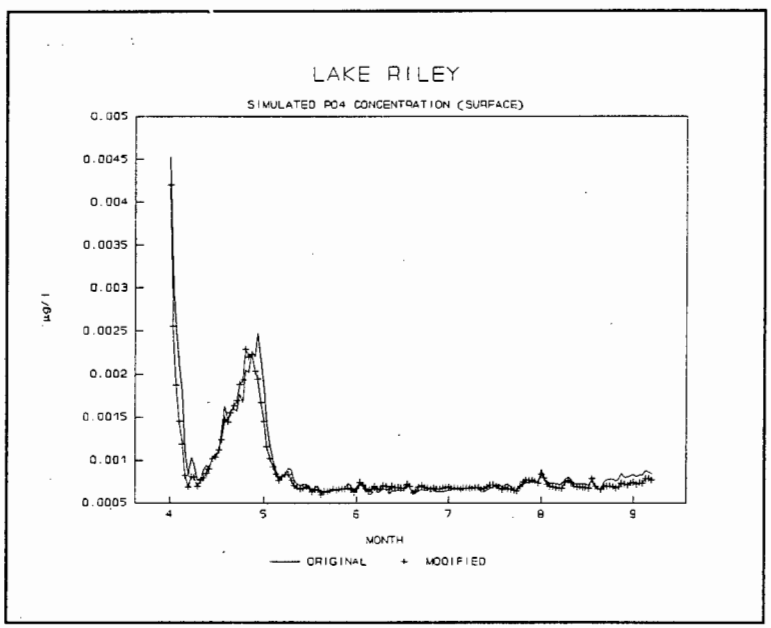

Figure 9.12
Simulated dissolved phosphate concentration obtained with the original and modified MINLAKE models.

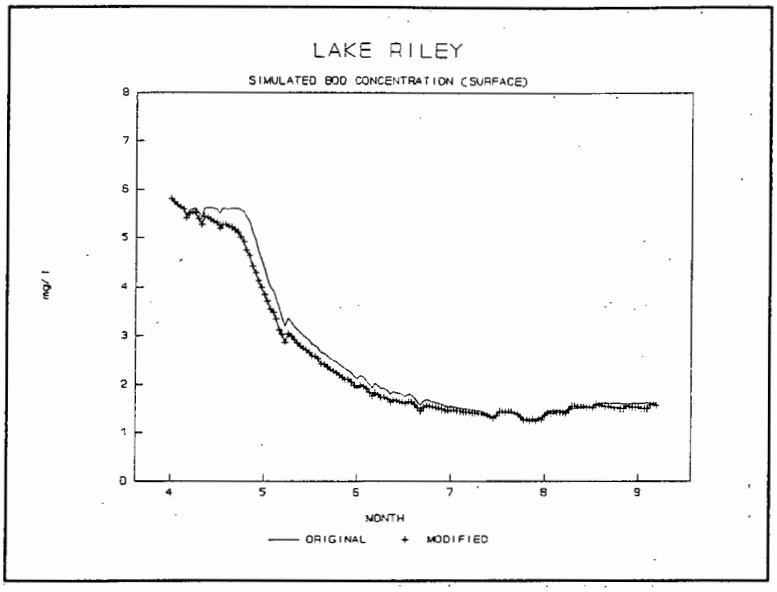

Figure 9.13
Simulated BOD obtained with the original and modified MINLAKE models.

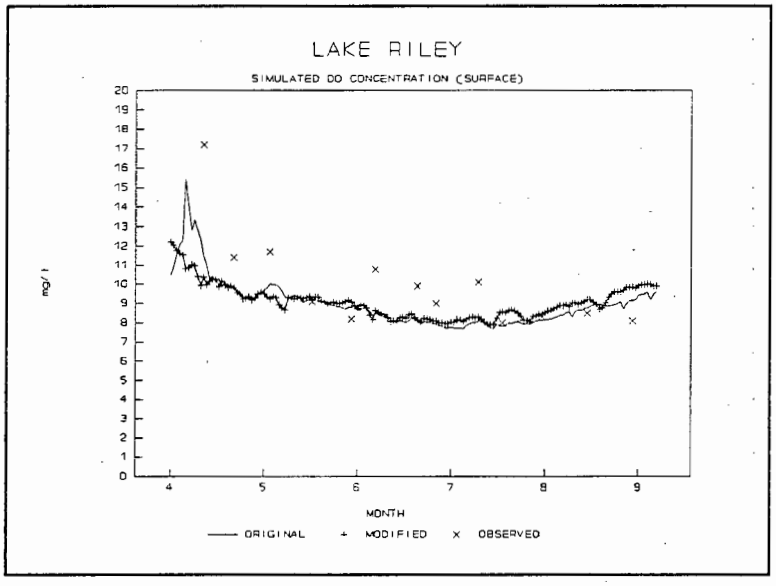

Figure 9.14
Simulated dissolved oxygen concentration obtained with the original and modified MINLAKE models.

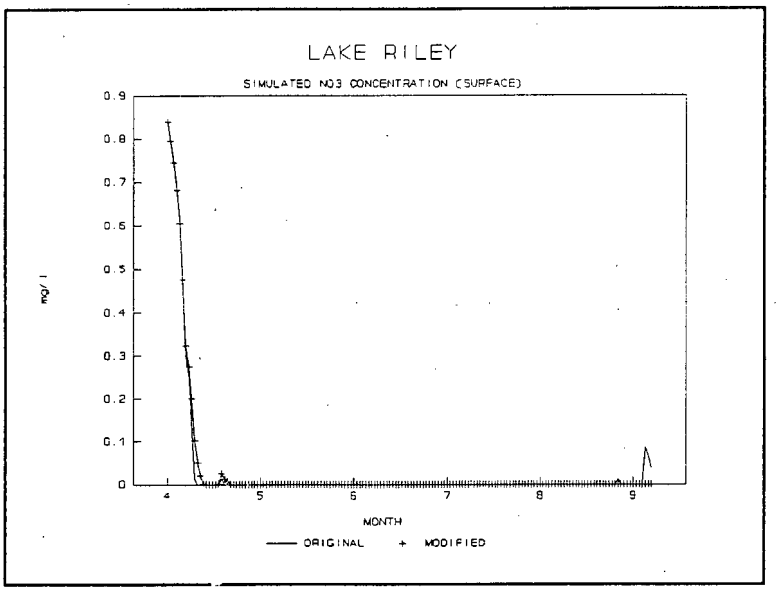

Figure 9.15
Simulated nitrate concentration obtained with the original and modified MINLAKE models.

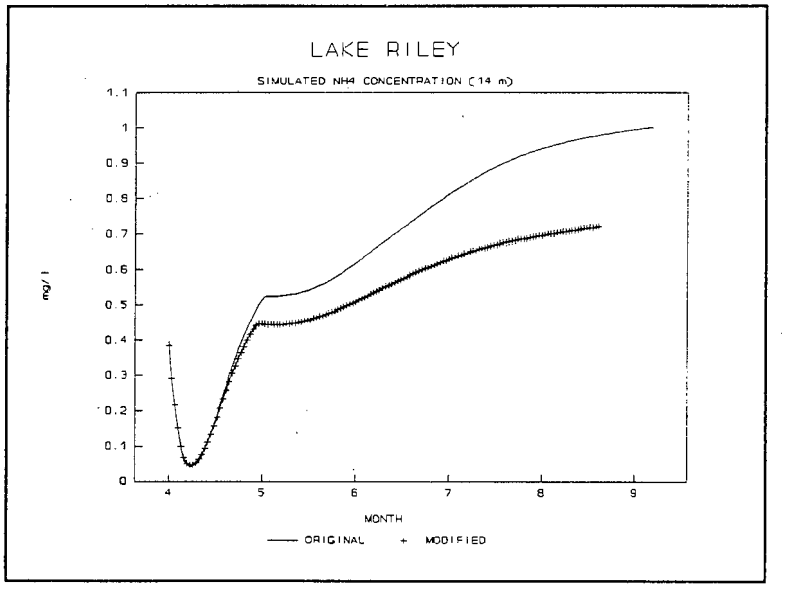

Figure 9.16
Simulated ammonia concentration obtained with original and modified MINLAKE models.

CHAPTER 10

SENSITIVITY OF MODEL OUTPUT TO INPUT DATA FREQUENCY

10.1 INTRODUCTION

A characteristic of water quality models such as MINLAKE is the large amount of data needed as input. Typically, five types of input data are needed, i.e, calibration coefficients, physical reservoir constants, reservoir profiles of the variables being simulated, and time-series measurements of several meteorological and inflow water quality variables. The calibration constants and physical reservoir constants required may vary between models, but these are single data inputs. Reservoir profiles are needed for comparison between measured and simulated data, and monthly data (or even less frequently) are needed. The time-series meteorological and inflow water quality data required by water quality models usually are very similar, and, because model predictions have a time step of one day, daily meteorological and inflow water quality data are needed. For instance, the MINLAKE model requires the following input data on a daily basis:

Meteorological data:

Air temperature
Dew point (other models may require relative humidity)
Precipitation
Wind speed
Wind direction
Percentage sunshine
Shortwave radiation

Inflow water quality data:

The MINLAKE model makes provision for the following:

Flow rate
Water temperature
Dissolved phosphate
Detritus
Dissolved oxygen
Total inorganic suspended sediment
Total dissolved salts
Nitrate
Ammonia
Chlorophyll-a (up to three classes)

In South Africa, meteorological data are monitored by the Weather Bureau via an extensive network of 2494 rainfall stations and 208 climate stations. Rainfall stations measure precipitation only. Climate stations provide a spectrum of measurements depending on the classification of the station, i.e. a first, second, or third order station (CSIR 1985):

First-order climate stations are manned by either full-time personnel or part-time weather observers. Observations are made at least three times daily: at 8h00, 14h00 and 20h00 South African Standard Time, but most of the variables are recorded autographically. Below is a list of the variables monitored, with the number of stations where these are measured, shown in brackets:

atmospheric pressure (105)
evaporation (82)
solar radiation (12)
wind speed and direction (21)
humidity (158)
sunshine hours (101)
cloud cover (?)

Second-order climate stations are manned by volunteer observers. Air temperature measurements are made daily at 08h00 and 14h00. Humidity, sunshine hours and rainfall are recorded autographically.

Third-order climate stations are manned by volunteer observers. Air temperature and rainfall are measured daily at 08h00.

Various other institutions, eg. the Department of Agriculture, municipalities, and airports, measure specific meteorological variables of important to their function.

River water quality data are monitored mainly by Department of Water Affairs. Local and regional authorities such as municipalities and regional Water Boards (eg Umgeni Water in Natal), operate monitoring programs in specific localities/areas.

Sample collection as done by the Department of Water Affairs, commenced during the 1950's and routine sampling at a large number of sites was initiated during the early 1970's. Currently, most of the registered sampling sites, in a country-wide monitoring network, are sampled routinely for a variety of water quality variables, at intervals which vary from daily to weekly to monthly (DWA, 1991). These variables are listed in Table 10.1.

TABLE 10.1 Water quality variables monitored by the Department of Water Affairs and Forestry in rivers and reservoirs.

CHEMICAL VARIABLES Rivers and Reservoirs	PHYSICAL VARIABLES Rivers	Reservoirs
pH	Conductivity	Conductivity
Calcium	Water temp.	Water level
Magnesium		Sampling depth
Potassium		Water temp
Sodium		
Chloride		
Fluoride		
Silicon		
Sulphate		
Total Phosphorus (as P)		
Ortho-phosphate (as P)		
Ammonium (as N)		
Nitrate plus Nitrite (as N)		
Total Kjeldahl Nitrogen (as N)		
Dissolved organic carbon (as C)		
Total alkalinity (H_2CO_3*alkalinity)		
Total dissolved salts(TDS)		

The extensive daily data required by water quality models often prohibit their general use. Although all the meteorological and inflow water quality variables are being monitored in South Africa, monitoring is not always done at the specific reservoir being modelled. Even if monitoring is done at the specific site, the required data may not be available on a daily basis, and/or the financial means to set up and maintain a monitoring network to supply daily data may be lacking. Thus, to obtain a set of daily data, infilling of data has to be done. This can be a time consuming procedure, as infilling has to be done by extrapolation from data from another site, or by finding a

relationship between variables with missing values and other variables with more complete values. Consequently, a study was undertaken to ascertain whether:

- frequency of data input can be reduced from daily to weekly, or even monthly, without serious loss of performance by the model
- site-specific hydrometeorological data are essential, or whether regional data will suffice

Simulated output data obtained during calibration of the modified MINLAKE model on Roodeplaat Dam, using daily meteorological and inflow water quality data, were used as a basis for comparisons. The frequency of meteorological and inflow water quality data was changed from daily, to, for instance, weekly, or even monthly, and the change in daily simulated output data was assessed. Thus, although the frequency of data input was changed, the model still provided output on a daily basis. The following simulated variables were used in the comparisons:

	Water temperature
Concentrations of:	Chlorophyll-a
	Dissolved phosphate
	Dissolved oxygen
	Total inorganic suspended sediment
	Total dissolved salts
	Nitrate
	Ammonia

10.2 SENSITIVITY OF MODEL OUTPUT TO FREQUENCY OF METEOROLOGICAL INPUT DATA

Generally, the following meteorological data are required by dynamic water quality models on a daily basis: Air temperature, dew point/relative humidity, precipitation, wind speed, wind direction, percentage sun, and short wave radiation. The general rationale in testing the sensitivity of the model output to frequency of meteorological data input was as follows:

The meteorological data base that was developed for calibration of the modified MINLAKE model on Roodeplaat Dam was used as a basis. This data base contains daily values of the meteorological variables. It was supposed that, instead of daily measurements, weekly measurements would be available. However, because of the structure of the model, and because model predictions are evaluated on a daily basis, the MINLAKE model requires input data on a daily basis. Thus, to test the effect of weekly meteorological measurements, for each variable the value of the variable on the first day of each week was entered as the value for each day of the rest of that week. The model output obtained with these input data, was compared to the model output obtained with the full set of individual daily input values. Similarly, to evaluate the effect of monthly meteorological measurements, for each variable the value of the variable on the first day of each month was entered as the value for each day for the rest of that month. The model output obtained with these input values was compared to the model output obtained with the full set of individual daily input values. The effect of these changes in the frequency of data input is discussed separately for each of the meteorological variables:

10.2.1 The effect of changing the data frequency of air temperature on model predictions

Air temperature is one of the meteorological variables that is measured by the Weather Bureau at all climate stations, therefore daily measurements of air temperature should always be available. However, because measurements may not be available at the specific site, and to test the sensitivity of the model to air temperature measurements, the model was run with weekly, and monthly, air temperatures entered on a daily basis, as described above. The frequency of the rest of the meterological data was not changed, nor was the frequency of the inflow water quality data changed.

The first step was to assess whether the change from daily to weekly or monthly air temperature data had any effect on the water budget: as indicated in Fig 10.1, changing the frequency of the air temperature from daily to weekly, or even monthly, did not cause any significant change in the water budget for Roodeplaat Dam.

Changing the air temperature from daily to weekly values (entered on a daily basis) caused no change whatsoever in any of the simulated output variables. Changing the air temperature from daily to monthly values resulted in small changes in dissolved oxygen concentration, and very slight changes in dissolved phosphate concentration (Fig 10.2 and 10.3 respectively)

The small change in dissolved oxygen concentration is probably due to the fact that saturated dissolved oxygen concentration is a function of water temperature, which is affected by air temperature. The change in dissolved phosphate concentration can be ascribed to the change in dissolved oxygen concentration - in the modified model the release/adsorption rate of phosphate by the bottom sediments has been linked to the aerobic/anaerobic state of the water.

Conclusion: Changing the data frequency of air temperature from daily to weekly does not cause any change in the simulated water budget, nor in any of the simulated variables. Changing the frequency from daily to monthly results in a small change in predicted concentrations of dissolved oxygen and dissolved phosphate. However, these changes are not significant. Therefore, if air temperature measurements are not available on a daily basis at the site of the reservoir being modelled, weekly, or even monthly, values may be substituted. Measurements from another, nearby site can also be substituted.

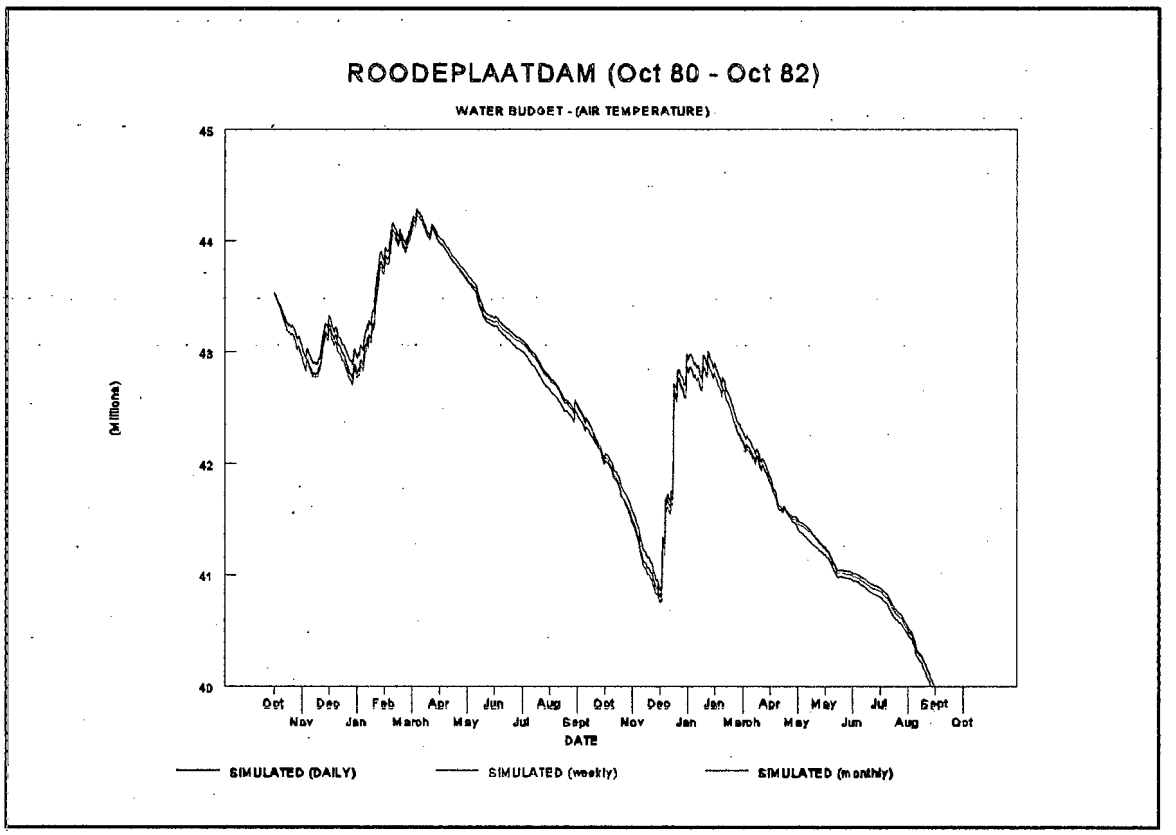

Figure 10.1
Change in simulated water budget obtained with the modified MINLAKE model as a result of changing air temperature input data frequency from daily to weekly/monthly.

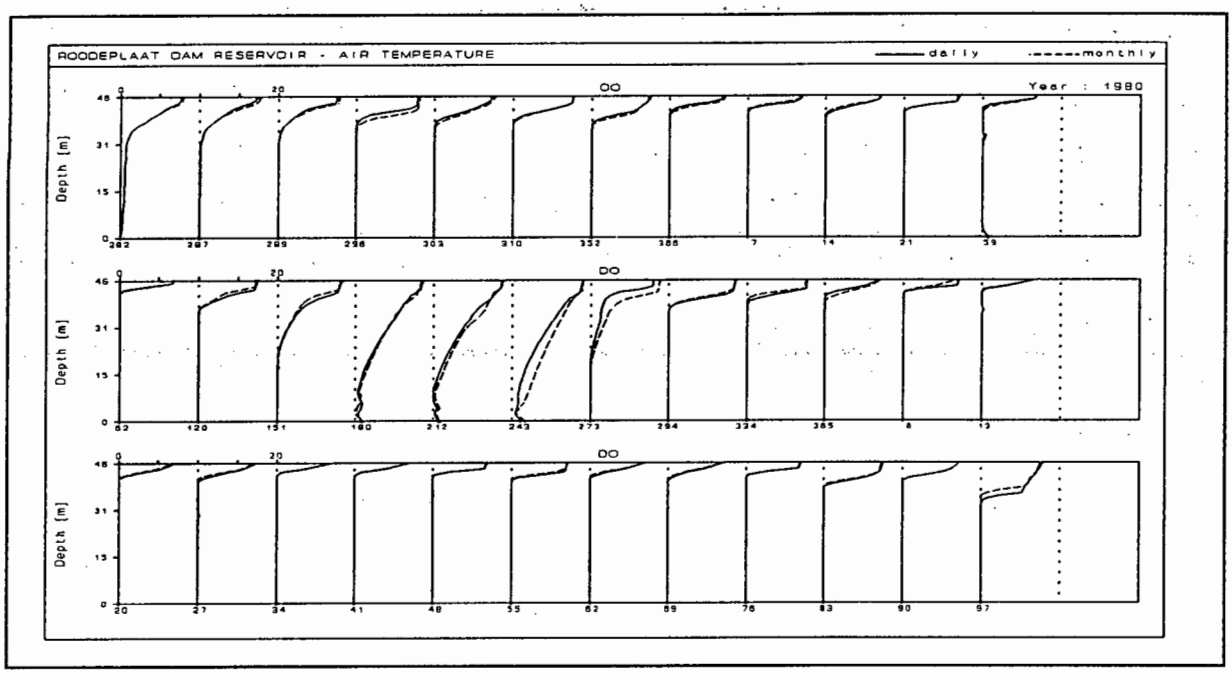

Figure 10.2
Simulated dissolved oxygen concentrations obtained with the modified MINLAKE model using daily and monthly air temperature input data

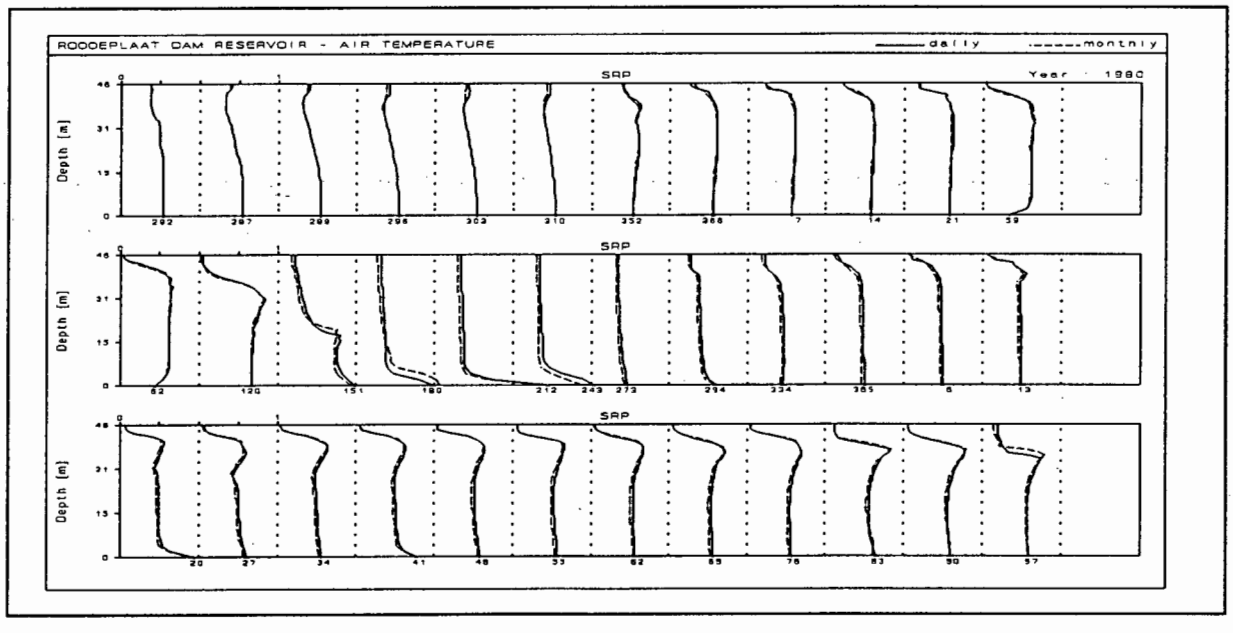

Figure 10.3
Simulated dissolved phosphate concentrations obtained with the modified MINLAKE model using daily and monthly air temperature input data

10.2.2 The effect of changing the frequency of dew point temperature data on model predictions

Both the original and the modified MINLAKE model require dew point temperature measurements. (Other models may require measurement of relative humidity instead of dew point temperature.) If dew point temperature measurements are not available, dew point temperature can be calculated from relative humidity. Relative humidity are measured autographically at first and second order climate stations (*cf* paragraph 10.1), therefore daily measurements of relative humidity should be available. However, as with air temperature, to test the sensitivity of the model to dew point temperature, the model was run with weekly, and monthly, dew point temperatures entered on a daily basis. The frequency of the rest of the meterological data was not changed, nor was the frequency of the inflow water quality data changed.

There was virtually no difference in the simulated water budget when using daily or weekly dew point temperatures. Monthly dew point temperatures (entered on a daily basis) led to a slight change in the water budget (Fig 10.4).

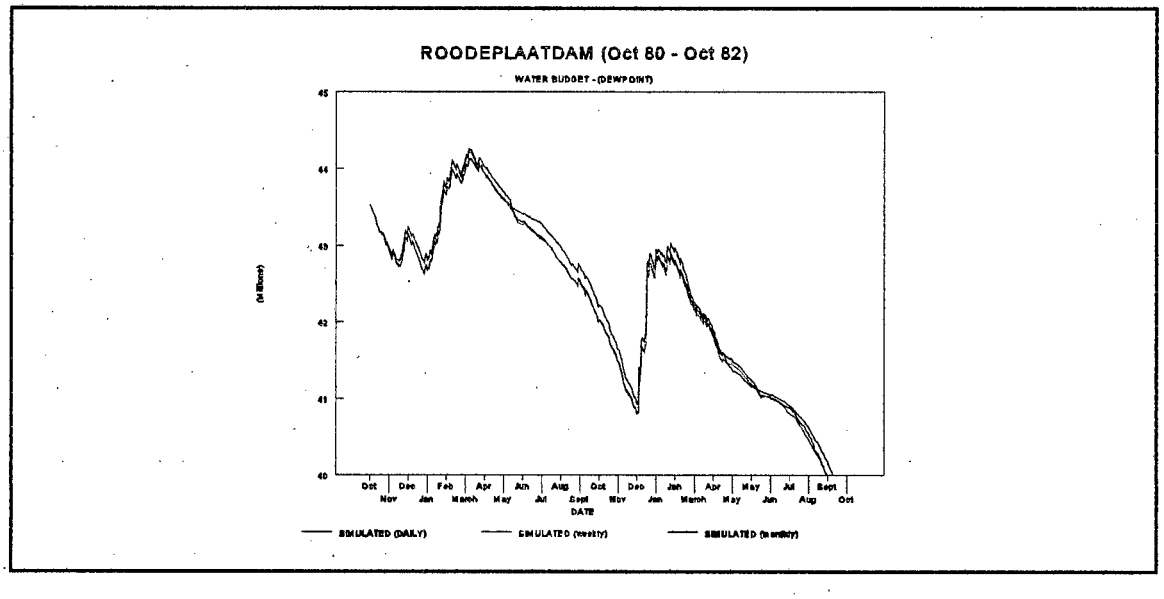

Figure 10.4
Simulated water budget obtained with the modified MINLAKE model using daily, weekly, and monthly dew point temperature input data.

Changing the frequency of dew point temperature data from daily to weekly (entered on a daily basis), did not result in any change in any of the simulated variables. However, changing the frequency from daily to monthly did have an effect: it caused a change in the simulated water temperature, especially during the period of overturn, as depicted in Fig 10.5, Julian days 151 - 243. The change in water temperature is to be expected, as dew point temperature is used in the model in calculation of evaporative heat loss. Furthermore, the change in simulated water temperature caused a change in simulated dissolved oxygen concentration (Fig 10.6), which was so significant that it caused changes in dissolved phosphate, nitrate, and ammonia concentration, mostly during the period of overturn (Julian days 151-243, Fig 10.7, 10.8, and 10.9). These changes occurred because the processes influencing the concentration of these compounds are linked to the dissolved oxygen concentration, for instance, nitrification of ammonia to nitrate occurs during aerobic periods only.

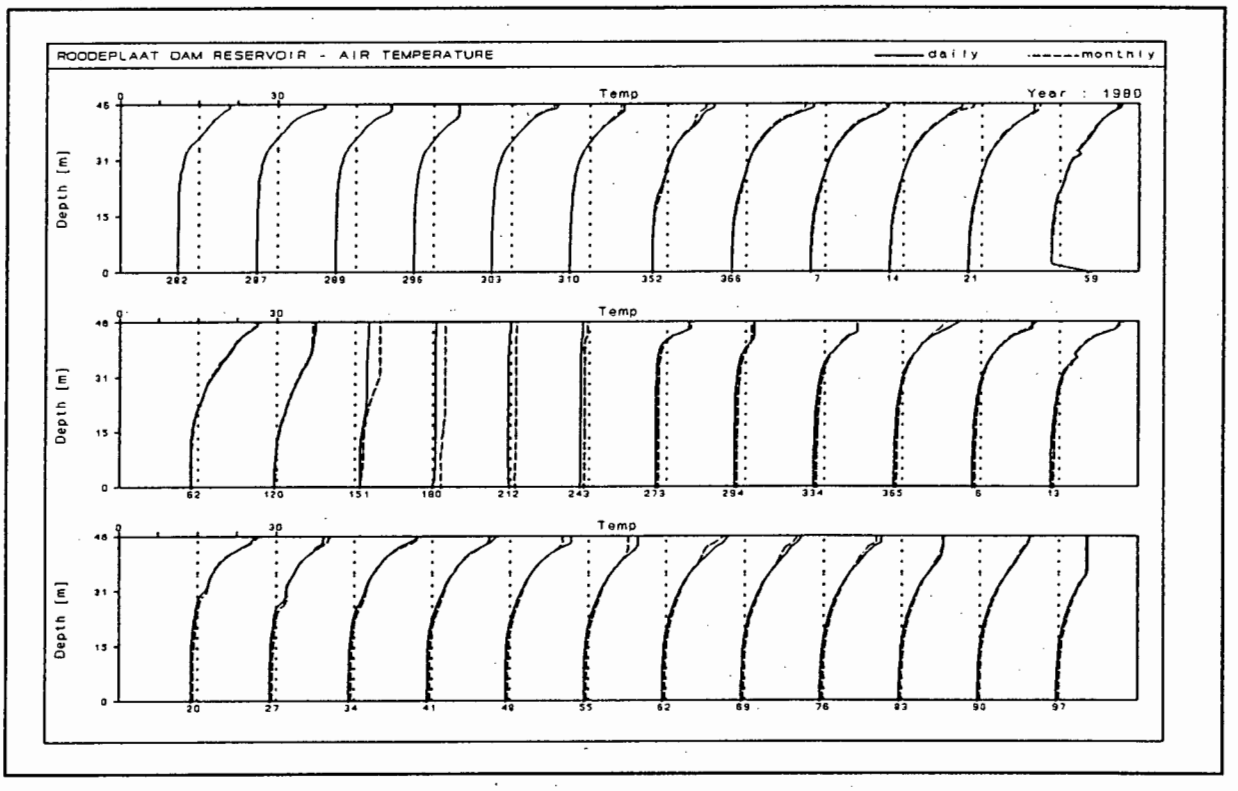

Figure 10.5
Simulated water temperatures obtained with the modified MINLAKE model using daily and monthly dew point input data.

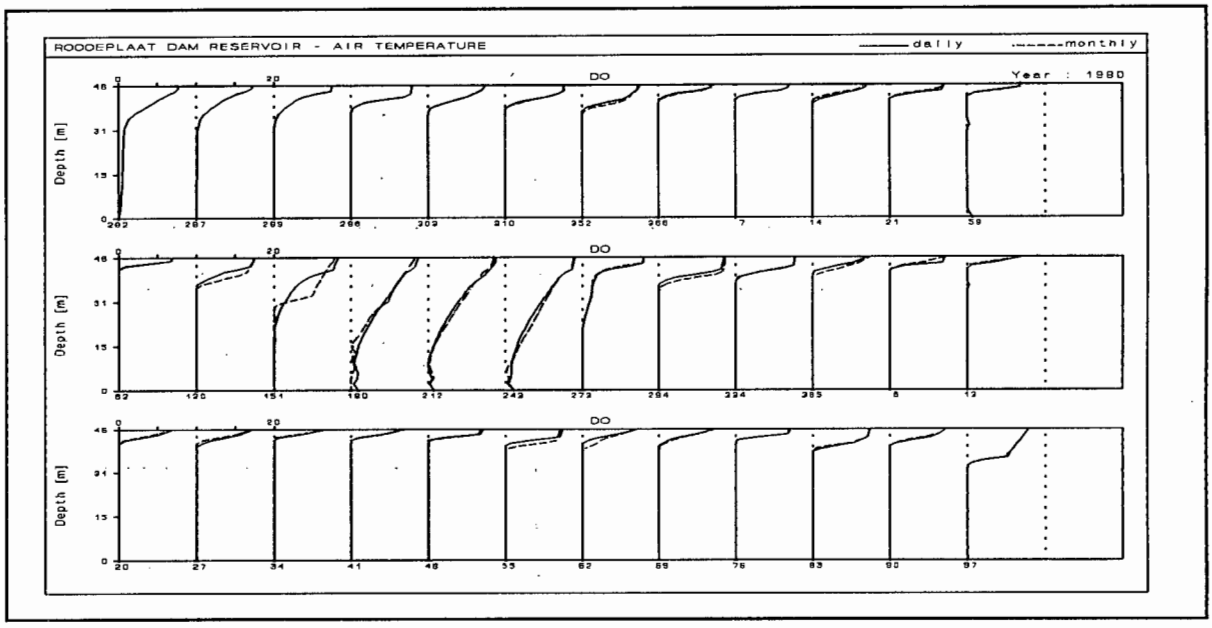

Figure 10.6
Simulated dissolved oxygen concentrations obtained with the modified MINLAKE model using daily and monthly dew point temperature input data.

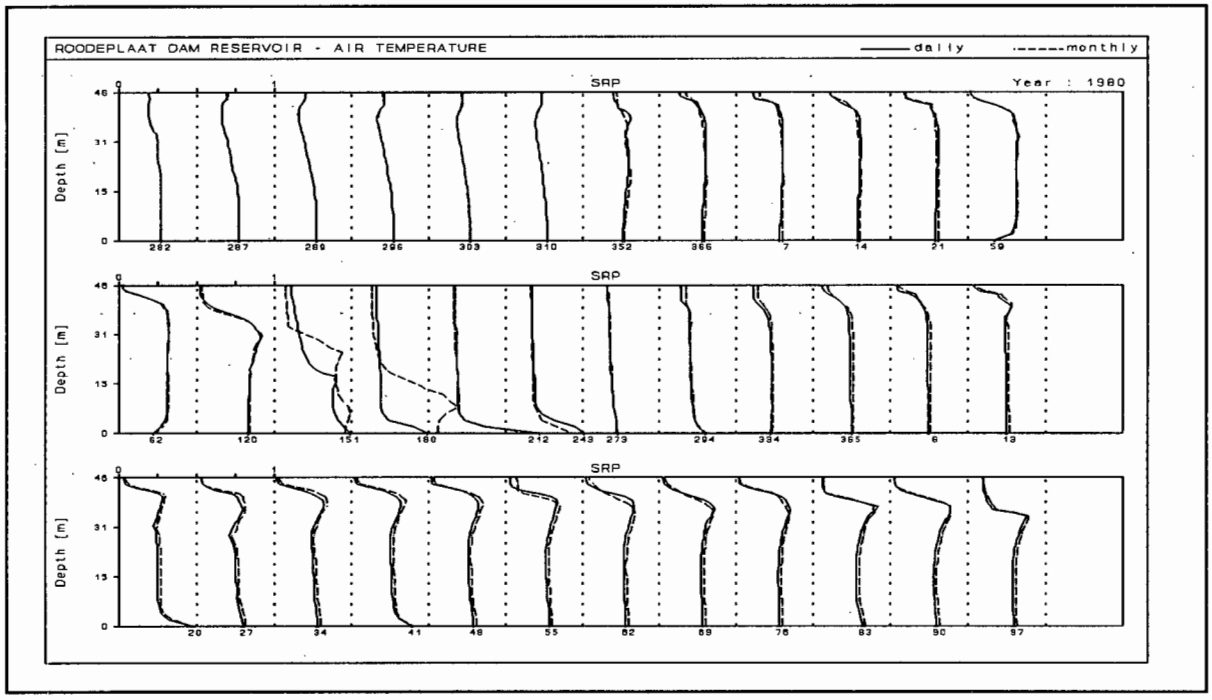

Figure 10.7
Simulated dissolved phosphate concentrations obtained with the modified MINLAKE model using daily and monthly dew point input data.

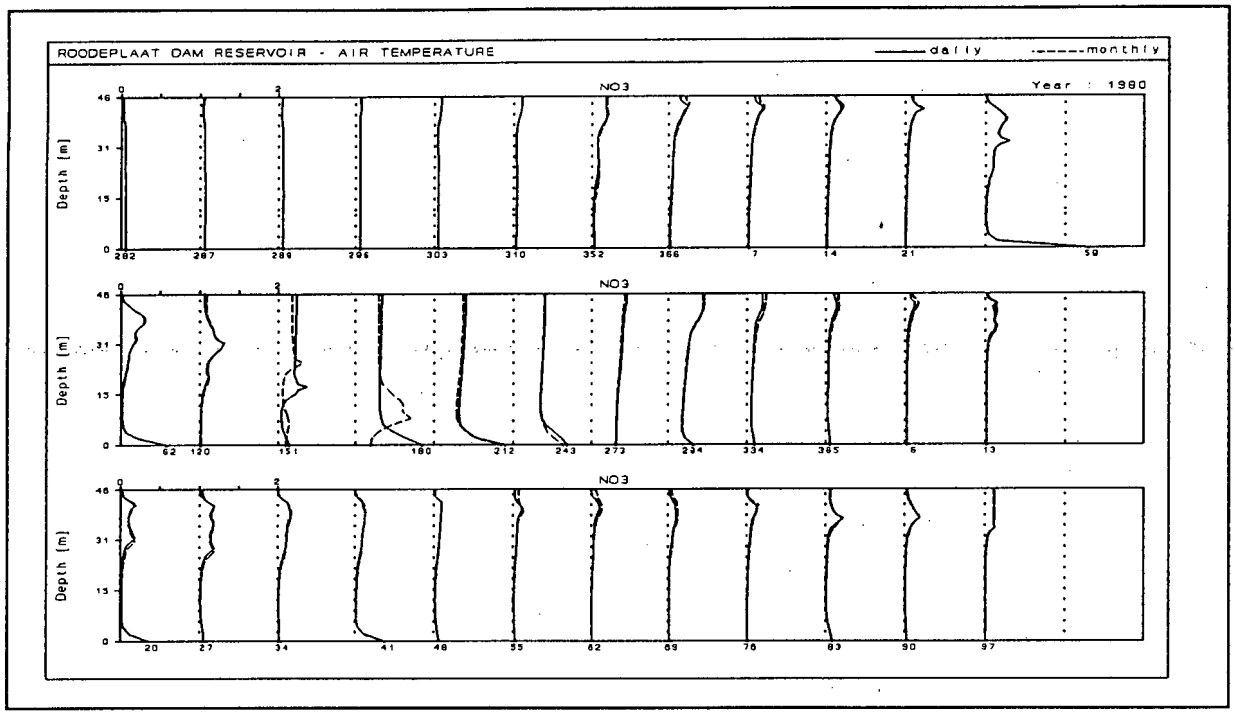

Figure 10.8
Simulated nitrate concentrations obtained with the modified MINLAKE model using daily and monthly dew point temperature input data.

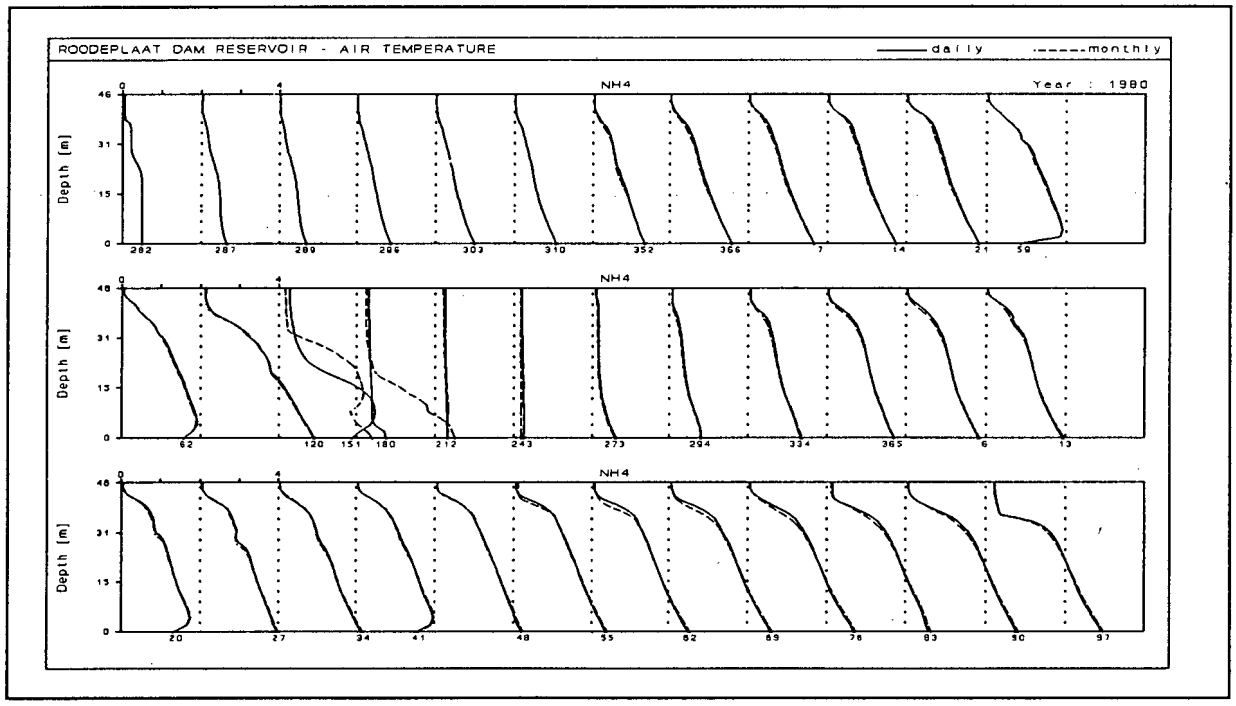

Figure 10.9
Simulated ammonia concentrations obtained with the modified MINLAKE model using daily and monthly dew point temperature input data.

Conclusion: If daily measurements of dew point temperature/relative humidity are not available, weekly values (entered on a daily basis) may be used. The use of monthly values (entered on a daily basis) is not recommended, as the simulated water temperature, as well as concentrations of dissolved oxygen, dissolved phosphate, nitrate and ammonia obtained with these monthly values differed significantly from those obtained with daily values.

10.2.3 The effect of changing the input frequency of precipitation data on model predictions

Precipitation is measured on a daily basis by the Weather Bureau at all climate stations, thus daily precipitation data for, or near, a particular site should always be available. However, to test the sensitivity of the model to precipitation, the following was done: instead of using weekly/monthly data, entered on a daily basis, in this case it was deemed more practical to use weekly/monthly **averaged** precipitation data, as it would be feasible to check a rain gauge weekly or monthly, which would give averaged data. Thus the **average** for each week/month was entered on a daily basis; the frequency of the other meteorological and inflow water quality variables was not changed.

Using weekly/monthly averaged precipitation data (entered on a daily basis), instead of daily data, resulted in no change in the simulated water budget, nor in any of the other simulated variables.

Conclusion: In the absence of daily precipitation data, **averaged** weekly, or even monthly, precipitation data may be entered on a daily basis in the modified MINLAKE model, as it will not cause any significant difference in the simulated output. Precipitation data from another, nearby site can be substituted also.

10.2.4 The effect of changing the input frequency of wind speed data on model predictions

In both the original and the modified MINLAKE model, wind speed has been identified as one of the main driving forces in the model. The model requires wind speed measured at 10 m height above land. In South Africa, often wind speed is measured at 1.8 m above land, necessitating conversion to wind speed at 10 m above land. Also, wind speed is measured at 21 climate stations only (CSIR 1985), thus it is quite likely that wind speed may not be measured at or near the reservoir being modelled. The only solution is to use wind speed measurements from the nearest site. However, due to topographical and climatic differences, these measurements may not be a true reflection of the wind speed at the reservoir being modelled. Ideally, wind speed should be measured at the reservoir being modelled. However, continuous autographic recording of wind speed is expensive (Quibell 1993), therefore the rationale in testing the sensitivity of the model to wind speed was as follows: it was assumed that it would be economically feasible to determine wind speed one day per week at the specific site, or at least one day per month. The wind speed in the original meteorological data base for Roodeplaat Dam was used as a basis. To evaluate the effect of one wind speed measurement per week, the wind speed on the first day of every week was entered for all the days of that week. The frequency of the rest of the meteorological and inflow water quality variables was not changed. Thereafter, to evaluate the effect of one wind speed measurement per month, the wind speed on the first day of each month was entered for all the days of that month. Again the frequency of the rest of the meteorological and inflow water quality variables was not changed.

Figure 10.10 depicts the simulated water budget obtained when the modified MINLAKE model was run on Roodeplaat Dam with daily, weekly, and monthly wind speed. There is virtually no change in the simulated water budget obtained with daily and weekly wind speeds. The simulated water budget obtained with monthly wind speed measurements differs slightly from the simulated water budget obtained with daily wind speed measurements.

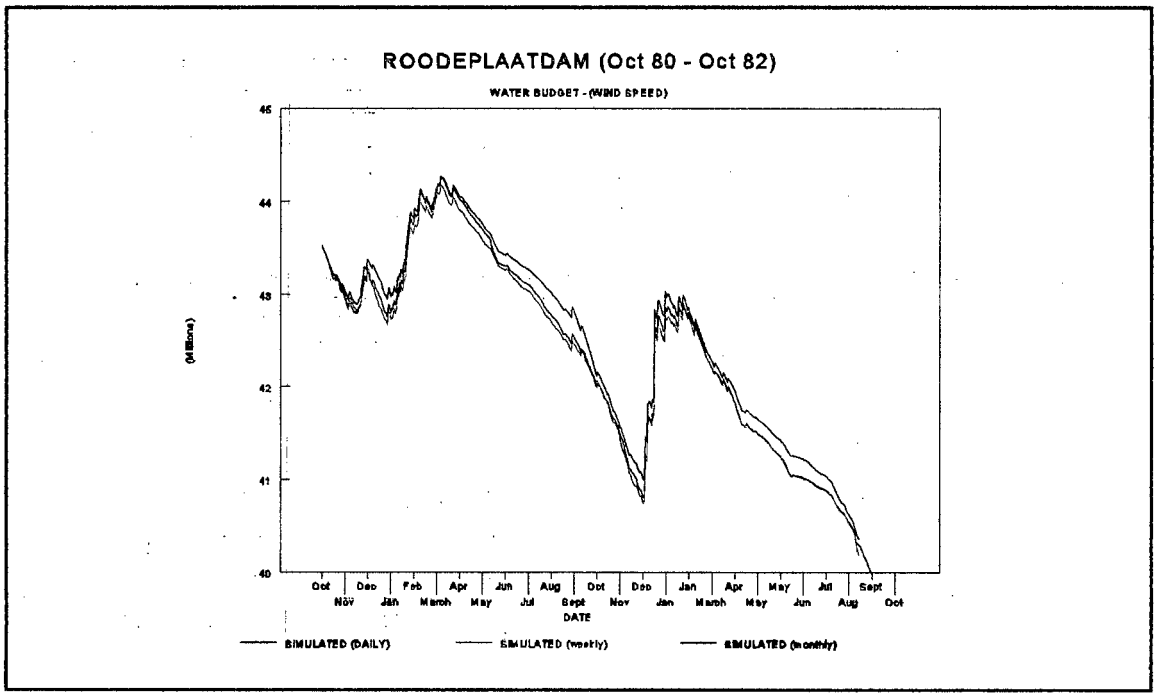

Figure 10.10
Simulated water budgets obtained with the modified MINLAKE model using daily, weekly, and monthly wind speed input data.

In both the original and the modified MINLAKE model, mixing depth is formulated, *inter alia,* as a function of wind speed. However, changing the frequency of wind speed data as described above did not affect the simulated mixing depth significantly.

With regard to the other simulated variables, changing the wind speed from daily to weekly data (entered on a daily basis) resulted in a small, but definite, change in water temperature (Fig 10.11). This change is to be expected, as, in the original and modified MINLAKE model, both evaporative and convective heat loss is a function of wind speed. The effect of changing the frequency of wind speed data on evaporative heat loss can be seen on Julian days 296 - 21 in Fig 10.11, where the water temperature in the surface layer changed. Convective heat loss was effected only when turnover started - Julian day 151 in Fig 10.11. The influence of a change in convective heat loss on water temperature is evident in the hypolimnion. The change in convective heat loss is large enough to cause a change in water temperature for the rest of the simulation period.

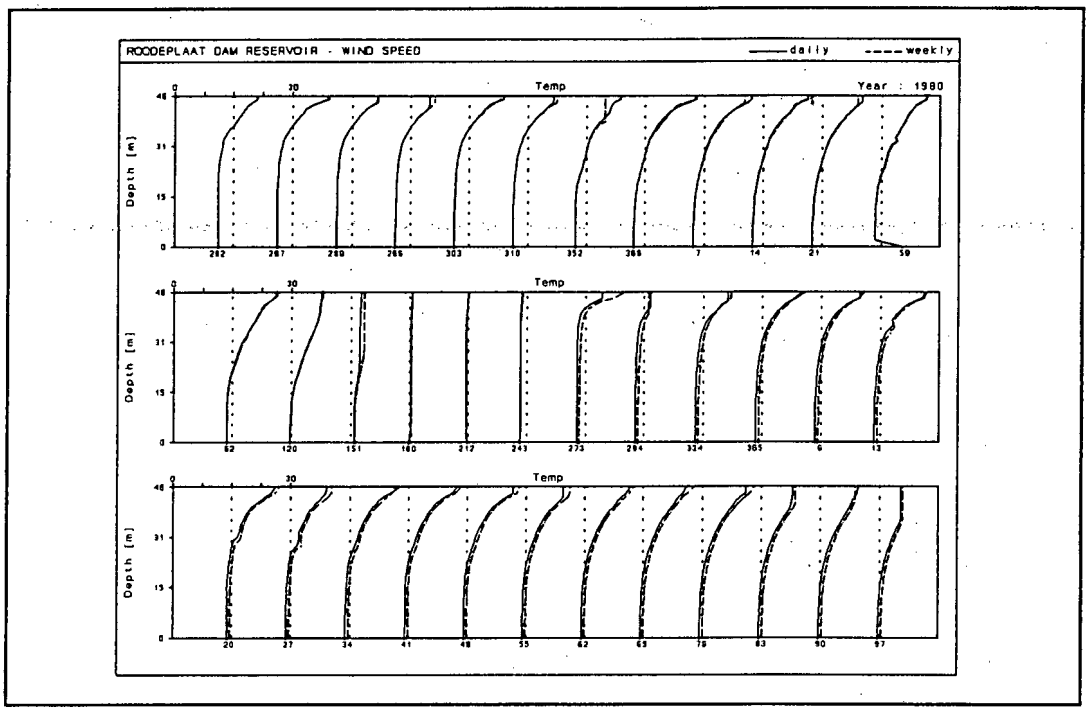

Figure 10.11
Simulated water temperature obtained with the modified MINLAKE model on Roodeplaat Dam using daily and weekly wind speed data.

Changing the wind speed data from daily to weekly also affected the simulated dissolved oxygen concentration (Fig 10.12). The change in dissolved oxygen concentration is probably due to both the change in wind speed data, which will affect the water-air surface interaction, and to the change in water temperature, as dissolved oxygen concentration is a function of water temperature.

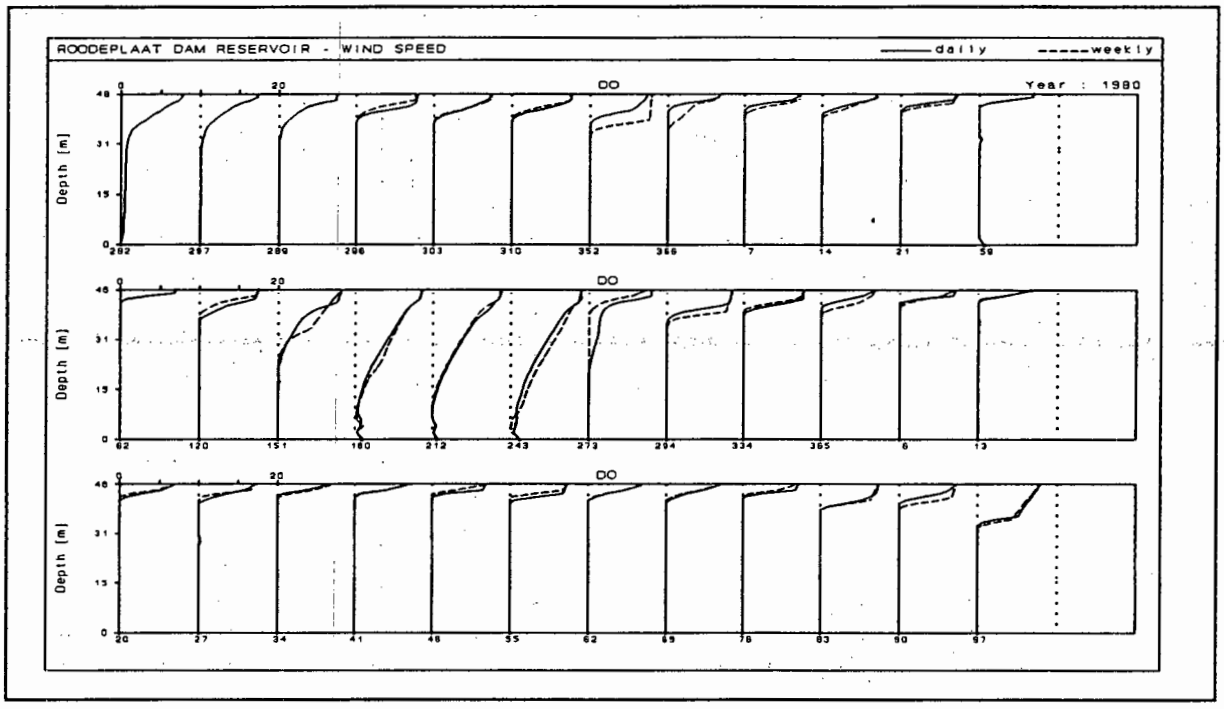

Figure 10.12
Simulated dissolved oxygen concentrations obtained with the modified MINLAKE model using daily and weekly wind speed data

Differences in simulated concentrations of dissolved phosphate, nitrate and ammonia are depicted in Fig 10.13 - 10.15. The reasons for these differences are twofold; firstly it is due to the change in dissolved oxygen concentration, as a number of processes, e.g. the release/adsorption of nutrients, is linked to the aerobic/anaerobic state of the water in the modified MINLAKE model. Secondly the differences were due to the change in water temperature which caused the water density to change, thereby affecting the rate of hypolimnetic diffusion. During calibration of the modified MINLAKE model on Roodeplaat Dam, hypolimnetic diffusion was identified as one of the most significant transport processes in the model.

The effect of a change in simulated dissolved oxygen concentration on, for instance, simulated dissolved phosphate, is evident on Julian days 352 - 21 in Fig 10.13, whereas the effect of a change in simulated water temperature (and hence in hypolimnetic diffusion) on simulated dissolved phosphate is evident from Julian days 273 onwards in Fig 10.13.

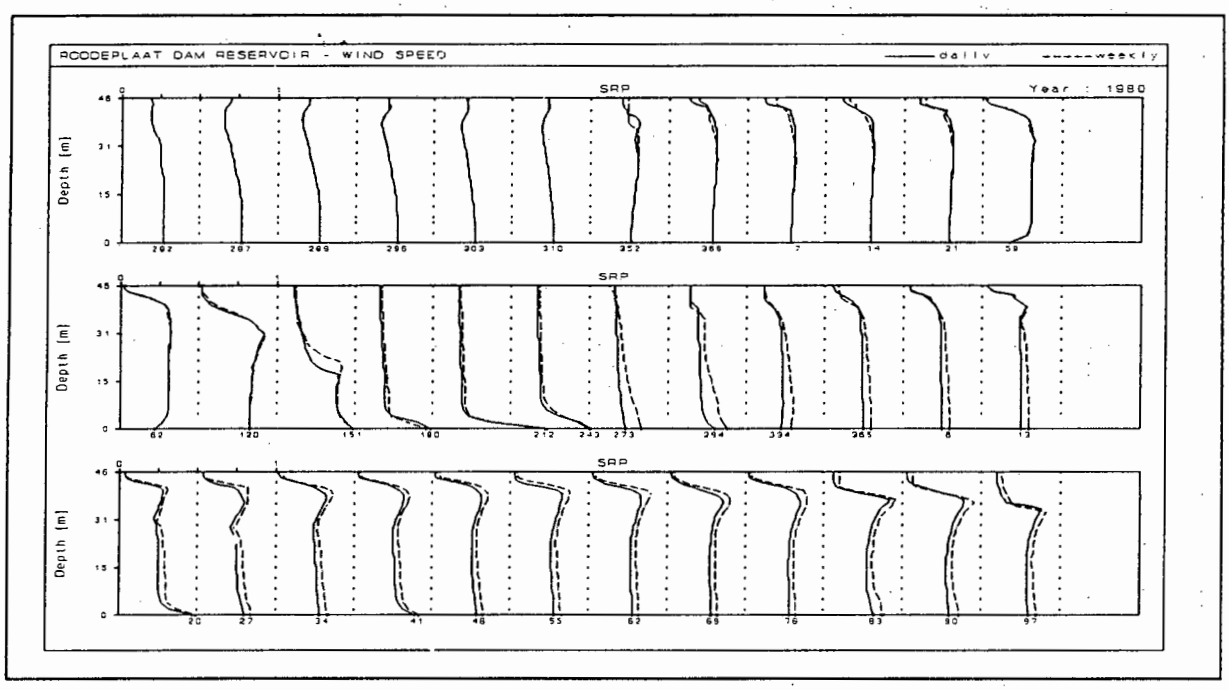

Figure 10.13
Simulated dissolved phosphate concentrations obtained with the modified MINLAKE model on Roodeplaat Dam using daily and weekly wind speed data.

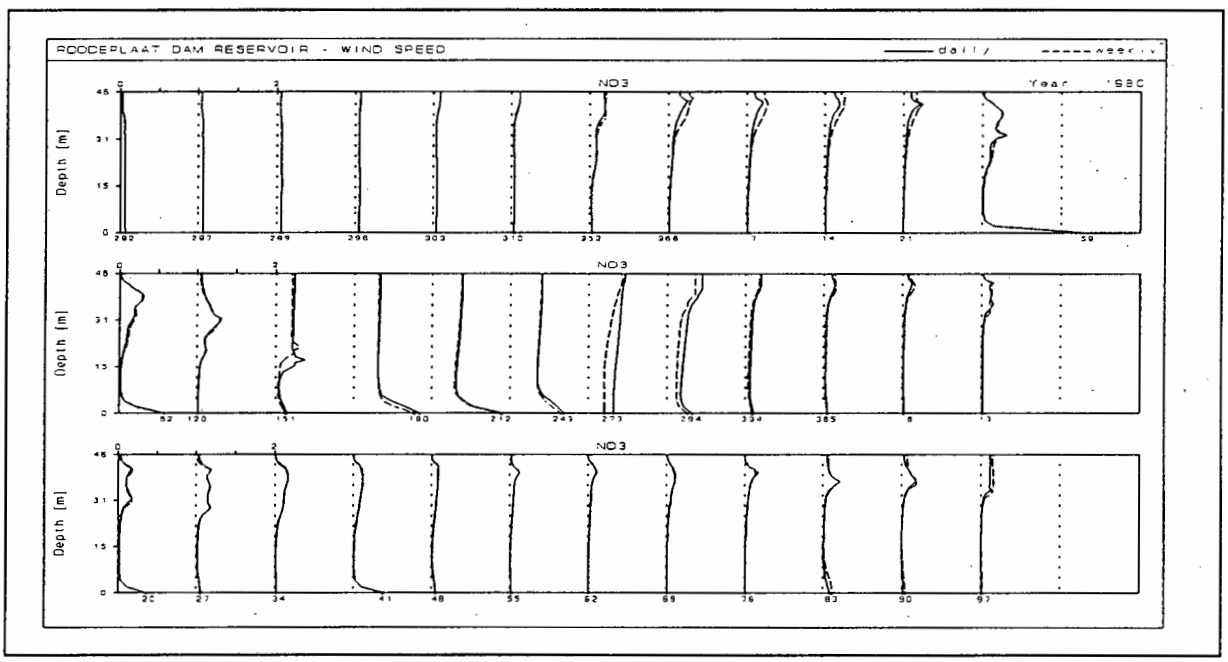

Figure 10.14
Simulated nitrate concentrations obtained with the modified MINLAKE model on Roodeplaat Dam using daily and weekly wind speed data.

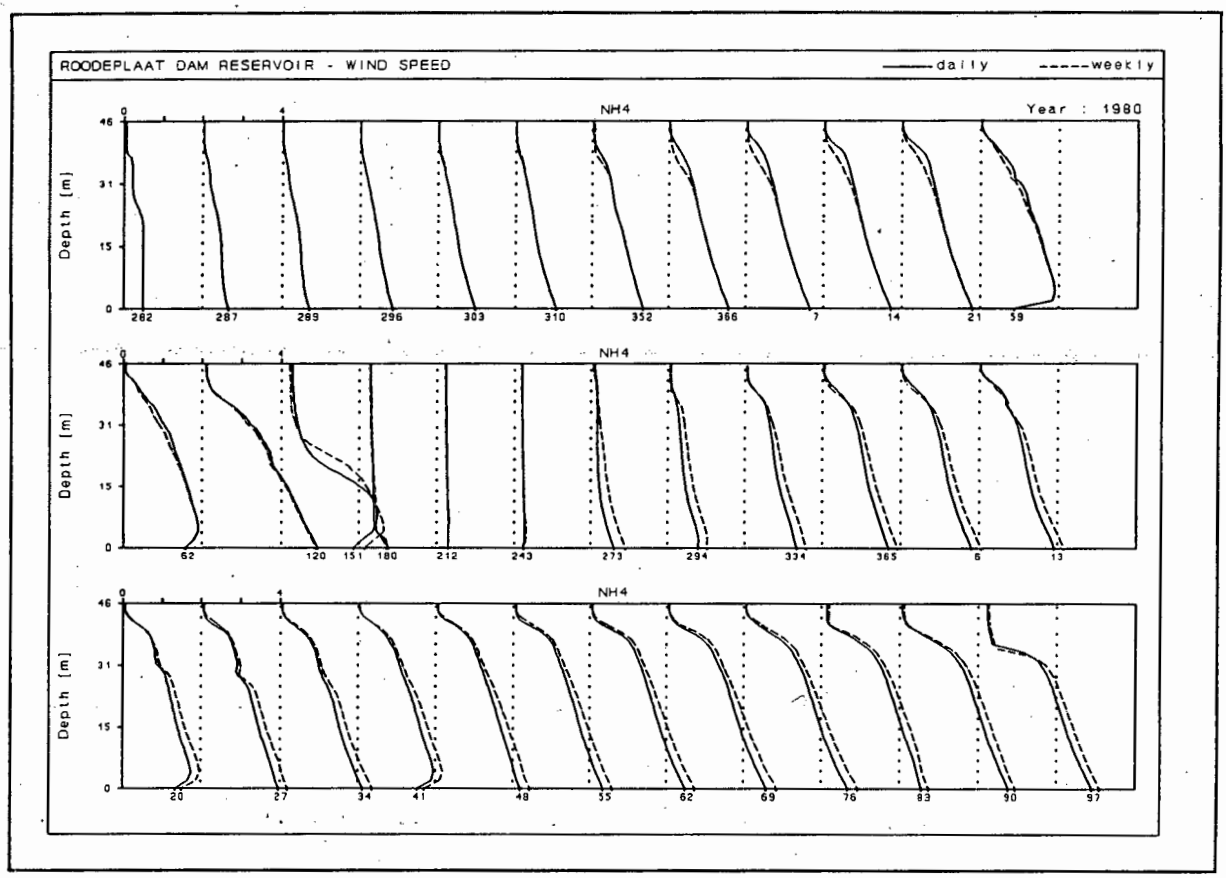

Figure 10.15
Simulated ammonia concentrations obtained with the modified MINLAKE model on Roodeplaat Dam using daily and weekly wind speed data.

Changing the frequency of wind speed data input from daily to monthly affected the same variables, i.e. water temperature, and concentrations of dissolved oxygen, dissolved phosphate, nitrate and ammonia, the differences being more significant (Fig 10.16 - 10.20) than with the change from daily to weekly wind speed input.

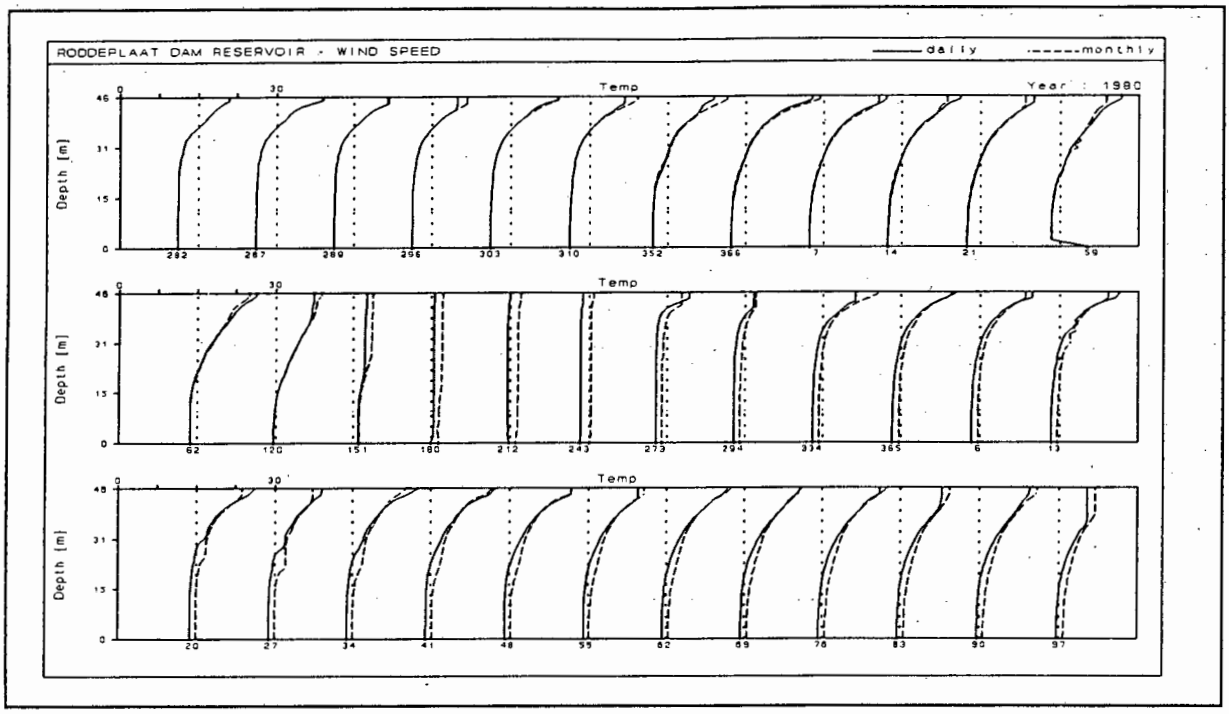

Figure 10.16
Simulated water temperature obtained with the modified MINLAKE model on Roodeplaat Dam using daily and monthly wind speed data.

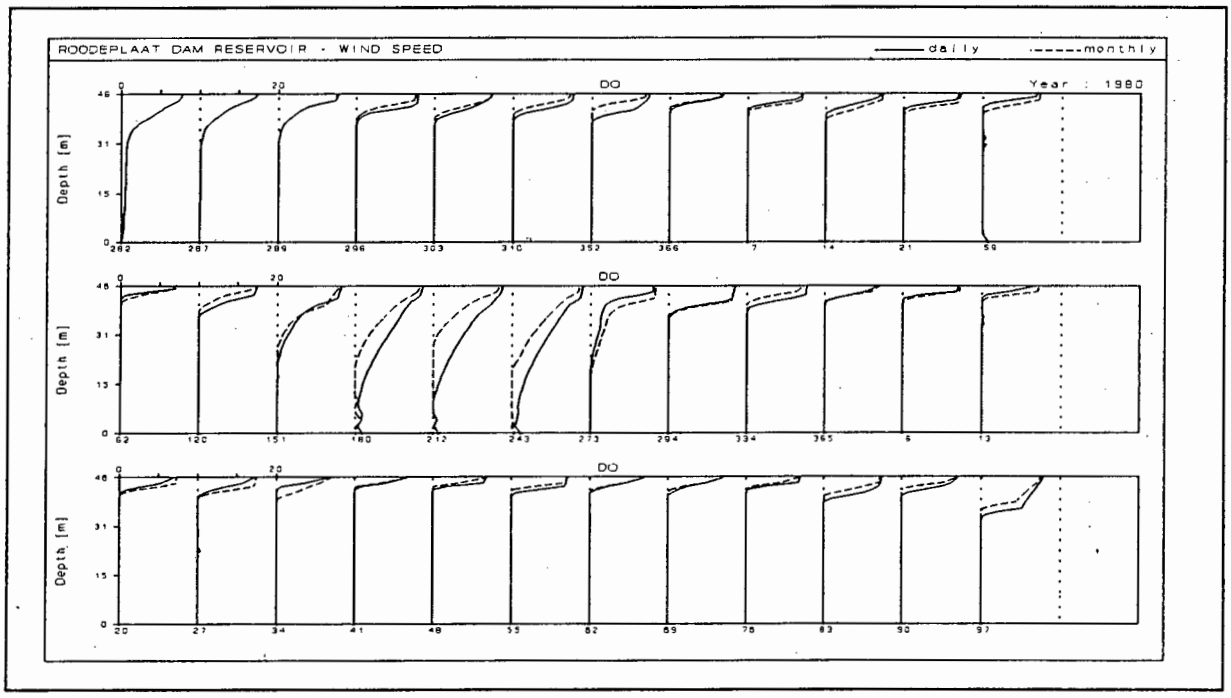

Figure 10.17
Simulated dissolved oxygen concentrations obtained with the modified MINLAKE model on Roodeplaat Dam using daily and monthly wind speed data.

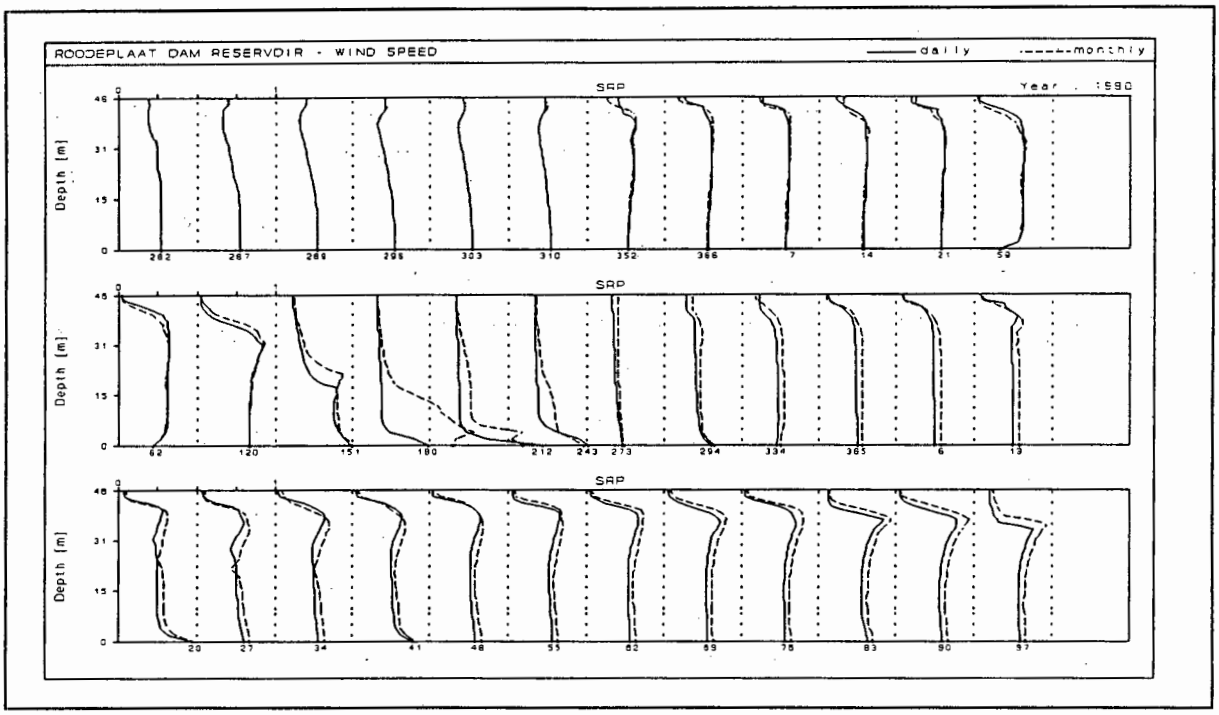

Figure 10.18
Simulated dissolved phosphate concentrations obtained with the modified MINLAKE model on Roodeplaat Dam using daily and monthly wind speed data.

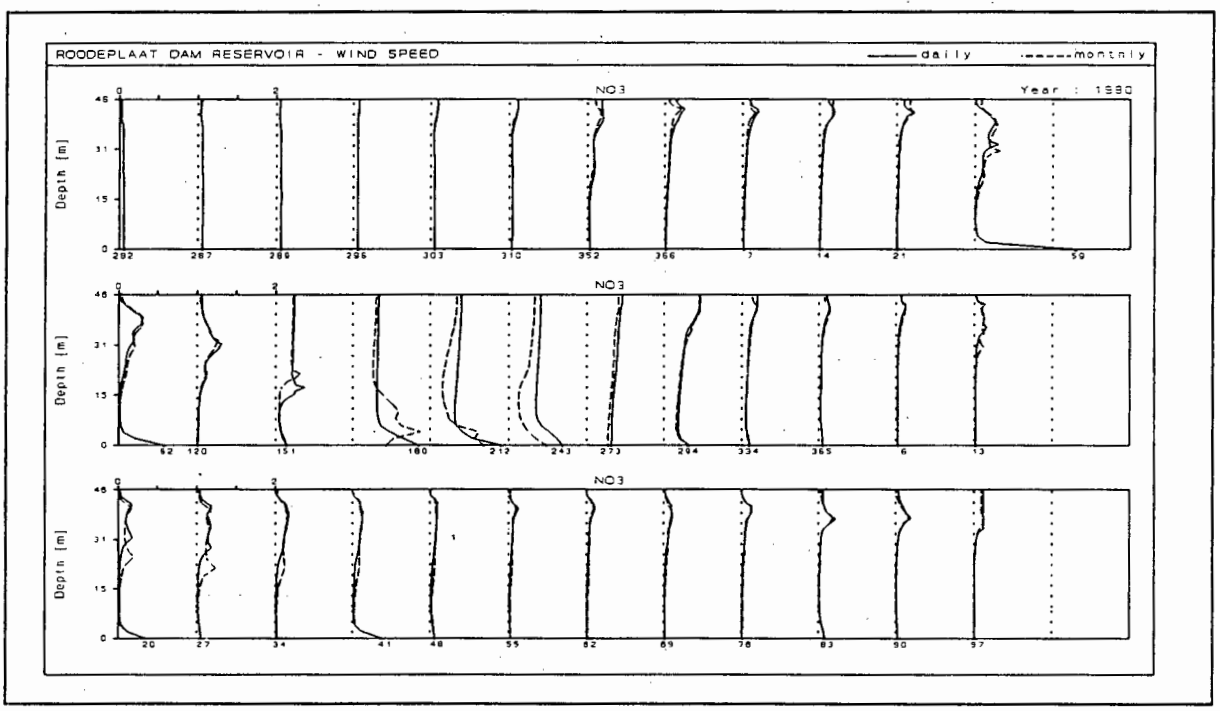

Figure 10.19
Simulated nitrate concentrations obtained with the modified MINLAKE model on Roodeplaat Dam using daily and monthly wind speed data.

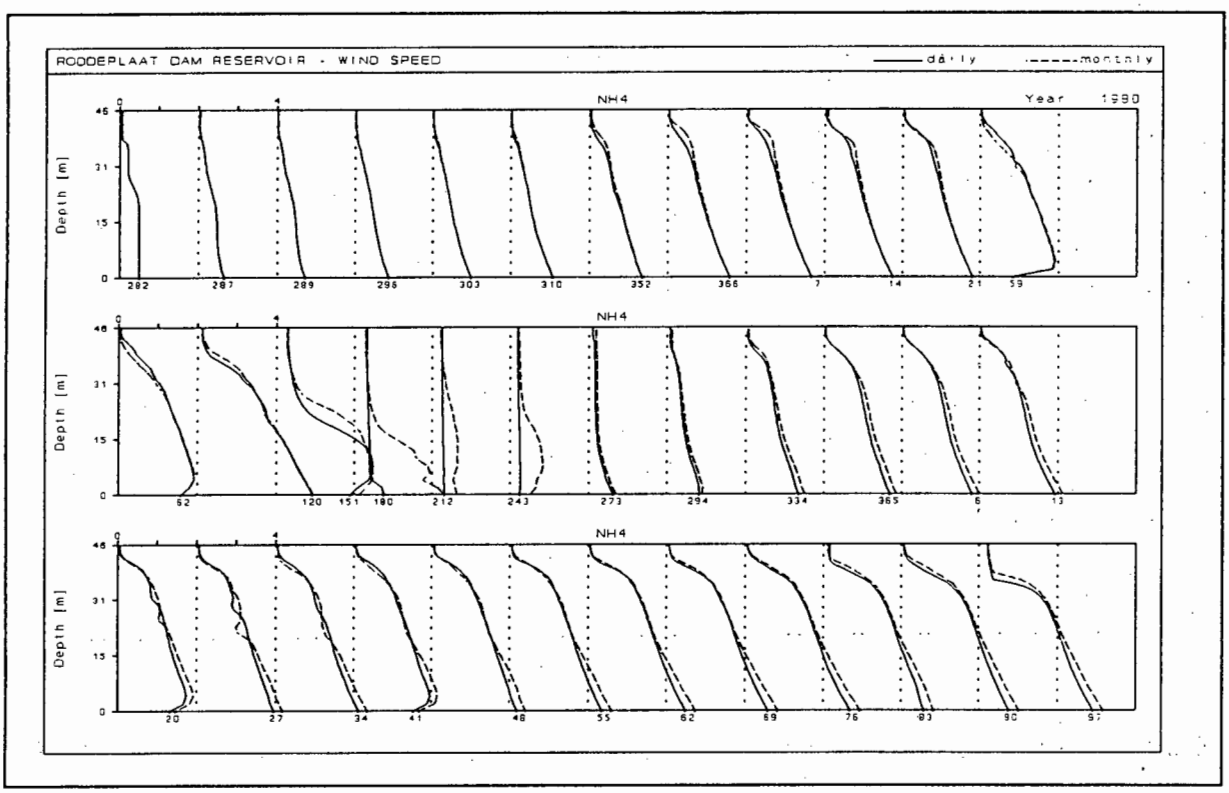

Figure 10.20
Simulated ammonia concentrations obtained with the modified MINLAKE model on Roodeplaat Dam using daily and monthly wind speed data.

Conclusion: Wind speed has been identified as one of the main driving forces in both the original and the modified MINLAKE models. During calibration of the modified model on Roodeplaat Dam, considerable time was spent on setting up the wind speed data base. Calibration of the model was possible only once the observed wind speed (measured at 1.8 m over land), was converted to wind speed at 10 m over land, as required by the model. In view of the proven importance of wind speed, it was expected that a change in the frequency of wind speed data would result in greater changes in the simulated variables than those reported here. However, it would seem that, although wind speed is one of the main driving forces of the model, the model is not that sensitive to minor variations in wind speed, i.e. the difference between daily wind speed measurements and weekly data (entered on a daily basis) is too small to

cause significant changes in the model output, whereas the difference between wind speed at 2 m and that at 10 m above land, is large enough to cause significant differences in the model output. Thus it is very important to ensure that, if the observed wind speed has not been measured at height required by the model, it is converted from the observed height to the required height. Once this has been done, in the absence of daily data, one weekly measurement of wind speed, entered into the model on a daily basis, should give satisfactory results.

The differences in simulated results between daily and monthly wind speed data (entered on a daily basis) are more significant. However, depending on the requirements of the user, even monthly wind speed data may be adequate.

In the absence of on-site measurements, care should be taken in using wind speed data from another, nearby site, depending on the surrounding topography. If for instance, the reservoir is situated in hilly terrain, wind speed from another site may not be representative of the wind speed at the reservoir site.

10.2.5 The effect of changing the input frequency of wind direction data on model predictions.

In South Africa, wind direction measurements are not done on a routine basis. Also, if wind direction is measured, the results are often in graphical format, whereas mathematical models usually require digital format. During calibration of the modified MINLAKE model on Roodeplaat Dam, considerable time was spent on digitising the wind direction data, and infilling missing data as accurately as possible. As with wind speed data, missing wind direction data have to be infilled from the nearest site where the wind direction has been measured. This may not be a true reflection of wind direction at the reservoir being modelled, due to topographical differences, and considerable time was spent to ensure that the infilled data was a good reflection of the wind direction at Roodeplaat Dam.

To test the sensitivity of the model to wind direction data, the original meteorological data file that was developed for Roodeplaat Dam was used as a basis. The wind direction on the first day of each week was entered as the wind direction for all the days of that week. Similarly, to evaluate the effect of one wind direction measurement per month, the wind direction on the first day of each month, was entered as the wind direction for all the days of that month. The frequency of the rest of the meteorological, as well as the inflow water quality variables, was not changed.

The changes in the frequency of the wind direction data did not result in any change to the simulated water budget, the simulated mixing depth, or any of the other simulated variables. The source code of the original MINLAKE model was checked to identify the formulations that utilized wind direction. It was found that, although wind direction data is entered into the model, it is never used in any of the process formulations in the main programme. The only advantage of reading wind direction data into the main programme, is that the user can specify wind fetch as a function of wind direction in the lake specific programme.

Conclusion: Wind direction data are not required in any of the process formulations in the model, but it does afford the user the opportunity of linking, for instance, wind fetch to wind direction. This may be of significance in non-symmetrical dams. Therefore, the frequency of wind direction data would depend on the requirements of the user, and in some instances wind direction data may not be required at all.

10.2.6 The effect of changing the input frequency of sunshine data on model predictions.

In both the original and modified model algal growth is calculated as a function of percentage sunshine. Percentage sunshine must be calculated by the user from observed sunshine hours and astronomical day length. Astronomical day length is the maximum number of hours of sunshine that can occur theoretically, and is calculated from the latitude of the reservoir being modelled (*cf* Chapter 4).

Sunshine hours are measured by the Weather Bureau at first and second-order climate stations, but data may not always be available at a specific reservoir site. To test the sensitivity of the model to the frequency of percentage sunshine, the observed sunshine hours on the first day of each week was entered as the value for all the days of that week. Thereafter the value on the first day of each month was entered as the value for all the days of that month. Daily data were used for the rest of the meteorological and inflow water quality variables.

Changing the frequency of observed sunshine data from daily to weekly did not result in any changes in the water budget, nor in any of the other simulated variables. Changing the frequency from daily to monthly did not affect the water budget, but it did cause a slight change in simulated chlorophyll-a concentration. This change is to be expected, as algal growth is formulated as a function of percentage sunshine. The change in simulated chlorophyll-a concentration led to small changes in the simulated concentration of dissolved oxygen, dissolved phosphate, nitrate and ammonia. However, these changes were not considered significant.

Conclusion: Although algal growth is calculated as a function of percentage sunshine, the model output does not seem to be very sensitive to this variable, therefore, if daily data on the number of hours of sunshine are not available, weekly, or even monthly, data can be used. In the absence of on-site data, data from another, nearby site can be used.

10.2.7 The effect of changing the input frequency of shortwave radiation data on model predictions.

Short wave radiation is one of the main driving forces of both the original and the modified MINLAKE models. Solar radiation is measured by the Weather Bureau at 12 first-order climate stations only, therefore it is quite likely that radiation data would not be available at the site of the reservoir being modelled. As with the other variables, to test the sensitivity of model to short wave radiation, the frequency of radiation data was changed from daily to weekly, and thereafter to monthly, whilst retaining a daily frequency for the other meteorological and inflow water quality variables.

Regarding the water budget, changing the frequency of radiation data from daily to monthly had a bigger effect on the simulated results than changing the frequency from daily to weekly (Fig 10.21).

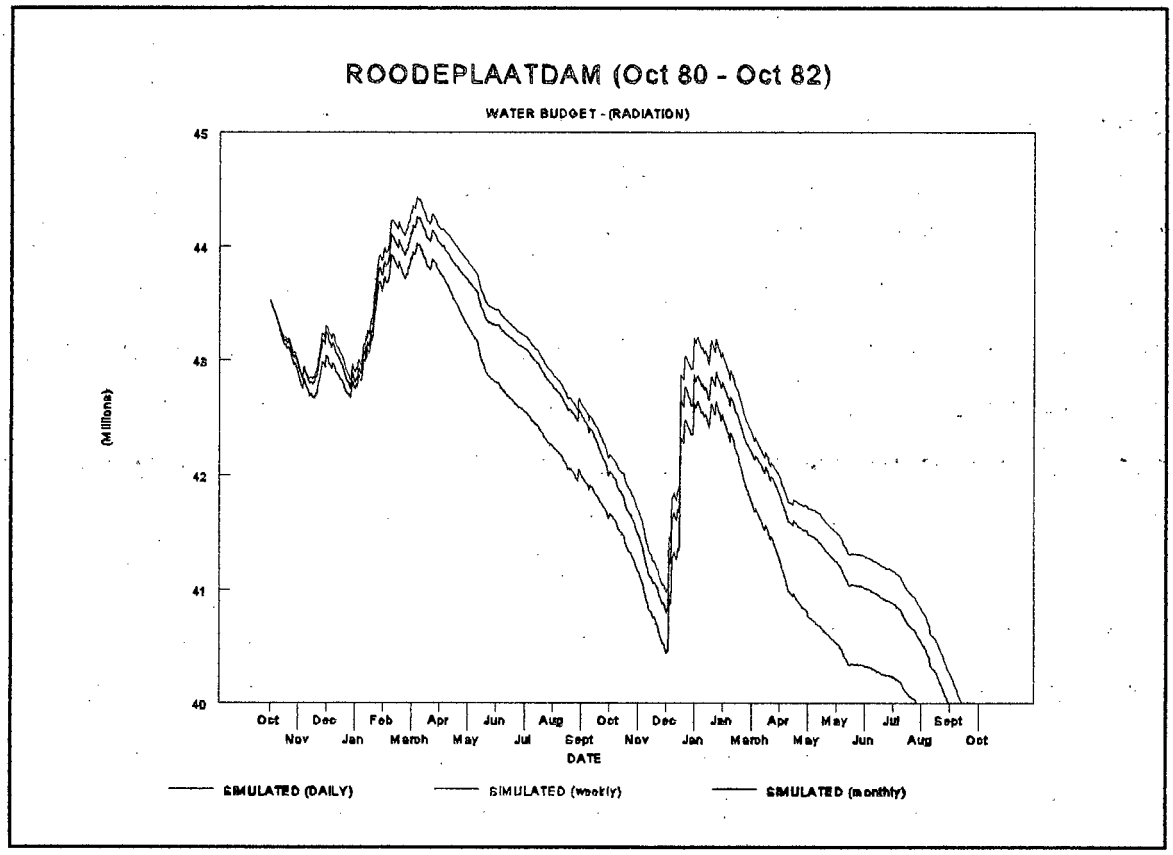

Figure 10.21
Water budget for Roodeplaat Dam as simulated with the modified MINLAKE model using daily, weekly, and monthly short wave radiation data.

Changing the frequency of radiation data leads to small, but significant changes in water temperature (Fig 10.22). This is to be expected, as water temperature is formulated as a function of short wave radiation in the model. The changes in simulated chlorophyll-a concentration are more significant (Fig 10.23). Again this is to be expected, as, in both the original and modified models, algal growth rate is a function of both water temperature and short wave radiation.

The changes in simulated water temperature and chlorophyll-a concentration caused a change in simulated dissolved oxygen concentration (Fig 10.24). All of these changes influence the concentrations of dissolved phosphate, nitrate and ammonia, because, in the modified MINLAKE model, these concentrations are functions of water temperature, chlorophyll-a concentration, and the aerobic/anaerobic state of the water (Fig 10.25 -10.27). The changes in simulated nutrient concentration are more prominent towards the end of the simulation period - this would indicate that the change in water temperature (and thus water density) is affecting the hypolimnetic diffusion rate.

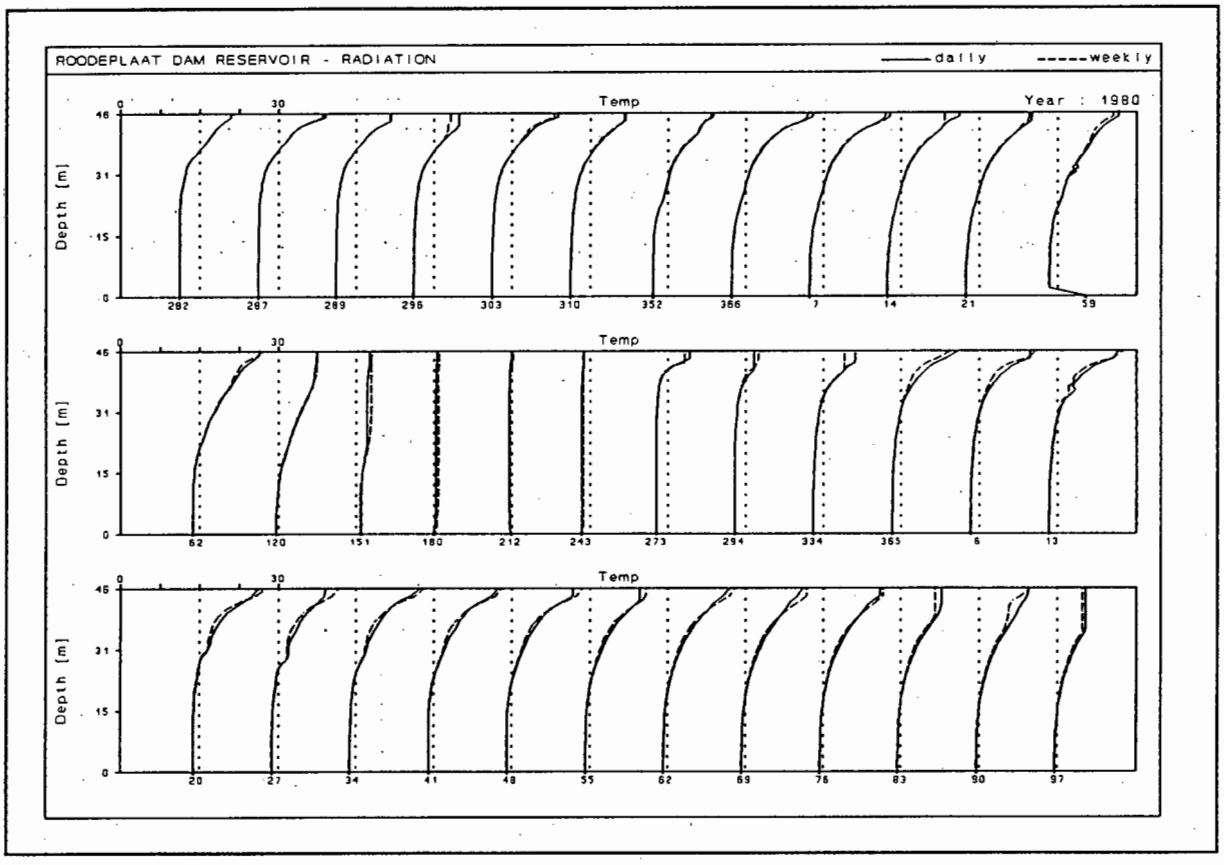

Figure 10.22
Simulated water temperatures obtained with the modified MINLAKE model on Roodeplaat Dam using daily and weekly radiation data.

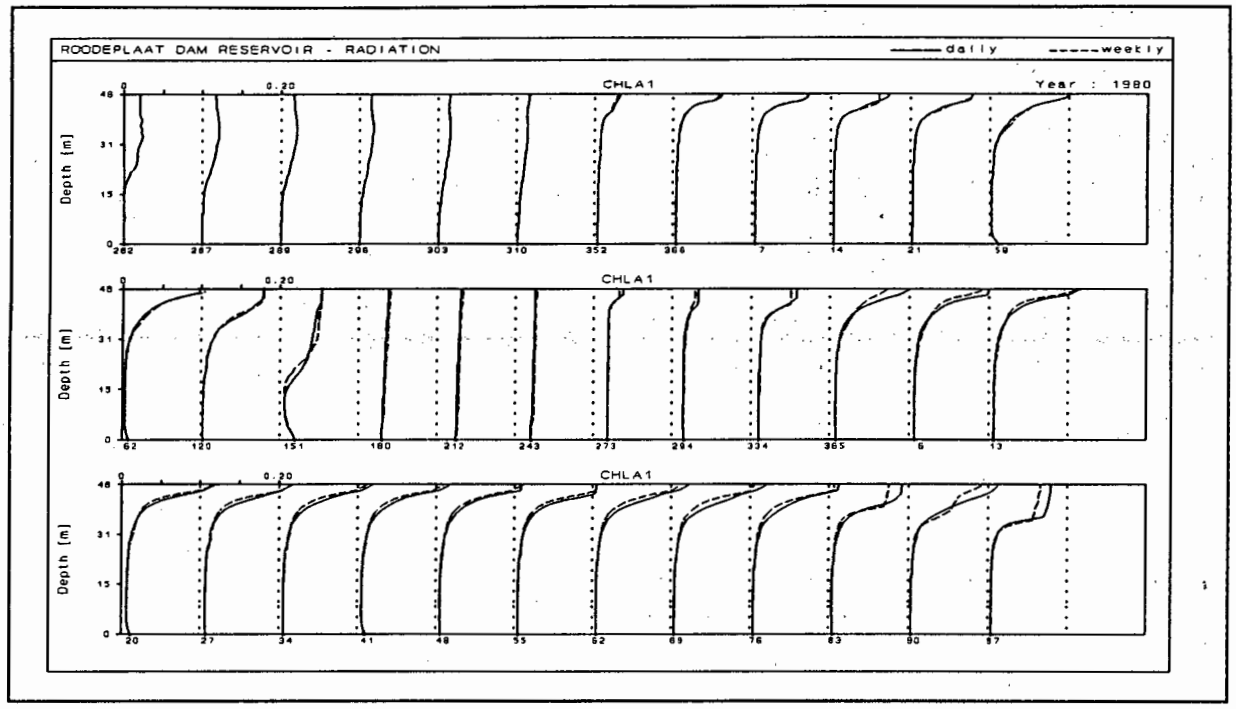

Figure 10.23
Simulated chlorophyll-a concentrations obtained with the modified MINLAKE model on Roodeplaat Dam using daily and weekly radiation data.

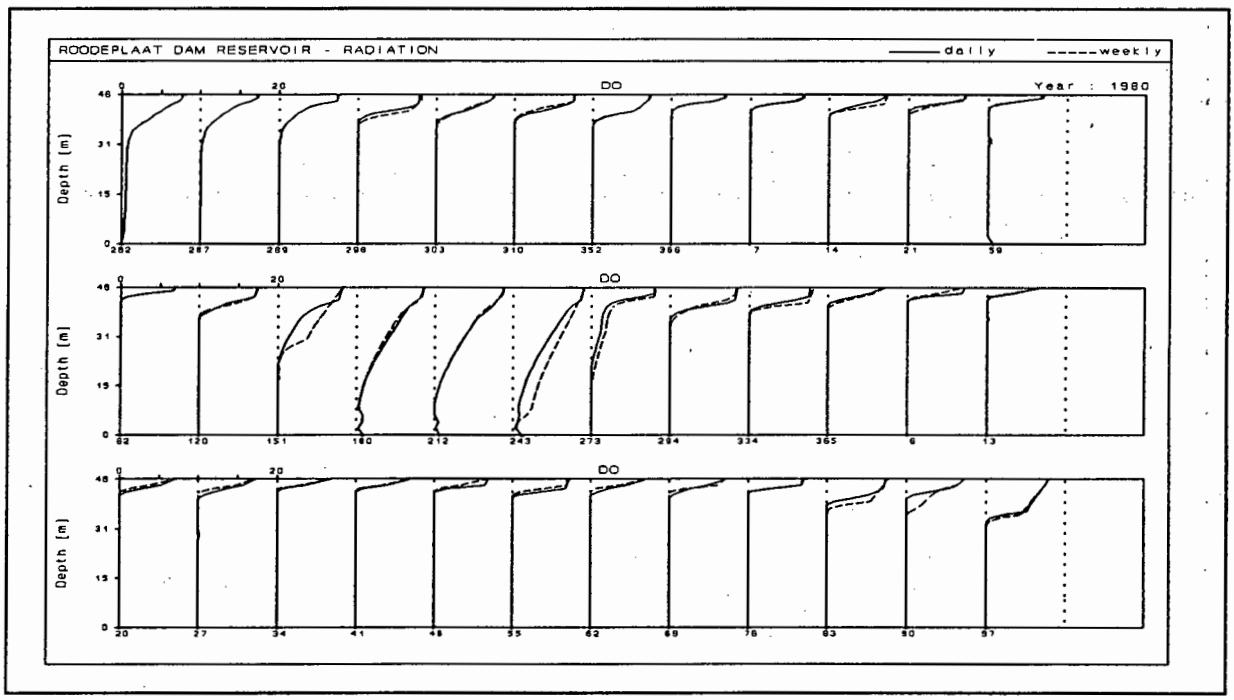

Figure 10.24
Simulated dissolved oxygen concentrations obtained with the modified MINLAKE model on Roodeplaat Dam using daily and weekly radiation data.

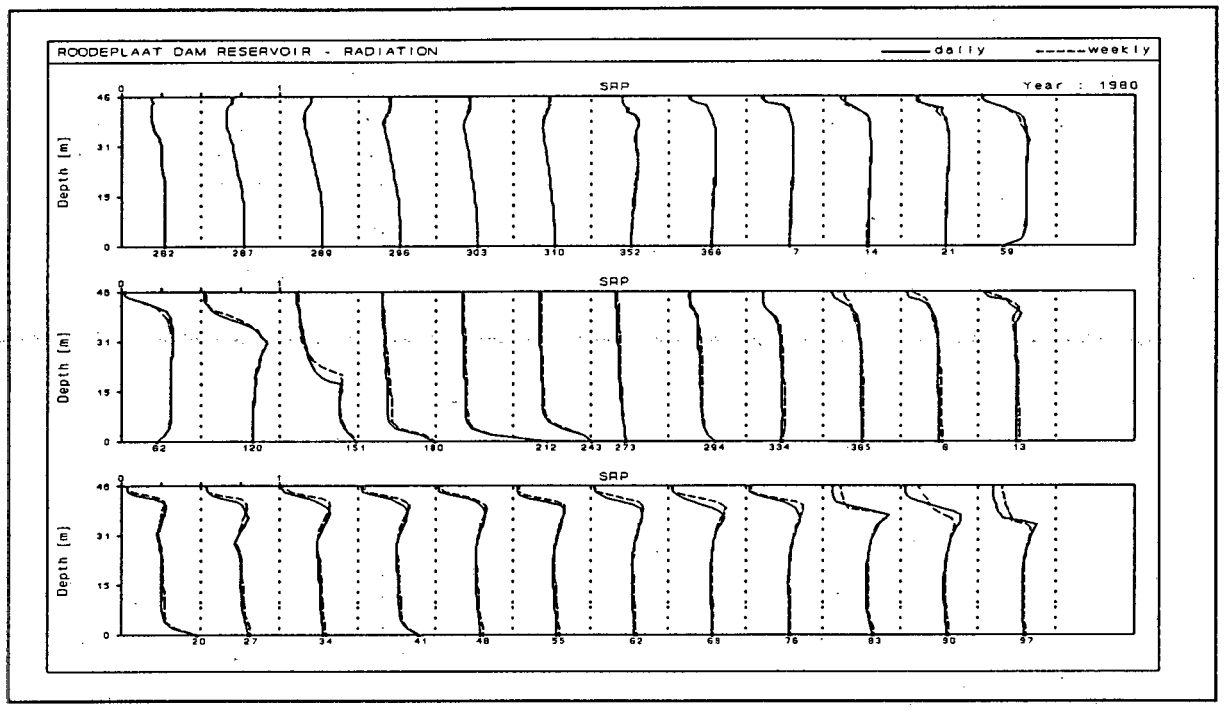

Figure 10.25
Simulated dissolved phosphate concentrations obtained with the modified MINLAKE model on Roodeplaat Dam using daily and weekly radiation data.

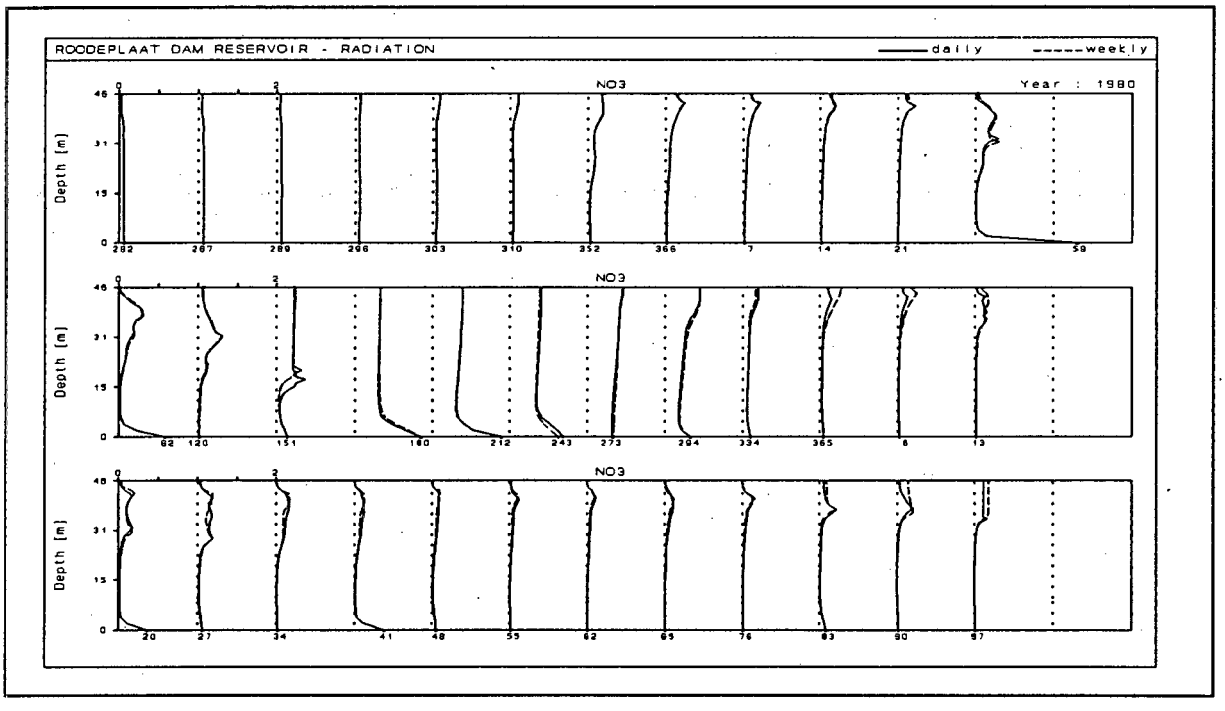

Figure 10.26
Simulated nitrate concentrations obtained with the modified MINLAKE model on Roodeplaat Dam using daily and weekly radiation data.

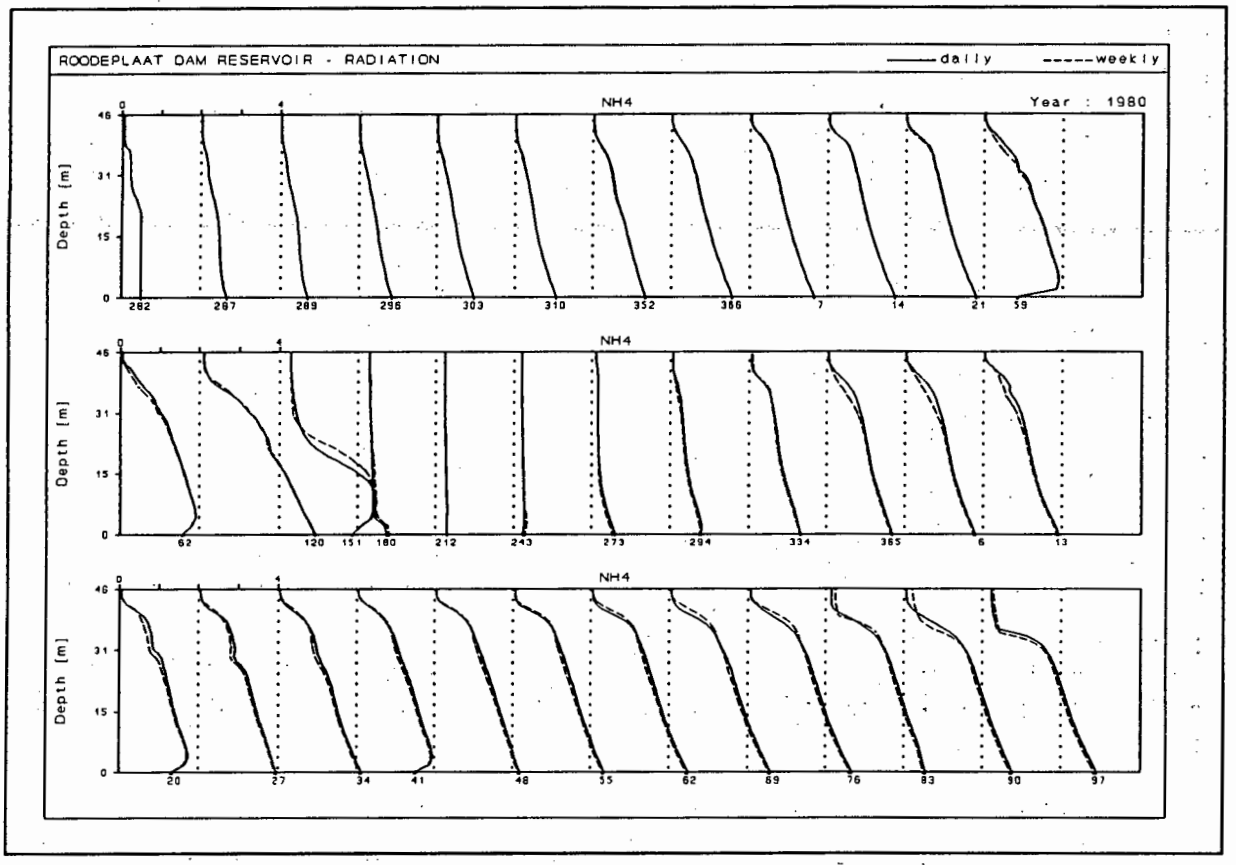

Figure 10.27
Simulated ammonia concentrations obtained with the modified MINLAKE model on Roodeplaat Dam using daily and weekly radiation data.

Changing the frequency of radiation data from daily to monthly led to slightly more prominent differences (Fig 10.28 - 10.33), but these differences were smaller than expected.

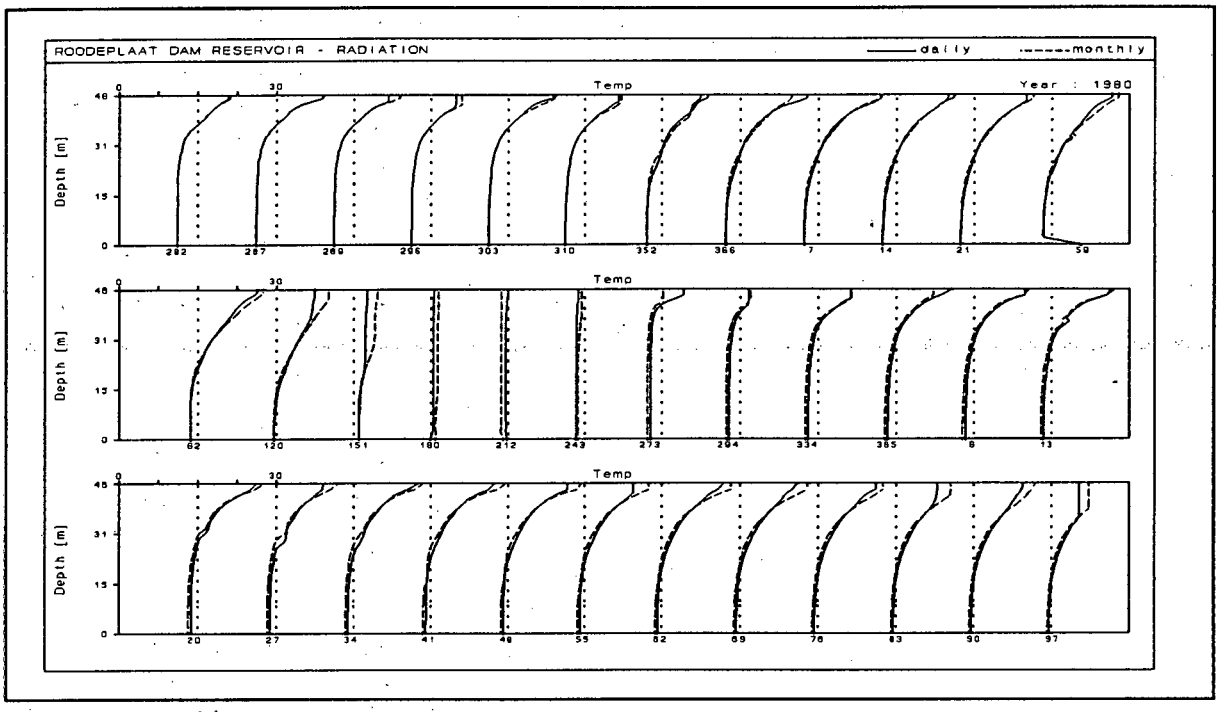

Figure 10.28
Simulated water temperature obtained with the modified MINLAKE model on Roodeplaat Dam using daily and monthly radiation data.

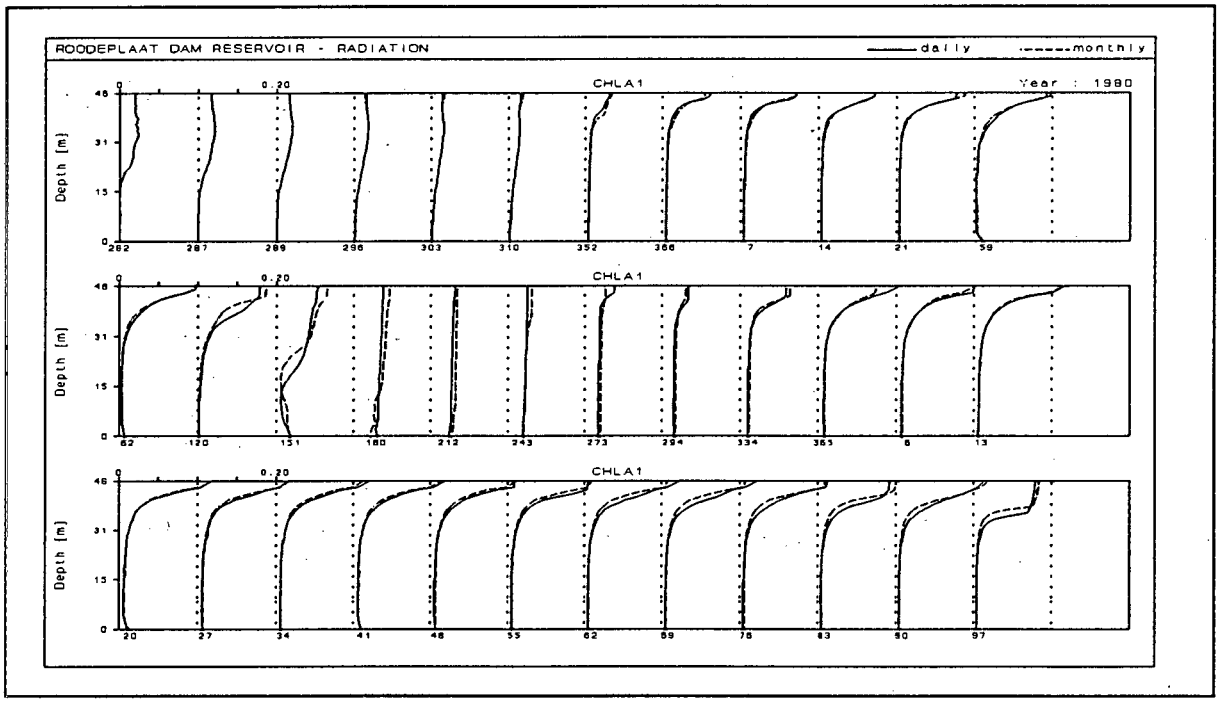

Figure 10.29
Simulated chlorophyll-a concentrations obtained with the modified MINLAKE model on Roodeplaat Dam using daily and monthly radiation data.

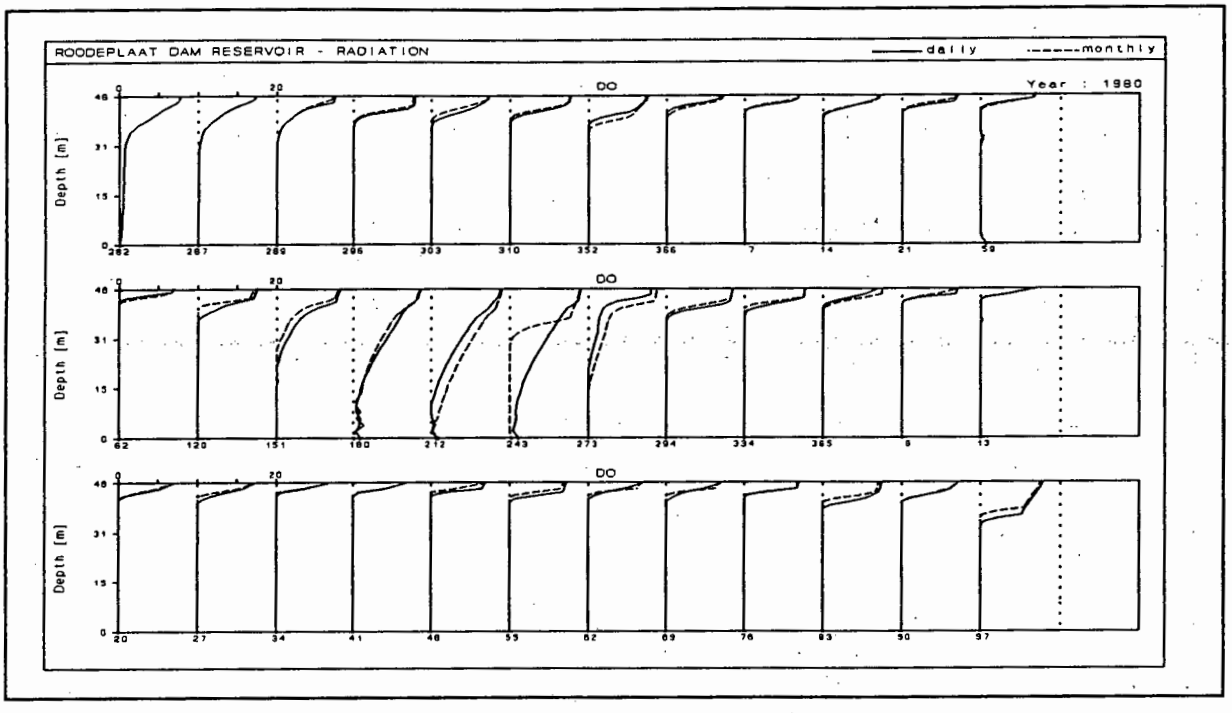

Figure 10.30
Simulated dissolved oxygen concentrations obtained with the modified MINLAKE model on Roodeplaat Dam using daily and monthly radiation data.

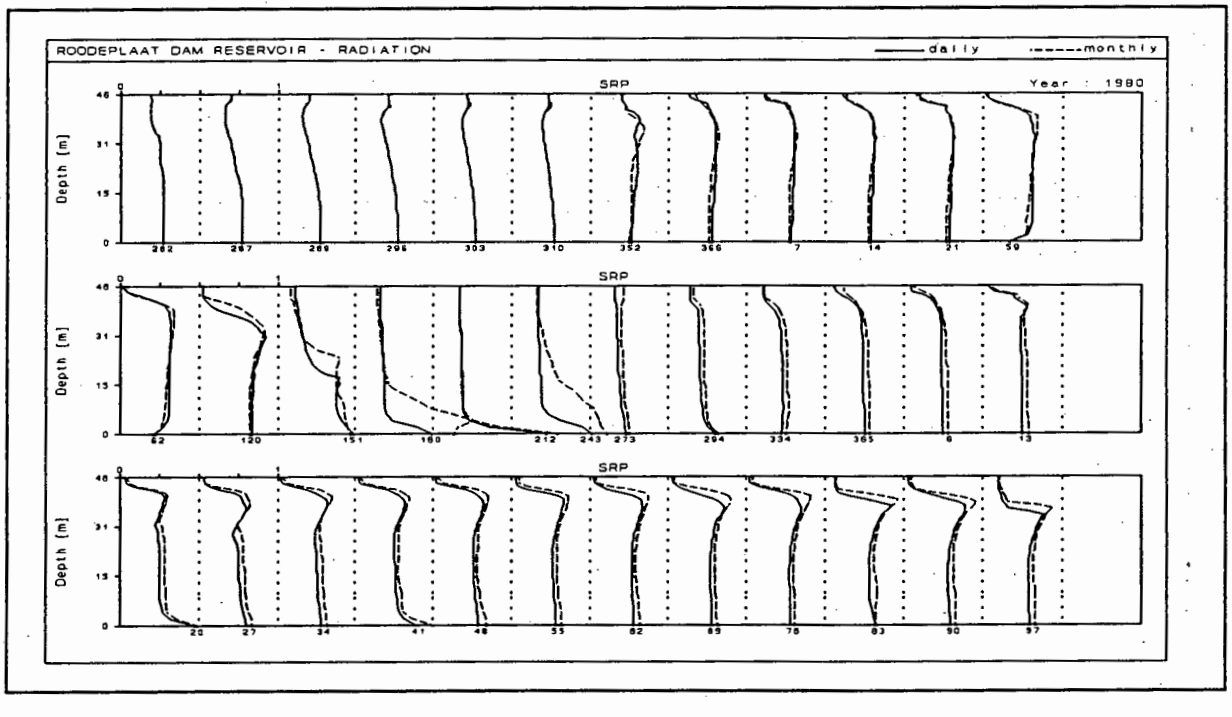

Figure 10.31
Simulated dissolved phosphate concentrations obtained with the modified MINLAKE model on Roodeplaat Dam using daily and monthly radiation data.

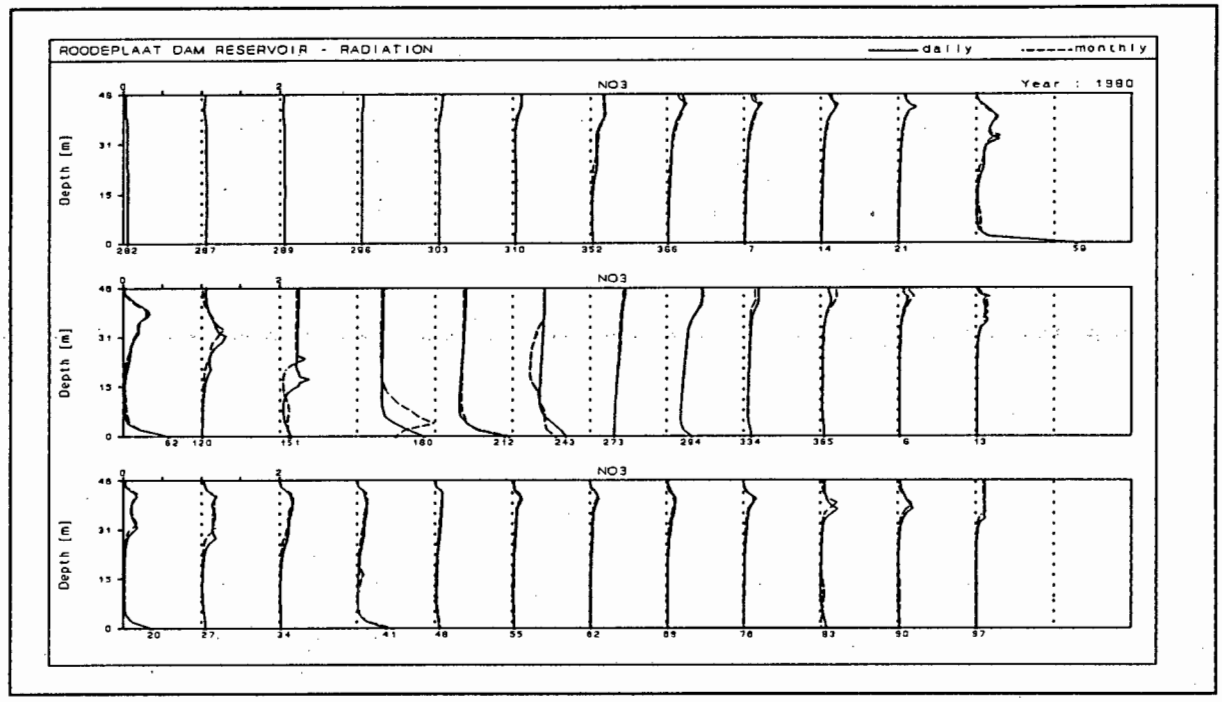

Figure 10.32
Simulated nitrate concentrations obtained with the modified MINLAKE model on Roodeplaat Dam using daily and monthly radiation data.

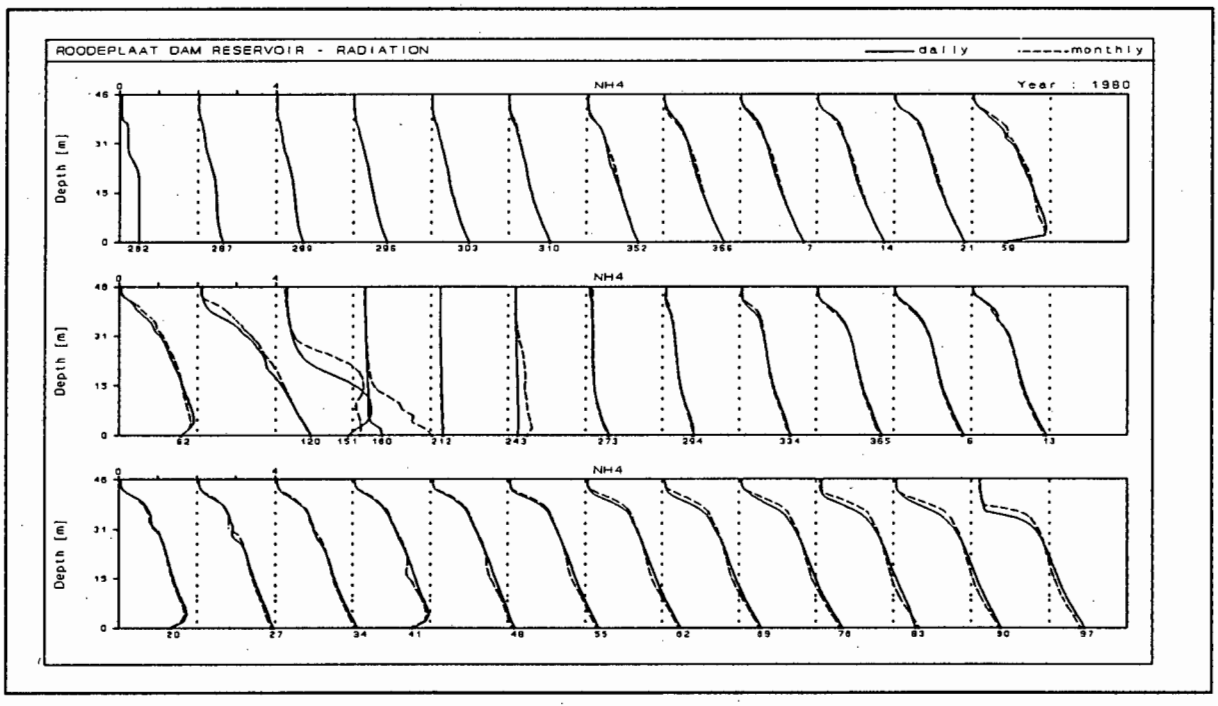

Figure 10.33
Simulated ammonia concentrations obtained with the modified MINLAKE model on Roodeplaat Dam using daily and monthly radiation data.

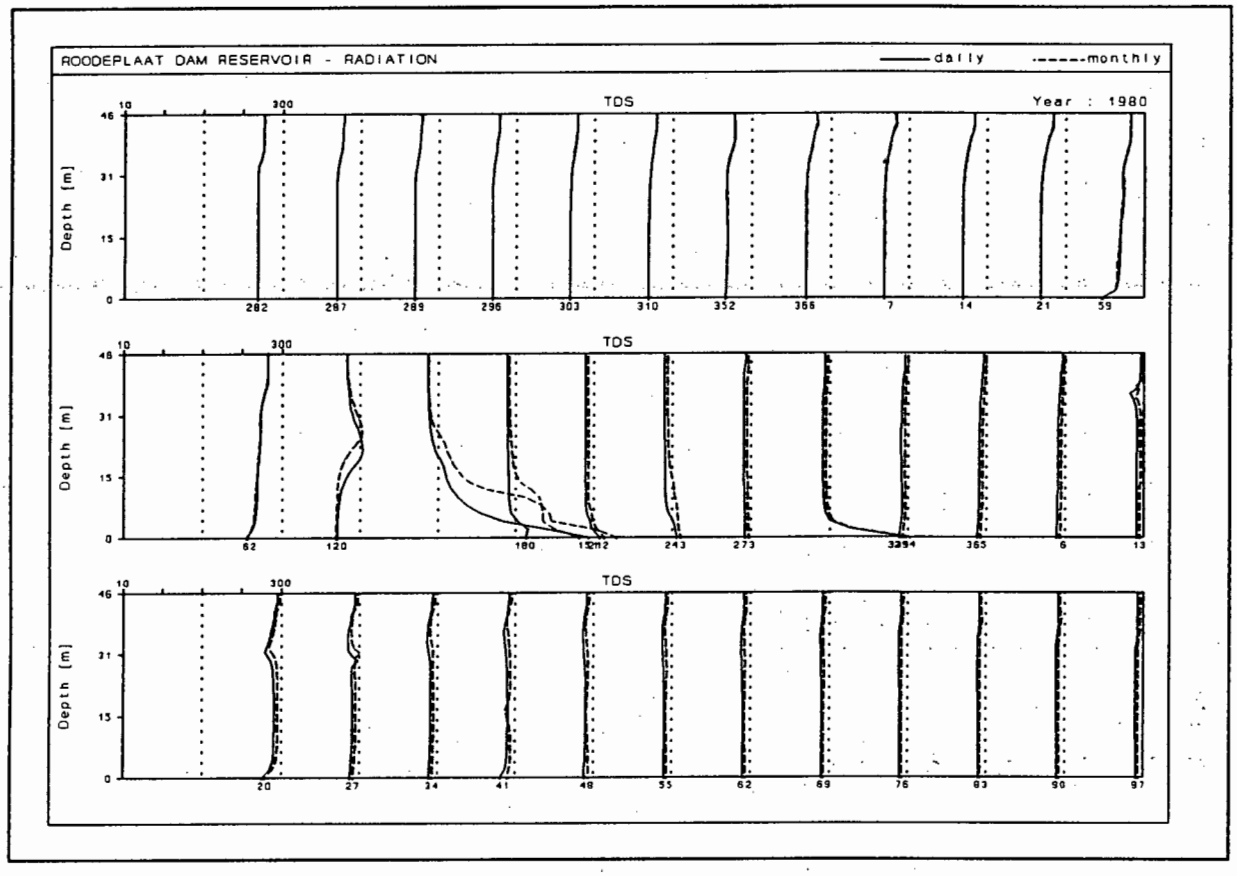

Figure 10.34
Simulated TDS concentrations obtained with the modified MINLAKE model on Roodeplaat Dam using daily and monthly radiation data.

Conclusion: Although changing the frequency of short wave radiation data from daily to weekly did not affect the water budget significantly, it did cause small, but significant changes in simulated water temperature, and concentrations of chlorophyll-a, dissolved oxygen, dissolved phosphate, nitrate, and ammonia. Changing to a monthly data input resulted in slightly more significant differences, specially in the simulated water budget. The difference in simulated chlorophyll-a concentration could be regarded as significant, but it would depend on the requirements of the user as to whether this difference, as well as the differences in the other simulated variables, should be regarded as meaningful.

If daily short wave radiation data are not measured at the reservoir being modelled, it would seem that data from another nearby site could be substituted, and that weekly, instead of daily, data can be used. However, care should be taken when using monthly data, as the water budget may be affected significantly.

10.2.8 The effect of changing the input frequency of all the meteorological variables on model predictions.

The meteorological data file consists of seven variables. In the above study, the effect of changing the input data frequency of a single variable, whilst keeping the data frequency of the other variables unchanged, was tested. However, in practice it is more likely that the frequency of all variables will be changed simultaneously.

Changing the data frequency of all the meteorological variables from daily to weekly did have a small effect on the water budget towards the latter half of the simulation period (Fig 10.35). Changing the data frequency of all meteorological variables from daily to monthly resulted in a significant change in the water budget, specially towards the end of the simulation period.

Regarding simulated variables: changing the data frequency of all variables from daily to weekly resulted in definite changes in simulated water temperature, and simulated concentrations of chlorophyll-a, dissolved oxygen, dissolved phosphate, nitrate, and ammonia (Fig 10.36 - 10.41). The change in dissolved phosphate was the most prominent. It is interesting to note that the changes become more significant towards the latter half of the simulation period, this probably being due to a change in the hypolimnetic diffusion rate, caused by changes in water temperature and water density.

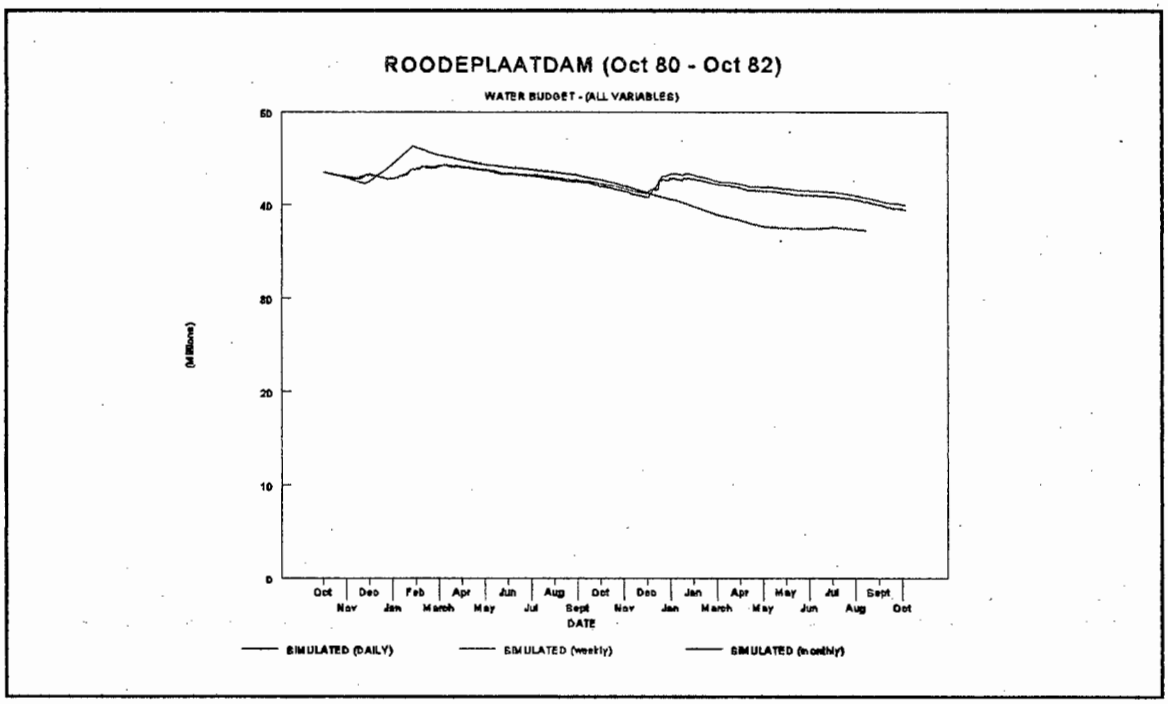

Figure 10.35
Water budget for Roodeplaat Dam as simulated with the modified MINLAKE model using daily, weekly, and monthly data for all the meteorological variables.

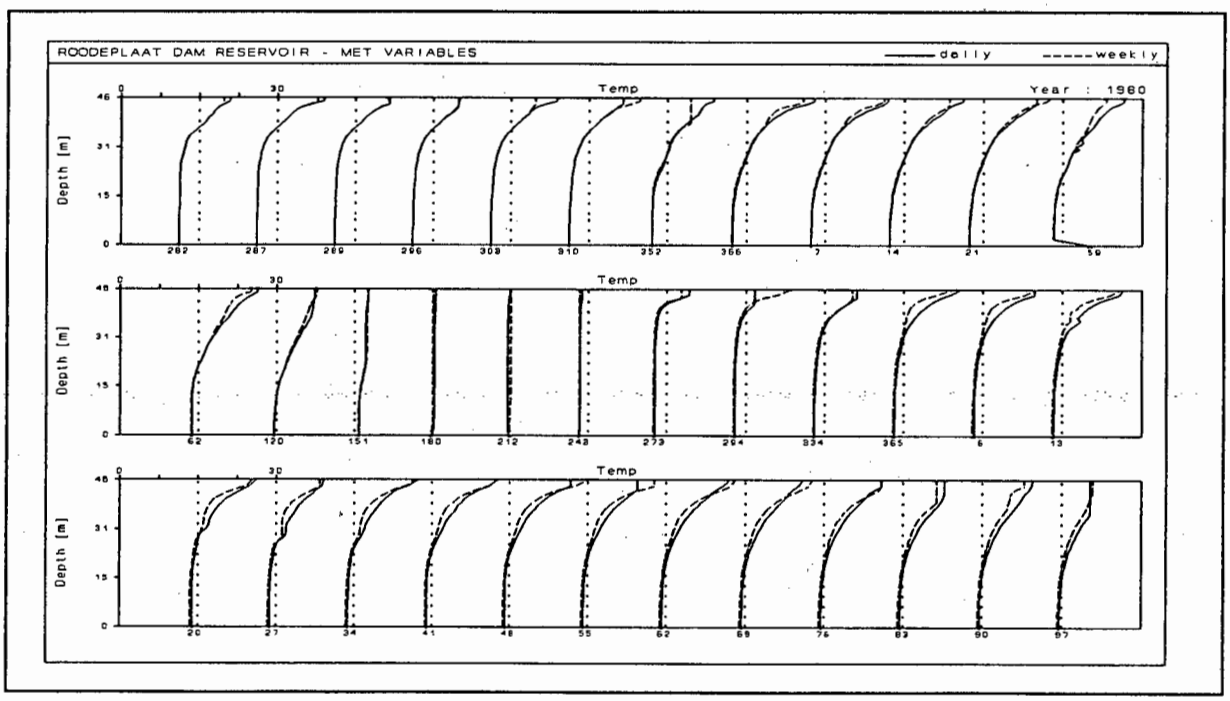

Figure 10.36
Simulated water temperatures obtained with the modified MINLAKE model on Roodeplaat Dam using daily and weekly data for all the meteorological variables.

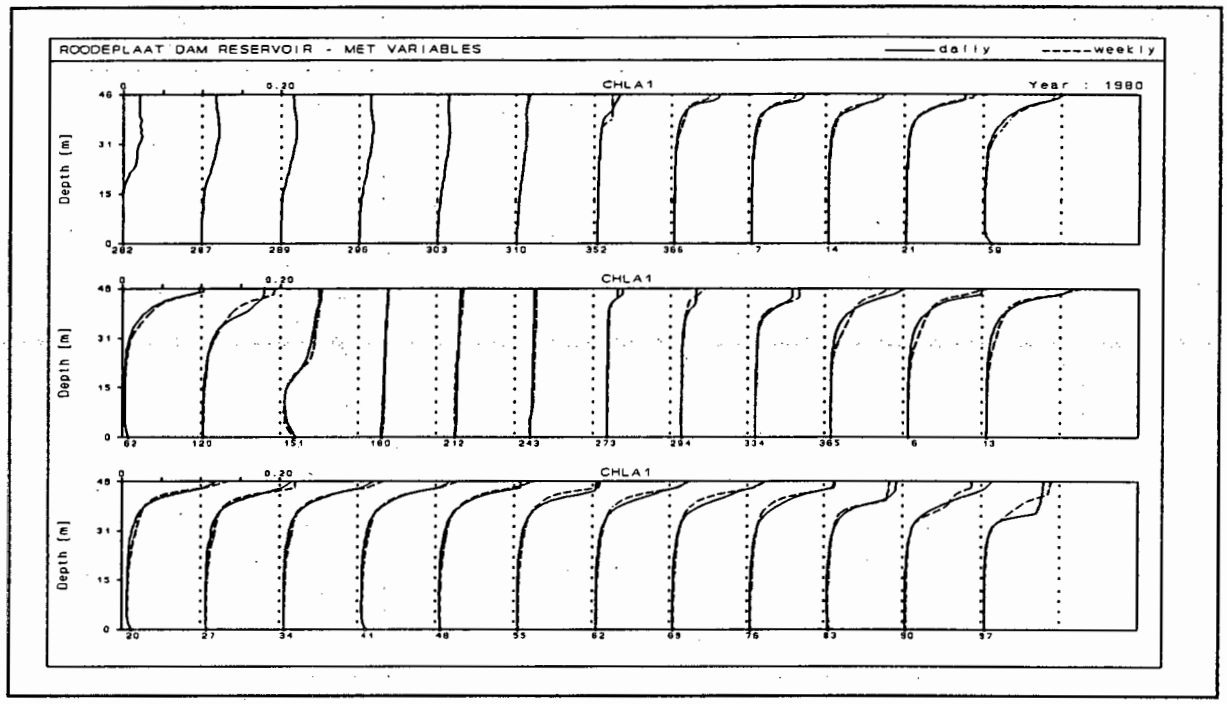

Figure 10.37
Simulated chlorophyll-a concentrations obtained with the modified MINLAKE model on Roodeplaat Dam using daily and weekly data for all the meteorological variables.

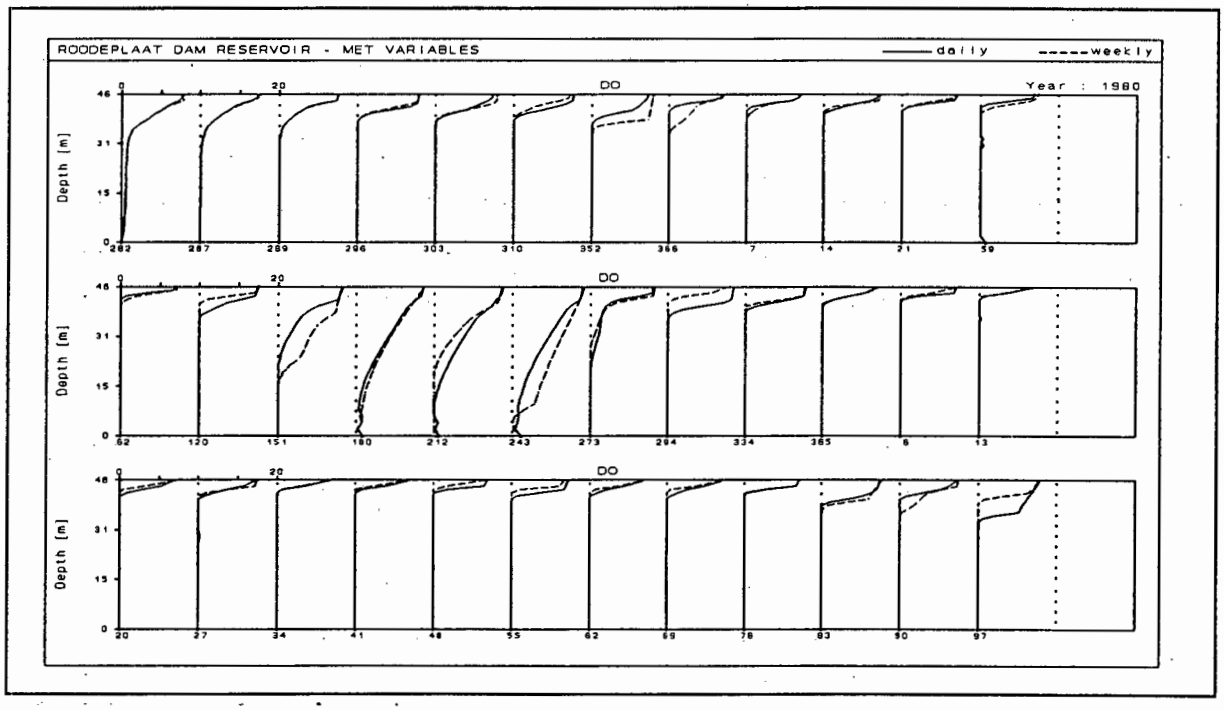

Figure 10.38
Simulated dissolved oxygen concentrations obtained with the modified MINLAKE model on Roodeplaat Dam using daily and weekly data for all the meteorologicl variables.

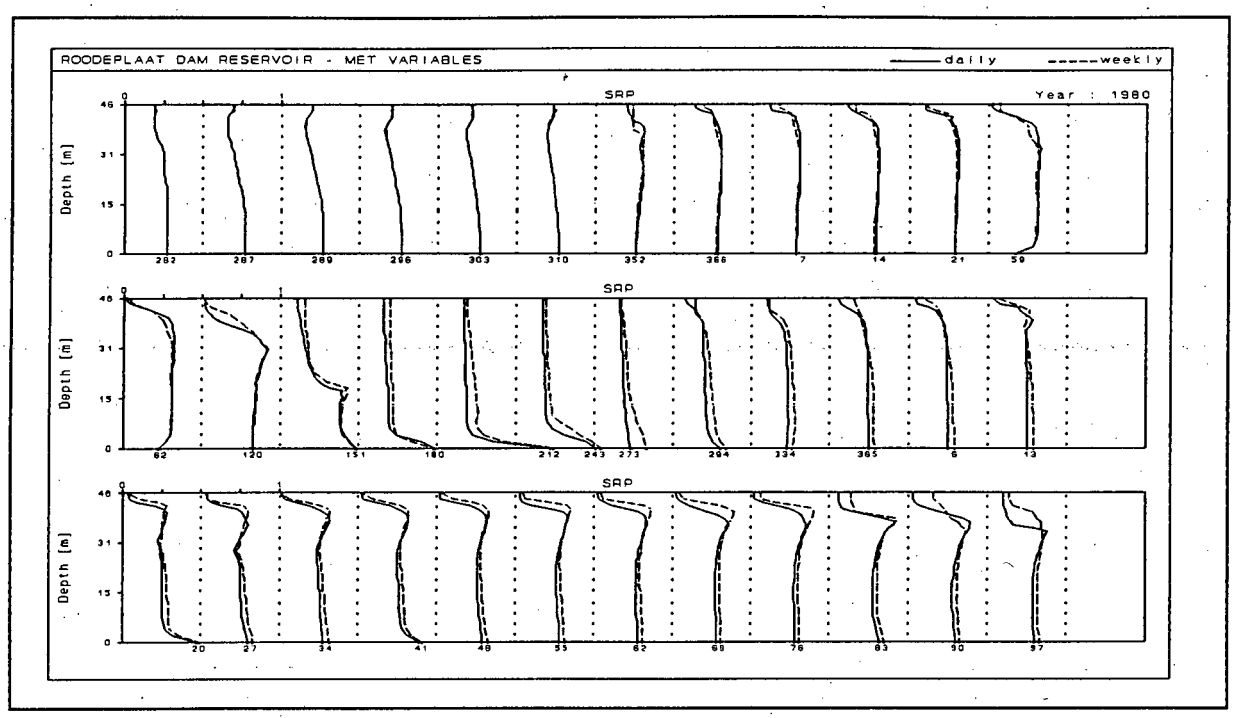

Figure 10.39
Simulated dissolved phosphate concentration obtained with the modified MINLAKE model on Roodeplaat Dam using daily and weekly data for all the meteorological variables.

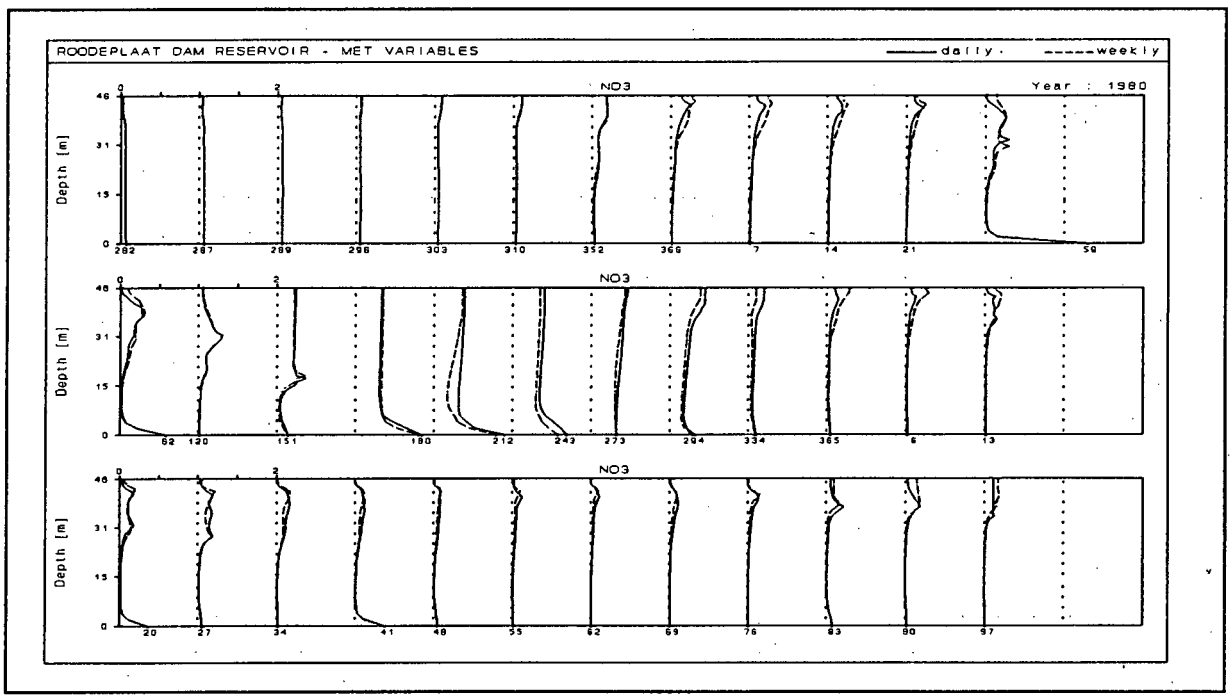

Figure 10.40
Simulated nitrate concentration obtained with the modified MINLAKE model on Roodeplaat dam using daily and weekly data for all the meteorological variables.

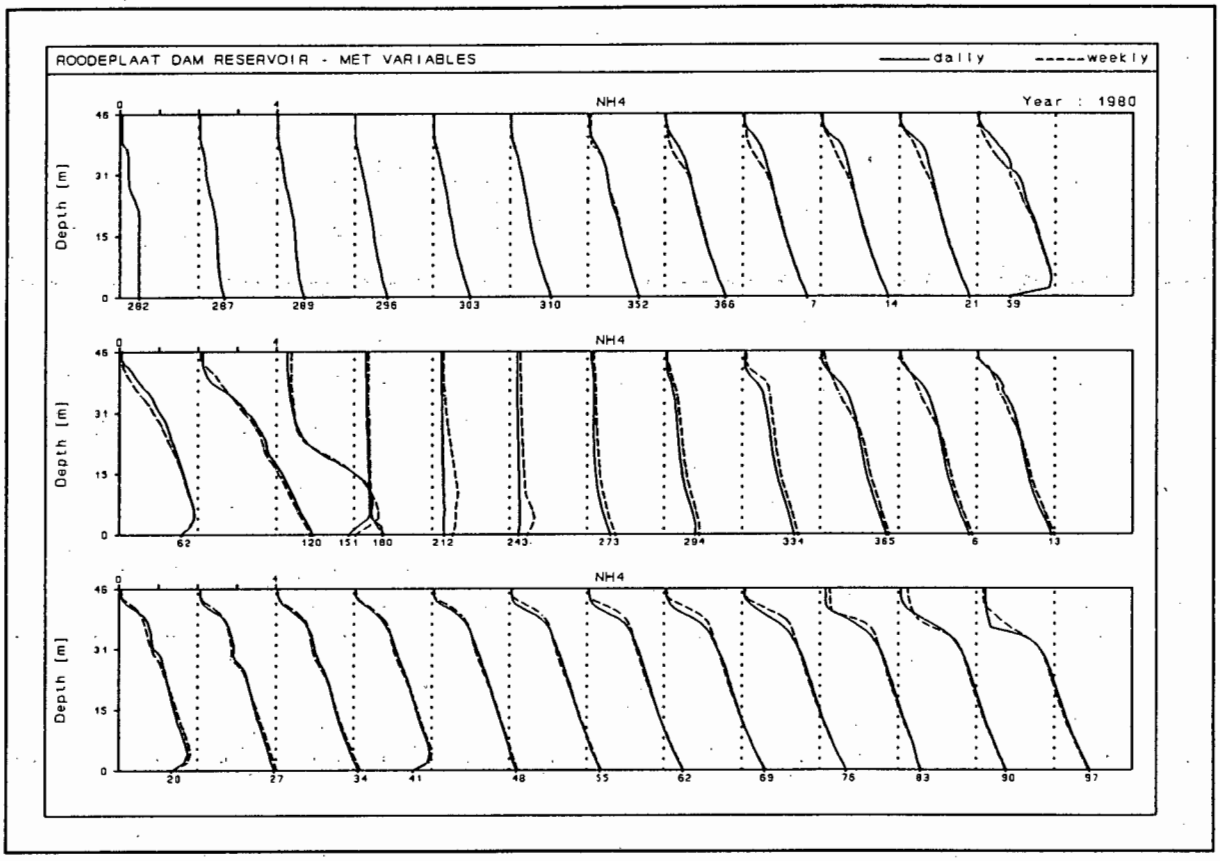

Figure 10.41
Simulated ammonia concentrations obtained with the modified MINLAKE model on Roodeplaat Dam using daily and weekly data for all the meteorological variables.

Changing the data frequency of all variables to monthly resulted in marked changes in all the simulated variables, as would be expected in view of the prominent change in the water budget (Fig 10.42 - 10.48)

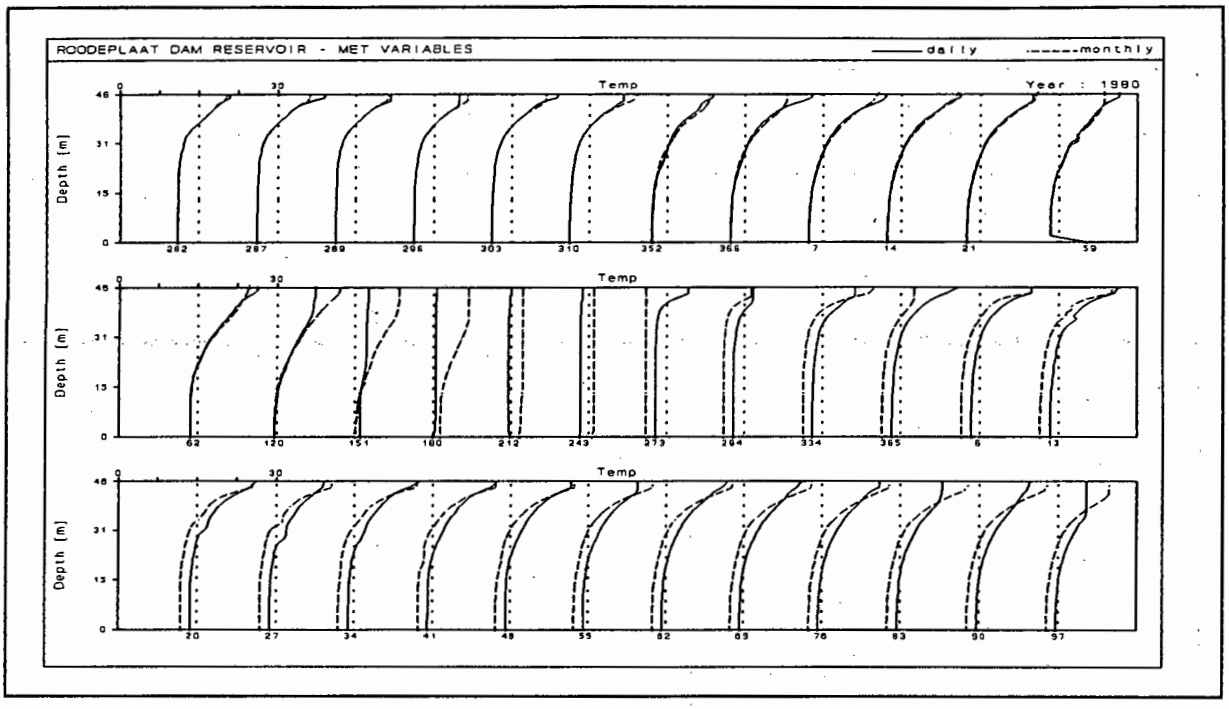

Figure 10.42
Simulated water temperature obtained with the modified MINLAKE model on Roodeplaat Dam using daily and monthly data for all the meteorological variables.

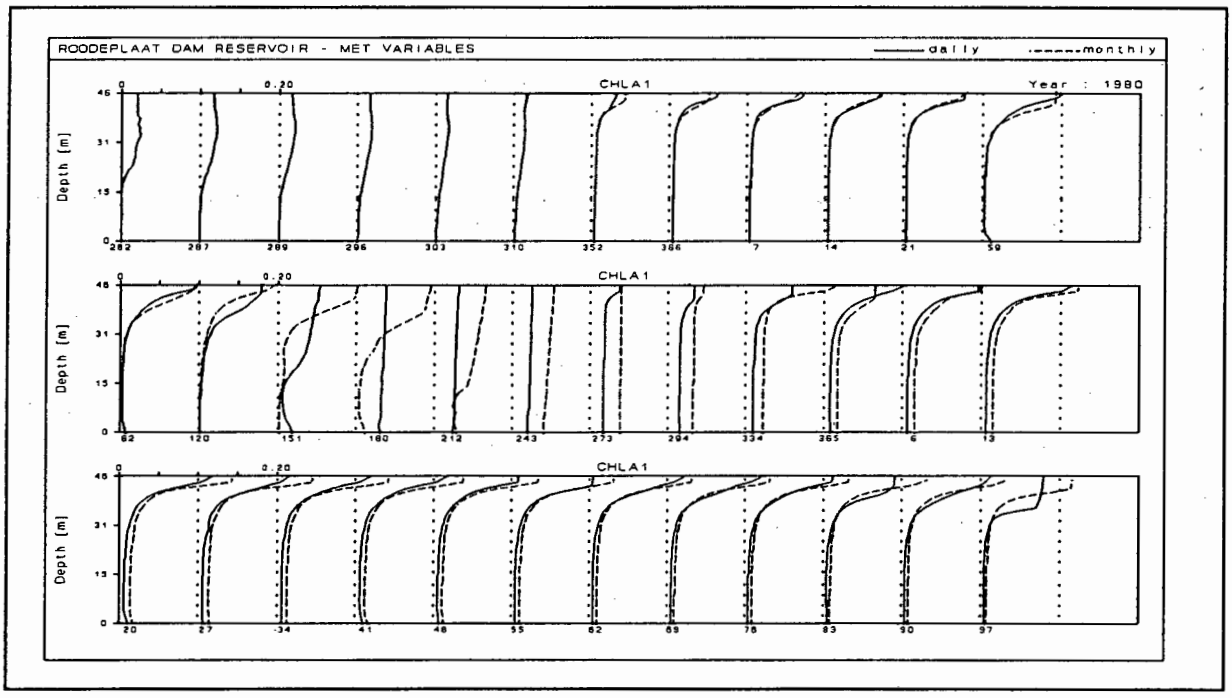

Figure 10.43
Simulated chlorophyll-a concentrations obtained with the modified MINLAKE model on Roodeplaat Dam using daily and monthly data for all the meteorological variables.

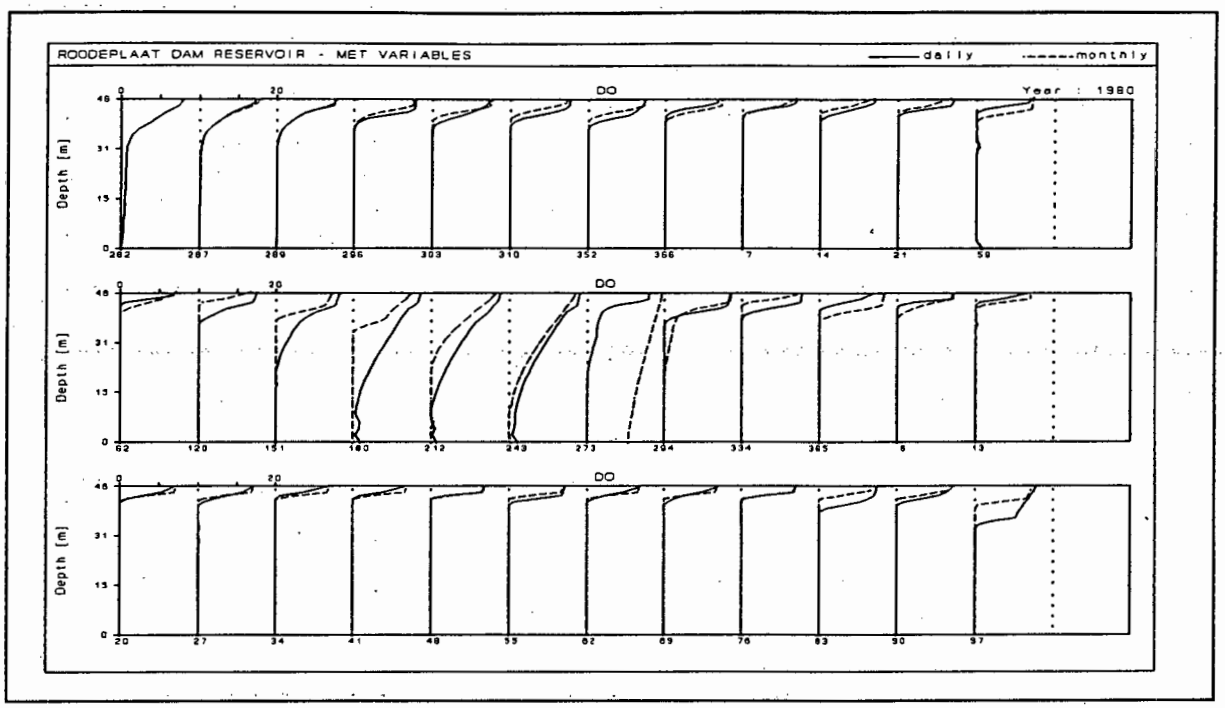

Figure 10.44
Simulated dissolved oxygen concentrations obtained with the modified MINLAKE model on Roodeplaat Dam using daily and monthly data for all the meteorological variables.

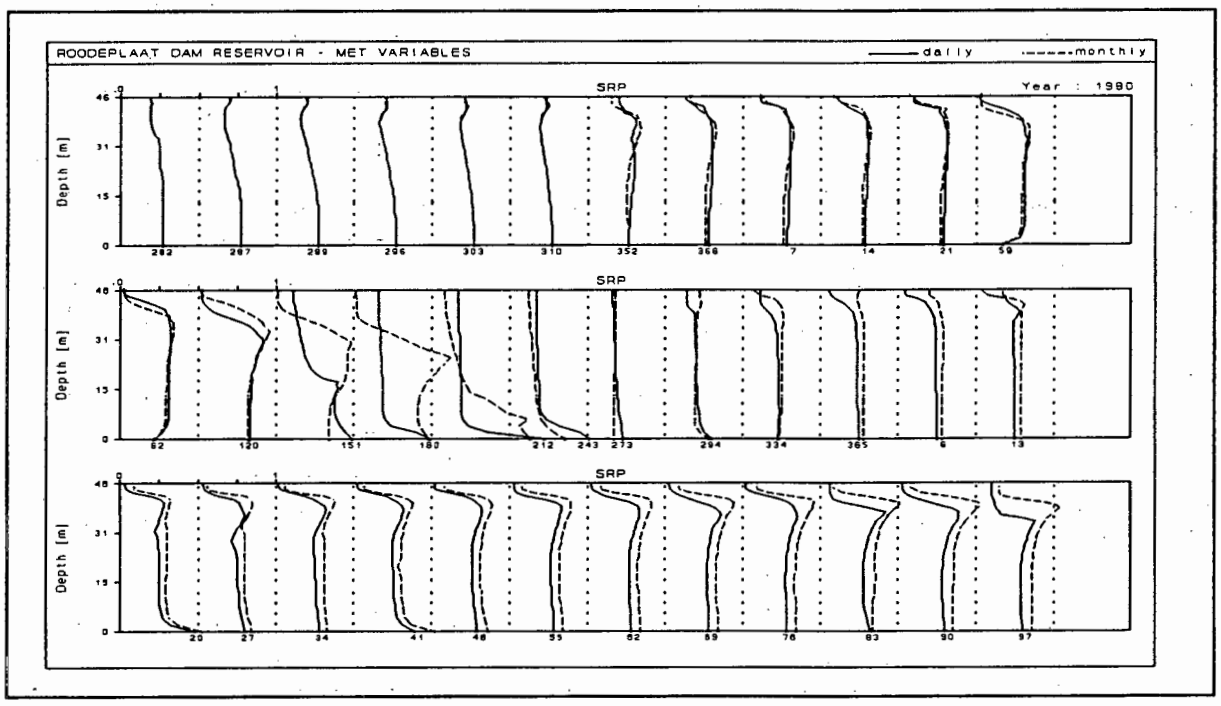

Figure 10.45
Simulated dissolved phosphate concentrations obtained with the modified MINLAKE model on Roodeplaat Dam using daily and monthly data for all the meteorological variables.

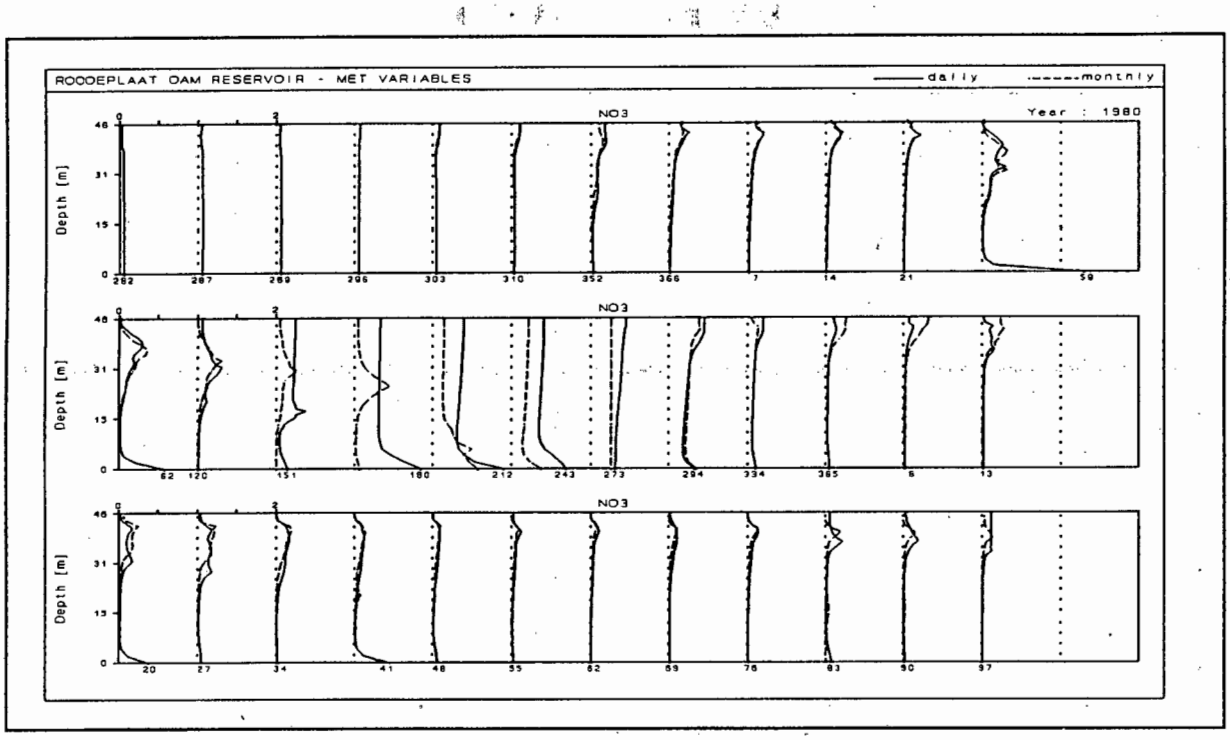

Figure 10.46
Simulated nitrate concentrations obtained with the modified MINLAKE model on Roodeplaat Dam using daily and monthly data for all the meteorological variables.

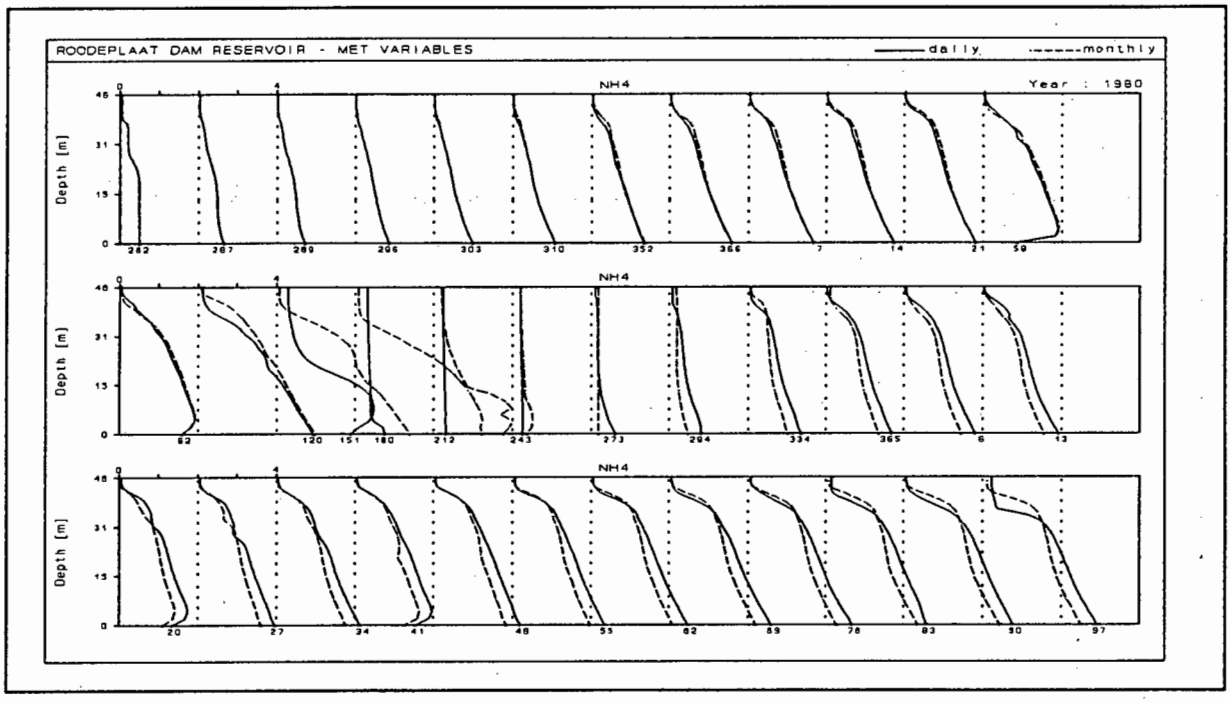

Figure 10.47
Simulated ammonia concentrations obtained with the modified MINLAKE model on Roodeplaat Dam using daily and monthly data for all the meteorological variables.

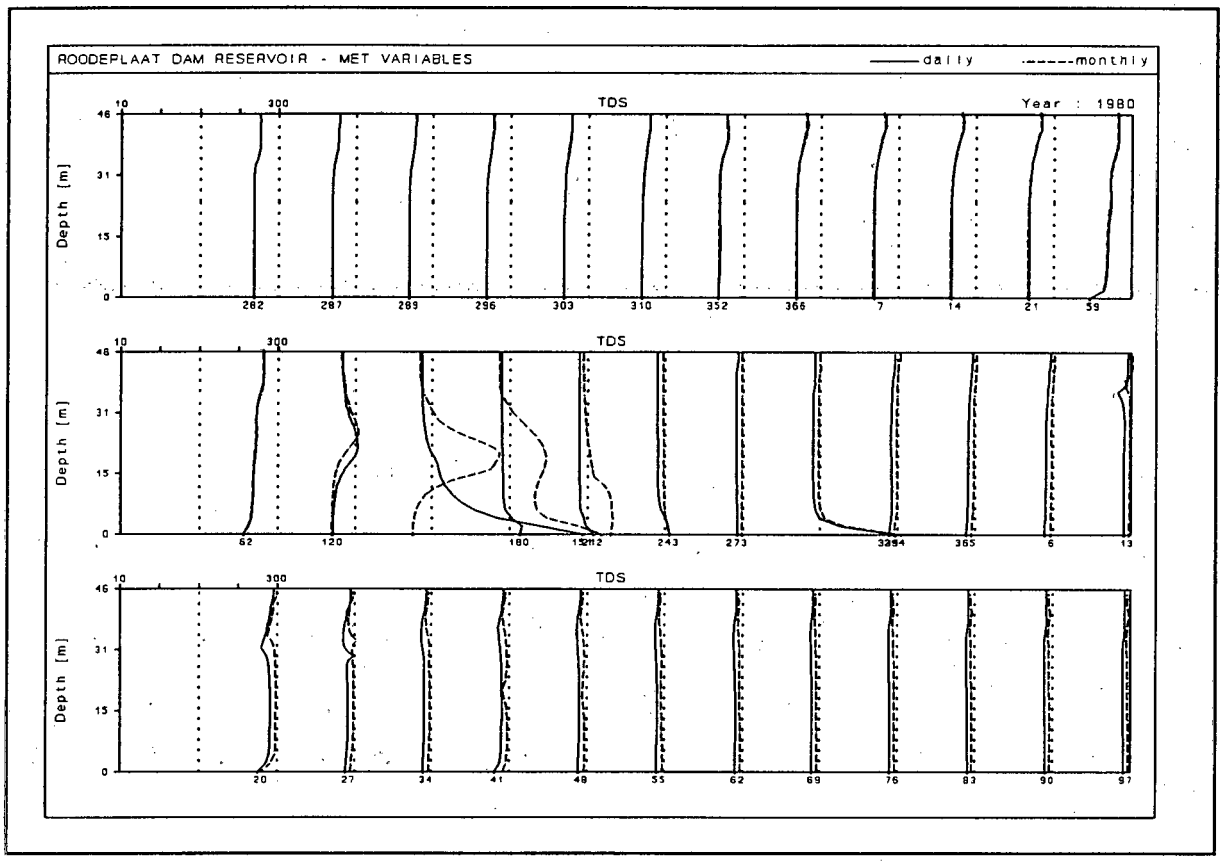

Figure 10.48
Simulated TDS concentrations obtained with the modified MINLAKE model on Roodeplaat Dam using daily and monthly data for all the meteorological variables.

Conclusion: Changing the data frequency of all the meteorological variables from daily to weekly did not affect the water budget to a great extent. It did result in small, but definite, changes in simulated water temperature, and concentrations of chlorophyll-a, dissolved oxygen, dissolved phosphate, nitrate, and ammonia. It would depend on the requirements of the user as to whether these changes should be regarded as significant. The changes became more prominent towards the latter half of the simulation period of 18 months, thus using weekly data for all the meteorological variables would probably suffice for shorter simulation periods, eg 9-12 months.

Changing the data frequency of all the meteorological variables from daily to monthly resulted in significant changes in the water budget, as well as in the simulated variables, and therefore the use of monthly data for all the meteorological variables is not recommended.

10.3 SENSITIVITY OF MODEL OUTPUT TO FREQUENCY OF INFLOW WATER QUALITY DATA

The modified MINLAKE model makes provision for the following data on inflow water quality: flow rate, water temperature, dissolved phosphate, detritus, dissolved oxygen, total inorganic suspended sediment (TSS), total dissolved salts (TDS), nitrate, and ammonia. Although most of these variables currently are being measured by the Department of Water Affairs and Forestry (with the exception of TSS, dissolved oxygen and detritus concentration, *cf* Table 10.1), measurements are not always done on a daily basis. During calibration of the modified MINLAKE model on Roodeplaat Dam, considerable time and effort were spent in infilling of missing inflow water quality data. Daily river flow rate was often used for infilling, as the flow records were complete, but a rather complicated three-stage time-dependent seasonal technique was required:

- First stage: infilling was done with a time-dependant seasonal nonlinear regression of grab sample against daily flow, for days with flow above a certain truncation level, but with the infilled values weighed by proximity to a grab sample value at either end of the missing period

- Second stage: data for days with flows below the truncation level were filled in by linear interpolation between measured values

- Third stage: The grab sample values are imbedded in the created series and discontinuities and seasonal transitions smoothed.

This complicated infilling technique was followed to ensure that the inflow water quality data base was as reliable as possible. It was surmised that reliable input data improve reliability in model output.

However, in view of the considerable time and effort required by the three-stage technique for infilling of missing inflow water quality data, the question arose whether less accurate inflow water quality data would affect the model output significantly. Two possibilities were examined:

- Instead of following a monitoring programme where each variable is measured daily for an unspecified length of time, it may be possible to set up an initial intensive, daily monitoring programme for a period of, for instance, one year only, and then reduce the intensity of the monitoring programme. The purpose of the initial intensive daily monitoring programme would be to establish the best possible relationships between flow rate and the other inflow water quality variables. If, as was the case with the rivers flowing into Roodeplaat Dam, a close relationship between flow rate and most of the variables could be established, then it should be possible to measure flow rate only on a daily basis. Instead of measuring the other water quality variables also on a daily basis, these could be calculated from daily flow rate measurements, using the relationships established during the intensive monitoring programme. Occasional measurements of all the inflow water quality variables could be done to ensure that the established relationships remain valid.

  To test this hypothesis, the relationships between the different inflow water quality variables and river flow rate that were established in setting up the MINLAKE data base for Roodeplaat Dam were used to calculate daily time-series data for each variable from the observed flow rate. The rationale was to use a simple regression that is not flow or season dependant. Also, because the surmise was that only calculated data should be used in the time-series, the observed data was not utilised, and thus discontinuities and seasonal transitions were not smoothed as was done with the original three-stage infilling

process. The calculated time-series data obtained with this basic method will be referred to as 'simple regression data', whilst the time-series data in the original data base obtained with the three-stage infilling technique, utilising both calculated and observed data, will be referred to as 'smoothed data'.

To test the sensitivity of the model to daily measurements of inflow water quality data, the model was run repeatedly with simple regression data for one inflow water quality variable, whilst the data for the other inflow water quality variables consisted of the original smoothed data.

- The question also arose as to whether, in a situation where, for instance, only weekly measurements were available, it was necessary to establish complicated flow and/or season dependant relationships between variables to infill the missing data, as was done with the aid of the three-stage technique mentioned above. To test the sensitivity of the model to sparse inflow data, the rationale was as follows:

  Although daily measurements of inflow water quality variables are not always available, weekly measurements often are. To evaluate the effect of using weekly measurements, the original inflow data base (consisting of smoothed data) was used as a basis, and, separately for each variable, the value on the first day of the week was entered for all the days of that week. The other inflow water quality variables were not changed.

Both the original and the modified MINLAKE models make provision for the following inflow water quality variables: flow rate, water temperature, and concentrations of dissolved phosphate, dissolved oxygen, total inorganic sediment, total dissolved salt, nitrate, and ammonia. When the inflow data base for Roodeplaat Dam was established, the majority of time was spent in infilling missing dissolved phosphate, nitrate, ammonia, and TDS data from flow rate data. For each of these variables, the model outputs obtained with inflow data calculated with the aid of a simple regression, and the outputs obtained with weekly observed values (entered on a daily basis), are

now compared to the original model output obtained with daily smoothed data during calibration of the modified MINLAKE model on Roodeplaat Dam.

10.3.1 The effect of changing dissolved phosphate data in the inflow on model output

Using calculated 'simple regression' dissolved phosphate data instead of 'smoothed' data: When the original inflow data base was established for Roodeplaat Dam during calibration of the modified MINLAKE model, much time was spent on infilling missing dissolved phosphate data as accurately as possible. Phosphate data was seen as very important, because algal growth rate often is limited by dissolved phosphate concentration. In establishing the original data base, elaborate linear regressions that were flow and season-dependant were established between the natural log of the flow rate and the natural log of observed dissolved phosphate data. Thereafter missing data were infilled with the aid of the three-stage technique mentioned earlier. In the present study, flow and seasonal dependency of the regression was discarded, and for each river, dissolved phosphate data was calculated from flow rate, using a simple linear regression between the natural log of flow rate and the natural log of observed dissolved phosphate. The linear regression used for each river is indicated in Table 10.2.

TABLE 10.2. Linear regression between ln flow and ln PO_4 for each river flowing into Roodeplaat Dam.

RIVER	DEPENDENT VARIABLE	INDEPENDENT VARIABLE	SLOPE	CONSTANT	R^2
Pienaars	ln PO_4	ln flow	0.43±0.03	0.27±0.69	0.15
Hartbees	ln PO_4	ln flow	0.289±0.017	-3.09±0.67	0.21
Edendale	ln PO_4	ln flow	0.39±0.03	-3.04±0.58	0.31

Time-series of dissolved phosphate data for Pienaars River obtained with the elaborate infilling procedure (i.e. smoothed data), and the data obtained employing the simple regression equation in Table 10.2, are shown in Figure 10.49.

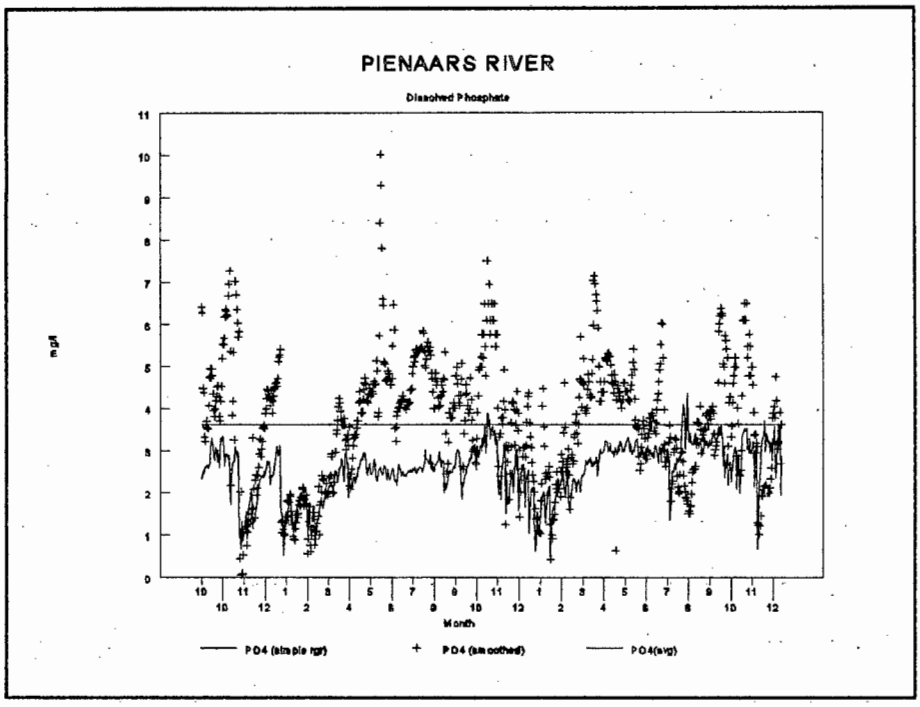

Figure 10.49
Time-series of dissolved phosphate data for the Pienaars River, obtained by elaborate infilling, and the data obtained by using a simple regression equation.

The modified MINLAKE model was run with the calculated dissolved phosphate data, i.e. no observed phosphate data were used. The other variables in the inflow data file were unchanged. Simulated water temperature and simulated concentrations of chlorophyll-a, dissolved oxygen, TSS, TDS, nitrate, and ammonia were not affected by changing the inflow phosphate data from 'smoothed data' to 'simple regression data'. Only simulated dissolved phosphate concentration was affected significantly (Fig10.50).

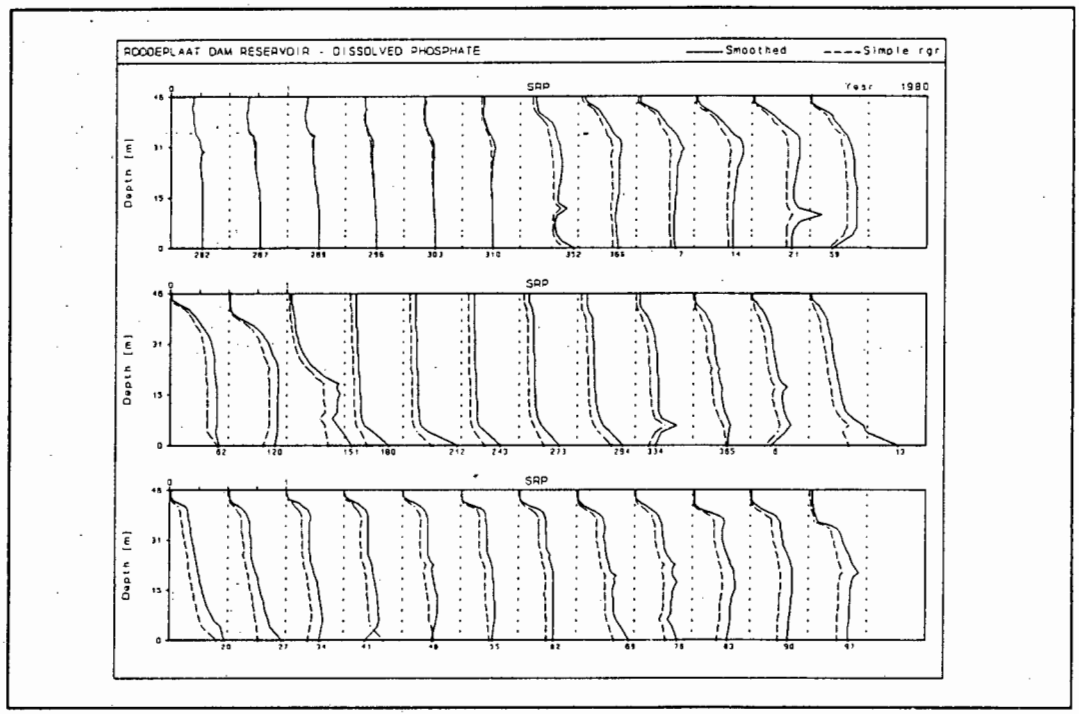

Figure 10.50
Simulated dissolved phosphate concentrations obtained with the modified MINLAKE model for Roodeplaat Dam using 'smoothed' and 'simple regression' dissolved phosphate data.

Using weekly values for dissolved phosphate data instead of daily values: To evaluate the effect of weekly, instead of daily, dissolved phosphate data being available, the value on the first day of each week was entered for all the days of that week. (The structure of the model requires a value to be entered for each day since model predictions are evaluated daily). Only the simulated dissolved phosphate concentration was affected by the change from daily to weekly dissolved phosphate data; the other simulated variables remained the same. The change in simulated dissolved phosphate concentration was not very significant (Fig 10.51).

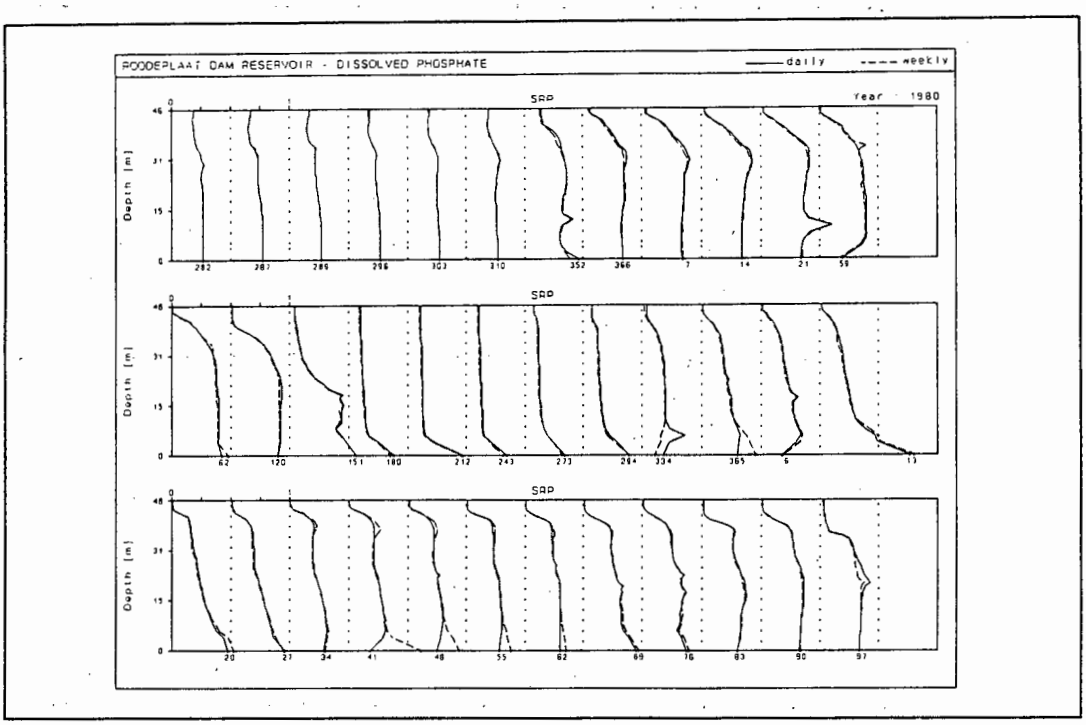

Figure 10.51
Simulated dissolved phosphate concentrations obtained with the modified MINLAKE model on Roodeplaat Dam using daily and weekly dissolved phosphate data.

Conclusion: Disregarding all observed dissolved phosphate data and using only dissolved phosphate data that was calculated from flow rate data with the aid of a simple regression, significantly affected simulated dissolved phosphate concentration. Changing from daily dissolved phosphate data to weekly data (entered on a daily basis) also affected simulated dissolved phosphate concentration only, but the change was not very significant. However, it should be noted that this conclusion may be true only for Roodeplaat Dam. In this reservoir, algal growth is not limited by the availability of dissolved phosphate (see Chapter 7 and 8). For reservoirs where algal growth is phosphate limited, a number of water quality variables most likely will be significantly influenced by changes in the inflow phosphate data.

10.3.2 The effect of changing nitrate data in the inflow on model output.

Using calculated 'simple regression' nitrate data instead of 'smoothed' data: In this study, observed nitrate data were discarded and, for each river, nitrate data were calculated from flow rate, using a simple linear regression that is neither flow nor season dependant (Table 10.3). The 'smoothed' nitrate data in the original inflow data base were substituted with these 'simple regression' nitrate data. The other variables in the inflow data file were unchanged.

TABLE 10.3. Linear regression between ln flow and ln NO_3 for each river flowing into Roodeplaat Dam.

RIVER	DEPENDENT VARIABLE	INDEPENDENT VARIABLE	SLOPE	CONSTANT	R^2
Pienaars	ln NO_3	ln flow	0.182±0.020	1.283±0.400	0.15
Hartbees	ln NO_3	ln flow	0.458±0.039	-0.29±0.85	0.15
Edendale	ln NO3	ln flow	-0.33±0.03	-2.04±1.11	0.15

Time-series of 'smoothed' vs 'simple regression' nitrate data for Pienaars River are shown in Figure 10.52.

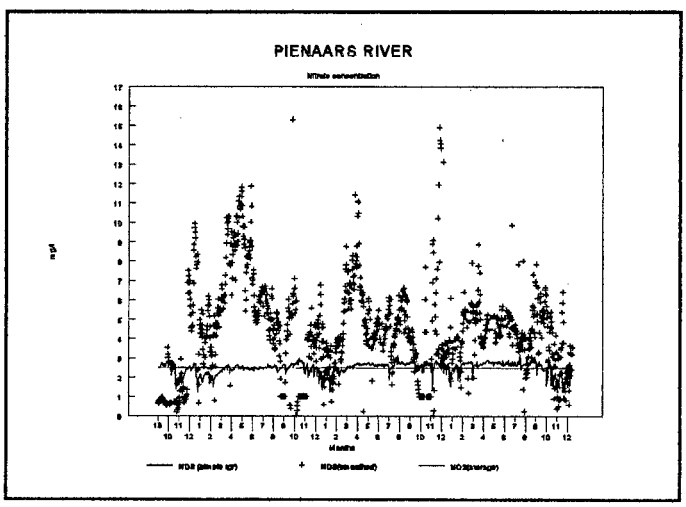

Figure 10.52
Time-series of 'smoothed' vs 'simple regression data for Pienaars River.

Using 'simple regression' data instead of 'smoothed' nitrate data in the inflow resulted in a very small, insignificant change in simulated nitrate concentration only. The other simulated variables were unaffected.

Using weekly values for nitrate data instead of daily values: To evaluate the effect of having weekly, instead of daily, nitrate data available, the value on the first day of each week was entered for all the days of that week. Changing inflow nitrate data from daily to weekly values affected simulated nitrate concentration only, and again the change was so small that it can be regarded as insignificant. The other simulated variables were not affected at all.

Conclusion: Using 'simple regression' instead of 'smoothed' nitrate data in the inflow had a minor effect on simulated nitrate concentration, and no effect on the other simulated variables. Using weekly, instead of daily, data affected simulated nitrate concentration minimally. It would therefore seem that nitrate data can be calculated from flow rate data using simple linear regression relationships, instead of using measured data. If weekly measurements are available, the value for each weekly measurement can be entered for all the days in that week, i.e. there is no need for elaborate infilling techniques to establish missing nitrate data.

10.3.3 The effect of changing ammonia data in the inflow on model output.

Using calculated 'simple regression' ammonia data instead of 'smoothed' data: As with dissolved phosphate and nitrate data, observed ammonia data were discarded and the model was run with ammonia data calculated from a simple regression (Table 10.4). The other variables in the inflow data file were unchanged.

TABLE 10.4. Linear regression between ln flow and ln NH_4 for each river flowing into Roodeplaat Dam.

RIVER	DEPENDENT VARIABLE	INDEPENDENT VARIABLE	SLOPE	CONSTANT	R^2
Pienaars	ln NH_4	ln flow	-0.54±0.01	1.30±1.77	0.04
Hartbees	ln NH_4	ln flow	0.078±0.031	02.25±0.68	0.01
Edendale	ln NH_4	ln flow	0.08±0.03	-3.04±0.47	0.05

Time-series of 'smoothed' vs 'simple regression' ammonia data for Pienaars River are shown in Figure 10.53.

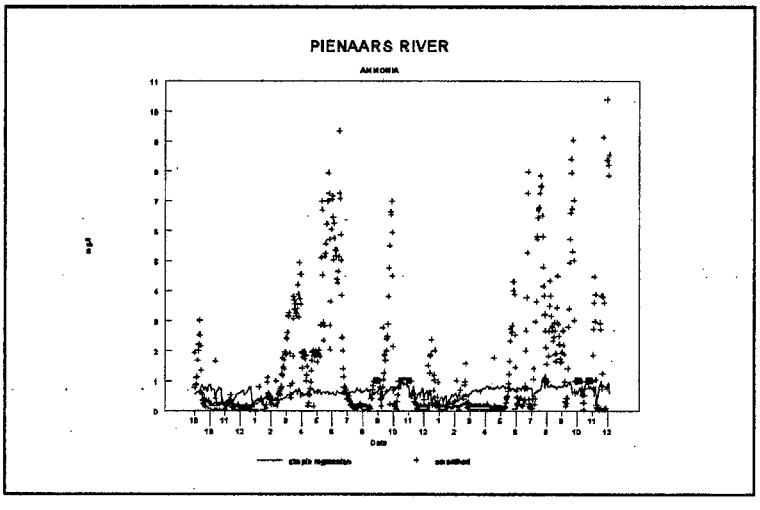

Figure 10.53
Time-series of 'smoothed' vs 'simple regression' ammonia data for Pienaars River.

Using 'simple regression' data instead of 'smoothed' data in the inflow file had a very small effect on simulated ammonia concentration (Fig 10.54), and no effect at all on the other simulated variables.

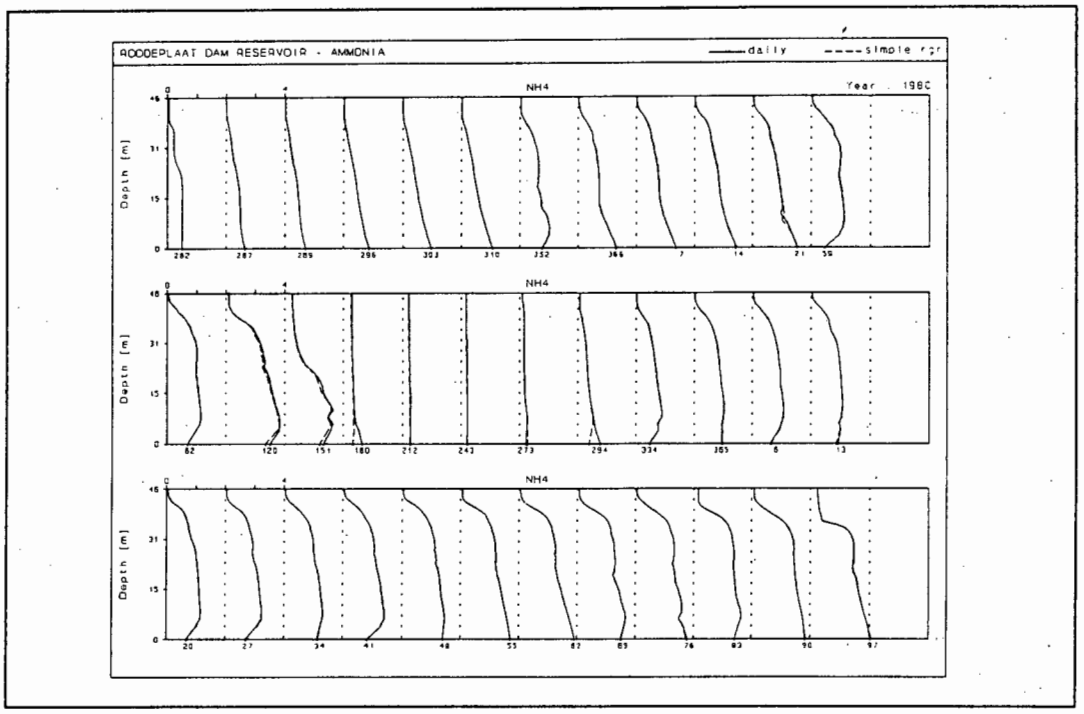

Figure 10.54
Simulated ammonia concentrations obtained with the modified MINLAKE model on Roodeplaat Dam using 'smoothed' and 'simple regression' ammonia data for the inflowing rivers.

Using weekly values for ammonia data instead of daily values:
Changing inflow ammonia data from daily to weekly values caused no change in any of the simulated variables, including simulated ammonia concentration.

Conclusion: Using 'simple regression' data instead of 'smoothed' ammonia data in the inflow basically had no effect on simulated ammonia concentration, and absolutely no effect on the other simulated variables. Using weekly, instead of daily input data, caused no change in any of the simulated variables. It would therefore seem that inflow ammonia data can be calculated from flow rate data using simple linear

regression relationships, instead of using daily measured data. If weekly measurements are available, the value for each weekly measurement can be entered for all the days in that week, i.e. as with nitrate, there is no need for elaborate infilling techniques to establish missing data.

10.3.4 Influence of inflow nitrogen on simulated output:

The changes in simulated output resulting from changes in nitrate and ammonia data in the inflow data file were less significant than expected. However, Roodeplaat Dam has been classified as a highly eutrophic dam, thus the internal load of nutrients from the bottom sediments may be quite high compared to the nutrient load entering the dam from the rivers, and therefore changes in the inflow concentrations would be small compared to the high internal nutrient load. This hypothesis is supported by the results of this study. However, it would also mean that the conclusions drawn from the above study on the effect of changes in water quality data on model output may be applicable only to dams where the internal nutrient concentration is much higher than the inflow nutrient concentration.

10.3.5 The effect of changing TDS data in the inflow on model output.

Using calculated 'simple regression' TDS data instead of 'smoothed' data: As with the other variables, observed data were discarded and inflow TDS data were calculated from flow rate data with the aid of a simple linear regression (Table 10.5). The other inflow variables were unchanged.

TABLE 10.5. Linear regression between ln flow and ln TDS for each river flowing into Roodeplaat Dam.

RIVER	DEPENDENT VARIABLE	INDEPENDENT VARIABLE	SLOPE	CONSTANT	R^2
Pienaars	ln TDS	ln flow	0.240±0.005	6.52±0.19	0.52
Hartbees	ln TDS	ln flow	0.231±0.011	5.39±0.39	0.30
Edendale	ln TDS	ln flow	-0.14	5.1	0.70

Time-series of 'smoothed' vs 'simple regression' TDS data for Pienaars River are shown in Figure 10.55.

Using 'simple regression' inflow TDS data instead of 'smoothed' data in the inflow file caused changes in simulated concentrations of ammonia, dissolved phosphate, nitrate and TDS (Fig 10.56 - 10.59). However, these changes were very small and probably are insignificant. The changes are due to a change in hypolimnetic diffusion rate, which is a function of water density. In the MINLAKE model, water density is formulated as a function of water temperature, and concentrations of TSS and TDS.

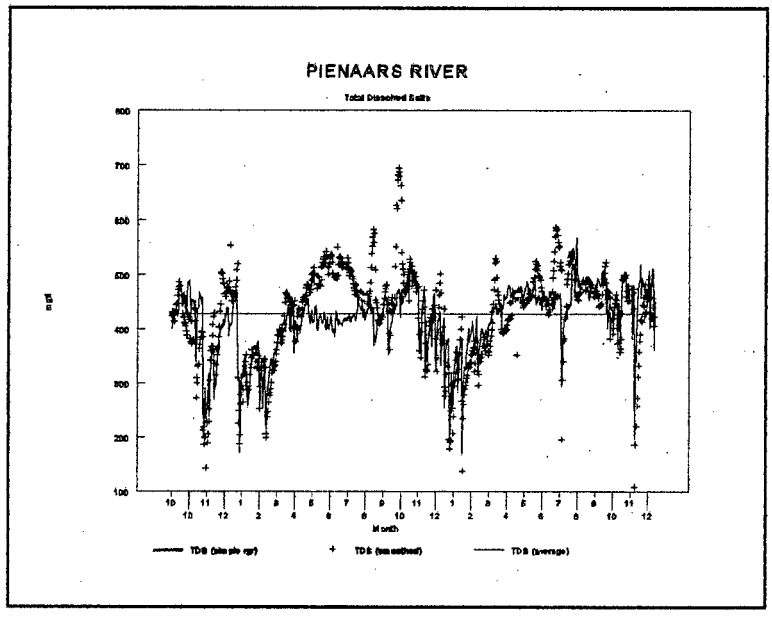

Figure 10.55
Time-series of 'smoothed' vs 'simple regression' TDS data for Pienaars River.

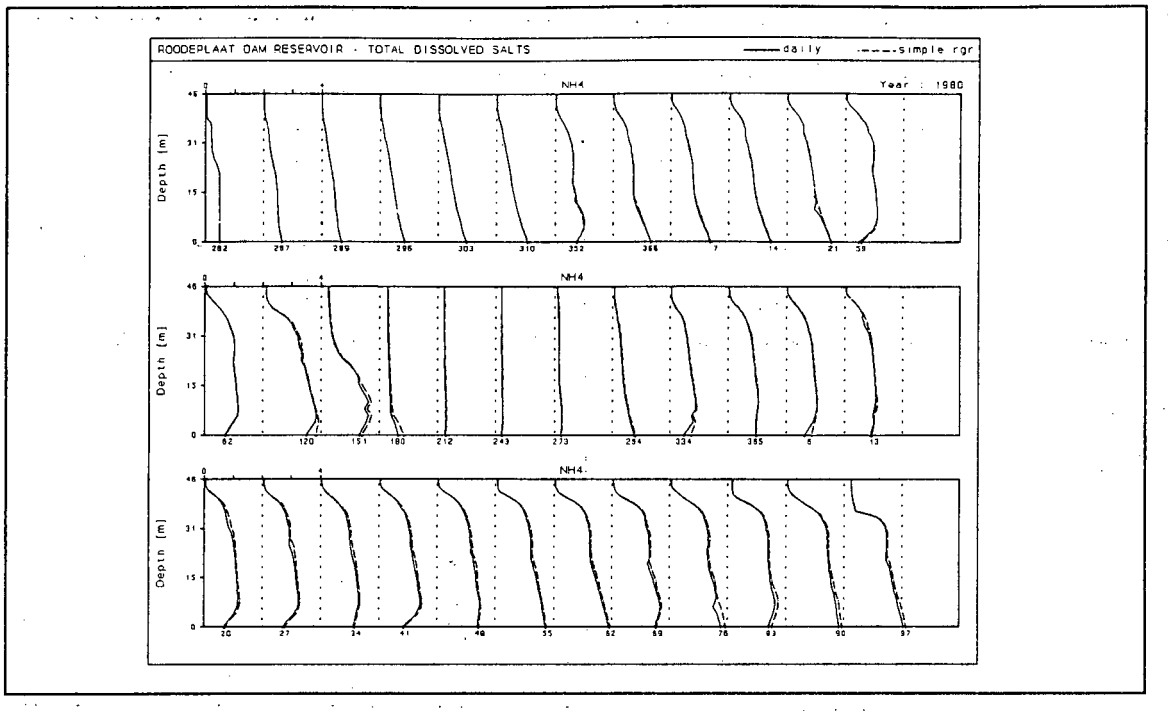

Figure 10.56
Simulated ammonia concentrations obtained with the modified MINLAKE model on Roodeplaat Dam using 'smoothed' and 'simple regression' TDS data for the inflowing rivers.

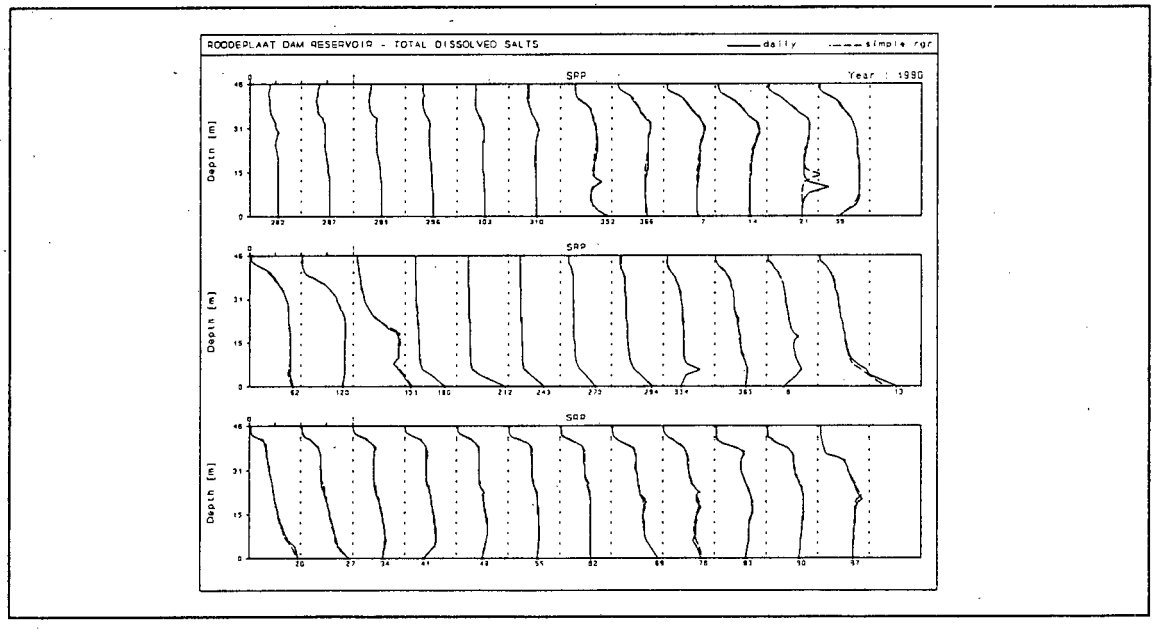

Figure 10.57
Simulated dissolved phosphate concentrations obtained with the modified MINLAKE model on Roodeplaat Dam using 'smoothed' and 'simple regression' TDS data for the inflowing rivers.

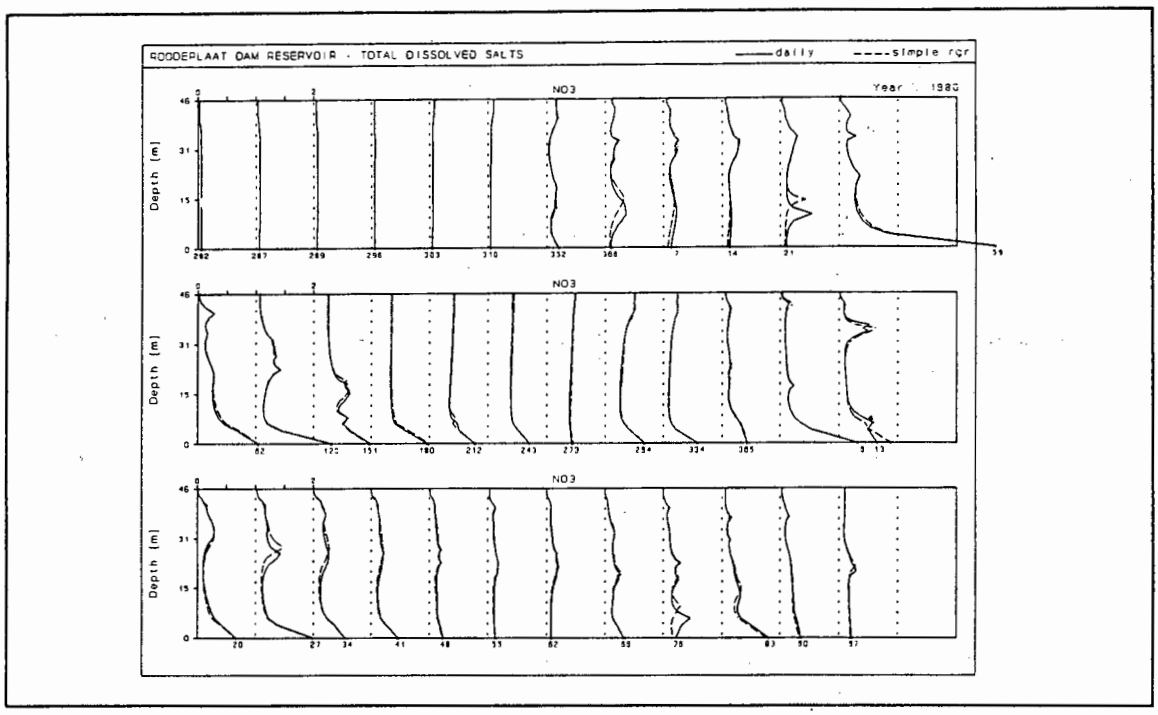

Figure 10.58
Simulated nitrate concentrations obtained with the modified MINLAKE model on Roodeplaat Dam using 'smoothed' and 'simple regression' TDS data for the inflowing rivers.

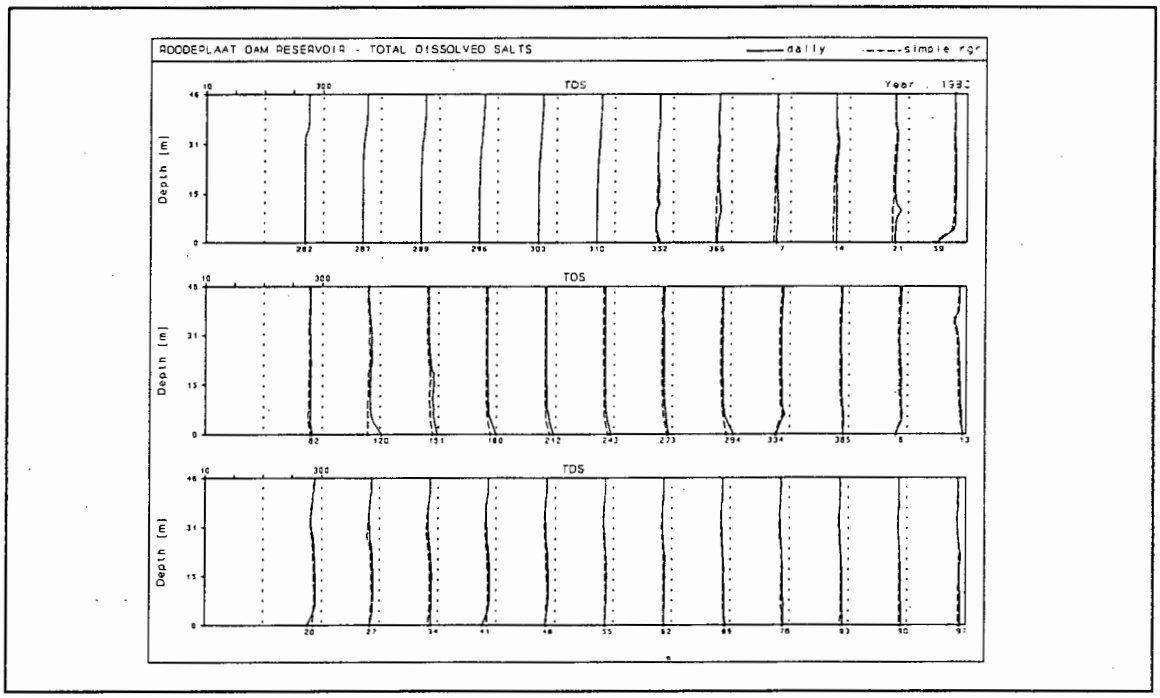

Figure 10.59
Simulated TDS concentrations obtained with the modified MINLAKE model on Roodeplaat Dam using 'smoothed' and 'simple regression' TDS data for the inflowing rivers.

Using weekly values for TDS data instead of daily values:

Changing inflow TDS data from daily to weekly values caused a very small change in simulated TDS concentration only (Fig 10.60).

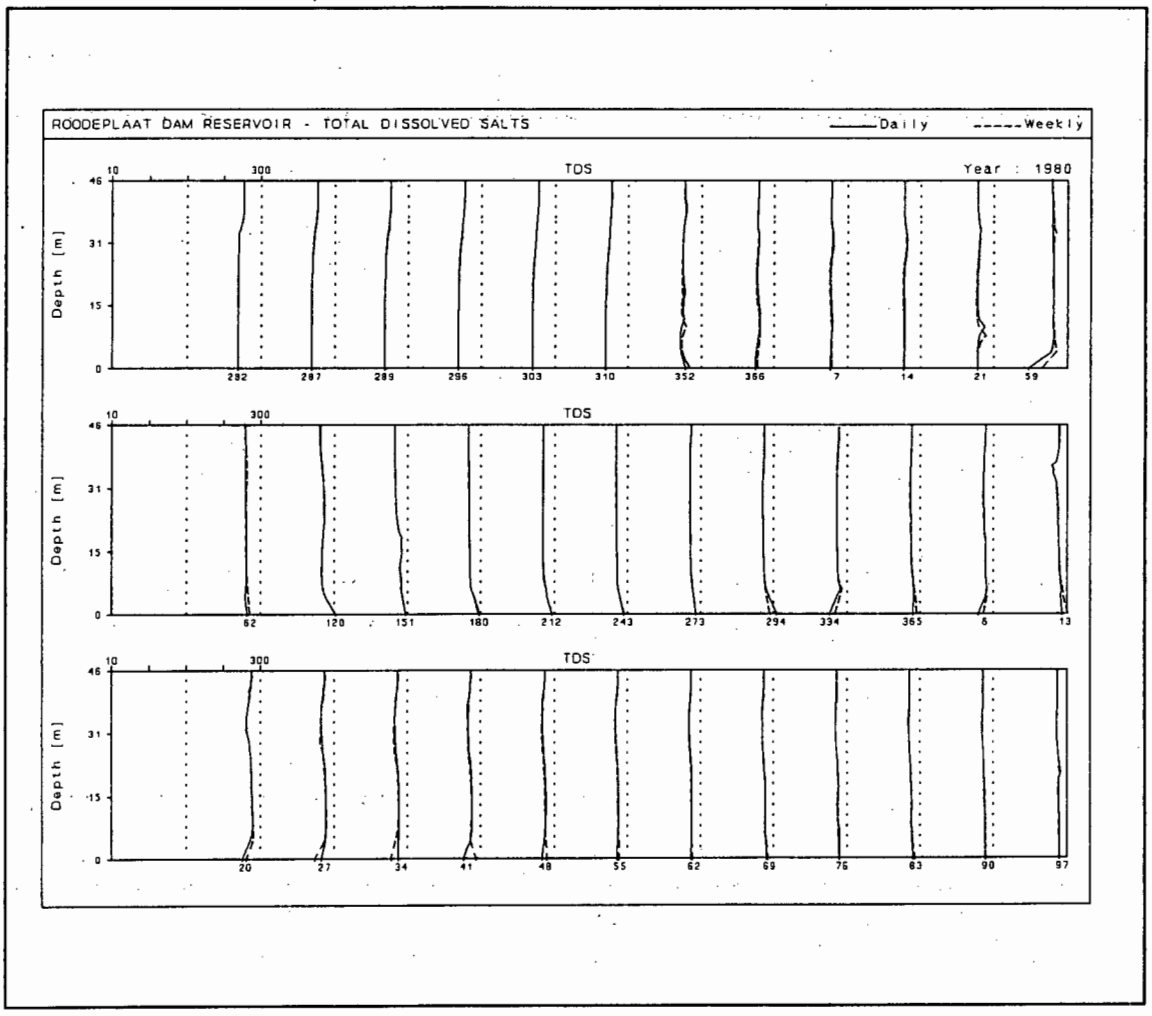

Figure 10.60
Simulated TDS concentrations obtained with the modified MINLAKE model on Roodeplaat Dam using daily and weekly TDS data.

Conclusion: Using calculated, instead of daily 'smoothed' TDS data in the inflow data file resulted in insignificant changes in simulated concentrations of ammonia, dissolved phosphate, nitrate and TDS. Changing from daily to a weekly TDS data virtually had no effect at all on the model output.

10.4 GENERAL CONCLUSIONS

The large amount of data needed as input by dynamic water quality models such as MINLAKE often limits their general use. Although most of the meteorological and inflow water quality variables required by these models are being measured in South Africa, daily measurements may not be available, or measurements may not be done at the site of the reservoir being modelled. In the above study, the sensitivity of the modified MINLAKE output to changes in the frequency of meteorological and inflow water quality data was tested, using daily calibrated output obtained with the modified MINLAKE model on Roodeplaat Dam as a basis. The following conclusions can be drawn from this study:

10.4.1 Meteorological input data

- Air temperature - instead of daily input data, weekly, or even monthly input data can be used. If measurements are not made at the site of the reservoir being modelled, data from another, nearby site can be substituted.

- Dew point temperature - weekly input data can be used, but the use of monthly data is not recommended, as it resulted in significant differences in model output. Care should be taken when using data from another site.

- Precipitation - weekly, or even monthly **averaged** data may be used instead of daily data, or data from another, nearby site can be substituted.
- Wind speed - if wind speed is not measured at the height required by the model, it is of the utmost importance to correctly convert the wind speed from the observed height to the required height. In the absence of daily measurements, weekly data can be used, but the use of monthly data is not recommended. Wind speed data from another nearby site may not be representative of wind speed at the site of reservoir being modelled, due to topographical differences.

- Wind direction - although wind direction data is entered into the model, it is not used in any of the formulations in the model. However, it does afford the user the opportunity of linking, for instance, wind fetch to the wind direction. This may be important in non-symmetrical dams.

- Sunshine hours - weekly, or even monthly data can be used. Data from another site can be substituted.

- Solar radiation - weekly data, or data from another, nearby site can be used. Depending on the requirements of the user, monthly measurements may be used.

- All meteorological variables - depending on the requirements of the user, weekly data for all the meteorological variables may be used, though care should be taken if the simulation period exceeds 9 - 12 months. The use of monthly data, or data from another site, for all the meteorological variables is not recommended.

10.4.2 Inflow water quality data

Regarding inflow water quality data, it is difficult to make a final conclusion that would be valid for all reservoirs on the basis of the study done on Roodeplaat Dam. For reservoirs such as Roodeplaat Dam, where the internal nutrient loads due to release from the bottom sediments are high in comparison with the inflow nutrient load, the following conclusion appears to be valid: Instead of daily inflow water quality data, weekly data can be used. In some instances daily data calculated with the aid of a simple regression can even be used. However, it is unlikely that this conclusion will be valid for reservoirs where the inflow nutrient load is comparable to the internal nutrient load.

CHAPTER 11

USE OF THE MODEL TO TEST TREATMENT OPTIONS

11.1 INTRODUCTION

The complex interaction between reservoir processes often makes selection of the most suitable treatment option and prediction of its effectiveness difficult. Also, any treatment strategy may have secondary and undesirable effects on other reservoir processes. Although it is difficult to foresee these effects, the problem can be resolved to a certain extent by modelling the behaviour of the reservoir. As an example of how a model can be used as an aid in management decisions, the MINLAKE model, as calibrated for Roodeplaat Dam Reservoir, was used to test the effect of certain treatment options on the trophic behaviour of the reservoir. The options investigated were:

- Reduction of inflow phosphate concentration.
- Reduction of inflow nitrate concentration.
- Reduction of inflow ammonia concentration.

11.2 TESTING THE EFFECT OF REDUCED PHOSPHATE CONCENTRATION IN THE INFLOW

High phytoplankton concentrations in reservoirs that are used as drinking water supplies, cause a multitude of problems (*cf* Chapter 1). To reduce the nuisance caused by algae in these reservoirs, a special effluent phosphate-P standard of 1 mg l^{-1} was introduced in certain sensitive catchments in 1985. The simulation period for Roodeplaat Dam Reservoir (October 1980 to October 1982) is prior to initiation of this standard. During the simulation period, Pienaars River, the river with the highest phosphate-P concentration of the three rivers flowing into the reservoir, sometimes

had a phosphate-P concentration as high as 10 mg l^{-1}, with an average concentration of 4 mg l^{-1} during the simulation period (Fig 11.1). The PO_4-P load from all three rivers for the entire study period was 63.5 tons.

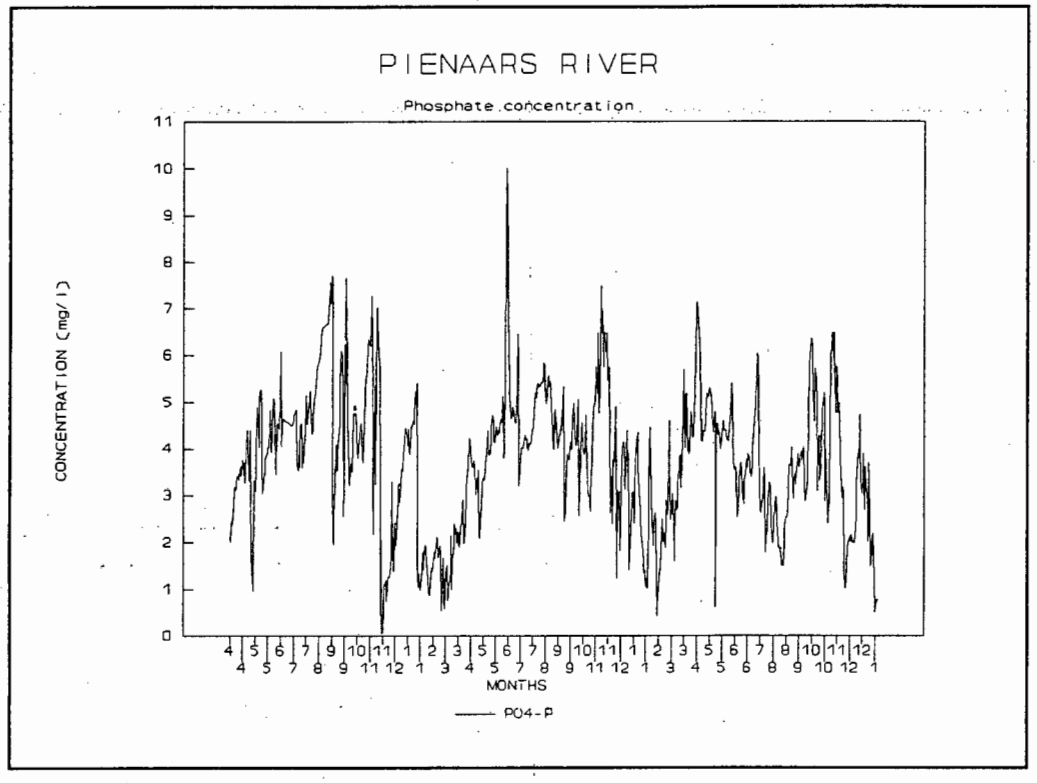

Figure 11.1
Observed phosphate concentration in Pienaars River.

To assess the effect of a reduction in inflow phosphate concentration on the trophic behaviour of the reservoir, a run was done with the inflow phosphate concentration arbitrarily set at 5% of the observed concentration, i.e. the PO_4-P load was reduced from 63.5 tons to 3.2 tons. The results are depicted in Fig 11.2 to 11.7.

The dissolved phosphate concentration in the reservoir declined rapidly and was negligible after only three months (Fig 11.2). However, it took 12 months for the chlorophyll-a concentration to decline (Fig 11.2). Regarding nitrate concentration, after 6 months there was a steady increase in nitrate concentration, to a concentration of about 1.5 mg l^{-1} at the end of the simulation period (Fig 11.3). The ammonia concentration does not appear to be affected (Fig 11.3).

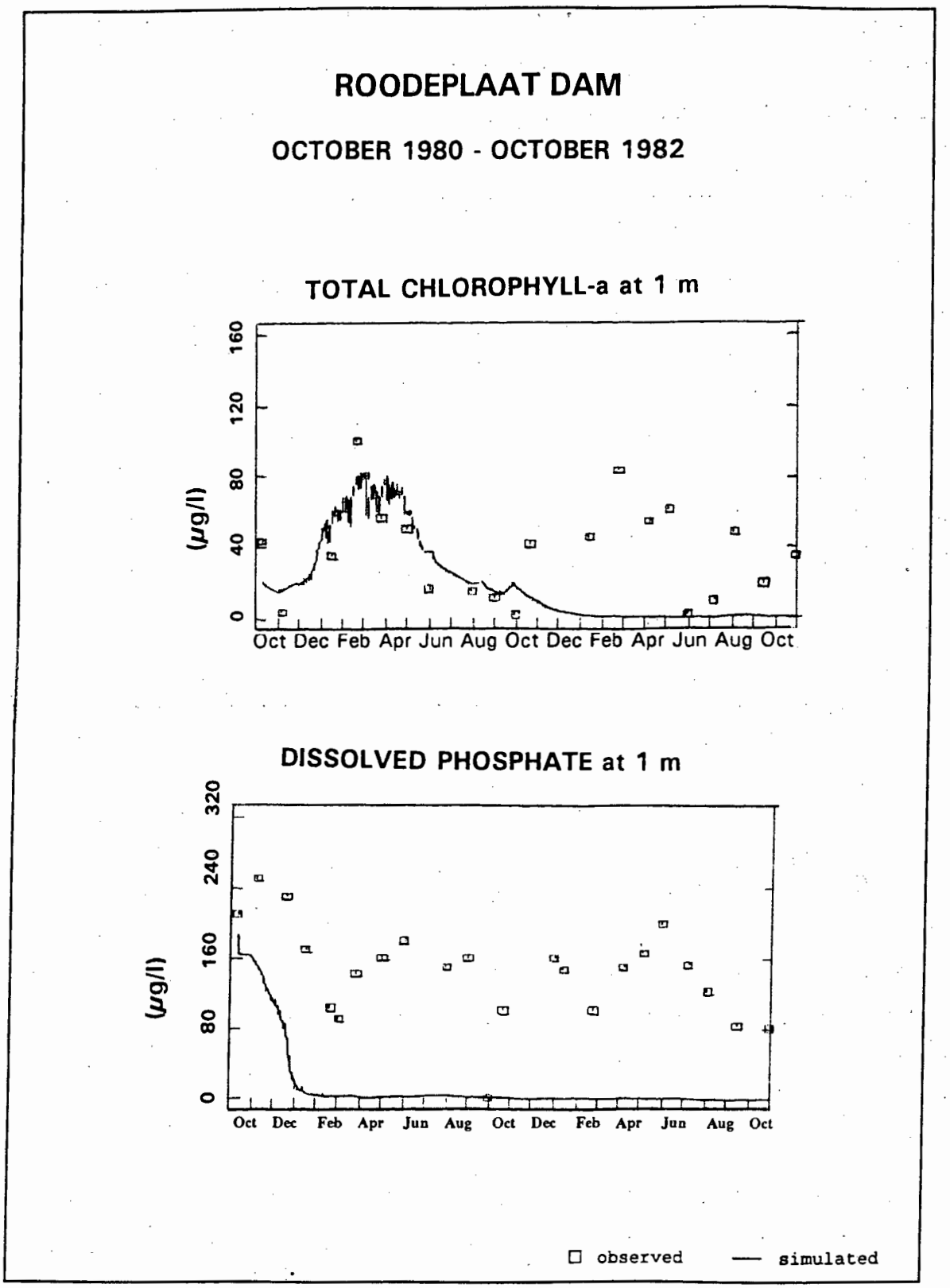

Figure 11.2
Plot of simulated vs observed chlorophyll-a and dissolved phosphate concentrations with inflow phosphate concentration set at 5% of the observed.

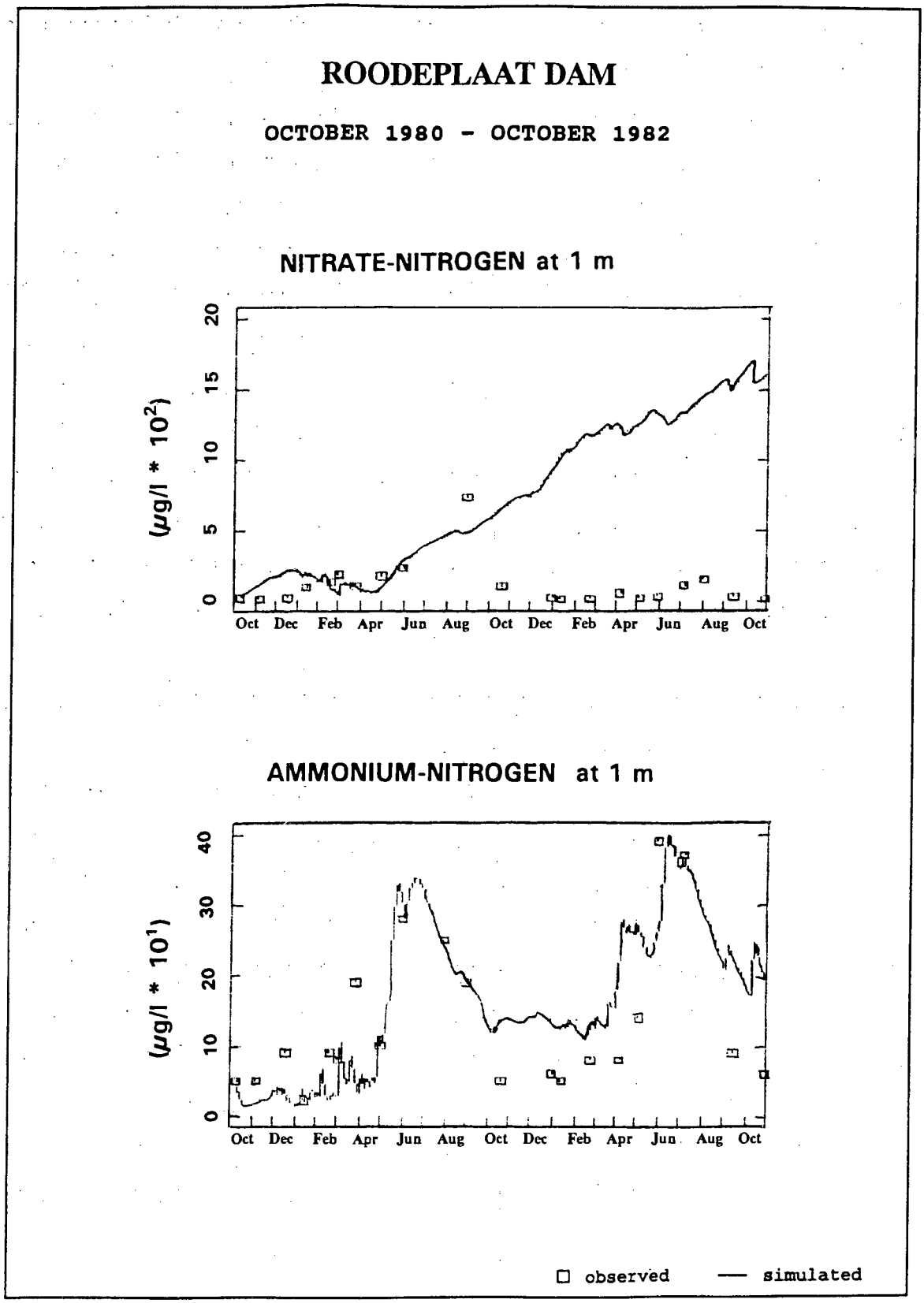

Figure 11.3
Plot of simulated vs observed nitrate and ammonia concentrations with inflow phosphate concentration set at 5% of the observed.

The decreased algal concentration had a major effect on the reservoir. The effect was not immediate - algal growth declined after 12 months only, probably because of luxury uptake of phosphorus by the algae, i.e., the algae had sufficient internally stored reserves of phosphate to sustain growth for a further 9 months after the concentration of external phosphorus declined to zero. However, because of the lower algal concentration, the concentration of detritus was lower, thus less oxygen was consumed in microbial decay of detritus, leading to an increase in the concentration of hypolimnetic oxygen, as is evident in Figure 11.4, Julian Day 273. (Figure 11.4 was obtained by plotting simulated oxygen concentration as obtained with the MINLAKE model on Roodeplaat Dam Reservoir with 'normal' inflow phosphate concentration as observed, and by plotting simulated oxygen concentration obtained with inflow phosphate reduced to 5% of the observed values. Similarly, Figure 11.5 to 11.7 depict plots of phosphate, nitrate, and ammonia concentrations simulated under 'normal' conditions, and with inflow phosphate concentration reduced to 5% of the observed).

The increased hypolimnetic oxygen concentration affected several other processes. For instance, the rapid decline in dissolved phosphate concentration is not due only to reduced phosphate in the inflow, but also to the increased oxygen concentration - in Roodeplaat Dam Reservoir, dissolved phosphate is released from the bottom sediments under anaerobic conditions, and adsorbed under aerobic conditions. Thus, because the hypolimnion does not become anaerobic, no phosphate is released from the bottom sediment. In fact, phosphate is adsorbed continuously by the sediments, and thus the sediments become a significant sink of phosphate. This is not necessarily an ideal situation, as, apart from the residual phosphate concentration in the sediments, the concentration of phosphate in the sediments will increase steadily. Should anaerobic conditions occur, the resultant sediment phosphate release could lead to a large increase in dissolved phosphate concentration, causing increased algal growth.

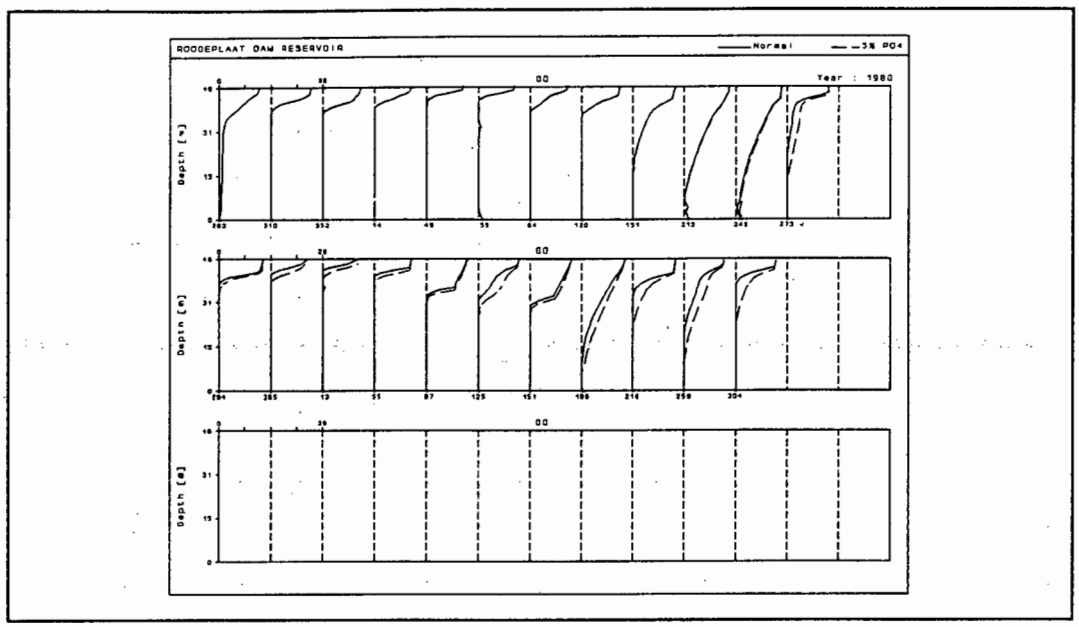

Figure 11.4
Plots of simulated oxygen concentration obtained with inflow phosphate concentration set at 5% of the observed, and with inflow phosphate concentration as observed.

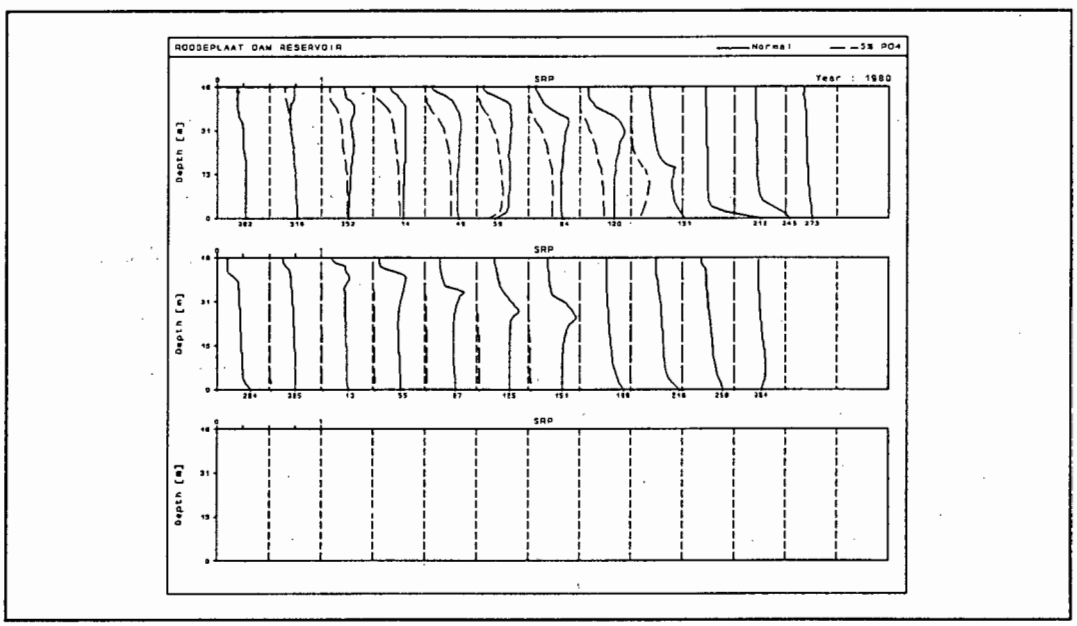

Figure 11.5
Plots of simulated phosphate concentration obtained with inflow phosphate concentration set at 5% of the observed, and with inflow phosphate concentration as observed.

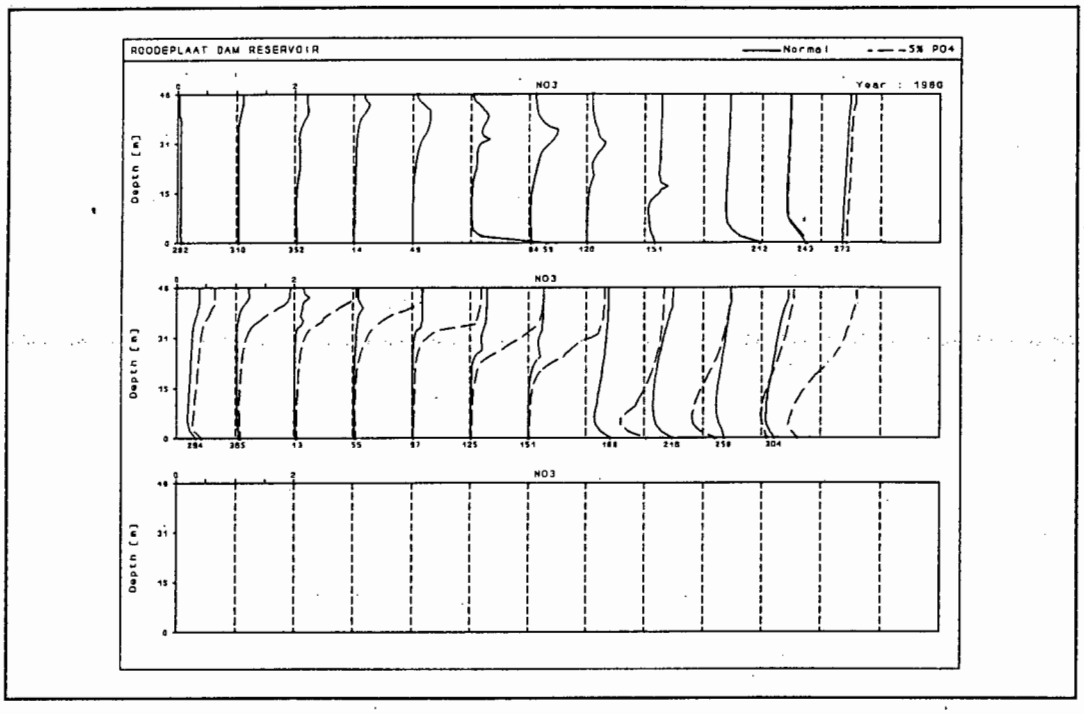

Figure 11.6
Plots of simulated nitrate concentration obtained with inflow phosphate concentration set at 5% of the observed, and with inflow phosphate concentration as observed.

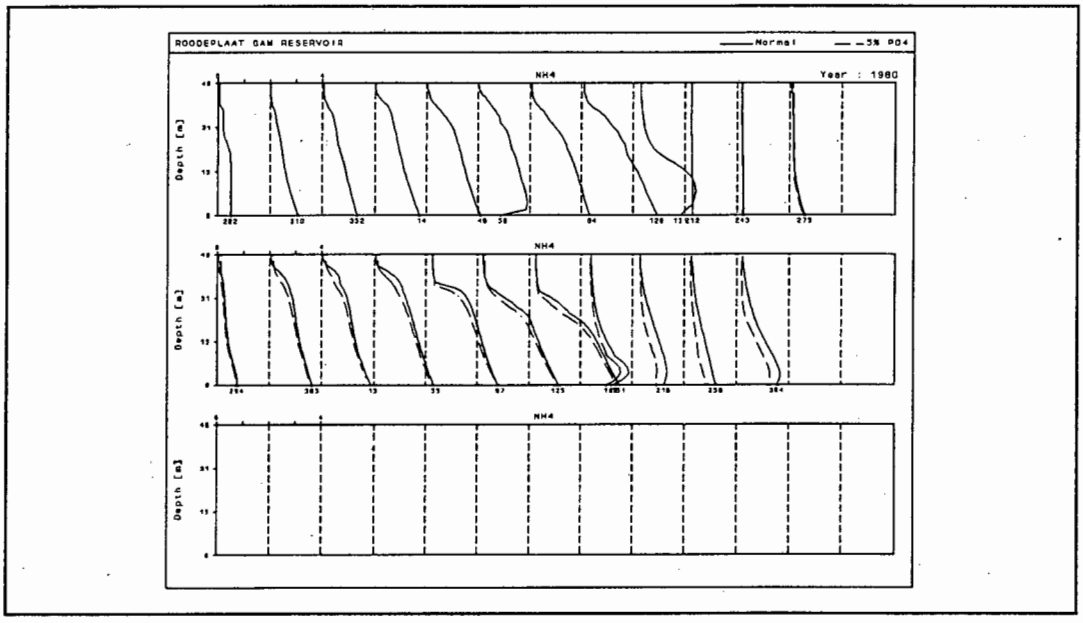

Figure 11.7
Plots of simulated ammonia concentration obtained with inflow phosphate concentration set at 5% of the observed, and with inflow phosphate concentration as observed

The increased nitrate concentration can be attributed also to the increase in hypolimnetic oxygen concentration. The sediments are a major source of ammonia (see discussion in Chapter 8). If the water above the sediments is aerobic, the surface layer of the sediments becomes aerobic also, thereby enabling nitrification of ammonia in the sediments. Thus the bottom sediments become a source of nitrate under aerobic conditions. Nitrification will occur in the water column as well, but no denitrification can occur under aerobic conditions. Thus the increased nitrate concentration can be attributed to increased nitrification in both the sediments and the water column, and decreased denitrification. The effect of increased oxygen concentration on the concentration of nitrate can be seen in Figures 11.4 and 11.6 - in Figure 11.4 the first significant change in oxygen concentration is seen to occur on Julian Day 273, and in Figure 11.6 the associated change in nitrate concentration on Julian Day 273 can be seen.

Regarding ammonia concentration, as can be seen in Figure 11.7, the change in ammonia concentration was not as marked as the change in nitrate concentration. The concentration of ammonia decreased slightly, probably because of increased nitrification, and decreased release from the sediments under aerobic conditions.

The large increase in nitrate concentration upon reduction of phosphate concentration leads to the question as to whether it would not be more beneficial to reduce the nitrate concentration in the inflow, as that should cause a decrease in algal growth also, and may result in a lower nitrate concentration than was observed under reduced phosphate conditions.

11.3 TESTING THE EFFECT OF REDUCED NITRATE CONCENTRATION IN THE INFLOW

During the study period, the average NO_3-N concentrations in the three rivers flowing into the Roodeplaat Dam was 4.54 mg l^{-1} (Pienaars River), 5.87 mg l^{-1} (Hartbeesspruit), and 0.14 mg l^{-1} (Edenvalespruit). The load entering the dam from all three rivers was 173 tons. The daily nitrate concentrations in the rivers were arbitrarily reduced to 5%,

i.e. a load of 8.7 tons. Compared to reduced phosphate concentration, reducing the inflow nitrate concentration to 5% of the observed had a smaller effect on the trophic behaviour of the reservoir. The effect of reduced nitrate concentration on algal concentration can be seen in Figure 11.8. Although there is a slight decrease in the concentration of blue-green algae, green algae were not really affected, probably because the concentration of ammonia was still sufficient for green algal growth. Because there was not a significant reduction in algal concentration, there is no associated decrease in detrital concentration, nor an increase in hypolimnetic oxygen, and thus concentrations of phosphate and ammonia were affected insignificantly. The effect of reducing the nitrate in the inflow can be seen in Figure 11.9 - the simulated concentration obtained with inflow nitrate as observed clearly shows an increase in nitrate concentration at the depth of inflow, but the simulations obtained with reduced inflow nitrate do not show the same effect at the depth of inflow.

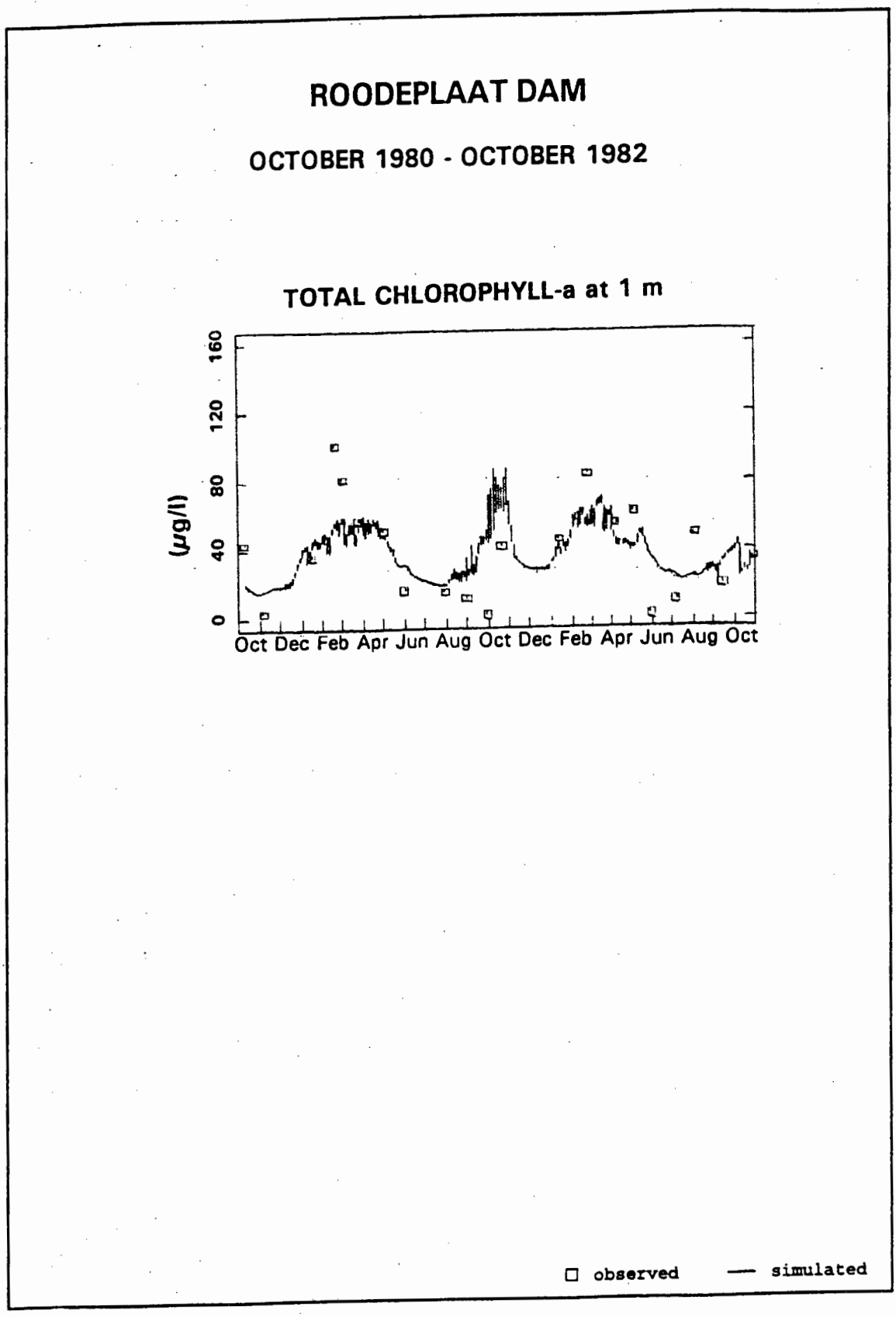

Figure 11.8
Plot of simulated vs observed chlorophyll-a concentrations with inflow nitrate concentration set at 5% of the observed.

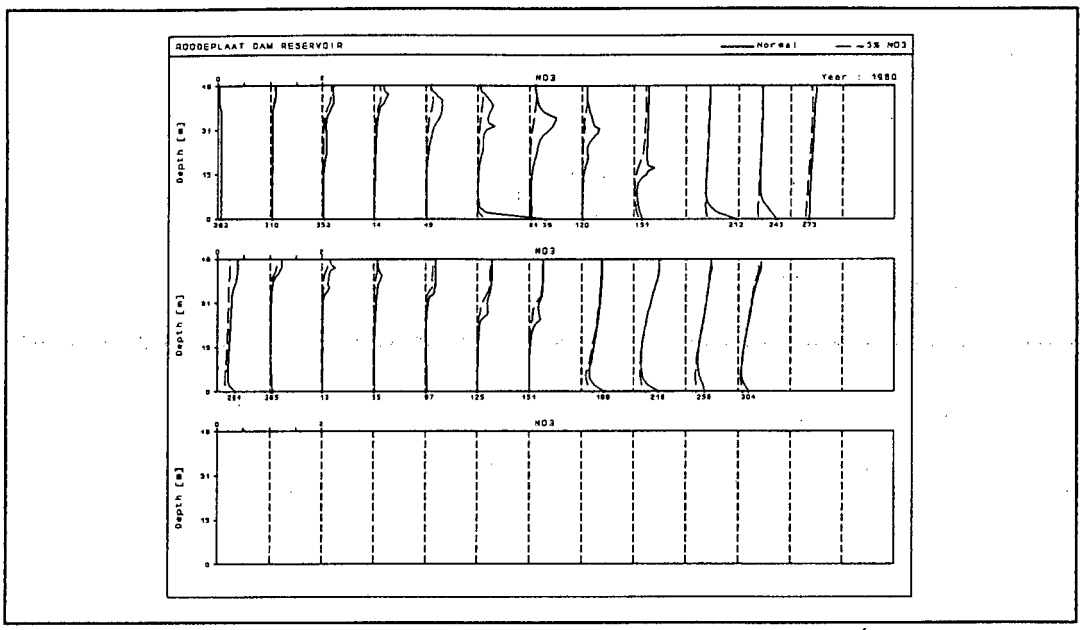

Figure 11.9
Plots of simulated nitrate concentration obtained with inflow nitrate concentration set at 5% of the observed, and with inflow nitrate concentration as observed

11.4 TESTING THE EFFECT OF REDUCED AMMONIA CONCENTRATION IN THE INFLOW

Reducing the concentration of nitrate in the inflow had very little effect on the trophic behaviour of the reservoir, and thus it was decided to test the effect of reduced ammonia in the inflow. As with phosphate and nitrate, a run was done with ammonia concentration in the inflows reduced to 5% of the observed, i.e. reducing the NH_4-N load during the study period from 37 to 1.85 tons. The results were compared with that obtained with observed ammonia concentrations.

As depicted in Figures 11.10 and 11.11, reducing the ammonia concentration in the inflow had an insignificant effect on the ammonia concentration in the reservoir, and hence on the trophic behaviour of the reservoir. Most likely this can be attributed to the eutrophic history of the reservoir, which means that the bottom sediments have become a major source of ammonia to the reservoir (see discussion in Chapter 8).

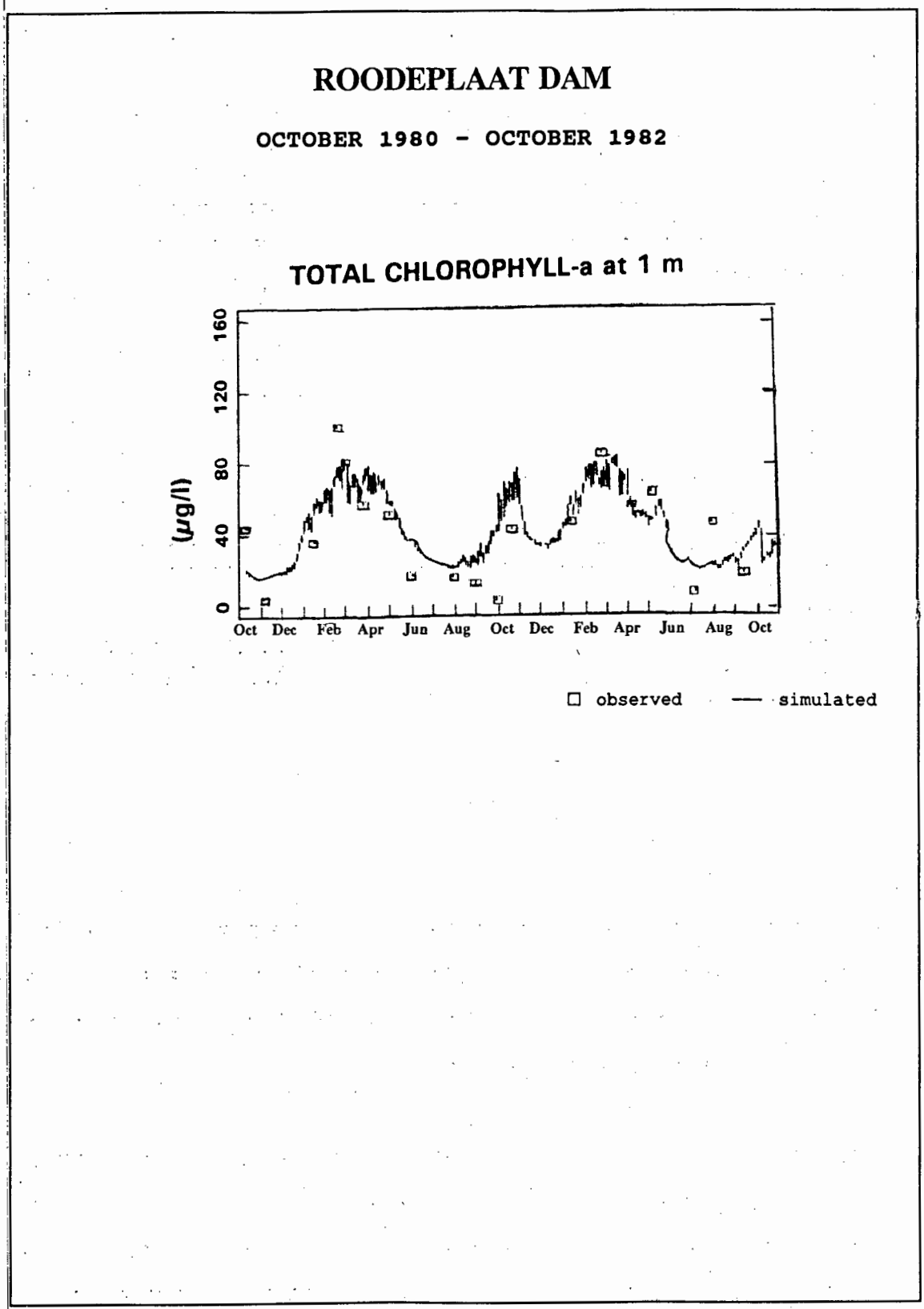

Figure 11.10
Plot of simulated vs observed chlorophyll-a concentrations with inflow ammonia concentration set at 5% of the observed.

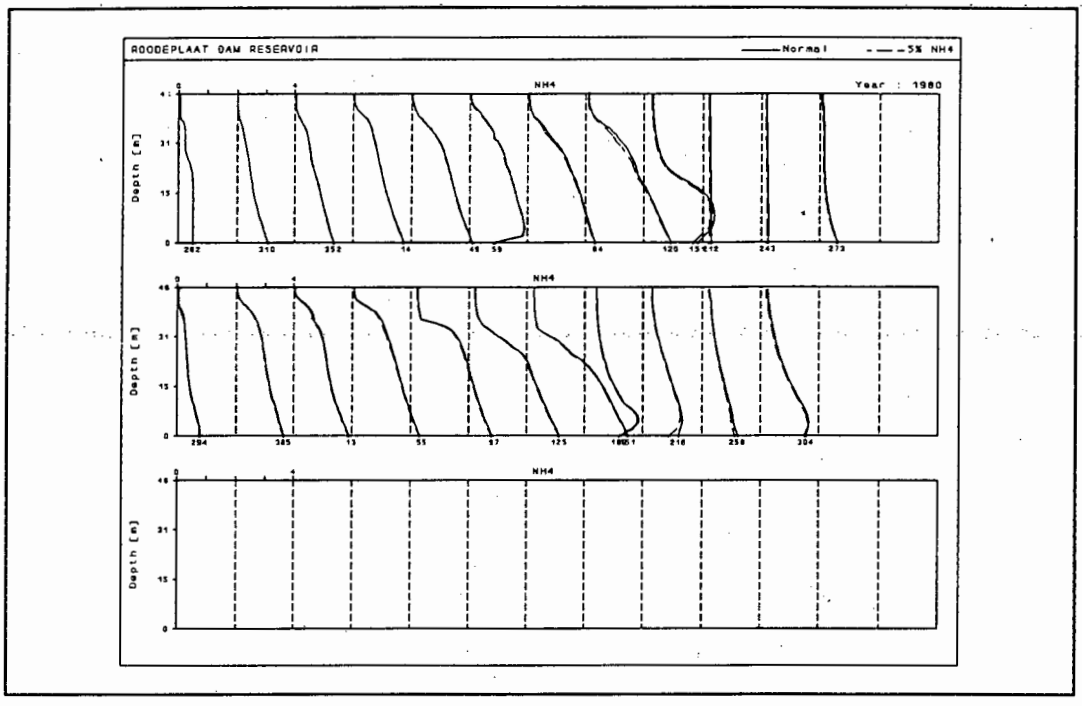

Figure 11.11
Plots of simulated ammonia concentration obtained with inflow ammonia concentration set at 5% of the observed, and with inflow ammonia concentration as observed

11.5 CONCLUSION

Reducing the phosphate concentration in the inflow had the most significant effect on the trophic behaviour of the reservoir, mainly because of the decreased algal growth that changed the aerobic/anaerobic state of the reservoir. A negative side effect of this treatment is a large increase in nitrate concentration.

Reducing the nitrate concentration in the inflow did not affect the trophic behaviour of the dam significantly. It lead to a decrease in nitrate concentration in the reservoir, and to a slight decrease in algal concentration. However, the decrease in algal concentration was not sufficient to cause a change in the aerobic/anaerobic state of the reservoir, and thus the concentration of other constituents such as phosphate and ammonia was not affected.

Reducing the concentration of ammonia in the inflow had the least affect, as it did not even cause a significant reduction in the concentration of ammonia in the reservoir, probably because of the eutrophic history of the reservoir, which means that the bottom sediments have become the main source of ammonia to the reservoir.

CHAPTER 12

CONCLUSIONS AND RECOMMENDATIONS

The objective of this study was to determine whether a one-dimensional eutrophication model such as the MINLAKE model (Minnesota Lake Water Quality Model), developed in a cold temperate climate in the northern USA, can simulate the trophic behaviour of a typical South African reservoir (Roodeplaat Dam, north of Pretoria) situated in a warm temperate/subtropical climate, or whether climatic differences would necessitate the MINLAKE model to be modified.

12.1 CONCLUSIONS

The following conclusions were drawn from the study:

12.1.1 Applicability

The MINLAKE model is a one-dimensional model, and the basic assumption of a 1D model is horizontal homogeneity at any depth. Despite the fact that Roodeplaat Dam has an irregular shape with multiple in/outlets in the main body of the dam, temperature profiles at different locations in the dam indicate support for the assumption of horizontal homogeneity. Disruptions of the 1D structure due to storm events are rapidly dissipated, and the dam returns to the 1D state within one or two days.

12.1.2 Hydrodynamic behaviour

The hydrodynamic behaviour of Roodeplaat Dam appears to be described adequately by the modified MINLAKE model. The temperature profiles in particular are described very well, and mixed layer depth is described adequately.

Simulation of the hydrodynamic behaviour of Roodeplaat Dam did not require any modifications to the hydrodynamic part of the original MINLAKE model, i.e. both the conceptual basis and formulation of the hydrodynamic part of the original model can be regarded as sound. However, a few technical modifications were required before the model could be applied to Roodeplaat Dam:

(i) The model requires wind speed at 10 m height, whereas wind speed in South Africa is measured at 1.8 m (6 ft). Accordingly it was necessary to convert the observed wind speed at 1.8 m to a wind speed at 10 m as required by the model. This conversion procedure can be applied to wind speed measured at any height.

(ii) The original MINLAKE model made provision for only one inflow or outflow, and accordingly the model was changed to allow multiple in/outflows, up to a maximum of 5. The outflows can be specified as either surface or subsurface at preselected depths.

(iii) The model was adapted to allow simulation at latitudes both north and south of the equator. The original model was hard-wired for the specific latitude of Lake Riley in the northern hemisphere.

12.1.3 Water quality behaviour

The original MINLAKE model was developed and tested on observations made on lakes situated in Minnesota in a cold temperate climate. Accordingly, only processes that reflected the behaviour observed in such a climate were included. When the model was applied to a hypertrophic dam in a warm temperate climate, it was clear that the original model had to be extended to incorporate processes that would reflect behaviour observed in a warm temperate climate but not in a cold temperate climate.

The principal extension was to take cognisance of the effect of the aerobic/anaerobic state of the water on various process rates, to consider the effect of temperature on certain process rates, and in particular incorporation of the process of denitrification.

Incorporation of these modifications appears to make the model more general. Application of the modified model to Lake Riley in Minnesota gave close correspondence between observed and simulated results - the simulated results were virtually identical to that obtained with the original model. It would appear that the modified model can be applied over a greater range of climatic conditions, from warm temperate to cold temperate.

12.1.4 Input data

12.1.4.1 Hydrodynamic input data:

Calibration confirmed that wind speed is a most important variable. There is little likelihood of obtaining realistic simulation of hydrodynamic and water quality behaviour if wind speed data are unreliable. It therefore seems to be essential that on-site measurements of wind speed (including seasonal variation) are performed. Furthermore, regardless of whether a dam is to be modelled or not, wind speed data *per se* can, with experience, assist in a subjective evaluation of the hydrodynamic and water quality behaviour of a dam.

An analysis of the sensitivity of the modified model to the input frequency of meteorological data (wind speed, wind direction, air temperature, dew point temperature, wind speed, wind direction, percentage sunshine, precipitation, and short wave solar radiation) indicated that, although the model requires these on a daily basis, the model output is not affected significantly if data taken at weekly intervals are substituted for the daily data over that week. Furthermore, except for wind speed, data taken from a nearby site would prove adequate also.

An analysis of the sensitivity of the model to wind direction indicates that the sensitivity varies with the shape of the dam. With approximately circular-shaped dams, wind direction is of little account, but in elongated or dendritic water bodies wind direction is important in that wind fetch becomes a function of wind direction. However, it would appear that great accuracy in wind direction data is not necessary.

12.1.4.2 Water quality input data:

The MINLAKE model makes provision for inflow water quality data on the following parameters for each of the inflowing rivers:

- river water temperature
- flow rate
- BOD

Concentrations of:

- dissolved phosphate
- dissolved oxygen
- ammonia
- nitrate
- total dissolved salts (TDS)
- total inorganic suspended sediment (TSS)
- chlorophyll-a

Inflow water quality data need to be supplied only for those parameters that are to be simulated.

Regarding the frequency of inflow water quality data, it is not possible to make a general statement regarding these. For highly eutrophic dams where the bottom sediments have become a major source of nutrients, data taken at weekly intervals would appear to be adequate, because the internal load from the sediments dominates over the load from the inflowing rivers. In younger dams where there has been little accumulation of nutrients in the bottom sediments, dam response will be more sensitive to inflow water quality data, and daily inflow water quality data would be important.

12.1.5 Model calibration

During both the hydrodynamic and water quality calibration, the importance of eddy diffusion as a mixing mechanism was confirmed. In both the original and the modified MINLAKE models, the user has to specify the maximum hypolimnetic eddy diffusion coefficient. It is important to calculate this coefficient with reasonable accuracy, else realistic simulation of nutrients and temperature with depth is not possible.

Simulation of nutrient kinetics was possible only if the effects of the aerobic/anaerobic states of the water were taken into account. Calibration of nitrogen kinetics was possible only once the process of denitrification was included.

Regarding the factors that limit algal growth in Roodeplaat Dam; in the model algal growth rate is calculated assuming that either phosphate, nitrogen or light is limiting. By comparing the growth rates as calculated by the model for phosphate, nitrogen and light, the limiting factor for a given day can be identified. Thus, with the aid of the model it was possible to determine that, during the study period, the concentration of dissolved phosphate was so high that it never was a limiting factor - growth was limited by nitrogen during part of the summer period, and by light for the rest of the annual cycle. The validity of this approach is supported in that simulated algal growth corresponded closely with the observed. Such analysis of growth limiting factors provides a tool for researchers to determine growth limiting factors (including light limitation) on a daily basis.

Regarding algal succession, one of the most useful features of the MINLAKE model is that it can simulate up to three algal classes simultaneously, thus it was possible to identify the factors that govern algal succession in Roodeplaat Dam during the study period, i.e. light and temperature. This finding is supported by the literature that states that, in the presence of high nutrient concentrations, often light and temperature become the factors that govern algal succession.

Successful simulation of algal succession requires a simulation period of at least one year, but preferably 18 months to two years.

Regarding the effect of inorganic suspended sediment (TSS), during calibration of algal growth kinetics, it was found that TSS concentration affects simulation of algal concentration significantly. This is to be expected, as algal growth in Roodeplaat Dam is light limited for significant periods. Calibration of TSS concentration was hampered severely because TSS concentration was not measured in the reservoir, nor in any of the three inflowing rivers, necessitating elaborate synthesizing procedures for calculating TSS data. Furthermore, in the original MINLAKE model, only one sediment particle diameter was specified in simulation of TSS concentration. However, under South African climatic conditions, sediment particles of different diameter are found under low and storm flow conditions. Realistic simulation of TSS concentration in Roodeplaat Dam was possible only if at least two sediment particle diameters were specified, one for low flow, and one for storm flow conditions.

Regarding the bottom sediments, calibration of nutrient kinetics, especially nitrogen, was not possible unless it is assumed that the bottom sediments are a major source of ammonium, and to a lesser extent, phosphate. Calibration of nutrient kinetics was severely hampered by the paucity of observed data in the hypolimnion.

12.2 RECOMMENDATIONS

Due to climatic differences between South Africa and Minnesota, the original MINLAKE model could not simulate the water quality behaviour of a typical South African Dam. As the many South African dams turn anearobic during part of the hydrological cycle, great care should be taken when selecting a model to simulate the behaviour of a South African dam to ensure the model takes cognisance of varying process rates under aerobic and anaerobic conditions. The modified MINLAKE model has been demonstrated to be effective in both the presence and absence of aerobic/anaerobic conditions, that is, it is effective over a wide range of climatic conditions, from cold temperate to warm temperate/subtropical.

At present the modified MINLAKE model is the only 1D model in South Africa that can simulate more than one algal class, and hence simulate algal succession. For these reasons, the modified MINLAKE model is recommended as a tool for simulating the eutrophic behaviour of dams in South Africa.

Apart from simulating the trophic behaviour of a dam, the model can be usefully applied for the following purposes also:

- Optimise monitoring programmes by determining the relative importance of the variables to be monitored, as well as the optimum frequency of monitoring.

- Waste load allocation studies and setting of water quality standards, because the response of each dam to a particular load will be unique, depending on factors such as climate and dam morphology.

- Determining the future water quality in a dam, and the effect this may have on the process design of water treatment facilities that use water from the dam as a raw water source.

- As an aid in siting and design of proposed dams.

- Evaluation of the effect of various treatment options to minimize eutrophication.

To enhance user confidence in model predictions, the modified MINLAKE model should be validated - world-wide, very few validation studies have been done, due to lack of time and data. However, Roodeplaat Dam has a data base that is adequate for validation of the model, and thus such a study is strongly recommended. If the model can be validated, it will greatly improve user confidence in model predictions, and encourage wider use of the model.

The original and modified MINLAKE models have been designed for simulation of deep, eutrophied dams. However, there are several shallow urban impoundments in South Africa (eg Zeekoeivlei in the Cape Peninsula) that will benefit greatly from eutrophication modelling. Therefore application of the modified MINLAKE to such an impoundment to assess the applicability of the model to shallow, unstratified impoundments is recommended.

Further collaboration with the developers of the original MINLAKE model is recommended, as they have done studies using the model to simulate the effects of artificial lake destratification, as well as simulating the behaviour of oxidation ponds. At present, no model is available in South Africa that can simulate the water quality response of a dam to artificial destratification. In view of the proposed destratification of Inanda Dam, such a model will be invaluable. Regarding simulation of the behaviour of oxidation ponds, oxidation ponds are used widely in South Africa and simulation of the behaviour of these ponds may be an invaluable aid in optimising situng, design and operation of such ponds. Information on using the model to simulate oxidation ponds may be of assistance also in applying the model to shallow urban impoundments.

CHAPTER 13

REFERENCES

Ahlgren G (1980). Effects on algal growth by multiple nutrient limitation. *Arch Hydrobiol.* **89**: 43-53.

Ahlgren I, and Abegaz Z (1993). Interactions of light, nutrients and stratification regimes in controlling phytoplankton production in eutrophic lakes. *Verh. Internat. Verein. Limnol.* **25**: 506 - 511.

Akiyama J, and Stefan H G (1984). Plunging flow into a reservoir: Theory. *ASCE Journal of Hydraulic Engineering* **110** No HY4: 484 - 499.

Allanson B R, Hart R C, O'Keefe J H, and Robarts R D (1990). *Inland Waters of Southern Africa: An Ecological Perspective.* Kluwer Academic Publishers, Dordrecht.

Ashton P J (1979). Nitrogen fixation in a nitrogen-limited impoundment. *Journal of the Water Pollution Control Federation*. **51** No 3: 570 - 579.

Ashton P J (1981). Nitrogen fixation and the nitrogen budget of a eutrophic impoundment. *Water Research.* **15:** 823 - 823.

Ashton P J (1985). Seasonality in Southern Hemisphere freshwater phytoplankton assemblages. *Hydrobiologia* **125**: 179 -190.

Ashton P J (1992). Personal communication, September 1992. Watertek, CSIR, Pretoria.

Ashton P J (1994). Personal communication, August 1994. Watertek, CSIR, Pretoria.

Barica J, Kling H, and Gibson J (1980). Experimental manipulation of algal bloom composition by nitrogen adition. *Canadian Journal of Fisheries and Aquatic Science* **37**: 1175 - 1183.

Barnes R S K, and Mann K H (1980). *Fundamentals of aquatic ecosystems*. Blackwell Scientific Publications, Oxford, England.

Barnes R S K, and Mann K H (1991). *Fundamentals of aquatic ecology*. Blackwell Scientific Publications, Oxford, England.

Barrow G M (1973). *Physical Chemistry.* McGraw-Hill, Tokyo.

Barta B (1994). Regional integration of water demands for adequate development of resources in South Africa. *Proc. IWRA Congress*, Cairo.

Bath A J (1989). *Phosphorus transport in the Berg River, Western Cape.* Technical Report Number TR143, Department of Water Affairs and Forestry, Pretoria.

Baudo R, Giesy J P, and Muntau H (1990). *Sediments: Chemistry and Toxicity of In-Place Pollutants.* Lewis Publishers, Ann Arbor, Boston.

Bedford K W, Sylees R M, and Libicki C (1983). Dynamic advective water quality model for rivers. *ASCE Journal of the Environmental Engineering Division* **109**: 535 - 554.

Bedford K W and Babajimopoulos C (1977). Vertical diffusivities in areally averaged models. *ASCE Journal of the Environmental Engineering Division* **103**: 113-125.

Bienfang P K (1975). Steady state analysis of nitrate-ammonium assimilation by phytoplankton. *Limnology and Oceanography*, **20** N0 3: 402 - 411.

Bierman V J (Jr), Verhoff F H, Poulson T L, and Tenney M W (1977). In *Modeling the eutrophication process.* Edited by: E J Middlebrooks, D H Falkenborg and T E Malone. Science Publishers Inc, Ann Arbor, Michigan.

Bingham R D, Lin C-H, and Hoag R S (1984). Nitrogen cycling and and algal growth modelling. *Journal WPCF* **56** No 10: 1118 - 1122.

Blom G, Van Duin E H S, and Lijkema L (1994). Sediment resuspension and light conditions in some shallow Dutch lakes. *Water Quality International '94 - IAWQ 17th Biennial International Conference.* 24-29 July 1994, Budapest, Hungary.

Boers P C M (1991). The influence of pH on phosphate release from lake sediments. *Water Research* **25** No 3: 309 - 311.

Bratby J (1977). Aeration in the activated sludge process. *Course CE 541: Wastewater treatment.* Dept of Civil Engineering, University of Cape Town.

Breen C M (1983). *Limnology of Lake Midmar.* South African National Scientific Programmes Report No 78. CSIR, Pretoria.

Brutsaert W (1982). *Evaporation into the atmosphere - Theory, history, and applications.* D Reidel Publishing Company, Dordrecht, Holland.

Brutsaert W, and Gour-Tsyh Y (1970). A power wind law for turbulent transfer computations. *Water Resources Research,* **6** No 5: 1387 - 1391.

Bureau for Information (1990). *This is South Africa.* Bureau for Information, Pretoria, RSA.

Bureau for Information (1991). *South African Profile.* Bureau for Information, Pretoria, RSA.

Butty M, and Walmsley R D (1979). *The limnological characteristics of 21 South African impoundments, Part 5.* CSIR/WRC Report No W 5/100/4/1/1, Pretoria.

Canale R P (1976). *Modeling biochemical processes in aquatic ecosystems*. Ann Arbor Science Publishers Inc. Ann Arbor, Michigan.

Casey T G, Ekama G A, Wentzel M C, and MArais GvR (1992). A hypothesis for the cause of low F/M filament bulking in nutrient removal activated sludge systems. *Water Research* **26**: 867 - 869.

Chiaudani G, and Vighi M (1974). The N:P ratio and tests with *Selenastrum* to predict eutrophication in lakes. *Water Research* **8**: 1063 - 1069.

Chiaudani G, and Vighi M (1982). Multistep approach to identification of limiting nutrients in Northern Adriatic eutrophied coastal waters. *Water Research* **16**: 1161 - 1166.

Chen C W, and Orlob G T (1975). Ecologic simulation of aquatic environments. *Systems Analysis and Simulation in Ecology* **3**, edited by B C Patten, New York Academic Press - as reviewed by G T Orlob (1983)

Chen C W, Lorenzen M, and Smith D J (1975). *A comprehensive water quality-ecologic model for Lake Ontario.* Report to Great Lakes Environmental Research Laboratory, National Oceanic and Atmospheric Administration. Tetra Tec Inc., as reviewed by G T Orlob (1983).

Chutter F M (1989). *Evaluation of the impact of the 1 mg l^{-1} phosphate-P standard on the water quality and trophic state of Hartbeespoort Dam.* Water Research Commission Report No 181/1/89, Pretoria.

Chutter F M, and Rossouw J N (1991). *The management of phosphate concentrations and algae in Hartbeespoort Dam*. Water Research Commission Report No 289/1/91, Pretoria.

CIRIA (1970). *The modern design of wind-sensitive structures.* Proceedings of the Seminar held on 18 June 1970 at The Institution of Civil Engineers, Great George Street, London. Construction Industry Research and Information Association.

Clarke K, Jarvis A C, Ashton P J, and Zohary T (1987). The use of TROFIC as an aid for the management of eutrophic lakes. *J. Limnol. Soc. sth. Afr.* **(13)2**: 106 - 110.

Cloot A, Schoombie S W, Pieterse A J H, and Roos J C (1992). A note on a light-temperature dependant model for algal blooms in the Vaal River. *Water SA* **18** No 4: 299-302.

Cochrane K L, Ashton P J, Jarvis A C, Twinch A J, and Zohary T (1987).
An ecosystem model of phosphorus cycling in a warm monomictic, hypertrophic impoundment. *Ecological Modelling* **37:** 207 - 233.

Cohen Y (1983). Mass transfer across a sheared, wavy air-water interface. *Int. J. Heat Mass Transfer.* **26**(9): 1289-1297.

Cole T M (1991). *User guide to CE-QUAL-W2* Instruction report, US Army Engineer, Waterways Experimental Station, Vicksburg, Mississippi (First Draft).

Conway H L (1974). *The uptake and assimilation of inorganic nitrogen by Skeletonema Costatum*. Dissertation, University of Seattle, as quoted by Jørgensen (1980).

CRC (1978). *Handbook of Chemistry and Physics*. 58th Edition, CRC Press Inc, West Palm Beach, Florida, USA.

CSIR (1985). *National Register for Weather, Climate and Atmosphere Numeric Data Sources.* Report No CSTI 88. Compiled by Brunt A G, Chalmers L, and Hetem J E. FRD/CSIR, Pretoria.

CWR (1991). *DYRESM 1-D Manual*. Coastal and Engineering Laboratory, Centre for Water Research, University of Western Australia.

Dake J M K, and Harleman D R F (1969). Thermal stratification in lakes: Analytical and laboratory studies. *Water Resources Research.* **5** No 2: 484-495.

Dake J M K (1972). Evaporative cooling of a body of water. *Water Resources Research.* **8** No 4: 1087-1091.

Danckwerts P V (1951). Significance of liquid-film coefficients in gas absorption. *Industrial and Engineering Chemistry.* **43** No 6: 1460 - 1467.

Davison I R (1991). Environmental effects on algal photosynthesis: temperature. *Journal of Phycology* **27**: 2 - 8.

De Groot C-J (1991). The influence of FeS in the inorganic phosphate system in sediments. *Verh. Internat. Verein. Limnol.* **24:** 3029 - 3035.

De Wet J S (1986). *Fitoplanktonproduktiwiteit en die faktore wat dit in Roodeplaatdam beïnvloed.* PhD-thesis, Department of Botany, University of the Orange Free State, South Africa.

Di Toro D M, O'Connor D J, Thomann R V, and Mancini J L (1975). Phytoplankton-zooplankton-nutrient interaction model for western Lake Erie. *Systems Analysis and Simulation in Ecology* **3**, edited by B C Patten, New York Academic Press, as reviewed by G T Orlob (1983).

Dold P L, Ekema G A, and Marais GvR (1980). A general model for the activated sludge process. *Prog. Wat. Tech.* **12**: 47 - 77.

Dold P L, Wentzel M C, Billing A E, Ekama G A, and Marais GvR (1991). *ACTIVATED SLUDGE SYSTEM SIMULATION PROGRAMS Nitrification and nitrification/denitrification systems, Version 1.* Water Research Commission Report TT 52/91.

Droop M R (1973). Some thoughts on nutrient limitation in algae. *J Phycol.* **9**: 264-272.

Droop M R (1983). 25 Years of algal growth kinetics - a personal view. *Botanica Marina* **XXVI**: 99 - 112.

Dudel G, and Kohl J-G (1991). Contribution of nitrogen fixation and denitrification to the N-budget of a shallow lake. *Verh. Internat. Verein. Limnol.* **24**: 884 - 888.

Dugdale R C, and MacIsaac J (1971). A computation model for the uptake of nitrate in the Peru Upwelling Region. *Investigasion Pesquerg*, Barcelona, Vol 3, as quoted by Jørgensen (1980).

DWAF (1981). *Water year + 10 and then?* Technical Report No 114, Department of Water Affairs and Forestry, Pretoria.

DWAF (HRI) (1984) *Roodeplaat Dam limnological data 1980 - 1984.* Compiled by Limnological Section, Hydrological Research Institute,[1] Department of Water Affairs and Forestry, Pretoria.

DWAF (1986). *Management of the Water Resources of the Republic of South Africa.* Department of Water Affairs, Pretoria.

[1] The Hydrological Research Institute (HRI) is presently known as the Institute for Water Quality Studies (IWQS).

DWAF (HRI) (1988). *Analytical Methods Manual.* Report No TR 136, Hydrological Research Institute, Department of Water Affairs and Forestry, Pretoria.

DWAF (HRI) - personal communication. Gavin Quibell, April 1992. Hydroligical Research Institute, Department of Water Affairs and Forestry, Pretoria.

DWAF (1990). *List of Hydrological Gauging Stations - July 1990.* Hydrological Information Publication No 15. Department of Water Affairs and Forestry, Directorate of Hydrology), Pretoria.

DWAF (1991). *Water Quality Data Inventory.* Technical Report No TR 146. Compiled by Swart S J, Van Veelen M and Nell U. Hydrological Research Institute, Department of Water Affairs and Forestry, Pretoria.

Eckenfelder W W, Malina J F, Gloyna E F , and Ford D L (1967). Physical, chemical and biological processes. *Report prepared for Poland Project-26, World Health Organization.* Austin, Texas.

Elliot W P (1958). The growth of the atmospheric internal boundary layer. *Transactions of the American Geophysical Union* **39**: 1048-1054.

Ellison T H, and Turner J S (1959). Turbulent entrainment in stratified flows. *Journal of fluid mechanics* **6**: 423 - 448.

Emerson S (1975). Gas exchange rates in small Canadian lakes. *Limnology and oceanography* **20** No 5: 754-761.

EPA (1985). *Rates, constants and kinetic formulations in surface water quality modelling.* USA EPA Document No 600/3-85/040. Environmental Research Laboratory, Athens, Georgia.

EPA (1987). *The enhanced stream water quality models QUAL2E and QUAL2E-UNCAS: Documentation and user model.* USA EPA Document No 600/3-87/007. Environmental Research Laboratory, Athens, Georgia.

Faafeng B A, and Hessen D O (1993). Nitrogen and phosphorus concentrations and N:P ratios in Norwegian lakes: Perspectives on nutrient limitation. *Verh. Internat. Verein. Limnol.* **25**: 465-469.

Farrel G J, and Stefan H G (1988). Mathematical modeling of plunging river flows. *ASCE Journal of Hydraulic Research* **26** No HY5: 525-537.

Fischer H B, List E J, Koh R C Y, Imberger J, and Brooks N H (1979). *Mixing in inland and coastal waters*. Academic Press, New York.

Flett R J, Schindler D W, Hamilton R D, and Campbell N E R (1980). *Canadian Journal of Fisheries and Aquatic Science* **37**: 494; as reviewed by Smith V H (1983).

Ford D E, and Stefan H (1980). Thermal predictions using integral energy model. *Proc. ASCE, J. Hyd.Div.* **106** No HY1: 39-55.

Freedman B (1989) *Environmental ecology: the impacts of pollution and other stress-system structure and function.* Academic Press, San Diego, California, USA.

Freney J R, and Galbally I E (1982). *Cycling of carbon nitrogen sulphur and phosphorus in terrestrial and aquatic ecosystems*. Australian Academy of Science, Springer Verlag.

Friedman G M, and Sanders J E (1978). *Principles of Sedimentology*. John Wiley and Sons, New York.

Galvez J A, Niell F X, and Lucena J (1993). C:N:P ratio of settling eston in a eutrophic reservoir. *Verh. Internat. Verein. Limnol.* **24:** 1390 - 1395.

Gardner R H, O'Neill R V, Mankin J B, and Carney J H (1981). A comparison of sensitivity analysis and error analysis based on a stream ecosystem model. *Ecological Modelling* **12**: 173-190.

Gargas E (1976). A three-box eutrophication model of a mesotrophic Danish Lake. Water Quality Institute, Hørsholm, Denmark, as quoted by Orlob (1983).

Geiger R (1965). *The climate near the ground*. Harvard University Press, Cambridge, Massachusetts.

Gibbs R J, Mathews M D, and Link D A (1971). The relationship between sphere size and settling velocity. *Journal of Sedimentary Petrology*. **41** No 1, as quoted by Riley (1988).

Goldman C R, and Horn A J (1983). *Limnology.* McGraw-Hill Book Company, New York.

Görgens A H M, Bath AJ, Venter A, De Smidt K, and Marais GvR (1993). *Applicability of hydrodynamic reservoir models for water quality management of stratified water bodies in South Africa*, Water Research Commission Report No 304/1/93.

Grobbelaar J U, and Toerien D F (1985). Carbon flow in a small man-made impoundment. *Hydrobiologia* **121:** 237 - 247.

Grobler D C (1985). Phosphorus budget models for simulating the fate of phosphorus in South African reservoirs. *Water SA* **11** No 4: 219.

Grobler D C (1986). Assessment of the impact of eutrophication control measures on South African impoundments. *Ecological modelling* **31**: 237 - 247.

Grobler D C, Toerien D F, and Rossouw J N (1987). A review of sediment/water quality interaction with particular reference to the Vaal River system . *Water SA* **13**: 15 - 22.

Grobler D C, and Davies E (1981). Sediments as a source of phosphate: A study of 38 impoundments. *Water SA* **7** No 1: 54 - 60.

Grobler D C, and Silberbauer M J (1984) *Impact of eutrophication control measures on South African impoundments.* Water Research Commission Report No 130/1/84, Pretoria.

Hamilton D P, and Schladow S G (1994). Modelling the sources of oxygen in an Australian reservoir. *Verh. Internat. Verein.Limnol.* **25**: 1282 - 1285.

Hanson M J, Riley M J, and Stefan H G (1987). An introduction to mathematical modeling of lake processes for management decisions. *Project Report No 249, Legislative Commission on Minnesota Resources,* St Anthony Falls Hydraulic Laboratory, University of Minnesota.

Harbeck G E and Meyers J S (1970). Present day evaporation techniques. *ASCE Journal of the Hydraulics Division* **96** Hy 7: 1381-1391.

Harleman D R F (1982). Hydrothermal analysis of lakes and reservoirs. *ASCE Journal of the Hydraulics Division.* **108** No HY3: 302-325.

Harris G P (1984). Phytoplankton productivity and growth measurements; past, present and future. *Journal of Plankton Research.* **6** No 2: 219-237.

Hart R C, and Allanson B R (Ed) (1984). *Limnological criteria for management of water quality in the southern hemisphere.* South African National Scientific Programmes Report No 93.

Hattingh W H J (1978). *Waterkwaliteit in die Republiek van Suid-Afrika.* Report B-N2/3/3/33. Hydrological Research Institute, Pretoria, RSA.

Hebbert B, Imberger J, Loh I, and Patterson J (1979). Collie River underflow into the Wellington Reservoir. *ASCE Journal of the Hydraulics Division* **105 No** HY5: 533 - 545.

Henderson-Sellers B (1984). *Engineering Limnology.* Pitman Publishing Limited, London.

Henze M, Grady C P L (Jr), Gujer W, Marais GvR and Matsuo T (1987). *Activated Sludge Model No 1* IAWPRC Scientific and Technical Report No 1, IAWPRC, London.

House W A (1990). The prediction of phosphate coprecipitation with calcite in fresh waters. *Water Research* **24** No 8: 1017 - 1023.

Humphreys W J (1940) *Physics of the air.* McGraw-Hill Book Company Inc, New York.

Hutchinson G E (1944). Limnological studies in Connecticut. *Ecology* **25** No 1: 3 - 26.

Hutchinson G E (1957). *A treatise on Limnology.* John Wiley and Sons, New York.

Imberger J (1987). *Hydrodynamics of lakes*. Centre for Water Research, The University of Western Australia.

Imberger J, and Hamblin P F (1982). Dynamics of lakes, reservoirs, and cooling ponds. *Ann Rev Fluid Mech*, **14**: 153 - 187.

Imberger J, and Patterson J C (1981). A dynamic reservoir simulation model - DYRESM: 5. *Transport models for inland coastal waters*. Academic Press Inc.

Imberger J, Patterson J, Hebbert B, and Loh I (1978). Dynamics of reservoir of medium size. *ASCE Journal of the Hydraulics Division* **104** No HY5: 725 - 743.

Imboden D M (1978). Modelling of vertical temperature distribution and its implication on biological processes in lakes. In: *State-of-the-art in ecological modelling*. Editor: S E Jørgensen 1980. Pergamon Press.

Jacobsen O S, and Jørgensen S E (1975). A submodel for nitrogen release from the sediments. *Ecological Modelling* **1**: 147 - 151.

Jain S C (1980). Plunging phenomena in reservoirs. *Proceedings of the Symposium on Surface Water Impoundments* Minneapolis, Minnesota, published by ASCE 1981; as quoted by Akiyama and Stefan 1984.

James A (1993). *An introduction to water quality modelling*. John Wiley and Sons, Chicester.

Jassby A, and Powell T (1975). Vertical patterns of eddy diffusion during stratification in Castle Lake, California. *Limnology and Oceanography* **20** No 4: 530 - 543.

Jeffries M, and Mills D (1990). *Freshwater Ecology - Principles and Applications.* Belhaven Press, London and New York.

Jokela J B and Patterson J C (1985). *Quasi-two-dimensional modelling of reservoir inflow*. Twenty-first IAHR Congress, Melbourne, Australia, 19-23 August 1985.

Jones C A, and Welch E B (1990). Internal phosphorus loading related to mixing and dilution in a dendritic, shallow prairie lake. *Research Journal WPCF* **62** No 7: 847 - 852.

Jones R A, and Lee G F (1984). Application of OECD eutrophication modelling approach to South African dams (reservoirs). *Water SA* **10** No 9: 109.

Jørgensen S E (1976). A eutrophication model for a lake. *Ecological modelling* **2,** 147-165.

Jørgensen S E (Ed) (1978). *State-of-the-art in ecological modelling*. Proceedings of the conference on Ecological modelling, Copenhagen, Denmark, 28 August - 2 September 1978. Pergamon Press, Oxford.

Jørgensen S E (1980). *Lake management - (Water development, supply and management; vol 14)*. Pergamon Press Ltd, Oxford.

Jørgensen S E, Kamp-Nielsen L, and Mejer H F (1982). Comparison of a simple and and a complex sediment phosphorus model. *Ecological modelling* **16**: 99 - 124.

Kamp-Nielsen L (1975). A kinetic approach to the aerobic sediment-water exchange of phosphorus in Lake Esrom. *Ecological Modelling* **1**: 153 - 160.

Kamp-Nielsen L (1980). The influence of changed phosphorus loading to hypertrophic Lake Glumsø. *Proceedings SIL Workshop on Hypertrophic Systems*. Växsjö, Sweden, as quoted by Jørgensen *et al* (1982).

Kamp-Nielsen L (1981). Sediment water exchange models. *Application of Ecological Models in Environmental Management*. Ed: S E Jørgensen, as quoted by Jørgensen *et al* (1982).

Kessel J F (1977). Factors affecting the denitrification rate in two water-sediment systems. *Water Research* **11:** 259 - 267.

Kirk J T O (1983). *Light and photosynthesis in aquatic ecosystems*. Cambridge University Press, Cambridge.

Klapper H (1991). *Control of eutrophication in inland waters*. Ellis Horwood, New York.

Kraus E B, and Turner J S (1967). A one-dimensional model of the seasonal thermocline - the general theory and its consequences. *Tellus* **XIX**: 98 - 105.

Krüger G H J, and Eloff J S (1978). The effect of temperature on specific growth rate and activation energy of *Microcystis* and *Synechococcus* isolates relevant to the onset of natural blooms. *Journal of the Limnological Society of Southern Africa* **4** No 1: 9 - 20.

Kufel L (1991). Nutrient sedimentation at the river inflow to a lake. *Verh. Internat. Verein. Limnol.* **24**: 1772 - 1774.

Kunikane S, Kaneko M, and Maehara R (1981). Steady state analysis of algal cultures grown under simulataneous limitation of nitrogen and phosphorus. *Verh. int. Ver. Limnol.* **2**: 1454-1457

Lathrop R C (1988). Evaluation of whole-lake nitrogen fertilization for controlling blue-green algal blooms in a hypereutrophic lake. *Canadian Journal of Fisheries and Aquatic Science* **45**: 2061 - 2075.

Lean D R S, and Pick F R (1981). Photosynthetic response of lake plankton to nutrient enrichment: A test for nutrient limitation. *Limnology and Oceanography*. **26** No 6: 1001 - 1019.

Le Cren E D, and Lowe-McConnel R H (Editors 1980). *The functioning of freshwater ecosystems (International biological programme; 22)* Cambridge University Press, New York.

Lee G F, and Jones K A (1980). *Determination of nutrient limiting maximum algal biomass in water bodies*. AWWA Quality Control in Reservoirs Committee Report.

Le Gourieres D (1982). *Wind power plants: theory and design.* Pergamon Press.

Lehman J T, Botkin D B, and Likens G E (1975). The assumption and rationales of a computer model of phytoplankton population dynamics. *Limnology and Oceanography.* **20** No 3: 343 - 364.

Lewis W K, and Whitman W G (1924). Principles of gas absorption. *Industrial and Engineering Chemistry* **16**, No 12: 1215 - 1220.

Lindholm R (1987). *A practical approach to sedimentology.* Allen and Unwin, London.

Linden P F (1973). The interaction of a vortex ring with a sharp density interface: A model for turbulent entrainment. *Journal of Fluid Mechanics* **60** Part 3: 467 - 480.

Livingstone D M, and Imboden D M (1993). The non-linear influence of wind speed variability on gas transfer in lakes. *Tellus* **45B:** 275 - 295.

Loewenthal R E, and Marais GvR (1976). *Carbonate chemistry of aquatic systems: Theory and Application.* Ann Arbor Sci Publishers, Michigan.

Louw W J (1965). *'n Ondersoek na die konstantes a en b in die Ångstrom tipe formule.* M Sc thesis, University of the Orange Free State.

Mann K H (1988). Production and use of detritus in various freshwater, estuarine, and coastal marine ecosystems. *Limnology and Oceanography* **33** No 4, part 2: 910 - 930.

Marais GvR (1970). Dynamic behaviour of oxidation ponds. *Proc. 2nd Int Symp on Waste Treatment Lagoons*. Kansas City, Kansas.

Markofsky J, and Harleman D J F (1973). Prediction of water quality in stratified reservoirs. *ASCE Journal of the Hydraulics Division* **99** No HY5: 729 - 745.

Martone C H (1976). *Studies related to the determination of biodegradability and long term BOD.* MSc-thesis, Tufts University, Medford, Massachusetts, as quoted by EPA (1985).

McEwen G F (1929). A mathematical theory of the vertical distribution of temperature and salinity in water under the action of radiation, conduction, evaporation and mixing due to the resultant convection. *Scripps Institute of Oceanography Technical Bulletin.* **2**: 197 - 306, as quoted by Orlob (1983).

Megard R O, Tonkyn D W, and Senft W H (1984). Kinetics of oxygenic photosynthesis in planktonic algae. *Journal of Plankton Research* **6** No 2: 325 - 337.

Mortimer C H (1942). The exchange of dissolved substances between mud and water in lakes. *Journal of Ecology* **30:** 147 - 201.

Murray F W (1967). On the computation of saturation vapor pressure. *Journal of Applied Meteorology* **6**, No 1, as quoted by Riley (1988).

Najarian T O, and Harleman D R F (1975). *A real time model of nitrogen-cycle dynamics in an estuarine system*. MIT Dept of Civil Engineering, R M Parsons Laboratory Report No 204, as quoted by Jørgensen (1980).

Nedwell D B, and Brown C M (1982). *Sediment Microbiology*. Published for the **Society for General Microbiology**, Academic Press, London.

Ninham Shand (1989). *Laing Dam: Application of a hydrodynamic model for planning purposes*. Report No NS 1521/4705. Ninham Shand Consulting Engineers.

NIWR (1985). *The Limnology of Hartbeespoort Dam.* South African National Scientific Programmes Report No 110, FRD/CSIR Pretoria.

Noble R D (1981). Comparison of two surface heat exchange models. *ASCE Journal of the Hydraulics Division* **107:** 361 - 366.

O'Connor D J (1983). Wind effects on gas-liquid transfer coefficients. *ASCE Journal of Environmental Engineering* **109** No 3: 731 - 752.

Odum E P (1971) *Fundamentals of Ecology*. Third Edition, Saunders College Publishing, Philidelphia.

Orlob G T and Selna L G (1970) Temperature variations in deep reservoirs. *ASCE Journal of the Hydraulics Division* No HY 2: 391 - 410.

Orlob G T (1983). *Mathematical Modelling of Water Quality: Streams, Lakes, and Reservoirs*. John Wiley and Sons, New York.

Ozmidov R V (1965). On the turbulent exchange in a stably stratified ocean. *J Atmos. Oceanic Phys*. **1**: 493 - 497, as quoted by Fischer *et al* (1979).

Patterson J C, Hamblin P F, and Imberger J (1984). Classification and dynamic simulation of the vertical density structure of lakes. *Limnology and Oceanography* **29** No 4: 845 - 861.

Penman H L (1948) Natural evaporation from open water, bare soil and grass. *Proceedings of the Royal Society* **A193:** 120 - 145.

Perry R H, and Chilton C H (1973) *Chemical Engineers' Handbook*. Fifth Edition. McGraw-Hill International Book Company.

Pieterse A J H, and Toerien D F (1978). The phosphorus-chlorophyll relationship in Roodeplaat Dam. *Water SA* **4** No 3: 105 - 112.

Pieterse A J H, and Röhrbeck M A (1990). Dominant phytoplankters and environmental variables in Roodeplaat Dam, Pretoria, South Africa. *Water SA* **16** No 4: 211 - 218.

Pitman W V (1995). Towards improved utilisation of South Africa's water resources. *SANCHIAS Conference*, September 1995, Grahamstown.

Pitman W V, Middleton B J, and Midgley D C (1981). *Surface water resources of South Africa*. Vol 3 Part 1. Report no 11/81. Hydrological Research Unit, University of the Witwatersrand, RSA.

Placke J F (1983). *Trophic status evaluation of TVA reservoirs*. Technical Report Series No TVS/ONR/WR-83/7. Regional Water Management Program, Chattanooga, Tennessee, as reviewed by Rossouw, L. (1986a).

Platzman G W (1963). The dynamic prediction of wind tides on Lake Erie. *Meteorology Monographs* **4** (26), as reviewed by G T Orlob (1983).

Pollinger U (1986). Phytoplankton periodicity in a subtropical lake (Lake Kinneret, Israel). *Hydrobiologia* 138: 127 - 138.

Powell T, and Jassby A (1974). The estimation of vertical eddy diffusivities below the thermocline in lakes. *Water Resources Research* **10,** No 2: 191 - 198.

Quibell G (1993). Personal communication, February 1993. Hydrological Research Institute, Department of Water Affairs and Forestry, Pretoria.

Reid P J MR (1981). *Energy aspects of water use efficiency.* Report No TR 111, Department of Environmental Affairs.

Reynolds A J (1974). *Turbulent flows in engineering.* John Wiley and Sons, London.

Reynolds C S (1984). *The ecology of freshwater phytoplankton.* University Press, Cambridge.

Reynolds C S (1986). Experimental manipulations of phytoplankton periodicity in large limnetic enclosures in Blelham Tarn, English Lake District. *Hydrobiologia* **138**: 43 - 64.

Rhee G-Y (1978). Effects of N:P ratios and nitrate limitation on algal growth, cell composition, and nitrate uptake. *Limnology and Oceanography* **23** No 1: 10 - 25.

Rheinheimer G (1971). *Aquatic microbiology*. John Wiley and Sons, London.

Richardson K, Beardall J, and Raven J A (1983). Adaption of unicellular algae to irradiance: an analysis of strategies. *New Phycology* **93:** 157 - 191.

Riley M J (1988). *User's manual for the dynamic water quality simulation program "MINLAKE"*. St Anthony Falls Hydraulic Laboratory, University of Minnesota.

Riley M J, and Stefan H G (1988). MINLAKE: a dynamic lake water quality simulation model. *Ecological modelling* **43:** 155 - 182.

Ritchie J C, McHenry J R, and Schiebe F R (1978). The vertical distribution of suspended sediments in reservoirs. *Journal of the Water Pollution Control Federation*: 734 - 738.

Robarts R D, and Ashton P J (1988). Dissolved organic carbon and microbial activity in a hypertrophic African reservoir. *Arch. Hydrobiol.* **113** No 4: 519 - 539.

Robarts R D, and Zohary T (1984. *Microcystis aeruginosa* and underwater light attenuation in a hypertrophic lake (Hartbeespoort Dam, South Africa). *Journal of Ecology* **72:** 1001 - 1017.

Rodney M W, and Stefan H G (1984). How wind can effect a sedimentation basin. *Journal WPCF* **56** No 11: 1204 - 1208.

Rooseboom A (1992). *Sediment transport in rivers and reservoirs - a Southern African perspective.* Water Research commission Report No 297/1/92, Pretoria.

Rossouw J N (1986). *Application of LAVSOE, an eutrophication model developed for shallow lakes in Denmark, on Bloemhof Dam, South Africa.* MSc Thesis, University of the Orange Free State, Bloemfontein, South Africa.

Rossouw J N (1990) *The development of management orientated models for eutrophication control.* Water Research Commission Report No 174/1/90, Pretoria.

Rossouw J N (1991). New PC program helps to control eutrophication in South Africa. *SA Water Bulletin.* September 1991: 12 - 15.

Rossouw L. (1986a) *A comparison of methods to determine nutrient limitation in impoundments.* Hydrological Research Institute, Department of Water Affairs and Forestry, Pretoria. Technical Report No 124. January 1986.

Rossouw J N, and Grobler D C (1988). *Evaluation of the impact of eutrophication control measures on water quality in Hartbeespoort Dam.* Report to the Department of Water Affairs, Pretoria.

Rossouw J N, and Meyer D H (1992). Development of the reservoir eutrophication model (REM) for South African reservoirs. *Water SA* **18** No,3: 155 - 164.

Ruttner F (1952). *Fundamentals of Limnology*. Third edition, University of Toronto Press, Toronto.

Ryan J R, Harleman R F, and Stolzenbach K D (1974). Surface heat loss from cooling ponds. *Water Resources Research* **10**(5): 930 - 938.

Salas H J, and Martino P (1991). A simplified phosphorus trophic state model forwarm-water tropical lakes. *Water Research* **25** No 3: 341 - 350.

Savage S B, and Brimberg J (1975). Analysis of plunging phenomena in water resources. *IAHR Journal of Hydraulic Research* **13** No 2: 187 - 204; as quoted by Akiyama and Stefan (1984).

Scavia D (1980). An ecological model of Lake Ontario. *Ecological Modelling* **8**: 49 - 78.

Schindler D W (1977). Evolution of phosphorus limitation in lakes. *Science* **195:** 260 - 262.

Schindler D W (1978). Factors regulating phytoplankton production and standing crop in the world's freshwaters. *Limnology and Oceanography* **23** Part 3: 476 - 486.

Schroeder F, Klages D, and Knauth H-D (1991). Contributions of sediments to the nitrogen budget of the Elbe estuary. *Verh. Internat. Verein. Limnol.* **24:** 3063 - 3066.

Scott W E, Seaman N T, Connell A D, Kohlmeyer S I, and Toerien D F (1977). The limnology of some South African impoundments. I. The physico-chemical limnology of Hartbeespoort Dam. *J. Limnol. Soc. sth Afr.* **3**, No 2: 43 - 58.

Seitzinger S P (1988). Denitrification in freshwater and coastal marine ecosystems: Ecological and geochemical significance. *Limnology and Oceanography* **33** Part 2: 702 - 724.

Shapiro J (1990). Current beliefs regarding dominance by blue-greens: The case for importance of CO_2 and pH. *Verh. Internat. Verein. Limnol.* **24**: 38 - 54.

Shaw E M (1994). *Hydrology in practice*. Third edition, Chapman and Hall, London.

Shaw J F H, and Prepas E E (1990). Relationships between phosphorus in shallow sediments and in the trophogenic zone of seven Alberta lakes. *Water Research* **24** No 5: 551 - 556.

Shelef G, Schwarz M, and Schechter M (1972). Prediction of photosynthetic production in biomass in accelerated algal-bacterial wastewater treatment system. *Proceedings of 6th International Synposium on Water Pollution Research.* Pergamon Press, Oxford, as quoted by Orlob (1983).

Simons T J (1973). Development of three dimensional numerical models of the Great Lakes *Canada Centre for Inland Waters Science Series No 12* Burlington, Ontario, Canada, as reviewed by G T Orlob (1983).

Simiu E, and Scanlan R H (1986). *Wind effect on structures*. John Wiley and Sons, New York.

Singh B, and Shah C R (1971). Plunging phenomenon in density currents in reservoirs. *La Houille Blanche* **26** No 1: 59 - 64; as quoted by Akiyama and Stefan (1984).

Sly P G (Ed) (1986). *Sediments and Water Interactions*. Proceedings of the Third International Symposium on Interactions between Sediments and Water, Geneva, Switzerland, August 27-31, 1984.

Smith I R (1975). *Turbulence in lakes and rivers*. Freshwater Biological Association Scientific Publication No 29. Titus Wilson and Son Ltd, Kendal.

Smith V H (1983). Low nitrogen to phosphorus ratios favor dominance by blue-green algae in lake phytoplankton. *Science* **221:** 669 - 671.

Smith V H (1986). Predicting the proportion of blue-green algae in lake phytoplankton. *Canadian Journal of Fisheries and Aquatic Science* **43**: 148 - 153.

Smith V H (1987). *Prediction of nuisance blue-green algal growth in North Carolina waters.* Report No 233, Water Resources Institute. University of North Carolina, as reviewed by Shapiro J (1990).

Spigel R H, and Imberger J I (1980). The classification of mixed-layer dynamics in lakes of small to medium size. *Journal of Physical Oceanography* **10:** 1104 -1121.

Steele J H (1974). *The structure of Marine Ecosystems*. Published by Blackwell Scientific Publications, Oxford, as quoted by Orlob (1983), and Jørgensen (1980).

Stefan H G, Dhamotharan S, and Schiebe F R (1982). Temperature/sediment model for a shallow lake. *ASCE Journal of Environmental Engineering Division.* **108** No EE4: 750 - 765.

Stefan H G, and Ford D E (1975). Temperature dynamics in dimictic lakes. *ASCE Journal of the Hydraulics Division* **101** No HY1: 97 - 114.

Stefan H G, and Fang X (1994). Dissolved oxygen model for regional lake analysis. *Ecological Modelling* **71**: 37 - 68.

Stefan H G, and Hanson M J (1981). Phosphorus loading in five shallow lakes. *ASCE Journal of Environmental Engineering Division* **107** No EE4: 713 - 730.

Steyn D J, and Toerien D F (1976). Eutrophication levels in some South African impoundments III. Roodeplaat Dam. *Water SA* **2** No 1: 1 - 6.

Stockner J G, and Hyatt K D (1984). Lake fertilization: state of the art after 7 years of application. *Can. Tech. Rpt. Fish. Aq. Sci No 1324,* as reviewed by Shapiro J (1990).

Stockner J G, and Shortreed K S (1988). Response of *Anabaena* and *Synechococcus* to manipulation of nitrogen:phosphorus ratios in a lake fertilization experiment. *Limnology and Oceanography* **33** Part 1: 1348 - 1361.

Straškraba M (1973). Limnological models of reservoir ecosystems. *Proceedings of international symposium on Eutrophication and Water Pollution Control*. Castle Reinhardsbrunn, DDR, as reviewed by G T Orlob (1983).

Straškraba M (1976). Development of an analytical phytoplankton model with parameters empirically related to dominant controlling variables. *Umweltbiophysik.* Akademie-Verlag, Berlin, as quoted by Orlob (1983).

Stumm W, and Morgan J J (1970). *Aquatic Chemistry.* Wiley-Interscience, New York.

Sundaram T R, and Rehm R G (1971). Formation and maintenance of thermoclines in temperate lakes. *AIAA Journal* **9** No 7: 1322 - 1330.

Sundaram T R, and Rehm R G (1973). The seasonal thermal structure of deep temperate lakes. *Tellus* **XXV** No 2: 157 - 167.

Suttle C A, Cochlan W P, and Stockner J G (1991). Size-dependant ammonium and phosphate uptake, and N:P supply ratios in an oligotrophic lake. *Canadian Journal of Fisheries and Aquatic Science* **48:** 1226 - 1234.

Suttle C A, and Harrison P J (1988). Rapid ammonium uptake by freshwater phytoplankton. *Journal of Phycology* **24**: 13 - 16.

Sykes R M, Bedford K W, and Smarkel K M (1978). *The turbulent transport and biological structure of eutrophication models Vol 2, Comparative study of the mathematical formulations for primary productivity in stratified lakes.* Dept of Civil Engineering, Ohio State University, Columbus. Coastal Engineering Research Report Series OSU/CE 5/78/6.

Taylor R, Best H J, and Wiechers H N S (1984). The effluent phosphate standard in perspective: Part 1. Impact, control and management of eutrophication. *IMIESA* **9**: 43-56.

Tchobanoglous G, and Schroeder E D (1985). *Water Quality.* Addison-Wesley Publishing Company, Reading, Massachusetts.

Tennessee Valley Authority (1972). *Heat and mass transfer between a water surface and the amosphere.* TN Report 14. TVA Water Resources Research Engineering Laboratory, Norris, as reviewed by G T Orlob (1983).

Thornton J A (1986). Nutrients in African Lake Ecosystems: Do we know all? *J. Limnol. Soc. sth. Afr.* **12** No 1/2: 6 - 21.

Thornton J A, and Walmsley R D (1982). Applicability of phosphorus budget models to southern African man-made lakes. *Hydrobiologia* **89**: 237 - 245.

Tilman D, Kilham S S, and Kilham P (1982). *Annu. Rev. Ecol. Syst.* **13**: 349; as reviewed by Smith V H (1983).

Toerien D F (1977) *A review of eutrophication and guidelines for its control in South Africa.* Special Report WAT 48. Division of Water Technology, CSIR, Pretoria.

Toerien DF, Hyman K L, and Bruwer M J (1975). A preliminary trophic status classification of some South African impoundments. *Water SA* **1**, No 1: 15 - 23.

Toerien D F, Steyn D J, and Visser J H (1976). Eutrophication levels of Some South African Impoundments III. Roodeplaat Dam. *Water SA* **2** No 1: 2 - 6.

Tomaszek J (1991). Oxygen consumption by bottom sediments. *Verh. Internat. Verein. Limnol.* **24**: 3045 - 3049.

Toms I P, Mindenhall M J, and Harman M M I (1975). *Factors affecting the removal of nitrate by sediments from rivers, lagoons and lakes.* Technical Report TR 14, Water Research Centre, Buckinghamshire, England.

Trimbee A M, and Harris G P (1984). Phytoplankton population dynamics of a small reservoir: effect of intermittent mixing on phytoplankton succession and the growth of blue-green algae. *Journal of Plankton Research* **6** No 4: 699 - 713.

Turner J S, and Kraus E B (1967). A one-dimensional model of the seasonal thermocline - A laboratory experiment and its interpretation. *Tellus* XIX: 88 - 97.

Twinch A J, and Breen C M (1980). *Advances in understanding phosphorus cycling in inland waters - their significance for South African limnology.* South African National Scientific Programmes Report No 42. CSIR, Pretoria.

Van der Molen D (1991). A simple, dynamic model for the simulation of the release of phosphorus from sediments in shallow, eutrophic systems. *Water Research* **25** No 6: 737 - 744.

Van Dorn W (1953). Wind stress on an artificial pond. *Journal of Marine Research* **12**: 249 - 276, as quoted by Henderson-Sellers (1984).

Van Haandel A C, Ekema G A, and Marais GvR (1981). THE ACTIVATED SLUDGE PROCESS - 3 Single sludge denitrification. *Water Research* **15**: 1135 - 1152.

Van Kessel J F (1978). Gas production in aquatic sediments in the presence and absence of nitrate. *Water Research* **12:** 291 - 297.

Vincent W F, Downes M T, and Vincent C L (1981). Nitrous oxide cycling in Lake Vanda, Antarctica. *Nature* **292**: 618 - 620.

Viner A B (1985). Thermal stability and phytoplankton distribution. *Hydrobiologia* **125**: 47 - 69.

Walmsley R D and Toerien D F (1978). The chemical composition of the waters flowing into Roodeplaat Dam. *Water SA* **4** No 3: 192 - 202.

Walmsley R D and Butty M (1980). *Guidelines for the control of eutrophication in South Africa*. Report No UDC 574-524 (680). Water Research Commission and National Institute of Water Research, CSIR, Pretoria

Walmsley R D and Butty M (1980a). *Limnology of Some Selected South African Impoundments.* Report No UDC 556.55(680). Water Research Commission and National Institute of Water Research, CSIR, Pretoria

Walmsley R D, Butty M, Van der Piepen H, and Grobler D (1980). Light penetration and the interrelationships between optical parameters in a turbid subtropical impoundment. *Hydrobiologia* **70**: 145 - 157.

Walmsley R D, and Thornton J A (1984). Evaluation of OECD-type phosphorus eutrophication models predicting the trophic status of southern African man-made lakes. *South African Journal of Science* **80**: 257 - 259.

Wang W (1979). Fractioning of sediment oxygen demand. *Water Research* **14**: 603 - 612.

Weisman R N (1975). Comparison of warm water evaporation equations. *ASCE Journal of the Hydraulics Division* **101** No HY 10: 1303 - 1313

Weiss C M (1969). Relation of phosphates to eutrophication. *Journal of American Water Works Association* **61** No 8: 387 - 391.

Welander P (1968). Theoretical forms for the vertical exchange coefficients in a stratified fluid with applications to lakes and seas. *Acta R. Soc. Litt. Gothob. Geophys.* **1**: 1 - 26; as reviewed by Jassby and Powell (1975).

Wiltshire K H (1991). Experimental procedures for the fractioning of phosphorus in sediments with emphasis an aerobic techniques. *Verh. Internat. Verein. Limnol.* **24**: 3073 - 3078.

Wu J (1969). Wind stress and surface roughness at air-sea interface. *Journal of Geophysical Research* **74**: 444 - 445; as quoted by Henderson-Sellers (1984).

Wunderlich W O, and Elder R A (1973). Mechanics of flow through man-made lakes. *Man-made lakes: Their problems and environmental effects*. W C Ackermann, G F White, and E B Worthington, eds., American Geophysical Union, Washington, DC; as quoted by Akiyama and Stefan (1984).

Zohary T, and Breen C M (1989). Environmental factors favouring the formation of *Microcystis aeruginosa* hyperscums in a hypertrophic lake. *Hydrobiologia* **178**: 179 - 192.

Zohary T, and Madeira A M P (1990). Structural, physical and chemical characteristics of *Microcystis aeruginosa* hyperscums from a hypertrophic lake. *Freshwater Lakes* **23**: 339 - 352.

APPENDIX A1

CONSTRUCTION OF A DATA BASE FOR ROODEPLAAT DAM

A1.1 INTRODUCTION

In this Appendix, the physical, chemical, and limnological characteristics of the dam chosen for the study (Roodeplaat Dam) are discussed, as well as the data requirements of the MINLAKE model, and construction of the required data base.

A1.2 PHYSICAL, CHEMICAL AND LIMNOLOGICAL CHARACTERISTICS OF ROODEPLAAT DAM

The dam selected for evaluation of the original MINLAKE model is Roodeplaat Dam, north of Pretoria. The reasons for choosing Roodeplaat Dam were as follows:

- When the data requirements of the MINLAKE model were compared to the data that were measured at Roodeplaat Dam, it was found that the measurements at Roodeplaat Dam match most of the MINLAKE data requirements. Monthly depth profiles of temperature and dissolved oxygen, as well as surface measurements of several other water quality parameters in the dam, were available. Flow rate was measured on a daily basis in the inflowing rivers, as well as a few water quality parameters, though the latter were mostly measured on a weekly or two-weekly basis. Meteorological data were measured on a daily basis for extended periods.

- Roodeplaat Dam receives both secondary treated domestic waste water effluent, and run-off from agricultural land. It is a popular recreational site and a source of irrigation water, and consequently there is concern about the water quality in the dam. In 1976 Roodeplaat Dam was ranked as the third most eutrophic dam in a study of 98 South African impoundments, with an algal growth potential (AGP) value of up to 200 mg l^{-1} (Steyn and Toerien 1976).

Accordingly, Roodeplaat Dam was selected as appropriate for the calibration and evaluation of the MINLAKE model.

A1.2.1 Physical characteristics of Roodeplaat Dam.

Roodeplaat Dam is situated 20 km north of Pretoria (23°58'S; 27°43'E). The reservoir lies in a summer rainfall region with an average annual rainfall of about 700 mm. The catchment area covers 668 km^2 of grassland, shrub-covered ridges and bushveld (Walmsley and Toerien 1978). Three rivers, the Pienaars River, Edenvalespruit and Hartbeesspruit, discharge into the reservoir. The Pienaars River flows through Mamelodi Township and then past the Baviaanspoort sewage works which treats effluent from the township. Edenvalespruit receives run-off from agricultural and grassland, while Hartbeesspruit originates in the urban areas of Pretoria, whereafter it flows through the industrial area of Silverton. The river inflow is strongly seasonal with flooding of the system during the rainy season in summer (Butty and Walmsley 1979). Roodeplaat Dam stratifies on an annual basis, with stratification occurring from August to April (Pieterse and Röhrbeck 1990).

The points of inflow for each river, as well as the shape of the dam and the different sampling points, are shown in Figure A1.1 Further characteristics of Roodeplaat Dam are presented in Table A1.1. Area, volume, and maximum and mean depth are indicated at full supply level.

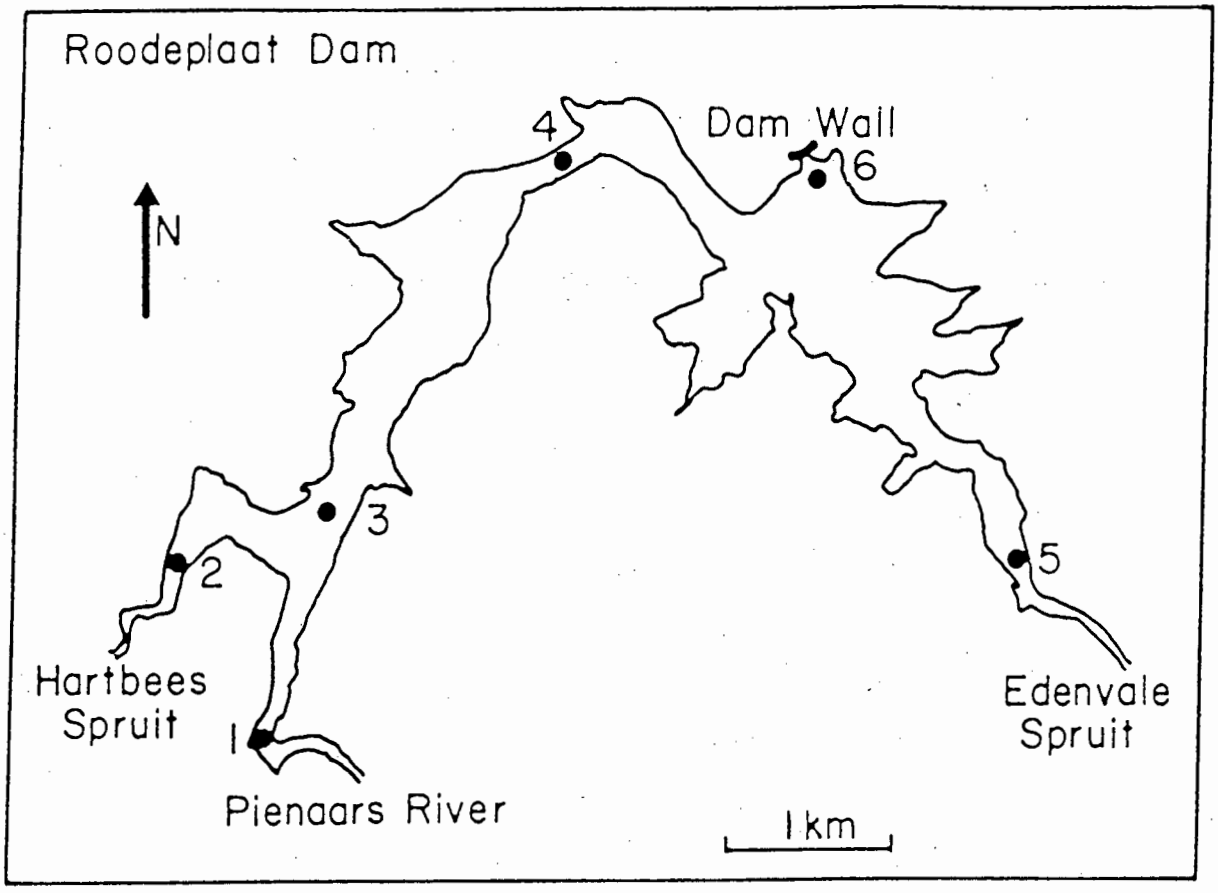

Figure A1.1
Map of Roodeplaat Dam, indicating main sampling stations and point of inflow for each river (After Pieterse and Röhrbeck 1990).

TABLE A1.1 PHYSICAL CHARACTERISTICS OF ROODEPLAAT DAM.

Area	396 ha
Volume	41,9 x 10^6 m^6
Maximum depth	43 m
Mean depth	10,6 m
Height above sea level	1214 m
Annual inflow	59,01 x 10^6 m^3
Annual outflow	55,68 x 10^6 m^3

A1.2.2 Limnological and chemical characteristics of Roodeplaat Dam.

Studies on Roodeplaat Dam indicated seasonal dominance by different algal groups during the study period (October 1980 to October 1982). Between January and May blue-green algae were dominant, but between September and November green algae were dominant, with the concentration of blue-green algae much higher than that of green algae. Of the blue-green algae, *Microcystis aeruginosa* was the most dominant (DWAF-HRI 1984, Pieterse and Röhrbeck 1990).

Regarding the chemical characteristics, during the stratified period (August to April) the hypolimnion becomes anoxic (Walmsley and Butty 1980a, Pieterse and Röhrbeck 1990). The Pienaars River is the major external nutrient source, contributing up to 75% of the annual dissolved nitrogen load, and up to 87% of the annual phosphorus load (Butty and Walmsley 1979). The average, as well as the maximum dissolved phosphate, ammonia, and nitrate concentrations in each river during the study period are indicated in Table A1.2.

Table A1.2. Average and maximum nutrient concentrations for the period October 1980 to October 1982 for each of the rivers flowing into Roodeplaat Dam

Nutrient	Pienaars River	Hartbeesspruit	Edenvalespruit
	Average concentration ($mg\ l^{-1}$)		
PO_4-P	3.69	0.04	0.02
NO_3-N	4.54	5.87	0.14
NH_4-N	1.31	1.43	0.05
	Maximum concentration ($mg\ l^{-1}$)		
PO_4-P	10.0	3.3	0.1
NO_3-N	15.3	15.9	1.71
NH_4-N	9.3	9.5	0.2

A1.3 DATA NEEDED BY THE MINLAKE MODEL

Four types of data are required by both the original and modified MINLAKE models i.e meteorological, inflow/outflow, in-dam profile data, and physical reservoir constants. Furthermore, process coefficients for particular processes must also be provided - these coefficients usually act as calibration parameters.

A1.3.1 Meteorological data

This group contains variables such as solar radiation (measured in Langley per day)[1] and wind speed (mph), which have been identified as the two main hydrodynamic driving forces in MINLAKE. Further meteorological data are:

- Air temperature (°F)
- Dew point temperature (°F)
- Precipitation (inches)
- Wind direction (degrees)
- Percentage sun

The units required are the units used by the National Weather Service in the USA.[2] Meteorological data are needed on a daily basis. If site specific meteorological data are not available, a site specific meteorological data base would need to be generated by interpolation from other data bases.

---

[1] Langley = cal cm^{-2}.

[2] Changing the model to allow data input to be in SI units was considered, as SI units are used generally in South Africa. However, this would be a major task, as changing the units of measurement would necessitate changing the values of the constants in model equations also.

A1.3.2 Inflow/outflow daily time series

Regarding inflow, average **daily** flow rate (cfs) and temperature of inflowing water (°C) are essential variables for the hydrodynamic part of MINLAKE. Provision is made for data on the following water quality variables in the inflowing rivers:

- Dissolved oxygen (mg/l)
- Total dissolved solids (mg/l)
- Suspended inorganic sediment (mg/l)
- Dissolved phosphate (mg/l)
- Nitrate-nitrite (mg/l)
- Ammonium (mg/l)
- Chlorophyll-a (mg/l)

Only those variables that have been identified as affecting the water quality of the reservoir significantly need to be included.

Regarding outflow, the flow rates of water being discharged, and of water flowing over the top of the dam wall, are entered as negative flow rates. Water quality variables are not specified in the outflow.

The original software makes provision for only one inflow/outflow. The model was subsequently modified to make provision for up to 5 inflows/outflows.

A1.3.3 Reservoir data

In order to check the simulated values provided by the model, depth profiles[3] of reservoir water quality variables of importance to the specific reservoir are required. Provision is made in the model for the following:

- Reservoir water temperature (°C)
- Dissolved oxygen (mg/l)
- Dissolved phosphate (mg/l)
- Total phosphorus (mg/l)
- Detritus as BOD (mg/l)
- Suspended inorganic solids (mg/l)
- Nitrate-nitrite nitrogen (mg/l)
- Ammonium nitrogen (mg/l)
- Three classes of chlorophyll-a (mg/l)

A1.3.4 Physical reservoir constants

The following constants must be specified by the user for each reservoir:

- Width of each inflowing river
- Maximum width of the reservoir perpendicular to the inflowing river
- Height of reservoir bottom above sea level
- Height of discharge outlets above sea level
- Width of discharge outlet
- Initial height of the reservoir water level (stage) above sea level
- Downstream slope of each inflowing river
- Manning's friction factor for each of the rivers

---

[3] Depth profiles are measurements taken at discrete intervals from the surface to the bottom of the reservoir.

A1.3.5 Calibration coefficients

In MINLAKE, many of the processes are simplified or even approximated, by the use of calibration coefficients, which must be specified by the user. Establishing values for the calibration coefficients constitutes calibration of the model; this is discussed in Chapters 6 and 7.

A1.3.6 Data format and model structure

A1.3.6.1 Input data:

The input data required are represented in three separate computer files, i.e. a meteorological file containing the meteorological data; an inflow file containing river water quality data, and an input file containing observed profiles of reservoir water quality variables, calibration coefficients, as well as the various reservoir specific constants.

The three data input files are standard ASCII data files, and the data format is in free form, i.e. data files can be constructed without concern for the spacing between data. The only requirement is that columns of data must be separated by at least one blank space. The free form format is particularly suited to using spreadsheet programs, such as Lotus or Quattro, to construct data input files.

The MINLAKE package also contains data file listing programs for each of the three data files. Errors in the data files will cause an error exit when the MINLAKE program is run. Considerable time can be spent in debugging data files, not only because the data files usually are quite large, but also because the data file containing an error often cannot be determined from the error exit code. The debugging of data files is facilitated by the use of the data listing programs provided. These programs list the contents of a data file to the screen, allowing the user to view the data. Errors in the data file will cause the data listing program to stop at the line where the error occurs.

Remark: It is recommended that, whenever an error exit occurs, the first step in tracking the error that caused the exit, should be the listing of the data files with the data listing program. An error exit is usually caused by an error in the data files.

To provide a bench mark example, test data files for each of the three data files, and for the lake specific subroutine are supplied for Lake Riley in Minnesota. This allows the user to gain familiarity with the MINLAKE program before attempting to run the program with own input.

A1.3.6.2 Output data:

Data output from the MINLAKE model is in the form of graphics and statistics, as well as in file format. Graphics, consisting of profiles as well as time-series, and statistics are displayed during operation of the model, and can be printed by request.

A1.3.6.3 Model structure:

The model is divided into two separate, but linked, computer programs. The first program contains the main MINLAKE program, and the second a lake specific subroutine.

Main MINLAKE program: The main program consists of 40 subroutines and two function routines. The subroutines calculate daily changes in states/concentration of various compounds, and the influence of inflows and outflows. The three input data files are accessed from the main program via these subroutines. Graphical and tabular output, as well as all statistical calculations are also done in the main program. (The user manual suggests that there should be no need to make modifications to the main program; the program is constructed in such a way that, should modifications be required, it can be done via the lake specific subroutine).

The lake specific subroutine: The main program makes periodic calls to the lake subroutine which allows the user to change processes, add processes, or add inflows and outflows. Reservoir specific features such as depth-area relationships and the fetch of the lake are dealt with in the lake specific subroutine.

A1.4 DATA RETRIEVAL AND DATABASE DEVELOPMENT FOR ROODEPLAAT DAM

A1.4.1 Retrieval of meteorological and inflow data

A summary of various institutions where meteorological and inflow data were obtained, the format of the obtained data, and the units of measurement, as opposed to the units required by MINLAKE, is given in Table A1.3.

TABLE A1.3 Summary of units and format of obtained data, and institutions where data were obtained.

Variable	Measured Unit	Required Unit	Institution*	Format of obtained data
River flow rate	m^3s^{-1}	cfs	DWAF	Floppy discs
River water temperature	°C	°C	DWAF/HRI	Copy of original handwritten record
PO_4,NO_3, NH_4, TDS	mg l^{-1}	mg l^{-1}	DWAF	Floppy discs
Air temperature	°C	°F	DWAF/HRI	Photostat copy of recorder charts
Dew point (calculated from humidity)	°C	°F	DWAF/HRI	Photostat copy of recorder charts
Precipitation	mm	inches	DWAF/HRI	Photostat copy of handwritten record
Wind speed	km h^{-1}	mph	DWAF/HRI	Mostly photostat copies of undigitised wind run chart
Wind direction	degrees	degrees	DWA/HRI	Mostly photostat copies of undigitised wind direction chart
Sun hours	hours	% sun	DWAF/HRI	Photostat copy of handwritten record
Solar radiation	Watt-hr m^{-2} Joule m^{-2}	Langley (cal cm^{-2})	DWAF/HRI WB	Photostat copy of original records

*Institutions:
DWAF: Department of Water Affairs and Forestry Head Office, Pretoria.
DWAF(HRI): Hydrological Research Institute, Department of Water Affairs and Forestry, Roodeplaat Dam. (Presently known as the Institute for Water Quality Studies - IWQS).
WB: The Weather Bureau, Department of the Environment, Pretoria.

A1.4.2 Processing of meteorological and inflow data

From Table A1.3 it is evident that the data that were needed, were lodged with various state departments, and that the data were not in a readily usable format. Only river flow rate and chemical water quality parameters were available in computerised format. Where photostat copies of original records were obtained, (i.e. river water temperature, sun hours and solar radiation), these had to be computerised. Because of the format of, for instance, solar radiation, this often was a laborious process. Where photostat copies of original recorder charts were obtained (i.e. wind speed and direction, air temperature and humidity), these had to be digitised.

Two meteorological variables required by the model, dew point temperature and percentage sun hours, were not available, and therefore had to be calculated. Daily dew point temperature was calculated from daily relative humidity data, using the Clausius-Clapeyron formulation (Barrow, 1973). Percentage sun is defined as the number of hours of observed sunshine per day, divided by the maximum number of hours of sunshine possible (astronomical day length). Observed sunshine data were obtained from the Department of Water Affairs and Forestry (HRI). Tables of the astronomical day length for Pretoria, as well as a general formula for calculating astronomical day length at any latitude, were obtained from the Observatory in Cape Town.

A1.4.3 Infilling of missing meteorological and inflow data

A summary of the availability of required inflow data, as well as meteorological data, is given in Tables A1.4 - A1.7. Though the required data were available on a daily basis for extensive periods during 1980 to 1984, there were still some periods in between where no data were available. The worst period was April to November 1984. No radiation data were available for this period, as well as no river water quality data for Hartbeesspruit and Edenvalespruit. The study period therefore had to be limited to January 1980 to December 1983. It was decided to use the data for the period

January 1980 to December 1982 for calibration of model, and the rest of the data for a later verification study.

Table A1.4 The availability of meteorological data for Roodeplaat Dam 1980-1983

MONTH	TEMP °C	DEW POINT °C	PRECIP mm	WIND km/h	DIR	%SUN	RAD Various
1980 1	**	**	**	**	**	**	**
2	**	**	**	**	**	**	**
3	**	**	**	**	**	**	**
4	**	**	**	**	**	**	**
5	**	**	**	6	7	**	**
6	**	**	**	**	**	**	**
7	**	**	**	**	**	**	**
8	**	**	**	**	**	**	**
9	**	**	**	**	**	**	**
10	**	**	**	**	**	**	**
11	**	**	**	**	8	**	**
12	**	**	**	**	3	**	**
1981 1	**	**	**	4	18	**	**
2	**	**	**	**	11	**	**
3	**	**	**	**	**	**	**
4	**	**	**	**	**	**	**
5	**	**	**	**	**	**	**
6	**	**	**	**	**	**	12
7	**	**	**	**	**	**	**
8	**	**	**	3	3	5	**
9	**	**	**	**	3	**	**
10	**	**	**	**	**	**	**
11	**	**	**	**	**	**	**
12	**	**	**	**	**	**	**

(continued...)

MONTH	TEMP	DEW POINT	PRECIP	WIND SPEED	DIR	%SUN	RAD
1982 1	**	**	**	**	**	**	**
2	**	**	**	**	**	**	**
3	**	**	**	6	**	3	**
4	**	**	**	9	9	**	**
5	**	**	**	**	4	**	**
6	**	**	**	**	**	**	**
7	**	**	**	**	**	**	**
8	**	**	**	**	**	**	**
9	**	**	**	**	**	**	**
10	**	**	**	4	**	**	**
11	**	**	**	7	6	**	**
12	**	**	**	8	6	**	**
1983 1	**	**	**	**	**	**	**
2	**	**	**	**	**	**	**
3	**	**	**	**	**	**	**
4	**	**	**	**	**	**	**
5	**	**	**	**	**	**	**
6	**	**	**	**	**	**	**
7	**	**	**	**	**	**	**
8	**	**	**	3	3	3	**
9	**	**	**	**	**	13	**
10	**	**	**	**	**	3	**

** : Data is available.
Number : Number of days of missing data (three or more consecutive days).
Blank : The variable was not monitored.

Table A1.5 The availability of inflow water quality data for Pienaars River.

MONTH	FLOW cfs	TEMP °C	PO4 mg/l	BOD	TSS mg/l	TDS mg/l	NO3 mg/l	NH4 mg/l	Chla mg/l
1980									
1	**	31	4			4	4	4	
2	**	29	**			**	**	**	
3	**	31	**			**	**	**	
4	**	30	**			**	**	**	
5	**	31	10			10	10	10	
6	**	30	19			19	19	19	
7	**	12	14			14	14	14	
8	**	**	18			18	18	18	
9	**	**	**			**	**	**	
10	**	**	**			**	**	**	
11	**	**	**			**	**	**	
12	**	**	6			6	6	6	
1981									
1	**	**	**			**	**	**	
2	**	**	**			**	**	**	
3	**	3	8			8	8	8	
4	**	**	**			**	**	**	
5	**	**	**			**	**	**	
6	**	**	**			**	**	**	
7	**	**	**			**	**	**	
8	**	**	**			**	**	**	
9	**	**	18			18	18	18	
10	**	**	**			**	**	**	
11	**	**	29			29	29	29	
12	**	**	9			9	9	9	

MONTH	FLOW	TEMP	PO4	BOD	TSS	TDS	NO3	NH4	Chla
1982									
1	**	**	**			**	**	**	
2	**	**	**			**	**	**	
3	**	**	**			**	**	**	
4	**	**	**			**	**	**	
5	**	**	**			**	**	**	
6	**	**	**			**	**	**	
7	**	**	**			**	**	**	
8	**	4	**			**	**	**	
9	**	**	**			**	**	**	
10	**	**	20			20	20	20	
11	**	**	23			23	23	23	
12	**	**	3			3	3	3	
1983									
1	**	**	16			16	16	16	
2	**	5	9			9	9	9	
3	**	**	**			**	**	**	
4	**	**	4			4	4	4	
5	**	**	**			**	**	**	
6	**	**	**			**	**	**	
7	**	**	**			**	**	**	
8	**	**	**			**	**	**	
9	**	3	3			3	3	3	
10	**	**	**			**	**	**	
11	**	**	**			**	**	**	
12	**	**	**			**	**	**	

** : Data is available
Number : Number of days of missing data (three or more consecutive days)
Blank : The variable was not monitored

Table A1.6. Inflow water quality data for Hartbeesspruit

MONTH	FLOW cfs	TEMP °C	PO4 mg/l	BOD	TSS mg/l	TDS mg/l	NO3 mg/l	NH4 mg/l	Chla mg/l
1980									
1	**	31	4			4	4	4	
2	**	29	**			**	**	**	
3	**	31	**			**	**	**	
4	**	30	**			**	**	**	
5	**	31	5			5	5	5	
6	**	30	19			19	19	19	
7	**	12	14			14	14	14	
8	**	**	18			18	18	18	
9	**	**	**			**	**	**	
10	**	**	5			5	5	5	
11	**	**	**			**	**	**	
12	**	**	5			5	5	5	
1981									
1	**	**	**			**	**	**	
2	**	**	5			5	5	5	
3	**	3	8			8	8	8	
4	**	**	**			**	**	**	
5	**	**	**			**	**	**	
6	**	**	**			**	**	**	
7	**	**	**			**	**	**	
8	**	**	**			**	**	**	
9	**	**	20			20	20	20	
10	**	**	**			**	**	**	
11	**	12	29			29	29	29	
12	**	**	9			9	9	9	

(continued...)

MONTH	FLOW	TEMP	PO4	BOD	TSS	TDS	NO3	NH4	Chla
1982									
1	**	**	**			**	**	**	
2	**	**	**			**	**	**	
3	**	**	**			**	**	**	
4	**	**	4			4	4	4	
5	**	**	3			3	3	3	
6	**	**	**			**	**	**	
7	**	**	**			**	**	**	
8	**	4	**			**	**	**	
9	**	11	10			10	10	10	
10	**	10	29			29	29	29	
11	**	**	23			23	23	23	
12	**	**	3			3	3	3	
1983									
1	**	**	27			27	27	27	
2	**	7	10			10	10	10	
3	**	20	20			20	20	20	
4	**	18	17			17	17	17	
5	**	27	20			20	20	20	
6	**	14	17			17	17	17	
7	**	14	14			14	14	14	
8	**	15	15			15	15	15	
9	**	25	26			26	26	26	
10	**	**	10			10	10	10	
11	**	**	**			**	**	**	
12	**	**				3	3	3	

** : Data is available
Number : Number of days of missing data (three or more consecutive days)
Blank : The variable was not monitored

Table A1.6 The availability of inflow water quality data for Edenvalespruit

MONTH	FLOW	TEMP	PO4	BOD	TSS	TDS	NO3	NH4	Chla
	cfs	°C	mg/l		mg/l	mg/l	mg/l	mg/l	mg/l
1980									
1	**	31	4			4	4	4	
2	**	29	**			**	**	**	
3	**	31	**			**	**	**	
4	**	30	**			**	**	**	
5	**	31	6			6	6	6	
6	**	30	19			19	19	19	
7	**	12	14			14	14	14	
8	**	**	18			18	18	18	
9	**	**	**			**	**	**	
10	**	**	**			**	**	**	
11	**	**	**			**	**	**	
12	**	**	9			9	9	9	
1981									
1	**	**	**			**	**	**	
2	**	**	5			5	5	5	
3	**	3	6			6	6	6	
4	**	**	**			**	**	**	
5	**	**	**			**	**	**	
6	**	**	**			**	**	**	
7	**	**	**			**	**	**	
8	**	**	**			**	**	**	
9	**	**	20			20	20	20	
10	**	**	**			**	**	**	
11	**	6	29			29	29	29	
12	**	9	9			9	9	9	

(continued...)

MONTH	FLOW	TEMP	PO4	BOD	TSS	TDS	NO3	NH4	Chla
1982									
1	**	**	**			**	**	**	
2	**	8	8			8	8	8	
3	**	25	25			25	25	25	
4	**	30	30			30	30	30	
5	**	31	31			31	31	31	
6	**	30	30			30	30	30	
7	**	27	27			27	27	27	
8	**	4	**			**	**	**	
9	**	**	**			**	**	**	
10	**	27	29			29	29	29	
11	**	30	30			30	30	30	
12	**	31	31			31	1	31	
1983									
1	**	24	29			29	29	29	
2	**	28	28			28	28	28	
3	**	31	31			31	31	31	
4	**	30	30			30	30	30	
5	**	31	31			31	31	31	
6	**	30	30			30	30	30	
7	**	31	31			31	31	31	
8	**	31	31			31	31	31	
9	**	30	30			30	30	30	
10	**	31	31			31	31	31	
11	**	8	9			9	9	9	
12	**	**	**			**	**	**	

** : The data is available
Number : The number of days of missing data (three or more consecutive days)
Blank : The variable was not monitored

Even though there were still some data missing from the period 1980 to 1983, infilling of data was possible. Table A1.8 gives a summary of the inflow and meteorological variables that needed infilling, the variables that were used to aid in the infilling, and the relationship that existed between the variables.

Exhaustive efforts were made to find relationships between variables with missing values and other variables with more complete values. Regarding inflow water quality data, often daily flow rate was used for infilling, as the flow records were complete (only three days missing from the entire record). When daily flow rate was used for infilling other data, it was done with the aid of a three-stage time-dependant seasonal technique.

- **First stage**: Infilling was done with a time-dependant seasonal nonlinear regression of grab sample against daily flow, for days with flow above a certain truncation level, but with the infilled values weighed by proximity to a grab sample value at either end of the missing period.

- **Second stage**: Data for days with flows below the truncation level were filled in by linear interpolation.

- **Third stage**: The grab sample values are imbedded in the created series and discontinuities and seasonal transitions are smoothed.

TABLE A1.8 Infilling of meteorological and water quality variables.

Parameter with missing data	Parameter used for infilling	Condition	R^2	Slope	Infilling technique
Water temp (Edenvale)	Average air temp.	-	0.80	0.96	Linear regression
Water temp (Hartbees)	Average air temp.	-	0.80	0.92	Linear regression
Water temp (Pienaars)	Average air temp.	-	0.86	0.96	Linear regression
ln** PO_4 (Pienaars)	ln flow	May-Nov flow<0.22m^3 s^{-1}	0.00	0.006	Interpolation
		May-Nov flow>0.22m^3 s^{-1}	0.40	-0.68	Program*
		Dec-April flow<0.25m^3 s^{-1}	0.04	0.66	Interpolation
		Dec-April flow>0.25m^3 s^{-1}	0.40	-0.79	Program
ln PO_4 (Hartbees)	ln flow	-	0.22	0.29	Program
ln PO_4 (Edenvale)	ln flow	-	0.31	0.39	Program
ln NH_4 (Pienaars)	ln flow	-	0.04	-0.54	Interpolation
ln NH_4 (Hartbees)	ln flow	-	0.01	0.078	Interpolation
ln NH_4 (Edenvale)	ln flow	-	0.05	0.08	Interpolation
ln NO_3 (Pienaars)	ln flow	-	0.15	0.182	Program
ln NO_3 (Hartbees)	ln flow	-	0.15	0.458	Program
ln NO_3 (Edenvale)	ln flow	-	0.15	-0.33	Program
ln TDS (Pienaars)	ln flow	-	0.52	-0.24	Program
ln TDS (Hartbees)	ln flow	-	0.30	-0.23	Program
ln TDS (Edenvale)	ln flow	-	0.72	-0.13	Program
Wind speed	Wind speed (Forum)***	Aug-Dec	0.44	0.22	Linear regression
Wind dir.	Wind dir. (Forum)	-			
%Sun hours	Radiation	-	0.84	0.005	Linear regression
Radiation	% Sun hours	-	0.84	166	Linear regression

* Program refers to the three-stage technique discussed below.

** 'ln' refers to the natural logarithm.

*** Forum refers to the Forum Building in Pretoria, the site where the wind data used for infilling were measured.

A1.4.3.1 Infilling of missing water temperature data:

Water temperature was determined from the 'average' air temperature as follows: The 'average' air temperature for a specific day was defined as the mean of the true average air temperature for that day and the true average air temperature for the preceding day. A satisfactory correlation of 0.96 was found between water temperature and this 'average' air temperature.

A1.4.3.2 Infilling of missing dissolved phosphate data:

Missing dissolved phosphate concentrations were filled in with the aid of river flow rate data. The best regression between phosphate concentration and river flow rate was obtained using the natural logarithm of the two variables. It was found that the regression for Pienaars River differed from the other two rivers. This difference probably is due to a point source of dissolved phosphate to the Pienaars River, namely effluent from a sewage works upstream from measuring point. A definite seasonal phosphorus/flow trend could be discerned in the regression analysis, for flows greater than 0.22 $m^3 s^{-1}$ for the period May to November, and for flows greater than 0.25 $m^3 s^{-1}$ for the period December to April (Table A1.8). It was found that the truncation level of the flow influenced the value of R^2 significantly. The final infilling was done with the aid of the three-stage technique mentioned previously, for the period May-November (flow > 0.22 $m^3 s^{-1}$) and for the period December-April (flow > 0.25 $m^3 s^{-1}$). Below these flows linear interpolation was used. No annual trend could be established.

The other two rivers did not show any seasonal phosphorus/flow dependence. In spite of exhaustive efforts, no discernable cause for the spread of data could be identified. The linear regression coefficient was low, $\approx$ 0.2 and $\approx$ 0.3 (Table A1.8). However, in view of the much lower dissolved phosphate concentration in these two rivers, the regression relationship between flow and dissolved phosphate was accepted.

A1.4.3.3 Infilling of missing ammonia (NH_4) data:

An attempt was made to infill missing ammonia data with the aid of river flow rate data. However, in spite of exhaustive efforts, a significant relationship between ammonia and

flow rate data could not be found, as is evident in the R^2 value for the linear regression between ammonia and flow rate (0.04). Consequently, missing ammonia data were infilled by linear interpolation between observed data at the beginning and end of the missing period.

A1.4.3.4 Infilling of missing nitrate (NO_3) data:

A better linear regression between nitrate and river flow rate data was obtained than was the case with ammonia data (R^2 value for nitrate 0.15 as opposed to 0.04 for ammonia). Even though this the correlation is still poor, missing nitrate data were infilled with the aid of river flow data.

A1.4.3.5 Infilling of missing total dissolved salt (TDS) data:

Although a very good linear regression between TDS and conductivity was found for each river, the regression relationship could not be used for infilling TDS data from conductivity data, because both TDS and conductivity were monitored at the same time, or both not at all. The missing values therefore had to be filled in with the aid of river flow rate, using the aforementioned three-stage approach. The regression relationship between TDS and river flow rate was also described best by the natural logarithm of the two variables. The regression coefficients for Pienaars River and Edenvalespruit were reasonable (R^2 = 0.52 and 0.72 respectively) but the R^2-value for Hartbeesspruit was low, ≈ 0.3.

A1.4.3.6 Infilling of missing inorganic suspended sediment (TSS) data:

No data on inorganic suspended sediment concentration were available. TSS is modelled as an implicit part of the processes that govern water quality and temperature distribution in a reservoir, therefore it was vital that some estimate of TSS be made in order to simulate the behaviour of the reservoir. Also, during calibration of the water quality part of the model, it was found that TSS concentration has a definite effect on simulation of algal growth kinetics - in view of the high TSS concentrations normally found in South African reservoirs, this finding is not unexpected.

The approach to find surrogate TSS data went through two phases; in the first phase, time-series data on the concentration of total suspended matter (TSM) in the reservoir were available. TSM is defined as comprising dead and alive phyto- and zooplankton, as well as inorganic suspended sediment and detritus (DWAF, 1988). TSM concentration was measured three times per week at points 6, 3 and 5 in the reservoir. (See map, Fig A1.1). Point 3 is near the confluence of Pienaars River and Hartbeesspruit and therefore it was concluded that TSM concentration at this point very likely approximated the weighted average TSM concentration of Pienaars River and Hartbeesspruit. The TSM data at point 5 should adequately reflect the TSM concentration of Edenvalespruit. Point 6 is well away from the effect of inflows and consequently TSM data at this point were used as field data to compare the simulated and observed TSS/TSM results. Missing time-series TSM data were filled in by linear interpolation. However, running the model with this set of TSM data did not result in any improvement in the correlation between observed and simulated chlorophyll- a concentration. Also, when the TSM data were compared with the flow data it did not reflect the relationship usually expected between TSS and flow. Upon investigation it was found that (DWAF (HRI) - personal communication):

- Total Suspended Matter at monitoring point 6 at Roodeplaat Dam consists of only algal biomass, and not phyto- and zooplankton, inorganic suspended sediment and detritus, as defined in TR 136: Analytical Methods Manual (DWAF (HRI), 1988)

- The assumption that TSM concentration at monitoring point 3 approximated the weighted average TSM concentration of Pienaars River and Hartbeesspruit is incorrect.

It was concluded that TSM cannot serve as a reliable measure of TSS, and therefore, and thus another approach to synthesize TSS data had to be followed.

The second phase of the search for surrogate TSS data centred on the synthesizing of daily TSS concentrations by use of the daily inflow record, as well as unit

streampower theory. The unit streampower equation, based on daily flows, as developed by Rooseboom, was calibrated against the surveyed sediment volume in Roodeplaat Dam for the period 1959 to 1980. Though this solved the problem of TSS concentration entering the Dam, it did not provide any TSS data in the Dam against which the performance of the model could be checked. However, monthly measurements of secchi disc depth in Roodeplaat Dam are available, and, under high sediment loads, secchi disc depth becomes a function of TSS concentration. The following relationship between secchi disc depth and TSS concentration has been established (Henderson-Sellers 1984, Stefan *et al* 1982):

$$TSS = 8\ d^{-1.6} \qquad \text{(A1.1)}$$

TSS = Total inorganic suspended sediment concentration (mg l^{-1})
d = Secchi disc depth (m)

This correlation is valid only in the absence of high algal concentrations. Using Eq. (1), TSS concentrations were calculated from secchi disc depth measurements for Roodeplaat Dam during periods when the chlorophyll-a concentration was less than 10 $\mu g\ l^{-1}$. These concentrations were then used as 'observed data' to check the simulation of suspended sediment in the upper layers of the Dam. (Also see discussion on TSS simulation in Chapters 7 and 8).

A1.4.3.7. Infilling of missing dissolved oxygen data:

Dissolved oxygen concentration was not measured in any of the three rivers. However, the concentration of dissolved oxygen in water is a function of water temperature, thus the concentration of dissolved oxygen in the rivers was approximated by the following equation (Riley 1988):

$$DO = (14.652 - T_s(0.41022 - T_s * ((7.99 * 10^{-3}) - 7.7774 * 10^{-5} * T_s))) \quad \text{(A1.2)}$$

DO = saturated dissolved oxygen concentration (mg l^{-1})
T_s = surface water temperature (°C)

A1.4.3.8 Infilling of missing wind speed data:

Monitoring of wind speed data was done at Roodeplaat Dam. Analysis of the wind speed (and wind direction) data required digitizing of the data from Roodeplaat Dam from the original wind recorder charts (an extremely time consuming process). Also, the data were not complete - see Table A1.3. To infill the missing data, it was found that, for the windy period, August to December, a slight correlation ($R^2 = 0.4$) existed between the daily wind speed measured at Forum Building in Pretoria, and wind speed measured at Roodeplaat Dam. For this period, infilling of missing data was done using the regression relationship between the wind speeds at the two locations. During the low wind period, January to July, the correlation between the wind speeds was near zero and accordingly infilling of Roodeplaat Dam wind speed was done by linear interpolation between the known wind speed at the beginning and end of the missing period.

Regarding the height where wind speed was measured - the model requires wind speed data measured at 10 meter above ground. However, the wind speed data at Roodeplaat Dam was measured at 1.8 meter (6 ft) above ground, therefore it had to be converted to wind speed at 10 meter [4]. The conversion was done using the Logarithmic Formula - see Appendix A2.

[4] If the observed wind speed was not measured at a height of 10 m, it is of extreme importance to convert the observed wind speed to wind speed at 10 m height - see discussion in Appendix A2.

A1.4.3.9 Infilling of missing wind direction data:

A study of the dominant monthly wind directions at Roodeplaat Dam and Forum Building in Pretoria showed a similarity only during the windy period from about August to January (Table A1.9). Missing wind direction data for the period August to January for Roodeplaat Dam therefore were filled in from the daily wind direction at Forum Building. For the low wind period (February to July) the dominant monthly wind direction at Roodeplaat Dam was used to fill in the daily missing values.

TABLE A1.9 Monthly dominant wind direction* at Forum Building in Pretoria and at Roodeplaat dam.

	J	F	M	A	M	J	J	A	S	O	N	Dec
1980												
Forum	3	7	7	25	7	7/25	3/7	3	3	3	3	3
Roode	3	16/3	12	12	16	16	16	3	3	3	3	3
1981												
Forum	3	7	7	7	7	25	3	7	25	7	3	3
Roode	16	16	16	21	16	21	21	21	3	7	3	3
1982												
Forum	3	7	3	25	25	25	3	25	3	3	3	3
Roode	16	16	16	16	16	16	16	16	16	7	3	3
1983												
Forum	3	7	7	3	21	25	25	25	3	3	3	3
Roode	16	12	16	16	16	16	16	16	16	3	3	16

* In degrees/10, with zero = north and angle of rotation clockwise

A1.4.3.10 Infilling of missing sun hour and solar radiation data:

The linear regression between sun hours and solar radiation is based on an Ångstrom-type formula, i.e.

$$\frac{Q}{Q_A} = a + b\left(\frac{S}{S_o}\right) \qquad \text{(A1.3)}$$

Q = Solar radiation as measured.

Q_A = Ångot value of radiation (radiation before passing through atmosphere).

S = Hours of sunshine as measured.

S_o = Astronomical (theoretical) day length.

a,b = Constants

The constants a and b are preferably calculated for each month. According to the literature, there may be a deviation from linearity when $(S/S_o) < 0.5$ (Louw 1965) or when $(S/S_o) < 0.2$ (Reid 1981). However, no significant difference could be found between the monthly values of a and b, and neither was the linearity improved by only considering values where $(S/S_o) > 0.5$ or 0.2. The infilling of both radiation and sun hours therefore were done by a straight regression correlation with no special conditions.

3.11.2 Reservoir characteristics, water quality variables and calibration coefficients:

Lake specific subroutine: The lake specific subroutine contains two lake-specific functions that must be developed and coded into the subroutine. These are:

a) The relationship between water surface area and depth:

The relationship was developed from hydrographic information received from Department of Water Affairs and Forestry, and 1:10 000 ortho maps.

b) Wind fetch as a function of wind direction:

The function was developed from 1:10 000 ortho maps of the reservoir, and varies with the wind direction.

Reservoir water quality: Depth profiles of the following variables were considered necessary for Roodeplaat Dam: water temperature, dissolved oxygen (DO), dissolved phosphate, nitrate, ammonia,inorganic suspended sediment and chlorophyll-a. Depth profiles of water temperature and DO were measured monthly and sometimes weekly, but only down to the thermocline. Concentrations of dissolved phosphate, nitrate-nitrite, ammonia, TDS and chlorophyll-a were mostly measured at the surface only. Occasionally an integrated sample from surface to 5 meters was taken. Depth profile data were obtained from the Hydrological Research Institute (Department of Water Affairs and Forestry).

APPENDIX A2

CONVERSION OF WIND SPEED

A2.1 INTRODUCTION

The surface of the earth exerts a horizontal drag force upon moving air, thereby slowing down the flow of air. The effect of the drag force is a function of surface roughness and decreases with increasing height above ground. It becomes negligible above a certain height (approximately 1 km) known as the *boundary layer of the atmosphere*. The atmosphere above the boundary layer is known as the free atmosphere (Geiger 1965, Simiu and Scanlan 1986).

As a result of the effect of the drag force decreasing with increasing height above ground, wind speed varies with height above ground also. Consequently, it is not possible to directly compare wind speed measured at a certain height with wind speed measured at a different height, a conversion has to be done so that both wind speeds are at the same height. Similarly, in the case of a mathematical model such as MINLAKE, (where the input wind speed should be the wind speed at 10 meter above ground), if the observed wind speed was not measured at 10 meters, the observed wind speed should be converted to wind speed at 10 meter height. Furthermore, because the effect of the drag force is influenced by surface roughness, wind speed at a certain height above ground will differ from wind speed above water at the same height. Some models, eg. MINLAKE, incorporate the adjustment of wind speed from land to water surface in the simulation program, whereas other models, eg. DYRESM, require the user to adapt the wind speed as part of the meteorological data.

Two formulae are generally used to adapt wind speed measurements with height, the Power Law formula, and the Logarithmic formula. Wind speed measured over land can

be adapted to wind speed over water at the same height, by using a relationship between the fetch and the roughness factor for land and water surfaces.

A2.2 THE POWER LAW.

The Power Law was first used in 1880 to describe the change in wind speed with height (Bruetsaert *et al*, 1970). It was derived empirically and gives a good approximation of the variation of wind speed with height, provided the terrain is horizontally homogeneous (Ciria, 1971). According to the power law (Le Gourieres, 1982):

$$\frac{V}{V_o} = \left(\frac{H}{H_o}\right)^n \qquad \text{A2.1}$$

V_o = measured wind speed at height H_o

V = wind speed at height H

n = a constant dependent upon roughness of terrain.

Different values of n for different terrains is given in Table A2.1

TABLE A2.1 Values of the Power Law exponent n for various terrains (Ciria, 1971).

Type of terrain	n
Water surface, eg. oceans and lakes	0.14
Open terrain with few obstacles, eg desert or open grass	0.16
Terrain uniformly covered with obstacles 10 to 15 m in height, eg small towns, small fields with bushes trees and hedges.	0.28
Terrain with large and irregular objects, eg. centres of large cities, very broken country with many tall trees.	0.4

In the Power Law (Eq A2.1), the value of n is constant for a given application, However, the value of n has been found to change with height (Geiger, 1965), therefore the Power Law only gives an approximation of the wind profile. Conditions under which the Power Law will give realistic results, can be summarized as follows (CIRIA, 1971):

"Provided the terrain is reasonably level, and of sufficiently uniform surface roughness to allow a state of dynamic equilibrium to be established between the drag and the stirring action of the surface, and the steady flow at high level determined by the isobar map, the variation of mean wind speed with height in neutral stability (high wind) conditions, can be satisfactorily represented by a simple power law."

If a model is sensitive to wind speed, most likely the Power Law will be inadequate.

A2.3. THE LOGARITHMIC LAW.

The Logarithmic Law is based on Prandtl's Logarithmic Law that states that the flow of air over a surface (i.e wind speed over a certain terrain) is expressed by (Simiu and Scanlan, 1986):

$$V = \frac{u_*}{k} \ln\left(\frac{H}{z_o}\right) \qquad \text{A2.2}$$

V	=	wind speed at height H above the surface
u.	=	wind shear velocity
k	=	Von Karman's constant (0.4)
z_o	=	roughness length

The shear velocity is indicative of the amount of turbulence, and its value is independent of height for a given profile. The roughness length is a function of the roughness of the surface and also is independent of height for a given profile. It is

determined empirically and has the dimensions of length, thereby expressing the roughness of the terrain as a numerical value. Different values of the roughness length for different terrains are given in Table A2.2.

Using Prandtl's law as a basis, the variation of wind speed with height for a given terrain can be expressed as:

$$\frac{V}{V_1} = \frac{\ln(\frac{H}{z_o})}{\ln(\frac{H_1}{z_o})} \qquad \text{A2.3}$$

V_1 = wind speed measured at height H_1

V = wind speed at the required height H

z_o = roughness length (from Table A2.2)

TABLE A2.2. Values of surface roughness length z_o in the Logarithmic Law (Simiu and Scanlan 1986).

Type of surface	z_o (cm)
Sand	0.01 - 0.10
Snow surface	0.10 - 0.60
Mown grass (~0.01 m)	0.10 - 1
Low grass, steppe	1 - 4
Fallow field	2 - 3
High grass	4 - 10
Palmetto	10 - 30
Pine forest (mean height of trees: 15 m; one tree per 10 m^2)	90 - 100
Sparsely built-up suburbs	20 - 40
Densely built-up suburbs, towns	80 - 120
Centres of large cities	200 - 300

A2.4 ADAPTING WIND SPEED FROM LAND TO WATER SURFACE

The relationship between wind speed over land and wind speed over water, at the same height, is expressed by (Ford and Stefan, 1980):

$$V_w = V_{10} \frac{\ln\frac{H}{z_2}\ \ln\frac{z_b}{z_1}}{\ln\frac{H}{z_1}\ \ln\frac{z_b}{z_2}} \qquad \text{A2.4}$$

V_w = wind speed over water at a height of 10 meters (m s^{-1})

V_{10} = wind speed measured over land at a height of 10 meters (m s^{-1})

z_2 = surface roughness of the water (~0.0001m)

z_1 = surface roughness of the land in meter. (From Table A2.2)

z_b = equivalent boundary layer over the water.

The equivalent boundary layer over the water is expressed by (Elliot 1958):

$z_b = 0.86(\text{Fetch})\ z_1^{0.23}$

z_b = equivalent boundary layer over water

Fetch = fetch of the wind over the water surface (m)

z_1 = surface roughness of the land (m)

APPENDIX A3

CALCULATION OF THE HYPOLIMNETIC EDDY DIFFUSION COEFFICIENT

A4.1 INTRODUCTION

The eddy diffusion coefficient increases with depth in the hypolimnion, reaching a maximum at about mid-depth in the hypolimnion. Both the original and the modified MINLAKE model requires the user to specify the maximum hypolimnetic eddy diffusion coefficient (*cf* paragraph 6.3.4.1). The eddy diffusion coefficient can be calculated from Eq 6.7 and 6.8. Table A4.1 below is an example of the calculation that was done for Roodeplaat Dam utilizing data observed on 13 October 1980. From dT/dZ (the change in temperature with depth), it would seem that the thermocline was situated between 6 and 7 meters. The molecular diffusion coefficient was taken to be 0.12×10^{-2} cm^2s^{-1}.

Table A4.1 Example of hypolimnetic eddy diffusion calculation for Roodeplaat Dam

13 OCT 1980 OBSERVED DATA							
Z	Temp	dT/dZ	dZ	Area(cm2)	Area*temp	∫(Area*Temp)	EDDY
0	21.7			4.03e+10	8.73e+11	7.42e+12	
1	21.3	-0.4	1	3.70e+10	7.89e+11	6.55e+12	
2	21	-0.3	1	3.41e+10	7.15e+11	5.76e+12	
3	20.9	-0.1	1	3.12e+10	6.53e+11	5.04e+12	
4	18.8	-2.1	1	2.85e+10	5.36e+11	4.39e+12	
5	17.8	-1	1	2.54e+10	4.53e+11	3.85e+12	
6	16.8	-1	1	2.29e+10	3.84e+11	3.40e+12	0.00
7	16.2	-0.6	1	2.09e+10	3.38e+11	3.02e+12	0.03
8	15.7	-0.5	1	1.88e+10	2.95e+11	2.68e+12	0.04

9	15.3	-0.4	1	1.72e+10	2.63e+11	2.38e+12	0.05
10	14.4	-0.9	1	1.57e+10	2.26e+11	2.12e+12	0.03
11	13.2	-1.2	1	1.43e+10	1.89e+11	1.90e+12	0.02
12	12.9	-0.3	1	1.27e+10	1.64e+11	1.71e+12	0.10
13	12.5	-0.4	1	1.14e+10	1.43e+11	1.54e+12	0.08
14	12.2	-0.3	1	1.07e+10	1.31e+11	1.40e+12	0.12
15	12.1	-0.1	1	9.82e+09	1.19e+11	1.27e+12	0.39
16	12	-0.1	1	9.05e+09	1.09e+11	1.15e+12	0.42
17	11.8	-0.2	1	8.45e+09	9.97e+10	1.04e+12	0.23
18	11.7	-0.1	1	7.96e+09	9.31e+10	9.41e+11	0.48
19	11.6	-0.1	1	7.49e+09	8.68e+10	8.48e+11	0.51
20	11.5	-0.1	1	6.93e+09	7.97e+10	7.61e+11	0.55
21	11.3	-0.2	1	6.28e+09	7.10e+10	6.82e+11	0.31
22	11.3	0	1	5.80e+09	6.55e+10	6.11e+11	ERR
23	11.3	0	1	5.46e+09	6.17e+10	5.45e+11	ERR
24	11.2	-0.1	1	5.05e+09	5.66e+10	4.84e+11	0.76
25	11.2	0	1	4.56e+09	5.11e+10	4.27e+11	ERR
26	11.2	0	1	4.11e+09	4.60e+10	3.76e+11	ERR
27	11.1	-0.1	1	3.83e+09	4.25e+10	3.30e+11	1.00
28	11.1	0	1	3.61e+09	4.01e+10	2.87e+11	ERR
29	11.1	0	1	3.06e+09	3.39e+10	2.47e+11	ERR
30	11.1	0	1	2.84e+09	3.15e+10	2.13e+11	ERR
31	11.1	0	1	2.60e+09	2.89e+10	1.82e+11	ERR
32	11	-0.1	1	2.26e+09	2.49e+10	1.53e+11	1.70